

Pertanika Journal of
**SCIENCE &
TECHNOLOGY**

JST

VOL. 25 (3) JUL. 2017



PERTANIKA
JOURNALS

A scientific journal published by Universiti Putra Malaysia Press

Journal of Science & Technology

About the Journal

Overview

Pertanika Journal of Science & Technology (JST) is the official journal of Universiti Putra Malaysia published by UPM Press. It is an open-access online scientific journal which is free of charge. It publishes the scientific outputs. It neither accepts nor commissions third party content.

Recognized internationally as the leading peer-reviewed interdisciplinary journal devoted to the publication of original papers, it serves as a forum for practical approaches to improving quality in issues pertaining to science and engineering and its related fields.

JST is a **quarterly** (January, April, July and October) periodical that considers for publication original articles as per its scope. The journal publishes in **English** and it is open to authors around the world regardless of the nationality.

The Journal is available world-wide.

Aims and scope

Pertanika Journal of Science and Technology aims to provide a forum for high quality research related to science and engineering research. Areas relevant to the scope of the journal include: bioinformatics, bioscience, biotechnology and bio-molecular sciences, chemistry, computer science, ecology, engineering, engineering design, environmental control and management, mathematics and statistics, medicine and health sciences, nanotechnology, physics, safety and emergency management, and related fields of study.

History

Pertanika was founded in 1978. A decision was made in 1992 to streamline Pertanika into three journals as Journal of Tropical Agricultural Science, Journal of Science & Technology, and Journal of Social Sciences & Humanities to meet the need for specialised journals in areas of study aligned with the interdisciplinary strengths of the university.

After almost 25 years, as an interdisciplinary Journal of Science & Technology, the revamped journal now focuses on research in science and engineering and its related fields.

Goal of *Pertanika*

Our goal is to bring the highest quality research to the widest possible audience.

Quality

We aim for excellence, sustained by a responsible and professional approach to journal publishing. Submissions are guaranteed to receive a decision within 14 weeks. The elapsed time from submission to publication for the articles averages 5-6 months.

Abstracting and indexing of *Pertanika*

Pertanika is almost 40 years old; this accumulated knowledge has resulted in Pertanika JST being abstracted and indexed in SCOPUS (Elsevier), Thomson (ISI) Web of Knowledge [BIOSIS & CAB Abstracts], EBSCO & EBSCOhost, DOAJ, ERA, Cabell's Directories, Google Scholar, MyAIS, ISC & Rubriq (Journal Guide).

Future vision

We are continuously improving access to our journal archives, content, and research services. We have the drive to realise exciting new horizons that will benefit not only the academic community, but society itself.

Citing journal articles

The abbreviation for Pertanika Journal of Science & Technology is *Pertanika J. Sci. Technol.*

Publication policy

Pertanika policy prohibits an author from submitting the same manuscript for concurrent consideration by two or more publications. It prohibits as well publication of any manuscript that has already been published either in whole or substantial part elsewhere. It also does not permit publication of manuscript that has been published in full in Proceedings.

Code of Ethics

The Pertanika Journals and Universiti Putra Malaysia takes seriously the responsibility of all of its journal publications to reflect the highest in publication ethics. Thus all journals and journal editors are expected to abide by the Journal's codes of ethics. Refer to Pertanika's **Code of Ethics** for full details, or visit the Journal's web link at http://www.pertanika.upm.edu.my/code_of_ethics.php

International Standard Serial Number (ISSN)

An ISSN is an 8-digit code used to identify periodicals such as journals of all kinds and on all media—print and electronic. All Pertanika journals have ISSN as well as an e-ISSN.

Journal of Science & Technology: ISSN 0128-7680 (*Print*); ISSN 2231-8526 (*Online*).

Lag time

A decision on acceptance or rejection of a manuscript is reached in 3 to 4 months (average 14 weeks). The elapsed time from submission to publication for the articles averages 5-6 months.

Authorship

Authors are not permitted to add or remove any names from the authorship provided at the time of initial submission without the consent of the Journal's Chief Executive Editor.

Manuscript preparation

Refer to Pertanika's **INSTRUCTIONS TO AUTHORS** at the back of this journal.

Most scientific papers are prepared according to a format called IMRAD. The term represents the first letters of the words **I**ntroduction, **M**aterials and **M**ethods, **R**esults, **A**nd, **D**iscussion. IMRAD is simply a more 'defined' version of the "IBC" [Introduction, Body, Conclusion] format used for all academic writing. IMRAD indicates a pattern or format rather than a complete list of headings or components of research papers; the missing parts of a paper are: *Title, Authors, Keywords, Abstract, Conclusions, and References*. Additionally, some papers include Acknowledgments and Appendices.

The *Introduction* explains the scope and objective of the study in the light of current knowledge on the subject; the *Materials and Methods* describes how the study was conducted; the *Results* section reports what was found in the study; and the *Discussion* section explains meaning and significance of the results and provides suggestions for future directions of research. The manuscript must be prepared according to the Journal's **INSTRUCTIONS TO AUTHORS**.

Editorial process

Authors are notified with an acknowledgement containing a *Manuscript ID* on receipt of a manuscript, and upon the editorial decision regarding publication.

Pertanika follows a **double-blind peer-review** process. Manuscripts deemed suitable for publication are usually sent to reviewers. Authors are encouraged to suggest names of at least three potential reviewers at the time of submission of their manuscript to Pertanika, but the editors will make the final choice. The editors are not, however, bound by these suggestions.

Notification of the editorial decision is usually provided within ten to fourteen weeks from the receipt of manuscript. Publication of solicited manuscripts is not guaranteed. In most cases, manuscripts are accepted conditionally, pending an author's revision of the material.

As articles are double-blind reviewed, material that might identify authorship of the paper should be placed only on page 2 as described in the first-4 page format in Pertanika's **INSTRUCTIONS TO AUTHORS** given at the back of this journal.

The Journal's peer-review

In the peer-review process, three referees independently evaluate the scientific quality of the submitted manuscripts.

Peer reviewers are experts chosen by journal editors to provide written assessment of the **strengths** and **weaknesses** of written research, with the aim of improving the reporting of research and identifying the most appropriate and highest quality material for the journal.

Operating and review process

What happens to a manuscript once it is submitted to *Pertanika*? Typically, there are seven steps to the editorial review process:

1. The Journal's chief executive editor and the editorial board examine the paper to determine whether it is appropriate for the journal and should be reviewed. If not appropriate, the manuscript is rejected outright and the author is informed.
2. The chief executive editor sends the article-identifying information having been removed, to three reviewers. Typically, one of these is from the Journal's editorial board. Others are specialists in the subject matter represented by the article. The chief executive editor asks them to complete the review in three weeks.

Comments to authors are about the appropriateness and adequacy of the theoretical or conceptual framework, literature review, method, results and discussion, and conclusions. Reviewers often include suggestions for strengthening of the manuscript. Comments to the editor are in the nature of the significance of the work and its potential contribution to the literature.

3. The chief executive editor, in consultation with the editor-in-chief, examines the reviews and decides whether to reject the manuscript, invite the author(s) to revise and resubmit the manuscript, or seek additional reviews. Final acceptance or rejection rests with the Editor-in-Chief, who reserves the right to refuse any material for publication. In rare instances, the manuscript is accepted with almost no revision. Almost without exception, reviewers' comments (to the author) are forwarded to the author. If a revision is indicated, the editor provides guidelines for attending to the reviewers' suggestions and perhaps additional advice about revising the manuscript.
4. The authors decide whether and how to address the reviewers' comments and criticisms and the editor's concerns. The authors return a revised version of the paper to the chief executive editor along with specific information describing how they have answered the concerns of the reviewers and the editor, usually in a tabular form. The author(s) may also submit a rebuttal if there is a need especially when the author disagrees with certain comments provided by reviewer(s).

5. The chief executive editor sends the revised paper out for re-review. Typically, at least one of the original reviewers will be asked to examine the article.
6. When the reviewers have completed their work, the chief executive editor in consultation with the editorial board and the editor-in-chief examine their comments and decide whether the paper is ready to be published, needs another round of revisions, or should be rejected.
7. If the decision is to accept, an acceptance letter is sent to all the author(s), the paper is sent to the Press. The article should appear in print in approximately three months.

The Publisher ensures that the paper adheres to the correct style (in-text citations, the reference list, and tables are typical areas of concern, clarity, and grammar). The authors are asked to respond to any minor queries by the Publisher. Following these corrections, page proofs are mailed to the corresponding authors for their final approval. At this point, **only essential changes are accepted**. Finally, the article appears in the pages of the Journal and is posted on-line.



EDITOR-IN-CHIEF

Mohd Adzir Mahdi

Physics, Optical Communications

CHIEF EXECUTIVE EDITOR

Nayan Deep S. Kanwal

Environmental Issues – Landscape Plant Modelling Applications

UNIVERSITY PUBLICATIONS COMMITTEE

Husaini Omar, Chair

EDITORIAL STAFF

Journal Officers:

Kanagamalar Silvarajoo, *ScholarOne*

Lim Ee Leen, *ScholarOne*

Tee Syin-Ying, *ScholarOne*

Editorial Assistants:

Zulinaardawati Kamarudin

Florence Jiyom

Ummi Fairuz Hanapi

Rahimah Razali

COPY EDITORS

Doreen Dillah

Crescentia Morais

Pooja Terasha Stanslas

PRODUCTION STAFF

Pre-press Officers:

Kanagamalar Silvarajoo

Nur Farrah Dila Ismail

Layout & Typeset:

Wong Wai Mann

WEBMASTER

Mohd Nazri Othman

PUBLICITY & PRESS RELEASE

Magdalene Pokar (*ResearchSEA*)

Florence Jiyom

EDITORIAL OFFICE

JOURNAL DIVISION

Office of the Deputy Vice Chancellor (R&I)

1st Floor, IDEA Tower II

UPM-MTDC Technology Centre

Universiti Putra Malaysia

43400 Serdang, Selangor Malaysia.

Gen Enq.: +603 8947 1622 | 1616

E-mail: executive_editor.pertanika@upm.my

URL: www.journals-td.upm.edu.my

PUBLISHER

Kamariah Mohd Saidin

UPM Press

Universiti Putra Malaysia

43400 UPM, Serdang, Selangor, Malaysia.

Tel: +603 8946 8855, 8946 8854

Fax: +603 8941 6172

E-mail: penerbit@putra.upm.edu.my

URL: <http://penerbit.upm.edu.my>



EDITORIAL BOARD

2015-2017

Abdul Halim Shaari

Superconductivity and Magnetism, Universiti Putra Malaysia, Malaysia.

Adem Kilicman

Mathematical Sciences, Universiti Putra Malaysia, Malaysia.

Ahmad Makmom Abdullah

Ecophysiology and Air Pollution Modelling, Universiti Putra Malaysia, Malaysia.

Ali A. Moosavi-Movahedi

Biophysical Chemistry, University of Tehran, Tehran, Iran.

Amu Therwath

Oncology, Molecular Biology, Université Paris, France.

Angelina Chin

Mathematics, Group Theory and Generalisations, Ring Theory, University of Malaya, Malaysia.

Bassim H. Hameed

Chemical Engineering: Reaction Engineering, Environmental Catalysis & Adsorption, Universiti Sains Malaysia, Malaysia.

Biswa Mohan Biswal

Medical, Clinical Oncology, Radiotherapy, Universiti Sains Malaysia, Malaysia.

Christopher G. Jesudason

Mathematical Chemistry, Molecular Dynamics Simulations, Thermodynamics and General Physical Theory, University of Malaya, Malaysia.

Hari M. Srivastava

Mathematics and Statistics, University of Victoria, Canada.

Ivan D. Rukhlenko

Nonlinear Optics, Silicon Photonics, Plasmonics and Nanotechnology, Monash University, Australia.

Kaniraj R. Shenbaga

Geotechnical Engineering, Universiti Malaysia Sarawak, Malaysia.

Kanury Rao

Senior Scientist & Head, Immunology Group, International Center for Genetic Engineering and Biotechnology, Immunology, Infectious Disease Biology and System Biology, International Centre for Genetic Engineering & Biotechnology, New Delhi, India.

Karen Ann Crouse

Chemistry, Material Chemistry, Metal Complexes – Synthesis, Reactivity, Bioactivity, Universiti Putra Malaysia, Malaysia.

Ki-Hyung Kim

Computer and Wireless Sensor Networks, AIOU University, Korea.

Kunnawee Kanitpong

Transportation Engineering-Road Traffic Safety, Highway Materials and Construction, Asian Institute of Technology, Thailand.

Megat Mohd Hamdan

Megat Ahmad Mechanical and Manufacturing Engineering, Universiti Pertahanan Nasional Malaysia, Malaysia.

Mirnalini Kandiah

Public Health Nutrition, Nutritional Epidemiology, UCSI University, Malaysia.

Mohamed Othman

Communication Technology and Network, Scientific Computing, Universiti Putra Malaysia, Malaysia.

Mohd. Ali Hassan

Bioprocess Engineering, Environmental Biotechnology, Universiti Putra Malaysia, Malaysia.

Mohd Sapuan Salit

Concurrent Engineering and Composite Materials, Universiti Putra Malaysia, Malaysia.

Narongrit Sombatsompop

Engineering & Technology: Materials and Polymer Research, King Mongkut's University of Technology Thonburi (KMUTT), Thailand.

Prakash C. Sinha

Physical Oceanography, Mathematical Modelling, Fluid Mechanics, Numerical Techniques, Universiti Malaysia Terengganu, Malaysia.

Rajinder Singh

Biotechnology, Biomolecular Sciences, Molecular Markers/ Genetic Mapping, Malaysia Palm Oil Board, Kajang, Malaysia.

Renuganth Varatharajoo

Engineering, Space System, Universiti Putra Malaysia, Malaysia.

Riyanto T. Bambang

Electrical Engineering, Control, Intelligent Systems & Robotics, Bandung Institute of Technology, Indonesia.

Sabira Khatun

Engineering, Computer Systems & Software Engineering, Applied Mathematics, Universiti Malaysia Pahang, Malaysia.

Shiv Dutt Gupta

Director, IHMR, Health Management, Public Health, Epidemiology, Chronic and Non-communicable Diseases, Indian Institute of Health Management Research, India.

Suan-Choo Cheah

Biotechnology, Plant Molecular Biology, Asiatic Centre for Genome Technology (ACGT), Kuala Lumpur, Malaysia.

Wagar Asrar

Engineering, Computational Fluid Dynamics, Experimental Aerodynamics, International Islamic University, Malaysia.

Wing Keong Ng

Aquaculture, Aquatic Animal Nutrition, Aqua Feed Technology, Universiti Sains Malaysia, Malaysia.

Yudi Samyudia

Chemical Engineering, Advanced Process Engineering, Curtin University of Technology, Malaysia.

INTERNATIONAL ADVISORY BOARD

2017-2019

Adarsh Sandhu

Editorial Consultant for Nature Nanotechnology and Contributing Writer for Nature Photonics, Physics, Magneto-resistive Semiconducting Magnetic Field Sensors, Nano-Bio-Magnetism, Magnetic Particle Colloids, Point of Care Diagnostics, Medical Physics, Scanning Hall Probe Microscopy, Synthesis and Application of Graphene, Electronics-inspired Interdisciplinary Research Institute (EIIRIS), Toyohashi University of Technology, Japan.

Graham Megson

Computer Science, The University of Westminster, U.K.

Kuan-Chong Ting

Agricultural and Biological Engineering, University of Illinois at Urbana-Champaign, USA.

Malin Premaratne

Advanced Computing and Simulation, Monash University, Australia.

Mohammed Ismail Elnaggar

Electrical Engineering, Ohio State University, USA.

Peter G. Alderson

Bioscience, The University of Nottingham, Malaysia Campus.

Peter J. Heggs

Chemical Engineering, University of Leeds, U.K.

Ravi Prakash

Vice Chancellor, JUIT, Mechanical Engineering, Machine Design, Biomedical and Materials Science, Jaypee University of Information Technology, India.

Said S.E.H. Elnashaie

Environmental and Sustainable Engineering, Penn. State University at Harrisburg, USA.

Suhash Chandra Dutta Roy

Electrical Engineering, Indian Institute of Technology (IIT) Delhi, India.

Vijay Arora

Quantum and Nano-Engineering Processes, Wilkes University, USA.

Yi Li

Chemistry, Photochemical Studies, Organic Compounds, Chemical Engineering, Chinese Academy of Sciences, Beijing, China.

ABSTRACTING/INDEXING

Pertanika is now over 39 years old; this accumulated knowledge has resulted the journals being indexed in abstracted in SCOPUS (Elsevier), Thomson (ISI) Web of Knowledge [ESCI, BIOSIS & CAB Abstracts], EBSCO & EBSCOhost, ERA, DOAJ, AGRICOLA (National Agric. Library, USA), Cabell's Directories, Google Scholar, MyAIS, Islamic World Science Citation Center (ISC), ASEAN Citation Index (ACI) & Rubriq (Journal Guide).

The publisher of *Pertanika* will not be responsible for the statements made by the authors in any articles published in the journal. Under no circumstances will the publisher of this publication be liable for any loss or damage caused by your reliance on the advice, opinion or information obtained either explicitly or implied through the contents of this publication.

All rights of reproduction are reserved in respect of all papers, articles, illustrations, etc., published in *Pertanika*. *Pertanika* provides free access to the full text of research articles for anyone, web-wide. It does not charge either its authors or author-institution for refereeing/publishing outgoing articles or user-institution for accessing incoming articles.

No material published in *Pertanika* may be reproduced or stored on microfilm or in electronic, optical or magnetic form without the written authorization of the Publisher.

Copyright © 2017 Universiti Putra Malaysia Press. All Rights Reserved.



Pertanika Journal of Science & Technology
Vol. 25 (3) Jul. 2017

Contents

Foreword	i
<i>Nayan Deep S. Kanwal</i>	
Review Article	
Implementation of Building Information Modelling (BIM) in Malaysia: A Review	661
<i>Nuzul Azam Haron, Raja Putri Zariyh Ana Raja Soh and Aizul Nahar Harun</i>	
Regular Articles	
Reliability, Technical Error of Measurement and Validity of Height Measurement Using Portable Stadiometer	675
<i>Azli Baharudin, Mohamad Hasnan Ahmad, Balkish Mahadir Naidu, Nurul Rufaidah Hamzah, Nor Azian Mohd Zaki, Ahmad Ali Zainuddin and Noor Safiza Mohd Nor</i>	
The value of ¹⁸ F-fluorodeoxyglucose –positron emission tomography/computed tomography (¹⁸ F- FDG PET/CT) in the staging and impact on the management of patients with nasopharyngeal carcinoma	687
<i>Sethu Thakachy Subha, Fathinul Fikri Ahmad Saad, Abdul Jalil Nordin and Saraiza Abu Bakar</i>	
Design of a Movable Swine Roasting Machine	697
<i>Bunkrachang, N. and Kitthawee, U.</i>	
Effect of inoculums content and screening of significant variables for simultaneous COD removal and H ₂ production from tapioca wastewater using Plackett-Burman Design	707
<i>Thanwised, P.</i>	
Comparison of Scoring Functions on Greedy Search Bayesian Network Learning Algorithms	719
<i>ChongYong, Chua and HongChoon, Ong</i>	
Selected Papers from the 2nd International Conference on Statistics in Science, Business and Engineering (ICSSBE 2015)	
Guest Editors: Yap Bee Wah & Sayang Mohd Deni	
Analysis of Malaysia's Single Stock Futures and Its Spot Price	735
<i>Marzuki, R. M., Mohd, M. A., Nawawi, A. H. M. and Redzwan, N. M.</i>	
Projecting Input-Output Table for Malaysia: A Comparison of RAS and EURO Method	745
<i>Shuja', N., Lazim, M. A. and Yap, B. W.</i>	

Relative Risk Estimation for Dengue Disease Mapping in Malaysia based on Besag, York and Mollié Model <i>Samat, N. A. and Pei Zhen, W.</i>	759
Effects of Baseline Correction Algorithms on Forensic Classification of Paper Based on ATR-FTIR Spectrum and Principal Component Analysis (PCA) <i>Lee, L. C., Liong, C-Y., Khairul, O. and Jemain, A. A.</i>	767
Deriving Partial Differential Equation for the Value of Salam Contract with Credit Risk <i>Hisham, A. F. B., Jaffar, M. M. and Othman, J.</i>	775
Combination of Forecasts with an Application to Unemployment Rate <i>Muniroh, M. F., Ismail, N. and Lazim, M. A.</i>	787
Complexity Index for Decision Making Method <i>Hanif, H. M., Mohamad, D. and Dom, R. M.</i>	797
Evaluation of Risk Factors for Prolonged Invasive Mechanical Ventilation in Paediatric Intensive Care Unit (PICU) <i>Ismail, I., Yap, B. W. and Abidin, A. S. Z.</i>	811
The Control Chart Technique for the Detection of the Problem of Bad Data in State Estimation Power System <i>Zahid Khan, Radzuan B. Razali, Hanita Daud, Nursyarizal Mohd Nor and Mahmud Fotuhi-Firuzabad</i>	825
Selected Papers from the International Conference on Science, Engineering, Law and Management (ICSELM 2017)	
Guest Editor: Hardeep Singh & Acmad Choerudin	
Guest Editorial Board: Pooja Sahni, Amit Wason, Surender Singh Saini, Elsanosy M. Elamin & Tolga Ensari	
Internet of Things – Technology Adoption Model in India <i>Singh, G., Gaur, L. and Ramakrishnan, R.</i>	835
Effect of Maghemite (γ -Fe ₂ O ₃) Nano-Powder Mixed Dielectric Medium on Tool Wear Rate (TWR) During Micro-EDM of Co- Cr-Mo <i>Elsiti, N. M., Noordin, M. Y. and Idris, A.</i>	847
Review of Channel Modelling for Optical Wireless Links <i>Miglani, R. and Malhotra, J. S.</i>	859
Dealing with Interdependency among NFR using ISM <i>Kaur, H. and Sharma, A.</i>	871
DNA and Bernoulli Random Number Generator Based Security Key Generation Algorithm <i>Sodhi, G. K. and Gaba, G. S.</i>	891
Analysis of MIMO FSO over different Modulation Techniques <i>Kaur, K., Miglani, R. and Malhotra, J. S.</i>	905

Performance Evaluation of Compressive Sensing based Channel Estimation Techniques in OFDM System for Different Channels <i>Jha, A., Kansal, L. and Gaba, G. S.</i>	921
Cost Estimation Model for Web Applications using Agile Software Development Methodology <i>Soni, D. and Kohli, P. J.</i>	931
Understanding Consumer Preferences using IoT SmartMirrors <i>Gaur, L., Singh, G. and Ramakrishnan, R.</i>	939
Selected Papers from the International Conference On Computational Methods In Engineering and Health Sciences (ICCMEH 2015)	
Guest Editor: Kamarul Ariffin Ahmad, Mohammad Zuber, Mohamad Ridzwan Ishak & Norkhairunnisa Mazlan	
Guest Editorial Board: Azmin Shakrine Mohd Rafie, Mohamed Thariq Hameed Sultan, Raghuvir Pai, Masaaki Tamagawa, Satish Shenoy, S. M. Abdul Khader & Satoshi Iikubo	
Investigation on Tapping of Al6061-SiC Metal Matrix Composite with HSS Taps <i>Melvin Paious, Raviraja Adhikari and Nagaraja</i>	949
Dynamic Performance Characteristics of Finite Journal Bearings Operating on TiO ₂ based Nanolubricants <i>Binu, K. G., Yathish, K., Shenoy, B. S., Rao, D. S. and Pai, R.</i>	963
Modal Behaviour of Vertical Axis Wind Turbine Comprising Prestressed Rotor Blades: A Finite Element Analysis <i>Torabi Asr, M., Masoumi, M. M. and Mustapha, F.</i>	977
A review study on diesel and natural gas and its impact on CI engine emissions <i>Hayder A. Alrazen and K. A. Ahmad</i>	983
Stability of water lubricated bearing using linear perturbation method under turbulent conditions <i>R. Mallya, B. S. Shenoy, R. S. Pai and R. Pai</i>	995
Estimation and Validation of Nearshore Current at the Coast of Carey Island, Malaysia <i>Fitri, A., Hashim, R. and Motamedi, S.</i>	1009
A Computational Fluid Dynamics Study of Combustion and Emission Performance in an Annular Combustor of a Jet Engine <i>M. Zuber, M. S. B. Hisham, N. A. M. Nasir, A. A. Basri and S. M. A. Khader</i>	1019
Effect of Silica Nanoparticles in Kenaf Reinforced Epoxy: Flexural and Compressive Properties <i>F. Bajuri, N. Mazlan and M. R. Ishak</i>	1029



Foreword

Welcome to the **Third Issue 2017** of the Journal of Science and Technology (JST)!

JST is an open-access journal for studies in science and technology published by Universiti Putra Malaysia Press. It is independently owned and managed by the university and is run on a non-profit basis for the benefit of the world-wide science community.

This issue contains **32 articles**, of which **one** is a review article and **five** are regular research articles. This issue also features **nine** selected papers from the 2nd International Conference on Statistics in Science, Business and Engineering (ICSSBE 2015), **nine** papers from the International Conference on Science, Engineering, Law and Management (ICSELM 2017) and **eight** papers from the International Conference On Computational Methods In Engineering and Health Sciences (ICCMEH 2015). The authors of these articles vary in country of origin, coming from **Malaysia, Iran, Indonesia, Hong Kong, Thailand, India, and Iraq**.

The review article in this issue discusses the implementation of building information modelling (BIM) in Malaysia (*Nuzul Azam Haron Raja Putri Zarifh Ana Raja Soh and Aizul Nahar Harun*).

The regular articles cover a wide range of topics. The first article is on the reliability, technical error of measurement and validity of height measurement using a portable stadiometer (*Azli Baharudin, Mohamad Hasnan Ahmad, Balkish Mahadir Naidu, Nurul Rufaidah Hamzah, Nor Azian Mohd Zaki, Ahmad Ali Zainuddin and Noor Safiza Mohd Nor*). The following articles look at the value of 18F-fluorodeoxyglucose-positron emission tomography/computed tomography (¹⁸F-FDG PET/CT) in staging and impact on the management of patients with nasopharyngeal carcinoma (*Sethu Thakachy Subha, Fathinul Fikri Ahmad Saad, Abdul Jalil Nordin and Saraiza Abu Bakar*); design of a movable swine-roasting machine (*Bunkrachang, N. and Kitthawee, U.*); effect of inoculum content and screening of significant variables for simultaneous COD removal and H₂ production from tapioca wastewater using the Plackett-Burman Design (*Thanwised, P.*); and comparison of scoring functions on greedy search Bayesian network learning algorithms (*ChongYong, Chua and HongChoon, Ong*).

I conclude this issue with 26 articles arising from selected international conferences featuring the following: an analysis of Malaysia's single stock futures and its spot price (*Marzuki, R. M., Mohd, M. A., Nawawi, A. H. M. and Redwan, N. M.*); a projecting input-output table for Malaysia comparing the RAS and EURO methods (*Shuja', N., Lazim, M. A. and Yap, B. W.*); relative risk estimation for dengue-disease mapping in Malaysia based on the Besag, York and Mollié models (*Samat, N. A. and Pei Zhen, W.*); the effects of baseline correction algorithms on forensic classification of paper based on the ATR-FTIR spectrum and principal component analysis (PCA) (*Lee, L. C., Liang, C-Y., Khairul, O. and Jemain, A. A.*); deriving partial differential equation for the value of a *salam* contract with credit risk (*Hisham, A. F. B., Jaffar, M. M. and Othman, J.*); combination of forecasts with an application to the unemployment rate (*Muniroh, M. F., Ismail, N. and Lazim, M. A.*); a complexity index for a decision-making method (*Harliza, M. H., Daud, M. and Rosma, M. D.*); evaluation of risk factors for prolonged invasive mechanical ventilation

in a paediatric intensive care unit (PICU) (*Ismail, I., Yap, B. W. and Abidin, A. S. Z.*); the control chart technique for the detection of the problem of bad data in a state estimation power system (*Zahid Khan, Radzuan B. Razali, Hanita Daud, Nursyarizal Mohd Nor and Mahmud Fotuhi Firuzabad*); the Internet of things, a look into a technology adoption model in India (*Singh, G., Gaur, L. and Ramakrishnan, R.*); the effect of iron (III) oxide (Fe_2O_3) nano-powder mixed dielectric medium on micro-electrical discharge machining (EDM) of cobalt-chrome-molybdenum (CoCrMo) (*Elsiti, N. M., Noordin, M. Y. and Idris, A.*); a review of channel modelling for optical wireless links (*Miglani, R. and Malhotra, J. S.*); dealing with interdependency among NFR using ISM (*Kaur, H. and Sharma, A.*); a DNA and Bernoulli random number generator-based security key generation algorithm (*Sodhi, G. K. and Gaba, G. S.*); an analysis of MIMO FSO over different modulation techniques (*Kaur, K., Miglani, R. and Malhotra, J. S.*); performance evaluation of compressive-sensing-based channel estimation techniques in an OFDM system for different channels (*Jha, A., Kansal, L. and Gaba, G. S.*); a cost estimation model for web applications using agile software development methodology (*Soni, D. and Kohli, P. J.*); understanding consumer preferences using IoT smart mirrors (*Gaur, L., Singh, G. and Ramakrishnan, R.*); investigation on tapping of Al6061-SiC metal matrix composite with HSS taps (*Melvin Paious, Raviraja Adhikari and Nagaraja*); dynamic performance characteristics of finite journal bearings operating on TiO₂-based nanolubricants (*Binu, K. G., Yathish, K., Shenoy, B. S., Rao, D. S. and Pai, R.*); a finite element analysis of the modal behaviour of vertical axis wind turbine comprising prestressed rotor blades (*Torabi Asr, M., Masoumi, M. M. and Mustapha, F.*); a review study of diesel and natural gas and their impact on CI engine emissions (*Hayder A. Alrazen and K. A. Ahmad*); the stability of water-lubricated bearing using the linear perturbation method under turbulent conditions (*R. Mallya, B. S. Shenoy, R. S. Pai and R. Pai*); estimation and validation of nearshore current and its characteristics at Carey Island (*Fitri, A., Hashim, R. and Motamedi, S.*); a computational fluid dynamics study of combustion and emission performance in an annular combustor of a jet engine (*M. Zuber, M. S. B. Hisham, N. A. M. Nasir, A. A. Basri and S. M. A. Khader*); and the effect of silica nanoparticles in kenaf-reinforced epoxy, looking specifically at its flexural and compressive properties (*F. Bajuri, N. Mazlan and M. R. Ishak*).

I anticipate that you will find the evidence presented in this issue to be intriguing, thought-provoking, and, hopefully, useful in setting up new milestones. Please recommend the journal to your colleagues and students to make this endeavour meaningful.

I would also like to express my gratitude to all the contributors, namely, the authors, reviewers and editors for their professional contribution towards making this issue feasible. Last but not least, the editorial assistance of the journal division staff is fully appreciated.

JST is currently accepting manuscripts for upcoming issues based on original qualitative or quantitative research that opens new areas of inquiry and investigation.

Chief Executive Editor

Nayan Deep S. KANWAL, [FRSA](#), [ABIM](#), [AMIS](#), Ph.D.

nayan@upm.my



Review Article

Implementation of Building Information Modelling (BIM) in Malaysia: A Review

Nuzul Azam Haron^{1*}, Raja Putri Zarifh Ana Raja Soh² and Aizul Nahar Harun³

¹*Department of Civil Engineering, Universiti Putra Malaysia, 43400 UPM, Serdang, Selangor, Malaysia*

²*Department of Civil and Construction Engineering, Universiti Putra Malaysia, 43400 UPM, Serdang, Selangor, Malaysia*

³*Department of Management of Technology, Malaysia-Japan International Institute of Technology, Universiti Teknologi Malaysia, 81310 UTM, Skudai, Johor, Malaysia*

ABSTRACT

This paper seeks to clarify Building Information Modelling (BIM) and its implementation in Malaysia. Most developed countries that have implemented BIM in the construction industry have found it effective. This paper reviews existing literature on the implementation of BIM and examines the implementation strategies that have been developed. The review highlights numerous advantages of BIM in construction, which include, among others, reducing cost, time, carbon burden and capital cost. BIM can also help increase broader efficiencies and improve coordination and communication between each party. However, implementing BIM is complicated and requires efforts from both the government and the private sector. While the implementation of BIM may reduce costs in developed countries, it may not do so in developing countries; in Malaysia, for instance, costs act as an initial barrier. Other obstacles to implementing BIM in Malaysia include application system requirements and lack of knowledge and readiness to change. To facilitate its implementation in the construction industry, the Malaysian government needs to hold seminars to promote a better understanding of BIM. They may also introduce a properly structured BIM course by preparing a standard code of practices and guidelines for BIM in the education sector.

Keywords: Building Information Modelling, cost reduction, time reduction, construction industry

Article history:

Received: 12 May 2016

Accepted: 3 November 2016

E-mail addresses:

nuzul@upm.edu.my (Nuzul Azam Haron),

rpzarifhana@yahoo.com (Raja Putri Zarifh Ana Raja Soh),

aizulnahaar.kl@utm.my (Aizul Nahar Harun)

*Corresponding Author

INTRODUCTION

This paper explains about Building Information Modelling, which is one of the methods used by companies to smoothly control and manage projects. Most developed

countries use this method in their construction field; Australia is the foremost in implementing BIM (18-75%), followed by the United States (31%), Europe (16%), the Middle East (11%) and India (9%) (Figure 1). Owing to increased consciousness about its advantages, construction companies in Malaysia have recently started to use BIM in their projects.

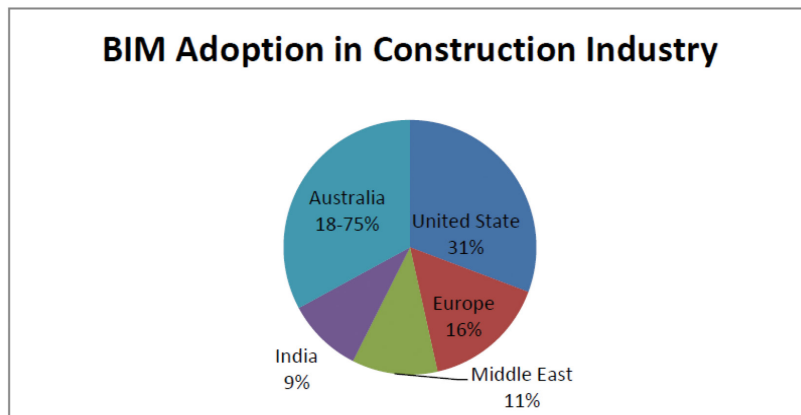


Figure 1. Countries that use BIM (Sawney, 2014)

In Malaysia, the progress of BIM has mainly been driven by the private sector since 2009. The idea to implement BIM in Malaysia was introduced by the Director of the Public Works Department (PWD) in 2007. The first government project to use BIM methodology was announced in 2010. BIM implementation requires the development of reliable tools for information exchange between different software tools while enabling efficient and direct coordination and monitoring processes between project participants and team members. An acceptable level of interoperability and standardisation of work methods must be developed for project participants and team members. The experience of project participants as a team allows us to define the decision-making process prior to BIM implementation in separate projects. It also makes it possible to make recommendations about the process of planning in an environment of small companies with different software and methods of work (Migilinskas et al., 2013).

One of the projects using BIM in Malaysia is the National Cancer Institute (NCI), as highlighted in seminars and workshops organised by CIDB regarding issues and challenges in implementing Building Information Modelling for small and medium enterprises (SMEs) in the construction industry (2014). According to Latiffi et al. (2013), BIM will be implemented in future projects such as the Healthcare Centre Type 5 at Sri Jaya Maran, Pahang, Administration Complex Project of Suruhanjaya Pencegah Rasuah Malaysia (SPRM) at Shah Alam, Selangor, the Primary School at Meru Raya Ipoh, Perak, and the Primary School at Tanjung Minyak 2, Melaka Tengah, Melaka. These are pilot projects and are part of the Malaysian government's initiative to expose government officers to BIM. The main objective of the present study is to understand the Building Information (BIM) as a technology for coordinating project development.

There are mixed perspectives of the benefits of BIM, creating a general misunderstanding of expected outcomes. The frequency and variety of definitions illustrate the existing confusion in defining and quantifying BIM and in considering its potential benefits. Any definition of BIM should not be unilateral, but instead, encompass key characteristics that have been attributed to it. There is a risk in offering a narrow definition of BIM, as that makes it more difficult to establish a baseline for comparisons. A narrow definition also makes it difficult, if not impossible, to improve BIM use by benchmarking (Abbasnejad et al., 2013). At the end of this study, the reader will understand BIM with regards to the benefits, barriers and solutions to its implementation in Malaysia.

REVIEW OF LITERATURE

Building Information Modelling (BIM)

According to Enegbuma et al. (2014), BIM is the process of generating and managing building data during its life cycle. Meanwhile, Sawney (2014) classifies BIM as not just a software tool or simply a technology that can be acquired and implemented. It is rather a paradigm that combines technology with people and process issues in the industry. This results in a tectonic shift in the way we deliver the built environment.

A seminar titled *Issues and Challenges in Implementing Building Information Modelling for Small and Medium Enterprises (SMEs)* organised by CIDB in 2014 presented BIM as one of the emerging technologies to be deployed in design, construction and facility management, in which a digital representation of the building is created to facilitate the exchange and interoperability of information in digital format. Thurairajah et al. (2013) stated that Building Information Modelling represents the formation of digital models used during the planning, design, construction and operation stages of a facility's life. Latiffi et al. (2013) referred to BIM as a set of digital tools that can help manage the effectiveness of a construction project. Zahrizan et al. (2014) stated that BIM can be viewed as a combination of advanced processes and technology that offers a platform for collaboration between different parties in construction projects by exploiting the use of information technology.

Arayici et al. (2012) stated that in the simplest of terms, BIM is the utilisation of a database infrastructure to encapsulate built facilities with specific viewpoints of stakeholders. It is a methodology to integrate digital descriptions of building objects and their relationship with others in a precise manner so that stakeholders can query, simulate, and estimate activities and their effects on the building process as a life-cycle entity. Therefore, BIM can help by providing the required value judgments that satisfy their owners and occupants for creating a more sustainable infrastructure.

BIM has many meanings and can be described in many different ways. Table 1 summarises the diversity of definitions.

Table 1
Summary of BIM Definitions

No.	Statement	Author
1.	The process of generating and managing building data during the building's life cycle	Enegbuma et al. (2014)
2.	BIM is not just a software tool or simply a technology that can be acquired and implemented.	Sawney (2014)
3.	BIM is one of the new emerging technologies to be deployed in design, construction and facility management, where a digital representation of the building is created to facilitate the exchange and interoperability of information in digital format.	CIDB (2014)
4.	Building Information Modelling (BIM) represents the formation of digital models for use during the planning, design, construction and operation stages of a facility's life.	Thurairajah et al. (2013)
5.	A set of digital tools that can manage the construction project's effectiveness	Latiffi et al. (2013)
6.	BIM can be viewed as a combination of advanced process and technology that offers a platform for collaboration between different parties in the construction project by exploiting the uses of Information Technology (IT).	Zahrizan et al. (2014)
7.	The utilisation of a database infrastructure to encapsulate built facilities with specific viewpoints of stakeholders	Arayici et al. (2012)

Based on the various definitions of BIM, it can be concluded that BIM is a software model that can be used in project planning, design, monitoring and control among construction project group stakeholders in order to ensure project success.

BIM Tools

Due to the complexity of gathering relevant information when working on a building project with BIM, some companies have designed software specifically to work within a BIM framework. In reference to the Autodesk Revit Manual Guidelines (2017), these packages include the Bentley AECOSim Building Designer, ArchiCAD, Tekla Structures, Autodesk Revit, Synchro PRO and Vector Works, among others. These software differs from other architectural drafting tools such as AutoCAD, as they allow the addition of further information such as time, cost, manufacturers' details, sustainability and maintenance information in the building mode.

Probably the greatest example of such software is Autodesk Revit. Autodesk Revit is building information modelling software for architects, structural engineers, MEP engineers, designers and contractors. It allows users to design a building structure and its components in 3D, annotate the model in 2D drafting element and get building information with access from the building model's database. Revit is built with drafting elements in 4D and contains tools to plan and track the various stages in the building's life cycle from concept to construction and, later, demolition. This is clarified in a research report by Latiffi et al. (2013).

In their research report, Latiffi et al. (2013) also highlighted the benefit of using Revit. Revit can be used as a collaboration tool between different disciplines in the sphere of building design. Implementation of BIM in the Malaysian construction industry can be carried out by players from different disciplines with support from BIM tools. Figure 2 shows the tools that can be used by each player. It approaches the programme from various unique perspectives. Each of these perspectives is focussed on completing the discipline's task. Companies that adopt software first examine the existing workflow process to determine if such an elaborate collaboration tool is required.

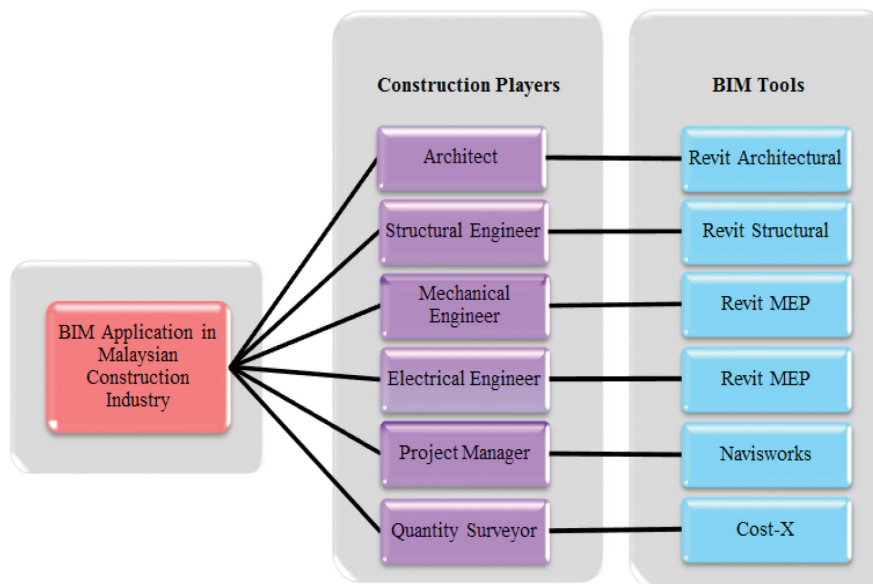


Figure 2. BIM tools suggested by the Director of Public Works Department (PWD) in 2007 (Latiffi et al., 2013)

METHODOLOGY

This section explains the research methodology that is adopted in this study. There are several ways to collect data. Data may be obtained from two sources. Primary data collection is the direct collection and process of information by the researcher, such as from observations, surveys, interviews and focus groups. Secondary data collection is the retrieval of information from pre-existing sources such as research articles, the Internet or library searches. Figure 3 shows the data collection process used in this paper, which was the use of secondary data sources.

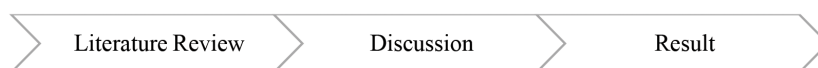


Figure 3. The process of data collection

A review of the literature was performed to analyse the current information available with regards to the implementation of BIM, with the aim 1) to determine the proper explanation and meaning of BIM; 2) to identify the problems faced by the players in implementing BIM; and 3) to assist players in the construction industry to implement BIM in Malaysia.

Over 100 sources of information were determined including journal articles, conference proceedings, published case studies, press releases, professional presentations and online articles. We narrowed these down to 40 sources that were published during the past 10 years. Overall, these mostly discuss the meaning, benefits, challenges and strategy connected to adopting BIM.

RESULTS AND DISCUSSION

Advantages of Implementing BIM in Malaysia

BIM helps in reducing cost and time and increasing broader efficiencies (Azhar, 2008; Barlish et al., 2012; Sawney, 2014; Chougule et al., 2015). Therefore, it is gaining popularity in the global built environment sector. It has impressed governments around the world, especially in developed nations, with the results encouraging strong steps to increase BIM adoption. The UK government has prepared a BIM strategy for the UK Government Construction Client Group to reduce the capital cost and carbon burden by 20% from the construction and operation of the built environment sector (Azhar, 2008; Mc Auley, 2012; Sawney, 2014; Dodia, 2015; Kathi, 2015).

Other than that, BIM can save the cost of design by benefiting from earlier access to the construction market. It can cut both time and cost of design by half (Yan et al., 2008). 'Half time at half cost' does not merely save money, it also reduces the time taken to be introduced to the market. BIM not only improves technology but also changes the process of design and build. Yan et al. (2008) stated that Building Information Modelling creates obtainable concurrent information on the performance of the project and the economic aspects of the project in the operation phase. BIM leaves a digital document trail resulting from transformations and developments during operation. Most users of BIM believe that it can reduce dependence on human resources during the entire operation phase.

The benefits of adopting BIM in development are that it can improve project coordination and communication with each side. These apply to the team of workers, where everyone is able to understand the project better. It allows fellow professionals to understand the proposal better (Autodesk, 2007; Becerik-Gerber et al., 2010; Dodia, 2015). According to some research reports, the Malaysian government encourages construction players to apply BIM in their construction projects because it can overcome construction problems such as delay, clash of design by different professionals and construction cost overrun (Becerik-Gerber et al., 2010; Latiffi et al., 2013; Elhag et al., 2014; Kathi et al., 2015). Activities with established duration are connected to a project network plan by taking into account relevant precedence relationships. Project duration is automatically determined from the generated network plan. A BIM model of the construction object is completed by upgrading the 3D model with defined schedules and cost data (Pučko et al., 2014). Thus, BIM helps increase construction project efficiency and the effectiveness of project management. In addition, it helps improve communication

and collaboration between construction players. With BIM, design change becomes a more efficient and smoother process, since different components are linked together and updated accordingly (Elhag et al., 2014).

Researchers conclude that BIM can overcome construction problems and boost the productivity level of the Malaysian construction industry to be at par with that of Australia and the US. Table 2 summarises the advantages of using BIM as suggested by different authors.

Table 2
Advantages of Using BIM in the Construction Industry

No.	Statement	Author
1.0	BIM helps to reduce cost and time and increases other broader efficiencies.	1) Anil (2014) 2) Azhar, S. (2008) 3) Dodia et al. (2015) 4) Kathi et al. (2015) 5) Yan et al. (2008) 6) Liu et al. (2015) 7) Barlish et al. (2012)
2.0	The UK has prepared a BIM strategy for the UK Government Construction Client Group for reducing capital cost and the carbon burden from the construction and operation of the built environment by 20%.	1) Anil (2014) 2) McAuley et al. (2012) 3) Azhar, S. (2008) 4) Dodia et al. (2015) 5) Kathi et al. (2015)
3.0	The two main benefits of adopting BIM in development are an improvement in coordination and communication.	1) Autodesk (2007) 2) Dodia et al. (2015) 3) Becerik-Gerber et al. (2010)
4.0	The Malaysian government encourages construction players to apply BIM to their construction projects because BIM can overcome construction project problems such as delay, clash of the design by different professionals and construction cost overrun.	1) Latiffi et al. (2013) 2) Kathi et al. (2015) 3) Becerik-Gerber et al. (2010) 4) Elhag et al. (2014)

Problems with Implementing BIM in Malaysia

Implementation of BIM in Malaysia is not without challenges. There is a lack of awareness and knowledge among users in the industry. This is consistent with findings of studies on barriers to the use of BIM in Iran (Hosseini et al., 2011) and Pakistan (Masood et al., 2014). The application of BIM in the industry becomes narrower if the government and its agencies consider it useless. Although the government has taken a role in the implementation of BIM, the pace of implementing BIM in Malaysia is still lagging.

In developing countries, one of the benefits of using BIM is cost. However, in Malaysia cost is one of the barriers to implementing BIM (Lindblad, 2013; Gardezi et al., 2014). Research by Liu et al. (2015) and Franco et al. (2015) corroborates this by showing that cost was the most critical barrier to the implementation of BIM. This is followed by the absence of

national standards and lack of skilled personnel. All participants in their research had a common awareness of the critical barriers and most agreed that cost was a critical factor. The initial cost of investing in new technology and time for training personnel is also significant. Table 3 displays the inter-related key variables stated by the participants as contributing to barriers in implementing BIM in construction. Among others, cost showed the highest percentage (26.2%), followed by IT components (23%), time (16.4%) and readiness (14.8%). Meanwhile, knowledge (8.2%), technology (8.2%) and information (3.3%) were among the lowest barriers (CREAM, 2014; Eadie, 2013; Salleh, 2014; Chougule et al., 2015; Hedayati, 2015). The CIDB seminar compiled the variables under four headings of barriers to BIM implementation in Malaysia, including cost, system requirements, lack of knowledge and readiness to change.

Table 3
Barriers to the Implementation of BIM (CIDB, 2014)

Variables	Percentage %
Cost	26.2
Time	16.4
IT (Software, Hardware, Computer)	23.0
Readiness	14.8
Knowledge	8.2
Technology	8.2
Information	3.3

According to Yan (2008) and Manu et al. (2014), about 40% of respondents from the USA and about 20% respondents from the UK believe that their companies need to allocate a lot of time and human resources to the training process. If the understanding of BIM and its possibilities is not well established in the organisation, there is a risk of losing the goal of BIM adoption (Lindblad, 2013). This category poses the largest latent barrier to the application of BIM. Decisions made in organisations are mainly derived from a business perspective (i.e. profit). The AEC industry is not glad to invest in BIM because of the lack of case study evidence of the financial benefit of BIM. Investment in BIM by the AEC industry will increase only when a good business case is made with case study evidence. There is also social and habitual resistance to change, as a number of architects are satisfied with traditional methods to design projects and increase the new functions and advantages of BIM.

Kushwaha (2016) says that Building Information Modelling has revolutionised the AEC industry, but the rate of implementation of BIM in the industry is low because of various barriers. He claims that the lack of initiative from government organisations and educational institutes is the major factor responsible for the limited awareness and implementation of BIM. In addition, shifting from traditional approaches to BIM is not an easy task; it requires collaborative efforts from government agencies as well as private organisations.

Table 3 shows that IT is also one of the challenges faced by construction players in the implementation of BIM. The lack of consistent standards and software incompatibility along the project supply chain remains an issue despite great improvements in recent years

(Manu, 2014; Smith, 2014; Ali, 2015). Fully-integrated project delivery with multi-disciplinary project teams working on a single integrated and compatible BIM model are essential for the optimal use of BIM. Currently, the scope for this remains limited. The use of BIM is considered to be more suited to larger projects with larger clients and contractors who have the scope to demand that all project participants have the necessary technological capability and compatible software. Some players claim that working with BIM projects is not effective against projects that work outside of the BIM model, due to incompatibility issues regarding software, standards and practices. This is also compounded by key parties in the project supply chain not meeting the capabilities required. All the researchers agreed that although these issues would continue to improve, they remained critical for successful BIM implementation across the industry.

Other challenges triggered by BIM adaptation that needs to be considered can be divided into four perspectives, namely (1) process-related obstacles; (2) social context obstacles; (3) technical obstacles; and (4) associated costs. Process-related challenges have three aspects (Talebi, 2014). First, BIM changes the traditional processes in building projects, and accordingly, construction organisations need to adapt to new business processes. However, due to the immaturity of users and absence of clear guidelines, it is difficult to foresee the consequences. Second, there is a need for building new roles; however, it is ambiguous as to how they should be integrated into current processes. The final issue in process-related obstacles is about the need for developing new contractual agreements for BIM-based projects. These agreements must be able to deal with the division of economic incentives and ownership of information.

For BIM to be adopted successfully, all construction players in a project must participate in this change. Therefore, there is a need for developing the ability to make requirements regarding how BIM is supposed to be used. If a single player is not contributing, much value in the models is lost because of the subsequent inability to use them as intended (Lindblad, 2013).

Solutions for Implementing BIM in Malaysia

The government and its agencies need to play the biggest role, as then the driving force in ensuring BIM technology will be successfully implemented in the construction industry (CREAM, 2014; Rogers, 2015). The government may strategically organise a series of awareness and motivation programmes such as seminars and workshops for various levels of industry players. Institutions of higher learning throughout Malaysia are encouraged to incorporate BIM courses in their syllabus to equip graduates to understand BIM technology as preparation for successful careers.

A proper structure of BIM courses for various grades of contractors and practitioners needs to be provided to give required knowledge in the study and application of BIM implementation. Besides that, a standard code of practices and guidelines of BIM is a prerequisite for standardising new output and enabling efficient communication and integration among stakeholders, thus ensuring that it will be easy to implement and manage.

The government, the AEC industry, educational institutions and BIM providers need to work together to reduce BIM implementation costs, establish BIM implementation strategies and promote BIM education (Mohd-Nor, 2012; Liu, 2015; Rogers, 2015). With investigation

and overcoming of the identified barriers, BIM will help the AEC industry evolve rapidly. Research results indicate that 92.63% of respondents believed that governments should play a vital role in the BIM implementation process and give it due recognition, indicating that respondents had expectations of government support. Besides that, more than half of the respondents (51.6%) believed that governments should play a leading role, which means that governments should take full advantage of their administrative function and actively participate in the promotion process. A further 39.1% of the respondents believed that governments should play a guiding role, which means there is a need not to lead but to inspire the development of the industry. All government staff thought governments should take a leading or guiding role in BIM implementation. Few industry staff thought that governments should not be involved in BIM implementation at all.

National leadership and coordination can also minimise inefficiencies and avoid the many problems created by piecemeal and disjointed approaches. Although government entities should primarily drive this leadership, it needs the support of and collaboration with major industry players, such as private sector clients, contractors and industry/professional associations (Smith, 2014; Rogers et al., 2015). Other than that, the implementation of BIM needs consistent national and global standards to achieve the efficiencies envisioned by the technology. It is contradictory for there to be a range of different systems and piecemeal approaches to BIM development. Global leadership can help ensure that collaboration occurs on a national and global scale. Clearly, if BIM is to be the future of international projects, then common standards need to be adopted. These papers also suggest providing BIM education, training and research to drive not only implementation but also the evolution of the industry. BIM education is required at the tertiary level so that graduates entering the industry have necessary BIM knowledge and capabilities.

We have discussed above how a number of factors obstruct the implementation of BIM. Cost is the major factor that obstructs implementation of BIM, followed by IT components. This major factor has been solved in developing countries such as the US. Agencies such as government agencies, developers and designers need to take up the implementation of BIM in Malaysia as a serious task. Table 4 summarises the solutions suggested in the literature to help construction players solve problems obstructing the implementation of BIM.

Table 4
Summary of Solutions to Barriers in Implementing BIM in the Construction Industry

No.	Solution	Source
1.0	Offer motivation programmes such as seminars and workshops	1) CIDB (2014)
	Incorporate BIM courses in the syllabus of educational institutions	2) Smith, P. (2014)
	Offer properly structured BIM courses at the university level	3) Rogers et al. (2015)
	Prepare a standard code of practices and guidelines for BIM	
2.0	Support and enforce the implementation of BIM by the government	1) Zahrizan et al. (2014)
	Promote BIM training programmes	2) Smith, P. (2014)
	Seek initiative of senior management and related industry players	

CONCLUSION

BIM has many benefits that can help contractors manage their projects effectively and effortlessly. BIM has the potential to be adopted in the construction field and expanded into the engineering field. Unfortunately, in Malaysia, BIM is lagging behind because of a few factors acting as barriers to its implementation. Cost is one of these factors. It appears that the best way to overcome obstacles to BIM implementation is that governmental agencies and private developers need to play bigger roles to uphold the role of BIM technology in Malaysia.

REFERENCES

- Abbasnejad, B., & Moud, H. I. (2013). BIM and basic challenges associated with its definitions, interpretations and expectations. *International Journal of Engineering Research and Application*, 3(2), 287–294.
- Ali, M., Mohamed, Y., Taghaddos, H., & Hermann, R. (2015). BIM obstacles in industrial projects: A contractor's perspective. In *Proceedings of ICSC15: The Canadian Society for Civil Engineering 5th International/11th Construction Specialty Conference* (pp. 1–10). <http://doi.org/10.14288/1.0076376>
- Arayici, Y., Egbu, C., & Coates, P. (2012). Building information modelling (BIM) implementation and remote construction projects: Issues, challenges, and critiques. *Electronic Journal of Information Technology in Construction*, 17(May), 75–92. <http://doi.org/ISSN 1874-4753>
- Autodesk. (2007). Revit Structure and BIM. *Architecture*, 0(0), 1–9.
- Azhar, S., Nadeem, A., Mok, J. Y. N., & Leung, B. H. Y. (2008). Building information modelling (BIM): A new paradigm for visual interactive modelling and simulation for construction projects. In *Proceedings of the First International Conference on Construction in Developing Countries (ICCIDC-I)* (pp. 435-446). Karachi, Pakistan.
- Barlish, K., & Sullivan, K. (2012). How to measure the benefits of BIM – A case study approach. *Automation in Construction*, 24, 149–159. <http://doi.org/10.1016/j.autcon.2012.02.008>
- Becerik-Gerber, B., & Rice, S. (2010). The perceived value of building information modelling in the US building industry. *Journal of Information Technology in Construction*, 15(February), 185–201. Retrieved from <http://www.itcon.org/2010/15>
- Chougule, N. S., & Konnur, B. A. (2015). A review of building information modelling (BIM) for construction industry. *International Journal of Innovative Research in Advanced Engineering*, 2(4), 98–102. Retrieved from <http://www.ijirae.com/volumes/Vol2/iss4/17.APAE10106.pdf>
- CREAM. (2014). *Issues and challenges in implementing building information modelling (BIM) for SME's in the construction industry*. Kuala Lumpur, Malaysia: Construction Research Institute (CREAM). Retrieved from <http://www.cidb.gov.my/images/pdf/announcement/BIM/bim>
- Dodia, S. M., & Hariharan, S. (2015). Evaluating effectiveness of BIM application in construction projects. *International Journal of Engineering and Computer Science*, 4(9), 14076–14078. <http://doi.org/10.18535/ijecs/v4i9.01>
- Eadie, R., Odeyinka, H., Browne, M., McKeown, C., & Yohanis, M. (2013). An analysis of the drivers for adopting building information modelling. *Journal of Information Technology in Construction*, 18(February), 338–352.

- Elhag, T., & Al-sharifi, M. (2014). The viability of BIM for UK contractors. In *Proceedings of International Conference on Construction in a changing World* (pp. 4-7). Retrieved from <http://www.cib2014.org/proceedings/>
- Enegbuma, W. I., Ologbo, A. C., Aliagha, U. G., & Ali, K. N. (2014). Product lifecycle management for a global market. In S. Fukuda, A. Bernard, B. Gurumoorthy, & A. Bouras (Eds.), *11th IFIP WG 5.1 International Conference, PLM 2014, revised selected papers* (pp. 51–62). Yokohama, Japan. Berlin, Heidelberg: Springer Berlin Heidelberg. http://doi.org/10.1007/978-3-662-45937-9_6
- Franco, J., Mahdi, F., & Abaza, H. (2015). Using building information modelling (BIM) for estimating and scheduling, adoption barriers. *Universal Journal of Management*, 3(9), 376–384. <http://doi.org/10.13189/ujm.2015.030905>
- Gardezi, S. S. S., Shafiq, N., Nurudinn, M. F., Farhan, S. A., & Umar, U. A. (2014). Challenges for implementation of building information modelling (BIM) in Malaysian construction industry. *Applied Mechanics and Materials*, 567(JUNE), 559–564. <http://doi.org/10.4028/www.scientific.net/AMM.567.559>
- Hedayati, A., Mohandes, S. R., & Preece, C. (2015). Studying the OBSTACLES TO IMPLEMENTING BIM in educational system and making some recommendations. *Journal of Basic Applied Science Research*, 5(3), 29–35.
- Hosseini, M. R., Azari, E., Tivendale, L., & Chileshe, N. (2011). Barriers to adoption of building information modelling (BIM) in Iran: Preliminary Results. In *proceedings of the The 6th International Conference on Engineering, Project, and Production Management (EPPM2015)* (pp. 384-394).
- Kathi, V., Vasam, S., Rao, K. J., & Rao, M. V. S. (2015). A critical review on new advancements in implementation of IT in construction industry: Integration of BIM with cloud computing. *International Journal of Research in Engineering and Technology*, 4(1), 145–150.
- Kushwaha, V. (2016). Contribution of building information modelling (BIM) to solve problems in architecture, engineering and construction (AEC) industry and addressing barriers to implementation of BIM. *International Research Journal of Engineering and Technology*, 3(1), 100-105.
- Latiffi, A. A., Mohd, S., Kasim, N., & Fathi, M. S. (2013). Building information modelling (BIM) application in Malaysian construction Industry. *International Journal of Construction Engineering and Management*, 2(A), 1–6. <http://doi.org/10.5923/s.ijcem.201309.01>
- Lindblad, H. (2013). *Study of the implementation process of BIM in construction projects: Analysis of the barriers limiting BIM adoption in the AEC industry*. (Unpublished Master's Thesis). University of Stockholm, Sweden. Retrieved from <http://kth.diva-portal.org/smash/get/diva2:633132/FULLTEXT01>
- Liu, S., Xie, B., Tivendal, L., & Liu, C. (2015). Critical barriers to BIM implementation in the AEC industry. *International Journal of Marketing Studies*, 7(6), 162–171. <http://doi.org/10.5539/ijms.v7n6p162>
- Manu, P., Wildin, K., Shelbourn, M., Navendren, D., & Mahamadu, A. M. (2014). Briefing: Towards exploring profession-specific BIM challenges in the UK. *Proceedings of the ICE - Management, Procurement and Law*, 167(4), 163–166. <http://doi.org/10.1680/mpal.14.00004>
- Masood, R., Kharal, M. K. N., & Nasir, A. R. (2014). Is BIM adoption advantageous for construction industry of Pakistan? *Procedia Engineering*, 77, 229–238. <http://doi.org/10.1016/j.proeng.2014.07.021>

- McAuley, B., Hore, A., & West, R. (2012). Use of building information modelling in responding to low carbon construction innovations: An Irish perspective. In *Proceedings of the Joint CIB W055, W065, W089, W118, TG76, TG78, TG8 International Conference on Management of Construction: Research to Practice* (pp. 523–538). Montreal. Retrieved from <http://arrow.dit.ie/beschrecon/9/>
- Migilinskas, D., Popov, V., Juocevicius, V., & Ustinovichius, L. (2013). The benefits, obstacles and problems of practical BIM implementation. *Procedia Engineering*, 57, 767–774. <http://doi.org/10.1016/j.proeng.2013.04.097>
- Mohd-Nor, M. F. I., & Grant, M. P. (2012). The development of digital architecture modelling in the Malaysian architecture industry. In *Recent Advances in Computer Engineering, Communications and Information Technology. World Scientific and Engineering Academy and Society* (pp. 77–84). Retrieved from <http://www.wseas.us/e-library/conferences/2014/Tenerife/INFORM/INFORM-10.pdf>
- Pučko, Z., Nataša, N., & Klanšek, U. (2014). Building information modelling based time and cost planning in construction projects. *Organization, Technology and Management in Construction: An International Journal*, 6(1), 958–971. <http://doi.org/10.5592/otmcj.2014.1.6>
- Rogers, J., Chong, H. Y., & Preece, C. (2015). Adoption of building information modelling technology (BIM). *Engineering, Construction and Architectural Management*, 22(4), 424–445. <http://doi.org/10.1108/ECAM-05-2014-0067>
- Salleh, H., & Fung, W. P. (2014). Building information modelling application: Focus-group discussion. *Journal of the Croatian Association of Civil Engineers*, 66(08), 705–714. <http://doi.org/10.14256/JCE.1007.2014>
- Sawhney, A. (2014). *State of BIM adoption and outlook in India* (pp. 1–32). India: RICS School of Built Environment, Amity University.
- Smith, P. (2014). BIM & the 5D project cost manager. *Procedia - Social and Behavioural Sciences*, 119, 475–484. <http://doi.org/http://dx.doi.org/10.1016/j.sbspro.2014.03.053>
- Smith, P. (2014). BIM implementation – Global strategies. *Procedia Engineering*, 85, 482–492. <http://doi.org/10.1016/j.proeng.2014.10.575>
- Talebi, S. (2014). Exploring advantages and challenges of adaptation and implementation of BIM in project life cycle. In *2nd BIM International Conference on Challenges to Overcome* (pp. 1–20). BIM Forum Portugal, Lisbon, Portugal.
- Thurairajah, N., & Goucher, D. (2013). Advantages and challenges of using BIM: A cost consultant's perspective. In *49th ASC Annual International Conference Proceedings* (pp. 1–8). California Polytechnic State University (Cal Poly) in San Luis Obispo, CA.
- Yan, H., & Damian, P. (2008). Benefits and barriers of building information modelling. In *12th International Conference on Computing in Civil and Building Engineering* (Vol. 161, pp. 1-5). Beijing.
- Zahrizan, Z., Ali, M., Haron, T., & Marshall-Ponting, A. (2014). Exploring the barriers and driving factors in implementing building information modelling (BIM) in the Malaysian construction industry: A preliminary study. *The Institute of Engineers, Malaysia*, 75(1), 1–10. <http://doi.org/10.1017/CBO9781107415324.004>



Reliability, Technical Error of Measurement and Validity of Height Measurement Using Portable Stadiometer

Azli Baharudin^{1*}, Mohamad Hasnan Ahmad¹, Balkish Mahadir Naidu¹,
Nurul Rufaidah Hamzah², Nor Azian Mohd Zaki¹, Ahmad Ali Zainuddin^{1,3}
and Noor Safiza Mohd Nor¹

¹Centre for Nutrition Epidemiology, Institute for Public Health, 50590 Jalan Bangsar, Kuala Lumpur, Malaysia

²Faculty of Computer and Mathematical Sciences, Universiti Teknologi MARA, Sri Iskandar, 32610 UiTM, Perak, Malaysia

³Universiti Teknologi MARA, 42300 UiTM, Bandar Puncak Alam, Selangor, Malaysia

ABSTRACT

This study sought to examine the reliability and validity of height measurements using a portable stadiometer as compared to a mechanical scale. Samples from 142 adults aged 22 to 57 were taken during data collection in November 2014. There was a high degree of reliability for the inter-examiner, intra-examiner and inter-instrument aspects with regards to mean difference, the inter correlation coefficient (ICC) and Bland-Altman Plot. For the inter-examiner aspect, the height measurement taken by the first examiner was 0.01 cm higher than that by the second examiner with an ICC of 0.999. For the intra-examiner aspect, the difference was 0.1 cm; this was higher in the first measurement compared to the second. The ICC was also 0.999. For the inter-instrument aspect, measurement taken by stadiometer was 0.61 cm higher than the measurement taken by mechanical scale and the ICC was 0.997. The Bland-Altman plot showed a distribution of differences between measurements in the inter-examiner, intra-examiner and inter-instrument aspects that were close to zero within the narrow range of $\pm 1.96SD$. The technical error of measurement (TEM), coefficient of reliability (R) and coefficient of variation (CV) for the inter-examiner, intra-examiner and inter-instrument aspects were within the acceptable limits. This study suggests that the portable stadiometer is reliable and valid for use in community surveys.

Article history:

Received: 22 October 2015

Accepted: 14 February 2017

E-mail addresses:

ps_azlibaharudin@moh.gov.my (Azli Baharudin),
mha.hasnan@gmail.com (Mohamad Hasnan Ahmad),
balkishmahadir@gmail.com (Balkish Mahadir Naidu),
nurulhamzah17@gmail.com (Nurul Rufaidah Hamzah),
norazianmz@moh.gov.my (Nor Azian Mohd Zaki),
ahmadali@moh.gov.my (Ahmad Ali Zainuddin),
safiza@moh.gov.my (Noor Safiza Mohd Nor)

*Corresponding Author

Keywords: Stadiometer, reliability, technical error of measurement, validity of height

INTRODUCTION

Anthropometry is an easy, fast and inexpensive way to assess the nutritional status of a person. Simple measurements such as height, weight,

waist circumference and hip circumference are constituents of anthropometric measurements. They can be easily measured and provide information such as body mass index (BMI) and waist-hip ratio for further health diagnosis (Ulijaszek & Kerr, 1999; Sanchez-Garcia et al., 2007).

Nevertheless, anthropometric measurement has its limitations, with the need for trained examiners and relatively high between-measurement technical errors and mechanical limitations (NYORC, 2006; Haniff et al., 2008). Surveys that involve a large number of samples require a group of skilled and trained people to do the measurement, and this can lead to measurement errors (Ulijaszek & Kerr, 1999). It was found that instrument error increased the variance of height, weight, and mean BMI generally (Biehl et al., 2013). Measurement precision and reliability refer to “the extent to which repeated measurements give the same value” while accuracy and validity mean “how close a measurement is to its ‘true’ value (Ulijaszek & Kerr, 1999; Cameron, 2002; Biehl et al., 2013).

Nowadays, numerous anthropometry instruments have been produced. Some of them have been modified for more practical use in certain places, situations or conditions. One of them is height measurement. The height measurement is estimated from a fixed rod on the wall to an adjusted and portable stadiometer. There is a concern about the reliability of stadiometers and the ensuing technical errors that may arise. As the usage of the instrument (SECA 213) for height measurement is still new in Malaysia, this study was aimed at assessing inter- and intra-examiner reliability, technical error of measurement and validity of the SECA Stadiometer 213 for measuring height in community surveys.

METHODOLOGY

This cross-sectional study was conducted among adults in a selected government clinic. Data collection was undertaken in November 2014. A total of 142 adults were recruited using convenient sampling. Respondents with no deformities affecting height were recruited. Adults with mental and terminal illness were excluded from this study. The sample size was estimated based on Walter et al. (1998), with two replicates per subject; an expected reliability coefficient (r) of at least 0.8 ($H1: \rho=0.8$), reliability of 0.7 ($H0: \rho=0.7$) or higher were required to be minimally acceptable, $\alpha=0.05$ and $\beta=0.2$ (corresponds to 80% power); this required a total number of 130 subjects. Using a 10% drop-out rate accounted for by poor response, the final target sample size was 142.

The height of respondents was obtained by using two instruments i.e. the portable SECA Stadiometer 213 as a ‘test’ instrument and the SECA Medical 703 Digital Column Scale as a ‘reference’ instrument, which is standardised and used widely in health facilities. A good stadiometer is able to read to 0.1 cm or 1/8th of an inch; it is stable and has a horizontal headpiece that can be brought into contact with the most superior part of the head.

Data collection was carried out in November 2014. Two trained examiners with a background in public health nursing conducted the measurement of height for each respondent. Not being a part of the study team, the two examiners were not aware of the study’s objectives. Height was measured to the nearest 0.1 cm from the subject head-to-toe in an upright position with five points of the subject’s body touching the wall.

On the day of data collection, each examiner measured the respondents' height individually. The first examiner measured the respondent's height, followed by the second examiner using the same instrument, the SECA Stadiometer 213. After that, the respondent was measured again, but this time using the SECA Medical 703 Digital Column Scale. The examiners were requested not to reveal their previous readings. The data capture form was designed in such a way that all the recordings of previous readings were obscured immediately after each recording; this was to minimise recall bias. A measurement form was provided to the examiners for their easier recoding and data management later.

Statistical analysis was reported using:

1. Absolute mean difference
 - Generally, absolute mean difference is the measure of a statistical dispersion difference of two random variables. In this paper, it is explained by the dispersion difference in inter-examiner, intra-examiner and inter-instrument aspects of height measurement using the SECA Stadiometer 213 and the SECA Medical 703 Digital Column Scale. It is the base analysis to verify the difference or similarity between two readings (Haniff et al., 2008).
2. Correlation coefficient (r)
 - This is commonly used to show the relationship (similarities) between two readings. Intra-class correlation (ICC) will be used for this purpose. The value of the reliability coefficient ranged from 0 to 1, where $ICC < 0$ indicated "no reliability", ≥ 0 but < 0.2 "slight reliability", 0.2 to < 0.4 "fair reliability", 0.4 to < 0.6 "moderate reliability", 0.6 to < 0.8 "substantial reliability" and 1 "almost perfect reliability" (MUSC, 2006; Geeta et al., 2009).
3. Bland-Altman plot (Bland, 1986)
 - This is a method to compare two measurement techniques or methods by plotting the differences between the two methods against the averages of the two methods. It is set as a model to show the spread of differences in the readings, the mean difference and the upper and lower limits of agreement for both inter- and intra-examiner reliabilities (Geeta et al., 2009).
4. Technical error of measurement (TEM)
 - This is an important analysis to represent the measurement quality and control dimension. It is a typical way to indicate the error margin in anthropometry that has been adopted by the International Society for the Advancement of Kinanthropometry for the accreditation of anthropometrists. It is indeed the standard deviation between repeated measures. The TEM index allows anthropometrists to verify the degree of accuracy when performing and repeating anthropometrical measurements (intra-examiner) and when comparing their measurement with measurements from other anthropometrists (inter-examiner). A relative TEM value less than 0.20 indicates that the measurements taken are acceptable (Geeta et al., 2009).

To determine the precise height measurement, four differences are commonly used, which are Technical Error of Measurement (TEM), the relative of Technical Error Measurement (rTEM), the Coefficient of Reliability (R) and the Coefficient of Validity (CV) (Ulijaszek & Kerr, 1999).

$$\text{Absolute TEM} = \sqrt{\frac{\sum d_i^2}{2n}} \quad (1)$$

where T_0 = Absolute TEM

d = difference between 1st and 2nd reading,

n = number of respondents,

i = the number of readings

From the equation (1) it was transformed into T_1 to obtain the error expressed as a percentage corresponding to the total average of the variable to be analysed. To compare TEM across anthropometric measurement or study occasions, we converted the absolute TEM (α) to %TEM (β). The equation (2) of β is shown:

$$\text{relative TEM (\% TEM)} = \frac{T_0}{\mu} \times 100 \quad (2)$$

where T_1 = relative TEM

μ = Average of measurement

Acceptable T_1 levels were 5% or less for skinfolds and 1% for other anthropometrical measure (Gore & Gore, 2000). The lower the T_1 obtained, the better the precision to perform the measurement.

From TEM, the coefficient of reliability (R) was very useful for comparing relative reliability of different measurements. Equation (3) is shown:

$$\text{Coefficient of reliability, R} = 1 - \left(\frac{(T_0)^2}{\sigma^2} \right) \quad (3)$$

If the range of R is close to 0 then the reading of the anthropometrical measure is considered as not reliable but if the range is close to one it is considered as being completely reliable. If the R values are greater than 0.95, this indicates that the measurement is sufficiently precise (Ulijaszek & Kerr, 1999).

Finally, the coefficient of variance (CV) was calculated to express sample variability relative to the mean of the sample, with the following formula. Equation (3) is shown:

$$\text{Coefficient of variability, CVs} = \frac{\sigma}{\mu} \times 100 \quad (4)$$

where σ = standard deviation,

The CVs provide a general view of the performance of the method. If the CVs are less than or equal to 5%, they generally imply good method performance, while CVs greater than or equal to 10% imply that the method did not perform well (Zady, 2006). In comparing methods, the percentage of the CVs is a good indicator (Bland, 2006).

RESULTS

Sample Characteristics

A sample of 142 adults aged 22 to 57 years were involved during the one-month data collection in November 2014. Among them, 44 (31%) were men and 98 (69%) were women. Mean height was 167.48 ± 5.71 cm and 156.38 ± 6.60 cm for men and women, respectively and it was not significantly different by gender.

Reliability

There were three ways in which the inter-examiner, intra-examiner and inter-instrument aspects were examined in this study. The first was by looking at the absolute mean difference. Absolute mean difference for the inter-examiner, intra-examiner and inter-instrument aspects were 0.01, 0.10 and 0.61, respectively as illustrated in Table 1. Although mean differences in the inter-instrument aspect was high, by independent t-test, the measurements were determined as being not significantly different between the stadiometer and mechanical scale.

The second method was by determination of the correlation coefficient. Results of the correlation coefficient of analysis of the inter-examiner, intra-examiner and inter-instrument aspects used the intra-class coefficient (ICC) as given in Table 1. All the ICCs were nearly in perfect agreement, which means a strong correlation between the two readings. This indicated a high degree of reliability between the two examiners, within examiners and between the two instruments.

Table 1
Absolute Mean Difference and Intra-Class Coefficient (ICC) of Height Measurement

Pair comparison	Summary statistic			Absolute mean diff. (1) – (2)	P value	ICC
	N	Mean (SD)	Median (Min, Max)			
Inter-examiner	142			0.01	0.989	0.999
Examiner#1 (1)		159.60 (7.85)	158.65 (141.75, 179.65)			
Examiner#2 (2)		159.59 (7.81)	158.58 (141.65, 179.60)			
Intra-examiner	142			0.10	0.915	0.999
1 st measurement (1)		159.55 (7.85)	158.60 (141.80, 179.60)			
2 nd measurement (2)		159.65 (7.85)	158.80 (141.70, 179.90)			
Inter-instrument	142			0.61	0.511	0.998
Stadiometer (1)		159.60 (7.85)	158.65 (141.75, 179.65)			
Stadiometer (2)		158.99 (7.92)	158.35 (141.95, 179.50)			

P value was obtained by independent t-test

Validity

The third method used was the Bland-Altman method. Figure 1 shows that the measurements taken by the first examiner were consistent with those taken by the second examiner, with an average difference of 0.012 cm, upper limit at 0.591 cm and lower limit at -0.566 cm. Figure 2 shows that the measurements taken by the first examiner at first reading were consistent with those of the second reading, with an average difference of -0.099 cm, upper limit at 0.436 cm and lower limit at -0.636 cm. Figure 3 shows that the measurements taken by mechanical scale were consistent with those taken by stadiometer with an average difference of 0.616 cm, upper limit at 1.775 cm and lower limit at -0.543 cm.

Inter-examiner. The Bland and Altman plot in Figure 1 shows that the differences between examiner 1 and examiner 2 were consistent for the measurements in which the data were collected. However, it was noted that there were many points outside the upper control limit of 0.51 cm and the lower control limit of -0.566 cm.

Intra-examiner. The Bland and Altman plot in Figure 2 shows that the differences between measurement 1 and measurement 2 were almost consistent for the measurements. However, it was noted that there were more points outside the upper control limit of 0.436 cm and lower control limit of -0.636 cm.

Inter-instrument. The Bland and Altman plot in Figure 3 shows that the differences between the Stadiometer and the Seca Mechanical Scale measurements were consistent for the measurements compared to when using the intra-examiner and inter-examiner aspects. Only several points were outside the lower control limit of -0.543 cm.

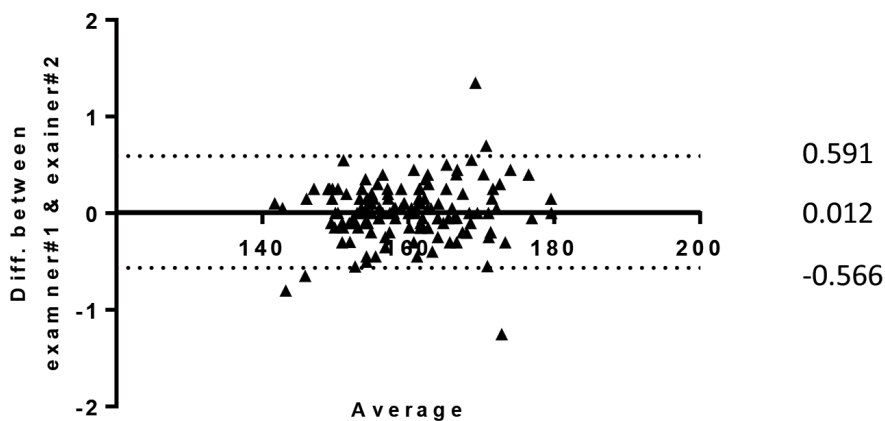


Figure 1. Bland-Altman plot difference vs average of first and second examiner

Height Measurement Reliability Using Portable Stadiometer

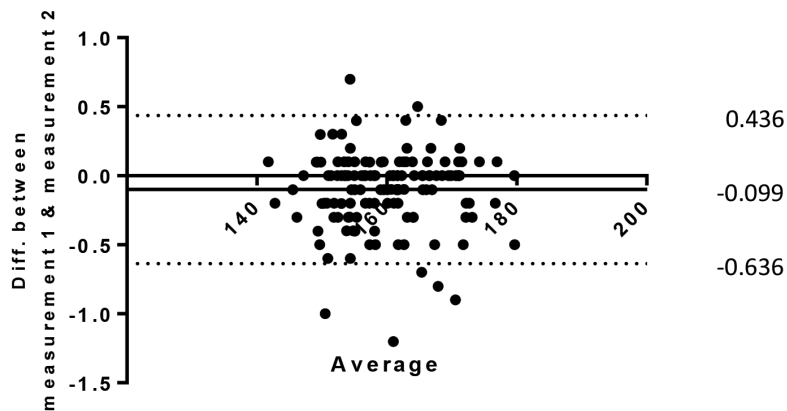


Figure 2. Bland-Altman plot difference vs average of first and second measurement

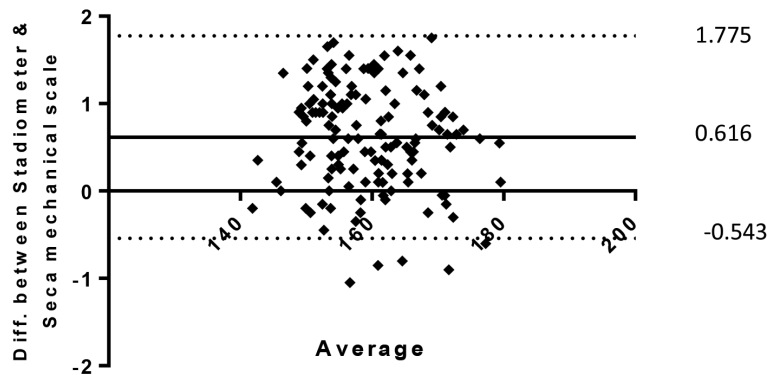


Figure 3. Bland-Altman plot difference vs average stadiometer and seca mechanical scale

Technical Error Measurement (TEM)

The results for the TEM are tabulated in Table 2. The relative TEMs (T_1) for the inter- and intra-examiner aspects were 0.13% and 0.13%, respectively, while for the inter-instrument aspect, it was 0.38%. The coefficient of reliability, (R), for inter, intra-instrument and inter-instrument aspects were 99.92%, 99.93% and 99.41%, respectively. The coefficients of variability (CVs) for the inter- and intra-examiner and inter-instrument aspects were 4.895%, 4.908% and 4.943%, respectively.

Table 2
Technical Error of Measurement (TEM) & Coefficient of Variation (CVs)

	Inter-examiner (Examiner 1 & Examiner 2)	Intra-examiner (1 st measurement & 2 nd measurement)	Inter-instrument (Stadiometer & Mechanical Scale)
Σ (Deviation) ²	12.31	11.95	102.94
Absolute TEM, T_0	0.21	0.21	0.60
VAV	159.60	159.60	159.30
Relative TEM %, T_r	0.13	0.13	0.38
Coefficient of reliability (R)	0.99929	0.999314	0.994155
Coefficient of variations (CVs)	4.895	4.908	4.943

DISCUSSION

Anthropometric measurements have different types of error. This study looked, in particular, at imprecision as one of the components of reliability. Imprecision is the variability of repeated measurements due to intra- examiner, inter-examiner and inter-instrument measurement differences (Ulijaszek, 1999) (Table 3). There are a few indices that are often used to assess intra- and inter-examiner and inter-instrument aspect variability. These include technical error of measurement (TEM), coefficient variation (CV), coefficient of reliability (R), intra-class correlation coefficient (ICC) and the Bland and Altman plot. There are only a handful of published articles on measurement errors. There is one landmark review article (Ulijaszek, 1999) that captured two anthropometric measurements among which were the Stadiometer and Mechanical Scale. This study examined the reliability of the inter-examiner, intra-examiner and inter-instrument aspects. The ICC is an estimate of the proportion of the combined variance for the true biological value for any anthropometric measure and for the measurement errors associated with it. We found that the ICC values were close to 1; 0.999 for the inter-examiner and 0.999 for the intra-examiner and 0.997 for the inter-instrument aspects. This indicates high variability between repeated measures on the same subject, which means the accuracy of the stadiometer varied between different examiners.

Table 3
Correlation of Coefficient of Inter- and Intra-Examiner and Inter-Instrument Measurement

Variables	N	Inter-examiner		N	Intra-examiner		N	Inter-instrument	
		ICC	Coefficient Variation		ICC	Coefficient Variation		ICC	Coefficient Variation
Height	137	0.999	5.15%	137	0.999	5.07%	137	0.997	5.07%

A number of methods of measuring inconsistency are available but the preferred method involves calculation of the intra- and inter-examiner and intra-instrument aspects. TEM gives information on the error margin of a trait and therefore is an accuracy index. Determination of acceptable levels of measurement errors is not straightforward and relates to the variable being studied as well as the height of the subjects (Ulijaszek & Kerr, 1999). However, Ulijaszek and Kerr (1999) have suggested acceptable intra- and inter-examiner limits for a range of anthropometric measure including height, weight and skinfold site (Ulijaszek & Kerr, 1999). The results of anthropometric measurements, TEM (T_0), rTEM (T_I), R and CVs values are presented in Table 1.

Changes in the mean, correlation coefficient and Bland and Altman plots revealed a high degree of inter-examiner reliability. The p values of the change in the mean showed no statistical significance. The Bland and Altman plot shown in the three graphs are valid because all the points are close to each other. This makes for high validity and was also found, by Bland and Altman, that the two examiners were consistent with an average of 0.012 cm and an upper limit of 0.591 cm to lower limit of -0.566 cm. However, the reading of an upper limit and lower limit was slightly bigger in difference. For intra-examiner reliability, the average is -0.99 cm with an upper limit of 0.436 cm to lower limit of -0.636 cm. It was found that the difference between mean upper limit and lower limit was more precise compared to those of the inter-examiner aspect. The reading was more valid because the same person took the reading. In addition, the mean inter-instrument average was 0.616 cm and upper limit 1.775 cm to lower limit -0.543 cm. This suggested that the examiner must have been poorly trained at handling the instrument. The ICC for both intra- and inter-examiner was almost perfect: 0.9900 and 0.9990, respectively. For inter-instrument was 0.954. All findings showed that the reliability of the three experiments was absolutely perfect.

All three relative TEM values were within the acceptable limit. Our findings of TEM values for the inter- and intra- examiner was 0.13% and for inter-instrument it was 0.38%. The inter-instrument reading was higher compared to that for inter- and intra- examiner, which was found to be due to different instruments. Comparison for intra- and inter-examiner and inter-instrument aspects showed that the inter-correlation coefficient gave a precise reading, which is close to 1. From the findings of R, the Coefficient of Reliability, all three measurements reported less than 5% error due to human measurement. These indicated close to perfect intra- and inter-examiner reliability for both measurements and inter-instrument. The CVs for three experiments were below 5% error. This shows that variability was low in this sample, which was the hypothesis. However, this study can conclude that the measurement of inter-instruments were less reliable than those for the inter- and intra-examiner aspects. On the part of validity, the intra- and inter-examiner readings were 4.895% and 4.908%, respectively. For inter-instrument, it was 4.943%. Our findings showed that the most valid measurement was that of the intra-examiner compared to the others.

The reporting of examiner measurement error was common, and it is this issue that should receive adequate attention in future studies using anthropometric measures as the main study outcome. For further research, observer or examiner measurement error should be minimised through close attention to every aspect of the data collection process, such as equipment calibration and the training of research personnel.

CONCLUSION

Anthropometric measurement errors are unavoidable and should be minimised through close attention to every aspect of the data collection process including selection of examiners. The inter-examiner, intra-examiner and inter-instrument correlation coefficients for height measurement were almost perfect. The R and CV value were also within acceptable range. Therefore, it was proven that the portable stadiometer had high degrees of reliability for measuring height and was valid to be interchanged with the SECA Mechanical scale.

ACKNOWLEDGEMENT

The authors would like to thank the Director General of Health, the Ministry of Health Malaysia, for permission to publish this paper. We are grateful to the subjects for participating in this survey.

REFERENCES

- Biehl, A., Hovengen, R., Meyer, H. E., Hjelmesæth, J., Meisfjord, J., Grøholt, E. K. ... & Strand, B. H. (2013). Impact of instrument error on the estimated prevalence of overweight and obesity in population-based surveys. *BMC Public Health*, 13(1), 1–6.
- Bland, M. J., & Altman, D. G. (1986). Statistical methods for assessing agreement between two methods of clinical measurement. *The lancet*, 327(8476), 307-310.
- Cameron, N. (2002). *Human growth and development*. United States of America, USA: Academic Press.
- Geeta, A., Jamaiyah, H., Safiza, M. N., Khor, G. L., Kee, C. C., Ahmad, A. Z., ... & Faudzi, A. (2009). Reliability, technical error of measurements and validity of instruments for nutritional status assessment of adults in Malaysia. *Singapore Medical Journal*, 50(10), 1013.
- Gore, C. J., & Australian Sports Commission (Eds.). (2000). *Physiological tests for elite athletes*. United Kingdom, UK: Human Kinetics.
- Haniff, J., Appannah, G., Nor, M., Safiza, N., Wong, N. F., Kee, C. C., ... & Abd Talib, R. (2008). Reliability and technical error of calf circumference and mid-half arm span measurements for nutritional status assessment of elderly persons in Malaysia. *Malaysian Journal of Nutrition*, 14(2), 137–150.
- MUSC. (2006). *Medical University of South Carolina*. Retrieved September 20, 2006 from www.musc.edu/dc/icrebm/index.html
- NYORC. (2006). *New York Obesity Research Center: Body composition unit*. Retrieved September 16, 2006 from www.nyorc.org/anthropometry.html
- Norton, K., & Olds, T. (1996). *Anthropometrica: A textbook of body measurement for sports and health courses*. Australia: UNSW press.
- Sánchez-García, S., García-Peña, C., Duque-López, M. X., Juárez-Cedillo, T., Cortés-Núñez, A. R., & Reyes-Beaman, S. (2007). Anthropometric measures and nutritional status in a healthy elderly population. *BMC Public Health*, 7(2), 1-9.

Height Measurement Reliability Using Portable Stadiometer

- Ulijaszek, S. J., & Kerr, D. A. (1999). Anthropometric measurement error and the assessment of nutritional status. *British Journal of Nutrition*, 82(03), 165–177.
- Walter, S. D., Eliasziw, M., & Donner, A. (1998). Sample size and optimal designs for reliability studies. *Statistics in Medicine*, 17(1), 101–110.
- Zady, M. F. (n.d.). *Z-4: Mean, standard deviation, and coefficient of variation*. Madison: Westgard QC. Retrieved March 6, 2014, from www.westgard.com/lesson34.htm#coefficient



The value of ^{18}F -fluorodeoxyglucose –positron emission tomography/computed tomography (^{18}F - FDG PET/CT) in the staging and impact on the management of patients with nasopharyngeal carcinoma

Sethu Thakachy Subha^{1*}, Fathinul Fikri Ahmad Saad², Abdul Jalil Nordin² and Saraiza Abu Bakar³

¹Department of Surgery/ENT, Faculty Medicine and Health Sciences, University Putra Malaysia, 43400 UPM, Serdang, Selangor, Malaysia

²Centre for Diagnostic Nuclear Imaging, University Putra Malaysia, 43400 UPM, Serdang, Selangor, Malaysia

³Department of ENT, Hospital Serdang, 43000 Serdang, Selangor, Malaysia

ABSTRACT

This study sought to prospectively evaluate the influence of contrasted fluorine-18 fluorodeoxyglucose positron emission tomography/computed tomography (^{18}F -FDGPET/CT) in the staging of and impact on the management plan for treatment in patients with nasopharyngeal carcinoma (NPC). A total of 14 histologically proven NPC patients (mean age: 44.64 ± 4.01 years) were included in the study. These patients underwent contrasted Computed Tomography (CT) as well as ^{18}F -FDGPET/CT imaging. Staging was based on the 7th edition of the American Joint Committee on Cancer Tumor Node Metastases (AJCC-TNM) recommendations. The oncologist was asked to prospectively assign a treatment plan for all patients being evaluated by CT and ^{18}F -FDGPET/CT. The treatment plans were compared with the incremental information supplied by the FDG-PET/CT. The maximum standardised uptake value (SUV_{max}) and the widest dimension of the primary tumour, cervical lymph nodes size and the distant metastatic lesions were quantified on the co-registered PET/CT images by two experienced nuclear radiologists. The contrasted ^{18}F -FDGPET/CT changed the management intent in nine patients (64.7%). A univariate analysis showed that there were significant correlations between SUV_{max} and the size of the metastatic lymph nodes ($R^2 = 0.0761$, $p < 0.01$), lymph node volume ($R^2 = 0.695$, $p < 0.01$) and the T-stage ($R^2 = 0.647$, $p < 0.01$). Multiple linear regression analysis revealed the tumour SUV_{max} to be the independent predictor

of the T-stage (adjusted $R^2 = 0.889$, $p < 0.05$). The SUV_{max} may potentially be a surrogate marker for the T-stage in the NPC patients. The use of the combined imaging modality, ^{18}F -FDGPET/CT, substantially impacted on the management strategy for treatment of NPC patients.

Keywords: ^{18}F -FDG PET/CT, nasopharyngeal carcinoma, AJCC-TNM staging), SUV_{max} , impact

Article history:

Received: 2 February 2016

Accepted: 5 December 2016

E-mail addresses:

subhast2@yahoo.com (Sethu Thakachy Subha),

ahmadsaadff@gmail.com; ainurff@gmail.com

(Fathinul Fikri Ahmad Saad),

drimaging@yahoo.com; abdjilil@upm.edu.my

(Abdul Jalil Nordin),

drsaraiza@yahoo.com (Saraiza Abu Bakar)

*Corresponding Author

INTRODUCTION

Nasopharyngeal carcinoma (NPC) is unique and distinguished from other head and neck malignant tumours because of its epidemiology, histopathological spectrum, clinical characteristics, therapy and biological behavior (Vokes et al., 2000; Yang et al., 2015). Distinct geographic variation in the incidence of NPC indicates an influence of genetic and environmental factors. Various reports revealed that the southern Chinese are an ethnically distinct and high-risk group for this particular tumour. The environmental factor is the ingestion of Cantonese-style salted fish especially in childhood. NPC presents most commonly as a neck lump in 50% to 70% of patients as a result of cervical lymph node metastases. The tumour may not be clinically apparent at the time of presentation (Goh et al., 2009). The symptoms are usually protracted and the disease manifests late in its course.

Positron Emission Tomography (PET) imaging has been reported to be the more sensitive imaging technique in detecting clinically occult metastatic disease, retropharyngeal lymph nodes, small volume lesions and distant metastases (Chang et al., 2005; Fathinul et al., 2009). The use of a glucose analogue (fluorodeoxyglucose, FDG) underpins the cancer cell reprogramming on the altered glycolytic metabolism, seen as areas of increased tracer uptake on the PET images. The standardised uptake value (SUV) is a measure of the FDG-intensity on the PET image and appears to be a reliable parameter in evaluating correlation with factors that determine the tumour's aggressiveness (Fathinul et al., 2013). All NPC cases in this study were regrouped into two histological types according to the WHO 1991 classification, namely keratinising squamous cell carcinoma (equivalent to WHO Type I) and non-keratinising carcinoma (pooling together WHO Type II non-keratinising and Type III undifferentiated carcinoma in the old terminology (Shanmugaratnam et al., 1991).

Although the five-year survival rate for overall NPC patients is high, around 90% of patients with distant metastases will die within one year (King et al., 2000). Thus, accurate staging and restaging of NPC are important for improving treatment and prognosis. As outlined by the AJCC (American Joint Committee on Cancer), the TNM staging system is the most important prognostic factor for appropriate treatment planning and survival prediction of NPC patients (Li et al., 2014). A revised AJCC-TNM staging 7th edition was released in 2009. There were several revisions in the new edition staging system compared to 6th edition. Li et al. compared the prognostic value of the TNM 6th edition and the TNM 7th edition for NPC patients. Their study demonstrated that the TNM 7th staging system is superior to the TNM 6th staging system in predicting the frequency of overall survival and distant metastases free survival (Li et al., 2014).

The superiority of the PET/CT to whole-body MRI in overall TNM staging supports the usefulness of ^{18}F -FDG PET/CT as a possible first-line modality for whole-body tumour staging (Antoch et al., 2003). The N stage was found to be prognostically significant even among patient groups stratified for the size and degree of fixation of the neck nodes involved (Antoch et al., 2003; Chen et al., 2007). Though irrelevant to the N staging of NPC, the SUV_{max} was correlated to the size of the lymph nodes and also related to the degree of differentiation of NPC

(Liu et al., 2012). Analysing the prognostic factors for nasopharyngeal carcinoma (Iacovelli et al., 2014) demonstrated that the most significant prognostic factors in nasopharyngeal carcinoma were patient age, T-stage of the primary tumour, presence of cervical lymphadenopathy and certain technical factors of irradiation. This study was set to evaluate the clinical application of FDG PET/CT in predicting the staging of NPC using SUV on the latest AJCC 7th edition and to determine its potential impact on the management strategy for treatment.

MATERIALS AND METHODS

Patient Accrual

This study was approved by the institutional ethical committee and obtained written consent from all the patients. We prospectively analysed the contrasted CT and ¹⁸F-FDGPET/CT findings from 14 consecutive patients (mean age: 44.64±4.01) with histologically proven NPC. The exclusion criteria were children, acute or chronic inflammatory disease, pregnant patients, lactating mothers, terminally ill patients and any previous malignancy. Staging of the disease was done based on the 7th edition AJCC-TNM (American Joint Committee on Cancer-Tumor size, Lymph Nodes, Metastases) staging system based on both imaging modalities. The oncologist was asked to outline the patients' treatment management intent based on CT as well after PET/CT. The change in management intent and incremental information obtained after PET/CT imaging were compared and analysed.

¹⁸F-FDG-PET/CT

All the subjects were required to fast for at least 6 hours prior to PET/CT, although oral hydration with glucose-free water was allowed. After verification of a normal blood glucose level in the peripheral blood (mean FBS), patients received an IV injection of 370 MBq (10 mCi) of FDG and then rested for approximately 60 minutes prior to the PET/CT imaging. Image acquisition was performed with an integrated PET/CT device (Siemens Biograph-64) consisting of a PET scanner (lutetium oxyorthosilicate) 64-MDCT scanner. The axes of both systems were aligned such that the patient could be moved from the CT scanner to the PET scanner with a movement of the examination table of up to 68 cm. Patients were allowed normal shallow respiration during acquisition of CT scan. The CT was performed with IV contrast (Iopamidol 300) at 5.0-mm spiral acquisition from base of skull to the proximal thigh for the purpose of anatomical localisation and attenuation correction to rescale the FDG-PET image attenuation. The PET emission was performed contemporaneously at 3 minutes per bed position acquisition. CT data were resized from a 512 × 512 matrix to a 128 × 128 matrix to match the PET data to allow image fusion and CT transmission maps were generated. PET image data sets were reconstructed iteratively with the ordered-subsets expectation maximisation algorithm with segmented measured attenuation correction (two iterations, 28 subsets) with the CT data. Co-registered images were displayed on the Siemens-Leonardo workstation.

Image Analysis

The SUV_{max} and the widest dimension of the primary tumour, size of the cervical lymph nodes and the distant metastatic lesions were quantified on the co-registered PET/CT images by two experienced nuclear radiologists who were blinded to the diagnosis. As for the CT, nodes with a short-axis diameter greater than 10 mm were defined as abnormal, and the presence of necrosis within a lymph node was considered a sign of malignancy, regardless of node size.

STATISTICS

Mean, SD, range and frequencies were used to describe the data. Differences in the mean of the variables were analysed via a non-parametric test (Kruskal Wallis) The clinical risk factors i.e. age, sex, SUV_{max} and tumour size were evaluated for independent predictors for the TNM staging (AJCC 7th edition) using the univariate and multivariate analysis. A two-sided p value of <0.05 was considered significant.

RESULTS

Patients Characteristics

Fourteen patients with nasopharyngeal carcinoma were included in this study with the mean age of 44.64 ± 4.01 years. They comprised four females and 10 males. Biopsy results were available for all patients with WHO (type 1) noted in one patient and WHO (type II) in the 13 others (Table 1). All the patients had pre-treatment CT and ^{18}F -FDG PET/CT for the purpose of TNM staging disease stratification for the intended management plan (Table 2).

Out of the 14 patients, five had early-stage disease (Stage I and Stage II) and of them, two were put on an altered treatment plan based on the PET-CT results. Nine patients were initially classified as having advanced stage disease (Stage III and Stage IV) and seven of these patients had their treatment altered following the findings of the PET-CT imaging. The PET-CT imaging accurately identified that the extension of the primary tumour and T staging had changed in the four patients. The PET-CT imaging had correctly identified the nodal stage in three patients and these patients benefitted by being having neoadjuvant chemotherapy added. Distant metastases were identified in four patients and thus, the management intent was changed from definitive to palliative intent. Nine (64.3%) patients had stage migration i.e. upstaging of the disease as shown in Table 3. There was no change in disease staging among five of the (35.3%) patients.

Table 1
Patient Characteristics

Parameter	Characteristic	n	%
Age	44.64 ± 4.01 (years)		
Sex	Male	10	71.42
	Female	4	28.57
Histology	WHO (Type 1)	1	7.14
	WHO (Type II)	13	92.85

Table 2
 Management Intent Based On CT and PET-CT

No	age	sex	CT staging	PET/CT staging		Management Intent	
				CT	PET/CT	CT	PET/CT
P1	44	M	T1N3M0 IVB	T1N3bM0 IVB	3 cycles neoadj Ct then CtRT	3 cycles neoadj Ct then CtRT	
P2	56	F	T1N2M0 III	T1N3bM0 IVB	CtRT	3 cycles neoadj Ct then CtRT	
P3	50	M	T2N1M0 II	T4N1M0 IVA	CtRT	3 cycles neoadj Ct then CtRT	
P4	70	M	T1N0M0 I	T1N0M0 I	RT alone	RT alone	
P5	39	M	T2N2M0 III	T4N2M0 IVA	CtRT	3 cycles neoadj Ct then CtRT	
P6	22	M	T1N1M0 I	T1N1M0 I	CtRT	CtRT	
P7	65	M	T3N2M0 III	T3N3M0 IVB	CtRT	3 cycles neoadj Ct then CtRT	
P8	46	M	T3N0M0 III	T4N0M1 IVC	CtRT	Chemotherapy – 6 cycles	
P9	42	M	T3N3M0 IVB	T4N1M0 IVA	3 cycles neoadj Ct then CtRT	3 cycles neoadj Ct then CtRT	
P10	55	F	T3N0M0 III	T4N0M1 IVC	CtRT	Chemotherapy – 6 cycles	
P11	54	M	T2N2M0 III	T2N2M1 IVC	CtRT	Chemotherapy – 6 cycles	
P12	22	M	T1N1M0 I	T2N1M0 II	CtRT	CtRT	
P13	26	F	T2N2M0 III	T2N2M0 III	CtRT	CtRT	
P14	34	F	T3N3M0 IVB	T3N3M1 IVC	3 cycles neoadj Ct then CtRT	Chemotherapy – 6 cycles	

Note. NPC: Nasopharyngeal Carcinoma; CT: Computed Tomography;
 PET/CT: Positron Emission Tomography/Computed Tomography;
 RT: Radiotherapy; Ct: Chemotherapy; neoadj: neoadjuvant
 CtRT: Chemoradiotherapy
 M-male, F-Female

Table 3
Influence of PET-CT Findings on the Impact of Management Intent

Number of patients	Stage Migration/ shift	Management intent with CT	Management intent with PET/ CT	Impact on management intent
2	11 -1VA	CtRT	Neoadj Ct &CtRT	High
3	111-1V B	CtRT	Neoadj CT &CtRT	High
3	111 -1VC	CtRT	Chemotherapy alone	High
1	1VB-1VC	Neoadj Ct &CtRT	Chemotherapy alone	High

CT: Computed Tomography; PET/CT: Positron Emission Tomography/Computed Tomography; RT: Radiotherapy; Ct: Chemotherapy neoadj: neoadjuvant; CtRT: Chemoradiotherapy

Correlation of SUV_{max} and the Clinical Risk Parameters

As shown in Table 4, the univariate analysis showed significant correlations between SUV_{max} of the primary tumour and the widest diameter of metastatic lymph nodes ($R^2=0.0761$, $p<0.01$) and the lymph node volume ($R^2=0.695$, $p<0.01$). There was no significant correlation with other continuous clinical risk parameters pertaining to the primary tumour with the SUV_{max} .

Table 4
Univariate Analysis of SUV_{max} Primary Tumour for Clinical Risk Variables

<u>SUV_{max} mean 14.28 ± 2.43</u>	Mean	P value
Clinical parameter/ R^2		
Lymph node size (d/cm)	1.14 ± 0.09	<0.01
Lymph node volume (cm^3)	3.05 ± 0.47	<0.01

SUV_{max} as a Predictive Marker

Multiple linear regression analysis revealed the tumour SUV_{max} to be the independent predictor of the T-stage (adjusted $R^2=0.889$, $p<0.05$). There was no influence of the other clinical parameters on the SUV_{max} . The details of these are shown in the Table 5.

Table 5
Multivariate Analysis of the SUV_{max} for the Clinical Risk Variables (n=14)

Clinical parameter	HR (95% CI)	p
Age	0.433 ± 0.315	0.711
Sex	22.217 ± 11.19	0.450
Lymph node size	44.420 ± 10.23	0.177
No of lymph node	1.808 ± 1.94	0.931
T stage	11.564 ± 0.17	*0.045
N stage	6.167 ± 7.38	0.833
M stage	18.085 ± 13.14	0.712

* Statistical significant value ($p<0.05$)

DISCUSSION

Nasopharyngeal carcinoma is a progressive epithelial malignancy that is often under-staged by clinical examination (Chen et al., 2006). Accurate timely diagnosis of TNM staging is of paramount importance for appropriate treatment planning and prognosis (Zeng et al., 2014). The main effective method of treatment for NPC is radiotherapy and a good outcome is indicated if the disease is detected early in its course. The five-year overall survival rate is about 50% to 70% (Phua et al., 2013).

As shown in our study, the SUV_{max} for this diseases is significantly correlated with the size and the volume of the metastatic lymph nodes. These indicate that SUV_{max} as a marker for an altered glucose metabolism is an important signalling marker of the PET that reflects the tumour aggressiveness. This evidence clearly shows that the prevalence of the nodal metastasis is proportionally associated with tumour aggressiveness as reflected on the TNM staging. Information gathered from PET imaging complements the questionable sub-centimeter lymph node that is vastly imperceptible on the CT. This was reflected in our study and is seen in Table 2 (P2, P7& P9) which shows that the patients were upstaged based on the N-stage. This is in line with previous reports that stated that FDG PET-CT has higher accuracy in detecting cervical Lymph nodes than conventional imaging (Chang et al., 2005).

SUV_{max} was determined to be the only independent parameter for the T-staging. The finding further emphasised that the aggressiveness of the primary tumour was reflected by the intensity of the SUV_{max} concentration of the primary tumour. In this context, SUV_{max} plays a potential role in T-staging as determined in our study. This is in accordance with other reports that established the association of ^{18}F -FDG PET/CT on the T staging of NPC (Phua et al., 2013). Chen et al. compared ^{18}F -FDG PET/CT, PET and CT in the detection of the primary site of NPC and reported that the T stage was accurately determined in 18 out of 20 cases with ^{18}F -FDG PET/CT. Both PET alone and CT alone correctly assessed the T-stage in 15 out of 20 cases (Chen et al., 2006).

The SUV_{max} was found to be a statistically insignificant marker for the M staging in our cohort of patients compared with those in other reports, which stated the contrary in other cancer cell lines. The explanation for this is that our study cohort included a small number of patients, in whom the PET findings were positive for metastatic disease. There were only four patients (P8, P10, P11 and P14) who were found to have positive metastatic deposits on PET but none was discerned from the CT. Although no correlation was found between the SUV_{max} and the M-staging, it is noteworthy to highlight that PET had accurately detected two patients with skeletal metastasis on the FDG-PET. This is supported by the study by Liu et al., whose report showed that ^{18}F -FDG PET was more sensitive in detecting bone metastases compared to skeletal scintigraphy (Liu et al., 2006). Two patients in our study group were detected to have mediastinal nodal metastases by PET/CT. The treatment for all four patients with distant metastases was subsequently altered to palliative intent.

Our ^{18}F FDG PET/CT study findings had altered the management intent of 64.7% [9/14] patients based on the TNM-AJCC 7th edition. Among them, the PET /CT findings disclosed further evidence of distant metastases in 28% [4/14] patients. This study suggested ^{18}F -FDG uptake as measured by SUV_{max} in the PET-CT could potentially play a significant role in providing appropriate staging and adequate treatment planning.

Limitations

There were some limitations to our study. Some of the influence of the SUV_{max} did not seem to influence clinical parameters as stated in other studies. The potential attribute for this may be due to the small sample size calculated for a significant statistical test. A more cohesive method in preparing the patients for the PET-CT scanning and the scanning procedures should be adopted as to minimise factors that lead to image degradation. This was observed when the scanning time varied from 45 minutes to 90 minutes and some of the suboptimal images were not repeated to yield an image of better quality. It would also have had been better to include an MRI study in the comparative analysis with the CT imaging as the former is known to have better soft tissue resolution than the latter, thus providing better image interpretation.

CONCLUSION

While the SUV_{max} may potentially be a surrogate marker for the T-stage in NPC patients based on the 7th edition of AJCC-TNM staging, the use of the contrasted ^{18}F -FDGPET/CT substantially impacted on the management strategy for treatment of the disease.

CONFLICT OF INTEREST STATEMENT

The authors report no conflicts of interest.

ACKNOWLEDGEMENT

This research was supported by the RUGS (Research University Grant Scheme) from the Research Management Centre, Technology Centre UPM-MTDC, University Putra Malaysia, 43400 UPM Serdang, Selangor, Malaysia. The abstract was presented at the International Cancer Imaging Society 2011 conference and 11th annual teaching course in October 2011 in Copenhagen (Cancer Imaging (2011, 11, S40)).

REFERENCES

- Antoch, G., Vogt, F. M., Freudenberg, L. S., Nazaradeh, F., Goehde, S. C., Barhausen, J., ... & Ruehm, S. G. (2003). Whole-body dual-modality PET/CT and whole body MRI for tumor staging in oncology. *The Journal of the American Medical Association*, 290(24), 3199–3206.
- Chang, J. T., Chan, S. C., Yen, T. C., Liao, C. T., Lin, C. Y., Lin, K. J., ... & Ng, S. H. (2005). Nasopharyngeal carcinoma staging by (18) F-fluorodeoxyglucose positron emission tomography. *International Journal of Radiation Oncology Biology Physics*, 62(2), 501–507.
- Chen, Y. K., Cheng, R. H., Chi, K. W., Liang, J. G., Wang, S. C., Shen, Y. Y., ... & Su, C. T. (2007). Application of 18F-FDG PET/CT in nasopharyngeal carcinoma. *Annals of Nuclear Medicine Science*, 20(1), 21–32.

- Chen, Y. K., Su, C. T., Ding, H. J., Chi, K. H., Liang, J. A., Shen, Y. Y., ... & Kao, C. H. (2006). Clinical usefulness of fused PET/CT compared with PET alone or CT alone in nasopharyngeal carcinoma patients. *Anticancer Research*, *26*(2B), 1471–77.
- Fathinul, F., & Lau, W. F. E. (2009). A subcentimetre single pulmonary nodule (SPN); Potentials of FDG- PET interpretative pitfalls in patients with a known extrapulmonary malignancy. *Biomedical Imaging and Intervention Journal*, *6*, e34.
- Fathinul, F., Nordin, A. J., & Lau, E. F. E. (2013). 18 [F] FDG-PET/CT is a useful molecular marker in evaluating tumour aggressiveness; A revised understanding of an in-vivo FDGPET imaging that alludes the alteration of cancer biology. *Cell Biochemistry and Biophysics*, *66*(1), 37–43.
- Goh, J., & Lim, K. (2009). Imaging of nasopharyngeal carcinoma. *Annals Academy of Medicine Singapore*, *38*(9), 809–16.
- Iacovelli, N. A., Bossi, P., Fallai, C., Gardani, G., & Orlandi, E. (2014). Emerging prognostic factors in nasopharyngeal carcinoma. *Journal of Nasopharyngeal Carcinoma*, *1*(8), e8. doi:10.15383/jnpc.8.
- King, W. W., Ku, P. K., Mok, C. O., & Teo, P. M. (2000). Nasopharyngectomy in the treatment of recurrent nasopharyngeal carcinoma: A twelve-year experience. *Head and Neck*, *22*(3), 215–222.
- Li, J., Zou, X., Wu, Y. L., Guo, J. C., Yun, J. P., Xu, M. ... & Chen, M. Y. (2014). A comparison between the sixth and seventh editions of the UICC/AJCC staging system for nasopharyngeal carcinoma in a Chinese cohort. *PloS one*, *9*(12), e116261.
- Liu, W. S., Wu, M. F., Tseng, H. C., Liu, J., T., Weng, J. H., Li, Y. C., & Lee, J. K. (2011). The role of pretreatment FDG-PET in nasopharyngeal carcinoma treated with intensity-modulated radiotherapy. *International Journal of Radiation Oncology Biology Physics*, *82*(2), 561–6.
- Liu, F. Y., Chang, J. T., Wang, H. M., Liao, C. T., Ng, S. K., Chan, S. C., ... & Yen, T. C. (2006). [18F] fluorodeoxyglucose positron emission tomography is more sensitive than skeletal scintigraphy for detecting bone metastasis in endemic nasopharyngeal carcinoma at initial staging. *Journal of Clinical Oncology*, *24*(4), 599–604.
- Phua, V. C. E., Loo, W. H., Yusof, M. M., Ishak, W. Z. W., Tho, L. M., & Ung, N. M. (2013). Treatment outcome for nasopharyngeal carcinoma in University Malaya Medical Centre from 2004-8. *The Asian Pacific Journal of Cancer Prevention*, *14*(8), 4567–4570.
- Shanmugaratnam, K., & Sobin, L. (1991). *Histological typing of tumours of the upper respiratory tract and ear* (2nd Ed.) (pp. 32-33). Berlin: Springer-Verlag.
- Vokes, E. E., Liebowitz, D. N., & Weichselbaum, R. R. (1997). Nasopharyngeal carcinoma. *The Lancet*, *350*(9084), 1087–1091.
- Yang, Z., Shi, Q., Zhang, Y., Pan, H., Yao, Z., Hu, S., ... & Hu, C. (2015). Pretreatment 18 F-FDG uptake heterogeneity can predict survival in patients with locally advanced nasopharyngeal carcinoma –a retrospective study. *Radiation Oncology*, *10*(4), 1-8.
- Zeng, F., & Cheng, M. (2014). Clinical application value and progress of PET/CT in nasopharyngeal carcinoma. *Journal of Nasopharyngeal Carcinoma*, *1*(2), e2. doi:10.15383/jnpc.2.





Design of a Movable Swine Roasting Machine

Bunkrachang, N.¹ and Kitthawee, U.^{2*}

¹*Faculty of Agriculture and Natural Resources, Rajamangala University of Technology Tawan-ok, Chon Buri 20110, Thailand*

²*Faculty of Science and Technology, Suan Dusit University, Dusit, Bangkok 10300, Thailand*

ABSTRACT

The objective of this research was to design a transportable swine-roasting machine. The methodology was in two parts. The first was to survey the local knowledge of roast swine and to examine the process. The second was to design a movable swine-roasting machine. The result showed that most manufacturers and distributors produced roast swine. Their daily income was about USD170 per day. The cost of the roast swine was USD5.5 per kilogram. The process involved slaughtering a swine that was approximately 25 kg, removing the offal and inserting lemongrass stalks into the carcass. The pig carcass was then roasted on hot charcoal for about 3 hours and turned by hand. The average chest diameters of 47 roast swine were 0.332, 0.307 and 0.244 m. (large, medium and small, respectively). The design concepts of a movable swine roaster involved equipment that allowed roasting on only two sides of the swine, which was supported by stainless steel pipes (the swine holder) rotated by a 0.5 hp electrical motor. The amount of charcoal for a transportable swine-roasting machine was between 14 and 18 kg depending on the weight of the swine to be roasted. The average temperature of the roaster was 260°C. The average weight of fresh pork to charcoal was around 1.46:1 kg. The roaster was easy to use and maintain.

Keywords: Roast pork, swine-roasting machine, swine, roaster, movable roaster

INTRODUCTION

By 2014, Thailand's swine industry was relatively mature and produced 15.8 million swine or 1.19 million tonnes of pork annually. In addition, the consumption of pork reached 1.18 million tonnes as reported by The Swine Raisers Association of Thailand in 2014. This is

equivalent to an average consumption of 17.9 kilograms per person per year. In the same year, Thailand exported 20,000 tonnes of pork and pork products, which were valued at around USD108 million or 1.67% of total production, and it was projected to increase steadily. Admittedly, a large number of pork

Article history:

Received: 10 May 2016

Accepted: 3 November 2016

E-mail addresses:

krumon38090@hotmail.com (Bunkrachang, N.),

udomsak_kit@dusit.ac.th (Kitthawee, U.)

*Corresponding Author

and pork products were manufactured for domestic consumption. Nakhon Pathom province, recognised as one of Thailand's top swine-producing provinces, experienced an oversupply of piglets in 2007. Local food consumption would have had a significant relationship within the context of daily living, thus reflecting the availability of natural resources and the development of local knowledge (Anantathanachai, 2010). Similarly, people in Tha Kham, Sam Phran and Nakhon Prathom provinces considered swine their most important resource. Relying on local wisdom, they successfully developed a delicious dish known as roast swine, which had a unique taste and quality as it was the result of using academic principles of food production. The traditional method of roasting swine was to cook the meat on the ground, which ran the risk of producing low-quality meat (Wessapan & Borirak, 2014).

Traditional meat products are developed using different processes. The success of such products can be seen at different levels (Chu-iad, 2008). Certainly, government agencies and local authorities are required to play a vital role in developing human resources in the industry while providing them with greater knowledge of operating and managing all aspects of the business. In addition, the production of roast swine was only appropriate for day-to-day selling (Kitthawee et al., 2013). Given that the majority of customers preferred fresh roast swine, the product was not meant to be kept overnight. Transportation and selling period became key factors in roast swine production. If transportation took more than 1 hr, the roast swine would be considered inferior in quality and thus, become less appealing. A swine-roasting machine was therefore developed to cook small pieces of meat (Teeboonma et al., 2006; Paengteeresukkamai, 2011; Wessapan & Borirak, 2014).

As the researcher had foreseen the significance and possible impact of the design of the mobile swine roaster on the roast swine industry, it was necessary to conduct a preliminary survey and gather vital information about the product. The aim of this research was to design a portable swine roaster to facilitate roasting at selling locations.

MATERIALS AND METHOD

Fundamental Information

The researcher conducted a preliminary survey on traditional roast swine at local markets and manufacturing venues with the assistance of the Tha Kham Subdistrict Administrative Organisation in Nakhon Pathom's Sam Phran district. The survey covered several topics including the production process, the preparation of raw materials and ingredients, the measurement of swine of different sizes prior to roasting and the determination of charcoal temperature at four positions in the roaster as well as swine temperature at two positions on the swine holder every 15 min for 3 hrs. The temperature was measured using an IR thermometer, CEM DT-8835.

Design Principles

The portable swine roaster was designed using principles similar to the traditional large roaster traditionally placed on the ground, as shown in Figure 1. Judging from the description in Figure

2, only the sides of the swine are exposed to heat using this method. Moreover, the fat does not drip directly onto the hot charcoal (Wessapan & Borirak, 2014). The swine is positioned to be turned slowly to receive heat from the burning charcoal (see the two arrows in Figure 2). However, heated charcoal is required at the lower middle part of the roaster. The other remaining sides of the swine are exposed to the heat acquired from the same position of the heated charcoal in the next round. As the heat is maintained at the same temperature, the whole body of the swine is roasted twice in one rotation.

The portable swine roaster is designed to maintain the heat from both sides, which can be controlled manually. The roaster is made of a steel sheet and other inexpensive materials chosen for their portability and heat-resistant properties. The portable swine roaster consists of a 9.5 mm (3/8 in) metal sheet designed in half cylinder, a metal roast set, a worm-gear speed reducer (40:1) powered by a simple pulley and belt system and a 0.5 hp electric motor that powers the continuous turning throughout the roasting period as shown in Figure 4.



Figure 1. Traditional roast-swine manufacturing

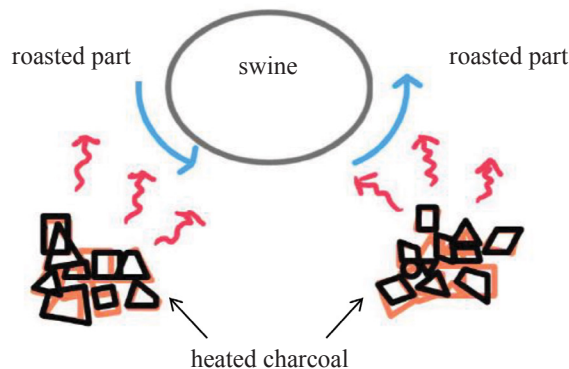
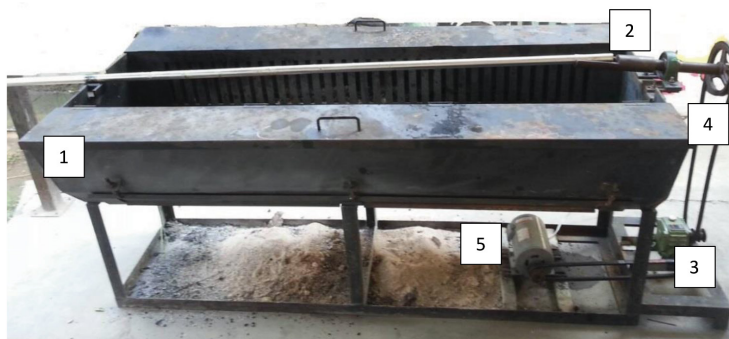
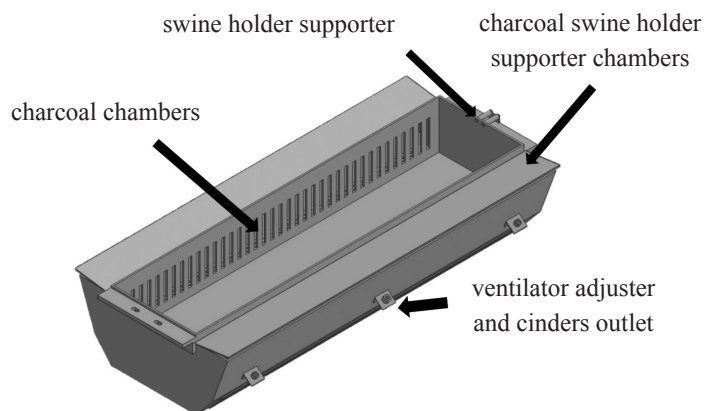


Figure 2. Concept of heat transfer from burning charcoal to swine



Figure 3. Roasting of swine by local manufacturer



1=metal sheet; 2= metal roaster set; 3=a worm gear; 4=belt system; 5=electric motor

Figure 4. Portable swine roaster

RESULTS AND DISCUSSION

The taste of the roast swine was similar to that of Trang-style roast pork, but the former had a richer herbal fragrance and a crispy skin commonly eaten with spicy sauce.

General Information

According to a survey conducted with eight families in Tha Kham, Sam Phran and Nakhon Prathom provinces, the families were able to earn up to USD170 daily from sale of roast swine. A selling place should be set up somewhere in the local market less than 30 km away from the manufacturing site. The retail-selling price of roast swine is around USD5.5 per kilogram, where 15 kg could be the weight of the swine after the roasting process. The average weight of the unprocessed swine is 25 kg and its cost is around USD37 per unit, as shown in Table 1.

Table 1
General Information About Roast-Swine Manufacturers

Specific Information	Average Value
Average income per family (USD)	170
Recommended daily selling period (hr)	6
Retail selling price per kilogram (USD)	5.5
Net weight after the roasting process (kg)	15
Net weight before the roasting process (kg)	25
Cost per unit (USD)	37

The manufacturing process takes about 3 to 4 hrs for each swine. The wine for slaughter should weigh around 20 to 25 kg. The swine's belly must be cut to remove its entrails. The belly is then filled with several types of herb such as lemongrass, kaffir lime leaves and banana leaves to replace the entrails that were removed. A swine holder, consisting of a long iron pipe is used to hold the swine longitudinally as it is roasted, as show in Figure 3. It is necessary that the swine be firmly placed on the iron pipe over the heated charcoal, which should not contain red flames that could cause the swine's skin to get burnt. Finally, while roasting, the operator must repeatedly turn the swine slowly to ensure that it is evenly and thoroughly cooked. A few drops of orange food colouring can be applied on the swine's skin to enhance the appearance of the product.

For this study, it was necessary to measure the size of 47 live swine with a focus on nose-to-tail length as well as pectoral and pelvic diameters (shown in Table 2). Swine of different sizes were categorised by the manufacturers.

Table 2
Sizes of Swine Prior to Roasting

Size (m)	Length (m)	Chest Diameter (m)	Hip Diameter (m)
Small	0.945 (0.780)*	0.244 (0.029)	0.273 (0.045)
Medium	1.090 (0.680)	0.307 (0.021)	0.351 (0.026)
Large	1.184 (0.120)	0.332 (0.023)	0.389 (0.034)

*Standard deviation of size

The researcher also measured the temperature of the heated charcoal at four positions: the front, back, left and right as well as the temperature of the roasting swine every 15 min for 3 hrs (shown in Table 3).

Table 3
Temperatures of Swine and Heated Charcoal Throughout the Roasting Period

Sample	Temperature (°C)											
	Min 15	Min 30	Min 45	Min 60	Min 75	Min 90	Min 105	Min 120	Min 135	Min 150	Min 165	Min 180
Swine	33.8 (3.9)*	70.0 (28.7)	127.5 (18.1)	149.1 (20.2)	161.3 (10.1)	164.7 (16.0)	168.7 (13.3)	167.8 (19.0)	169.7 (17.4)	162.4 (22.3)	158.0 (24.7)	156.1 (32.7)
Charcoal	45.5 (5.5)	57.3 (3.3)	66.3 (5.5)	85.0 (17.7)	376.5 (39.1)	611.8 (69.1)	652.5 (70.5)	681.0 (72.8)	695.5 (79.8)	679.6 (68.6)	657.8 (61.6)	643.4 (31.9)

*Standard deviation of temperatures

Roast-Swine Machine

The portable swine roaster consisted of a 9.5 mm (3/8 in.) metal sheet shaped into a half cylinder and a metal roasting set (Figure 4). The metal roasting set was able to support a 12.7-mm (1/2 in) stainless steel pipe with a length of 2 m and a 1.60×0.50×0.50 m³ roast. The roaster's height was 0.7 m above the ground and it was more convenient to operate than a traditional roaster. It also featured a worm-gear speed reducer (40:1) powered by a simple pulley-and-belt system as well as a 0.5 hp electric motor and two charcoal chambers installed on the front of the roaster. There were two ventilator adjusters and cinder outlets at the bottom of the charcoal chambers. Rollers were installed at both ends of the roaster to support the swine holder to ensure that the stainless steel pipe was rotating slowly throughout the roasting period.

The research continued with the roasting of three uncut swine with individual weights of no more than 40 kg as shown in Figure 5. The charcoal was heated in the charcoal chambers before the swine was firmly placed on the stainless steel pipe of the swine holder, where the

12.7-mm (1/2 in.) roller was installed on one side of the roaster. With the assistance of the 0.5 hp electric motor, no fat dropped on the heated charcoal or the smoke along the roasting platform.

Figure 4 shows the appropriate temperatures for different types of meat. Generally, pork requires up to 85°C for thorough cooking. According to the roasting results, the temperature of the swine meat (T_m), the swine skin (T_s) and the roaster (T_o) should increase consistently with the roasting time as it increases. For the swine, the temperature should increase heavily during the first roasting hour and drop after 2.5 hrs. The temperature seemed to stabilise after 2.5 hrs of roasting. Figure 7 records a high temperature of 100°C and 74°C for the swine skin and the swine meat, respectively. It took about 3.5 hrs to achieve equal temperature for the swine meat and the swine skin, while the temperature of the roaster was estimated to rise by three times higher than the temperature of the swine skin. This characteristic temperature is normal for a meat roaster (Teeboonma et al., 2006). However, at least 2 hrs is required to cook the swine thoroughly, as the meat can only maintain temperatures of up to 70°C. The movable roaster machine has the same the characteristic temperature as a traditional roaster, and this ensures that the crispiness and taste of the swine are similar. Fortunately, the manufacturer cooked the swine at a local market using the movable roaster machine.

Based on Table 4, 4.5 hrs were needed to roast the swine thoroughly using the movable roasting machine, during which the amount of charcoal required ranged from 14-18 kg., depending on the weight of the swine being roasted. In other words, 1 kg of charcoal was required to roast 1.46 kg of fresh swine to produce a roast of equal characteristics as traditional roast swine.

The advantages of using this roasting machine were that it allowed for a higher height, which is ergonomically better than the position required for the traditional method; a uniform roast was possible because of the continuous turning during roasting, and; the process was more hygienic as it avoided ash and dust from the burning charcoal.

The portable swine-roasting machine was delivered to manufacturers for their use, and many were satisfied with its easy-to-use operation. However, the roaster needs further development in terms of weight and heat delivery, for which a shorter roasting period and greater awareness of skin burning are also needed.



Figure 5. Roasting of swine



Figure 6. Levels of temperature suitable for cooking different types of meat

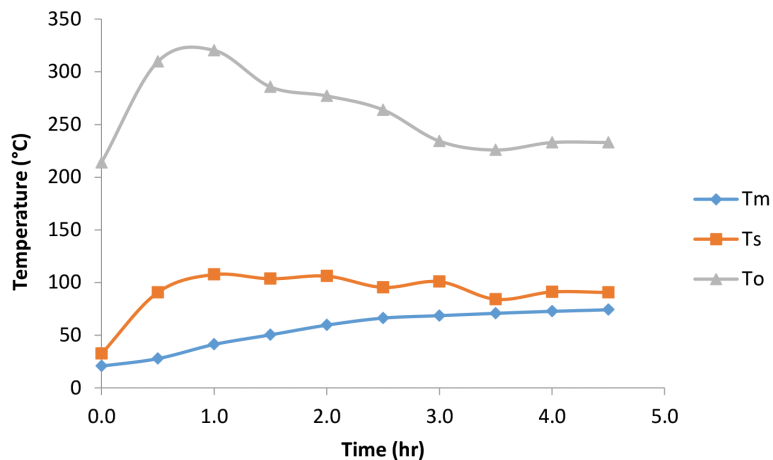


Figure 7. Relative temperature of swine meat (T_m), swine skin (T_s) and roaster (T_o)

Table 4
Results of Roast Swine on Machine

No.	Weight (kg)			Roasting period (hr.)	Amount of charcoal (kg)	Average temperature of roaster (°C)	Average temperature of swine (°C)	Fresh meat weight to charcoal* (kg:kg)
	Live swine	Before roasting	After roasting					
1	35.00	25.00	15.10	4.50	18.00	319.22	75.67	1.39
2	25.00	22.00	16.00	4.50	17.00	257.44	80.10	1.29
3	28.00	24.00	19.00	4.50	14.00	203.07	70.67	1.71
Average	29.33	23.67	16.70	4.50	16.33	259.91	75.48	1.46

*Weight ratio of fresh meat and required charcoal to cook the meat (kg:kg)

CONCLUSION

The goal of this research was to promote the invention of a movable swine machine developed to facilitate roasting at selling locations. According to a survey conducted among manufacturers and distributors of roast swine, they are able to earn up to USD170 in daily income from the sale of the meat. The average amount of roast swine is expected to be sold on a daily basis, where the retail-selling price is USD5.5 per kilogram. The process of manufacturing each roast swine takes about 3 to 4 hrs. First, a live swine weighing around 20 to 25 kg is slaughtered. Then its entrails are removed and replaced with several types of herb. Then the manufacturer uses a swine holder, which is a long iron pipe used for roasting swine that is slowly and repeatedly turned by hand. The swine is divided into three major size categories, including small (0.945 m, 0.244 m and 0.273 m), medium (1.090 m, 0.307 m and 0.351 m) and large (1.184 m, 0.332 m and 0.390 m). The average temperature of heated charcoal and the swine meat is 437°C and 135.5°C, respectively. The portable swine roaster is powered by a simple pulley-and-belt system and is powered by a 0.5 hp electric motor, and its metal roast set possesses a bearing to support a 12.7-mm (1/2 in.) stainless steel pipe with a length of 2 m and a 1.60×0.50×0.50 m³ roast. The amount of charcoal needed is 14 to 18 kg depending on the weight of the swine to be roasted, and the average temperature of the roaster is 260°C. The average weight ratio of the fresh pork and charcoal to cook the meat is around 1.46:1 kg. The roasted swine made with the movable roaster is the same as swine cooked with a traditional roaster that has less manpower and product mobility, thus making the roast swine more accessible to the public.

ACKNOWLEDGEMENT

This research was achieved by financial support from the National Research Council of Thailand and the Research and Development Institute, Suan Dusit University. We would like to express our thanks to the Sakon Nakhon Rajabhat University International Conference 2015 (SNRU-IC 2015) for help in preparation of documents, feedback, proof-reading and submission of this paper.

REFERENCES

- Anantathanachai, R. (2010). Thai cuisine healthy development based on sufficiency economy and community context. *SDU Research Journal Sciences and Technology*, 3(1), 59–74.
- Chu-iad, N. (2008). *Local wisdom on management and development of traditional processed meat products for commercial purpose, Kalasin province*. (Master's Thesis). Mahasarakham University.
- Kitthawee, U., Virayawat, N., & Phuhinkhon, V. (2013). Preliminary quality evaluation of local grilled-swine. *SDU Research Journal Sciences and Technology*, 6(1), 1–9.
- Paengteeresukkamai, P. (2011). *Development and construction of porker on fire machine semi-automatic*. (Research Report). Faculty of Engineering, Rajamangala University of Technology Phra Nakhon, Thailand.
- The Swine Raisers Association of Thailand. (2014, October-December 25-26). Production of 2014. *Magazine Pig* (In Thai).

Bunkrachang, N. and Kitthawee, U.

Teeboonma, U., Suwanakoot, T., & Soponronnarit, S. (2006). Beef drying using infrared radiation. *KKU Engineering Journal*, 33(2), 169–180.

Wessapan, T., & Borirak, T. (2014, January 16-17). Design and fabricate a continuous pork roaster using infrared heating. In *International Conference on Computer, Communications and Information Technology (CCIT 2014)*. Beijing, China.



Effect of inoculums content and screening of significant variables for simultaneous COD removal and H₂ production from tapioca wastewater using Plackett-Burman Design

Thanwised, P.

Program of Environmental Science, Faculty of Science and Technology, Sakon Nakhon Rajabhat University, 680 Nittayo Road, Mueang District, Sakon Nakhon, 47000, Thailand

ABSTRACT

The effect of four selected variables on Chemical Oxygen Demand (COD) removal and H₂ production by anaerobic mixed cultures from tapioca wastewater in batch mode (viz. ferrous sulphate (FeSO₄), initial pH, sodium bicarbonate (NaHCO₃) and nutrient solution with two inoculums (3,750 mgVSS/L and 7,500 mgVSS/L) were sought. Identification and screening of significant variables were conducted using the Plackett-Burman Design. An independent sample t-test was applied using 12 trials to evaluate inoculums content to determine the optimum level of the main variables and inoculum content at the steepest ascent. FeSO₄ and initial pH both had a statistically significant ($P < 0.05$) influence on COD removal and H₂ production. COD removal and H₂ production was greater at 7,500 mgVSS/L inoculums content than at 3,750 mgVSS/L ($P < 0.05$). An initial pH of 10 and FeSO₄ at 2.5 g/L yielded the maximum H₂ production potential (443.37 mL H₂/L) and COD removal (61.54 %).

Keywords: Initial pH, ferrous sulphate (FeSO₄), sodium bicarbonate (NaHCO₃), nutrient solution, Plackett-Burman Design, inoculums content

INTRODUCTION

The world is burning fossil fuels at an unprecedented rate, belching 34 billion tons of CO₂ into the atmosphere in 2011, accelerating global warming (Olivier, 2012). Biogas technology from fermentative hydrogen production (Kim & Kim, 2013) derived from animal waste (Sirirote et al., 2010), food production (Zhu et al., 2011), cassava detoxification (Wang et al., 2012) and corn processing (Cheng et al., 2012) is an alternative source of energy. It has a high heating value of 142 KJ/g and does not release greenhouse gasses during combustion (Singh et al., 2013).

Fermentative hydrogen production is influenced by many factors such as inoculum, substrate, alkalinity, reactor type, organic

Article history:

Received: 13 May 2016

Accepted: 22 November 2016

E-mail address:

thanwised56@gmail.com (Thanwised, P.)

loading rate, pH and temperature (Mohammadi et al., 2012). When microorganisms degrade, organic substrates electrons (COD removal), which need to be disposed of to maintain electrical neutrality, are produced. Tapioca is grown in almost every tropical country; its biodegradable starch is an important source of carbohydrates for livestock (Blagbrough, Bayoumi, Rowan, & Beeching, 2010). The tapioca starch-processing industry in Thailand is the world's largest (DAO, 2015). Tapioca's highly organic wastewater is an effective substrate for H₂ production through dark fermentation (Chavalparit & Ongwandee, 2009; Show, Lee, Tay, Lin, & Chang, 2012).

Iron is an important nutrient element needed to form hydrogenase and other enzymes, and a small additional amount of FeSO₄ at high cell concentration is sufficient to enhance H₂ production (Sinha & Pandey, 2011). NaHCO₃ can maintain pH at a favourable range for hydrogenesis (Li, Jiang, Xu, & Zhang, 2008; Mohammadi, Ibrahim, & Mohamad Annuar, 2012). The Plackett-Burman experimental design has had the greatest impact on screening variables (Kevin & Dennis, 2015). The lack of information on tapioca wastewater vis-à-vis H₂ production required us to statistically screen for significant variables for simultaneous COD removal and H₂ production.

The main objectives of the current study were to assess the effect of (a) iron (II) sulphate (FeSO₄); (b) initial pH; (c) sodium bicarbonate (NaHCO₃); and (d) nutrient amendments on COD removal and H₂ production efficiency using tapioca wastewater as the substrate with the Plackett-Burman Design. Low (3,750 mgVSS/L) and high (7,500 mgVSS/L high) inocula content was assessed for its effect on COD removal and H₂ production.

MATERIALS AND METHOD

Seed Mixed Culture Inoculum

Anaerobic seed sludge was collected from a tapioca starch factory's full-scale, up-flow anaerobic sludge blanket (UASB) reactor. The factory was in Kalasin Province, Thailand. Normally, this UASB produces methane. To inactivate methanogenic microbes, the sludge was heated to 105°C for 2 hr, after which it was cooled in a desiccator at room temperature. Inoculum preparation followed the method of Thanwiset, Wirojanagud and Reungsang (2012).

Tapioca Wastewater

In the current study, tapioca wastewater was obtained from the tapioca factory as recommended by Thanwiset, Wirojanagud and Reungsang (2012). It was immediately transferred to the laboratory and stored at 4°C until needed. The characteristics of the tapioca wastewater was as follows: pH 4.58±0.29, COD 9,277±414 mg/L, BOD₅ 5,800±256 mg/L, TS 13,430±1018 mg/L and TSS 1,524±581 mg/L.

Biohydrogen Production and COD Removal

A working volume of 70 mL in 120 mL serum bottles was used for the H₂-production experiment. The H₂ production medium contained a respective 3,750 mgVSS/L and 7,500 mgVSS/L of inoculum. Different concentrations of FeSO₄, NaHCO₃ and nutrient amendments were added and the initial pH adjusted according to the experimental design.

Analytical Methods

Biogas composition was measured via gas chromatograph (GC-2014, Shimadzu) as per Thanwised, Wirojanagud and Reungsang (2012). Standard methods (APHA, 21st Ed., 2005) were used for measuring COD and hydrogen gas production calculated as per Zheng and Yu (2005).

Kinetic Modelling

A modified Gompertz Eq. [1] was used as per Zheng and Yu (2005):

$$H(t) = P \exp\{-\exp[(R_m e/P)(\lambda-t)+1]\} \quad [1]$$

where, H represented the cumulative volume of hydrogen produced (mL); P_s the hydrogen production potential (mL); R_m the maximum production rate (mL/h); λ the lag-phase time (h); t the incubation time (h), and; e equalled 2.718281828.

Screening and Identifying Procedure

The current study used the Plackett–Burman Design to identify and screen for significant variables vis-à-vis COD removal and H₂ production by mixed cultures in tapioca wastewater. The parameters investigated included nutrient addition, initial pH, FeSO₄ and NaHCO₃ concentration. Composition of nutrient solution modified from Lin and Lay (2004) as recommended by Thanwised, Wirojanagud and Reungsang (2012). The Plackett-Burman experimental design based on the first-order model followed Plackett and Burman (1946) Eq. 2:

$$Y = \beta_0 + \sum \beta_i X_i \quad [2]$$

where, Y was the response (hydrogen production); β₀ the model intercept; β_i the linear coefficient, and; x_i the level of the independent variable. The initial pH (X₁), nutrient addition (X₂), iron (II) sulphate (FeSO₄) (X₃) and sodium bicarbonate (NaHCO₃) (X₄) were examined to determine if they had any effect on hydrogen production and/or COD removal. Based on the Plackett–Burman Design, each factor was prepared in two levels: -1 for low levels and +1 for high levels (Table 1). A centre point was run to evaluate the linear and curvature effects of the variables (Plackett & Burman, 1946). In the present study, four assigned variables were screened in 12 experimental runs in addition to three runs at their centre points. Hydrogen production was carried out in triplicate and the average value was used to represent the response. The factors significant at the 95% level (P<0.05) were considered to have a significant effect on hydrogen production and COD removal.

Table 1
Regression Coefficient, Estimated Effect and Corresponding F and P Values

Table 1A
H₂ Production

Code	Variable	Unit	Low Level (-1)	High Level (+1)	Coefficient		Effect (E _{xi})		F-value		P-value Prob>F	
					Low	High	Low	High	Low	High	Low	High
X ₁	Initial pH	-	5	7	39.64	49.42	79.28	98.83	13.17	15.9979	0.0084	0.0052
X ₂	Nutrient	ml/L	1	10	-11.32	-17.44	-22.63	-34.89	1.07	1.9937	0.3346	0.2008
X ₃	FeSO ₄	g/L	0.5	1	17.94	27.48	35.88	54.96	2.70	4.9478	0.1445	0.0615
X ₄	NaHCO ₃	g/L	1	5	-4.51	-4.40	-9.01	-8.79	0.17	0.1267	0.6923	0.7324

Table 1B
COD Removal

Code	Variable	Unit	Low Level (-1)	High Level (+1)	Coefficient		Effect (E _{xi})		F-value		P-value Prob>F	
					Low	High	Low	High	Low	High	Low	High
X ₁	Initial pH	-	5	7	2.78	2.68	5.56	5.37	15.49	13.8836	0.0056	0.0074
X ₂	Nutrient	ml/L	1	10	-0.67	-0.40	-1.34	-0.79	0.89	0.3025	0.3758	0.5994
X ₃	FeSO ₄	g/L	0.5	1	2.24	1.33	4.48	2.66	10.05	3.4146	0.0157	0.1071
X ₄	NaHCO ₃	g/L	1	5	-1.29	-0.92	-2.59	-1.83	3.35	1.6146	0.1099	0.2444

Note. Low = low inoculum = 3,750 mg-VSS/L and High = high inoculum = 7,500 mg-VSS/L

The effect of each variable was determined as per Eq. [3] and a tool for statistical analysis by Saraphirom and Reungsang (2010):

$$E_{(X_i)} = 2(\Sigma M_{i+} - M_{i-})/N \tag{3}$$

where, E_{X_i} was the concentration effect of the tested variable; M_{i+} and M_{i-} were P_s from runs where the variable (X_i) measured was present at the high and low concentration, respectively, and; N was the number of runs (12).

Comparison of Inoculums Content

SPSS version 22 was used to calculate the independent samples t-test for 12 trials so as to evaluate the varying significance levels of inoculums content on COD removal and H₂ production (Table 2).

Table 2
Observed and Predicted H₂ Production and COD Removal

Run	X ₁	X ₂	X ₃	X ₄	H ₂ Production (mL H ₂ /L)			COD removal (%)			
#	Initial pH	Nutrient	FeSO ₄	NaHCO ₃	Low inoculum		High inoculum	Low inoculum		High inoculum	
	(ml/L)	(g/L)	(g/L)	(g/L)	Observed	Predicted	Observed	Observed	Predicted	Observed	Predicted
1	7	1	0.5	1	241.35±1.71	191.94±2.07	351.06±1.57	50.00±0.62	48.84±0.59	53.88±0.35	53.21±0.33
2	5	10	0.5	5	113.14±1.11	81.02±1.13	201.01±1.34	40.87±0.81	39.36±0.79	46.83±0.85	45.21±0.83
3	7	10	0.5	5	126.19±1.18	160.30±1.22	230.70±0.78	43.64±0.68	44.92±0.65	50.00±0.31	50.58±0.28
4	5	1	0.5	1	88.50±0.84	112.66±0.82	171.75±0.90	40.79±0.33	43.28±0.43	45.30±0.33	47.84±0.43
5	7	1	1.0	5	181.63±1.29	218.81±1.36	311.35±1.06	46.83±0.19	50.73±0.16	50.00±0.12	54.04±0.27
6	7	10	1.0	1	205.70±0.02	205.19±0.02	334.61±0.45	51.85±0.07	51.98±0.06	55.56±0.25	55.08±0.23
7	5	10	1.0	1	147.99±0.76	125.91±0.74	253.09±0.98	46.34±0.04	46.42±0.04	49.59±0.06	49.71±0.06
8	5	1	1.0	1	121.26±0.94	148.54±0.94	229.75±0.80	48.78±0.55	47.76±0.52	52.03±0.80	50.50±0.78
9	5	10	1.0	5	116.85±0.00	116.90±0.00	189.81±0.69	43.29±0.29	43.84±0.27	46.51±0.72	47.88±0.69
10	5	1	0.5	5	100.94±0.09	103.65±0.09	194.47±0.07	41.27±0.31	40.69±0.29	46.88±0.46	46.01±0.43
11	7	10	0.5	1	148.75±0.71	169.31±0.68	222.49±1.30	48.02±0.27	47.50±0.26	52.38±0.02	52.41±0.02
12	7	1	1.0	5	260.73±1.45	218.81±1.61	382.66±1.12	54.37±0.95	50.73±0.66	57.54±0.84	54.04±0.36
Determination coefficient (R²)					0.97	0.96	0.96	0.98	0.98	0.98	0.98
Adjusted determination coefficient (Adjusted R²)					0.95	0.96	0.96	0.97	0.97	0.97	0.97

Note. Low inoculum = 3,750 mg-VSS/L and high inoculum = 7,500 mg-VSS/L

Path of Steepest Ascent

This step was used to determine the optimum level for the main variable. In the current study, this was done by increasing the initial pH (from 1 to 11) and FeSO₄ concentrations (from 1.0 to 3.0 g/L) based on the high level (as per positive signs, Table 1) for improving COD removal and H₂ production potential.

RESULTS AND DISCUSSION

Diagnostic Checking of the Fitted Model

The multiple regression analysis was applied to the data in Table 2 and the attained second-order polynomial equation could well explain the COD removal and hydrogen production as per Eq. [4] to [7]:

$$Y_1 = 50.54 + 2.68 X_1 - 0.40 X_2 + 1.33 X_3 - 0.92X_4 \quad [4]$$

$$Y_2 = 46.34 + 2.78X_1 - 0.67X_2 + 2.24X_3 - 1.29X_4 \quad [5]$$

$$Y_3 = 256.06 + 49.42 X_1 - 17.44 X_2 + 27.48 X_3 - 4.40 X_4 \quad [6]$$

$$Y_4 = +154.42 + 39.64 X_1 - 11.32 X_2 + 17.94 X_3 - 4.51 X_4 \quad [7]$$

where, Y_1 and Y_2 were the predicted COD removal; Y_3 and Y_4 were the predicted H₂ production of high and low inocula content, and; X_1 , X_2 , X_3 and X_4 were the coded values of initial pH, nutrient, FeSO₄ and NaHCO₃, respectively.

The R^2 value of 0.97, 0.96 and 0.98 (Table 2) indicated good agreement between the experimental and predicted values and implied that the mathematical model predicted the hydrogen production rate (Saraphirom & Reungsang, 2010; Zhang, Liu, & Shen, 2005), while a high value of the adjusted determination coefficient of 0.95, 0.96 and 0.97 suggested the significance of the model (Saraphirom & Reungsang, 2010).

Effect of Main Variables on COD Removal and H₂ Production

The P -value (Table 1) indicated the relative importance of the initial pH, nutrient addition, FeSO₄ and NaHCO₃ concentration on COD removal and H₂ production. The P -value of the initial pH (both low and high inoculums content) was less than 0.05 ($P < 0.05$) (Table 1A); this means that initial pH had a significant effect on H₂ production. This was not surprising since pH is the most important factor in hydrogen production due to its effects on Fe-hydrogenase activity, metabolic pathways and the duration of the lag phase (Liu & Shen, 2004).

Table 1B shows that a *P*-value for both the initial pH and FeSO₄ was less than 0.05 ($P < 0.05$), indicating that both variables had a significant effect on COD removal. The effect sign was positive, meaning that the influence of initial pH and FeSO₄ on COD removal and H₂ production was greater at the high level. Iron is an important factor for biohydrogen production (Saraphirom & Reungsang, 2010; Zhang, Liu, & Shen, 2005), as microorganisms degrade organic substrates for energy (electrons) (i.e. COD removal), which need to be disposed of in order to maintain electrical neutrality. In anoxic environments, protons can act as electron acceptors to produce molecular H₂ in the presence of hydrogenase enzyme. These two variables were therefore selected for the next path of steepest ascent. Observed and predicted H₂-production and COD removal is recorded in Table 2.

Comparative of Inocula Content

Both COD removal and H₂ production at high inoculums content were greater than at low inoculums content ($P=0.022$ and 0.001 , respectively) (Table 3). Hence, a higher inoculums content was seen to have provided greater microbial activity, leading to increased COD removal and H₂ production. Previous research demonstrated substantially improved performance and stability of an anaerobic reactor by inoculums (O-Thong, Prasertsan, Intrasingkha, Dhamwichukorn, & Birkeland, 2008; Zheng & Yu, 2005). The next steepest ascent experiment should inoculate at 7,500 mgVSS/L. The COD content at low vs. high inoculums content is presented in Figure 1. The respective COD for low vs. high inoculums content was decreased from the initial $9,277 \pm 414$ mg/L to $4,968 \pm 332$ mg/L and $4,670 \pm 434$ mg/L after 120 hours.

Table 3
Independent-Sample t-Test for H₂ Production and COD Removal

Parameter	Inoculum	Mean	Standard Deviation	Sig. (2-tailed)
H ₂ Production (mL H ₂ /L)	Low	154.42	6.02	0.001
	High	256.06	7.76	
COD _{removal} (%)	Low	46.34	4.47	0.022
	High	50.54	3.85	

Note. Low inoculum = 3,750 mg-VSS/L and high inoculum = 7,500 mg-VSS/L

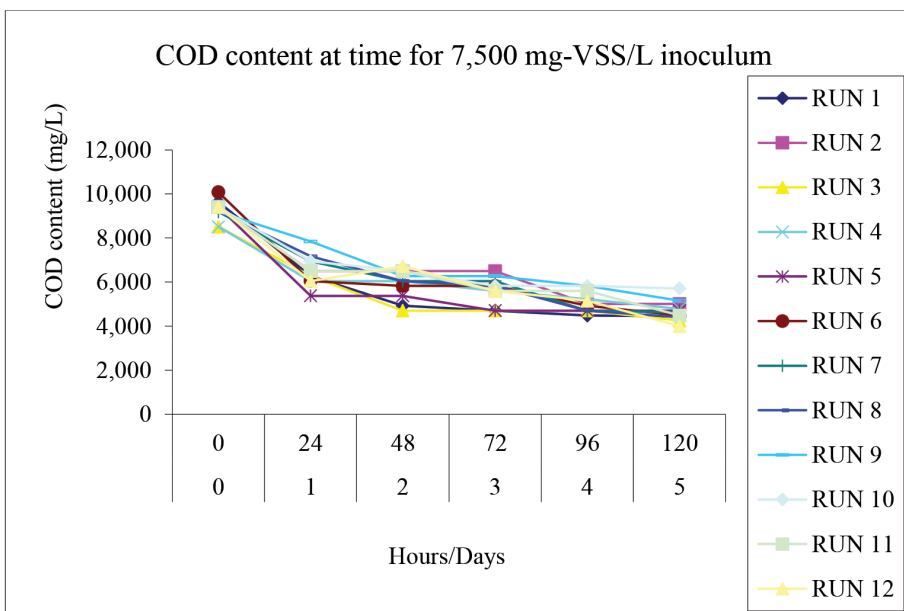
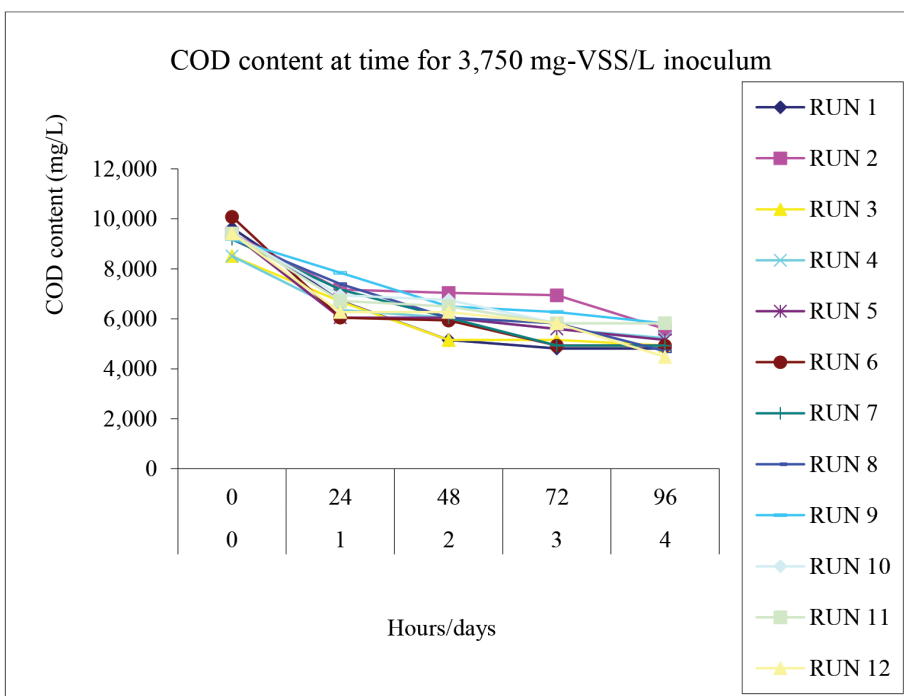


Figure 1. COD content at low and high inoculums content

The Path of Steepest Ascent

The results indicated that Run 4, with an initial pH of 10 and FeSO₄ of 2.5 g/L (Table 4), yielded the greatest H₂ production potential (443.37 mL H₂/L) and COD removal (61.54 %). A higher hydrogen production rate occurred at a higher initial pH because the latter was sufficient to rapidly buffer the acid production accompanying hydrogen production so that hydrogen production was not inhibited (Li et al., 2008). The *in vivo* activity of hydrogenase in fermentative bacteria was found to decrease with a reduction in Fe. Hydrogen was evolved as the final product of reductant disposal from hydrogenase or nitrogenase activity in which the primary electron donor for both enzymes was ferredoxin (Saraphirom & Reungsang, 2010).

Table 4
H₂ Production and Percentage of COD Removal at Steepest Ascent

Trials	Initial pH	FeSO ₄ (g/L)	P _{s1} (mL H ₂ /L)	P _{s2} (% COD removal)
1	7	1.0	119.09	38.46
2	8	1.5	128.00	42.86
3	9	2.0	258.03	50.00
4	10	2.5	443.37	61.54
5	11	3	47.25	16.67

CONCLUSION

Two significant variables affecting COD removal and H₂ production by anaerobic mixed cultures from tapioca wastewater (i.e. FeSO₄ and initial pH) were selected through experiments using the Plackett-Bruman Design. COD removal and H₂ production of 7,500 mgVSS/L inoculums content were significantly greater than 3,750 mgVSS/L ($P < 0.05$). An initial pH of 10 and FeSO₄ concentration of 2.5 g/L resulted in the maximum H₂ production potential (443.37 mL H₂/L) and COD removal (61.54 %). The next optimisation of COD removal and H₂ production by anaerobic mixed cultures from tapioca wastewater should use FeSO₄ and initial pH variables with 7,500 mgVSS/L inoculums content.

ACKNOWLEDGEMENT

The author thanks (a) Sakon Nakhon Rajabhat University, Thailand, for its support; (b) Associate Professor Dr. Wanpen Virojanagud and Professor Dr. Alissara Reungsang from Khon Kaen University, Thailand for their guidance; (c) the Sakon Nakhon Rajabhat University International Conference 2015 (SNRU-IC 2015), and; (d) Mr. Bryan Roderick Hamman for assistance with the proofreading of the manuscript.

REFERENCES

- APHA. (2005). *Standard methods for examination of water and wastewater* (21st Ed.). Washington, DC: American Public Health Association.
- Blagbrough, I. S., Bayoumi, S. A. L., Rowan, M. G., & Beeching, J. R. (2010). Cassava: An appraisal of its phytochemistry and its biotechnological prospects. *Phytochemistry*, *71*(17), 1940–1951.
- Chavalparit, O., & Ongwandee, M. (2009). Clean technology for the tapioca starch industry in Thailand. *Journal of Cleaner Production*, *17*(2), 105–110.
- Cheng, X. Y., Li, Q., & Liu, C. Z. (2012). Coproduction of hydrogen and methane via anaerobic fermentation of cornstalk waste in continuous stirred tank reactor integrated with up-flow anaerobic sludge bed. *Bioresource Technology Journal*, *114*, 327–333.
- DOA. (2015). Database of agriculture: Starch. *Thailand Department of Agriculture, Ministry of Agriculture and Cooperatives*. Retrieved from http://www.doa.go.th/data-doa/starch/stat/st0_4.htm.
- Kim, D. H., & Kim, M. S. (2013). Development of a novel three-stage fermentation system converting food waste to hydrogen and methane. *Bioresource Technology Journal*, *127*, 267–274.
- Li, Y. Q., Jiang, H. X., Xu, Y. Q., & Zhang, X. H. (2008). Optimization of nutrient components for enhanced phenazine-1-carboxylic acid production by *gac A* inactivated *Pseudomonas sp.* M18G using response surface method. *Applied Microbiology and Biotechnology*, *77*(6), 1207–1217.
- Li, Z., Wang, H., Tang, Z., Wang, X., & Bai, J. (2008). Effects of pH value and substrate concentration on hydrogen production from the anaerobic fermentation of glucose. *International Journal of Hydrogen Energy*, *33*(24), 7413–7418.
- Lin, C. Y., & Lay, C. H. (2004). A nutrient formulation for fermentative hydrogen production using anaerobic sewage sludge microflora. *International Journal of Hydrogen Energy*, *30*(3), 285–292.
- Liu, G. Z., & Shen, J. Q. (2004). Effects of culture and medium conditions on hydrogen production from starch using anaerobic bacteria. *Journal of Bioscience and Bioengineering*, *98*(4), 251–256.
- Mohammadi, P., Ibrahim, S., & Annuar, M. S. M. (2012). Effects of biomass, COD and bicarbonate concentrations on fermentative hydrogen production from POME by granulated sludge in a batch culture. *International Journal of Hydrogen Energy*, *37*(23), 17801–17808.
- Olivier, J. G. (2012). *Trends in global CO₂ emissions: 2012 report* (p. 40). Hague: PBL Netherlands Environmental Assessment Agency.
- Owen, W. F., Stuckey, D. C., Healy Jr., J. B., Young, L. Y., & McCarty, P. L. (1979). Bioassay for monitoring biochemical methane potential and anaerobic toxicity. *Water Research*, *13*(6), 485–493.
- Plackett, R. L., & Burman, J. P. (1946). The design of optimum multifactorial experiments. *Biometrika*, *33*(4), 305–325.
- Quinlan, K. R., & Lin, D. K. (2015). Run order considerations for Plackett and Burman designs. *Journal of Statistical Planning and Inference*, *165*, 56–62.
- Saraphirom, P., & Reungsang, A. (2010). Optimization of biohydrogen production from sweet sorghum syrup using statistical methods. *International Journal of Hydrogen Energy*, *35*(24), 13435–13444.
- Show, K. Y., Lee, D. J., Tay, J. H., Lin, C. Y., & Chang, J. S. (2012). Biohydrogen production: Current perspectives and the way forward. *International Journal of Hydrogen Energy*, *37*(20), 15616–15631.

- Singh, L., Wahid, Z. A., Siddiqui, M. F., Ahmad, A., Rahim, M. H. A., & Sakinah, M. (2013). Biohydrogen production from palm oil mill effluent using immobilized *Clostridium butyricum* EB6 in polyethylene glycol. *Process Biochemistry Journal*, 48(2), 294–8.
- Sinha, P., & Pandey, A. (2011). An evaluative report and challenges for fermentative biohydrogen production. *International Journal of Hydrogen Energy*, 36(13), 7460–7478.
- Sirirote, P., Thanaboripat, D., Klinkroon, N., & Tripak, S. (2010). The production of biogas from cassava tubers. *KMITL Science and Technology Journal*, 10(1), 30–36.
- Sompong, O., Prasertsan, P., Intrasungkha, N., Dhamwichukorn, S., & Birkeland, N. K. (2008). Optimization of simultaneous thermophilic fermentative hydrogen production and COD reduction from palm oil mill effluent by Thermoanaerobacterium-rich sludge. *International Journal of Hydrogen Energy*, 33(4), 1221–1231.
- Tchobanoglous, G., Burton, F. L., & Stensel, H. D. (2003). *Inc.: Waste water engineering: Treatment and reuse* (4th Ed.). New York: McGraw-Hill.
- Thanwiset, P., Wirojanagud, W., & Reungsang, A. (2012). Effect of hydraulic retention time on hydrogen production and chemical oxygen demand removal from tapioca wastewater using anaerobic mixed cultures in anaerobic baffled reactor (ABR). *International Journal of Hydrogen Energy*, 37(20), 15503–15510.
- Wang, W., Xie, L., Luo, G., Zhou, Q., & Lu, Q. (2012). Optimization of biohydrogen and methane recovery within a cassava ethanol wastewater/waste integrated management system. *Bioresource Technology Journal*, 120, 165–172.
- Zhang, Y. F., Liu, G. Z., & Shen, J. Q. (2005). Hydrogen production in batch culture of mixed bacteria with sucrose under different iron concentrations. *International Journal of Hydrogen Energy*, 30(8), 855–860.
- Zheng, X. J., & Yu, H. Q. (2005). Inhibitory effects of butyrate on biological hydrogen production with mixed anaerobic cultures. *Journal of Environmental Management*, 74(1), 65–70.
- Zhu, H., Parker, W., Conidi, D., Basnar, R., & Seto, P. (2011). Eliminating methanogenic activity in hydrogen reactor to improve biogas production in a two-stage anaerobic digestion process co-digesting municipal food waste and sewage sludge. *Bioresource Technology Journal*, 201(14), 7086–7092.
- Zhu, Y., & Yang, S. T. (2004). Effect of pH on metabolic pathway shift in fermentation of xylose by *Clostridium tyrobutyricum*. *Journal of Biotechnology*, 110(2), 143–157.



Comparison of Scoring Functions on Greedy Search Bayesian Network Learning Algorithms

ChongYong, Chua* and HongChoon, Ong

School of Mathematical Sciences, Universiti Sains Malaysia, 11800 USM, Penang, Malaysia

ABSTRACT

Score-based structure learning algorithm is commonly used in learning the Bayesian Network. Other than searching strategy, scoring functions play a vital role in these algorithms. Many studies proposed various types of scoring functions with different characteristics. In this study, we compare the performances of five scoring functions: Bayesian Dirichlet equivalent-likelihood (BDe) score (equivalent sample size, ESS of 4 and 10), Akaike Information Criterion (AIC) score, Bayesian Information Criterion (BIC) score and K2 score. Instead of just comparing networks with different scores, we included different learning algorithms to study the relationship between score functions and greedy search learning algorithms. Structural hamming distance is used to measure the difference between networks obtained and the true network. The results are divided into two sections where the first section studies the differences between data with different number of variables and the second section studies the differences between data with different sample sizes. In general, the BIC score performs well and consistently for most data while the BDe score with an equivalent sample size of 4 performs better for data with bigger sample sizes.

Keywords: Bayesian network, greedy search, heuristic search, score-based, scoring function, structure learning

INTRODUCTION

Since its introduction by Pearl (1985), the Bayesian Network (BN) has had a huge impact on data mining as one of the best mining tools. Numerous studies have been done on learning BN in the last few decades. Constraint-based and score-based algorithms are two major classes of BN structural learning algorithms while hybrid-based algorithms that combined

both is later introduced. Despite advantages and disadvantages of each algorithm, score-based algorithms, especially the greedy search type algorithm that constantly looks for the most improvement in each iteration, are used frequently due to its simplicity and

Article history:

Received: 11 July 2016

Accepted: 5 December 2016

E-mail addresses:

cychua91@hotmail.com (ChongYong, Chua),

hcong@usm.my (HongChoon, Ong)

*Corresponding Author

effectiveness. With score-based algorithms such as Hill Climbing (Daly & Shen, 2007) and K2 algorithm (Cooper & Herskovits, 1992), a scoring function is chosen to calculate the joint probability distribution using a BN structure from its corresponding database, and then a network searching approach is used to maximise this function. To this end, most score-based algorithm research is done on improving the search phase but scoring functions play a vital role as well. A good search approach can help to sidestep local maxima while a good scoring function can decide which network is closer to the true network. In real world applications, a network with a higher score does not always imply a good output. Instead, a network that can define the true causal relationship of the problem studied is a better output.

Scoring functions are usually derived from basic assumptions on the network parameter distribution. Based on multinomial sampling and dirichlet distribution assumptions, Heckerman et al. (1995) proposed the BD score and further improved it to the BDe score after including the likelihood equivalence assumption. Cooper and Herskovits (1992) introduced the K2 score, which is a particular case of BD score in their K2 algorithm paper. In other cases without the assumption of distribution, log-likelihood score is one of the established scores available. However, it does not represent a good score in BN learning as it leads to overfitting due to its tendency of favouring a complete network. To limit the overfitting problem, AIC score (Akaike, 1974) and BIC score (Schwarz, 1978) are proposed by introducing a penalising term in the log-likelihood score function.

In most cases, improvement of BN structural learning is done independently for searching mechanism and scoring functions. However, there is a relationship between searching mechanism and scoring functions. Each scoring function has its own characteristics and advantages that fit into certain learning algorithms. In this study, we were interested in identifying which scoring function worked better for a greedy search type algorithm. The rest of this paper is organised as follows. Section 2 introduces some preliminary concepts, assumptions and notations of Bayesian networks and scoring functions used. This is followed by Section 3, which shows the results of our experiment and discusses the results, and lastly, Section 4 consists of the conclusion.

MATERIALS AND METHODS

Bayesian Network

BN, also known as Bayesian Belief Network (BBN), is a powerful data mining tool for reasoning under uncertainty (Heckerman, 1996). BN is a directed acyclic graph (DAG) that consists of two parts $G = \langle S, \Theta \rangle$. For a set of variables $X = \{X_1, X_2, \dots, X_n\}$ from data D , a network structure, S , is a set of arcs connecting nodes or variable X , which indicates that there exists a dependent relationship between the nodes. Θ is the conditional probability associated with each variable. Suppose that X_i denotes a variable and its corresponding node, π_i is the parent of each node X_i in S as well as the variable corresponding to the parents. Given the structure S , the joint probability distribution for X is given by:

$$f(X) = \prod_{i=1}^n f(X_i | \pi_i) \quad [1]$$

BN is then constructed based on the conditional independence concept, which is defined below:

Definition 1 (Conditional Independence)

Two variables X_1 and X_2 are conditionally independent given if the variable X_3

$$f(X_1 | X_3) = f(X_1 | X_2, X_3) \quad [2]$$

Bayesian Network Structural Learning

Structural learning in BN refers to selecting the structure that most accurately defines the causal relationships between variables from a set of structure candidates. Typically, a structural learning algorithm can be separated into three major categories, which are constraint-based, score-based and hybrid-based. The constraint-based structural learning algorithm learns the network structure by analysing the probabilistic relations entailed by the Markov property of BN with a conditional independence test and then constructs a graph that satisfies the corresponding d-separation statement (Scutari, 2010). A few common conditional independence tests used for constraint-based algorithms are mutual information (Kullback, 1959) and Pearson's χ^2 (Spirtes et al., 1993). These tests are able to determine the existence of an edge between two nodes based on the conditional independence property as defined in Definition 1. A constraint-based algorithm begins with learning the skeleton of the network that is a completely undirected network. Most of the learning algorithms restrict the search to the Markov blanket of each node (including the parents, the children and the parents of the children of that particular node). The next step is to set the direction of the arcs that are a part of the v-structure (a triplet of nodes incident on a converging connection $X_j \rightarrow X_i \leftarrow X_k$). Lastly, direction of other arcs will be set to satisfy the acyclicity constraint (Neapolitan, 2004). The Incremental Association Markov Blanket by Tsamardinos et al. (2003) and PC algorithm by Spirtes and Glymour (1991) are among the well-established and most applied constraint-based algorithms.

On the other hand, the score-based algorithm works differently from the constraint-based algorithm. This algorithm is a type of maximisation problem that assigns a score to each network structure candidate and tries to maximise it with a certain heuristic search algorithm. Hill-climbing and Tabu search (Glover & Laguna, 1993) are known as greedy search algorithms while the Genetic algorithm (Goldberg, 1989) and Particle Swarm Optimisation (Kennedy & Eberhart, 1995) are examples of metaheuristic algorithms. Greedy search algorithms always opt for the best improvement of each iteration, which is referred to as the greedy property while metaheuristic algorithms explore the search space with simple or complex procedures inspired by natural phenomena. The score of a network structure is a guideline or criterion used to measure the fitness of the structure to prior knowledge and data. A score-based algorithm begins with an empty or a random structure and modifies the structure afterwards. Some transition functions such as adding arcs, deleting arcs or reversing arcs will be applied to the network structure to improve the structure's score. The iteration stops when the score converges at one point. However, one of the disadvantages of score-based algorithms is the iteration might be stuck at the local maxima and not return an optimum solution.

The hybrid-based algorithm is a combination of both score-based and constraint-based algorithms. It begins with constructing a skeleton or partially directed DAG (PDAG) using a conditional independence test. It then continues with performing a constrained score-based algorithm on the network obtained in the previous stage. MMHC (Tsamardinos et al., 2006) and H2PC (Gasse et al., 2014) are examples of hybrid-based algorithms. Despite the existence of various learning algorithms, score-based algorithms are frequently used in real-life applications compared to other methods. Constraint-based algorithms are efficient and faster especially when the data consist of a large number of variables, but it is strongly dependent on sample size of the data, where the results of conditional independence tests used are not entirely reliable with finite data (Fast, 2010). This weakness is crucial as most real-life data are limited and even incomplete. Although score-based algorithms suffer from limited data as well, the impact is not as significant as constraint-based algorithms. Hybrid-based algorithms on the other hand are not well established yet and have limited a choice of algorithms compared to the previous two types of algorithm. Hence, we are interested in improving score-based algorithms by reviewing existing scoring functions and their relationship with learning algorithms, specifically, greedy search algorithms.

Data Assumptions

The following are a few assumptions about the data considered in this study.

- I. All variables X_i , $i = 1, 2, \dots, n$ are discrete and observable and X_i has r_i possible values.
- II. All data are complete i.e. all instances have values for all variables that have no missing data. There are no latent variables in the database.
- III. All cases occur independently given a Bayesian network model.

Scoring Functions

Bayesian Dirichlet likelihood-equivalence (BDe). As an extension of the the Bayesian Dirichlet score, the BDe score included two more assumptions:

Assumption 1: Likelihood equivalence

Given two directed acyclic graphs, G and G' , such that $P(G) > 0$ and $P(G') > 0$, if G and G' are equivalent then $P(\Theta|G) = P(\Theta|G')$.

Assumption 2: Complete structural possibility

For any complete directed acyclic graph G , we have $P(G) > 0$.

The BDe score with equivalent sample size, , can be expressed (Heckerman et al., 1995) as:

$$P(G, D) = P(G) \times \prod_{i=1}^n \prod_{j=1}^{q_i} \left(\frac{\Gamma(N'_{ij})}{\Gamma(N_{ij} + N'_{ij})} \times \prod_{k=1}^{r_i} \frac{\Gamma(N_{ijk} + N'_{ijk})}{\Gamma(N'_{ijk})} \right) \quad [3]$$

where N_{ijk} denotes the number of instances in the database D where the variable x_i assigned its k th value ($k = 1, 2, \dots, r_i$), and its parent π_i assigned its j th value ($j = 1, 2, \dots, q_i$), $N_{ij} = \sum_{k=1}^{r_i} N_{ijk}$, $N'_{ijk} = N' \times P(X_i = x_{ik}, \Pi_{X_i} = w_{ij}|G)$ and $N'_{ij} = \sum_{k=1}^{r_i} N'_{ijk}$.

Akaike Information Criterion (AIC) & Bayesian Information Criterion (BIC). Log-likelihood (LL) score in BN is a measure of likelihood in log form between the network and data parameter. The LL score is written as:

$$LL(G|D) = \sum_{i=1}^n \sum_{j=1}^{q_i} \sum_{k=1}^{r_i} N_{ijk} \log\left(\frac{N_{ijk}}{N_{ij}}\right) \quad [4]$$

The LL score has decomposable property, where the score is the summation of conditional probability of each node given their parent sets. It also assumes likelihood equivalence assumption as explained in Assumption 1. Due to its likelihood equivalence and decomposable property, the LL score is computational efficient when used in structure learning. However, the LL score is not commonly used in BN structure learning as it tends to favour a complete network. When used in a structural learning algorithm, it tends to generate a fully connected DAG, causing overfitting problem. In order to eliminate overfitting problem, a penalised term is introduced to limit the number of arcs in the final network. A general penalised LL score, PLL, is shown as follows:

$$PLL(G|D) = LL(G|D) - f(N)|G| \quad [5]$$

where, $|G| = \sum_{i=1}^n (r_i - 1)q_i$ denotes network complexity, which is the number of parameters in Θ for the network G and $f(N)$ is a non-negative penalisation function. When $f(N)=1$, the penalised score function is the Akaike Information Criterion score (AIC) as shown below (Akaike, 1974):

$$AIC(G|D) = LL(G|D) - |G| \quad [6]$$

Later on, Schwarz (1978) proposed a stricter penalised scoring function, Bayesian Scoring Criterion score (BIC), which is given as:

$$BIC(G|D) = LL(G|D) - \frac{1}{2} \log(N) \cdot |G| \quad [7]$$

K2 Score. Cooper and Herskovits (1992) proposed the K2 score, which is a particular case of BD score with the uninformative assignment $N'_{ijk} = 1$ (corresponding to zero pseudo-counts). The K2 score can be expressed as:

$$K2(G, D) = \log(P(B)) + \sum_{i=1}^n \sum_{j=1}^{q_i} \left(\log\left(\frac{(r_i - 1)!}{(N_{ij} + r_i - 1)!}\right) + \sum_{k=1}^{r_i} \log(N_{ijk}!) \right) \quad [8]$$

Decomposability of the K2 score makes it a computational efficient scoring function but it does not have a score equivalence property as the previous three scoring functions. However, score equivalence property might or might not help in network learning. When we want to

learn the causal relationship between variables, we would need to eliminate the equivalence network from the true network as they infer a different causal relationship; score equivalence property skips this process. On the other hand, score equivalence property can reduce the time consumed if we only need the inference of one variable given another as either equivalence network can do this task.

RESULTS AND DISCUSSION

Experimental Design

In this experiment, five scoring functions were compared on seven sets of data ranging from 8 to 417 variables using three benchmark structure learning algorithms. The five scoring functions compared were the BDe score (ESS of 4), BDe (ESS of 10), AIC score, BIC score and K2 score. Hill Climbing (HC), Tabu Search (TS) and the K2 algorithm were used to test the accuracy of each scoring function. Since the optimal equivalent sample size (ESS) of the BDe score was unknown, we identified the ESS value by including two variations of the BDe score in this study with an ESS of 4 and 10, respectively. The length of the Tabu list used in the TS was set as 10 as a simple test was conducted to show that a Tabu list of more than 10 does not improve the quality of the network learnt. Node ordering required for K2 algorithm was obtained from the true network such that, if x_i preceded x_j in the ordering, x_j must not be in the parent sets of the x_i . True network in this study referred to the original network constructed by the authors of the paper of each dataset. True networks for each dataset are shown in Figures 1 to 7. Since all variables in the datasets studied did not have a number of parents exceeding 10 in their respective true network, the maximum number of parents for each algorithm was capped at 10.

The end result of networks generated by each scoring function and learning algorithm was compared with the true network using the Structural Hamming Distance (SHD) from “bnlearn” package in R. A brief explanation of SHD is quoted from Tsamardinos et al. (2006):

SHD directly compares the structure of the learned and the true networks and its use is fully oriented toward discovery rather than inference. SHD between two PDAGs is defined as the number of the following operators required to make the PDAGs match: add or delete an undirected edge, and add, remove, or reverse the orientation of an edge. Thus, an algorithm will be penalized by an increase of the score by 1 for learning a PDAG with an extra un-oriented edge and by 1 for not orienting an edge that should have been oriented. Algorithms that return a DAG are converted to the corresponding PDAG before calculating this measure. The reason for defining the SHD on PDAGs instead of DAGs is so that we do not penalize for structural differences that cannot be statistically distinguished.

The first section of this experiment studied the effect of scoring functions on different types of datasets with varying numbers of variables as summarised in Table 1. Each dataset was run with three learning algorithms using five scoring functions. The final network of each simulation was compared to the true network using SHD as explained in the previous

paragraph. The smaller the SHD between the network obtained and the true network, the better the score. The second section of this experiment investigated the effect of scoring functions on same datasets with different sample sizes. We selected three datasets (Alarm, Win95pts and Andes) for this study. For each dataset, we generated three sets of data with 5,000, 10,000 and 20,000 instances, respectively, based on the conditional probability table of the true network. The method for comparing is the same as the first section of the experiment with different sets of data.

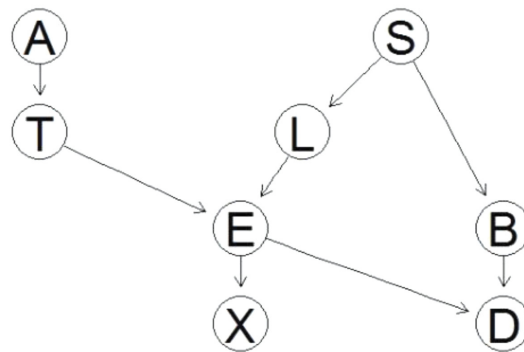


Figure 1. Asia

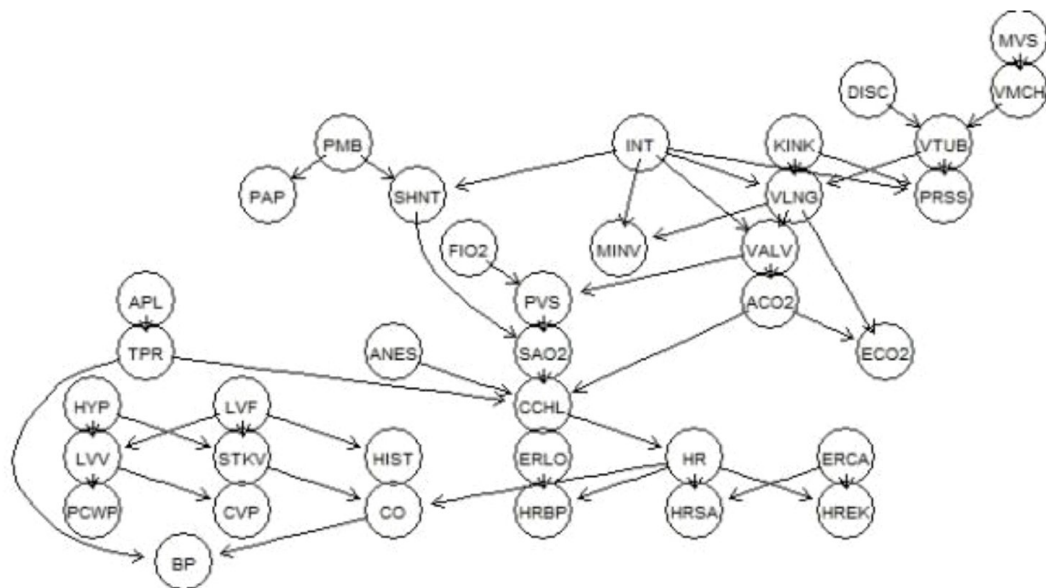


Figure 2. Alarm

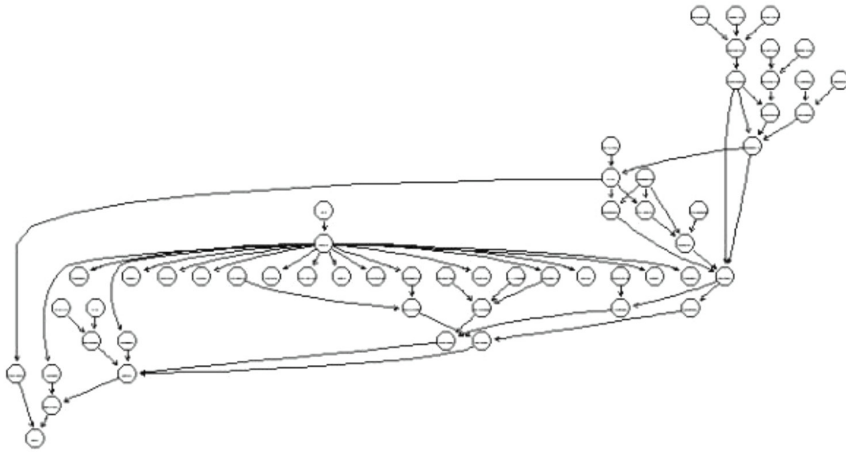


Figure 3. Hailfinder

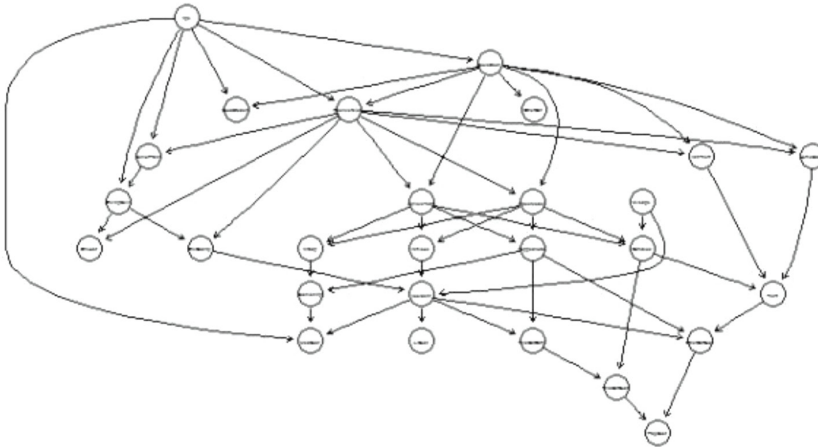


Figure 4. Insurance

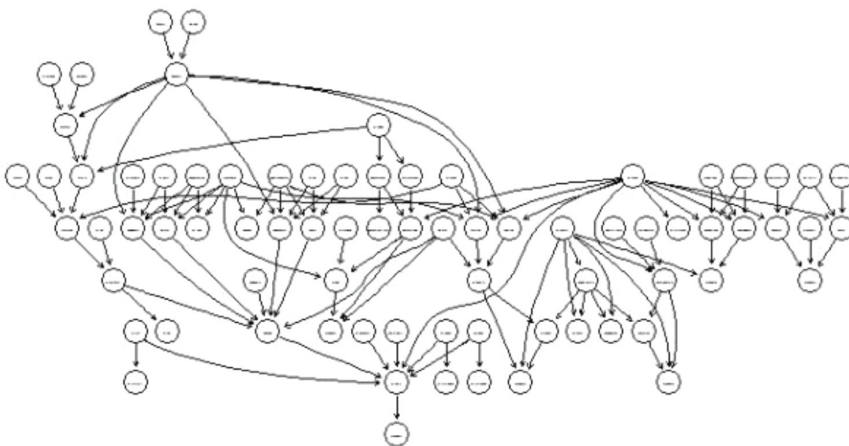


Figure 5. Win95pts

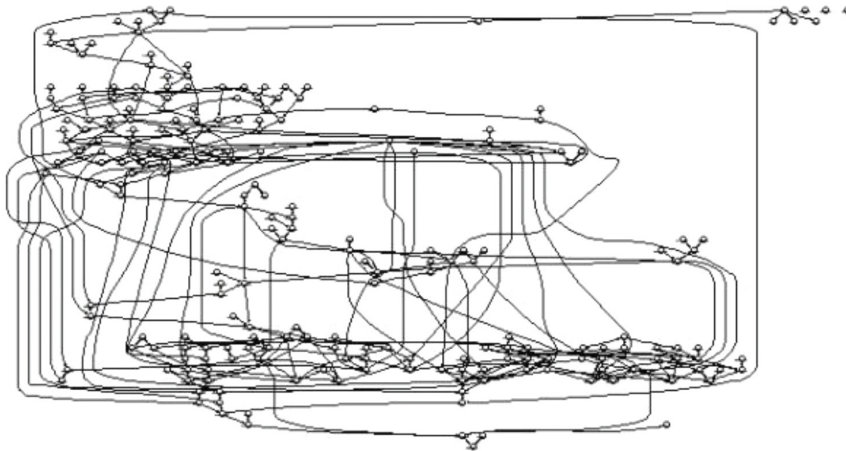


Figure 6. Andes

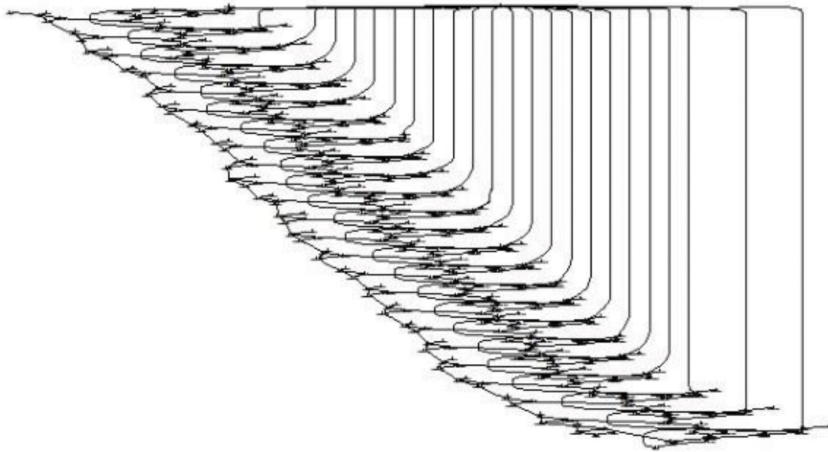


Figure 7. Diabetes

Table 1
Summary of Datasets

Data	No. of Variables	No. of Instances	Reference
Asia	8	5 000	Lauritzen and Spiegelhalter (1988)
Insurance	27	20 000	Binder et al. (1997)
Alarm	37	20 000	Beinlich et al. (1989)
Hailfinder	56	20 000	Abramson et al. (1996)
Win95pts	76	20 000	Developed at Microsoft Research and contributed to the community by Jack Breese.
Andes	223	20 000	Conati et al. (1997)
Diabetes	417	20 000	Andreassen et al. (1991)

Experiment Results

As explained in the previous section, the experiment was divided into two sections. In order to simplify the evaluation of the results, we categorised the data into small data (less than 50 variables), medium data (51-100 variables) and large data (more than 100 variables). The results of the first section are tabulated in Table 2 with bold font indicating the lowest SHD for each row.

For small data, the BDe score (ESS of 4) gives the best performance by generating 7 out of 9 networks with the lowest SHD. This is followed by the BIC score and K2 score with four and two networks of the lowest SHD, respectively. However, the BDe score with an ESS of 4 does not outperform other scoring functions as the differences were not convincing. For medium and large data, the BIC score performed best by generating seven networks with the smallest SHD from a total of 12 networks. Albeit only seven networks generated by BIC score had the smallest SHD, the difference between the BIC score and other scoring functions was significant with minimal exception. Surprisingly, the AIC score generated networks with the lowest SHD for data on diabetes but it did not differ much from the BIC score and both BDe scores.

The BDe score was asymptotically equivalent to the BIC score but one of the reasons the BDe with an ESS of 4 performed better for smaller data was due to the relatively larger sample size. BIC scores tend to penalise complex networks more heavily compared to BDe scores especially for smaller sample sizes. Since all datasets except Asia had the same sample size, which was 20,000 instances, the performance of the BDe score dropped as the number of variables increased. On the other hand, BIC scores favour a simpler network for larger data with a smaller sample size. Hence, the BIC score performed better than the BDe score as the number of variables increased.

In terms of an ESS parameter for the BDe score, an ESS of 4 outperformed an ESS of 10 for all networks generated. According to two studies done on finding the optimal ESS for BDe scores (Steck & Jaakkola, 2002; Silander et al., 2007), a lower ESS tended to favour deletion of arcs while a higher ESS favoured addition of arcs. With a large sample, the learnt network becomes an empty graph as the ESS approaches zero and tends to become a fully connected graph as the ESS increases. This explains why 4 is better than 10 as the ESS for the BDe score in this study as nearly all the networks generated had overfitting problem. Hence, a smaller number of ESS reduced the complexity of networks generated and was closer to the true network.

In the comparison with structural learning algorithms, the BIC score performed well for both Hill Climbing and Tabu search. Meanwhile, the K2 score occasionally performed better when the K2 algorithm was used. Although the K2 score performed better for certain data, the difference was small and the time consumed for the K2 score was significantly higher than for the others. For the second section of this experiment, the results are tabulated in Table 3. The results of different sample sizes on the Alarm data once again strengthened the belief that the BDe score performed better for larger sample sizes. For Alarm data with 20,000 instances, the BDe score with an ESS of 4 performed better with HC and TS. However, when the sample size was reduced to 10,000, the BIC score started to perform better and this was proven when the sample size was reduced to 5,000.

Table 2
Comparison Between Datasets

Data	Structural learning algorithm	Structural hamming distance (SHD)				
		BIC	AIC	BDe(4)	BDe(10)	K2
Asia	HC	1	4	1	8	8
	TS	1	4	1	8	8
	K2	1	4	1	8	4
Insurance	HC	45	43	42	45	39
	TS	44	42	36	39	39
	K2	9	11	10	29	10
Alarm	HC	35	53	25	38	33
	TS	31	49	14	37	33
	K2	6	19	10	14	7
Hailfinder	HC	12	25	19	19	39
	TS	12	44	35	42	39
	K2	12	15	18	18	25
Win95pts	HC	38	106	125	187	66
	TS	38	106	125	188	66
	K2	19	90	109	154	19
Andes	HC	30	512	112	192	216
	TS	30	515	113	194	216
	K2	21	473	94	168	53
Diabetes	HC	497	445	431	464	695
	TS	497	445	431	464	695
	K2	176	77	111	149	118

Table 3
SHD Comparison Between Sample Sizes

Data	Structural learning algorithm	Structural hamming distance (SHD)				
		BIC	AIC	BDe(4)	BDe(10)	K2
Alarm20000	HC	35	53	25	38	33
	TS	31	49	14	37	33
	K2	5	19	10	14	7
Alarm10000	HC	12	36	18	18	23
	TS	14	36	13	15	23
	K2	2	23	12	13	2
Alarm5000	HC	12	32	15	32	28
	TS	12	32	15	33	21
	K2	4	24	6	24	5
Win95pts20000	HC	38	106	125	187	66
	TS	38	106	125	188	66
	K2	21	90	109	154	19
Win95pts10000	HC	46	114	146	212	86
	TS	46	114	147	212	88
	K2	23	89	121	181	40
Win95pts5000	HC	48	100	148	217	80
	TS	48	100	152	217	80
	K2	27	86	152	197	36
Andes20000	HC	30	512	112	192	216
	TS	30	515	113	194	216
	K2	21	473	94	168	53
Andes10000	HC	45	493	127	240	267
	TS	45	493	134	242	267
	K2	31	443	110	211	65
Andes5000	HC	72	521	173	297	262
	TS	72	525	174	298	262
	K2	57	455	152	259	105

CONCLUSION

In this paper, five scoring functions were compared: BIC, AIC, BDe (ESS of 4), BDe (ESS of 10) and the K2 score. Two factors were manipulated to study the effects of scoring functions on data with a different number of variables and sample sizes. The first part of this study compared the performance of scoring functions between seven sets of data with different numbers of variables, while the second part of the study compared the scoring functions between three sets of data with different sample sizes.

The performance of the scoring functions in this study were measured using structural hamming distance (SHD) between the network generated for each scoring function and the true network. A smaller number of SHD indicated better similarities between the two networks, which implied that a better network was learnt. Albeit the higher scoring was advocated in network learning, defining a true causal relationship was more important as an overfitting network does not always imply true causal relationship.

When the sample size was relatively large, the BDe score with an ESS of 4 performed well. But as the number of variables increased, the data sample size was relatively smaller and the performance of the BDe score descended. On the other hand, the BIC score performed well and was consistent for all data regardless of the number of variables and sample size. Most of the networks generated using the AIC score was too complex and faced the problem of overfitting. Although the K2 score performed better with the K2 algorithm in certain cases, it is not recommended for use as the difference was insignificant while the time consumed was significantly greater. Different greedy search learning algorithms used have minimal impact on the performance of scoring functions. Based on the results, all networks generated had more arcs than the true network. In this case, it implies that stricter penalised terms tend to produce a network more similar to the true network. However, the penalised term is hard to determine as strict terms will produce barely connected network for data with few variables while loose terms will produce a fully connected graph for a large network in extreme cases. In summary, the BIC score is definitely the best benchmarked score for a greedy search type network learning algorithm and the BDe score can perform equally well provided the sample size is large.

REFERENCES

- Abramson, B., Brown, J., Edwards, W., Murphy, A., & Winkler, R. L. (1996). Hailfinder: A Bayesian system for forecasting severe weather. *International Journal of Forecasting*, 12(1), 57–71. doi: 10.1016/0169-2070(95)00664-8. doi:10.1016/0169-2070(95)00664-8 doi:10.1016/0169-2070(95)00664-8 doi:10.1016/0169-2070(95)00664-8
- Akaike, H. (1974). A new look at the statistical model identification. *IEEE Transactions on Automatic Control*, 19(6), 716–723. doi: 10.1109/TAC.1974.1100705
- Andreassen, S., Hovorka, R., Benn, J., Olesen, K. G., & Carson, E. R. (1991). A model-based approach to insulin adjustment. In *Proceedings of the 3rd Conference on Artificial Intelligence in Medicine*, Springer-Verlag (pp. 239–248). doi: 10.1007/978-3-642-48650-0_19

- Beinlich, I. A., Suermondt, H. J., Chavez, R. M., & Cooper, G. F. (1989). The ALARM monitoring system: A case study with two probabilistic inference techniques for belief networks. In *Proceedings of the 2nd European Conference on Artificial Intelligence in Medicine, Springer-Verlag* (pp. 247–256). doi: 10.1007/978-3-642-93437-7_28
- Binder, J., Koller, D., Russell, S., & Kanazawa, K. (1997). Adaptive probabilistic networks with hidden variables. *Machine Learning*, 29(2-3), 213–244. doi: 10.1023/A:1007421730016
- Conati, C., Gertner, A. S., Van Lehn, K., & Druzdzel, M. J. (1997). On-line student modeling for coached problem solving using Bayesian networks. In *Proceedings of the 6th International Conference on User Modeling, Springer-Verlag* (pp. 231–242). doi: 10.1007/978-3-7091-2670-7_24
- Cooper, G. F., & Herskovits, E. (1992). A Bayesian method for the induction of probabilistic networks from data. *Machine Learning*, 9(4), 309–347. doi: 10.1007/BF00994110
- Daly, R., & Shen, Q. (2007). Methods to accelerate the learning of Bayesian network structures. In *Proceedings of the 2007 UK Workshop on Computational Intelligence, Imperial College, London* (pp. 1-9). Retrieved from <http://hdl.handle.net/2160/421>
- Fast, A. (2010). *Learning the structure of Bayesian networks with constraint satisfaction*. (Ph.D. thesis). University of Massachusetts Amherst, Department of Computer Science, U.S.A.
- Gasse, M., Aussem, A., & Elghazel, H. (2014). A hybrid algorithm for Bayesian network structure learning with application to multi-label learning. *Expert Systems with Applications*, 41(15), 6756–6772. doi: 10.1016/j.eswa.2014.04.032
- Glover, F., & Laguna, M. (1993). Tabu search. In C. R. Reeves (Ed.), *Modern heuristic techniques for combinatorial problems* (pp. 70-150). Oxford: Blackwell Scientific Publishing.
- Goldberg, D. E. (1989). *Genetic algorithms in search, optimisation and machine learning*. Boston: Addison-Wesley Longman.
- Heckerman, D. (1996). A tutorial on learning Bayesian networks. *Microsoft Research, Technical Report: MSRTR-95-06*. Retrieved from <https://www.microsoft.com/en-us/research/publication/a-tutorial-on-learning-with-bayesian-networks/>
- Heckerman, D., Geiger, D., & Chickering, D. M. (1995). Learning Bayesian networks: The combination of knowledge and statistical data. *Machine Learning*, 20(3), 197–243. doi: 10.1023/A:1022623210503
- Kennedy, J., & Eberhart, R. C. (1995). Particle swarm optimization. In *Proceedings of the IEEE International Conference on Neural Networks* (pp. 1942–1948).
- Kullback, S. (1959). *Information theory and statistics*. New York: Wiley.
- Lauritzen, S., & Spiegelhalter, D. (1988). Local computation with probabilities on graphical structures and their application to expert systems (with discussion). *Journal of the Royal Statistical Society: Series B (Statistical Methodology)*, 50(2), 157–224. Retrieved from <http://www.jstor.org/stable/2345762>
- Neapolitan, R. E. (2004). *Learning Bayesian networks*. New Jersey: Pearson Prentice Hall.
- Pearl, J. (1985). Bayesian networks: A model of self-activated memory for evidential reasoning. In *Proceedings of the 7th Conference of the Cognitive Science Society, University of California, Irvine* (pp. 329–334).
- Schwarz, G. E. (1978). Estimation of the dimension of a model. *Annals of Statistics*, 6(2), 461–464. Retrieved from <http://www.jstor.org/stable/2958889>

- Scutari, M. (2010). Learning Bayesian network with the BNlearn r package. *Journal of Statistical Software*, 35(3), 1–22. doi: 10.18637/jss.v035.i03
- Silander, T., Kontkanen, P., & Myllymaki, P. (2007). On sensitivity of the MAP Bayesian network structure to the equipment sample size parameter. In *Proceedings of the 23rd Conference on Uncertainty in Artificial Intelligence* (pp. 360–367). Retrieved from arXiv:1206.5293
- Spirtes, P., & Glymour, C. (1991). An algorithm for fast recovery of sparse causal graphs. *Social Science Computer Review*, 9(1), 62–72. doi: 10.1177/089443939100900106
- Spirtes, P., Glymour, C., & Scheines, R. (1993). *Causation, prediction and search*. New York, NY: Springer.
- Steck, H., & Jaakkola, T. S. (2002). On the Dirichlet prior and Bayesian regularization. In *Advances in Neural Information Processing Systems 15, MIT Press* (pp. 697–704). Retrieved from <http://hdl.handle.net/1721.1/6702>
- Tsamardinos, I., Aliferis, C. F., & Statnikov, A. (2003). Algorithms for large scale Markov blanket discovery. In *The 16th International FLAIRS Conference, St. Augustine, Florida* (pp. 376–381).
- Tsamardinos, I., Brown, L. E., & Aliferis, C. F. (2006). The max-min hill-climbing Bayesian network structure learning algorithm. *Machine Learning*, 65(1), 31–78. doi: 10.1007/s10994-006-6889-7



Analysis of Malaysia's Single Stock Futures and Its Spot Price

Marzuki, R. M., Mohd, M. A. *, Nawawi, A. H. M. and Redzwan, N. M.

Faculty of Computer and Mathematical Sciences, Universiti Teknologi MARA, 40450 UiTM, Shah Alam, Selangor, Malaysia

ABSTRACT

Single Stock Futures (SSFs) was introduced in Bursa Malaysia on 28th April 2006. There have been many studies on derivative instruments in Malaysia; however, none is on SSFs. Various statistical methods have been used to analyse the SSFs and its spot returns, namely Descriptive Statistics, Unit Root test, VAR, Johansen and Juselius Co-integration test, Granger Causality test, Variance Decomposition test, VECM, and GARCH model. This study analyses the SSFs and spot returns of eight companies listed in Bursa Malaysia. It found that Berjaya Sports Toto Bhd and Genting Bhd have no long-run and short-run causality (Genting Bhd has bi-directional causality) while AirAsia Bhd and AMMB Holdings Bhd's spot returns' volatility decreased after the introduction of SSFs; it increased in the other seven companies. In addition, only AMMB Holdings Bhd futures return did not affect its spot return. Bursa Malaysia Bhd and RHB Capital Bhd spot returns lead their futures returns

Keywords: Single Stock Futures, SSF, VAR, Granger Causality, GARCH

INTRODUCTION

Futures are linked to two types of financial market: The Equity (known as Stock Market) and the Futures Market. Futures can be a driver to hedge a portfolio and to capture market opportunities. Basically, the value of derivatives is derived in a contractual manner from one or more underlying asset while Single Stock Futures (SSFs), as explained by Securities Commission Malaysia, is an agreement that the price of a stock, either to buy or sell in a future time, is agreed today and that particular underlying stock is listed on the exchange. Just like any other futures contracts, each SSFs has its expiry date. Investors are said to be able to have the rights in the underlying stock even though they do not own its shares and able to benefit from the rise in value of the price. However, because SSFs' holders are not

Article history:

Received: 27 May 2016

Accepted: 14 November 2016

E-mail addresses:

musfirah_marzuki@yahoo.com (Marzuki, R. M.),

azri_mohd@salam.uitm.edu.my (Mohd, M. A.),

halim@tmsk.uitm.edu.my (Nawawi, A. H. M.),

khairunnisa@tmsk.uitm.edu.my (Redzwan, N. M.)

*Corresponding Author

the real shareholders of the company, they do not have the right to receive dividends as well as any other rights. The SSFs are also standardised contracts of exchange-traded derivatives which are easier to deal because no discussion nor negotiation are involved outline the contract's specifications, terms and conditions. Since the futures markets are considered to be more volatile than the spot market, they can also be a source of volatility for the spot market. This study investigates whether the stock futures increases or decreases the spot market's volatility.

Awan and Rafiq (2013) stated that that derivatives generally increases stock prices. However, due to mixed empirical evidence, there is no agreement among researchers on this matter. Isa (2003) for instance, examined the impact of the introduction of derivative instruments on the cash markets of Bursa Malaysia. He concluded that the market efficiency has increased while the level of volatility has decreased. In this study, the relationship between Single Stock Futures and the underlying stock and the volatility level after the introduction of Single Stock Futures is examined and to discover whether the movement of Single Stock Futures price affects the underlying asset price, or vice versa.

LITERATURE REVIEW

The introduction of SSFs in the market has increased the force of arbitragers (Ang & Cheng, 2005). They found stock returns decreased resulting in lowest interest for investors while the arbitrages were more interested in trading. There are different types of risks as well as the restriction on investors, making it difficult to fully identify the impact of futures in the stock market (see McKenzie, Barailsford & Faff, 2001; Antonio, Koutmos & Pericli, 2005). Khan (2006) studied the effect of futures trading in Pakistan to identify their volatility. He stated that futures market influenced the spot market in terms of integrating new information. In addition, futures market does not affect spot market's volatility, and also the outgrowth of spot market affects the volatility of futures market. Khan and Hijazi (2009) found that the volatility of stock price declined after the introduction of futures trading. They noted a positive relationship between volatility of spot and volumes of spot. Mazouz and Bowe (2006) used GARCH (1,1) to investigate the futures trading's volatility effect, and found that there was an increase on residual variance in current news, and they proved that the listing of futures market improves the stock market. There was also a bidirectional causality between the spot market and futures market (Pizzi, Oconomopoulos & O'Neill, 1998). They also found that the spot led the futures for three to four minutes, while the futures led the spot for 20 minutes.

DATA AND METHODOLOGY

A qualified sample must not have any missing data (Chang, Cheng Pinegar, 1999). Data from ight companies was used for this research. Maxis Communications Bhd and Scomi Group Bhd were rejected because in the middle of observations, both companies were delisted from SSFs. The daily end spot prices data was retrieved from Datastream of UiTM between 17th March 2005 and 31st December 2013 because of data availability. The daily end futures prices data for the study was from 1st January 2007 to 31st December 2013 because even though SSFs was introduced on 28th April 2006, not all counters began their trading on that date. All eight

counters had complete data starting 1st January 2007, with 1,826 observations. Statistical analysis will use data from 1st January 2007 to 31st December 2013, except for GARCH model; the spot prices from 17th March 2005 to 8th June 2007 was used. Before the analysis began, the logarithmic returns were calculated for both spot prices and futures prices to prevent the non-stationary problem in raw data that usually happens to monetary data. Natural logarithm of two following after one another (consecutive) days is as follows:

$$R_t = \ln\left(\frac{P_t}{P_{t-1}}\right) \quad (1)$$

R_t is the SSFs return for the given period of t , P_t is the SSFs end price at time t , and P_{t-1} is the SSFs closing price at time $t-1$. Descriptive statistic is use to explain the behaviour of SSFs data, or in other words, it is the SSFs's characteristics summarisation. In this research, Johansen and Juselius Co-integration test will be used. This test depends on two types of test: trace test and maximum-eigenvalue test. Vector auto regression (VAR) of order n will be assumed as it consists of the trace test and maximum-eigenvalue test on SSFs data. The null hypothesis states that there are no cointegration between the SSF and its spot if the trace value is less than the critical value (0.05) and vice versa.

Granger Theorem's principal explains that there is a causal relationship between two variables, two or at least one direction, if that two variables are co-integrated. However, the co-integration does not interpret the lead relationship that is essential in price discovery, even though it does capture the existence of a long-run relationship. The Granger Cause is to detect whether, x precedes y , y precedes x , or if the movement occurs at the same time. Variance Decomposition test provides information on the importance of each random innovation that affects variables in VAR. The variance decomposition test explains the proportion of the movements in one variable (dependent variable) that are due to its own shocks versus shocks due to the other variables (independent variable). The variance decomposition is considered a better tool for the cumulative effect of shocks. Vector Error Correction Model (VECM) captures the short-term relationship of the SSFs. A VECM is part of multiple time series model that approximate the speed of SSFs to get back to equilibrium after the changes in spot market. There are three things that can be interpreted from the VECM result, namely the long-run causality, short-run causality and coefficient value. Null hypothesis states that there is a long-run causality for spot and futures returns if the first coefficient, $C(1)$, is negative and the probability is less than 0.05. The null hypothesis states that there is short run causality if the probability for the chi-square is less than 0.05 (accept null hypothesis) and vice versa (there is no short-run causality between spot and futures returns of the SSFs if chi-square is more than 0.05). The coefficient value indicates the correcting disequilibrium from previous day to current day, or in other words, how fast the changes from yesterday will affect today's SSFs price. The greater the value, the faster the change will be.

In the GARCH Model, volatility is measured through variance. A bigger value of variance indicates a high volatility and the market is said to be riskier. It can be used to detect the difference before and after the introduction of SSFs and in this study, the latter's pre-event variance and post event variance. The assumption of expected value of residual must be

zero, it is a constant variance of residual terms (heteroskedasticity), and also there is no auto-correlation in the data series like the assumptions made in OLS regression. The basis for ARCH and GARCH models is the breach of homoscedasticity assumption. The ARCH effect must not have heteroskedasticity. The null hypothesis for heteroskedasticity test is that there is no ARCH effect if the probability value is more than 0.05 (accept null hypothesis) and vice versa. Therefore, the GARCH model can be used in the analysis. Basic GARCH (1, 1) specification:

The mean equation;

$$y_t = \alpha + \beta y_{t-1} + \varepsilon_t \dots \dots \varepsilon_t(0, h_t) \tag{2}$$

Where y_t the return on SSFs and its spot is, α is a constant, βy_{t-1} is the autoregressive coefficient explanatory (lagged), ε_t is the residual term. Brooks in 2008 explained the variance equation as:

$$h_t = \omega + \alpha \varepsilon_{t-1}^2 + \beta h_{t-1} + \theta D_t \dots \dots \omega > 0, \alpha > 0, \beta \geq 0(10) \tag{3}$$

Whereby h_t represent the conditional variance in period t , ω is the constant, βh_{t-1} is then the persistence coefficient GARCH(1,1) term and θD_t is the dummy variable. Thus, the unconditional constant variance of error term:

$$\text{var} = \frac{\omega}{1 - \alpha - \beta} \tag{4}$$

The variance equation consists of three terms, namely a constant, ω , information regarding previous period volatility (ARCH term) and forecasted variance of last period (GARCH term).

$$\text{var}(\varepsilon_t) = \frac{\omega + \delta}{1 - \alpha - \beta} \tag{5}$$

δ represent the coefficient and D_t represents the dummy variable on the tested data series. The use of dummy in the variance equation is because of it is assumed that mean structure or volatility break is the cause of event. Economic researchers believe a long-term stable mean structure is better in the calculation of economic time series, as the temporary events should not be easily affecting. Finally, if the total GARCH parameters ($(\alpha + \beta)$ is greater than 0.9 it is an indication that the persistence of the shock to the volatility is permanent (Engle & Bollerslev, 1986).

ANALYSIS

Descriptive Statistics

Descriptive statistics was applied to both spot and futures returns (eight companies) with a total of 1,826 observations as seen in Table 1. The results show that in terms of spot return, the top three companies, namely Telekom Malaysia Bhd, RHB Capital Bhd, and AMMB Holding, have the highest average daily returns of 0.0589%, 0.0469%, 0.046% with 1.39%, 1.67% and 1.62% risk level respectively. However, their futures return recorded a - 0.031%, 0.0459%,

and 0.045% with risk level of 3.01%, 1.68%, and 1.51% respectively. AirAsia Bhd and IOI Corporation Bhd futures return record an average daily returns of 0.0215%, 6.84% with 2.37% -and 0.074% risk level respectively, whereas their spot average daily returns are 0.0206%, 0.0264% with 2.13% and 1.98% risk level respectively. Same goes to Genting Bhd and Bursa Malaysia Bhd where the average daily spot returns are higher than average daily futures returns, yet, their futures returns' risk level are higher than spot returns' risk level. Berjaya Sports Toto Bhd recorded negative average daily returns for both spot return (-0.00432%) and futures return (-0.00944%), with 1.5% and 0.78% risk level respectively. Only AirAsia Bhd spot and futures, Bursa Malaysia Bhd futures, Genting Bhd spot, RHB Capital Bhd spot and futures, and Telekom Malaysia Bhd spot have positive value in skewness (long right tail, higher tendency or probability of positive returns).

Table 1
Results of Descriptive Statistics

	Mean	Std. Dev.	Skewness	Kurtosis	Prob.
AA_FR	0.0002150	0.0237	2.4453	65.8105	0
AA_SR	0.0002060	0.0213	0.1014	6.4679	0
AMMB_FR	0.0004500	0.0151	-2.4784	150.1889	0
AMMB_SR	0.0004600	0.0162	-0.2785	12.3041	0
BM_FR	0.0000081	0.0202	2.3506	128.7121	0
BM_SR	0.0000121	0.0183	-0.0183	9.2133	0
BST_FR	-0.0000944	0.0078	-1.6392	85.9735	0
BST_SR	-0.0000432	0.0150	-0.3664	117.0728	0
G_FR	-0.0006330	0.0410	-33.1577	1308.9740	0
G_SR	0.0002420	0.0189	0.3025	5.8990	0
IOI_FR	-0.0007400	0.0684	-7.2668	507.1818	0
IOI_SR	0.0002640	0.0198	-0.0743	19.5952	0
RHB_FR	0.0004690	0.0167	0.3605	97.9842	0
RHB_SR	0.0004590	0.0168	0.2826	10.3678	0
TM_FR	-0.0003100	0.0301	-31.1359	1179.0600	0
TM_SR	0.0005890	0.0139	0.9867	51.2713	0

The remaining returns are negatively skewed (long left tail, higher probability of negative returns). All companies show kurtosis value of more than 3, and it is known as leptokurtosis to explain that all companies have fatter tail and lesser risk of extreme outcomes. Any small changes are less likely to happen. However, it is not favoured by conservative investors who tend to overestimate at high levels of significance, whereas in a normal distribution, low levels of significance will usually be overestimated. The reported probability is the probability for Jarque-Bera. Since all the returns have 0 probabilities, which is less than 0.05, it means that the returns are not normal.

Unit Root, Vector Auto Regression, Co-Integration & Granger Causality

Figure 1 shows the illustration of granger causality test. There are two unidirectional granger cause, one bi-directional granger cause and five no causality. Based on Table 2 and Table 3, we rejected the null hypothesis since the probability values are less than 0.05, no co-integration equation, and there is one co-integration equation. The probability values are all less than 0.05, hence, we rejected the null hypotheses to show that all eight companies have a long-run relationship.

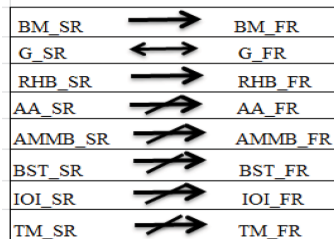


Figure 1. Simplified Granger Causality Test

Table 2
Trace Test

Company	Hypothesised No. of CE(s)	Eigenvalue	Trace Statistic	0.05 Critical Value	Prob.
AA	None *	0.194064	652.8156	15.49471	0.0001
AMMB	None *	0.175497	632.0589	15.49471	0.0001
BM	None *	0.194372	682.251	15.49471	0.0001
BST	None *	0.237961	827.031	15.49471	0.0001
G	None *	0.191526	711.5693	15.49471	0.0001
IOI	None *	0.225153	644.5632	15.49471	0.0001
RHB	None *	0.192731	665.3697	15.49471	0.0001
TM	None *	0.170849	575.7637	15.49471	0.0001

Table 3
Maximum Eigen-value Test

Company	Hypothesised No. of CE(s)	Eigenvalue	Max-Eigen Statistic	0.05 Critical Value	Prob.**
AA	None *	0.194064	392.8833	14.2646	0.0001
AMMB	None *	0.175497	351.4068	14.2646	0.0001
BM	None *	0.194372	393.5778	14.2646	0.0001
BST	None *	0.237961	494.8703	14.2646	0.0001
G	None *	0.191526	387.157	14.2646	0.0001
IOI	None *	0.225153	463.4991	14.2646	0.0001
RHB	None *	0.192731	389.8742	14.2646	0.0001
TM	None *	0.170849	340.9829	14.2646	0.0001

Hence, we can say that the spot returns may forecast the futures returns for Bursa Malaysia Bhd and Genting Bhd. While the futures return of Genting Bhd and RHB Capital Bhd may forecast their spot returns and play an important role in price discovery (determining the spot price).

Variance Decomposition Test & Vector Error Correction Model

Impulse or shock to futures returns are said to be 100% of variation explained by its own lag returns than by the lag returns of spot. We can say that all eight companies are in an exogenous (determined by external factors) market as majority of the shocks are explained by their own innovations, or in other words, the shocks can be explained by the decision of the company. The standard error for all eight companies are lower, which also means it is good because the smaller the standard error, the more it will represent the sample population, as it measures accuracy.

Table 4 shows the results of Vector Error Correction Model. There is a long-run causality for spot and futures returns if the first coefficient is negative and the probability is less than 0.05. Therefore, we can say that only Berjaya Sports Toto Bhd has no long-run causality while the remaining seven companies have a long-run causality. The coefficient values also indicate the percentage of correcting disequilibrium from previous day to current day. It is quite fast for five companies: 66.4183% for AirAsia Bhd, 35.2816% for AMMB Holdings Bhd, 79.6967% for Bursa Malaysia Bhd, 48.3434% for IOI Corporation Bhd, and 50.499% for Telekom Malaysia Bhd. It is very slow for the remaining three companies. From Table 5, there is no short-run causality between spot and futures returns for both Berjaya Sports Toto Bhd and Genting Bhd; because the probability for the chi-square is more than 0.05, we reject the null hypothesis.

Table 4
Vector Error Correction Model Results

	Coefficient	Std. Error	t-Statistic	Prob.
AA	-0.664183	0.034005	-19.53196	0
AMMB	-0.352816	0.026085	-13.5257	0
BM	-0.796967	0.036085	-22.08585	0
BST	-0.001908	0.003468	-0.550196	0.5823
G	-0.000992	0.000495	-2.005356	0.0451
IOI	-0.483434	0.029657	-16.30108	0
RHB	-0.072357	0.011996	-6.031744	0
TM	-0.502499	0.02946	-17.05679	0

Table 5
Short Run Causality

	Chi-square	Probability
AA	206.7796	0
AMMB	105.1169	0
BM	161.9309	0
BST	0.182172	0.9129
G	1.257373	0.5333
IOI	167.4725	0
RHB	33.28363	0
TM	140.6512	0

Table 6
Results of GARCH Test

		ω	α	β	Volatility	$\alpha + \beta$
AA	Before	0.8942	0.1750	0.0000	1.0411	0.1750
	After	0.0964	0.0000	0.0000	0.3105	0.0000
AMMB	Before	0.2032	0.1067	0.2037	0.5428	0.3104
	After	0.0054	0.0000	0.0000	0.0735	0.0000
BM	Before	0.4642	0.3063	0.0000	0.8180	0.3063
	After	0.8045	0.0000	0.0000	0.8969	0.0000
BST	Before	0.0844	0.0016	0.0952	0.3057	0.0968
	After	0.8769	0.0000	0.0000	0.9364	0.0000
G	Before	0.2724	0.0000	0.0000	0.5219	0.0000
	After	0.7280	0.0000	0.0000	0.8532	0.0000
IOI	Before	0.1181	0.0478	0.0000	0.3522	0.0478
	After	0.9535	0.0000	0.0000	0.9765	0.0000
RHB	Before	0.6825	0.2381	0.7675	0.0000	1.0056
	After	0.2990	0.0019	0.0000	0.5473	0.0019

Table 7
Futures Return Affecting Spot Return

Hypothesis	Probability
AA_FR Affects AA_SR	0.7484
AMMB_FR Affects AMMB_SR	0
BM_FR Affect BM_SR	0.1007
BST_FR Affects BST_SR	0.9252
G_FR Affects G_SR	0.1287
IOI_FR Affects IOI_SR	0.1058
RHB_FR Affects RHB_SR	0.3874

GARCH Model

Table 6 shows that before the introduction of SSFs, AirAsia Bhd, AMMB Holdings Bhd, Bursa Malaysia Bhd, and RHB Capital Bhd, the previous day's information does not influence the current day's volatility. However, after the introduction of SSFs, those companies' previous information does affect the current day's volatility. On the other hand, the remaining companies' volatilities are affected by the previous day's information. From Table 7, it can be concluded that only AMMB Holdings Bhd futures return does not affect its spot return whereas, the remaining seven companies' futures returns affect their spot returns.

CONCLUSION

The study has achieved its objectives, where we know that even though all eight companies' spot and futures returns are moving together in the long-run because the price of futures is determined by the price of stock market, both Berjaya Sports Toto Bhd and Genting Bhd have no long-run and short-run causalities. In addition, the volatility of majority of spot returns increases after the introduction of SSFs, except for AirAsia Bhd and AMMB Holdings Bhd Only AMMB Holdings Bhd futures return does not affect its spot return while the remaining companies' spot returns are affected by their futures returns. The study also shows that Bursa Malaysia Bhd and RHB Capital Bhd. spot returns lead their futures returns and Genting Bhd has bi-directional causality.

ACKNOWLEDGEMENT

This research is funded by the Fundamental Research Grant Scheme (FRGS) that is managed by the Research Management Centre, Universiti Teknologi MARA (600-RMI/FRGS 5/3 (5/2012).

REFERENCES

- Ang, J. S., & Cheng, Y. (2005). Single stock futures: Listing selection and trading volume. *Finance Research Letters*, 2(1), 30-40.
- Antoniou, A., Koutmos, G., & Pericli, A. (2005). Index futures and positive feedback trading: Evidence from major stock exchanges. *Journal of Empirical Finance*, 12(2), 219-38.
- Awan, A., & Rafiq, A. (2013). The Volatility effect of Single Stock Futures Trading on Pakistani Stock Market. *Business Review*, 8(1), 94 – 122.
- Chang, E. C., Cheng, J. W., & Pinegar, J. M. (1999). Does futures trading increase stock market volatility? The case of the Nikkei stock index futures markets. *Journal of Banking & Finance*, 23(5), 727-753.
- Engle, R. F., & Bollerslev, L. (1986). Modelling the persistence of conditional variance. *Econometric Reviews*, 5(1), 1-50.
- Isa, Z. (2003). The Impact of the Introduction of Derivatives Instruments on the Level of Spot Market Volatility: An empirical Study on Bursa Malaysia. *Sains Malaysiana*, 35(1), 95-105.
- Khan, S. (2006). Role of the futures market on volatility and price discovery of the spot market: Evidence from Pakistan's Stock Market. *The Lahore journal of Economics*, 11(2), 107-21.
- Khan, S., & Hijazi T. S. (2009). Single stock futures trading and stock price volatility: Empirical analysis. *The Pakistan Development Review*, 48(4), 553-563.
- Marzuki, R. M. (2015). *Relationship of single stock futures with the spot price*. (Master's Thesis). Faculty of Computer and Mathematical Sciences, Universiti Teknologi MARA, Malaysia.
- Mazouz, K., & Bowe, M. (2006). The volatility effect of futures trading: evidence from LSE traded stocks listed as individual equity futures contracts on LIFFE. *International Review of Financial Analysis*, 15(1), 1-20.
- McKenzie, M., Brailsford, T., & Faff, R. (2001). New insights into the impact of the Introduction of futures trading on stock price volatility. *Journal of Futures Markets*, 21(3), 237-255.

Marzuki, R. M., Mohd, M. A., Nawawi, A. H. M. and Redzwan, N. M.

Pizzi, M. A., Economopoulos, A. J., & O'Neill, H. M. (1998). An examination of the relationship between stock index cash and futures markets: A cointegration approach. *Journal of Futures Markets*, 18(3), 297-305.

Projecting Input-Output Table for Malaysia: A Comparison of RAS and EURO Method

Shuja', N.^{1*}, Lazim, M. A.² and Yap, B. W.³

¹ *Economic Indicators Division, Department of Statistics Malaysia, 43300 Seri Kembangan, Selangor, Malaysia*

² *Faculty of Computer and Mathematical Sciences, Universiti Teknologi MARA, 40450, Shah Alam, Selangor, Malaysia*

³ *Advanced Analytics Engineering Centre, Faculty of Computer and Mathematical Sciences, Universiti Teknologi MARA, 40450, Shah Alam, Selangor, Malaysia*

ABSTRACT

Input-Output analysis provides important information about the structure of a country's economy. The construction of input-output tables based on detailed census or surveys is a complex procedure requiring substantial financial outlay, human capital, and time. This is the main reason why Malaysia Input-Output (MIO) Table is produced and published on average once every five years. For policy makers past data is not seen as suitable for planning economic policies. The aim of this study is to compare RAS and Euro methods to project input-output tables for Malaysia. The data for the study are MIO table and Gross Domestic Product for the years 2000, 2005 and 2010. The RAS and Euro method were used to project the MIO table 2005 using MIO table 2000 and also projection of MIO table 2010 using MIO table 2005. The projection of I-O tables involved an intensive iterative procedure using Excel Visual Basic programming. The projection performance of RAS and Euro methods were assessed based on Mean Absolute Deviation (MAD), Root Mean Squared Error (RMSE) and Dissimilarity Index (DI). The results show that Euro method performed better than the RAS method in the projection of MIO table.

Keywords: Euro method, projecting input-output table, RAS method

Article history:

Received: 27 May 2016

Accepted: 14 November 2016

E-mail addresses:

yatishuja@stats.gov.my (Shuja', N.),

dralias@tmsk.uitm.edu.my (Lazim, M. A.),

beewah@tmsk.uitm.edu.my (Yap, B. W.)

*Corresponding Author

INTRODUCTION

Input-output (I-O) table is an important tool in economic analysis. I-O table provides information about the structure of the economy useful for policy development and decision making. Currently, producing a benchmark I-O table is expensive and time consuming. This is the main reason why

Malaysia Input-Output (MIO) Table is produced and published on average every five years. Generally, the latest I-O tables available would reflect data of a previous year. For example, MIO table for 2010 was released in 2014 (Department of Statistics Malaysia, 2014) making its application to be inaccurate.

This study will focus on projecting the MIO table using past I-O table to project the I-O table of the current year. The projection methods used are the bivariate method, namely the RAS technique and the EURO procedure which is a stochastic method. The RAS method was selected for this study because this technique is simple and widely used (Bacharah, 1970) whilst Euro method is a robust procedure and data requirement is minimal. It involves no arbitrary changes of input coefficients (Beutel, 2002; Eurostat, 2008). This paper is structured as follows. Reviews on projection of input-output tables are provided in Section 2, followed by the methodology in Section 3. Section 4 presents the results and findings. Finally, the conclusion is given in Section 5.

I-O tables are usually published five years after the reference period. The long time lag, its complexity as well as the tediousness and high costs of compiling survey-based input-output tables have motivated researchers to focus on projecting input-output tables. In their early study, Deming and Stephen (1940) proposed using least squares approach to adjust sample frequency table where marginal totals are known. Their approach involves the solution of normal equations. They also proposed an iterative method of adjustment and conclude that it is better than solving the normal and condition equations. However, Stephen (1942) reported that the iterative approach by Stephen and Deming (1940) only provides an approximation, they do not satisfy the normal equations. He then proposed a method of that converges to the least squares values and showed examples using the two and three dimensional cases. Stone and Brown (1962) then adapted the work by Stephen (1942) and proposed a biproportional adjustment of input-output coefficients and is well-known as the RAS procedure. The updating of input-output tables using RAS is known as non-survey or partial-survey method and has been the subject of long discussions and as a result, the alternative non-survey methods have been developed (Oosterhaven et al., 1986).

Meanwhile, Beutel (2002) introduced a new projection Euro method. The basic idea of this new approach is to derive I-O table using official information or macroeconomic data. The rows and columns of the input-output table use scale factors to derive the unknown rates for input and output from the gross value added by industries and final demand by use category. The advantages of Euro method are low costs involves, simple and robust updating procedure, relatively few data requirements for projection and only official data sources are used.

In order to be able to draw conclusions regarding projection techniques it is necessary to firstly assess their relative performance. Parikh (1979) applied RAS method in forecasting and examines an updating of the 1959 absorption flow matrices of nine European countries to the 1965 Input-Output table. The updated matrices were compared with the corresponding figures based on the actual 1965 tables at a 19-sectors level of aggregation. The percentage mean square errors between updated and actual coefficients were used to evaluate the methods. Butterfield and Mules (1980) also studied on cell by cell accuracy in the input-output matrices through a series of statistical tests and applied them to three non-survey estimates of input-output tables for the Australian State of Western Australia. The RAS method, the H-M (McMenamin-Haring)

method and the N (Naïve) method were used to estimate the I-O coefficients. The sign test is the first test to gauge consistency. The second test, pertains to the regression analysis on the relationship between the estimated coefficient and benchmark coefficients. The third test termed as chi-square contingency table. Finally, the Mean Absolute Difference (MAD) and Standardized Mean Absolute Difference (SMAD) measures the absolute distance between estimated and benchmark coefficients. Based on these statistical tests, the results suggest that RAS is the best method.

Temurshoev et al. (2011) presented the relative performance of eight methods using Dutch and Spanish Supply & Use Tables (SUT). The eight methods of projecting or updating SUTs are: (i) EUKLEMS method; (ii) Euro method; (iii) Generalised RAS (GRAS); (iv) Improved Normalized Squared Differences (INSD); (v) Improved Squared Differences (ISD); (vi) Improved Weighted Squared Differences (IWSD); (vii) Harthoorn and Van Dalen's method; and (viii) Kuroda's method. The measures of Mean Absolute Percentage Error, Weighted Absolute Percentage Error, Standardized Weighted Absolute Difference, The Psi Statistic, RSQ (or coefficient of determination and N_0 – number of zero elements in the estimated matrix X , whose corresponding elements are nonzero in the actual matrix X^{true} were used to assess their relative performance. They reported that GRAS, Harthoorn and Van Dalen and Kuroda methods provide good estimates in terms of projecting the SUT. GRAS is a popular bi-proportional technique proposed by Gunluk-Senesen and Bates (1988) and formalized by Junius and Oosterhaven (2003) which allows for negative elements in I-O tables.

METHODOLOGY

In this study, the MIO table for the year 2000, 2005 and 2010 were used as the base years for the iteration procedure for the compilation of a projected input-output table. The output matrix of domestic production at basic prices calculated for industry-by-commodity at basic prices calculated for commodity-by-industry were used to derive symmetry and industry-by-industry input-output table of domestic production at basic prices. The industries and commodities of the I-O tables were aggregated to 12 industries and 12 commodities in order to make the tables as comparable as possible for year 2000, 2005 and 2010. For example, there are 94 industries and 94 commodities for MIO table 2000, 120 industries and 120 commodities for MIO table 2005, and 124 industries and 124 commodities for MIO table 2010. For this study MIO table for 2000 was used as the base year to project the MIO table 2005. Similarly, MIO table 2005 was used to project the MIO table 2010. The industrial classification for the year 2000, 2005 and 2010 were aggregated in term of (1) Agriculture, Forestry and Logging; (2) Mining and Quarrying; (3) Manufacturing; (4) Electricity, Gas and Water; (5) Construction; (6) Wholesale and Retail; (7) Hotel and Restaurant; (8) Transport and Communication; (9) Finance and Insurance; (10) Real Estate and Ownership of Dwellings; (11) Business and Private Services; and (12) Government Services.

The data comes from MIO table for 2000, 2005 and 2010 as well as microeconomic data, viz., Gross Domestic Product (GDP) for 2005 and 2010 at current prices. This study involved two phases. In the first phase two projection methods, the RAS procedure and EURO method were used to project the MIO table 2005 using MIO table 2000 and then project the MIO

table 2010 using MIO table 2005. The projection of I-O tables involved an intensive iterative procedure using Microsoft Excel Visual Basic programming. In the second phase, the projection performance of RAS and EURO methods were assessed based on Mean Absolute Deviation (MAD), Root Mean Squared Error (RMSE) and Dissimilarity Index (DI) (Saari et al., 2014).

The simplified input-output table is shown in Table 1. The row sectors of intermediate input are the producing sectors of inputs, while the column sectors of intermediate demand are consuming sectors of output.

Table 1
Simplified Input-Output Table

Absorption Matrix of Domestic Production at Basic Prices (Industry by Industry)		Intermediate Demand					Final Demand (f)					Total Output (X _i)	
		Industry	Agriculture	Mining	...	Services	Total Intermediate Demand (d)	Private Consumption	Government Consumption	Gross Fixed Capital Formation	Changes Inventory		Exports
Intermediate Input	Industry	<i>j=1</i>	<i>j=2</i>	...	<i>j=m</i>		<i>k=1</i>	<i>k=2</i>	<i>k=3</i>	<i>k=4</i>	<i>k=5</i>		
	Agriculture	<i>i=1</i>	<i>x₁₁</i>	<i>x₁₂</i>	...	<i>x_{1m}</i>	<i>d₁</i>	<i>f₁₁</i>	<i>f₁₂</i>	<i>f₁₃</i>	<i>f₁₄</i>	<i>f₁₅</i>	<i>X₁</i>
	Mining	<i>i=2</i>	<i>x₂₁</i>	<i>x₂₂</i>	...	<i>x_{2m}</i>	<i>d₂</i>	<i>f₂₁</i>	<i>f₂₂</i>	<i>f₂₃</i>	<i>f₂₄</i>	<i>f₂₅</i>	<i>X₂</i>
	⋮	⋮	⋮	⋮	⋮	⋮	⋮	⋮	⋮	⋮	⋮	⋮	⋮
	Services	<i>i=n</i>	<i>x_{n1}</i>	<i>x_{n2}</i>	...	<i>x_{nm}</i>	<i>d_n</i>	<i>f_{n1}</i>	<i>f_{n2}</i>	<i>f_{n3}</i>	<i>f_{n4}</i>	<i>f_{n5}</i>	<i>X_n</i>
Total Intermediate Input (u)		<i>u₁</i>	<i>u₂</i>	...	<i>u_m</i>	<i>ud</i>	<i>f₁</i>	<i>f₂</i>	<i>f₃</i>	<i>f₄</i>	<i>f₅</i>	<i>uX</i>	
Imported Products (m)		<i>m₁</i>	<i>m₂</i>	...	<i>m_m</i>	<i>md</i>	<i>mf₁</i>	<i>mf₂</i>	<i>mf₃</i>	<i>mf₄</i>	<i>mf₅</i>	<i>mX</i>	
Taxes less Subsidies on Products (t)		<i>t₁</i>	<i>t₂</i>	...	<i>t_m</i>	<i>td</i>	<i>tf₁</i>	<i>tf₂</i>	<i>tf₃</i>	<i>tf₄</i>	<i>tf₅</i>	<i>tX</i>	
Gross Value Added (v)		<i>v₁</i>	<i>v₂</i>	...	<i>v_m</i>	<i>vd</i>	<i>vf₁</i>	<i>vf₂</i>	<i>vf₃</i>	<i>vf₄</i>	<i>vf₅</i>	<i>vX</i>	
Total Input (X _j)		<i>X₁</i>	<i>X₂</i>	...	<i>X_m</i>	<i>Xd</i>	<i>Xf₁</i>	<i>Xf₂</i>	<i>Xf₃</i>	<i>Xf₄</i>	<i>Xf₅</i>	<i>XX</i>	

RAS Method

RAS is an iterative procedure which involves two diagonal matrices, that is, a diagonal matrix of row multipliers, \hat{r} and a diagonal matrix of column multipliers, \hat{s} (Stone, 1962; Stone and Brown, 1962). It is named after the typical sequence of matrices, where the matrix of input coefficients, A(1) is obtained by pre-multiplying the corresponding matrix of A(0) by \hat{r} to obtain $\hat{r}A(0)$ and post-multiplying $\hat{r}A(0)$ by \hat{s} to obtain $\hat{r}A(0)\hat{s}$. The estimation process of obtaining A(1) from A(0) involves achieving convergence using proportional adjustment of the base year I-O matrix elements successively along the rows and columns. After several iterations, the cells in the adjusted matrix will sum up to the required row and column totals of the current year. The data required for RAS is the shaded area of the simplified I-O table shown in Table 1 which includes total intermediate input, total intermediate demand, final

demand, gross value-added, taxes less subsidies on products, imported commodities, total input and total output.

Let $A(0)$ be the input coefficient matrix corresponding to the base year I-O table and $A(1)$ is the projected input coefficients matrix corresponding to the projected I-O table. Then,

$$A(1) = \hat{r}A(0)\hat{s} \tag{1}$$

where, \hat{r} is diagonal matrix of row multipliers

\hat{s} is diagonal matrix of column multipliers

In matrix notation,

$$A(1) = \begin{bmatrix} r_1 & 0 & \cdots & 0 \\ 0 & r_2 & \cdots & 0 \\ \vdots & \vdots & \ddots & \vdots \\ 0 & 0 & \cdots & r_n \end{bmatrix} \times \begin{bmatrix} a_{11} & a_{12} & \cdots & a_{1n} \\ a_{21} & a_{22} & \cdots & a_{2n} \\ \vdots & \vdots & \ddots & \vdots \\ a_{n1} & a_{n2} & \cdots & a_{nn} \end{bmatrix} \times \begin{bmatrix} s_1 & 0 & \cdots & 0 \\ 0 & s_2 & \cdots & 0 \\ \vdots & \vdots & \ddots & \vdots \\ 0 & 0 & \cdots & s_n \end{bmatrix}$$

$$= \begin{bmatrix} r_1 a_{11} s_1 & r_1 a_{12} s_2 & \cdots & r_1 a_{1n} s_n \\ r_2 a_{21} s_1 & r_2 a_{22} s_2 & \cdots & r_2 a_{2n} s_n \\ \vdots & \vdots & \ddots & \vdots \\ r_n a_{n1} s_1 & r_n a_{n2} s_2 & \cdots & r_n a_{nn} s_n \end{bmatrix}$$

From matrix notation, it can be seen that each row of the matrix has a common r factor and each column has a common s factor. The r factors are called the *substitution* factors because they adjust each column for substitution effects and s factors are called the *fabrication* factors because they always change the fabricants of production.

The elements of $A(0)$ is obtained as follows:

$$A(0) = \begin{bmatrix} a_{11} & a_{12} & \cdots & a_{1n} \\ a_{21} & a_{22} & \cdots & a_{2n} \\ \vdots & \vdots & \ddots & \vdots \\ a_{n1} & a_{n2} & \cdots & a_{nn} \end{bmatrix}$$

where $a_{ij} = \frac{\sum_{j=1}^n z_{ij}}{X_j}$,

z_{ij} is intermediate input and X_j is total input

Let $Z(1)$ be the input-output flow matrix of the projected year which is unknown, $Y(1)$ is the known output vector and $A(1)$ is the new coefficient matrix to be estimated corresponding to $Z(1)$. If $Y(1)$ is converted into a diagonal matrix and indicated by the sign $\hat{\cdot}$ over it, hence,

$$\begin{aligned} Z(1) &= A(1)\hat{Y}(1) \\ &= [\hat{r}A(0)\hat{s}]\hat{Y}(1) \end{aligned} \tag{2}$$

Let d^* to be the row total of intermediate demand of matrix $Z(1)$, then

$$\begin{aligned} d^* &= Z(1)i \\ &= [\hat{r}A(0)\hat{s}]\hat{Y}(1)i \\ &= [\hat{r}A(0)\hat{Y}(1)]\hat{s}i \\ &= \hat{r}[A(0)\hat{Y}(1)]\hat{s} \end{aligned} \tag{3}$$

where, i is a column vector in which each element is equal to 1.

Vector i is used to sum the flow matrix across the rows, that is to obtain the row sums of the flow matrix $Z(1)$.

Let u^* to be the column totals of $Z(1)$, then

$$\begin{aligned} u^* &= Z(1)'i \quad \text{and} \\ u^* &= i'Z(1) \\ &= r'[A(0)\hat{Y}(1)]\hat{s} \end{aligned} \tag{4}$$

where, r' is a row vector

Equations [3] and [4] consist of two unknown r and s , the known information on the coefficient matrix, $A(0)$, the new row and column constraints d^* and u'^* and the new output level, $Y(1)$. Thus, if these equations are solved simultaneously, then the values of the r and s vectors can be calculated and then the projected matrix $A(1)$ can be derived on the basis of equation (1). By repetition of equation (1), we would find (Source: Miller and Blair, 2009),

$$\begin{aligned} A(1) &= \hat{r}^1 A(0) \hat{s} \\ A(2) &= \hat{r}^1 A(0) \hat{s}^1 \\ A(3) &= [\hat{r}^2 \hat{r}^1] A(0) [\hat{s}^1] \\ A(4) &= [\hat{r}^2 \hat{r}^1] A(0) [\hat{s}^1 \hat{s}^2] \\ &\vdots \\ A(2n) &= [\hat{r}^n \dots \hat{r}^1] A(0) [\hat{s}^1 \dots \hat{s}^n] \end{aligned} \tag{5}$$

Euro Method

The Euro method was developed by Beutel (2002). It corresponds to the basic idea of RAS approach. The fundamental aim is to develop a series of reliable and consistent input-output tables, which is dependent on official macroeconomic data (GDP). However, to ensure a consistent system, any arbitrary adjustments of input coefficients are avoided. The beginning point of the iteration procedure is an I-O table consisting of value added by industry and total final demand by use. The iteration procedure commences with the assumption that, in the first iteration, the given growth rates for value added by sectoral, final demand by use categories and total value added as the starting point for the unknown growth rates characterising the activity levels of input and output sectors. The growth rates will be marginally adjusted until the projected exogenous variables are reproduced.

The data required for EURO is the projected year t , that is, vectors of gross value added by industries, v_j , totals of final demand by use category, Xf_j , and total gross value added, vY . Thus, the original base year I-O table at basic prices consist of intermediate input (z_{11}, \dots, z_{nm}), final demand (f_{11}, \dots, f_{n5}) and value added (v_1, \dots, v_m).

$$\text{The growth rates is defined as, } p = \frac{v(1)_j}{v(0)_j} \quad (6)$$

where, $v(0)_j$ is actual value j for base year, $j=1, \dots, m$

$v(1)_j$ is macroeconomic statistics j for projected year t , $j=1, \dots, m$

is the basis for updating the intermediate input, z_{11}, \dots, z_{nm} , and final demand, f_{11}, \dots, f_{n5} . The growth rates for input is $W0$ and for output is $W1$. The growth rates for the activity levels of the corresponding input and output sector for each element in the I-O table is weighted in an iterative procedure. On completion of weighting the transactions, the resulting input-output table might not be expected to be consistent. Therefore, a traditional input-output model with projected I-O table is solved to guarantee the consistency of the system in terms of supply and demand.

The I-O matrix is then weighted with row multipliers for inputs, $T2$, where, $T2=W0*T1$ and column multipliers for outputs, $T3$, where, $T3=T1*W1$. By calculating the average I-O matrix weighted with row multipliers, $T2$, and column multipliers, $T3$, we obtain inconsistent I-O table, $T4$, where, $T4=(T2+T3)/2$.

Based on inconsistent I-O table, input coefficient and Leontief inverse are calculated.

$$a_{ij} = x_{ij} / X_j \quad (7)$$

$$\text{Leontief inverse} = (I - A)^{-1}$$

where, a_{ij} is input coefficients for domestic goods and services

z_{ij} is intermediate input of goods and services

X_j is total input of goods and services

I is identity matrix,

A is matrix of input coefficient

The Leontief inverse was then multiplied with vector of final demand to derive total output,

$$Y = (I - A)^{-1} f \quad (8)$$

where, Y is total output of goods and services

f is column vector of final demand.

The consistent I-O table is established through several adjustments of row multiplier and column multiplier in n iterations. The rates used are then adjusted in an iterative procedure in which the difference between the actual and the projected rates is minimal (less than one per cent).

The deviation, d , between macroeconomic variables of projected year and base year is defined as,

$$d = \frac{p0}{p1} \quad (9)$$

where, d is deviation

$p0$ is growth rates between projected year (before iteration) and base year

$p1$ is growth rates between projected year (after iteration) and base year

The observed deviations are used to correct the rates of $W0$ and $W1$ during the iteration. Hence, a convex adjustment function is recommended to adjust the rates. If the model underestimates or overestimates the projected macroeconomic variables, the corresponding rates, $W0$ and $W1$ respectively are increased or decreased according to the convex adjustment function. The adjustment function is defined as,

$$af = 1 - \frac{[(1-d)100]c}{100} \quad \text{if } d < 0 \quad (10)$$

$$af = 1 + \frac{[(d-1)100]c}{100} \quad \text{if } d > 0 \quad (11)$$

where, af is adjustment function

d is deviation

c is adjustment elasticity (for this study, $c=0.9$ is used based on simulation results)

Based on the adjustment function, the revised row multipliers for input, $W0(2)=W0*af$ and revised column multipliers for output, $W1(2)=W1*af$ are then calculated. With revised row and column multipliers, revised I-O matrix is obtained. The rates for input and output are marginally changed during the iteration until the projected rates for gross value added and final demand correspond with macroeconomic data. Each iteration begins with computing new correction factors, which is then multiplied by the row and column adjustment multipliers from the previous iteration. The iteration is completed if the deviation of projected and macroeconomic variables is within the one percent margin.

Assessing Projection Method

The RAS and EURO methods produce different MIO table estimates, thus it is desirable to assess their relative performance. There are several forms of error measures being used for evaluation. However, no particular error measure has been found to be best under all situations and for all types of data (Armstrong, 2006). In most applications, they tend to produce different results for different method type. Thus, in this study, the three statistics used were MAD, RMSE and DI to measure the performance of RAS and EURO methods based on the closeness of the estimates to the actual matrices.

RESULTS

The application of the RAS procedure and EURO method were done using Excel and Excel Visual Basic Programming. The rows and columns entries were iteratively changed until convergence was reached between the row and column sums of the new total. However, due to space constraint, only the projected I-O table for 2010 using EURO method is displayed in Table 2.

Table 2
Projected Malaysia Input-Output Table 2010 using EURO Method

INDUSTRY	PROJECTED USE MATRIX OF DOMESTIC PRODUCTION AT BASIC PRICES												TOTAL INTERMEDIATE DEMAND						TOTAL FINAL DEMAND					
	1	2	3	4	5	6	7	8	9	10	11	12	13	14	15	16	17	18	19	20				
12 INDUSTRY x 12 INDUSTRY (RM Million)	Agriculture, Fishery & Forestry	Mining & Quarrying	Manufacturing	Electricity, Gas & Water	Construction	Wholesale & Retail Trade	Hotel & Restaurants	Transport & Communication	Finance & Insurance	Real Estate & Ownership of Dwellings	Business & Private Services	Government Services	Private Consumption	Government Consumption	Gross Fixed Capital Formation	Change in Inventories	Exports	Imports	Government Expenditure	Household Expenditure				
1 Agriculture, Fishery & Forestry	12,749	407	64,033	39	202	2,536	20	103	165	9	18	618	80,900	12,255	1	2,864	(7,226)	18,589	26,483	107,382				
2 Mining & Quarrying	211	548	44,110	820	2,289	469	31	151	175	18	44	363	49,229	1,019	0	6,654	1,277	57,366	66,316	115,545				
3 Manufacturing	11,368	11,872	359,820	10,576	28,194	7,038	4,512	15,989	2,992	1,078	2,701	11,804	467,944	111,640	445	13,748	6,174	559,545	691,553	1,159,497				
4 Electricity, Gas & Water	566	273	10,187	8,992	356	993	2,548	1,572	710	563	981	2,367	30,108	15,608	181	36	(47)	2,888	18,667	48,775				
5 Construction	12	2,030	8,743	2,366	640	522	56	3,974	47	7,605	171	11,490	37,657	20,301	-	39,429	2	81	59,813	97,470				
6 Wholesale & Retail Trade	2,589	5,779	58,823	596	3,126	5,738	624	2,272	3,159	253	937	5,376	89,271	12,739	1	8,018	375	22,420	43,552	132,823				
7 Hotel & Restaurants	5	22	328	182	572	3,147	11,721	244	120	84	125	1,235	17,786	31,922	47	21	1	309	32,299	50,085				
8 Transport & Communication	1,197	1,534	23,198	585	3,985	4,684	1,533	38,653	6,883	504	3,934	5,824	92,725	29,699	26	3,652	109	29,439	62,925	155,649				
9 Finance & Insurance	1,265	61	12,014	196	3,031	2,703	1,318	18,793	33,934	1,116	1,557	620	76,009	13,723	42	0	(0)	21,972	35,737	112,346				
10 Real Estate & Ownership of Dwellings	0	95	16	45	0	1,695	3,152	3,445	1,276	3,674	1,567	2,557	17,522	28,112	0	0	(0)	0	28,112	45,634				
11 Business & Private Services	306	1,112	4,785	822	3,683	2,457	1,660	4,832	3,873	922	13,250	5,966	43,770	5,679	2,238	1,308	0	30,913	40,138	83,908				
12 Government Services	10	93	510	213	460	573	324	2,666	494	393	776	8,456	14,970	14,734	88,733	11	3,265	7,593	114,335	129,305				
TOTAL INTERMEDIATE INPUT	30,279	23,827	586,565	25,432	46,548	32,555	27,500	92,996	53,830	16,219	26,062	56,675	1,018,490	297,431	91,714	75,741	3,931	751,114	1,219,930	2,238,420				
13 Imported Products	6,704	5,975	374,371	4,103	23,644	5,474	1,944	11,829	877	1,127	13,353	13,942	463,243	60,993	9,262	101,280	-	28,440	199,975	663,218				
14 Taxes less Subsidies on Products	1,325	106	11,347	212	518	162	89	368	166	16	814	42	15,165	18,796	1,049	2,757	-	1,951	24,553	39,718				
15 Gross Value Added	69,075	85,636	187,214	19,028	26,760	94,632	20,662	50,456	57,473	28,272	43,679	58,646	741,522	-	-	-	-	-	-	741,522				
TOTAL INPUT	107,382	115,545	1,159,497	48,775	97,470	132,823	50,085	155,649	112,346	45,634	83,908	129,305	2,238,420	377,220	102,026	179,778	3,931	781,504	1,444,458	3,682,878				

In order to determine whether the RAS or EURO method performs better in projecting the MIOT for 2005 and 2010, they were evaluated using three error measures - the MAD, RMSE and DI methods. The results shown in Table 3 and Table 4 indicate the EURO method has on the average the smallest MAD, RMSE and DI. In 2005, the EURO method registered a smaller MAD (0.020), RMSE (0.036) and DI (0.421). Similarly, in 2010 the MAD (0.018), RMSE (0.031) and DI (0.460) also registered smaller values of error measures. Therefore, we can conclude that the EURO method performed better than RAS based on the smaller value of MAD, RMSE and DI.

Table 3

Assessment of RAS and EURO Method for year 2005

2005		MAD		RMSE		DI	
Sector		RAS	EURO	RAS	EURO	RAS	EURO
1	Agriculture, Fishery & Forestry	0.013	0.009	0.028	0.016	0.651	0.514
2	Mining & Quarrying	0.013	0.012	0.024	0.024	0.604	0.486
3	Manufacturing	0.010	0.018	0.019	0.043	0.364	0.307
4	Electricity, Gas & Water	0.045	0.031	0.065	0.052	0.556	0.452
5	Construction	0.010	0.011	0.013	0.014	0.317	0.302
6	Wholesale & Retail Trade	0.018	0.018	0.024	0.027	0.598	0.441
7	Hotel & Restaurant	0.052	0.045	0.086	0.074	0.491	0.509
8	Transport & Communication	0.033	0.026	0.055	0.050	0.396	0.442
9	Finance & Insurance	0.035	0.012	0.070	0.018	0.544	0.399
10	Real Estate & Ownership of Dwelling	0.033	0.017	0.050	0.041	0.522	0.339
11	Business & Private Services	0.024	0.017	0.036	0.028	0.506	0.451
12	Government Services	0.036	0.021	0.046	0.031	0.597	0.414
Average		0.027	0.020	0.043	0.035	0.512	0.421

Table 4

Assessment of RAS and EURO Method for year 2010

2010		MAD		RMSE		DI	
Sector		RAS	EURO	RAS	EURO	RAS	EURO
1	Agriculture, Fishery & Forestry	0.015	0.011	0.024	0.019	0.530	0.528
2	Mining & Quarrying	0.037	0.011	0.092	0.019	0.673	0.534
3	Manufacturing	0.030	0.016	0.071	0.033	0.304	0.335
4	Electricity, Gas & Water	0.038	0.025	0.086	0.045	0.561	0.561
5	Construction	0.010	0.018	0.016	0.026	0.370	0.517
6	Wholesale & Retail Trade	0.023	0.014	0.042	0.031	0.860	0.390
7	Hotel & Restaurant	0.015	0.040	0.021	0.065	0.389	0.562
8	Transport & Communication	0.028	0.011	0.052	0.018	0.284	0.344
9	Finance & Insurance	0.048	0.009	0.078	0.012	0.427	0.488
10	Real Estate & Ownership of Dwelling	0.024	0.027	0.046	0.051	0.509	0.451
11	Business & Private Services	0.026	0.014	0.042	0.026	0.793	0.397
12	Government Services	0.054	0.023	0.086	0.030	0.809	0.413
Average		0.029	0.018	0.055	0.031	0.542	0.460

CONCLUSION

Our empirical application of RAS procedure and EURO method to project Malaysia's Input-Output tables, suggest that the EURO method gives the best projection estimates. The EURO method has been found to be robust, less expensive, minimal data requirement and not requiring arbitrary changes of input coefficients. Hence, the EURO method is suggested for the projection of the I-O table for Malaysia to assist in economic planning and decision-making.

REFERENCES

- Armstrong, J. S. (2006). Findings from evidence-based forecasting: Methods for reducing forecast error. *International Journal of Forecasting*, 22(3), 583–598.
- Bacharach, M. (1970). *Biproportional Matrices and Input-Output Change*. New York, NY: Cambridge University Press.
- Beutel, J. (2002). *The Economic Impact of Objective 1 Interventions for the Period 2000-2006*. Report to the Directorate-General for Regional Policies, Konstanz.
- Butterfield, M., & Mules, T. (1980). A Testing Routine for Evaluating Cell by Cell Accuracy in Short-Cut Regional Input-Output Tables. *Journal of Regional Science*, 20(3), 293-310.
- DOSM. (2011). *Malaysia Input-Output Tables, 2010*. Department of Statistics, Malaysia.
- DOSM. (2010). *Malaysia Input-Output Tables, 2005*. Department of Statistics, Malaysia.
- DOSM. (2005). *Malaysia Input-Output Tables, 2000*. Department of Statistics, Malaysia.
- DOSM. (2014). *Annual National Accounts Gross Domestic Product (GDP), 2005-2013*. Department of Statistics, Malaysia.
- Deming, W. E., & Stephan, F. F. (1940). On a Least Squares Adjustment of a Sampled Frequency Table when the Expected Marginal Totals are Known. *The Annals of Mathematical Statistics*, 11(4), 427-444.
- Eurostat. (2008). *European Manual of Supply, Use and Input-Output Tables, Methodologies and Working Papers*. Luxembourg: European Communities.
- Gunluk-Senesen, G., & Bates, J. M. (1988). Some Experiments with Methods of Adjusting Unbalanced Data Matrices. *Journal of the Royal Statistical Society, Series A*, 151(3), 473-490.
- Junius, T., & Oosterhaven, J. (2003). The Solution of Updating or Regionalizing A Matrix with Both Positive & Negative Entries. *Economic System Research*, 15(1), 88-96.
- Miller, R. E., & Blair, P. D. (2009). *Input-Output Analysis - Foundations and Extensions*. United States of America (USA): Cambridge University Press.
- Oosterhaven, J., Pick, G., & Stelder, D. (1986). Theory and Practice of Updating Regional Versus Interregional Interindustry Tables. *Papers of the Regional Science Association*, 59(1), 57-72.
- Parikh, A. (1979). Forecast of Input-Output Matrices Using the R.A.S. Method. *The Review of Economics and Statistics*, 61(3), 477-481.
- Saari, M. Y., Hassan, A., Rahman, M. D. A., & Mohamed, A. (2014). Evaluation of the Relative Performance of RAS and Cross-Entropy Techniques for Updating Input-Output Tables of Malaysia. *Malaysian Journal of Economic Studies*, 51(2), 217-229.

- Stephan, F. F. (1942). An Iterative Method of Adjusting Sample Frequency Tables when Expected Marginal Totals are Known. *The Annals of Mathematical Statistics*, 13(2), 166-178.
- Stone, R. (1961). *Input-Output and National Accounts*. Paris: Organization for European Economic Cooperation.
- Stone, R., & Brown, A. (1962). *A computable model of economic growth* (Vol. 1). London: Chapman and Hall.
- Temurshoev, U., Webb, C., & Norihiko, Y. (2011). Projection on Supply and Use Tables: Methods & their Empirical Assessment. *Economic Systems Research*, 23(1), 91-123.
- Temurshoev, U., Miller, R. E., & Bouwmeester, M. C. (2013). A Note on the GRAS Method. *Economic Systems Research*, 25(3), 361-367.





Relative Risk Estimation for Dengue Disease Mapping in Malaysia based on Besag, York and Mollié Model

Samat, N. A.* and Pei Zhen, W.

Department of Mathematics, Faculty of Science and Mathematics, Universiti Pendidikan Sultan Idris, 35900 Tanjung Malim, Perak, Malaysia

ABSTRACT

In the study of disease mapping, relative risk estimation is the focus of analysis. Many methods have been introduced to estimate relative risk. In this paper, one of the common spatial models known as Besag, York and Mollié (BYM) model is discussed, and its application to dengue data for epidemiology weeks 1 to 52 of the year 2013 for 16 states in Malaysia is studied. Findings show that Selangor has the highest relative risk of dengue in comparison with other states. Data on the estimated relative risks are presented in the form of risk maps which can be used as a tool for the prevention and control of dengue.

Keywords: Relative risk estimation, disease mapping, dengue disease, BYM model

INTRODUCTION

Disease mapping is the visual representation of the spatial and geographic distribution of specified diseases and the corresponding risk. In recent years, disease mapping has become an important tool and technique of epidemiologists, biostatisticians, medical demographics and academics working on disease epidemiology and health services. A disease map displays the geographic areas with high and low incidence, prevalence or mortality rates of a specific diseases. In this paper, dengue is the disease of interest.

Dengue is a major global health problem in which the viruses are transmitted by the infective bite of female mosquito of species genus *Aedes*. This paper investigates the dengue disease mapping in Malaysia. In this research, Besag, York and Mollié (BYM) model is used as the alternative method to estimate the relative risk of dengue occurrence in human populations in Malaysia.

First, a brief introduction to the BYM method will be discussed. Data on dengue cases in Malaysia are used to estimate relative risk using WinBUGS software to carry out Markov chain Monte Carlo (MCMC)

Article history:

Received: 27 May 2016

Accepted: 14 November 2016

E-mail addresses:

norazah@fsm.upsi.edu.my (Samat, N. A.),

Peizhen123@yahoo.com (Pei Zhen, W.)

*Corresponding Author

computations of Bayesian models. Expected disease risk is presented and analysed using graph and risk map. The disease risk map will display the high and low disease risk incidences of the dengue diseases in 16 states of Malaysia.

BESAG, YORK AND MOLLIE (BYM) MODEL

In this paper, the Besag, York and Mollie model is applied to the observed dengue disease data to estimate the relative risks for the 16 states in Malaysia. This model was first introduced by Clayton & Kaldor (1987) as an empirical Bayesian and later developed to a fully Bayesian setting by Besag, York and Mollie (Besag, York, & Mollie, 1991).

There are three stages of the BYM model which are described in Lawson, Browne & Rodeiro (2003). In the first stage, for $i = 1, 2, \dots, M$ study regions, the observed numbers of dengue cases y_i are assumed to follow a Poisson distribution. The mean and variance for this distribution are the same which is $e_i \theta_i$. Here, e_i represents the expected number of new infective, while θ_i refers to the relative risk. Hence, the model is formulated as follows:

$$y_i \sim \text{Poisson}(e_i \theta_i) \tag{1}$$

$$\log(\theta_i) = \alpha + u_i + v_i \tag{2}$$

From Equation (2), the term α represents the intercept of the model which is an overall level of the relative risk, while the terms u_i and v_i represent the correlated and uncorrelated heterogeneities, respectively.

In the second stage, a Bayesian model needs specification of prior distribution for the random effects and intercept term. Here, the distribution model for v_i does not depend on geographic location and is assumed to follow a normal distribution which can be written as follows.

$$v_i \sim N(0, \tau_v^2) \tag{3}$$

While for the spatial correlation structure, u_i is used. Here, the risk estimation in any area depends on the spatial correlation between neighbouring areas. This distribution model is called the conditional autoregressive (CAR) model which is written in Equation (4).

$$[u_i | u_{p, i \neq j}, \tau_u^2] \sim N(\bar{u}_i, \tau_i^2) \tag{4}$$

where

$$\bar{u}_i = \frac{\sum_j u_j \omega_{ij}}{\sum_j \omega_{ij}}, \quad \tau_i^2 = \frac{\tau_u^2}{\sum_j \omega_{ij}}$$

For each u_i , the prior mean is in the form of weighted average of the other u_j in which $i \neq j$. The weightage, w_{ij} , defines the relationship between the areas i and its adjacent areas j based on the following scheme.

$$w_{ij} = \begin{cases} 1 & \text{if } i, j \text{ are adjacent} \\ 0 & \text{otherwise} \end{cases}$$

The variability for the random effect is controlled by the precision parameters τ_u^2 .

Finally, in the final stage, as a fully Bayesian analysis, the model specification is completed by adding hyper-prior distributions to the parameters τ_v^2 and τ_u^2 . As suggested by Johnson (2004), the Gamma hyper prior distribution was chosen.

APPLICATION OF RELATIVE RISK ESTIMATION TO DENGUE DISEASE MAPPING

This section displays the result of relative risk estimation based on the application of Besag, York and Mollié (BYM) model to observed dengue data in Malaysia.

Data Set

The data used in this analysis were provided by the Ministry of Health Malaysia, consisting of the observed count dengue data for every state in Malaysia from epidemiology week 1 to epidemiology week 52 of the year 2013. 16 states were involved in this study, which were Perlis, Kedah, Pulau Pinang, Perak, Kelantan, Terengganu, Pahang, Selangor, Kuala Lumpur, Putrajaya, Negeri Sembilan, Melaka, Johor, Sarawak, Labuan and Sabah.

Analysis and Results: Relative risk estimation based on BYM Model

This section presents the results of the analysis based on the BYM model. Figure 1 depicts the time series plot of cases of dengue disease for all 16 states in Malaysia from epidemiology week 1 to epidemiology week 52. It can be seen for every epidemiology week, Selangor had the highest number of cases. The number of cases shows an increasing trend and reached the peak in epidemiology week 52 with 1408 cases. While for other states, most states had less than 200 cases for most of the epidemiology weeks in 2013. The lowest number of cases is in Labuan, which reported only 14 cases of dengue. It is free from dengue for the first 20 weeks to increase to by week 49.

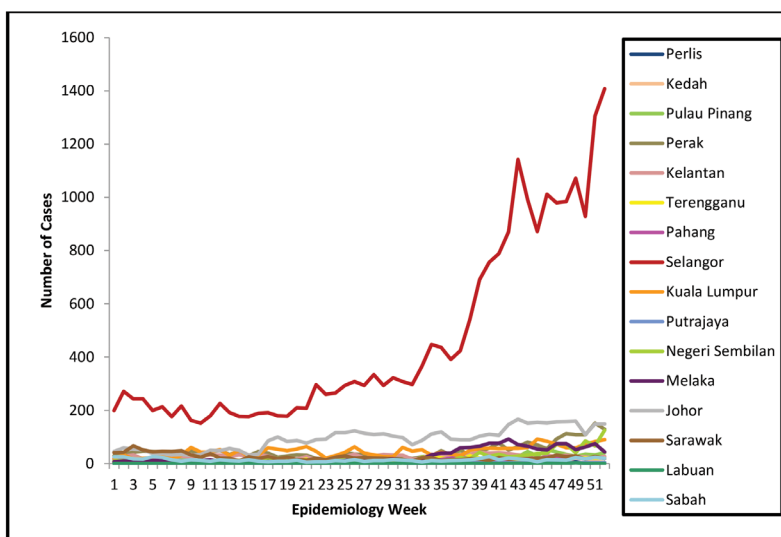


Figure 1. Time series plot for the number of dengue cases for all states in Malaysia

Figure 2 represents the time series graph of the estimated relative risk based on Besag, York and Mollié (BYM) model for dengue disease in Malaysia in 2013. The graph shows that Selangor had the highest number of relative risk of contracting dengue having relative risks above 2 for most epidemiology weeks. Based on the definition of relative risk found in Samat & Percy (2012) and Samat & Ma'arof (2013), a relative risk greater than 2 means that people in these states have a higher likelihood of contracting dengue compared to the rest of the country.

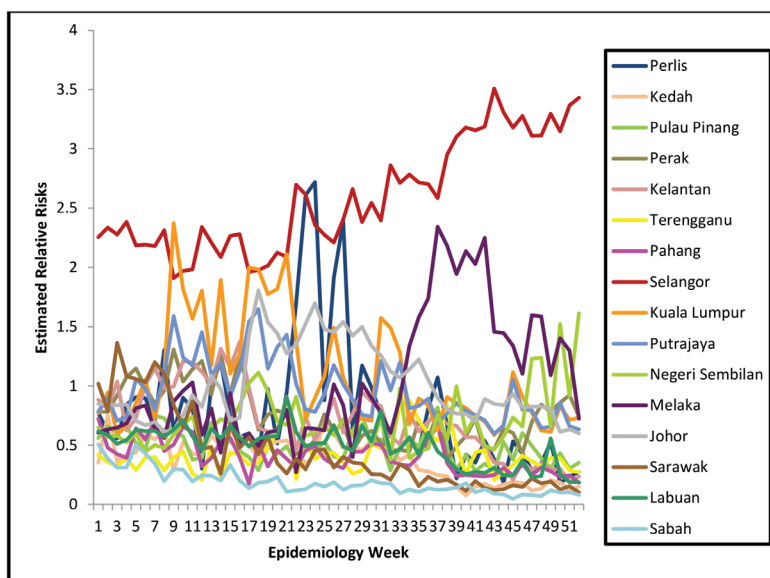


Figure 2. Time series plots for the estimated relative risks based on the BYM Model for all states in Malaysia

Table 1 shows the posterior means for the relative risk in 16 states of Malaysia obtained using the BYM model. The results give specific estimated relative risks for epidemiology week 52 and it can be seen that the state of Selangor has the highest risk.

Table 1
Estimated Relative Risks Based On BYM Model for Epidemiology Week 52

States	Relative Risk	Standard Deviation
Perlis	0.2738	0.1154
Kedah	0.1507	0.0313
Pulau Pinang	0.3535	0.0539
Perak	0.7407	0.0648
Kelantan	0.2354	0.0436
Terengganu	0.2723	0.0571
Pahang	0.1830	0.0398
Selangor	3.4310	0.0924
Kuala Lumpur	0.7309	0.0771
Putrajaya	0.6341	0.2851
Negeri Sembilan	1.6130	0.1439
Melaka	0.7242	0.1081
Johor	0.6006	0.0496
Sarawak	0.1018	0.0230
Labuan	0.1879	0.1242
Sabah	0.0812	0.0180

Dengue Risk Maps

In this section, the estimated relative risks are displayed in a form of risk maps. It provides a quick overview of the collected information, so that further attention and action can be given to these priority states. The interpretation of the maps is based on the tone of colours used. Darkest colour represents very high risk while the lightest colour represents very low risk.

Figures 3 and 4 show thematic risk maps for dengue disease based on the number of observed cases and the expected relative risk estimated by BYM model, respectively. Both maps demonstrate the results for epidemiology week 52 in the year 2013 for all 16 states in Malaysia. The relative risks are categorized into five different levels of risk, which are very low, low, medium, high and very high with respective intervals.

Figure 3 represents the risk map for dengue disease based on the number of cases for epidemiology week 52. The five category of risk are determined based on the intervals of $[0,300)$, $[300,600)$, $[600,900)$, $[900,1200)$, and $[1200,\infty)$, respectively. This figure depicts that state with very high risk for dengue occurrences is Selangor. The other 15 states are classified as very low risk areas.

Furthermore, Figure 4 represents the risk map for dengue disease based on BYM model for epidemiology week 52. There are five categories of risk area which are determined based on the intervals of $[0.0, 0.5)$, $[0.5, 1.0)$, $[1.0, 1.5)$, $[1.5, 2.0)$, and $[2.0, \infty)$, respectively. From this figure, Selangor showed has a very high risk area of dengue occurrence, followed by Negeri Sembilan with high risk. States with low risk include Perak, Kuala Lumpur, Putrajaya, Melaka and Johor. The other states with very low risk are Perlis, Pulau Pinang, Kelantan, Terengganu, Sarawak, and Labuan in Sabah.

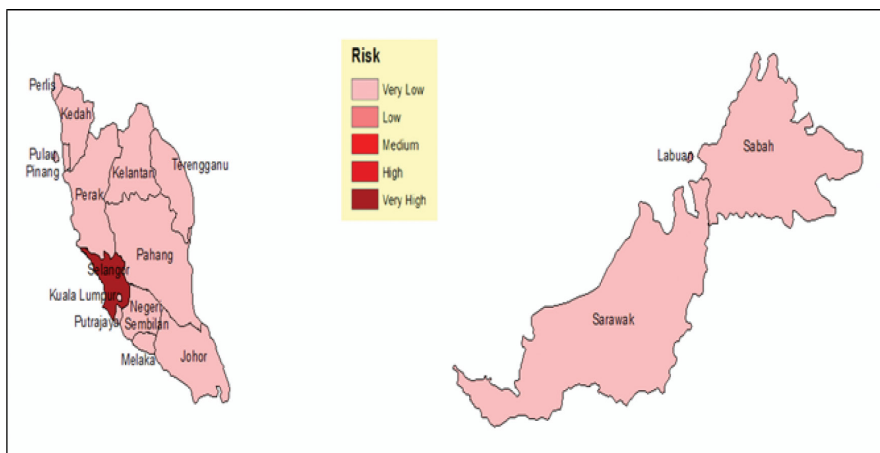


Figure 3. Risk map for dengue disease based on number of cases for Epidemiology Week 52

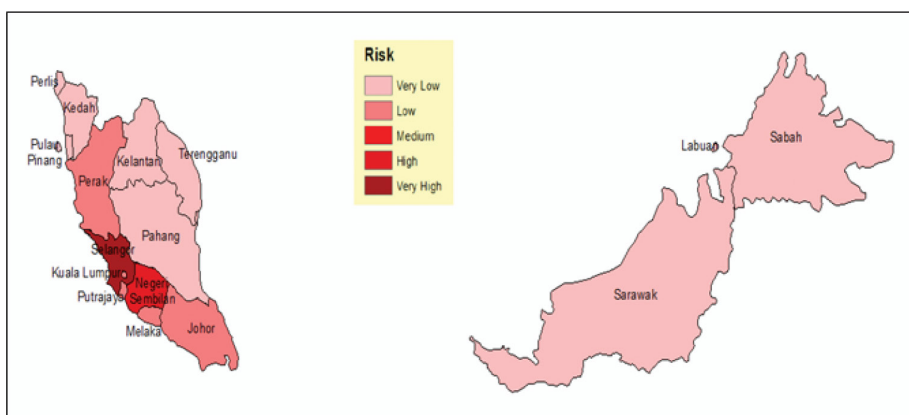


Figure 4. Risk map for dengue disease based on BYM model for Epidemiology Week 52

Comparisons among the map of Figures 3 and 4, specifically for epidemiology week 52, demonstrate no obvious differences in terms of the estimated risks for dengue disease in 16 states. However, further action and precautionary steps need to be implemented in every state, particularly in Selangor in which the people has very high risk to contract with dengue disease compared to people in overall population.

DISCUSSION AND CONCLUSION

Dengue is a major public health issue in Malaysia and is likely to remain endemic for a long time. The production of an accurate disease map relies on statistical modelling used to estimate the relative risk. The purpose of exploratory disease mapping is to provide insight into possible causes, effects and trends, and impression of the geographical or spatial distribution of disease.

In this paper, Besag, York and Mollié (BYM) model was used to estimate the relative risk of dengue. The results of the analysis showed that Selangor has very high risk of dengue, arising from higher rainfall, humidity, temperature, and urbanization. In order to avoid the spread of dengue surrounding area should be clean and free of water reservoir, requiring public and community commitment to hygiene. Disease risk maps can be useful for prevention and control strategies of dengue.

ACKNOWLEDGEMENT

The authors acknowledge Universiti Pendidikan Sultan Idris and the Ministry of Higher Education in Malaysia for their financial support in respect of this study.

REFERENCES

- Besag, J., York, J., & Mollié, A. (1991). Bayesian Image Restoration, With Two Applications in Spatial Statistics. *Annals Of The Institute Of Statistical Mathematics*, 43(1), 1-20.
- Clayton, D., & Kaldor, J. (1987). Empirical Bayes Estimates of Age-Standardized Relative Risks for Use in Disease Mapping. *Biometrics*, 43(3), 671-681.
- Johnson, G. D. (2004). Small Area Mapping of Prostate Cancer Incidence in New York State (USA) using Fully Bayesian Hierarchical Modelling. *International Journal of Health Geographics*, 3(1), 1-12.
- Lawson, A. B., Browne, W. J., & Rodeiro, C. L. V. (2003). *Disease mapping with WinBUGS and MLwiN* (Vol. 11). England: John Wiley & Sons.
- Samat, N. A., & Ma'arof, S. M. I. (2013). Dengue Disease Mapping with Standardized Morbidity Ratio and Poisson-gamma Model: An Analysis of Dengue Disease in Perak, Malaysia. *International Journal of Mathematical Science and Engineering*, 7(8), 1299-1303.
- Samat, N. A., & Percy, D. F. (2012). Dengue Disease Mapping in Malaysia Based on Stochastic SIR Models in Human Populations. *International Conference on Statistics in Science, Business, and Engineering (ICSSBE 2012)* (pp. 1-5). IEEE.





Effects of Baseline Correction Algorithms on Forensic Classification of Paper Based on ATR-FTIR Spectrum and Principal Component Analysis (PCA)

Lee, L. C.¹, Liong, C-Y.^{2*}, Khairul, O.¹ and Jemain, A. A.²

¹Forensic Science Program, Faculty of Health Sciences, Universiti Kebangsaan Malaysia, 50300 Kuala Lumpur, Malaysia

²School of Mathematical Sciences, Faculty of Science and Technology, Universiti Kebangsaan Malaysia, 43600 UKM, Bangi, Selangor, Malaysia

ABSTRACT

Spectral data is often required to be pre-processed prior to applying a multivariate modelling technique. Baseline correction of spectral data is one of the most important and frequently applied pre-processing procedures. This preliminary study aims to investigate the impacts of six types of baseline correction algorithms on classifying 150 infrared spectral data of three varieties of paper. The algorithms investigated were Iterative Restricted Least Squares, Asymmetric Least Squares (ALS), Low-pass FFT Filter, Median Window (MW), Fill Peaks and Modified Polynomial Fitting. Processed spectral data were then analysed using Principal Component Analysis (PCA) to visually examine the clustering among the three varieties of paper. Results show that separation among the three varieties of paper is greatly improved after baseline correction via ALS, FP and MW algorithms.

Keywords: Forensic science, paper, baseline correction, principal component analysis (PCA), IR spectroscopy

INTRODUCTION

Forensic document examination is often used in cases of financial fraud. Cheques, certificates and other important documents are examples of forged document often encountered by a forensic document examiner. Fourier transform infrared (FTIR) spectroscopy coupled with attenuated total reflectance (ATR) is one of the preferred non-destructive tools to examine forged documents objectively (Kher et al., 2001; Kher et al., 2005; Causin et al., 2010).

Article history:

Received: 27 May 2016

Accepted: 14 November 2016

E-mail addresses:

lc_lee@ukm.edu.my (Lee, L. C.),

lg@ukm.edu.my (Liong, C-Y.),

khairros@ukm.edu.my (Khairul, O.),

azizj@ukm.edu.my (Jemain, A. A.)

*Corresponding Author

Pre-processing of spectral data has become one of the popular mathematical pre-treatment methods to eliminate variation that does not originate from the analysed chemicals. If the spectral data are not pre-processed in a correct manner, the important information might be masked by irrelevant noises which is not of interest to the analyst (Rinna et al., 2008). There are three loosely defined categories of methods for data pre-processing: (1) signal-to-noise ratio (SNR) enhancing methods; (2) spectral normalisation and differentiation, and (3) methods for variable selection and dimensionality reduction. The fundamental aim of all pre-processing methods is to remove the variation that is detrimental to model performance (Trygg et al., 2009). The effectiveness of derivative on forensic classification of paper based on infrared (IR) spectrum has been studied by Kher et al. (2005). Their study shows that derivation methods can improve discrimination between papers based on their IR spectra by enhancing the relative variations within the data in the different spectral regions (Kher et al., 2005). In fact, there are many well-established pre-processing techniques available (Trygg et al., 2009; Rinna et al., 2009; Engel et al., 2013), but have not yet been applied in the field of forensics.

The objective of this preliminary study is to investigate the effects of six selected baseline correction algorithms: Iterative Restricted Least Squares (IRLS), Asymmetric Least Squares (ALS), Low-pass FFT Filter (FFT), Median Window (MW), Fill Peaks (FP) and Modified Polynomial Fitting (MPF), on classifying paper samples based on IR spectrum.

METHODOLOGY

Paper Samples

Three varieties of papers were purchased from a stationery shop in Kuala Lumpur. Table 1 displays information about the paper samples. More than 15 sheets of papers were sampled from each of the three varieties. For both surfaces of each sheet, one single point was selected randomly to be analysed using ATR-FTIR spectroscopy. Each IR spectrum was composed of 2701 wavenumbers which form the input variables.

Table 1
Paper Samples of Different Brands Analysed in This Study

Code	White Copy Paper Sample	
	Brand	Number of IR spectrum
IY	IK Yellow	29 x 2 = 58
OP	One Paper	29 x 2 = 58
SP	Save Pack	17 x 2 = 34

Software

The IR spectral data were exported to the comma separated values text files (.csv) format; further pre-processing and statistical analysis were performed using the R software environment for statistical computing and graphics (<http://www.r-project.org>) (R Core Team, 2015). This is an open-source project under the GNU General Public License. R has become the de facto standard among statisticians and has a rapidly increasing number of user-submitted packages for all kinds of statistical analyses. The “baseline” package is available on the Comprehensive R Archive Network (<http://cran.r-project.org>) (Liland et al., 2015).

Baseline Correction Algorithms

The baseline in a spectrum is expected to be of zero measurements, is often affected by additive baseline offsets (Engel et al., 2013). IR spectral data obtained from repeated analysis on the same chemicals seldom present a flat baseline. Due to imperfections of analytical instruments and/or other unknown factors, the baseline of the spectra of the same chemicals that were expected to be of zero measurements could attain a positive value. In this preliminary study, only six types of baseline algorithms were studied. Descriptions of the selected baseline algorithms can be found in Liland et al. (2015). A total of 150 IR spectra were subjected to six types of baseline correction algorithms. The lists of studied algorithms that are freely available in “baseline” R package are shown in Table 2.

Table 2

List of Pre-processing Algorithms that are Available from the “Baseline” R Package

Code	Baseline correction algorithm	
	Name	Parameters
b1	Iterative restricted least squares (IRLS)	-
b2	Asymmetric least squares (ALS)	-
b3	Low-pass FFT filter (FFT)	-
b4	Median window (MW)	Window half width for local medians (hwm)
b5	Fill peaks (FP)	2 nd derivative penalty for primary smoothing (lambda), half window (hwi), iteration (it)
b6	Modified polynomial fitting (MPF)	Degree of polynomial (degree)

Principal Component Analysis (PCA)

Principal Component Analysis (PCA) was used to visually examine the separation of the three different varieties of paper. The PCA score plots allow visualisation of the spatial distribution of clusters (Wehrens, 2011; Bro & Smilde, 2014).

RESULTS AND DISCUSSION

IR Spectrum

In general, IR spectra of all three varieties of paper (Figure 1(a)) appeared to present similar spectral patterns. However, minor differences in the form of peak shape and relative peak height were observed in the region between 1200-1500 cm^{-1} . Figures 1 and 2 show the same set of average IR spectra of three varieties of paper in raw format and that were pre-processed with the six studied baseline correction algorithms respectively. In comparison to the raw IR spectra data, spectra processed with baseline correction algorithms showed different spectral patterns, except those that were corrected using IRLS (Figure 1(b)) and MPF (Figure 2(d)) algorithms, respectively. On the other hand, ALS (Figure 1(c)) and FP-processed (Figure 2(c)) spectra appear to have flatter baselines than that observed in raw IR spectra.

Principal Component Analysis (PCA)

The effects of each studied baseline correction algorithms were evaluated by plotting their respective PCA scores plot. The most effective algorithms would cluster the set of IR spectral data by the brand of the paper, i.e. into three well-separated groups. Data were then examined with 2-D and 3-D PCA plots. After a careful examination, it was found that PC2's contribution was not as significant as PC3. Additionally, the 3-D plot did not improve the visualisation of clustering. As such, all results were studied based on PC1 versus PC3 scores plot, i.e. by just using only 2-D plot.

Figure 3 illustrates the clustering of data based on raw IR spectral data in which only OP was separated from IY and SP, while IY and SP were clustered into one single group. Figure 4 shows the separation of the three varieties of papers based on PCA score plots and the total variance explained by each respective PCA, calculated from IR spectral data that have been processed with the six different baseline correction algorithms. Obviously, IRLS (Figure 4(a)) and MPF (Figure 4(f)) processed spectra data show the worst separation, i.e. IY and SP were clustered into one group and the OP was not clustered within its own cluster. This was supported by the fact that the general patterns of their respective IR spectra (Figure 1(b) and 2(d)) are very similar to the raw one (Figure 1(a)). The best separation was achieved with ALS, MW and FP (Figure 4(b), (d) and (e)) algorithms. Each of the three paper types is well placed in their own cluster with partially overlapping regions.

Baseline Correction Algorithms Effects on Forensic Classification

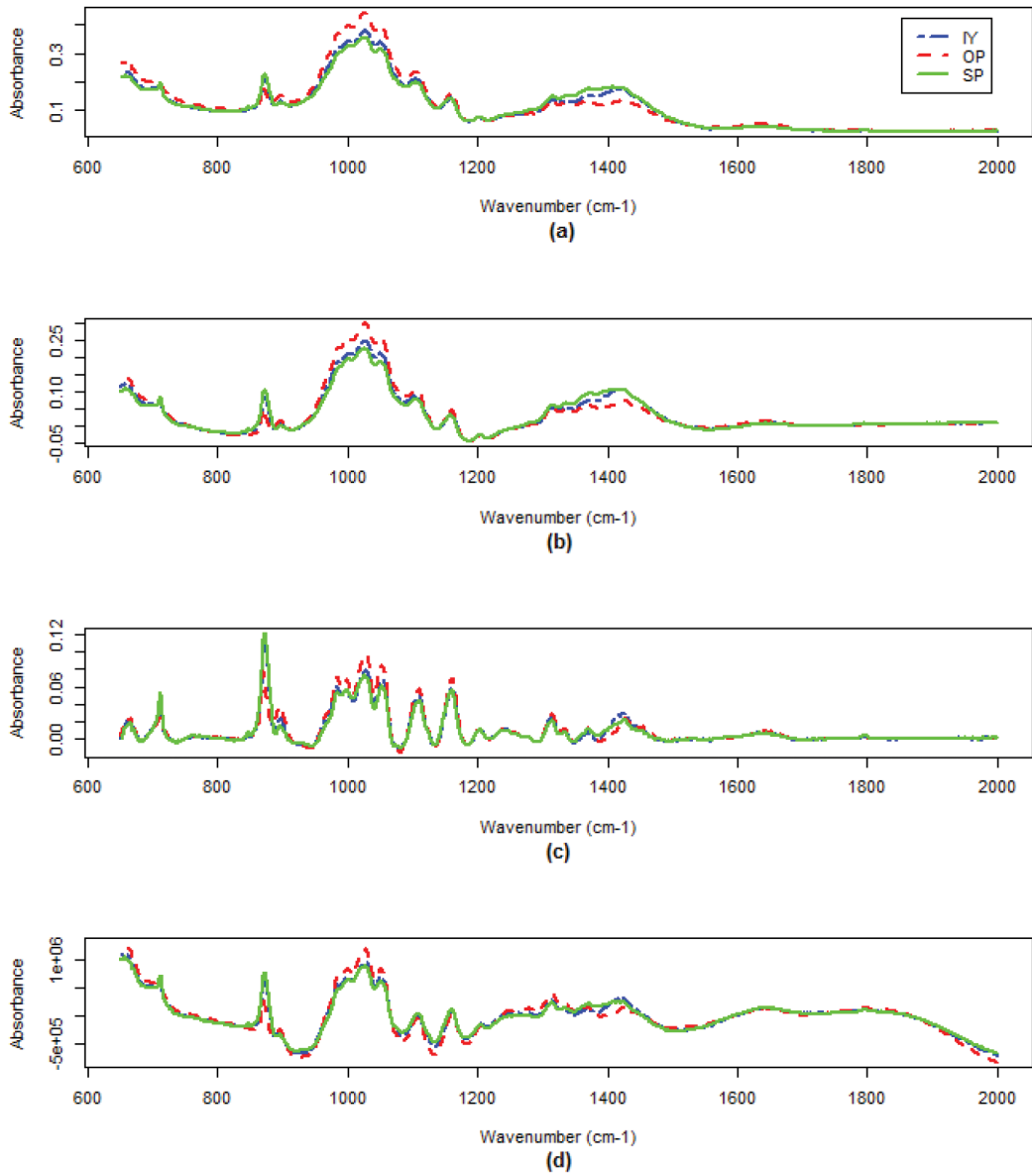


Figure 1. Comparison between average IR spectra of three varieties of paper: (a) raw untreated, against the ones that have the baseline corrected via (b) IRLS, (c) ALS, and (d) FFT, algorithms

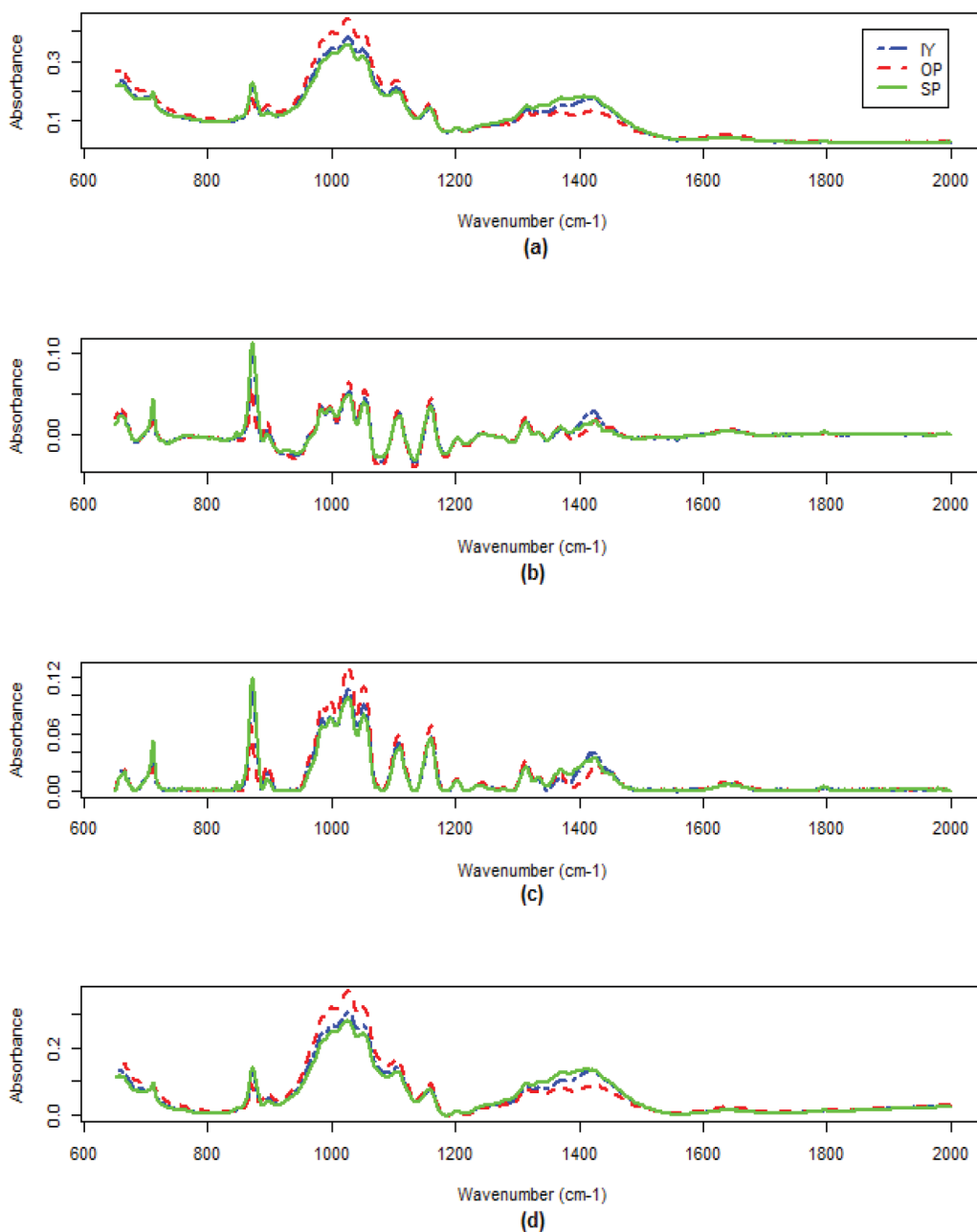


Figure 2. Comparison between average IR spectra of three varieties of paper: (a) raw untreated, against the one that have the baseline corrected via (b) MW, (c) FP, and (d) MPF, algorithms

Baseline Correction Algorithms Effects on Forensic Classification

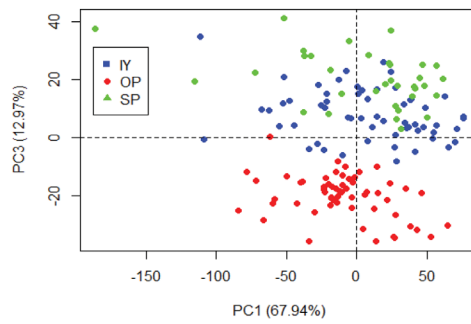


Figure 3. Score plots for three varieties of paper based on raw IR spectral data

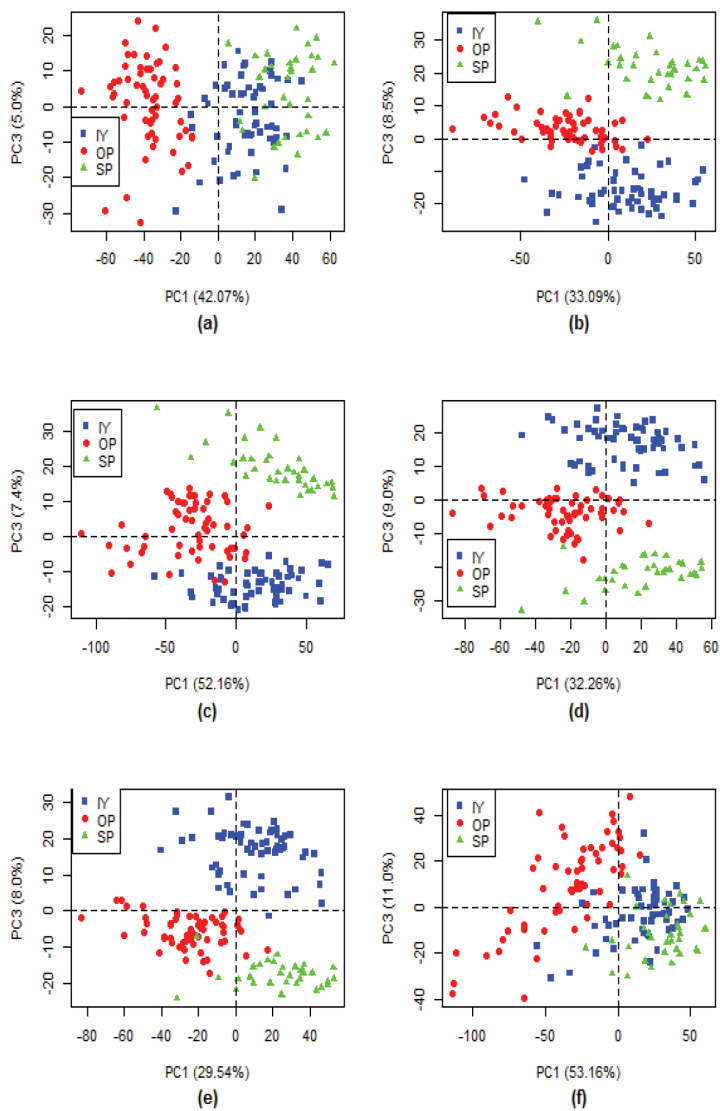


Figure 4. Scores plots for the three varieties of paper based on IR spectral data after being pre-processed with (a) IRLS, (b) ALS, (c) FFT, (d) MW, (e) FP and (f) MPF, algorithms

CONCLUSION

In this preliminary study, six types of baseline correction algorithms were investigated in the R environment for classifying the paper samples according to their manufacturer. The best separation is achieved with IR spectral data that are corrected with ALS, MW and FP algorithms respectively. It is recommended that future research conduct a more in-depth analysis on this topic with more advanced statistical techniques, for instance, with linear discriminant analysis or support vector machine, which would help in identifying the best algorithm based on quantitative figure of merits. This preliminary study has provided insights on the importance of implementing appropriate baseline correction algorithm to spectral data in the field of forensics.

ACKNOWLEDGEMENT

We are thankful to SAC Narenasagaran A/L Thangaveloo, Supt. Shaikh Abdul Adzis bin Shaikh Abdullah and Mr. Rizal (PDRM Forensic Laboratory, Cheras, Malaysia) for their help in acquiring IR data. We would also like to record our gratitude to UKM and KPTM for the financial support (FRGS/2/2013/ST06/UKM/02/1).

REFERENCES

- Bro, R., & Smilde, A. K. (2014). Principal component analysis. *Analytical Methods*, 6(9), 2812-2831.
- Causin, V., Marega, C., Marigo, A., Casamassima, R., Peluso, G., & Ripani, L. (2010). Forensic differentiation of paper by X-ray diffraction and infrared spectroscopy. *Forensic Science International*, 197(1), 70-74.
- Engel, J., Gerretzen, J., Szymanska, E., Jansen, J. J., Downey, G., Blanchet, L., & Buydens, L. M. C. (2013). Breaking with trends in pre-processing. *Trends in Analytical Chemistry*, 50, 96-106.
- Kher, A., Mulholland, M., Reedy, B., & Maynard, P. (2001). Classification of document papers by infrared spectroscopy and multivariate statistical techniques. *Applied Spectroscopy*, 55(9), 1192-1198.
- Kher, A., Stewart, S., & Mulholland, M. (2005). Forensic classification of paper with infrared spectroscopy and principal components analysis. *Journal of Near Infrared Spectroscopy*, 13(4), 225-229.
- Liland, K. H., Mevik, B. H., & Canteri, R. (2015, January 21). *Package 'baseline'* [Online]. Retrieved from <http://cran.r-project.org/web/packages/baseline/baseline.pdf>
- Rinna, A., van den Berg, F., & Engelsen, S. B. (2009). Review of the most common pre-processing techniques for near-infrared spectra. *Trends in Analytical Chemistry*, 28(10), 1201-1222.
- Rinna, A., Norgaard, L., van den Berg, F., Bro, R., & Engelsen, B. (2008). Data Pre-processing. In D. W. Sun (Ed.), *Infrared spectroscopy for food quality analysis and control* (pp. 29-48). Amsterdam: Elsevier.
- Team, R. C. (2015). *R: A language and environment for statistical computing*. R Foundation for Statistical Computing, Vienna, Austria. [Online]. Retrieved from <http://www.R-project.org/>
- Trygg, J., Gabrielsson, J., & Lundstedt, T. (2009). Background estimation, denoising and preprocessing. In S. D. Brown, R. Tauler, & B. Walczak (Eds.), *Comprehensive Chemometrics Chemical and Biochemical Data Analysis* (pp. 1-8). Amsterdam: Elsevier.
- Wehrens, R. (2011). Principal Component Analysis. In R. Wehrens (Ed.), *Chemometrics with R: Multivariate Data Analysis in the Natural Sciences and Life Sciences* (pp. 43-65). Heidelberg: Springer.

Deriving Partial Differential Equation for the Value of *Salam* Contract with Credit Risk

Hisham, A. F. B.^{1*}, Jaffar, M. M.¹ and Othman, J.²

¹Faculty of Computer and Mathematical Sciences, Universiti Teknologi MARA, 40450 UiTM, Shah Alam, Selangor, Malaysia

²Arshad Ayub Graduate Business School, Universiti Teknologi MARA, 40450 UiTM, Shah Alam, Selangor, Malaysia

ABSTRACT

There are many research papers on implementing the *salam* structure in the financial system. This study introduces a mathematical model of *salam* contract with credit risk that can be used as an Islamic financial derivative. It explores the properties of *salam* contract and the credit model that represents it, that is, the structural model with the default event on maturity of the *salam* contract.

Keywords: *Salam* contract, partial differential equation, credit risk model, Islamic derivative

INTRODUCTION

Salam is a syariah compliant financial contract based on deferred sale. It is an agreement between two parties to carry out a transaction at the future date (maturity) at a price determined today, according to Bacha (2013). The predetermined price or *salam* price $\overline{S(0)}$ has to be paid by the buyer at the initiation of the contract. This is the major difference between *salam* agreement and conventional forwards and futures contract (Hisham & Jaffar, 2014) and believed to help finance small entrepreneur working capital (Bacha, 1999; Yaksick, 1999). According to study done by Yaksick (1999) and Bacha (2013), the payoff or the value of *salam* contract $F(S(t), t)$ at the delivery date $t = T$ is given by:

$$F(S(T), T) = S(T) - \overline{S(0)} \quad (1)$$

where $S(T)$ is the underlying asset spot price at maturity. As we can see, the payoff of *salam* contract is the same with the forwards contract, therefore it closely resembles forwards rather than futures (Bacha, 1999). The *salam* agreement gains if the underlying price at maturity is priced greater than

Article history:

Received: 27 May 2016

Accepted: 14 November 2016

E-mail addresses:

aziemohzie14@gmail.com (Hisham, A. F. B.),

maheran@tmsk.uitm.edu.my (Jaffar, M. M.),

jaizah068@salam.uitm.edu.my (Othman, J.)

*Corresponding Author

the *salam* price $S(t) > \overline{S(0)}$ and losses when the spot price at maturity is less than the predetermined *salam* price $S(t) < \overline{S(0)}$.

As there exist some similarities between *salam* and conventional futures and forwards contract, a comparative research has been done. Ebrahim and Rahman (2005) have investigated the pareto optimality between synthetic futures contract and *salam* contract. Their synthetic future contract was formed by combining future contract on Islamic permissible commodities and Islamic cost-plus sale contract (Bai Murabaha). Their proposed synthetic futures have dominated *salam* contract on efficiency and welfare issues. However, the result is contrary to the intuition that under competitive markets, arbitrage free first order condition leads to pareto neutral (arbitrage free) of both contracts. Dali and Ahmad (2005) have proposed the application of *salam* contract in dinar economy as it can reduce price uncertainty and need for advance prepayment of capital. Susanti (2010) has proposed the implementation of *salam* agreement in murabahah financing contract, while Muneeza, Nurul Atiqah Nik Yusuf and Hassan (2011) highlight the possibility of *salam* application in the Malaysian Islamic banking system to assist farmers with working capital.

This study introduces a mathematical model to ascertain a *salam* contract with credit risk and therefore as an alternative Islamic derivative. The paper is organized as follows: 1) The definition and properties of *salam* contract, 2) the appropriate credit risk model that resembles the properties of *salam* structure, 3) the partial differential equation that describes the value of *salam* contract with credit risk.

CREDIT RISK MODEL

Based on prepayment at the beginning of the contract, the *salam* price is expected to be lower than the prevailing spot price at maturity (Bacha, 1999; Yaksick, 1999). Since the buyer has fully paid *salam* price at the beginning of the contract, he is exposed to the possibility of not receiving the goods at maturity from the seller (credit default risk). Hence, a discount from spot price which would compensate for credit risk (Vogel & Hayes, 1998) to overcome the potential default, syariah allows for the buyer to ask for guarantee such as mortgage and collateral (Bacha, 1999). In modeling *salam* contract this study adopts the method used in credit risk models; the structural model and reduced form model. The default in structural model is determined based on the evolution of the firm's structural variables (assets, liabilities and equities), whereby the reduced form model has assumed that default event is controlled by a Poisson process (Liang & Ren, 2007). In this study, we try to focus on the structural model as default risk in the *salam* contract, where the seller failed to deliver the agreed goods at the maturity leading to a default event.

In the structural model proposed by Merton (1974) default only occurs at the maturity of the contract. Using this approach, Jonson and Stulz (1987) have priced the option with default risk by assuming that the option buyer's claim is the only liability. Klein (1996) by assuming that there exist other liabilities other than the buyer claim, describes the option value by the stochastic process of both the option writer's asset while the default only occurs when option writer's asset falls below the fixed default boundary. Assuming a stochastic interest rate, Klein

and Inglis (1999) have modeled a defaultable option. Klein and Inglis (2001) have also modeled a vulnerable European option that allows for the total liabilities of the option writer to depend on the value of the option holder claim.

The second approach is the first passage time model introduced by Black and Cox (1976) where default can occur at any time prior to maturity. The firm will default when the value of the firm's asset crosses the default barrier. Longstaff and Schwartz (1995) and Briys and Varenne (1997) have extended this approach by assuming that the interest rate is stochastic in pricing bonds with credit risk. Liao and Huang (2005) have modeled a vulnerable option that can cause default prior to maturity by considering the correlation between the option writer's asset, the underlying asset and the value of the default-free zero coupon bond. Liang and Ren (2007) introduced a more practical default barrier where the default event occurs based on price fluctuations of the option value. In constructing a *salam* model with credit risk, this study will consider the structural model of the first approach as the default event only occur at the maturity of *salam* contract.

THE MODEL

In this section, the assumptions underlying Klein and Inglis (2001) for valuing European options subject to credit risk are used with adaptations to incorporate the default mechanism of *salam* contract. It follows the assumptions of Black and Scholes (1973), Merton (1974), Johnson and Stulz (1987), Klein (1996), Lio and Huang (2005) and Liang and Ren (2007).

Assumption 1 (*Salam* contract)

Consider a *salam* contract written on the underlying asset $S(t)$ with predetermined *salam* price $\overline{S(0)}$ and maturity time T . We assume that the underlying asset at time t , $S(t)$ follows the diffusion process by the following stochastic differential equation:

$$dS(t) = \mu(S)S(t)dt + \sigma(S)S(t)dW(t) \quad (2)$$

where $\mu(S)$ is the instantaneous expected return on the underlying asset, $\sigma(S)$ is the volatility of the underlying asset and $W(t)$ is a standard Wiener process for underlying asset.

Assumption 2 (*Salam* writer's asset)

The *salam* contract is issued by the *salam* writer. Let $V(t)$ denote the market value of all *salam* writer's assets at time t . The dynamic of $V(t)$ is described by:

$$dV(t) = \mu(V)V(t)dt + \sigma(V)V(t)dZ(t) \quad (3)$$

where $\mu(V)$ is the instantaneous expected return on the assets of *salam* writer, $\sigma(V)$ is the volatility of the *salam* writer's assets and $Z(t)$ is the standard wiener process for *salam* writer's asset. Since $Z(t)$ has the standard Brownian motion in the same space with $W(t)$, hence they are correlated with:

$$\text{cov}(dW(t), dZ(t)) \equiv E[dW(t) \cdot dZ(t)] = \rho(S, V)dt \quad (4)$$

Where $\rho(S, V)$ is the correlation coefficient between the two Brownian motion with $|\rho(S, V)| < 1$.

Assumption 3

It is assumed that both $S(t)$ and $V(t)$ are traded. Although $V(t)$ is not directly traded however the market value of the assets of counterparty behaves as if it is a traded asset (Klein, 1996).

Assumption 4

Trading of assets happen in continuous time and the market for traded assets are perfect with no transaction costs and taxes (Black & Scholes, 1973; Merton, 1974).

Assumption 5

It is possible to have unrestricted borrowing and lending of funds at the same instantaneous risk-free profit rate, r (Black & Scholes, 1973; Merton, 1974). However, to eliminate the element of *riba* in this *salam* contract transaction, we will replace it with the Islamic interbank rate.

Assumption 6

Claim of the *salam* contract holder is the only liability of *salam* writer.

Assumption 7

Due to the prepayment of predetermined *salam* price $\overline{S(0)}$ at the beginning of the contract $t = 0$, *salam* holder is exposed to the risk that the seller won't deliver the agreed underlying asset at the maturity. Hence, in order to overcome the potential of default from the seller, the *salam* writer's assets will take as the collateral of this *salam* contract.

Assumption 8

Salam contract matures at time T at which it pays $S(T) - \overline{S(0)}$ if the *salam* writer solvent where his total assets value greater than the *salam* holder claim at maturity ($V(T) > S(T) - \overline{S(0)}$). If *salam* writer failed to deliver the claim of *salam* holder at maturity (default) ($V(T) < S(T) - \overline{S(0)}$), *salam* holder will receive the assets of *salam* writer which have the value of $V(T)$ at time T .

Assumption 9

Underlying asset $S(t)$ and *salam* writer asset $V(t)$ cannot take negative value

$$S(t) \geq 0, \quad V(t) \geq 0$$

This is because the value of any assets can only take nonnegative values (Merton, 1974).

Assumptions 6, 7 and 8 are due to the unique properties of *salam* contract.

RISK NEUTRAL VALUATION

In this section, the stochastic differential equation (2) and (3) for the dynamic of *salam* contract value can be combined with a replication portfolio to eliminate the uncertainty represented by $dW(t)$ and $dZ(t)$. This results with a dynamic partial differential equation for a *salam* contract value which is deterministic. The partial differential equation will give the changes of *salam* contract value with credit risk as a function of underlying asset, *salam* writer’s assets and time $F(S(t), V(t), t)$.

Change of Measure

In adopting the risk neutral valuation for valuing the value of *salam* contract, we must transform first the real diffusion process describing the underlying asset and *salam* writer’s assets into the risk neutral process. According to Hilliard and Reis (1998) the expected growth of the underlying in the risk neutral world is given by $\mu(S) - \lambda(S)\sigma(S)$ where $\lambda(S)$ is the market price of risk associated with the underlying asset. Since the underlying asset behaves as the traded security that provides a return r then it can be written that:

$$r = \mu(S) - \lambda(S)\sigma(S)$$

Thus,

$$\mu(S) = r + \lambda(S)\sigma(S) \tag{5}$$

$$\lambda(S) = \frac{\mu(S) - r}{\sigma(S)} \tag{6}$$

Substituting (5) and (6) into (2), the following is obtained:

$$dS(t) = rS(t)dt + \sigma(S)S(t) \left(dW(t) + \frac{\mu(S) - r}{\sigma(S)} dt \right) \tag{7}$$

By comparing the terms in (2) and (7), Thus the relationship of Brownian motion for underlying asset in true probability measure $dW(t)$ and martingale probability measure $dW^*(t)$ is given by:

$$dW^*(t) = dW(t) + \frac{\mu(S) - r}{\sigma(S)} dt$$

$$dW(t) = dW^*(t) - \frac{\mu(S) - r}{\sigma(S)} dt \tag{8}$$

where $\frac{\mu(S) - r}{\sigma(S)}$ deducts the market price per unit of underlying asset risk (Bjerk Sund, 1991; Cuthbertson & Nitzsche, 2001; Hosseini, 2007). Hence, from (7) and (8), the appropriate risk neutral process for the purpose of valuing the *salam* contract depending on $S(t)$ is given by:

$$dS(t) = rS(t)dt + \sigma(S)S(t)dW^*(t) \tag{9}$$

Based on **Assumption 3**, the *salam* writer's assets have behave like a traded asset, hence the expected growth rate of the *salam* writer's assets in the risk neutral world is given by $\mu(V) - \lambda(V)\sigma(V)$ that can be written as:

$$r = \mu(V) - \lambda(V)\sigma(V)$$

$$\mu(V) = r + \lambda(V)\sigma(V) \tag{10}$$

$$\lambda(V) = \frac{\mu(V) - r}{\sigma(V)} \tag{11}$$

where $\lambda(V)$ is a constant market price of *salam* writer's assets risk. By substituting (10) and (11) into (3) it will get:

$$dV(t) = rV(t)dt + \sigma(V)V(t) \left(dZ(t) + \frac{\mu(V) - r}{\sigma(V)} dt \right) \tag{12}$$

The terms in (3) and (12) are compared, thus the relationship of Brownian motion for *salam* writer's assets in true probability measure $dZ(t)$ and martingale probability measure $dZ^*(t)$ is given by:

$$dZ^*(t) = dZ(t) + \frac{\mu(V) - r}{\sigma(V)} dt$$

$$dZ(t) = dZ^*(t) - \frac{\mu(V) - r}{\sigma(V)} dt \tag{13}$$

where $\frac{\mu(V) - r}{\sigma(V)}$ deducts the market price per unit of *salam* writer's assets risk. Therefore, the risk neutral process of *salam* writer's assets that will use for valuing *salam* contract is given by:

$$dV(t) = rV(t)dt + \sigma(V)V(t)dZ^*(t) \tag{14}$$

Both standard Brownian motion process $dW^*(t)$ and $dZ^*(t)$ are correlated with:

$$\text{cov}(dW^*(t), dZ^*(t)) \equiv E[dW^*(t) \cdot dZ^*(t)] = \rho(S, V)dt \tag{15}$$

The Process of $\ln S(t)$ and $\ln V(t)$

Based on the conjecture that the underlying asset has a log normal stationary distribution (Wilmott, 2007), defining $X = \ln S(t)$ where $X(S(t))$. Then, we have:

$$\frac{dX}{dS(t)} = \frac{1}{S(t)} \tag{16}$$

$$\frac{d^2 X}{dS^2(t)} = -\frac{1}{S^2(t)} \tag{17}$$

By applying one-dimensional Itô lemma (Segupta, 2005) on $X(S(t))$, we get:

$$dX = \frac{\partial X}{\partial S(t)} dS(t) + \frac{1}{2!} \left[\frac{\partial^2 X}{\partial S^2(t)} (dS(t))^2 \right] + \dots \tag{18}$$

where $(dt)^2 = 0$, $dt dW^*(t) = 0$ and $dW^*(t)dW^*(t) = dt$. By substituting the risk neutral process of underlying asset in equation (9) into the Itô lemma process in (16), (17) and (18) we have:

$$d[\ln S(t)] = \left(r - \frac{1}{2} \sigma^2(S) \right) dt + \sigma(S)dW^*(t) \tag{19}$$

where the process of $\ln S(t)$ can be described by equation (19). For *salam* writer's assets, based on the same conjecture as above whereby, it is assumed that *salam* writer's assets have a log normal stationary distribution. Therefore, defining $Y = \ln V$ where $Y(V(t))$

$$\frac{dY}{dV(t)} = \frac{1}{V(t)} \tag{20}$$

$$\frac{d^2 Y}{dV^2(t)} = -\frac{1}{V^2(t)} \tag{21}$$

Then, applying one-dimensional Itô lemma on $Y(V(t))$ we have:

$$dY = \frac{\partial Y}{\partial V(t)} dV(t) + \frac{1}{2!} \left[\frac{\partial^2 Y}{\partial V^2(t)} (dV(t))^2 \right] + \dots \tag{22}$$

where $(dt)^2 = 0$, $dt dZ^*(t) = 0$ and $dZ^*(t)dZ^*(t) = dt$. By substituting the risk neutral process of *salam* writer's assets in equation (14) into the Itô lemma process in (20), (21) and (22) we have:

$$d[\ln V(t)] = \left(r - \frac{1}{2} \sigma^2(V) \right) dt + \sigma(V) dZ^*(t) \tag{23}$$

Therefore, the process of $\ln V(t)$ can be described by equation (23). Based on equation (19) and (23), it is shown that $\ln S(t)$ and $\ln V(t)$ follow log normal diffusion process.

Partial Differential equation Governing the Salam Contract Value

When both underlying asset $S(t)$ and *salam* writer's assets $V(t)$ are shown to follow log normal diffusion process, it is possible to construct a perfect hedge portfolio of *salam* contract. There are several methods that can be used to form the partial differential equation for the price of the derivative.

Merton (1974) has constructed a replication portfolio that contains of three securities which are the firm, particular security and the riskless debt on pricing the corporate debt. Hilliard and Reis (1998) have been using the same approach as Hull and White (1987) and Scott (1987) by forming a non-arbitrage portfolio that consists of two futures contracts on different maturities and the spot commodity. Cuthbertson and Nitzsche (2001) and Willmott (2007) in their studies have constructed a synthetic portfolio consisting of underlying asset and bond or some derivative to eliminate the underlying uncertainty and then forming a dynamic partial differential equation for the price of derivative.

However, in forming the partial differential equation describing the *salam* contract value, this study adopts the same method in contingent claim analysis as in Gibson and Schwartz (1990), Bjerksund (1991), Hosseini (2007) and Tassis (2013). By invoking the assumption that the price of contingent claim $P(S(t), V(t), t)$ is twice continuously differentiable function of $S(t)$ and $V(t)$ (Gibson & Schwartz, 1990; Bjerksund, 1991), the instantaneous change value can be formed by applying the multi-dimensional Itô lemma (Segupta, 2005) given by:

$$\begin{aligned} dP = & \frac{\partial P}{\partial S(t)} dS(t) + \frac{\partial P}{\partial V(t)} dV(t) + \frac{\partial P}{\partial t} dt + \frac{1}{2!} \left[\frac{\partial^2 P}{\partial S^2(t)} (dS(t))^2 + \frac{\partial^2 P}{\partial S(t) \partial V(t)} \right. \\ & dS(t)dV(t) + \frac{\partial^2 P}{\partial S(t) \partial t} dS(t)dt + \frac{\partial^2 P}{\partial V^2(t)} (dV(t))^2 + \frac{\partial^2 P}{\partial V(t) \partial S(t)} dV(t)dS(t) \\ & \left. + \frac{\partial^2 P}{\partial V(t) \partial t} dV(t)dt + \frac{\partial^2 P}{\partial t^2} (dt)^2 + \frac{\partial^2 P}{\partial t \partial S(t)} dt dS(t) + \frac{\partial^2 P}{\partial t \partial V(t)} dt dV(t) \right] + \dots \end{aligned} \tag{24}$$

where $(dt)^2 = 0$, $dt dW^*(t) = 0$, $dt dZ^*(t) = 0$, $dW^*(t)dZ^*(t) = \rho(S,V)dt$, $(dW^*(t))^2 = dt$ and $(dZ^*(t))^2 = dt$. By substituting the correlated risk neutral process of underlying asset and *salam* writer asset as in (9) and (14) into the multi-dimensional Itô lemma (24), we have:

$$\begin{aligned}
 dP = & \left[(rS(t) \frac{\partial P}{\partial S(t)} + rV(t) \frac{\partial P}{\partial V(t)} + \frac{\partial P}{\partial t} + \frac{1}{2} S^2(t) \sigma^2(S) \frac{\partial^2 P}{\partial S^2(t)} \right. \\
 & + \rho(S, V) S(t) V(t) \sigma(S) \sigma(V) \frac{\partial^2 P}{\partial S(t) \partial V(t)} + \frac{1}{2} V^2(t) \sigma^2(V) \\
 & \left. \frac{\partial^2 P}{\partial V^2(t)} \right] dt + \sigma(S) S(t) \frac{\partial P}{\partial S(t)} dW^*(t) + \sigma(V) V(t) \frac{\partial P}{\partial V(t)} dZ^*(t)
 \end{aligned}
 \tag{25}$$

Equation (25) above describes the instantaneous change of the value of contingent claim $dP(S(t), V(t), t)$. Based on perfect market assumption which imply in the absence of arbitrage and considering the interest rate is not stochastic, the portfolio strategy $W(t) = W^*(t)$ and $Z(t) = Z^*(t)$ are chosen such that the coefficient of $dW(t)$ and $dZ(t)$ are always zero (Merton, 1974; Cuthbertson & Nitzsche, 2001). This strategy can be shown as in our risk neutral process in equation (9) and (14). Therefore, the value of the contingent claim will only be left with the deterministic term as below:

$$\begin{aligned}
 dP = & \left[(rS(t) \frac{\partial P}{\partial S(t)} + rV(t) \frac{\partial P}{\partial V(t)} + \frac{\partial P}{\partial t} + \frac{1}{2} S^2(t) \sigma^2(S) \frac{\partial^2 P}{\partial S^2(t)} \right. \\
 & \left. + \rho(S, V) S(t) V(t) \sigma(S) \sigma(V) \frac{\partial^2 P}{\partial S(t) \partial V(t)} + \frac{1}{2} V^2(t) \sigma^2(V) \frac{\partial^2 P}{\partial V^2(t)} \right] dt
 \end{aligned}
 \tag{26}$$

By applying no arbitrage argument, set up a risk-free portfolio as:

$$dP = rPdt
 \tag{27}$$

Equation (27) above describes that, if we have a completely risk free change dP in the portfolio value P then it must be the same as the growth that we would get if we put the equivalent amount of cash in the risk-free interest bearing account. Hence, by substituting (26) into (27), the market value of that contingent claim must satisfy the partial differential equation as below:

$$\begin{aligned}
 rS(t) \frac{\partial P}{\partial S(t)} + rV(t) \frac{\partial P}{\partial V(t)} + \frac{\partial P}{\partial t} + \frac{1}{2} S^2(t) \sigma^2(S) \frac{\partial^2 P}{\partial S^2(t)} \\
 + \rho(S, V) S(t) V(t) \sigma(S) \sigma(V) \frac{\partial^2 P}{\partial S(t) \partial V(t)} + \frac{1}{2} V^2(t) \sigma^2(V) \frac{\partial^2 P}{\partial V^2(t)} - rP = 0
 \end{aligned}
 \tag{28}$$

According to Cuthbertson and Nitzsche (2001) and Hosseini (2007), the change in the value of replication portfolio must match with the change in the value of derivative contract:

$$dP(S(t), V(t), t) = dF(S(t), V(t), t)
 \tag{29}$$

Hence, under the same market condition and applying the same no arbitrage argument as in (26) and (27), it can be shown that the value of *salam* contract with credit risk $F(S(t), V(t), t)$

must satisfies the following two-dimensional partial differential:

$$rS(t)\frac{\partial F}{\partial S(t)} + rV(t)\frac{\partial F}{\partial V(t)} + \frac{\partial F}{\partial t} + \frac{1}{2}S^2(t)\sigma^2(S)\frac{\partial^2 F}{\partial S^2(t)} + \rho(S,V)S(t)V(t)\sigma(S)\sigma(V)\frac{\partial^2 F}{\partial S(t)\partial V(t)} + \frac{1}{2}V^2(t)\sigma^2(V)\frac{\partial^2 F}{\partial V^2(t)} - rF = 0 \quad (30)$$

Under equivalent martingale theory (Bjerk Sund, 1991; Cuthbertson & Nitzsche, 2001) the current value of *salam* contract with credit risk of a claim on a future delivery at time T is given by:

$$F(S(t),V(t),t) = e^{-r(T-t)}E^*(S(t),V(t),t)[\text{payoff at } T] \quad (31)$$

where $E^*(S(t),V(t),t)[.]$ is the expectation taken under equivalent martingale probability measure. Therefore, equation (31) can be solved by considering the payoff of *salam* contract with credit risk at maturity as in equation (1), the claim in **Assumption 6**, the collateral as in **Assumption 7**, the default condition in **Assumption 8** and the non-negativity condition as in **Assumption 9**.

CONCLUSION

In constructing the partial differential equation to describe the dynamic behavior of *salam* contract value and credit risk, the diffusion process of the underlying asset and the *salam* writer's assets are reduced to risk neutral process. The properties of underlying asset and *salam* writer's assets process are investigated and a hedging portfolio constructed to eliminate uncertainty. The partial differential equation that describes the dynamic of *salam* contract value with credit risk was constructed based on perfect market conditions. This study aims to solve the two dimensional partial differential equation as in (30), by considering the payoff equation (31) subjects to **Assumption 6, 7, 8 and 9** to provide a model of *salam* contract with credit risk.

ACKNOWLEDGEMENT

The authors would like to acknowledge the financial support received from Ministry of Higher Education of Malaysia, Fundamental Research Grant Scheme 600-RMI/FRGS 5/3 (65/2013) and Tabung Amanah Pembangunan Pelajar (TAPA), Universiti Teknologi MARA.

REFERENCES

- Bacha, O. I. (1999). Derivative instruments and Islamic finance: some thoughts for a reconsideration. *International Journal of Islamic Financial Services*, 1(1), 9-25.
- Bacha, O. I. (2013). Risk management, derivatives and shariah compliance. In *Proceedings of the 20th National Symposium on Mathematical Sciences, AIP Conference Proceedings* (pp. 17-28). AIP

- Bjerk Sund, P. (1991). *Contingent claims evaluation when the convenience yield is stochastic: analytical results*. Bergen-Sandviken: Institutt for foretaksøkonomi, Institute of Finance and Management Science.
- Black, F., & Cox, J. C. (1976). Valuing corporate securities: Some effects of bond indenture provisions. *The Journal of Finance*, 31(2), 351-367.
- Black, F., & Scholes, M. (1973). The pricing of options and corporate liabilities. *Journal of Political Economy*, 81(3), 637-654.
- Briys, E., & De Varenne, F. (1997). Valuing risky fixed rate debt: An extension. *Journal of Financial and Quantitative Analysis*, 32(02), 239-248.
- Cuthbertson, K., & Nitzsche, D. (2001). *Financial engineering, derivatives and risk management*. United Kingdom, UK: John Wiley & Sons, Ltd.
- Dali, N. R. S. M., & Ahmad, S. (2005). A Review of Forward, Futures, and Options From The Shariah Perspective. "From Complexity to Simplicity". In *Conference on Seminar Ekonomi & Kewangan Islam* (pp.29-30).
- Ebrahim, M. S., & Rahman, S. (2005). On the pareto-optimality of the futures contracts over Islamic forward contracts: implications for the emerging muslim economies. *Journal of Economic Behavior and Organization*, 56(2), 273-295.
- Gibson, R., & Schwartz, E. S. (1990). Stochastic convenience yield and the pricing of oil contingent claims. *The Journal of Finance*, 45(3), 959-976.
- Hilliard, J. E., & Reis, J. (1998). Valuation of Commodity Futures and Options under Stochastic Convenience Yields, Interest Rates, and Jump Diffusions in the Spot. *Journal of Financial and Quantitative Analysis*, 33(1), 61-86.
- Hisham, A. F. B., & Jaffar, M. M. (2014, December). A review on mathematical methods of conventional and Islamic derivatives. In *International Conference On Quantitative Sciences And Its Applications (ICOQSIA 2014): Proceedings of the 3rd International Conference on Quantitative Sciences and Its Applications* (pp. 308-315). AIP.
- Hosseini, M. (2007). *Stochastic Modeling of Oil Futures Prices*. (Master Thesis). Department of Mathematics, Uppsala University.
- Hull, J., & White, A. (1987). The pricing of options on assets with stochastic volatilities. *The Journal of Finance*, 42(2), 281-300.
- Johnson, H., & Stulz, R. (1987). The pricing of options with default risk. *The Journal of Finance*, 42(2), 267-280.
- Klein, P. (1996). Pricing Black-Scholes options with correlated credit risk. *Journal of Banking and Finance*, 20(7), 1211-1229.
- Klein, P., & Inglis, M. (1999). Valuation of European options subject to financial distress and interest rate risk. *The Journal of Derivatives*, 6(3), 44-56.
- Klein, P., & Inglis, M. (2001). Pricing vulnerable European options when the option's payoff can increase the risk of financial distress. *Journal of Banking and Finance*, 25(5), 993-1012.
- Liang, G., & Ren, X. (2007). The credit risk and pricing of OTC options. *Asia-pacific Financial Markets*, 14(1), 45-68.

- Liao, S. L., & Huang, H. H. (2005). Pricing Black–Scholes options with correlated interest rate risk and credit risk: an extension. *Quantitative Finance*, 5(5), 443-457.
- Longstaff, F. A., & Schwartz, E. S. (1995). A simple approach to valuing risky fixed and floating rate debt. *The Journal of Finance*, 50(3), 789-819.
- Merton, R. C. (1974). On the pricing of corporate debt: The risk structure of interest rates. *The Journal of Finance*, 29(2), 449-470.
- Muneeza, A., Yusuf, N. N. A. N., & Hassan, R. (2011). The possibility of application of salam in Malaysian Islamic banking system. *Humanomics*, 27(2), 138-147.
- Scott, L. O. (1987). Option pricing when the variance changes randomly: Theory, estimation, and an application. *Journal of Financial and Quantitative analysis*, 22(4), 419-438.
- Sengupta, A. (2005). *Pricing derivatives: The financial concepts underlying the mathematics of pricing derivatives*. United States: McGraw-Hill.
- Susanti, D. O. (2010). Pelaksanaan Perjanjian Pembiayaan Murabahah Dengan Sistem Bai' u Salam (Studi Pada PT. BPRS Daya Artha Mentari Bangil-Pasuruan). *Risalah Hukum: Jurnal Hukum*, 6(2), 96-110.
- Tassis, D. (2013). *Pricing Of Commodities Futures: An Empirical Study*. (Master thesis). University of Piraeus, Greece.
- Vogel, F. E., & Hayes, S. L. (1998). *Islamic law and finance: religion, risk, and return*. The Netherland: Kluwer Law International.
- Wilmott, P. (2007). *Introduces qualitative finance* (2nd Ed.). New Jersey: John Wiley & Sons Ltd.
- Yaksick, R. (1999). The Islamic Commodity Trust with Application to Crude Oil Forward Sales. In *Proceedings of the third Harvard University Forum of Islamic finance: Local challenges, global opportunities* (pp.213-222). Center for Middle Eastern Studies, Harvard University.



Combination of Forecasts with an Application to Unemployment Rate

Muniroh, M. F.^{1*}, Ismail, N.² and Lazim, M. A.³

¹Actuarial and Statistics Branch, Department of Risk and Research, Social Security Organizational, Kuala Lumpur, Malaysia

²School of Mathematical Sciences, Faculty of Sciences and Technology, Universiti Kebangsaan Malaysia, 43600 Bangi, Selangor, Malaysia

³Department of Statistics and Decisions Sciences, Faculty of Computer and Mathematical Sciences, Universiti Teknologi MARA, 40450 UiTM, Shah Alam, Selangor, Malaysia

ABSTRACT

Combining forecast values based on simple univariate models may produce more favourable results than complex models. In this study, the results of combining the forecast values of Naïve model, Single Exponential Smoothing Model, The Autoregressive Moving Average (ARIMA) model, and Holt Method are shown to be superior to that of the Error Correction Model (ECM). Malaysia's unemployment rates data are used in this study. The independent variable used in the ECM formulation is the industrial production index. Both data sets were collected for the months of January 2004 to December 2010. The selection criteria used to determine the best model, is the Mean Square Error (MSE), Root Mean Squared Error (RMSE) and Mean Absolute Percentage Error (MAPE). Initial findings showed that both time series data sets were not influenced by the seasonality effect.

Keywords: Combination forecast, unemployment rate, error correction model

INTRODUCTION

Forecasting is an important tool for making decisions in a variety of fields. It helps government and top management of firms, in their decision making for strategic planning purposes. There are tremendous diversities in forecasting applications, such as in marketing where it plays a key role in determining the sales targets, pricing and advertising expenditure, in sales and services that allows salespersons to estimate sales to be achieved.

Governments use forecasts to guide monetary and fiscal policy and make plans for

Article history:

Received: 27 May 2016

Accepted: 14 November 2016

E-mail addresses:

Muniroh.fadzil@gmail.com, Muniroh.fadzil@perkeso.gov.my

(Muniroh, M. F.),

ni@ukm.edu.my (Ismail, N.),

dralias@tmsk.uitm.edu.my (Lazim, M. A.)

*Corresponding Author

the country's future directions while private firms use them to determine prices and product demand. Currently, there are many forecasting methods but not all are able to provide the best results. This has made the issue pertaining to the accuracy of forecasts to become a major topic in forecasting research. Study done by Dimitrios & John (2004), to compare the forecasting performance of the Naïve model, ARIMA model and Transfer Function (TF) model. In the Transfer Function they were interested in the contemporaneous relationship among variables such as Gross Domestic Product (GDP), Consumer Price Index (CPI), Industrial Production Index (IPI), Real Cost Labour, and OECD Industrial Production Index.

The availability of various forecasts methods allows the forecasters to examine their respective performance and hence to identify strengths and weaknesses. ARIMA models are based on autocorrelations while exponential smoothing is based on a structural view of the data to include level, trend and events. Exponential smoothing attempts to estimate the trend as a part of the modelling process in comparison with the ARIMA methodology which attempts to eliminate the trend before constructing the model. One suggestion regarding forecasting performance is to combine forecast values. This study aims to compare the performance of the combined univariate models with the more complex multivariate models using data of the unemployment rate. The four univariate models analysed are Naïve model, Single Exponential Smoothing, Holt-Winter Smoothing, Autoregressive Moving Average (ARIMA). The multivariate models studied using industrial production index (IPI) as the independent variable is the Error Correction Model (ECM).

Assis, Amran, Remali and Affendy (2010) compared the performance of four models in their prediction of the Cocoa Bean prices. The data used were Tawau Cocoa Bean prices graded SMC 18 for the period of January 1992-December 2006. The four univariate models used to make the comparisons were Single Exponential Smoothing, ARIMA, GARCH and Mixed ARIMA/GARCH models.

From the result, it was found that mixed ARIMA/GARCH model outperformed the Single Exponential Smoothing, ARIMA and GARCH models. The best result is indicated by the smallest error measures, the Root Mean Squared Error (RMSE), Mean Absolute Percentage Error (MAPE), Mean Absolute Error (MAE) and statistics. This is in agreement with the findings of the study done by Zhou, He & Sun (2006). Zhou, He & Sun (2006) Fatimah and Roslan (1986), Shamsuddin, Rosdi & Ann (1992), and Kahforoushan, Zarif & Mashahir (2010). On the other hand, Kamil, & Noor (2006) found that the GARCH model type has good predictive accuracy.

To assess the forecasting performances of each of the models that were developed various error measures were used, and the best model was ascertained on the out-of sample forecast evaluation procedure. Clemen (1989) found that combining forecast can produce better and more accurate results.

The performance of a single variable model such as Naïve, Exponential Smoothing, the ARIMA model and all univariate models show a diversity in their level of accuracy. The inclusion of exogenous and endogenous variables like the Error Correction Model (ECM) can make them better. The forecasting performances of these models are measured using several statistical criteria such as Akaike Info Criterion (AIC), Schwarz Criterion (BIC) and F-statistics. The objective of this study is to compare the performance of the models based

on the out-of-sample evaluation. This paper is organized as follows: Section 2 provides the data and methodology, section 3 presents the empirical results from the various methods of combining forecasts values and section 4 is the conclusion.

METHODOLOGY

An observation on the time series data to ascertain the presence of a trend, seasonal pattern was made. Following this five models, namely the Naive model, Single Exponential Smoothing, Holt Method, Autoregressive Moving Average (ARIMA) and Error Correction Model were used to fit the data. Analyses was done using EViews software to develop statistical models from the data and forecast the future values of the series.

The Data Series

Data used in this project was obtained from the Department of Statistics, Malaysia for months January 2004 till December 2010.

Modelling Procedures

The development of the five models suitable for forecasting purposes using the data series were based on the three step procedure described below:

1. Firstly the data series was split into two parts. The first part is called model estimation part where all models studied are estimated and fitted. The second part is called the evaluation part where the fitted models are compared out-of-sample to determine which model gives on the average, the best forecast values. In this study, the monthly data from January 2004 until December 2009 were used as the fitted (estimation) part, whereas data from January 2010 until December 2010 is the evaluation part. The sample size of the estimation part comprises of 72 observations and the sample size for the evaluation part 12 observations.
2. Secondly five models, namely Naive model, Single Exponential Smoothing, Holt Method, Autoregressive Integrated Moving Average (ARIMA), acted as univariate models while the Error Correction Model was the multivariate model. These models will be estimated on the estimation part of the data set, comprising 72 observations. In the multivariate model, the study adopted simple model to see the relationship between x_t and y_t where x_t is industrial production index while y_t is unemployment rate. To express this relationship, Error Correction Model (ECM) will be used.
3. Thirdly, these models were evaluated based on out-of sample procedure. The model that produces the best results will be declared the most suitable. The decision to pick the best model will be based on the minimum of the error measures. The error measures used are the Mean Squared Error (MSE), Root Mean Squared Error (RMSE) and Mean Absolute Percentage Error (MAPE).

The Model Used

Naive Model. This model is founded on the belief what happens today will happen again tomorrow or any other time in the future. Frechtling (1996) Summarized that the forecast value using the naive method is equal to the actual value from the last period available. This model can be used in a stable data series, which include seasonal component or any pattern. Naive model is also used as a benchmark for forecasting model. Mathematically, the model is represented as,

$$F_{t+m} = y_t \quad (1)$$

where m refers to the number of periods into future for which the forecast is desired and y_t is actual value at time t . For the one-step-ahead forecast model can present as $F_{t+1} = y_t$ where $m=1$.

Single Exponential Smoothing. In single exponential smoothing models, the forecast for the next and all subsequent periods are determined by adjusting the current period forecast by a portion of the difference between the current forecast and the current actual value. The formula for simple exponential smoothing is;

$$F_{t+m} = \alpha y_t + (1 - \alpha) F_t \quad (2)$$

where, F_{t+m} is the single exponentially forecast value in period m (this is also defined as the forecast value when generated out-of-sample), for $m = 1, 2, 3 \dots, t$. y_t is the actual value in time period t , α is unknown smoothing constant to be determined for value between 0 and 1, i.e. ($0 \leq \alpha \leq 1$) and F_t is the forecast value at period t .

Holt Methods. Holt method provides more flexibility in selecting the parameter value, which include the trend and slopes. This method also can be used to forecast when linear trend is present in the data. The application of the Holt's Method requires three equations;

The exponentially smoothed series;

$$S_t = \alpha y_t - (1 - \alpha)(S_{t-1} + T_{t-1}) \quad (3)$$

The trend estimate;

$$T = \beta(S_t - S_{t-1}) + (1 - \beta)T_{t-1} \quad (4)$$

The forecast for m period;

$$F_{t+m} = S_t + T_t * m \quad (5)$$

Autoregressive Moving Average (ARIMA). The Box-Jenkins methodology of forecasting differs from the methods described earlier because it does not assume any particular pattern in the historical data of the series to be forecast. It uses an iterative approach to identify a possible model from a general class of models. The chosen models are then checked against the historical data to see whether they accurately describe the series. This model also requires expert criteria, stationary data, models' diagnostic and etc. Funke (1992) and Floros (2005) also used a univariate ARIMA model to forecast the German and United Kingdom unemployment rates respectively.

As with any good modelling practice the first step when developing a Box-Jenkins model is to understand the characteristics of the series involved, that is how it behaves over time. Basically, it is assumed that the data series is stationary. A series is said to be 'stationary' if it does not show growth or decline over time. In other words, the data series does not indicate presence of trend component. A series that does not depict this characteristic is called 'non-stationary series' and such series can be made stationary (by removing the trend) by taking successive differences of the data. The basic model of Box-Jenkins methodology comprises of the autoregressive (AR) part and the moving average (MA) part. However, when the variable is non-stationary, then the differencing or integrated part is also included.

The general Autoregressive (AR) model of p^{th} term is given as,

$$y_t = \mu + \phi_1 y_{t-1} + \phi_2 y_{t-2} + \dots + \phi_p y_{t-p} + \varepsilon_t \tag{6}$$

The general Moving Average (MA) of q^{th} term is given as,

$$y_t = \mu + \varepsilon_t - \theta_1 \varepsilon_{t-1} - \theta_2 \varepsilon_{t-2} - \dots - \theta_q \varepsilon_{t-q} \tag{7}$$

Mixed Autoregressive and Moving Average (ARMA) model of p^{th} and q^{th} term, respectively (Where y_t is assumed stationary) is given as,

$$y_t = \mu + \phi_1 y_{t-1} + \phi_2 y_{t-2} + \dots + \phi_p y_{t-p} + \varepsilon_t - \theta_1 \varepsilon_{t-1} - \theta_2 \varepsilon_{t-2} - \dots - \theta_q \varepsilon_{t-q} \tag{8}$$

Mixed Autoregressive Integrated Moving Average (ARIMA)

$$w_t = \mu + \phi_1 w_{t-1} + \phi_2 w_{t-2} + \dots - \theta_1 \varepsilon_{t-1} - \theta_2 \varepsilon_{t-2} - \dots + \varepsilon_t \tag{9}$$

where $w_t = y_t - y_{t-1}$ is stationary and y_t is the original series p and q can take any value which define the lag length of y_t and ε_t , respectively, y_{t-p} is the p^{th} order of the lagged dependent and μ, ϕ_p and θ_q are unknown parameters to be estimated.

Error Correction Model (ECM). According to Engle & Granger (1987) if the set of series x_t and y_t are co-integrated, then there exists a generating mechanism called 'Error Correction Model', which forces the variables to move closer over time whilst allowing a range of short run dynamics. For example, if two variables y_t and x_t are co-integrated of order one, that is $\sim CI(1, 1)$, then the general error correction model (ECM) can be written as:

$$\Delta y_t = \alpha_0 + \phi v_{t-1} + \sum_{j=1}^J \gamma_j \Delta y_{t-j} + \sum_{k=1}^K \sum_{j=1}^{J_k} \beta_{kj} \Delta x_{k(t-j)} + \varepsilon_t \quad (10)$$

where $\Delta y_t = y_t - y_{t-1}$, $\Delta x_t = x_t - x_{t-1}$, $\varepsilon_t \sim iid(0, \sigma^2_\varepsilon)$ ϕ necessarily negative and $v_t = \hat{y}_t - (\beta_0 + \hat{\beta}_1 t)$

Combining Forecasts. Following the discussions made earlier in this study, this section continues with the discussion on combining the forecasts in order to obtain much better forecast values. Combination of forecasts will involve four models of univariate type and the result obtained will be compared against the Error Correction model. In this study, a simple procedure to combine the forecasts used is to take the average of the four models. To generate the average forecast values, assume all forecasts are independent with the same σ^2 . A arithmetic mean of these four forecast values are calculated as,

$$SAM = \frac{f_1 + f_2 + f_3 + f_4}{4} \quad (11)$$

Another method of combining forecast is to use the regression analysis. The most common procedure used to estimate the combining weight is to perform the Ordinary Least Squares (OLS) regression. The Regression Method (RM) can be expressed by the following equation:

$$y_{t+1} = a_0 + \sum_{j=1}^k a_j f_{t,j} + \varepsilon_{t+1} \quad (12)$$

where $f_{t,j}$ is the one step ahead forecasts made at time t of y_{t+1} with model i : a_0 is a constant term and a_j is the regression coefficient. As an improvement to the combining methods, Granger and Ramanathan (1984) showed that the optimal method is equivalent to a least squared regression in which the constant is suppressed and the weight are constrained to sum to one. They point out that values from discarded forecasting models still obtain useful information about the behaviour of y_t . If the biased forecasts are included in the least squares equation, the intercept adjusts for the bias. Hence, it is important to use least squares method with an intercept. Therefore, this study used both combination methods to evaluate the performance of forecast models. The smallest error measure is the criterion used to show that the combined of univariate model is better than the single complex models.

ANALYSIS AND RESULTS

Figure 1 shows the monthly observations of Malaysia's Unemployment Rate from January 2004 until November 2010. From the plot, it was found that the Malaysia's Unemployment rate had been on the decline with the exception of the periods Dec 2005 until Mac 2006 where the rate recorded its highest levels. The series however, does not indicate presence of seasonality

effect, though significantly large values in June and February in year 2007 and 2008 respectively were observed. This phenomenon could be explained by the fact that labour market conditions had weakened at end of year 2008 as reflected in higher retrenchments whilst demands for labour were moderate.

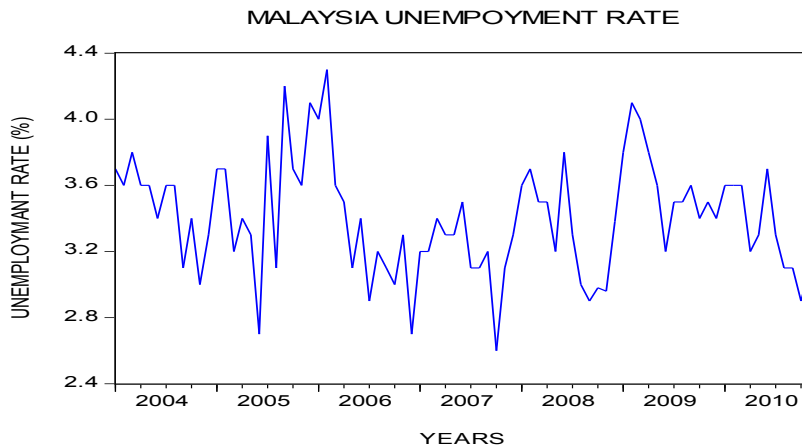


Figure 1. Malaysia unemployment rate

Table 1

Results of Unit Root ADF Test for Unemployment Rate and Industrial Production Indices

Variables	ADF Test Statistics	t-statistics	Probability
Unemployment Rate			
Before differencing	-3.4753	-3.1803	0.0980
After 1 st Differencing	-3.4753	-14.2636	0.0001
Industrial Production Indices (IPI)			
Before differencing	-3.4805	-0.2539	0.9903
After 1 st Differencing	-3.4805	-4.5019	0.0033

Table 2

Results of Unit Root ADF Results Test for Co-Integrated

Variables	ADF Test Statistics Critical Value at 5% Level	t-statistics	Probability
Before differencing	-3.4753	-3.4501	0.0531
After 1 st Differencing	-3.4753	-14.5626	0.0001

ECM versus Univariate Models

Table 3
The Estimation and Evaluation Models

Model Types	Error Measure		
	MSE	MAE	MAPE
Estimation Period: January 2004-December 2009			
Naïve Model	0.167800	0.289634	8.475200
Single Exponential Smoothing Alpha = 0.5100	0.033300	0.138410	4.112000
Holt Method (Alpha=0.52)	0.025100	0.121633	3.610700
ARIMA (1,1,3)	0.071560	0.201220	6.006736
ECM	0.085671	0.219243	6.523044
Combination Forecast (SAM)	0.004878	0.051120	1.553687
Combination Forecast (RM)	0.000531	0.016369	0.484067
Evaluation Period: January 2010-December 2010			
Naïve Model	0.049400	0.162993	4.984000
Single Exponential Smoothing Alpha = 0.5100	0.012400	0.081667	2.506600
Holt Method (Alpha=0.52)	0.012240	0.080419	2.935200
ARIMA (1,1,3)	0.035928	0.145557	4.388857
ECM	0.029192	0.114284	3.464466
Combination Forecast (SAM)	0.000996	0.022435	0.675566
Combination Forecast (RM)	0.000077	0.007968	0.238952

For the Error Correction Model, both unemployment rate and industrial production indices show that they are co-integrated. That is proven using the ADF test which shows that at least two variables are integrated of the first order (Table 1 and Table 2). Looking at the results of the model evaluation from the table, we can see that the ECM performed worst when compared against the deterministic models of Single Exponential Smoothing and Holt Method. However, both ARIMA (1,1,3) and the ECM were beaten when pitted against the combined (in this case the average forecast) forecast of all the deterministic models. The table also shows that the combined Simple Average Method and Regression Method forecasts are superior than ARIMA (1,1,3) and ECM. But, the combination forecasts from Regression Methods perform slightly better when compared to Simple Average Method.

CONCLUSION

In this study five univariate models were estimated and evaluated. The univariate models are Naive, Single Exponential Smoothing, Holt Method, Autoregressive Integrated Moving Average (ARIMA) and the multivariate model is the Error Correction Model (ECM).

From the results it can be concluded that the Holt Method shows the best result. However, after combining the forecasts using Simple Average Method and Regression Method, the combined forecast values explain better than Holt Method, proving combining several competing forecasts can help reduce errors and improve accuracy. In this regard the regression method of combination proved better than the simple average method.

The study also shows that variations in performance between univariate and multivariate analysis show that combining forecast provides better results.

REFERENCES

- Assis, K., Amran, A., Remali, Y., & Affendy, H. (2010). A Comparison of Univariate Time Series Methods for Forecasting Cocoa Bean Prices. *Trends in Agricultural Economics*, 3(4), 207-215.
- Clemen, R. T. (1989). Combining Forecasts: A Review and Annotated Bibliography. *International Journal of Forecasting*, 5(4), 559-583.
- Engle, R. F., & Granger, C. W. (1987). Co-Integration and Error Correction: Representation, Estimation, and Testing. *Econometrica*, 55(2), 1057-1072
- Fatimah, M. A., & Roslan, A. G. (1986). Univariate Approach towards Cocoa Price Forecasting. *The Malaysian Journal of Agricultural Economics*, 3, 1-11.
- Floros, C. (2005). Forecasting the UK Unemployment Rate: Model Comparisons. *International Journal of Applied Econometrics and Quantitative Studies*, 2(4), 57-72.
- Frechtling D. C. (1996). *Practical Tourism Forecasting*. Great Britain: Butterworth-Heinemann.
- Funke, M. (1992). Time-Series Forecasting of the German Unemployment Rate. *Journal of Forecasting*, 11(2), 111-125.
- Granger, C. W., & Ramanathan, R. (1984). Improved Methods of Combining Forecasts. *Journal of Forecasting*, 3(2), 197-204.
- Kahforoushan, E., Zarif, M., & Mashahir, E. B. (2010). Prediction of Added Value of Agricultural Subsections using Artificial Neural Networks: Box-Jenkins and Holt-Winters Methods. *Journal of Development and Agricultural Economics*, 2(4), 115-121.
- Kamil, A. A., & Noor, A. M. (2006). Time Series Modeling of Malaysian Raw Palm Oil Price: Autoregressive Conditional Heteroskedasticity (ARCH) Model Approach. *Discovering Mathematics*, 28(2), 19-32.
- Shamsudin, M. N., Rosdi, M. L., & Ann, T. C. (1992). An Econometric Analysis of Cocoa Prices: A Structural Approach. *Malaysia Journal of Economic*, 25(June 1992), 3-17.
- Thomakos, D. D., & Guerard, J. B. (2004). NaïVe, ARIMA, Nonparametric, Transfer Function and VAR Models: A Comparison of Forecasting Performance. *International Journal of Forecasting*, 20(1), 53-67.

Muniroh, M. F., Ismail, N. and Lazim, M. A.

Zhou, B., He, D., & Sun, Z. (2006). *Modelling and Simulation Tools for Emerging Telecommunication Networks*. United States of America, USA: Springer.



Complexity Index for Decision Making Method

Hanif, H. M.*, Mohamad, D. and Dom, R. M.

Faculty of Computer and Mathematical Sciences, Universiti Teknologi MARA, 40450 UiTM, Shah Alam, Selangor, Malaysia

ABSTRACT

Complexity has been discussed in decision making, computational, task complexity, activity network, supply chain, imaging, project management and mechanical. This paper reviews the definition of complexity and the preliminary-related definitions of complexity index in decision making. It proposes a complexity index for decision making, its properties, and implementation.

Keywords: Complexity index, decision making method

INTRODUCTION

Complexity determines whether the procedure or method surpasses others in term of performance. Though complexity has been investigated measuring it in decision making methods with multi granular term sets is difficult. (Francisco Herrera, Herrera-viedma, Martinez, Mata, & Pedro, 2004; F. Herrera, Alonso, Chiclana, & Herrera-Viedma, 2009; Massanet, Riera, Torrens, & Herrera-Viedma, 2014) have addressed complexity in decision making. In this paper, a brief survey of complexity is presented and followed with a complexity index for decision making based on three factors; information, function and step. The discussion on its implementation follows and ends with the conclusion.

COMPLEXITY IN GENERAL

Decision Making

Complexity in decision making method has been addressed in Francisco Herrera et al., 2004 They claimed that decision making methods that involve multi-granular linguistic term sets are highly complex and tried to solve them by transforming each fuzzy set into a linguistic 2-tuple using a central value

Article history:

Received: 27 May 2016

Accepted: 14 November 2016

E-mail addresses:

harlizahanif@gmail.com, harlizaaj86@yahoo.com

(Hanif, H. M.),

daud@tmsk.uitm.edu.my (Mohamad, D.),

rosma@tmsk.uitm.edu.my (Dom, R. M.)

*Corresponding Author

computed by means of a weighted average, where the weights are the membership degrees of the fuzzy set. In F. Herrera et al., 2009 the question that has been raised is whether it is possible to minimize the computation efforts in order to obtain the final choices using multi-granular linguistic term sets. Massanet et al., 2014 proposed a less complex multi-granular linguistic term set method by transforming it to discrete fuzzy numbers to reduce the complexity of the method in terms of the linguistic representation and the aggregation.

Computational

In computational Hartmanis & Stearns, 1965 examined a scheme of classifying sequences according to how hard they are to compute. According to them, their scheme can be generalized to classify numbers, functions, or recognition problems according to their computational complexity. A sequence of the computational complexity is measured by how fast a multi-tape Turing machine can print out the terms of the sequence.

Task Complexity

Task complexity has been classified as the determinants of the performance of method. Wood, 1986 divided the task complexity into three types. The first one is component complexity which direct function of the number of distinct acts that needs to be executed in performance of the task. The general formula which captures the aggregated effects of component complexity at each levels are presented as follows:

$$TC_1 = \sum_{j=0}^{j=p} \sum_{i=1}^{i=n} W_{ij} \tag{1}$$

where n is the number of distinct acts of subtask j , W_{ij} is the number of information cues to be processed in the performance of the i^{th} act of the j^{th} subtask and p is number of subtask in the task.

The second type of complexity is the coordinative complexity where it is defined as the nature of relationships between task inputs and task product (Oeser & O'Brien, 1967). At this level, timing, frequency, intensity and location requirements for performances of required acts will be included. Complexity is represented by:

$$TC_2 = \sum_{i=1}^{i=n} r_i \tag{2}$$

where n is number of acts in the task and r_i is number of precedence relations between the i^{th} act and all other acts in the tasks.

Dynamic complexity is the third type of complexity. It is due to changes in the states that have an effect on the relationship between task inputs and products. Knowledge about changes in the component and coordinative complexities of a task over time is required. The formula is as follows:

$$TC_3 = \sum_{f=1}^{f=m} |TC_{1(f+1)} - TC_{1(f)}| + |TC_{2(f+1)} - TC_{2(f)}| \tag{3}$$

where TC_1 is component complexity measured in standardized units, TC_2 is coordinate complexity measured in standardized units, f is the number of time periods over which the task is measured and TC_3 is dynamic complexity.

The overall complexity should be weighted such that a unit of TC_3 contributes more than a unit of TC_2 , which, in turn contributes more than a unit in TC_1 .

$$TC_t = \alpha TC_1 + \beta TC_2 + \gamma TC_3 \tag{4}$$

where $\alpha > \beta > \gamma$.

Activity Network

In activity network De Reyck & Herroelen, 1996 defined complexity index as the minimum number of node reductions necessary to transform a general activity network to a series-parallel network in activity network.

Supply Chain

Based on Efstathiou, Calinescu, & Blackburn, 2002 supply chain complexity can be divided into three types. Structural complexity is the first type and defined as the expected amount of information needed to describe the schedule state of the facility. The probability of each resource being in each of its allowed states need to be obtained as follows

$$S = - \sum_{j=1}^M \sum_{i=1}^{S_j} P_{ij} \log_2 P_{ij} \tag{5}$$

where M is the number of facility (such as machines or work centres), P_{ij} is the probability of resource j being in state i and S_j is for resource j there are S_j possible states.

Dynamic complexity is the second type of complexity that can be obtained using an expression similar to that for structural complexity. The formula is as follows:

$$D = - \sum_{j=1}^M \sum_{i=1}^{S_j} p'_{ij} \log_2 p'_{ij} \tag{6}$$

where p' is a probability estimates based on observed states rather than scheduled states.

The final type of complexity in supply chain is the decision-making complexity. The definition can be viewed in two perspectives. The first one is from a production process perspective where a systematic characteristic which integrates fundamental dimensions of the manufacturing world, including size, variety, concurrency, objectives, information, cost and value. The second perspective is from an information-theoretic perspective. It is defined as a measure of the volume and structure of the information that needs to be taken into account when creating the schedule for a given period or equivalently, as the difficulty embedded in creating the schedule. The formula is as follows:

$$DM = - \sum_{i=1}^m \sum_{j=1}^m \sum_{k=1}^{2^r-1} \sum_{l=1}^n \tilde{\pi}_{ijkl} \log \tilde{\pi}_{ijkl} \tag{7}$$

where m is total number of operations associated with a part mix, n is the number of parts to be concurrently produced in the manufacturing system, r is total number of resource associated with a given part set and $\tilde{\pi} = \{\tilde{\pi}_{y_{kl}}, \forall_i = \overline{l, m}, \forall_j = \overline{l, m}, \forall_k = \overline{l, r}, \forall_l = \overline{l, n}\}$ represent the normalized set of processing requirements with $\sum_{i=1}^m \sum_{j=1}^m \sum_{k=1}^{2^{i-1}} \sum_{l=1}^n \tilde{\pi}_{y_{kl}} = 1$.

Imaging

In imaging, complexity is not only relevant to the stimulus spatial properties but as an emerging factor affecting the human perceiver’s cognitive operations, it can also include the temporal dimensions (Cardaci, Gesù, Petrou, & Tabacchi, 2006). The formula proposed is as follows

$$G_0(\pi) = -\frac{1}{\log(2)} \times (\pi \log(\pi) + (1 - \pi) \log(1 - \pi)) \cdot [7]z \tag{8}$$

$$G_1(\pi) = \frac{2\sqrt{e}}{e-1} (\pi e^{1-\pi} - \pi e^{\pi-1}) \tag{9}$$

$$G_2(\pi) = 4\pi(1 - \pi) \tag{10}$$

where $\pi = \frac{1}{n} \sum_{i=1}^n |h_i|$ and h_i are the grey levels of the image pixels normalized is the range [0,1].

Project Management

Vidal, Marle, & Bocquet, 2011 defined complexity as the property of a project which makes it difficult to understand, foresee and keep under control its overall behaviour, even when given reasonably complete information about the project system in project management. They introduced project complexity index based on the following formula

$$CI_i = \frac{S(i)}{\max(S(i))} \rightarrow 0 \leq CI_i \leq 1 \tag{11}$$

where $S(i)$ is the priority source of alternative A_i obtained from to Analytic Hierarchy Process (AHP) calculations ($0 \leq CI_i \leq 1$).

Mechanical

In mechanical area Little, Tuttle, Clark and Corney (1998) proposed the complexity index for quantifying the geometric complexity of a three-dimensional solid model. This measure may be compared one with another, in relation to their relative complexity using the following formula

$$FCI = C. D_r T \quad (\text{summation}) \tag{12}$$

where FCI is Feature Complexity Index, T is an alphabetic one design to indicate the types of geometry found in a body; a is planar faces, b is cylindrical faces, c is other geometry type.

COMPLEXITY INDEX FOR DECISION MAKING METHOD

In this section, a method to measure the complexity for decision making method is proposed. The contributory factor, preliminary related definitions, the proposed complexity index, properties and implementation are presented accordingly.

Contributory Factor

There are several complexity contributory factors that has been listed out by researches. Wood, 1986 listed three types of task complexity: component complexity, dynamic complexity and coordinative complexity. The component complexity is a direct function of the number of distinct acts that need to be executed in performance of the task. In activity network, Kolisch, Sprecher and Drexl (1992) stated that the number of activities (steps to be taken) is the factor that resulting in a higher complexity. In 1996, De Reyck and Herroelen (1996) mentioned that the number of node (activity) needs to be reduced in order to transform a general activity network to a series-parallel network. In developing an algorithm, Chakraborty and Choudhury (2000) stated that the execution time and minimum number of operations to compute a given function is necessary to reduce the complexity of the algorithm.

Efstathiou et al. (2002) listed three types of complexity for a supply chain. One, structural complexity, defined as the expected amount of information needed to describe the schedule state of the facility. Two, dynamic complexity obtained using an expression similar to structural complexity. Three, is defined as a systematic characteristic which integrates fundamental dimensions of the manufacturing world, including size, variety, concurrency, objectives, information, cost and value. Meanwhile, Fortnow and Homer (2003), claimed that time can be measured by the number of steps as a function of the length of the input. On the other hand, Guo and Nilsson (2004) defined the algorithm complexity as the average number of search sub-lattices per symbol vector. The number of computational steps required in order to achieve a pre-determined fixed probability of success is defined to be the complexity of an algorithm (Shenvi, Brown, & Whaley, 2003).

The number of evaluation on line per symbol vector is defined by (Guo & Nilsson, 2004) as the definition of algorithm complexity. Jongho, Park, Lee and Song (2011) chose minimum integer in order to keep the computational complexity as low. Meanwhile, Herrera et al. (2009) raised a question that "Is it possible to minimize the computation efforts required to obtain the final choices using multi-granular linguistic information?" (p.354). In project management, Vidal et al. (2011) defined project complexity as the property of a project. Table 1 summarized the complexity contributory factors.

Table 1
The Summary of Complexity Contributory Factors

References	Factors		
	Information	Function	Step
Hartmanis & Stearns, 1965	√	√	
Wood, 1986		√	
Kolisch et al., 1992			√
De Reyck & Herroelen, 1996			√
Chakraborty & Choudhury, 2000		√	√
Efstathiou et al., 2002	√	√	
Shenvi et al., 2003			√
Fortnow & Homer, 2003			√
Guo & Nilsson, 2004			√
Jongho et al., 2011		√	
F. Herrera et al., 2009			√
Vidal et al., 2011		√	

Preliminary Related Definitions

This section listed the related definition and remarks that will be utilized in the proposed complexity index for decision making method.

Definition 1. The complexity index in decision making is the summation of quantity of information and also step times by function of a proposed method.

To calculate the complexity of a method, the following elements are taken into consideration: unification, aggregation and evaluation.

The Proposed Complexity Index

The proposed formula is based on the three contributory factors that are variable, function and step. Based on Wood (1986), the complexity index can be defined as a summation of the three types of complexity (Eqn. 1-4) and the proposed complexity index will be based on the same approach.

According to Efstathiou et al. (2002), one of the factors contributing to complexity in the supply chain is the expected amount of information needed to describe the schedule state of the facility. In decision making, the amount of information is the quantity of the input that can be translated into the number of variables involved. The formula, definition and properties of quantity of information are as follows.

$$\text{variable} = \sum v, \quad 0 < v < \infty \tag{13}$$

where *v* is considered as the number of information.

Definition 2. The quantity of information, ν is the number of variables used in a method.

Assumptions

1. The quantity of information is in between zero to infinity ($0 < \nu < \infty$)
2. Since the evaluation in decision making maybe in the form of fuzzy numbers, the number of variables will depend on the chosen type of fuzzy numbers. For example, a triangular fuzzy number (a, b, c) is considered to have three information meanwhile a trapezoidal fuzzy number (a, b, c, d) has four information.
3. For each section, if the information is redundant from the previous section, it counts as a number of information in the new section. However, if the same information is used repeatedly in the same section, it is considered as only one information.

Several researchers (Hartmanis & Stearns, 1965), (Wood, 1986), (Chakraborty & Choudhury, 2000), (Efstathiou et al., 2002), (Jongho et al., 2011) and (Vidal et al., 2011) claimed that the function used in decision making method is one of the contributory factors for complexity. Function in decision making method is translated into quantity of formula. However, an argument of simply counting the number of operations is not enough is valid if the operation is different making it necessary to give an index to the number of operations.

In solving mathematical formulation, it is frequent to question where to begin (in terms of the operations of arithmetics). BODMAS is an acronym creates to help memorize the ordering of the operations of arithmetics. According to Gamble, 2011 BODMAS stands for Brackets, Orders, Division, Multiplication, Addition, Subtraction. There are also other acronyms exists such as;

- i. BIMDAS (Brackets, Indices, Multiplication, Division, Addition, Subtraction),
- ii. BEDMAS (Brackets, Exponents, Division, Multiplication, Addition, Subtraction)
- iii. PODMAS (Parentheses, Orders, Division, Multiplication, Addition, Subtraction)
- iv. *Please Excuse My Dear Aunt Sally* (Parentheses, Exponents, Multiplication, Division, Addition, Subtraction),

Based on (Holt, 2015), there are three levels in BODMAS. The three levels are as follows; Brackets (First Level); Order, Divide and Multiply (Second Level); Addition and Subtract (Third Level)

As mentioned earlier, indices and exponent (taken from other acronyms) are synonymous for orders which implies to be in the second level. In addition, Gamble (2011) mentioned that for each level, it has the same precedence. Such as addition and multiplication are on the same level, thus it has the same precedence which implies the same weightage (index). The other level (higher level) includes order, indices, exponents, division and multiplication are on the other level.

Since the third level (addition and subtraction) is the lowest level, thus for the purpose of the index of formula operation, the index is one. The second level that includes order, indices, exponents, division and multiplication are index two. For the exponent with power more than two, the index depends on the power since it may result in longer operation due to it embedded the multiplication process in it. For example; $a^3 = a \times a \times a$, this implies multiplication operation

is involve for the three elements. Thus, the index is three. For other mathematical operation such as absolute and maximum and minimum, the index is one since it involves a simple mathematical operation only. For each of the function involves, the operation is index proposed according to Table 2.

Table 2
The Index of Formula Operation

	Operation	Index
1	Addition	1w
2	Subtraction	1w
3	Multiplication	2w
4	Division	2w
5	Exponent; Power of less than 1	2w
	Exponent; Power of 2	2w
	Exponent; Power of 3	3w
	Exponent; Power of n	nw
6	Trigonometric, logarithmic	2w
7	Absolute	1
8	Min, Max	1

where w is the number of element of in the type of number used. For real/crisp number, w is considered as 1, a triangular fuzzy number has three elements (a, b, c), thus, w is 3 and for trapezoidal fuzzy number, it has four elements (a, b, c, d), where w is 4.

Example

Example of calculation of index of operation is as follows:

Let $x = \frac{f}{\sqrt{a+b}}$ be a function used in method where f is a triangular fuzzy number (p, q, r) and a, b are scalars. The ‘ $a+b$ ’ addition has index of 1. ‘ $\sqrt{a+b}$ ’ square root has index of 2. Since f consists of three values (p, q, r) and each of the value undergo the division process, thus there are six operations involved. Thus, the total index for this operation is $1+2+6= 9$.

According to Chakraborty and Choudhury (2000), developing the least asymptotic execution time algorithm is important for a method to be effective. The time can be measured by the number of steps as a function of the length of the input (Fortnow & Homer, 2003). For Shenvi et al. (2003), the number of computational steps required in order to achieve a pre-determined fixed probability of success is defined as the complexity of an algorithm. On the other hand, Guo and Nilsson (2004) defined the algorithm complexity as the average number of search sub-lattices. Meanwhile, Jongho et al. (2011) chose minimum integer in order to keep the computational complexity as low. In addition, Herrera et al. (2009) raise the question: “Is it possible to minimize the computation efforts required to obtain the final choices using

multi-granular linguistic information?" (p.354). Thus, the quantity of step is considered from both computational and non-computational part.

In decision making, the usage of the function relates to the number of steps. Hence for each step, the index of function is embedded together in the step. If the step does not require any formula, it is considered as one. The formula, definition and properties of quantity of function and steps are as follows.

$$\text{function and step} = \sum fs, \quad 0 < f < \infty, \quad 0 < s < \infty \quad (14)$$

where f is the number of function and s is the number of step.

Assumptions

1. The quantity of function is in between zero to infinity ($0 < f < \infty$)
2. The quantity of step is in between zero to infinity ($0 < s < \infty$)
3. The index of operation is counted as per applied in each step.
4. If the step does not involve any formula, it is considered as 1.

The summation of the contributory factors is divided by 1000 for capping purposes so that the output index has a reasonable and acceptable value. Any calculated value of more than 1000 may be considered as highly complex which is due to partially or fully by the contributing factors. Hence, the overall complexity index, CI is defined as the summation of quantity of information, v , function, f and step, s and is given as

$$CI = \frac{\sum v + \sum fs}{1000}. \quad (15)$$

The result of the complexity index may be categorized as; $(0,0.25)$ = low complexity, $[0.25,0.5)$ = marginal complexity, $[0.5,1)$ = medium complexity and $[1,\infty)$ = high complexity.

Remark

1. The measurement of the complexity index is considered the worst-case scenario.
2. The complexity index of any two methods can only be compared when the basis is equal, for instance, the number of alternatives, criteria and sub-criteria under consideration are equal.

Properties

The proposed complexity index has the following properties;

1. $CI \neq 0$ since v, f and $s > 0$
2. $\sum fs + \sum v = \sum v + \sum fs$
3. $\sum fs = \sum sf$

4. $\sum v + \sum fs \geq 2$ since v, f and $s > 0$, the min value for v, f and s is 1. Thus;
 $CI = \sum v + \sum fs = 1 + 1(1) = 2$
5. $CI \in [0.002, \infty)$ since in relation to properties no. 4, the minimum value of $\sum v + \sum fs$ is 2.

Illustrative Examples

In order to implement the complexity index, the index will be implemented to crisp model of Technique for Order of Preference by Similarity to Ideal Solution (TOPSIS) and Analytic Hierarchy Process (AHP) first. Then the complexity index will be implemented to decision making method that used fuzzy numbers.

This research will implement Shyur (2006), and Ding and Kamaruddin (2014) for TOPSIS and for AHP (Chaghooshi, Janatifar, & Dehghan, 2014; Escobar & Moreno-Jimenez, 2007). For decision making method based on fuzzy numbers it will implement the index to single decision maker by Tseng and Klein (1989). For homogeneous group decision making method, this research will implement the method of Hanif et al. (2013) and Chen and Chen (2009). As for heterogeneous group decision making is used (Herrera, Herrera-Viedma, & Martínez, 2000; Jiang, Fan, & Ma, 2008; Massanet et al., 2014). The results are illustrated in Table 3 and 4 respectively.

Table 3
Single Versus Group Decision Making Crisp Topsis Method

Method	DM	Alt	Crt	CI
Shyur, 2006	1	3	3	0.291
Ding & Kamaruddin, 2014	3	3	3	0.362

DM-decision maker, Atl-alternatives, Crt-criteria.

Table 4
Single Versus Group Decision Making Crisp Ahp Method

Method	DM	Alt	Crt	CI
Chaghooshi et al., 2014	1	3	3	0.541
Escobar & Moreno-Jimenez, 2007	3	3	3	1.316

DM-decision maker, Atl-alternatives and Crt-criteria.

The method of Shyur, 2006 has lower complexity index compared with Ding and Kamaruddin (2014) because it is a single decision maker method while that of Ding and Kamaruddin (2014) is a group decision making method of TOPSIS. With similar argument, for AHP Chaghooshi et al. (2014) has lower complexity index compared with Escobar adandoreno-Jimenez (2007). In general, TOPSIS has lower complexity index (smaller range) compare to AHP (bigger range). Table 5 shows the result of complexity index for single versus group decision making fuzzy number method.

Table 5
Single Versus Group Decision Making Fuzzy Number Method

Method	DM	Alt	Crt	CI
(Tseng & Klein, 1989)	Single	3	1	0.111
(Hanif et al., 2013)	GHM	3	3	0.339
(Chen & Chen, 2009)	GHM	3	3	0.245
(F. Herrera et al., 2000)	GHT	3	1	0.861
(Jiang et al., 2008)	GHT	3	1	0.212
(Massanet et al., 2014)	GHT	3	1	0.557

DM - decision maker, Atl-alternatives, Crt-criteria, GHM-group homogeneous method, GHT-group heterogeneous method.

From Table 5, the method of Tseng and Klein (1989) has the lowest complexity index as it is a single decision making method. As for homogeneous group decision making (Hanif et al., 2013) has complexity index of 0.339. Meanwhile, it has 0.245 for complexity index (Chen & Chen, 2009). For heterogeneous group decision making, (Herrera et al., 2000) 0.861 complexity index. Herrera et al. (2000) proposed among the earliest method of heterogeneous group decision making. It is also a heterogeneous group decision making but with a low complexity index of 0.212, according to Jiang et al. (2008). Their method is based on fuzzy set and goal programming methods and claimed to have lower complexity due to this. According to Massanet et al. (2014), this is based on heterogeneous group decision making with a 0.553 complexity index. Their method used discrete fuzzy number which produces a lesser complexity index.

CONCLUSION

This paper elaborates general complexity in decision making, computational, task complexity, activity network, supply chain, imaging, project management and mechanical (what? Describe). A complexity index for decision making is proposed based on three factors which are the quantity of information, v , function, f and step, s . The complexity index proposed may justify the complexity level for the decision-making method. Illustrative examples are included in this paper to describe its usefulness. Since this is the first attempt to introduce a complexity index for decision making method, more improvement needs to be made in the future.

REFERENCES

- Cardaci M., Di Gesù V., Petrou M., Tabacchi M. E. (2006). On the Evaluation of Images Complexity: A Fuzzy Approach. In I. Bloch, A. Petrosino, & A. G. B. Tettamanzi (Eds.), *Fuzzy Logic and Applications* (Vol. 3849, pp. 305-311). Berlin, Heidelberg: Springer. Retrieved from http://link.springer.com/chapter/10.1007/11676935_38
- Chaghoooshi, A. J., Janatifar, H., & Dehghan, M. (2014). An Application of AHP and Similarity-Based Approach to Personnel Selection. *International Journal of Business Management and Economics*, 1(1), 24–32.

- Chakraborty, S., & Choudhury, P. P. (2000). A Statistical Analysis of an Algorithm's Complexity. *Applied Mathematics Letters*, 13(5), 121–126.
- Chen, S. M., & Chen, J. H. (2009). Fuzzy risk analysis based on ranking generalized fuzzy numbers with different heights and different spreads. *Expert Systems with Application*, 36(3), 6833–6842.
- De Reyck, B., & Herroelen, W. (1996). On the use of the complexity index as a measure of complexity in activity networks. *European Journal of Operational Research*, 91(2), 347–366. [http://doi.org/10.1016/0377-2217\(94\)00344-0](http://doi.org/10.1016/0377-2217(94)00344-0)
- Ding, S. H., & Kamaruddin, S. (2014). Assessment of distance-based multi-attribute group decision-making methods from a maintenance strategy perspective. *Journal of Industrial Engineering International*, 11(1), 73-85. <http://doi.org/10.1007/s40092-014-0078-2>
- Efstathiou, J., Calinescu, A., & Blackburn, G. (2002). A web-based expert system to assess the complexity of manufacturing organizations. *Robotics and Computer-Integrated Manufacturing*, 18(3-4), 305–311. [http://doi.org/10.1016/S0736-5845\(02\)00022-4](http://doi.org/10.1016/S0736-5845(02)00022-4)
- Escobar, M. T., & Moreno-Jimenez, J. M. (2007). Aggregation of individual preference structures in AHP-group decision making. *Group Decision and Negotiation*, 16(4), 287–301.
- Fortnow, L., & Homer, S. (2003). A Short History of Computational Complexity. *European Association for Theoretical Computer Science*, 80, 95–133.
- Gamble, G. (2011). BODMAS , BOMDAS and DAMNUS ... the sequel. *Mathematical Association of Western Australia*, 21(1), 7–11.
- Guo, Z., & Nilsson, P. (2004). Reduced Complexity Schnorr – Euchner Decoding Algorithms for MIMO Systems. *IEEE Communications Letters*, 8(5), 286–288.
- Hanif, H. M., Mohamad, D., Sulaiman, N. H., Mohd, H., Mohamad, D., & Hashimah, N. (2013). Solving Decision Making Problems using Fuzzy Numbers with Area Dominance Approach. In *20th National Symposium on Mathematical Sciences* (pp. 229–236). Universiti Kebangsaan Malaysia, Malaysia. <http://doi.org/10.1063/1.4801128>
- Hartmanis, J., & Stearns, R. E. (1965). On The Computational Complexity of Algorithms. *Transactions of the American Mathematical Society*, 117(May), 285–306.
- Herrera, F., Alonso, S., Chiclana, F., & Herrera-Viedma, E. (2009). Computing with words in decision making: foundations, trends and prospects. *Fuzzy Optimization and Decision Making*, 8(4), 337–364. <http://doi.org/10.1007/s10700-009-9065-2>
- Herrera, F., Herrera-Viedma, E., & Martínez, L. (2000). A fusion approach for managing multi-granularity linguistic term sets in decision making. *Fuzzy Sets and Systems*, 114(1), 43–58. [http://doi.org/10.1016/S0165-0114\(98\)00093-1](http://doi.org/10.1016/S0165-0114(98)00093-1)
- Herrera, F., Herrera-viedma, E., Martinez, L., Mata, F., & Pedro, J. S. (2004). A Multi-Granular Linguistic Decision Model for Evaluating the Quality of Network Services. In D. Ruan & X. Zeng (Eds.), *Intelligent Sensory Evaluation* (pp. 71-91). Germany: Springer Berlin Heidelberg.
- Holt, J. (2015). *Steps into Numeracy: What Do I Do First BODMAS*. University of East Anglia, Norwich, United Kingdom. Retrieved from <https://portal.uea.ac.uk/dos/learning-enhancement/study-resources/maths-stats/numeracy/what-do-i-do-first-bodmas>
- Jiang, Y. P., Fan, Z. P., & Ma, J. (2008). A Method for Group Decision Making with Multi-Granularity Linguistic Assessment Information. *Information Sciences*, 178(4), 1098–1109.

- Jongho, O., Park, S. R., Lee, S. R., & Song, I. (2011). Decoding With Hypothesis Testing : A Near ML Decoding Scheme for MIMO Systems. *IEEE Transactions on Vehicular Technology*, 60(3), 1251–1257.
- Kolisch, R., Sprecher, A., & Drexl, A. (1992). *Characterization and generation of a general class of resourceconstrained project scheduling problems: Easy and hard instances*. (Technical Report 301). Manuskripte aus den Instituten fuer Betriebswirtschaftslehre.
- Little, G., Tuttle, R., Clark, D. E. R., & Corney, J. (1998). A feature complexity index. *Proceedings of the Institution of Mechanical Engineers, Part C: Journal of Mechanical Engineering Science*, 212(5), 405–412. <http://doi.org/10.1243/0954406981521321>
- Massanet, S., Riera, J. V., Torrens, J., & Herrera-Viedma, E. (2014). A new linguistic computational model based on discrete fuzzy numbers for computing with words. *Information Sciences*, 258, 277–290. <http://doi.org/10.1016/j.ins.2013.06.055>
- Oeser, O. A., & O'Brien, G. (1967). A Mathematical Model for Structural Role Theory, III. *Human Relations*, 20(1), 83–97.
- Shenvi, N., Brown, K. R., & Whaley, K. B. (2003). Effects of Random Noisy Oracle on Search Algorithm Complexity. *Physical Review A*, 68(5), 1–17.
- Shyur, H. J. (2006). COTS evaluation using modified TOPSIS and ANP. *Applied Mathematics and Computation*, 177(1), 251–259. <http://doi.org/10.1016/j.amc.2005.11.006>
- Tseng, T. Y., & Klein, C. M. (1989). New algorithm for the ranking procedure in fuzzy decisionmaking. *IEEE Transactions on Systems, Man, and Cybernetics*, 19(5), 1289–1296.
- Vidal, L. A., Marle, F., & Bocquet, J. C. (2011). Measuring project complexity using the Analytic Hierarchy Process. *International Journal of Project Management*, 29(6), 718–727. <http://doi.org/10.1016/j.ijproman.2010.07.005>
- Wood, R. E. (1986). Task Complexity: Definition of the Construct. *Organizational Behavior and Human Decision Process*, 37(1), 60–82.





Evaluation of Risk Factors for Prolonged Invasive Mechanical Ventilation in Paediatric Intensive Care Unit (PICU)

Ismail, I.^{1*}, Yap, B. W.² and Abidin, A. S. Z.³

¹ Faculty of Computer and Mathematical Sciences, Universiti Teknologi MARA, 18500 UiTM, Machang, Kelantan, Malaysia

² Advanced Analytics Engineering Centre, Faculty of Computer and Mathematical Sciences, Universiti Teknologi MARA, 40450, Shah Alam, Selangor, Malaysia

³ Faculty of Medicine, Universiti Teknologi MARA, 47000 UiTM, Sungai Buloh, Selangor, Malaysia

ABSTRACT

Prolonged mechanical ventilation (PMV) is associated with increase in mortality and resource utilisation as well as hospitalisation costs. This study evaluates the risk factors of PMV. A retrospective study was conducted involving 890 paediatric patients comprising 237 neonates, 306 infants, 223 of pre-school age and 124 who are of school going age. The data mining decision trees algorithms and logistic regression was employed to develop predictive models for each age category. The independent variables were classified into four categories, that is, demographic data, admission factors, medical factors and score factors. The dependent variable is the duration of ventilation where it is categorized 0 denoting non-PMV and 1 denoting PMV. The performances of three decision tree models (CHAID, CART and C5.0) and logistic regression were compared to determine the best model. The results indicated that the decision tree outperformed the logistic regression model for all age categories, given its good accuracy rate for testing dataset. Decision trees results identified length of stay and inotropes as significant risk factors in all age categories. PRISM 12 hours and principal diagnosis were identified as significant risk factors for infants.

Keywords: Mechanical ventilation, prolonged mechanical ventilation, paediatric, logistic regression, decision tree

INTRODUCTION

The Paediatric Intensive Care Unit (PICU) provides care for infants, children and adolescents who are critically ill or injured. There are several conditions that usually cause critical illness such as severe infection, poisoning, drug overdose, trauma, extensive

Article history:

Received: 27 May 2016

Accepted: 14 November 2016

E-mail addresses:

idari512@kelantan.uitm.edu.my (Ismail, I.),

beewah@tmsk.uitm.edu.my (Yap, B. W.),

anis739@salam.uitm.edu.my (Abidin, A. S. Z.)

*Corresponding Author

surgery, congenital anomalies and immunological disorders. The first PICU was developed in 1955 in Gothenburg, Sweden to provide intensive care for polio patients, new-borns diagnosed with respiratory distress syndrome (RDS), postoperative children and severe pneumonia (Lin and Hsieh, 2009). In the United States, it was reported that 276 PICUs were established in 1989, 306 PICUs in 1995 and 349 in 2001 (Randolph et al., 2003).

The first PICU in Malaysia was established in University Hospital Kuala Lumpur (now known as University Malaya Medical Centre) in 1980. The PICU in University Malaya Medical Centre has the capacity to ventilate 10 patients with 24-hour Paediatric Intensivist coverage. This ten-bed multidisciplinary unit provides care for patients with hepatobiliary-gastrointestinal, haemato-oncology, cardiology, respiratory, genetic & metabolic, general surgery, otolaryngology, ophthalmology subspecialties and those undergoing bone marrow transplant.

Mechanical ventilation (MV) is usually used for a few days to help patients with acute serious illness. It can be applied as negative pressure on the outside of the thorax. Mostly, mechanical ventilation is applied as positive pressure to the airway where positive pressure ventilation can be invasive and non-invasive. The use of MV with positive pressure in PICU has increased [3]. Invasive ventilation is delivered via endotracheal tube or tracheostomy while non-invasive ventilation helps the patients to breathe with the help of a face mask.

Several previous studies found that children who require mechanical ventilation have increased. Farias et al., (2004) found that 35% of children or 659 out of 1893 patients were ventilated for 12 hours while Traiber et al., (2009) reported that the proportion of children in three Brazilian paediatric intensive care unit (PICU) who required mechanical ventilation for > 21 days was 2.5% or 192 of 7598 admissions. In a study by Payen et al. (2012), they found nearly similar results whereby 30% for all PICU admissions (315 patients) were ventilated for 12 hours and 2.9% for at least 21 days.

The use of mechanical ventilation can result in several complications such as airways, barotrauma, and nosocomial infections. Complications arising from the use of mechanical ventilation may cause prolonged mechanical ventilation (PMV), and lead to an increase in length of hospitalization and mortality rates (Kipps et al., 2011). A study by Chelluri et al., (2004) revealed that mortality rate for patients who received mechanical ventilation > 48 hours increased with age and number of comorbidities. Tracheostomy in children results in higher mortality and complication rates (Putra et al., 2006). There are several complications that may arise from PMV such as pneumothorax, airway injury, alveolar damage, and ventilator-associated pneumonia. According to Lum et al., (2011), invasive mechanical ventilation is associated with ventilator-induced and ventilator-associated pneumonia where a tracheal tube may cause subglottic and tracheal injury and ineffective clearance of secretions.

This study focuses on developing models for predicting duration of invasive mechanical ventilation and determining risk factors associated with PMV for patients in a PICU in Malaysia.

METHODS

Data Source

A retrospective study was conducted with e data retrieved from clinical records of paediatric patients admitted at Paediatric Intensive Care Unit (PICU) in a local hospital in Kuala Lumpur, Malaysia from August 2008 to June 2012. The data was extracted from the patients' forms which recorded information on demography, admissions, information on mechanical ventilation, patient related procedure, patient related therapy surgery, ICU acquired infection and death. The patients' forms were filled by the nurses at the unit.

Population and Sample of Study

All patients who were below 18 years old and requiring invasive mechanical ventilation were included in this study. A total of 1931 patients were admitted to PICU from August 2008 to June 2012. Of 1931 patients, 994 of them required invasive ventilation. This study only focuses on patients who needed invasive ventilation. Among the 916 patients included in this study, 447 needed ventilation ≥ 72 hours (PMV) and 496 patients required < 72 hours (non-PMV). Since there are only 26 adolescents, these adolescents were not included in the process of building the predictive models.

Theoretical Framework. The variables were classified into four categories (demographic data, admission factors, medical factors and score factors). The theoretical framework proposed in this study is presented in Figure 1. There are 4 continuous predictors (age, weight, length of stay and PRISM III-12) and the remaining predictors are categorical. The predictors involve (Age, Gender, Ethnicity and Weight, Admission source (Elective, Non-Elective), Admission type (Emergency, Ward, Referral), Surgery (Yes/No), VAP (Yes/No), BSI(Yes/No), Inotropes (Yes/No), Shock(Yes/No), Principal Diagnosis (respiratory, cardiovascular, gastroenterology, neurology and others), length of stay and PRISM III-12. The Paediatric Risk of Mortality (PRISM) is physiology-based predictor for PICU patients. This composite score use the death rate as an outcome measure. Using for evaluation within 24 hours after admission, PRISM III is a score between 0-38 where it comprises of 17 physiological data. The 17 physiological data consist of 5 clinical parameters which are systolic blood pressure, heart rate, Glasgow Coma Scale, papillary reflexes and temperature and the other 12 variables are acid-base status (pH, CO₂, PCO₂, and PaO₂), chemistry tests (glucose, potassium, creatinine, blood urea nitrogen) and haematology tests (white blood cell count, platelet count, prothrombin time and partial thromboplastin time). The dependent variable is Duration of Ventilation. If duration of ventilation is ≥ 72 hours it is coded as 1 (PMV) while 0 (Non- PMV) represents ventilation < 72 hours.

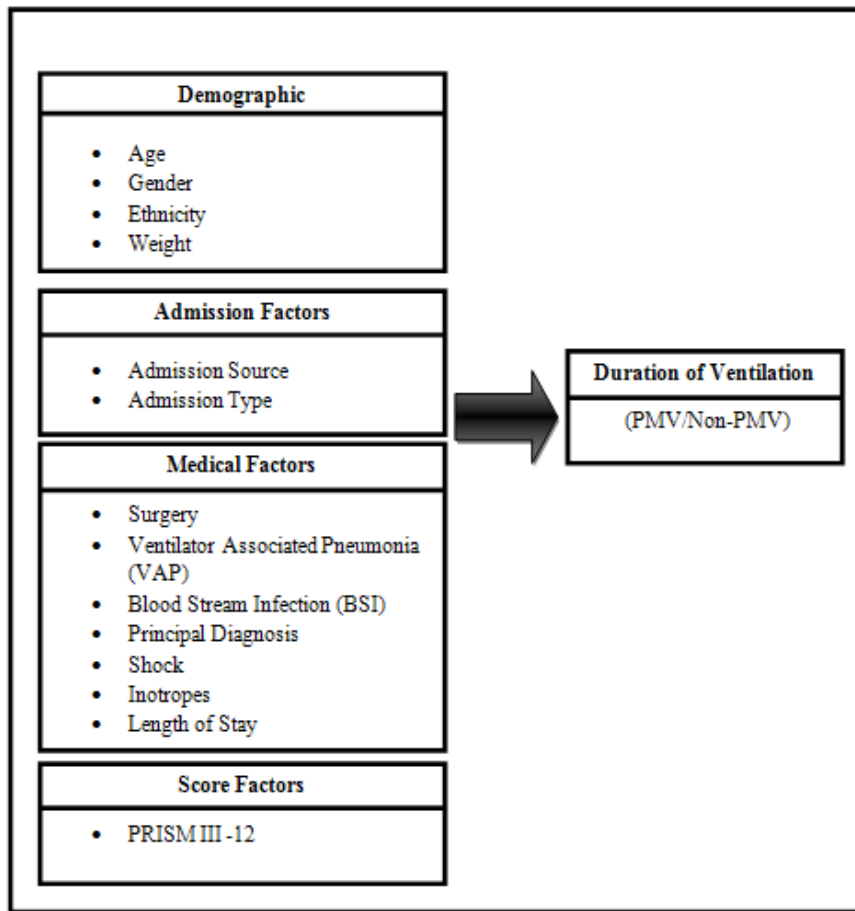


Figure 1. Theoretical Framework

Statistical Analysis

The analysis was carried out for four different age categories. Table 1 presents the age range for each age category. The predictive models include logistic regression and decision trees.

Table 1
Age Category

Age Category	Age Range
Neonate	0 -30 days
Infant	1 - 12 months
Pre-School Age	1 - 5 years
School-Age	6 - 12 years

Logistic Regression

Logistic regression is widely used in modelling a dichotomous dependent variable (Hair et al., 1998). The use of logistic regression is appropriate for predicting disease state (diseased/healthy) and decision making (yes/no) (Bagley et al., 2001). Due to its ability to model binary outcomes, it is widely implemented in health sciences study and for determining risk factors in medical studies (Lin et al., 2011; Camdeviren et al., 2007). The logistic regression model is developed based on the values of a set of predictor variables. The predictor variables in logistic regression can be either continuous, categorical or combination of both. For the purpose of developing logistic regression equation, the maximum-likelihood estimation was employed and Wald's statistic was used to determine the significance of the variables (Hosmer & Lemeshow, 2000). Logistic regression may be thought of as an approach that is similar to that of multiple linear regression but the difference is the dependent variable in logistic regression is categorical. The odds-ratio in logistic regression model provides important information on the effect of the risk factors.

The logistic regression model is written as follows:

$$\log\left(\frac{p_i}{1 - p_i}\right) = \beta_0 + \beta_1 X_{i1} + \beta_2 X_{i2} + \dots + \beta_k X_{ik} \quad (1)$$

where $p_i = P(Y_i = 1)$.

In this study, Y is the dependent variable (duration of ventilation) which is categorized as ventilation ≥ 72 hours (PMV) and ventilation < 72 hours (non-PMV).

Thus, by solving the logit in Equation (1), the probability of event $Y=1$ is obtained as follows:

$$P(Y_i = 1) = \frac{1}{1 + e^{-z}} \quad (2)$$

In this study, $P(Y_i = 1)$ is defined as the probability of requiring PMV, $z = \beta_0 + \beta_1 X_{i1} + \dots + \beta_k X_{ik}$.

β_0 = the constant of the equation

β_{ik} = the coefficient for predictor variable

x_{ik} = the predictor variable

β_0 is a constant and $\beta_1, \beta_2, \dots, \beta_k$ are the regression coefficients of the independent variables X_1, X_2, \dots, X_k . where the regression coefficient explains the size of contribution of the predictor variables to the outcome (Ayer et al., 2010). The criterion that is commonly used in measuring and testing statistical significance of the coefficients of the variables is Wald's statistics with $p \leq 0.05$.

Decision Tree

Decision tree is a powerful classification algorithm and widely used in classification problems. This non-linear discrimination method is used to split sample into smaller segments where the process of splitting is based on a set of independent variable (Ture et al, 2005). Decision tree has become a popular method for the purpose of classification and prediction by implementing a sequence of simple rules (Ibrahim et al., 2008). This machine learning technique recursively

splits the sample in branches or segments in order to develop a tree in a process known as recursive partitioning. Quinlan’s ID3, C4.5, C5 and Breinman et al.’s CART are some of the popular decision tree algorithms.

In this study, three commonly used algorithm constructing decision trees that is Chi-Square Automatic Interaction Detector (CHAID), Classification and Regression Tree (CART), and C5.0 were performed. As the dependent variable is a binary categorical variable, the decision trees generated in this study are called a classification tree.

CHAID will select the predictor that is the most significant with the smallest p-value to perform the first split. The process of constructing CHAID tree is done by repeatedly splitting subsets into two or more child nodes. CHAID has an ability to handle large number of predictors and appropriate to be employed when non-linear or complex relationship exists.

The construction of CART begins with the entire data set and repeatedly split subsets of the data based on independent variables to develop two child nodes (Ture et al., 2005). The selection of best predictor in CART can be done using several impurity measures such as Gini, twoing, ordered twoing and least-squared deviation (Kurt et al., 2008). In this study, Gini impurity measure was employed where Gini impurity can be applied for categorical dependent variable.

C5.0 algorithm is the improved version of C4.5 and ID3 algorithm where it is the most recent version of a machine learning program. It uses entropy as a measure of impurity when splitting subsets of observations into child nodes. The process of splitting the subsets repeats until the subsets cannot be split further. At the final stage, the lowest-level splits are reviewed and those that do not contribute significantly to the value of model are removed.

Model Performance Evaluation

The data was partitioned into 70% training and 30% validation samples. The evaluation was based on levels of accuracy, sensitivity, and specificity. The best decision tree model was then compared with logistic regression model. Sensitivity is defined as the proportion of patients who received ventilation ≥72 hours (PMV) correctly predicted by the model. Specificity is defined as the proportion of patients with ventilation < 72 hours (non-PMV) correctly predicted by the model. Classification accuracy, sensitivity and specificity are calculated by referring to the confusion table.

Table 2
Confusion Matrix

		Predicted		Total
		PMV	Non-PMV	
Actual	PMV	TP (True Positives)	FN (False Negatives)	TP + FN
	Non-PMV	FP (False Positives)	TN (True Negatives)	FP + TN
Total		TP + FN	FN + TN	TN+FP+FN+TP

$$\text{Accuracy} = \frac{TP+TN}{TP+TN+FP+FN}, \quad \text{Sensitivity} = \frac{TP}{TP+FN}, \quad \text{Specificity} = \frac{TN}{TN+FP}$$

RESULTS

Table 3 presents some descriptive statistics for each group.

Logistic Regression Analysis

This section discusses the result of logistic regression where ENTER, FORWARD, BACKWARD was used as selection methods in developing the models. The logistic models obtained were employed to identify risk factors associated with PMV.

Table 3
Descriptive Statistics

Age Category	Variable Name	Mean \pm Standard Deviation
Neonates	Weight(Kilogram)*	2.82 \pm 0.62
	Length of Stay(Days)	13.70 \pm 30.54
	PRISM III 12 hours	7.54 \pm 5.54
Infants	Weight(Kilogram)*	5.18 \pm 2.10
	Length of Stay(Days)	12.25 \pm 24.73
Pre -School Age	PRISM 12 hours	5.2 \pm 5.05
	Weight(Kilogram)*	11.85 \pm 24.59
	Length of Stay(Days)	9.69 \pm 17.73
	PRISM 12 hours	4.96 \pm 4.94
School Age	Weight(Kilogram)*	27.80 \pm 12.30
	Length of Stay(Days)	9.41 \pm 19.12
	PRISM 12 hours	5.67 \pm 5.82

Note: PRISM- Paediatric Risk of Mortality

* Data for weight was questionable and thus excluded in predictive modelling analysis.

Table 4 presents the summary of logistic regression results which includes the accuracy rate, sensitivity and specificity values. The logistic regression with ENTER selection method were chosen as the best model for all age categories.

Table 4
Performance of Logistic Regression Models

Age Category	Model	Training Set			Testing Set		
		Accuracy (%)	Sensitivity (%)	Specificity (%)	Accuracy (%)	Sensitivity (%)	Specificity (%)
Neonate	ENTER	76.40	73.26	80.00	68.42	65.42	72.41
	FORWARD	73.91	69.77	78.67	67.11	59.57	79.31
	BACKWARD	73.91	69.77	78.67	67.11	59.57	79.31
Infant	ENTER	77.99	70.48	85.58	77.32	66.67	87.76
	FORWARD	77.99	69.52	86.54	75.26	58.33	91.84
	BACKWARD	77.99	69.52	86.54	75.26	58.33	91.84
Pre-School Age	ENTER	77.63	59.70	91.76	71.83	71.43	72.22
	FORWARD	76.32	53.73	94.12	77.46	68.57	86.11
	BACKWARD	76.32	53.73	94.12	77.46	68.57	86.11
School Age	ENTER	84.09	75.76	89.09	66.67	47.06	84.21
	FORWARD	78.41	60.61	89.10	72.22	47.06	94.74
	BACKWARD	78.41	60.61	89.10	72.22	47.06	94.74

The significant risk factors found in the best logistic regression model for each age categories are summarized in Table 5.

Table 5
Significant Variables

NEONATE (ENTER)	INFANT (ENTER)	PRE-SCHOOL AGE (ENTER)	SCHOOL AGE (ENTER)
<ul style="list-style-type: none"> • PRISM III-12 • Admission Source = Ward • Inotropes = Yes 	<ul style="list-style-type: none"> • Length of Stay 	<ul style="list-style-type: none"> • PRISM III-12 • Inotropes = Yes • Principal Diagnosis = Cardio 	<ul style="list-style-type: none"> • Length of Stay • Inotropes = Yes

Table 6 presents the interpretation of the odds ratio for significant variables found in the logistic regression results.

Table 6
Interpretation of Odds Ratio

NEONATE	PRE-SCHOOL AGE
<ul style="list-style-type: none"> • PRISM 12 Hours (OR = 1.155) Neonates with higher PRISM III-12 score are more likely to receive PMV. • Admission Source (OR = 0.260) Neonates who admitted to PICU from ward are less likely to receive PMV compared to neonates admitted from referrals. • Inotropes (OR = 4. 223) Neonates who required inotropes are 4 times more likely to receive PMV compared to neonates who do not require inotropes. 	<ul style="list-style-type: none"> • PRISM III 12 Hours (OR = 1.135) Pre-school age patients with higher PRISM III-12 score are more likely to receive PMV. • Inotropes (OR = 11.508) Pre-school age patients who required inotropes are 12 times more likely to receive PMV compared to those who do not require inotropes. • Principal Diagnosis = Cardiovascular (OR = 5.964) Pre-school age patients diagnosed with cardiovascular are 6 times more likely to receive PMV compared to those who were diagnosed with other principal diagnosis.
INFANT	SCHOOL AGE
<ul style="list-style-type: none"> • Length of Stay (OR = 1.188) Infants with longer length of stay are more likely to receive PMV. 	<ul style="list-style-type: none"> • Length of Stay (OR = 1.071) School age patients with longer length of stay are more likely to receive PMV. • Inotropes (OR = 9.675) School age patients who required inotropes are 10 times more likely to receive PMV compared to those who do not require inotropes.

Decision Tree Analysis

In this study, three algorithms were used to generate decision tree CHAID, CART and C5.0. Table 7 compares the accuracy, sensitivity and specificity for training and testing dataset of decision tree models. Below are results for each age categories.

Table 7
Decision Tree Performance

Age Category	Model	Training Set			Testing Set		
		Accuracy (%)	Sensitivity (%)	Specificity (%)	Accuracy (%)	Sensitivity (%)	Specificity (%)
Neonate	CHAID	85.09	94.19	74.67	85.53	91.49	75.86
	CART	85.09	94.19	77.33	85.53	91.49	79.31
	C5.0	85.09	94.19	74.67	85.53	91.49	75.86
Infant	CHAID	84.69	89.52	79.81	80.41	70.83	89.80
	CART	82.30	77.14	87.50	72.16	52.08	91.84
	C5.0	79.90	82.86	76.92	79.38	70.83	87.76
Pre-School Age	CHAID	84.87	88.06	82.35	81.69	91.43	72.22
	CART	86.84	92.54	82.35	78.87	94.29	63.89
	C5.0	86.18	94.03	80.00	80.28	97.14	63.89
School Age	CHAID	88.64	69.70	100.00	75.00	52.94	94.73
	CART	90.91	78.79	98.18	80.56	70.59	89.47
	C5.0	88.64	78.79	94.55	83.33	76.47	89.47

For neonate, all three decision tree models gave same accuracy rate and sensitivity rate for both datasets. CART gave the best specificity rate for both datasets. While CHAID produced the best accuracy and sensitivity rate for training and testing sets for infants. For pre-school age patients, CART produce the best accuracy rate for training set while the best accuracy rate in testing set was given by CHAID. CART gave the best accuracy in training dataset for school age patients. C5.0 gave the best accuracy and sensitivity rate for testing dataset for pre-school age.

CART and C5.0 are chosen as the best decision tree model for neonate and school age patients respectively. While, for infant and pre-school age patients, CHAID is chosen as the best model due to slightly higher accuracy rate in testing dataset.

The interpretation of the best decision tree model for each category is presented in Table 8 respectively.

Table 8
Decision Tree Rules

NEONATE (CART)

- If neonates had length of stay for more than 4 days AND did not require inotropes, THEN these neonates received ventilation ≥ 72 hours (PMV).
- If neonates had length of stay for more than 4 days AND required inotropes, THEN these neonates received ventilation ≥ 72 hours (PMV).
- If neonates had length of stay for less or equal to 4 days AND did not require inotropes, THEN these neonates received ventilation < 72 hours (non- PMV).

Table 8 (*continue*)

INFANT (CHAID)
<ul style="list-style-type: none"> • If infants had length of stay for more than 10 days AND had PRISM 12 hours score of more than 0, THEN these infants received ventilation ≥ 72 hours (PMV). • If infants had length of stay for more than 4 days and less or equal to 10 days AND had principal diagnosis of respiratory OR cardiovascular OR neurology OR gastroenterology, THEN these infants received ventilation ≥ 72 hours (PMV). • If infants had length of stay more than 10 days AND had PRISM 12 hours score of 0, THEN these infants received ventilation < 72 hours (non- PMV). • If infants had length of stay for more than 4 days and less or equal to 10 days AND had principal diagnosis except of respiratory, cardiovascular, neurology and gastroenterology, THEN these infants received ventilation < 72 hours (non-PMV). • If infants had length of stay for more than 3 days and less or equal to 4 days, THEN these infants received ventilation < 72 hours (non-PMV). • If infants had length of stay for less or equal to 3 days, THEN these infants received ventilation < 72 hours (non-PMV).
PRE-SCHOOL (CHAID)
<ul style="list-style-type: none"> • If pre-school age patients had length of stay more than 6 days AND required inotropes, THEN these school age patients received ventilation ≥ 72 hours (PMV). • If pre-school age patients had length of stay more than 4 days and less or equal to 6 days, THEN these school age patients received ventilation ≥ 72 hours (PMV). • If pre-school age patients had length of stay more than 2 days and less or equal to 4 days, THEN these school age patients received ventilation < 72 hours (non-PMV). • If pre-school age patients had length of stay less than 2 days, THEN these school age patients received ventilation < 72 hours (non-PMV). • If pre-school age patients had length of stay more than 6 days AND did not require inotropes, THEN these school age patients received ventilation < 72 hours (non-PMV).
SCHOOL AGE (C5.0)
<ul style="list-style-type: none"> • If school age patients had length of stay less or equal 4days AND required inotropes, THEN these school age patients received ventilation ≥ 72 hours (PMV). • If school age patients had length of stay more than 4 days, THEN these school age patients received ventilation ≥ 72 hours (PMV). • If school age patients had length of stay less or equal 4days AND did not required inotropes, THEN these school age patients received ventilation < 72 hours (non-PMV).

Model Comparison

The performance of logistic model and the best models resulted from decision tree analysis is summarized in Table 9. For all age categories, the decision tree models outperformed the logistic regression model in which the decision tree models had better accuracy, sensitivity and specificity rate for testing set. Thus, decision tree models were found to be better predictive models compared to the traditional statistical technique, logistic regression in predicting risk factors for PMV.

Table 9
Model Evaluation

Age Category	Model	Training Set			Testing Set		
		Accuracy (%)	Sensitivity (%)	Specificity (%)	Accuracy (%)	Sensitivity (%)	Specificity (%)
Neonate	Logistic Regression (ENTER)	76.40	73.26	80.00	68.42	65.96	72.41
	CART	85.09	94.19	77.33	85.53	91.49	79.31
Infant	Logistic Regression (ENTER)	77.99	70.48	85.58	77.32	66.67	87.76
	CHAID	84.69	89.52	79.81	80.41	70.83	89.80
Pre-School Age	Logistic Regression (ENTER)	77.63	59.70	91.76	71.83	71.43	72.22
	CHAID	84.87	88.06	82.35	81.69	91.43	72.22
School Age	Logistic Regression (ENTER)	84.09	75.76	89.09	66.67	47.06	84.21
	C5.0	88.64	78.79	94.55	83.33	76.47	89.47

CONCLUSION AND RECOMMENDATION

This study found that five out of twelve potential risk factors examined in logistic regression analysis are significantly associated with PMV for all age categories. The five significant risk factors include PRISM III 12 hours, inotropes, length of stay, admission source, and principal diagnosis. Four significant risk factors (PRISM III 12 hours, inotropes, length of stay and principal diagnosis) were also found to be significant in decision tree making it better than logistic regression model. The predictive models developed in this study show the potential of the decision tree model in medical research.

Future study could consider potential risk factors such as Paediatric Index Mortality (PIM) and PRISM III 24 hours. A larger sample size is also recommended in order to validate the results of this study. Other data mining classification technique can be employed such as Artificial Neural Network (ANN) and Support Vector Machine (SVM).

REFERENCES

- Ayer, T., Chhatwal, J., Alagoz, O., Kahn, C. E. Jr, Woods, R. W., & Burnside, E. S. (2010). Informatics in radiology: comparison of logistic regression and artificial neural network models in breast cancer risk estimation. *Radiographic*, 30(1), 13-22.
- Bagley, S. C., White, H., & Golomb, B. A. (2001). Logistic regression in the medical literature : Standards for use and reporting, with particular attention to one medical domain. *Journal of Clinical Epidemiology*, 54(10), 979-985.
- Camdeviren, H. A., Yazici, A. C., Akkus, Z., Bugdayci, R., & Sungur, M. (2007). Comparison of logistic regression model and classification tree: An application to postpartum depression data. *Expert Systems with Applications*, 32(4), 987-994.
- Chelluri, L., Im, K. A., Belle, S. H., Schulz, R., Rotondi, A. J., Donahoe, M. P., ... & Pinsky, M. R. (2004). Long-term mortality and quality of life after prolonged mechanical ventilation. *Pediatric Critical Care Medicine*, 32(1), 61-69.
- Farias, J. A., Baltodano, A., Esteban, A., Frutos, F., Flores, J. C., Retta, A., ... & Johnson, M. (2004). What is the daily practice of mechanical ventilation in pediatric intensive care units? A multicenter study. *Intensive Care Medicine*, 30(5), 918-925.
- Hair, J. F., Anderson, R. E., Tatham, R. L., & Black, W. (1998). *Multivariate Data Analysis* (5th Edition). Upper Saddle River, NJ: Prentice Hall.
- Hosmer, D. W., & Lemeshow, S. (2000). *Applied Logistic Regression* (2nd edition). New York, NY: John Wiley & Sons, Inc.
- Ibrahim, N. A., Kudus, A., Daud, I., & Bakar, M. R. A. (2008). Decision tree for competing risks survival probability in breast cancer study. *World Academy of Science, Engineering and Technology*, 38, 15-19.
- Kipps, A. K., Wypij, D., Thiagarajan, R. R., Bacha, E. A., & Newburger, J. W. (2011). Blood transfusion is associated with prolonged duration of mechanical ventilation in infants undergoing reparative cardiac surgery. *Pediatric Critical Care Medicine*, 12(1), 52-56.
- Kurt, I., Ture, M., & Kurum, A. T. (2008). Comparing performances of logistic regression, classification and regression tree, and neural networks for predicting coronary artery disease. *Expert Systems with Applications*, 34(1), 366-374.
- Lin, C., & Hsieh, K. (2009). Pediatric critical care - A new frontier. *Pediatrics and Neonatology*, 50(5), 184-189.
- Lin, W. T., Wu, Y. C., Zheng, J. S., & Chen, M. Y. (2011). Analysis by data mining in the emergency medicine triage database at a Taiwanese regional hospital. *Expert Systems with Applications*, 38(9), 11078-11084.
- Lum, L. C., Abdel-Latif, M. E., de Bruyne, J. A., Nathan, A. M., & Gan, C. S. (2011). Noninvasive ventilation in a tertiary pediatric intensive care unit in a middle-income country. *Pediatric Critical Care Medicine*, 12(1), e7-e13.
- Payen, V., Jouviet, P., Lacroix, J., Ducruet, T., & Gauvin, F. (2012). Risk factor associated with increased length of mechanical ventilation in children. *Pediatric Critical Care Medicine*, 13(2), 152-157.
- Putra, S., Wong, C. Y., Hazim, M., Shiraz, M., & Goh, B. S. (2006). Paediatric tracheostomy in Hospital University Kebangsaan Malaysia-A changing trend. *Medical Journal of Malaysia*, 61(2), 209-213.

- Randolph, A. G., Meert, K. L., & O'neil, M. E. (2003). The feasibility of conducting clinical trials in infants and children with acute respiratory failure. *American journal of respiratory and critical care medicine*, 167(10), 1334-1340.
- Traiber, C., Piva, J. P., Fritsher, C. C., Garcia, P. C., Lago, P. M., Trotta, E. A., ... & Lisboa, B. D. (2009). Profile and consequences of children requiring prolonged mechanical ventilation in three Brazilian pediatric intensive care units. *Pediatric Critical Care Medicine*, 10(3), 375-80.
- Ture, M., Kurt, I., Kurum, A. T., & Ozdamar, K. (2005). Comparing classification techniques for predicting essential hypertension. *Expert Systems with Applications*, 29(3), 583-588.

The Control Chart Technique for the Detection of the Problem of Bad Data in State Estimation Power System

Zahid Khan^{1*}, Radzuan B. Razali¹, Hanita Daud¹, Nursyarizal Mohd Nor² and Mahmud Fotuhi-Firuzabad³

¹Department of Fundamental and Applied Sciences, Universiti Teknologi PETRONAS, 31750 UTP, Tronoh, Perak, Malaysia

²Department of Electrical Engineering, Universiti Teknologi PETRONAS, 31750 UTP, Tronoh, Perak, Malaysia

³Department of Electrical Engineering, Sharif University of Technology, 11155-1639 Tehran, Iran

ABSTRACT

State estimation plays a vital role in the security analysis of a power system. The weighted least squares method is one of the conventional techniques used to estimate the unknown state vector of the power system. The existence of bad data can distort the reliability of the estimated state vector. A new algorithm based on the technique of quality control charts is developed in this paper for detection of bad data. The IEEE 6-bus power system data are utilised for the implementation of the proposed algorithm. The output of the study shows that this method is practically applicable for the separation of bad data in the problem of power system state estimation.

Keywords: Nonlinear estimation, weighted least squares method, bad data, Chi-square test, normalised residual test, Gauss-Newton algorithm

INTRODUCTION

The risk of blackouts in grids has increased the desperate need of monitoring the power system. State estimation is a fundamental method for online system monitoring, analysis and control functions. It is a technique of evaluating field data and developing a precise estimation of the system's parameters. The state variables estimated in this way are used to calculate other key functions of the power flow analysis. With the estimated power quantities, the operator in the control centre will be able to get information about the current status of the system and take necessary

Article history:

Received: 27 May 2016

Accepted: 14 November 2016

E-mail addresses:

zahidkhan_g02731@utp.edu.my, zahid.hazara@gmail.com

(Zahid Khan),

radzuan_razali@petronas.com.my (Radzuan B. Razali),

hanita_daud@petronas.com.my (Hanita Daud),

nursyarizal_mnor@petronas.com.my (Nursyarizal Mohd Nor),

fotuhi@sharif.edu (Mahmud Fotuhi-Firuzabad)

*Corresponding Author

measurements in case of abnormal overloading and save the system from probably blackouts. It is fundamentally based for providing a reliable and accurate real-time data base, which in turn will be used by all other energy management system (EMS) functions.

The mathematical algorithm which is used by the state estimator is based on the weighted least squares (WLS) method. The WLS method works on the assumption that noisy measurements follow the Gaussian distribution. In the presence of noisy measurements only, the WLS provides reliable estimations for the state parameters. However, the final results of WLS in the existence of gross errors will be biased. Therefore, the detection of gross errors that cause bad data in SCADA measurements is also an important subject of interest in state estimation of a power system. The demand for electric energy is increasing because of the increased demand of consumers and their lifestyles. Thus, a power system must be able to generate enough energy to meet the required load for a region.

The revolutionary work of Schweppe (Schweppe & Rom, 1970; Schweppe & Wildes, 1970) has become the basis for using state estimation in the supervisory control unit of a power system. This model is built on measurements from snapshots that show the current status of the system (Monticelli, 2000). One of the key functions of state estimation is to detect bad data and eliminate them if possible (Mili, Van Cutsem, & Ribbens-Pavella, 1985). Sometimes, data are corrected by eliminating a bad value prior to estimation. An excellent discussion of these techniques can be found in Huang, Shih, Lee and Wang (2010).

The main objective of these techniques is saving iteration cost. Post estimation bad data techniques are based on residual analysis. The largest normalised residual is used to find the suspected measurement (Carvalho & Bretas, 2013). The normalised residual test does not always perform well (Khan, Razali, Daud, Nor, & Fotuhi-Firuzabad, 2015). The hypothesis-testing method is also used to find bad measurements in an iterative way (Mili & Van Cutsem, 1988). In the presence of bad data, many researchers also worked on the use of some robust methods like the least median squares and least trimmed squares estimator in calculating system state parameters, the details of which can be seen in several studies (Baldick, Clements, Pinjo-Dzgal, & Davis 1997; Kotiuga & Vidyasagar, 1982; Mili, Cheniae, & Rousseeuw 1994). A comparative study of these estimators in case of large and small bad measurements has been summarised in Habiballah and Irving (2000). There are a number of other robust estimators like the S -estimators, τ -estimators, and L -estimators that have reasonably high breakdown points that may be suitably applicable in the presence of bad values. The concept of outlier detection and leverage points within the context of robust regression is also a very important area. Introductory literature on these topics can be studied in statistical applications (Klebanov, Rachev, & Fabozzi 2009; Staudte & Sheather, 2011).

Most of the aforementioned research work is addressed towards numerical efficiency. In this work, we have, therefore, proposed a technique for detection of bad data in a statistical point of view which is based on the structure of the data generating model and its modified assumptions.

The overall contribution of this work is to provide a new detection technique for bad data in state estimation environments. This method will be effective in time and cost savings. This approach will be new information for the power system engineers who in turn can apply the technique to many other related studies.

The rest of this article is structured as follows. Section 2 describes the mathematical formulation of the state estimation problem; Section 3 explains the procedure for the construction of the control chart for detection of bad data; Section 4 is related to the presentation of the proposed algorithm and its implementation on the IEEE 6-bus power system. Finally, a conclusion is drawn in Section 5.

MATHEMATICAL MODEL AND ESTIMATION METHOD

Noisy data have been collected from different measuring devices that were installed at different locations of a transmission system. The exact value of any physical measurement was not known. Therefore, the stochastic model that is used in power system state estimation was given by:

$$Z = HX + e \tag{1}$$

where $H = \frac{\partial h(X)}{\partial X}$ is the Jacobian matrix, $Z = [z_1, z_2, \dots, z_n]^T$ is the vector of measurements, $X = [x_1, x_2, \dots, x_k]^T$ is an unknown state vector consisting of complex components of voltages of all the buses except the slack bus, $e = [e_1, e_2, \dots, e_n]^T$ is a Gaussian error vector with the following assumptions:

$$E(e) = 0 \text{ (mean vector) and } E(ee^T) = \sigma^2 \text{diag} \{ \sigma_1^2, \sigma_1^2 \dots \sigma_n^2 \} \text{ (covariance matrix).}$$

Here, it is worth mentioning that weights are the known figures in the power system state estimation problem. Contrary to a conventional weights matrix we defined the weight for the i^{th} observation as:

$$w_i = \frac{1}{\sigma_i^2}.$$

Here, σ_i^2 is a measurement to reflect the accuracy of the i^{th} measuring instrument. These values of σ_i^2 , $1 \leq i \leq n$ are known numbers where σ^2 is either estimated by its maximum likelihood estimate in case of sample data or found directly from the data in case of a fully observable system. The objective function in matrix notation can be written as:

$$J(X) = [Z - h(X)]^T W [Z - h(X)] \tag{2}$$

where W is a weight matrix.

The Gauss Newton algorithm is conventionally used in system state estimation for estimating the state of the power system (Monticelli, 2000).

In the Gauss Newton iterative scheme, the solution of X at r^{th} iteration is as given below:

$$X^{r+1} = X^r - [G(X^r)]^{-1} g(X^r) \tag{3}$$

where $g(X^r) = -H^T(X^r)W[Z - h(X^r)]$ and $G(X^r) = \frac{\partial g(X^r)}{\partial X} = H^T(X^r)W H(X^r)$.

The most important sub-function of a state estimator is detection of bad data. Our objective function can be written as:

$$\varphi(X) = \frac{\sum_{i=1}^n w_i \left(z_i - h_i(\hat{X}) \right)^2}{n - k}$$

which follows the Chi-square distribution with $n - k$ degree of freedom. If the calculated value of the objective function at optimum value of the state vector X is greater than that of the set critical value, it is implied that at least one bad value is suspected in the measurements. The Chi-square test is only an indication of the existence of bad data. It does not indicate which value is the bad one. The other test that is used in state estimation of power is the normalised residual test (Carvalho & Bretas, 2013). Based on a sensitivity analysis we found a covariance matrix for residuals whose diagonal elements represented the corresponding variances of estimated residuals. Normalised residuals were then calculated as given below:

$$r_i^N = \frac{|r_i|}{\sqrt{\phi_{ii}}}; \quad r^N \sim N(0,1) \tag{4}$$

where ϕ_{ii} is the corresponding diagonal element of the variance covariance matrix of i^{th} residual. The largest normalised residual was in accordance with the value polluted by gross error. Thus, in this way, the value corresponding to the largest normalised residual was deleted from the data or corrected by its appropriate substitute.

PROPOSED METHOD FOR IDENTIFICATION OF BAD DATA

Our proposed method was based on the control chart methodology. The control charts are used for monitoring shifts either in the mean or standard deviation of an assumed distribution. A control chart is a useful statistical technique for monitoring the process/system in terms of statistical control. The term statistical control means the capability of the chart to figure out whether the system is operating under variation of chance causes only or not. In statistical terms, a process is said to be “out-of-control” if it is functioning in the presence of assignable causes. If bad measurements are not detected properly, the results of the state estimator will not be valid and in return the power system security analysis may be misguided. The question that came to mind as to which observation would be considered a bad one in context of state estimation of power. The value in which a gross error is higher than the expected accuracy of the meter would be considered bad.

In model form we can write it as:

$$z^{meas} = z^{true} + c\sigma$$

where c is the amount of bad data measured in terms of standard deviation, z^{meas} is the available value from the metering device and z^{True} is a value obtained from the measurement function $h(x)$.

Thus, the available meter measurement is the sum of the true value of z and the Gaussian random variable. So, the addition of an amount will shift the Gaussian curve to the right or left depending on the sign of the added term. The shape of the curve will remain the same i.e. a bad observation will not alter the scale of distribution. Hence, we put in the effort to monitor only the mean of the process. This method was based on post estimation because it used the residuals in its analysis. Here, the out-of-control process referred to the data that were used to find the state parameters of a power system that was not of good quality. Hence, the estimation based on bad quality data would not be reliable. A single realisation of n pairs of $(z_i, h_i(x))$ can be represented as:

$$z_i = h_i(x) + e_i$$

where $h_i(x)$ has a specific known form that depends on the type of measurement and e_i is a normally distributed error term with a mean of zero and variance σ_i^2 . Thus, the very observation that is used in the state estimation is a measurement of the dependent variable z at the non-linear measurement function $h(x)$. This relationship, in terms of statistical quality control, is called a profile. Thus, our proposed control chart was based on non-linear profiles monitoring through the residuals of a non-linear model given in Equation (1). The general model control chart for a quality characteristic that is described by the sample statistics states that P is given by (Montgomery, 2009):

$$\begin{aligned} UCL &= \mu_p + c\sigma_p \\ CL &= \mu_p \\ LCL &= \mu_p - c\sigma_p \end{aligned} \tag{5}$$

where μ_p is the mean and σ_p is the standard deviation of the statistic p . The model that is used in state estimation is just like the one used in multivariate weighted non-linear regression. Consider the following transformed form of Equation (1):

$$J(X) = [Z_t - h_t(X)]^T [Z_t - h_t(X)] \tag{6}$$

where $Z_t = W^{1/2}Z$, $h_t(X) = W^{1/2}h(X)$ and $W^{1/2}$ is the Cholesky factor matrix of W .

In this way, the solution is reduced to the estimation by the ordinary least squares (OLS) method. The OLS estimation of Equation (6) is thus given by:

$$\hat{X}_t = (H^TWH)^{-1} H^TWZ$$

The value of this estimation can be calculated using the Gauss Newton algorithm after linearising the objective function as given in Equation (6). Now let the following residuals vector from Equation (1):

$$r_w = Z - \hat{Z}_w \tag{7}$$

where $\hat{Z}_w = H \hat{X}_t$, which is an unbiased estimator of Z .
 The Equation (7) implies that:

$$r_w = (I - H^*)e = Ke \tag{8}$$

where K is the sensitivity matrix of the residuals which is symmetric and idempotent. By utilising the properties of Equation (8), the variance covariance matrix of the residuals can be found as:

$$vcov(r_w) = \sigma^2 KW^{-1} \tag{9}$$

Hence from Equation (8) and Equation (9), it yields that: $r_w \sim N(0, \sigma^2 S)$, where, $S = KW^{-1}$

Since each residual has its own variance, therefore, we defined the i^{th} studentised residual as:

$$r_{wi}^s = \frac{r_{wi}}{\hat{\sigma} \sqrt{S_{ii}}}, \quad i = 1, 2, 3 \dots n \tag{10}$$

where $\hat{\sigma}$ is independently computed at the optimum value of the state vector X . Since each $r_{wi}^s \sim N(0,1)$, therefore, from Equation (5), the parameters of the control chart of the individual studentised residuals are given as:

$$UCL = 3, \quad CL = 0, \quad LCL = -3$$

where UCL and LCL signify the upper and lower control limits of the studentised residuals chart.

The value falling outside these limits was suspected to be a bad value. It needs correction or exclusion from the data and a re-estimation of the WLS on the corrected data. The residuals in Equation (9) are different from the conventional normalised residuals in Equation (3) because they also take into account the measurement of the closeness of the actual and estimated residuals into calculation.

IMPLEMENTATION OF RESIDUAL BASED CONTROL CHART

We developed a programme in MATLAB for estimating the model and finding the residuals as explained in the previous section. The algorithm of our technique can be summarised in the following steps:

- Step 1: Initialise the values by taking $r = 0$, flat start of state vector X^o and convergence quantity ϵ .
- Step 2: Calculate the measurement function $h(X^r)$, Jacobian function and gain matrix $G(X^r)$ as given in Equation (2).

- Step 3: Solve Equation (2), for new values of state variable X and check the solution convergence by comparing $|\Delta X^r| \leq \varepsilon$; if the solution converges, extract residuals from the model; otherwise, go to step 2, updating $r = r + 1$.
- Step 4: Construct residual-based control chart. If the process is in control, display the output for X ; otherwise, display the control chart for the out-of-control process and go to step 3.
- Step 5: Update the measurements vector by deleting the corresponding bad value from the data in accordance with the largest studentised residual and go to step 2.

The IEEE 6-bus standard test network was selected for the implementation of the results obtained in Section 3. The data on the used test network and system's topology can be found in Wood and Wollenberg (2012). The main features of this system are shown in Table 1.

Table 1
Main Features of IEEE 6-Bus Test Network

Types of Measurement	STD
Voltage measurement	2 kV
Real and reactive power injections	3 MV
Real and reactive power flows	3MVR

For the implementation of WLS, we assumed that each observation in both systems was weighted by the accuracy measurement of its corresponding measuring meter. These weights were defined in terms of the standard deviation (STD) of the measurements as given in Table 2.

Table 2
Weights of Different Measurements

Features	IEEE 6-bus test network
Total nodes	6
Total branches	11
Total measurements	62
Total parameters to be estimated	11

These values of weights, like the other measurements, were also converted in per unit system for their usage in the elaborated algorithm in Section 3 by dividing them by their base case values of 230 kV, 100 MV and 100 MVR. The termination criteria as stated in the algorithm was set at 10^{-4} for the convergence of the values of the vector. The actual values were assumed from the results of load-flow analysis whereas the noisy measurements were generated by perturbing the values with normal distribution random generation having a mean parameter equal to zero and variance corresponding to defined weights for each measurement as shown in Table 2. For the inclusion of a single bad value in the measurements, a value of the real power injection at bus 1 of the IEEE 6-bus system, was corrupted intentionally by adding 10 times its per unit standard deviation. The algorithm was converged at the third iteration and the results obtained as shown in Table 3.

Table 3
State Estimation Results with and Without Bad Data

\hat{X} without bad data	\hat{X} with bad data
1.0449	1.0477
1.0478	1.0473
1.0685	1.0677
0.9864	0.9863
1.0021	0.9792
-3.7282	1.0013
-4.2486	-4.3158
-3.7282	-4.9734
-4.2883	-4.8452
-5.3444	-5.9877
-5.8367	-6.5629
$\chi^2 = 52.1745$	$\varphi(X) = 88.8270$

The computed value of the Chi-square statistic showed that bad data were suspected when actually our data had a bad value. However, we did not know which value was actually bad and how bad it was. In order to answer questions on the detection and identification of bad value, we constructed the studentised residual-based control chart with the parameters as listed in Section 3. The control charts, which were the output of our proposed algorithm, are shown in Figure 1 and Figure 2.

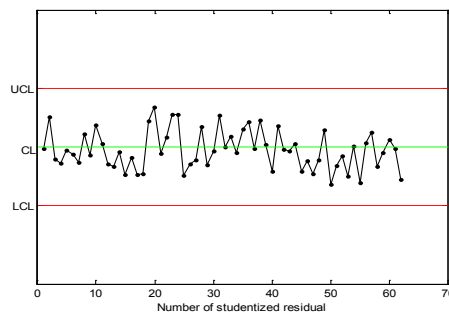


Figure 1. The snapshot of in-control data for the IEEE 6-bus system

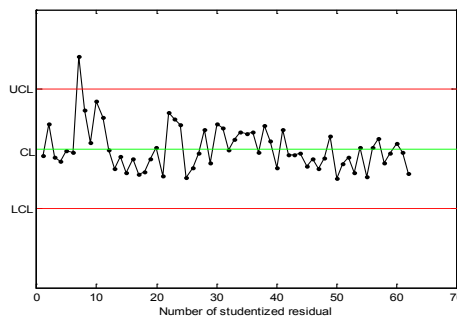


Figure 2. The snapshot of out-of-control data for the IEEE 6-bus system

The structure of the points in the control chart as given in Figure 2 showed that the quality of data was out of control at the seventh studentised residual. Hence, the corresponding value of the residual was suspected to be bad and it needed to be deleted from the data. Our proposed method has a visualisation feature that may help the operator in the separation of good and bad values. This method is better in the sense of having both properties of detection and identification of bad values whereas the Chi-square test has only the feature of sounding the alarm at the presence of bad data. Although the normalised residual test also had both properties, there was a risk of deletion of those values that were actually not bad whereas our proposed method had a clear benchmark limits to decide bad values. Our test was a modified form of the normalised residual test because it included mean square error (MSE) in its calculation. As the value of bad data increased, the MSE also increased in the denominator of the proposed studentised residual, which kept the ratio within the defined limits.

CONCLUSION

State Estimation has become a significant part of the controlling, monitoring and planning of modern power systems. Therefore, to rely on the results of a state estimator, it is mandatory to study those factors that can alter the results of the state estimator. One of these main factors is the existence of bad data. In view of its importance, a new algorithm has been proposed in this work for sounding the alarm in case of the existence of bad values in measurements. The technique has additional features of visualisation and clear threshold limits to discriminate between good and bad values. The algorithm on one hand is a new technique for power engineers for separation of bad data and is compatible with the conventional method of WLS in state estimation of power, but on the other, it is an extension of applications of the control chart in statistical process control (SPC) for monitoring non-linear profiles.

REFERENCES

- Baldick, R., Clements, K. A., Pinjo-Dzagal, Z., & Davis, P. W. (1997). Implementing non-quadratic objective functions for state estimation and bad data rejection. *IEEE Transactions on Power Systems*, 12(1), 376–382.
- Carvalho, B., & Bretas, N. (2013). Analysis of the largest normalized residual test robustness for measurements gross error processing in the WLS state estimator. *Journal of Systemics, Cybernetics and Informatics*, 11(7), 1–6.
- Habiballah, I. O., & Irving, M. R. (2000). A comparative study of three LS-based power system state estimators for bad data identification. *Electric Machines and Power Systems*, 28(2), 105–114.
- Huang, C. H., Shih, K. K., Lee, C. H., & Wang, Y. J. (2010). Application of Kalman filter to bad data detection in power system. In V. Kordic (Ed.), *Kalman filter* (pp. 127–144). Croatia: InTech.
- Khan, Z., Razali, R. B., Daud, H., Nor, N. M., & Fotuhi-Firuzabad, M. (2015). The largest studentized residual test for bad data identification in state estimation of a power system. *ARPN Journal of Engineering and Applied Sciences*, 10(21), 10184–10191. Retrieved from http://www.arpnjournals.org/jeas/research_papers/rp_2015/jeas_1115_3046.pdf

- Klebanov, L. B., Rachev, S. T., & Fabozzi, F. J. (2009). *Robust and non-robust models in statistics*. United States of America, USA: Nova Science Publishers.
- Kotiuga, W. W., & Vidyasagar, M. (1982). Bad data rejection properties of weighted least absolute value techniques applied to static state estimation. *IEEE Transactions on Power Apparatus and Systems, PAS-101*(4), 844–853.
- Mili, L., Cheniae, M. G., & Rousseeuw, P. J. (1994). Robust state estimation of electric power systems. *IEEE Transactions on Circuits and Systems I: Fundamental Theory and Applications, 41*(5), 349–358.
- Mili, L., & Van Cutsem, T. (1988). Implementation of the hypothesis testing identification in power system state estimation. *IEEE Transactions on Power Systems, 3*(3), 887–893.
- Mili, L., Van Cutsem, T., & Ribbens-Pavella, M. (1985). Bad data identification methods in power system state estimation: A comparative study. *IEEE Transactions on Power Apparatus and Systems, PAS-104*(11), 3037–3049.
- Montgomery, D. C. (2009). *Introduction to statistical quality control* (7th Ed.). New York, NY: John Wiley & Sons.
- Monticelli, A. (2000). Electric power system state estimation. *Proceedings of the IEEE, 88*(2), 262–282.
- Schweppe, F. C., & Rom, D. B. (1970). Power system static-state estimation, Part II: Approximate model. *IEEE Transactions on Power Apparatus and Systems, PAS-89*(1), 125–130.
- Schweppe, F. C., & Wildes, J. (1970). Power system static-state estimation, Part I: Exact model. *IEEE Transactions on Power Apparatus and Systems, PAS-89*(1), 120–125.
- Staudte, R. G., & Sheather, S. J. (2011). *Robust estimation and testing* (Vol. 918). New York, NY: John Wiley & Sons.
- Wood, A. J., & Wollenberg, B. F. (2012). *Power generation and control*. New York, NY: John Wiley & Sons.



Internet of Things – Technology Adoption Model in India

Singh, G., Gaur, L. and Ramakrishnan, R.*

Amity International Business School, Amity University, Noida, Uttar Pradesh 201313, India

ABSTRACT

Internet of Things (IoT) is the biggest ICT revolution that the world is witnessing with potential to be the next biggest technology disruptor that will improve productivity and efficiency across different industries and services sector. The purpose of this paper is to study adoption of Internet of Things (IoT) enabled technologies in the corporate sector in India and also to identify factors influencing its adoption rate. It prescribes a suitable model serving as a blue print for enterprises. The methodology used is exploratory research as significance of Technology Adoption Model (TAM) in IoT projects is still not studied to lay the groundwork for future studies. Literature review proposed different models based on TAM or their abridged versions. In this study, a team of five experts in IoT project adoption proposed factors crucial to successful IoT project implementation. Based on these, questionnaires were developed and sent to respondents who are senior officers at their respective selected companies. Data obtained was used to validate existing and proven TAM research model. Based on this, the study proposed a new model (IOT-TAM). Variables namely Perceived utility, Perceived ease of use, intrinsic variables and external organization were developed. First generation multivariate method of multiple regressions was used to assess reliability and validity of the model measures.

Keywords: Indian enterprises, internet of things, technology adoption, technology adoption model

INTRODUCTION

Internet of Things (IoT) is a new age communication paradigm that refers to objects, sensors, actuators and assemblies communicating in bi-directional mode with each other, generating and transmitting data and interacting across a digital network. Each of the objects is uniquely identifiable and has the capacity and willingness to broadcast information about itself or its surroundings for further decision making.

Andrea et al. (2014), noted that IoT has many applications including Smart Cities (A **smart city** is an urban development vision to integrate information and communication

Article history:

Received: 29 December 2016

Accepted: 21 April 2017

E-mail addresses:

gsingh@amity.edu (Singh, G.),

lgaur@amity.edu (Gaur, L.),

ravi.ramakrishnan@gmail.com (Ramakrishnan, R.)

*Corresponding Author

technology (ICT) and Internet of things (IoT) technology in a secure fashion to manage a city's assets), planning for safety of buildings, waste management, traffic congestion, noise monitoring, energy conservation and smart parking.

The major focus of IoT studies has been on technology, infrastructure and supplier innovation but little has been studied on the awareness of this technology among manufacturers in India. Adoption of IoT is beneficial to these companies as it offers many advantages such as cost competitiveness and a shift from traditional labour intensive business process to technology aided and automated business processes. This is in line with the Government of India's resolve to shift to Smart Manufacturing. However, there is a lack of a framework for Indian policy makers to determine the facilitators for adoption of IoT. The purpose of this paper is therefore to build on the Technology Adoption Model (TAM) and suggest a framework for adoption of IoT among businesses in India. The paper begins with a discussion of established TAM model that shows how users accept and use a technology. Next, it proposes a model IoT-TAM based on a IoT implementation case and then uses a survey method to gather data about the current state of IoT adoption in India and finally uses this data to validate the IoT-TAM model and its variables. The results of the survey were analysed using SPSS.

Internet of Things aims to transform the real-world objects into intelligent virtual objects. The IoT aims to unify everything in our world under a common infrastructure (Somayya, 2015).

Nunberg (2012) defines IoT as a network of networks that consists of millions of private, public, academic, business, and government networks, of local to global scope, that are linked by a broad array of electronic, wireless and optical networking technologies.

Kosmatos, Tselikas and Boucouvalas (2011) have described broad applications of IoT using RFID integrated with smart objects while Aggarwal and LalDas (2012) show that though IoT applications have many benefits, there are also security issues which are a significant determinant of user ease of acceptance of the technology.

The Technology Acceptance Model

Technology Acceptance Model (TAM) is one of the successful measurements for effective computer usage among end users. It is modelled after Everett Rogers's (1983) theory on diffusion of innovation where technology adoption is a function of a variety of factors including Relative advantage and ease of use.

It is necessary for organisations to evaluate technology adoptions as they spend a huge amount of resources implementing new technologies. This also helps predict the extent to which users will use the system provided to them. Understanding people's behaviour in accepting or rejecting computer related technologies is one of the most challenging issues in information systems (Swanson, 1988). This includes user beliefs and attitude, satisfaction measures, adaptation to change, role of culture, education and awareness.

The TAM is a modification of the Theory of Reasoned Action (TRA) which is a widely studied social psychology model concerned with the determinants of consciously intended behaviour.

According to TRA, a person's performance of a specific behaviour is determined by his/her behavioural intention (BI) to perform the behaviour and BI which is jointly determined by the person's attitude (A) and subjective norm (SN) concerning the behaviour.

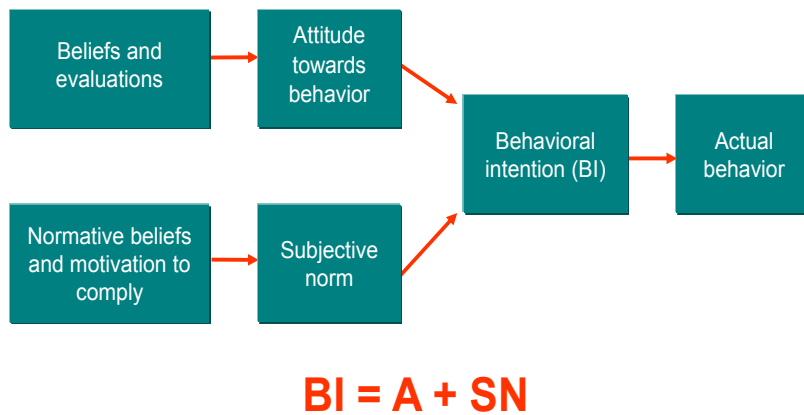


Figure 1. Theoretical Framework (TRA)

Literature Review

Davis (1989) has discussed the TAM theory in information systems and suggested that two main factors, Perceived Usefulness (PU) and Perceived Ease of use (PEOU), drive the adoption of a technology.

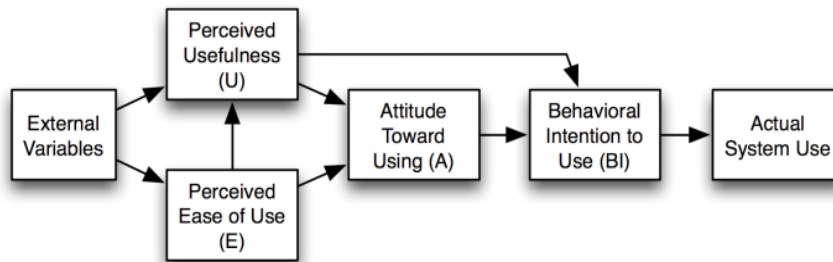


Figure 2. Original Technology Acceptance Model (TAM)

Venkatesh et al. (2000) examined the TAM model and proposed “Unified theory of acceptance and use of technology” (UTAUT) which has four key constructs to explain user intentions to use an Information system and subsequent usage behaviour which are performance expectancy, effort expectancy, social influence and facilitating conditions. The theory was a consolidation of the constructs of eight models of earlier research to explain information systems usage behaviour (theory of reasoned action, technology acceptance model, motivational model, theory of planned behaviour, a combined theory of planned behaviour / technology acceptance model, model of personal computer use, diffusion of innovations theory, and social cognitive theory).

Gaur and Ramakrishnan (2016) have explained the practical application of IoT in areas of manufacturing quantifying benefits and its relevance and adoption in the context of Industry 4.0.

Ferguson (2002), has emphasised the importance of objects having the ability to communicate as a major factor for companies to become more efficient, speed up processes, reduce error, prevent theft, and incorporate complex and flexible organisational systems through IoT.

Rahman (2014) has developed a conceptual model based on TAM for adoption of healthcare IT systems with emphasis on proposed perceived usefulness and perceived ease of use.

Zanella et al. (2014) has showcased IoT as the building block for Smart Cities in the near future where objects will be primarily driving everyday life activities.

Willis (2008) has done a comprehensive evaluation of TAM as a means to understanding online social networking behaviour. His findings suggest that TAM is a reasonable model of acceptance of online social networking systems, but the subjective norm component was not predictive of acceptance.

Park (2009) has used the TAM model to understand the behavioural intention of students to implement and use e-Learning in institutions and formulated a generic model.

Biddlecomb (2005) has discussed the concept of networking of individual machines making them readable and traceable on the Internet. Butler (2006) foresees tiny computers that constantly monitor ecosystems, buildings and even human bodies by 2020. Want (2006) has described the use of RFID as an initial evolution of object-to-object communication and its utility while Moeinfar (2012) has discussed the use of active RFID in container tracking.

Dodson (2008) has explained how billions of objects uniquely identified by EPC codes and IPV6 numbering can make objects as simple as razors or soft drink cans detectable and viewable by computers.

Gershenfeld (2011) on the other hand has reflected on aspects of privacy, trust and interaction when using IoT devices. He also discussed data exchange possibilities due to the pervasive and ubiquitous nature of these objects.

Andrea (2014) explained that the Internet of Things (IoT) shall be able to incorporate transparently and seamlessly a large number of different and heterogeneous end systems, while providing open access to selected subsets of data for the development of a plethora of digital services; this opens a huge opportunity for data based services on IoT.

METHODS

Research Methodology

Purpose of research. The purpose of this research is to suggest a technology adoption model (based on TAM) for IoT projects which are becoming one of the biggest technology disruptors of this decade. It is descriptive in nature whereby a survey method was used to understand the current status of IoT adoption among Indian organisations and using the data to propose and validate an IoT-TAM model.

Data collection method. Cross sectional survey method was used to collect data from participants with good knowledge of IoT to assess how they have overcome technology acceptance barrier for IoT in their respective organisations. The respondents were either business

leaders or technology leaders with decision making powers Responses were combination of nominal (mode central tendency), ordinal (illustrated median) and five point Likert-type scales.

Proposed model. In the study, an IoT-TAM model is proposed. A set of five organisational constructs was selected by expert opinion to develop hypothesis, research model and survey questions:-

- Perceived Usefulness of IoT (PUIOT),
- External Organisation variables (EOVIOT),
- Internal Organisation variables (IOVIOT)
- Perceived ease of use (PEUIOT) which is dependent on the current IT landscape and its strategic role and finally
- Behavioural intention to use (BIUIOT).

The model is supported by the TAM and UTAUT model.

Table 1
Constructs of the model and sample questions

Constructs	Summary	Survey Questions
PUIOT	Perceived usefulness	<i>How would you rate IoT adoption as being extremely useful in your organisation?</i> <i>Do you agree that IoT can help decrease operating costs?</i> <i>Do you agree that IoT adoption can help improve efficiency of employees and machines?</i> <i>Do you think that IoT adoption can encourage new business models in traditional organisations?</i>
EOVIOT	External Organisation Variables	<i>Do you agree that the industrial environment is conducive for organisations to adopt IoT?</i> <i>Do you agree that generally organisations who have adopted IoT or implementing IoT projects are likely to be successful?</i> <i>Do you consider IoT as an important enabler for organisations with global scope of operations and hence involvement of cross cultural employees?</i>
IOVIOT	Internal Organization Variables	<i>Do you consider your organisation's maturity in using IT technologies helped expedite adoption of IoT ?</i> <i>As a CIO did your role and personal belief play an important part in IoT adoption in your enterprise?</i> <i>Do you have budgets for new initiatives such as IoT as a regular practice and did that help in adoption?</i>
PEUIOT	Perceived ease of use	<i>Do you consider that enough IoT skills exist in Indian markets?</i> <i>Do you agree that no technical challenges exist for IoT adoption in India?</i> <i>Do you agree that no security challenges exist in IoT adoption?</i>
BIUIOT	Behavioural Intention to use	<i>Would you be looking at implementing or adopting an IoT project more aggressively in the coming year?</i> <i>Would you be considering marking major budgets for IoT adoption this year?</i> <i>Have you planned for upgrade of skills for IoT adoption in your internal IT team?</i>

The model below shows the relation between the above five constructs.

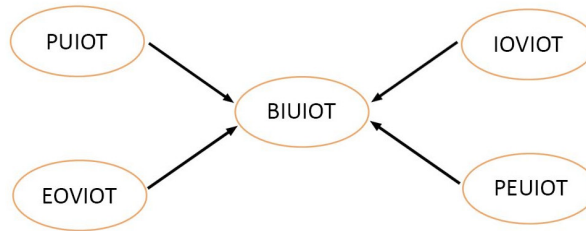


Figure 3. Constructs and relationship

Hypothesis

- H1: Perceived usefulness of IOT (PUIOT) positively affects the behavioural Intention to use IoT (BIUIOT)
- H2: A more robust Internal IT organisation (IOVIOT) variables positively influence BIUIOT
- H3: Complexity of External Organisational variables (EOVIOT) positively influence BIUIOT
- H4: Perceived ease of use of IOT (PEUIOT) positively influence BIUIOT

Sampling size and survey. In this study, the sample target was executives and business leaders who work in IT companies and have knowledge of IoT and implementing an associated project after understanding the above constructs.

The survey was conducted online using Google Forms and to ensure a higher response rate, convenience sampling was used to identify respondents.

The survey questionnaires were completed by 171 participants and showed a confidence rate of 90% which was found to be sufficient. Data was refined from manipulation and null or repetitive responses to get around 168 valid responses whereby:

- 50 respondents were CMO (Chief Marketing Officers) and equivalent
- 45 were Operations Head or Line Heads
- The rest consisted of department Managers and executives .

Sample distribution. Of the respondents, most of them were from other categories (mode).

Table 2
Sector wise respondents

Sector	Frequency	Percent
Financial Services	16	9.5
Telecommunications	32	19.0
Process Manufacturing	44	26.2
Discreet Assembly	12	7.1
Pharma Life sciences	12	7.1
Others	52	31.0
Total	168	100.0

Majority of the organisations had a turnover of over 1000 crores.

Table 3
Size of business

Size of Business	Frequency	Percent
< 250 crores INR	28	16.7
250-1000 crores INR	34	20.2
1000-6000 crores INR	70	41.7
>6000 crores INR	36	21.4
Total	168	100.0

The organisations have global operations

Table 4
Scope of operations

Scope of Operations	Frequency	Percent
Global Operations and Manufacturing	22	13.1
India-only operations	52	31.0
India manufacturing but global exports	94	56.0
Total	168	100.0

The respondents were mainly from the operational and strategic sections indicating that these organisations view IT as a business enabler.

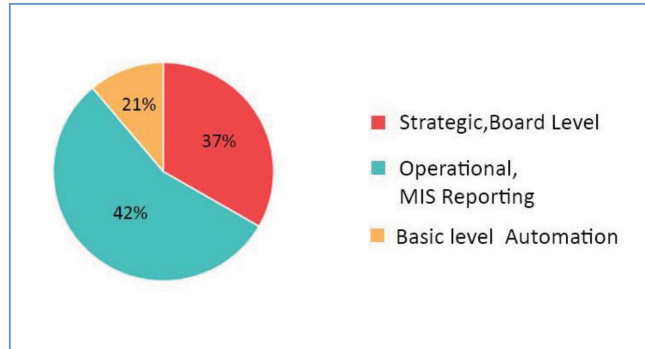


Figure 4. Role of IT

Factor and Reliability Analysis

The determinant value is 3.99E-05 which is greater than 0.00001 and hence, no singularity exists and there is no need for eliminating any questions. Value of KMO is .755 which shows the sample is adequate. We have used the Principal components analysis with Varimax rotation method.

DISCUSSION

The dependent variables have been considered as Behavioural Intention to use IoT (BIUIOT) while the independent variables are grouped as Perceived usefulness of IoT, External Organisation Variables (EOVIOT), Internal Organisation Variables (IOVIOT) and Perceived ease of use of IoT technology (PEUIOT).

In order to examine the relationship between the variables and adoption of IoT, this study adopts research statistical methods by Chin (1998), Pedhazur(1982) , Joreskog (1989), Stevens (2002) and Tabachnick (2001).

First Generation multiple regression analysis was used on the data appropriate for evaluating first the constructs, and secondly, the relationships between individual constructs.

Table 5
Calculation of R

Model Summary^e

Model	R	R Square	Adjusted R Square	Std. Error of the Estimate	Change Statistics					Durbin Watson
					R Square Change	F Change	df1	df2	Sig. F Change	
1	0.535 ^a	0.286	0.259	0.975	0.286	10.600	6	159	0.000	2.016
2	0.613 ^b	0.376	0.332	0.926	0.091	4.473	5	154	0.001	
3	0.637 ^c	0.405	0.346	0.916	0.029	1.839	4	150	0.124	
4	0.659 ^d	0.434	0.338	0.921	0.029	0.790	9	141	0.626	

The table above shows the model summary whereby R is the correlation between the observed and predicted values of the dependent variable. R square is proportion of variance in the dependent variable (BIUIOT) which can be predicted from the independent variables; 25.9% variance in BIUIOT can be explained from the variable 1, 37.6% from the variable 2, 40.5% from variable 3 and 43.4% from variable 4. The Adjusted R square is a more accurate value, the standard error of the estimate, also called the root mean square error, is the standard deviation of the error term, and is the square root of the Mean Square Residual.

Table 6
Analysis of Variance

ANOVA^a

Model		Sum of Squares	Df	Mean Square	F	Sig.
1	Regression	60.426	6	10.071	10.600	.000 ^b
	Residual	151.068	159	0.950		
	Total	211.494	165			
2	Regression	79.584	11	7.235	8.447	.000 ^c
	Residual	131.910	154	0.857		
	Total	211.494	165			
3	Regression	85.752	15	5.717	6.820	.000 ^d
	Residual	125.742	150	.838		
	Total	211.494	165			
4	Regression	91.788	24	3.824	4.505	.000 ^e
	Residual	119.706	141	0.849		
	Total	211.494	165			

Sum of Squares associated with the three sources of variance, Total, Model and Residual, for the regression sum of squares is 10.071 for variable 1 while the sum of squares for residual is .950. The p-value associated with this F value is very small (0.0000). These values are used to answer the question “is the independent variable reliably predicting the dependent variable?”. The answer is yes since the p value is less than the alpha level.

Model 1 which relates to the H1 hypothesis of positive correlation between perceived usefulness and behavioural intent to adopt IoT shows an R value of .259 which shows that 25.9% of the variances in adoption of IoT are explained by independent variable PUIOT and the significance value of regression model is 0 which shows a significant positive correlation.

Model 2 which relates to the H2 hypothesis of positive correlation between external organisation variables and behavioural intent to adopt IoT shows an R value of .332 which indicates that 33.2% of the variances in adoption of IoT are explained by independent variable EOVIOT and the significance value of regression model is 0 which shows a significant positive correlation.

Model 3 which relates to the H3 hypothesis of positive correlation between internal organisation variables and behavioural intent to adopt IoT shows a R value of .346 which indicates that 34.6% of the variances in adoption of IoT is explained by independent variable EOVIOT and the significance value of regression model is 0 which shows a significant positive correlation.

Model 4 which relates to the H4 hypothesis of positive correlation between perceived ease of use variables and behavioural intent to adopt IoT shows a R value of .338 which shows that 33.8% of the variances in adoption of IoT is explained by independent variable EOVIOT and the significance value of regression model is 0 which shows a significant positive correlation.

All four have a positive and significant correlation with IoT adoption and all four hypotheses are fully supported. The organisations' ability to adopt IoT for different use in their organisation is positively influenced by the traditional TAM model determinants i.e. perceived usefulness and perceived ease of use as with other information technology projects. Apart from the two other factors which play a major role in IoT adoption are the maturity levels of the organisation which is indicated by the role of IT executive and their influence in the organisation and current investments in cutting edge IT applications. A higher degree of evolution of IT is a positive influencer. Also, organisations are positively influenced where the external conducive environment be it technology adopted by competitors, infrastructure for supporting IT such as data network and skilled resource pool or government thrust area and incentives is conducive for adoption of smart technologies.

CONCLUSION

The findings of this study are consistent with the TAM model (Venkatesh and Davis 2000, 2004). whereby there is greater user involvement, system acceptance, and system success (Swanson, 1974; Ives & Olson, 1984; Hartwick & Barki, 1994). As countries across the world move towards Smart Cities, Smart Transportation, Smart Water management and Energy management and Industry 4.0, each stake holder has a role to play in getting interested parties to adopt IoT in their workplaces. A key to successful adoption has been determined by the above study and hence a healthy ecosystem comprising skilled resources which can be ensured by imparting education in IoT technologies as part of courses, robust infrastructure and data networks, government incentives based on measurable benefits and finally encouraging leading organisations to set trends for others to follow must be adopted holistically.

This study has proposed a model for successful IoT adoption by first validating the existing TAM model in organisations having implemented IoT projects. Based on survey results, an amended version of IoT-TAM is proposed. This research can be a foundation for future research which can validate the model and also determine which of the above four components carries more weight. This model can also help consulting companies who are implementing IoT projects or management of companies to successfully create a blue print for IoT implementation based on other intrinsic factors in the organisation. Any organisation which scales up well on the four dependent variables can be sure of success in the independent variable which is acceptance of IoT. Future research can also validate the model from specific industry sector and country perspective.

REFERENCES

- Aggarwal, R., & Das, M. L. (2012, August). RFID security in the context of internet of things. In *Proceedings of the First International Conference on Security of Internet of Things* (pp. 51-56). ACM.
- Biddlecombe, E. (2005, 17 November). UN predicts Internet of Things. *BBC News*. Retrieved from <http://news.bbc.co.uk/2/hi/technology/4440334.stm>
- Butler, D. (2006). 2020 computing: Everything, everywhere. *Nature*, 440(7083), 402-405.

- Chin, W. W. (1998). The partial least squares approach to structural equation modeling. *Modern methods for business research*, 295(2), 295-336.
- Davis, F. D., Bagozzi, R. P., & Warshaw, P. R. (1989). User acceptance of computer technology: a comparison of two theoretical models. *Management science*, 35(8), 982-1003.
- Dawood, M., Hossein, S., & Fatemeh, N. (2012). Design and implementation of a low-power active RFID for container tracking at 2.4 GHz Frequency. *Advances in Internet of Things*, 2(2), 13-22.
- Dodson, S. (2008, October). The Net shapes up to get physical. *The Guardian*. Retrieved from <https://www.theguardian.com/technology/2008/oct/16/internet-of-things-ipv6>
- Ferguson, G. T. (2002, June). Have your objects call my object. *Harvard Business Review*. Retrieved from <https://hbr.org/2002/06/have-your-objects-call-my-objects>
- Gershenfelo, N., Krikorian, R., & Cohen, D. (2004). The Internet of Things-The principles that run the Internet are now creating a new kind of network of everyday devices, an” Internet-O.”. *Scientific American*, 291(4), 46-51.
- ITU. (2005, November). *The Internet of Things*. International Telecommunication Union. Retrieved from <https://www.itu.int/net/wsis/tunis/newsroom/stats/The-Internet-of-Things-2005.pdf>
- Jöreskog, K. G., & Sörbom, D. (1989). *LISREL 7: A guide to the program and applications*. Spss.
- Kosmatos, E.A., Tselikas, N.D. and Boucouvalas, A.C. (2011). Integrating RFIDs and smart objects into a unified internet of things architecture. *Advances in Internet of Things: Scientific Research*, 1(1), 5-12.
- Li, B., & Yu, J. (2011). Research and application on the smart home based on component technologies and internet of things. *Procedia Engineering*, 15, 2087-2092.
- Madakam, S., Ramaswamy, R., & Tripathi, S. (2015). Internet of Things (IoT): A literature review. *Journal of Computer and Communications*, 3(5), 164-173.
- Nunberg, G. (2005, November 19). *The advent of the internet*. Retrieved from <http://wiki.lib.sun.ac.za/images/1/12/NunbInternet11-20.pdf>
- Park, S. Y. (2009). An analysis of the technology acceptance model in understanding university students’ behavioral intention to use e-learning. *Educational Technology & Society*, 12(3), 150-162.
- Pedhazur, E. J. (1982). *Multiple regression in behavioral research: Explanation and prediction* (2nd Ed.). New York, NY: Holt, Rinehart and Winston.
- Ramakrishnan, R., & Gaur, L. (2016). Application of Internet of Things (IoT) for Smart Process Manufacturing in Indian Packaging Industry. In S. C. Satapathy, J. K. Mandal, S. K. Udgata, & V. Bhateja (Eds.), *Information Systems Design and Intelligent Applications* (pp. 339-346). India: Springer.
- Stevens, J. P. (2012). *Applied multivariate statistics for the social sciences*. United States of America, USA: Routledge.
- Syed, M., R. (2008). *Multimedia technologies: Concepts, methodologies, tools, and applications*. United States of America, USA: Hershey.
- Tabachnick, B., G., & Fidell, L., S. (2001). *Using multivariate statistics* (4th Ed.). Needham Heights, MA: Pearson.
- Venkatesh, V., Morris, M. G., Davis, G. B., & Davis, F. D. (2003). User acceptance of information technology: Toward a unified view. *MIS quarterly*, 27(3), 425-478.

Singh, G., Gaur, L. and Ramakrishnan, R.

- Want, R. (2006). An introduction to RFID technology. *IEEE pervasive computing*, 5(1), 25-33.
- Willis, T. J. (2008). *An evaluation of the technology acceptance model as a means of understanding online social networking behavior*. (Doctoral Dissertation). University of South Florida, USA.
- Zanella, A., Bui, N., Castellani, A., Vangelista, L., & Zorzi, M. (2014). Internet of things for smart cities. *IEEE Internet of Things journal*, 1(1), 22-32.

Effect of Maghemite ($\gamma\text{-Fe}_2\text{O}_3$) Nano-Powder Mixed Dielectric Medium on Tool Wear Rate (TWR) During Micro-EDM of Co-Cr-Mo

Elsiti, N. M.^{1*}, Noordin, M. Y.¹ and Idris, A.²

¹Department of Materials, Manufacturing and Industrial Engineering, Faculty of Mechanical Engineering, Universiti Teknologi Malaysia, 81310 UTM, Skudai, Malaysia

²Department of Bioprocess Engineering, Faculty of Chemical Engineering, Universiti Teknologi Malaysia, 81310 UTM, Skudai, Malaysia

ABSTRACT

Micro Electro Discharge Machining (micro-EDM) is widely used for producing different types of micro features and micro components. Tool wear rate (TWR) is an important factor that affects the accuracy of machining as well as the productivity of micro-EDM process. This study examines the effects of process parameters and the use of Maghemite ($\gamma\text{-Fe}_2\text{O}_3$) nano-powder mixed dielectric medium on tool wear rate when micro-EDM Co-Cr-Mo. A Copper electrode with 300 μm diameter and positive polarity was used to evaluate the machining process by focusing on TWR. Two different concentrations of nano-powder (i.e., 2 g/l and 4 g/l) were added to the dielectric. Results showed that increasing the discharge current and voltage leads to a corresponding increase in TWR, while the presence of $\gamma\text{-Fe}_2\text{O}_3$ nano-powder in the dielectric liquid decreases TWR. Mixed micro-EDM with 2 g/l of nano-powder achieved a lower TWR.

Keywords: Cobalt Chromium Molybdenum (Co-Cr-Mo), Maghemite ($\gamma\text{-Fe}_2\text{O}_3$) nano-powder, powder-mixed-EDM, tool wear rate (TWR)

INTRODUCTION

Electrical discharge machining (EDM) is a process currently applied to the production of various tools and moulding used in industries for machining electrically-conductive parts. This method is capable of generating complex shapes with no limitation in the material hardness (Baseri & Sadeghian, 2016). One of the most proficient modern machining processes regarding the size and the precision of products is the micro-EDM process, which outperforms other fabrication processes such as laser, LIGA and ultrasonic ion beam, among others. The

Article history:

Received: 29 December 2016

Accepted: 21 April 2017

E-mail addresses:

nagwa.mejid@yahoo.com (Elsiti, N. M.),

noordin@fkm.utm.my (Noordin, M. Y.),

aniidris@utm.my (Idris, A.)

*Corresponding Author

advantage of this process is its low cost, though it is slow (Jahan, Rahman, & Wong, 2011). Micro-EDM is broadly applied in the field of micro-mould making and the generation of dies, cavities, and complex 3D structures (Alting, Kimura, Hansen, & Bissacco, 2003). One of the latest developments in the technology of EDM is powder-mixed electric discharge machining (PMEDM) that works with the addition of powder particles to the dielectric for improving machining rate, surface quality, and precision. Suspended particles cause a reduction in the dielectric overall electrical resistivity, allowing sparking from a distance. Flushing conditions and the improved spark frequency together with multiple sparks lead to the simultaneous improvement of both surface quality and material removal rate (Talla, Gangopadhyay, & Biswas, 2016). In recent years, alloys that are based on cobalt have been used considerably in the metallurgical and biomedical fields as they are tough and their strength is retained at high temperatures. Additionally, they are biocompatible and resistant to wear and corrosion (Agarwal & Ocken, 1990). The alloys are also used in aerospace and nuclear industries (Rees, 2011). In numerous studies, the effects of powder materials on the characteristics of PMEDM have been investigated, taking into account the reduction in tool wear rate (TWR). Jeswani (1981) examined the impact of adding 4 g of Gr powder to each liter of kerosene oil for EDM of steel. Findings showed that the material removal rate (MRR) and TWR are enhanced by 60% and 15% respectively, whereas the wear ratio (i.e., TWR/MRR) decreased by about 28%. Han-Ming Chow et al. (2000) studied the effects of powder that was added to kerosene for the micro-slit machining of titanium alloy by means of EDM. Findings showed that kerosene with either Al or SiC powder added in EDM could result in fine surface finish, enhance the material removal depth, and reduce TWR. Kung, Horng and Chiang, (2009) examined MRR and TWR during conventional PMEDM of cobalt bonded tungsten carbide (WC-Co) by means of Al powder of 1.5–2 μm and 10–20 g/L. Results showed an increase in MRR when aluminium powder concentration is increased and the EWR value tended to reduce with the aluminium powder concentration down to a minimum value after which it tended to increase. Tiwary, Pradhan and Bhattacharyya, (2015) investigated the impact of a variety of process parameters into TWR, MRR, overcut (OC), and taper of micro-hole during EDM process of Ti-6Al-4V. The Central Composite Design (CCD) technique was used to design the experiment, and Response Surface Methodology (RSM) was applied for mapping the relationships between the input and out process parameters. Jahan et al. (2011) investigated the improvement and enhancing the carbide surface characteristics in sinking and milling micro-EDM by using Gr nano-powder-mixed dielectric. Results showed both Ra and Rmax reduced with an increase in the powder concentration up to certain values; then they increased again. The EWR was decreased at certain concentrations; but at higher concentration, it tended to increase. According to Tzeng and Lee (2001), amongst SiC, Al, and chromium (Cr) powders, the use of Cr provides the highest MRR while the SiC powder produces the lowest MRR; and the SiC powder had the most significant effect on the tool wear followed by Al and Cr respectively. Figure 1 shows very few studies have been conducted on nano-powder-mixed EDM while there is no published work on effects of $\gamma\text{-Fe}_2\text{O}_3$ nano-powder-mixed EDM. Thus, the present paper examines and discusses the feasibility of obtaining low TWR when micro-EDM of CoCrMo through the addition of $\gamma\text{-Fe}_2\text{O}_3$ nano-powder to the dielectric medium. The TWR was observed with and without powder-mixed micro-EDM.

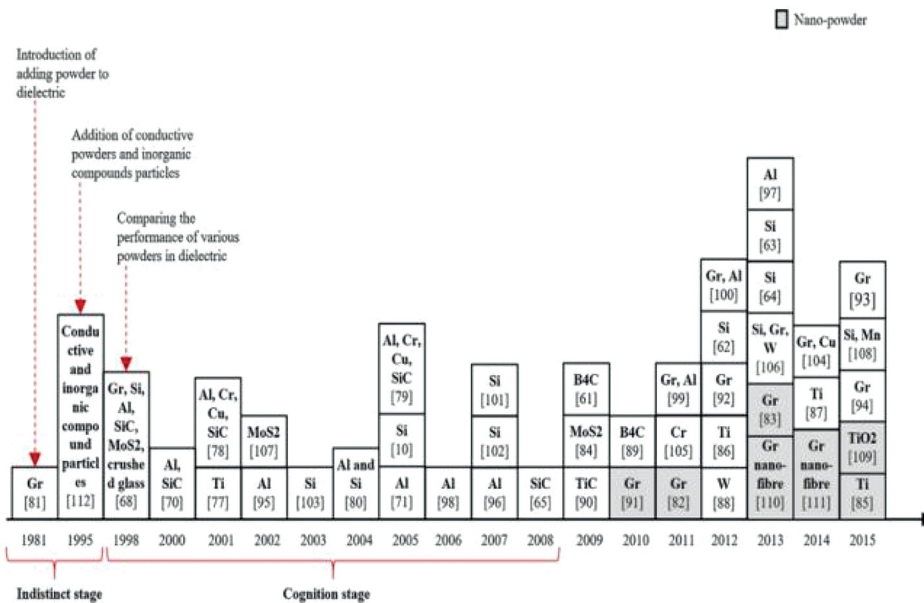


Figure 1. Studies conducted on PMEDM between 1981 and 2015 (Marashi, Jafarlou, Sarhan, & Hamdi, 2016)

METHODS: EXPERIMENTAL SETUP

The experiments in the current research were performed using an AG40L Sinkler EDM (Figure 2), and the samples were the CoCrMo alloy; the latter was cut into slides with dimensions of 50 mm x 90 mm x 1mm, and the electrode was from copper with 6 mm length and 300 μm diameter. The electrode had positive polarity, and oil-based dielectric fluid mixed with two percentages of γ-Fe₂O₃ nano-powder, which were 2g/l and 4g/l respectively were utilised. In the first group, the EDM dielectric was utilised, and in the second group, γ-Fe₂O₃ nano-powder with size less than 10 nm was mixed with the dielectric medium. The PMEDM experiments were carried out in working tank with dimensions of 46 cm × 35 cm × 24 cm made up of 1.5 mm thick stainless steel sheets. During the tests, a stirrer was employed to maintain a consistent suspension of Fe₂O₃ nano-powder in the tank,. The working tank is depicted in Figure 3. The input variables of the study were current, voltage, and pulse on time. The experiments were designed using a 2-level factorial design that comprised 11 runs including 8 points (2³) and 3 centre points. In order to calculate TWR for all experimental runs, equation 1 was used. A precision electronic balance was used to measure the electrode weights.

$$TWR = [(W1 - W2) \times 1000] / (T \times \rho) \tag{1}$$

Where W2 and W1 stand for the weights of the tool after and before machining respectively (in grams) while ρ denotes the density of workpiece in gm/cc, and T signifies the experiment time in minutes.



Figure 2. AG40L Sinker EDM



Figure 3. Working tank

Table 1
Machining Parameters

Description	Input Factors	Unit	Value		
			Low	Centre	High
A	Current	A	1.5	2.25	3
B	Voltage	V	60	90	120
C	Pulse On	μ s	10	105	200

Table 2
Experimental Results

Exp No	TWR1 Without nano-powder (mm^3/min)	TWR2 2g/l- nano-powder (mm^3/min)	TWR3 4g/l- nano-powder (mm^3/min)
1	0.000617	0.000322	0.00032
2	0.003713	0.00041	0.004998
3	0.007163	0.001821	0.029149
4	0.054019	0.011946	0.033762
5	0.006726	0.000252	0.000198
6	0.000676	0.000661	0.002478
7	0.025621	0.000539	0.000229
8	0.026912	0.015995	0.017812
9	0.009497	0.000868	0.00997
10	0.009586	0.0009	0.00646
11	0.007062	0.002563	0.006719

RESULTS AND DISCUSSIONS

Tables 1 and 2 respectively show the experimental parameters results obtained for TWR. Calculation was done for TWR1 (without nano-powder), TWR2 (adding 2 g of γ -Fe₂O₃ nano-powder to each liter of oil), and TWR3 (adding 4 g of γ -Fe₂O₃ nano-powder to each liter of oil). Design-Expert Software Ver. 7 was used to analyse the dependent variables. ANOVA (Analysis of variance) was carried out in order to examine the significance of the micro-EDM and PME-micro-EDM of Co-Cr-Mo model, individual model terms, and the lack of fit. The ANOVA results of TWR1, 2 and 3 are presented in tables 3, 4, and 5 respectively. Table 3 and Figure 4 show TWR1 increased with an increase in the peak current and gap voltage, whereas the effects of the pulse on time on TWR1 were insignificant. When current settings were high, more electric current (energy) passing through the gap resulted in a large amount of workpiece and electrode material removal through evaporation and melting. This is why the increased current led to higher TWR (Unses & Cogun, 2015). In addition, low TWR1 was obtained once the pulse on was 10 μ s and the current was 1.5 A. Based on Table 4 and Figure 5, (A, B, AB) factors had a significant effect on TWR2. The TWR2 value increased with an increase in the peak current and spark gap voltage. Higher heat energy is subjected to both electrodes when machining is done with higher values of the discharge current. It increases the volume of the molten and ejected metal from both electrodes (Habib, 2009). Table 5 and Figure 6 show the factors of A, B, C, and BC were significant. The TWR3 was increased with an increase in the current and gap voltage, whereas it was reduced once the pulse on time was increased. Increasing the pulse on time values decreases the TWR3 values. When values of pulse duration are small, more negatively charged particles in motion strike the positive tool electrode, which leads to an increase in the rate of melting of the electrode material (Habib, 2009). R-squared values for TWR1, TWR2 and TWR3 (0.9873, 0.9124, 0.9409 respectively) that are near to 1 which is desirable. There is a small difference between Pred R-squared and Adj R-squared (less than 0.2), which means there is an acceptable transaction between the input and output parameters. An Adeq precision greater than 4 is desired. Regression models regarding the actual factors for TWR1, TWR2 and TWR3 predictions are displayed as below:

$$\text{Sqrt(TWR1)} = -0.0215 - 0.0204 * \text{Current} - 0.00028 * \text{Voltage} + 0.00096 * \text{Pulse On} + 0.00095 * \text{Current} * \text{Voltage} + 0.000413 * \text{Current} * \text{Pulse On}$$

$$\text{Ln(TWR2)} = -7.981 - 0.95266 * \text{Current} - 0.013101 * \text{Voltage} + 0.022584 * \text{Current} * \text{Voltage}$$

$$\text{TWR3} = -0.038112 + 0.0048 * \text{Current} + 0.00049 * \text{Voltage} + 0.000104 * \text{Pulse On} - 0.00000181 * \text{Voltage} * \text{Pulse On}$$

Table 3
Analysis of Variance (ANOVA) Test for TWR1

Response: TWR1						
Source	Sum of Squares	DF	Mean Square	F Value	Prob > F	
A (Current)	0.002173	1	0.002173	17.85	0.0134	
B(Voltage)	0.025	1	0.025	205.46	0.0001	
C(Pulse On)	0.0001073	1	0.0001073	0.88	0.4009	
AB	0.003685	1	0.003685	30.26	0.0053	
AC	0.006957	1	0.006957	57.13	0.0016	
Residual	0.000487	4	0.0001218			
Lack of Fit	0.000362	2	0.0001814	2.92	0.2551	not significant
R-Squared	0.9873	Adj R-Squared	0.9715	Pred R-Squared	0.8428	Adeq Precision 23.45

Table 4
Analysis of Variance (ANOVA) Test for TWR2

Response: TWR2						
Source	Sum of Squares	DF	Mean Square	F Value	Prob > F	
Model	17.55	3	5.85	20.84	0.0014	significant
A (Current)	5.25	1	5.25	18.69	0.005	
B (Voltage)	10.24	1	10.24	36.47	0.0009	
AB	2.07	1	2.07	7.36	0.035	
Residual	1.68	6	0.28			
Lack of Fit	0.93	4	0.24	0.61	0.6964	not significant
R-Squared	0.9124	Adj R-Squared	0.8687	Pred R-Squared	0.7186	Adeq Precision 10.868

Table 5
Analysis of Variance (ANOVA) Test for TWR3

Response: TWR3						
Source	Sum of Squares	DF	Mean Square	F Value	Prob > F	
A (Current)	0.0001062	1	0.0001062	6.63	0.0498	
B (Pulse On)	0.0006653	1	0.0006653	41.50	0.0013	
C-Voltage	0.0002822	1	0.0002822	17.6	0.0085	
BC	0.0002229	1	0.0002229	13.9	0.0136	
Residual	0.000080	5	0.00001603			
Lack of Fit	0.000072	3	0.00002417	6.32	0.1397	not significant
R-Squared	0.9409	Adj R-Squared	0.8936	Pred R-Squared	0.6144	Adeq Precision 12.649

Effect of (Fe₂O₃) Nano-Powder

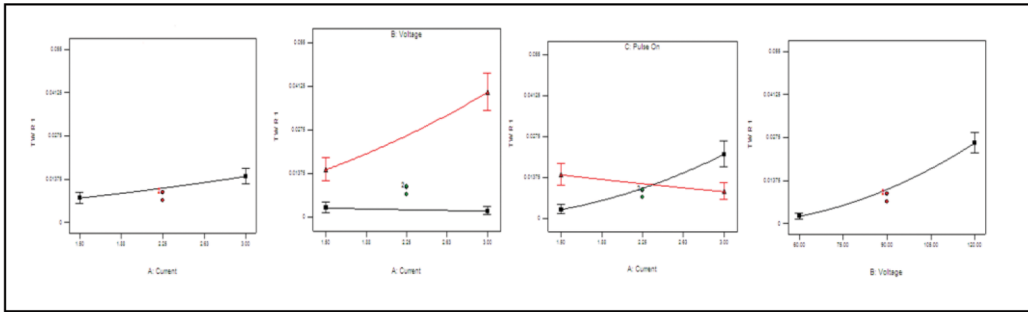


Figure 4. Effect plot showing variation of TWR1 with process parameters

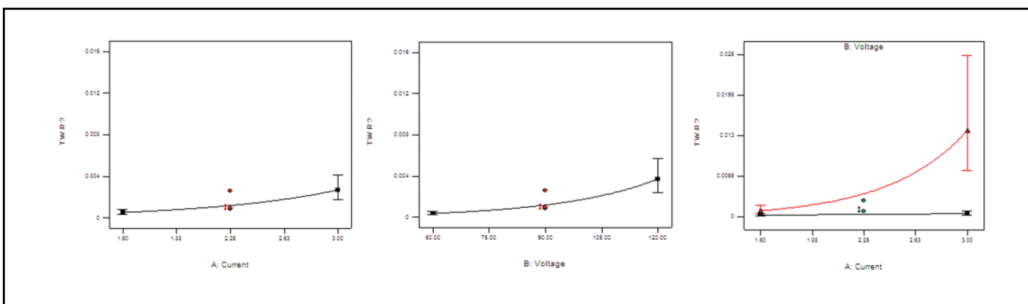


Figure 5. Effect plot showing variation of TWR2 with process parameters

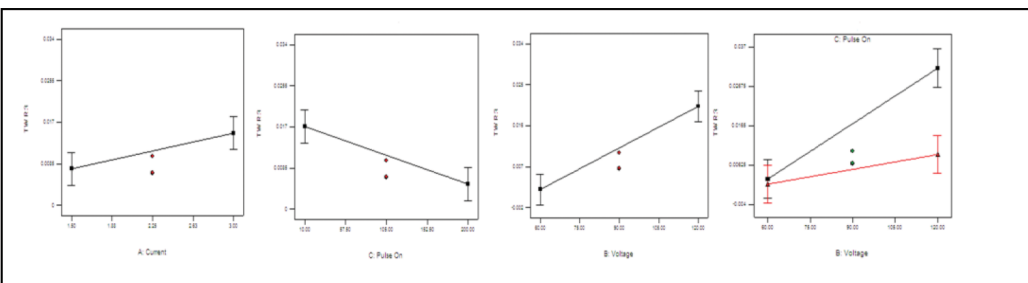


Figure 6. Effect plot showing variation of TWR3 with process parameters

Figure 7 shows that the residuals follow a roughly straight line in the normal probability plot, which indicates they are distributed in a normal way. The residuals have a constant variance since they are randomly scattered around zero in residuals versus predicted values. Therefore, there is no error due to the time or data collection order.

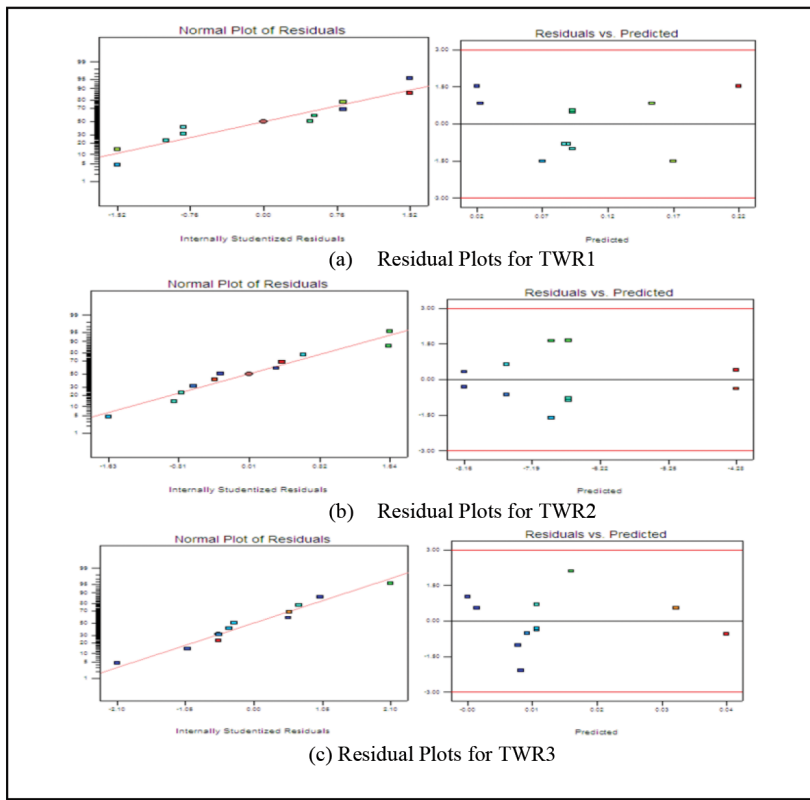


Figure 7. Normal plots of Residual for TWR

Figure 8 compares the amounts of TWR generated with the addition of various concentrations of Fe_2O_3 nano-powder to dielectric. Findings indicate that the addition of 2 g/l of Fe_2O_3 nano-powder to dielectric fluid causes lower TWR, whereas if 4g/l is added to the dielectric, the TWR values are increased, as shown in Figure 9. During micro-EDM, if conductive or semi-conductive powders exist in the working gap, the breakdown strength of dielectric can be reduced, resulting eventually in a higher spark gap. The decrease in TWR due to adding powder is because of the decrease of ineffective pulses at higher spark gap and the improved flushing, while the increased trend of TWR at higher concentration is because of the settlement of powder in the spark gap (Jahan et al., 2011; Yih-fong & Fu-chen, 2005)

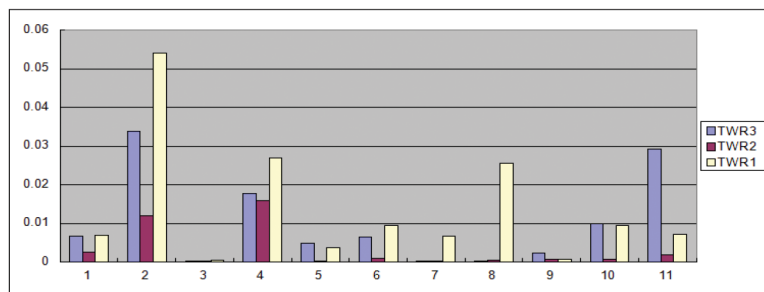


Figure 8. Comparison between TWR values

Effect of (Fe₂O₃) Nano-Powder

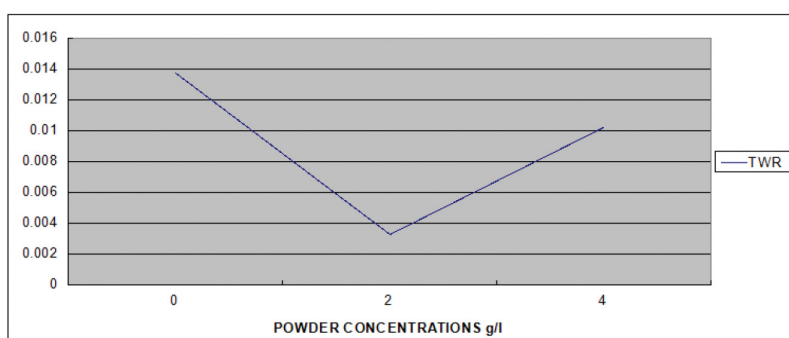


Figure 9. Effect of the powder concentration on TWR

Optimal Parameters and Confirmation Runs

Optimisation is aimed at exploring an appropriate set of conditions that can achieve all of the defined goals. The ANOVA results indicate that voltage, current, and pulse were significant. The input variables were adjusted to obtain desirable values of TWR in the optimisation process. The voltage and current were set as minimum values, while the pulse was set in range for TWR1 and TWR2; however, for TWR3, the pulse on time was set at maximum. When the desired value nears 1, the setting parameters provide the desirable responses. In Figure 10, the red area displays the best desirable values of parameters. For verification of the model's adequacy, two confirmation experiments were carried out on TWR1, TWR2, and TWR3, and data from the confirmation runs are listed in Table 6. The maximum deviation of the predicted results from the experimental results is -13.52%.

Table 6
Analysis of Confirmation Experiments for TWR

IP	V	Ton	Powder %	Response	Actual	Predict	%error
1.5	70	10	0	TWR1	0.0217	0.0215	2.52
1.88	60	10	0	TWR1	0.02161	0.0245	-13.52
1.5	70	10	2	TWR2	0.0025	0.0026	-7.32
1.88	60	10	2	TWR2	0.0039	0.0037	5.12
1.5	70	200	4	TWR3	0.02156	0.0207	3.98
1.88	60	200	4	TWR3	0.0297	0.0314	-5.91

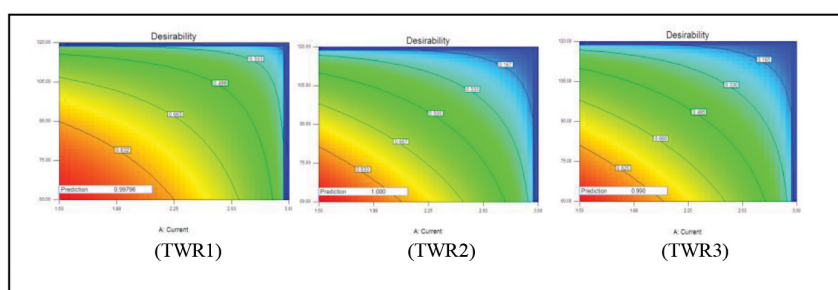


Figure 10. Desirability graphs for TWR1, TWR2 and TWR3

CONCLUSION

The present study shows that a decreasing tool wear rate (TWR) is achievable during the EDM process of CoCrMo using Fe₂O₃ nano-powder. It also examined the impacts of process parameters on TWR. Below is the summary of the findings of this study:

- As indicated by the ANOVA analysis for TWR responses, current and voltage were the significant factors. By setting the current at 3A and voltage at 120V, the highest value of TWR was obtained. With an increase in current, the TWR increased; this was because using higher values of current during machining process meant higher heat energy was subjected to both electrodes. As result, the material that is removed from both electrodes increased too.
- During the powder-mixed micro-EDM of Co-Cr-Mo, adding γ -Fe₂O₃ nano-powder to the dielectric liquid caused a reduction in TWR. 2 g of nano-powder reduced the TWR, whereas 4 g/l of γ -Fe₂O₃ nano-powder increased the TWR.

ACKNOWLEDGEMENT

The authors express their gratitude to the Centre for Graduate Studies of Universiti Teknologi Malaysia for its support in the conduct of this research.

REFERENCES

- Agarwal, S. C., & Ocken, H. (1990). The microstructure and galling wear of a laser-melted cobalt-base hardfacing alloy. *Wear*, 140(2), 223-233.
- Alting, L., Kimura, F., Hansen, H. N., & Bissacco, G. (2003). Micro Engineering. *CIRP Annals - Manufacturing Technology*, 52(2), 635-657.
- Baseri, H., & Sadeghian, S. (2016). Effects of nanopowder TiO₂-mixed dielectric and rotary tool on EDM. *The International Journal of Advanced Manufacturing Technology*, 83(1), 519-528.
- Chow, H. M., Yan, B. H., Huang, F. Y., & Hung, J. C. (2000). Study of added powder in kerosene for the micro-slit machining of titanium alloy using electro-discharge machining. *Journal of Materials Processing Technology*, 101(1-3), 95-103.
- Habib, S. S. (2009). Study of the parameters in electrical discharge machining through response surface methodology approach. *Applied Mathematical Modelling*, 33(12), 4397-4407.
- Jahan, M. P., Rahman, M., & Wong, Y. S. (2011). Study on the nano-powder-mixed sinking and milling micro-EDM of WC-Co. *The International Journal of Advanced Manufacturing Technology*, 53(1), 167-180.
- Jeswani, M. L. (1981). Effect of the addition of graphite powder to kerosene used as the dielectric fluid in electrical discharge machining. *Wear*, 70(2), 133-139.
- Kung, K. Y., Horng, J. T., & Chiang, K. T. (2009). Material removal rate and electrode wear ratio study on the powder mixed electrical discharge machining of cobalt-bonded tungsten carbide. *The International Journal of Advanced Manufacturing Technology*, 40(1), 95-104.

- Marashi, H., Jafarlou, D. M., Sarhan, A. A., & Hamdi, M. (2016). State of the art in powder mixed dielectric for EDM applications. *Precision Engineering*, 46, 11-33.
- Rees, A. (2011). *Micro Electrical Discharge Machining: Axissymmetric component manufacture and surface*. (Doctor of Philosophy). University of Wales, Cardiff United Kingdom, Cardiff School of Engineering, Manufacturing Engineering Centre, University of Wales, Cardiff.
- Talla, G., Gangopadhyay, S., & Biswas, C. K. (2016). Effect of Powder-Suspended Dielectric on the EDM Characteristics of Inconel 625. *Journal of Materials Engineering and Performance*, 25(2), 704-717.
- Tiwary, A. P., Pradhan, B. B., & Bhattacharyya, B. (2015). Study on the influence of micro-EDM process parameters during machining of Ti-6Al-4V superalloy. *The International Journal of Advanced Manufacturing Technology*, 76(1), 151-160.
- Tzeng, Y. F., & Lee, C. Y. (2001). Effects of Powder Characteristics on Electrodischarge Machining Efficiency. *The International Journal of Advanced Manufacturing Technology*, 17(8), 586-592.
- Unses, E., & Cogun, C. (2015). Improvement of Electric Discharge Machining (EDM) Performance of Ti-6Al-4V Alloy with Added Graphite Powder to Dielectric. *Strojniški vestnik-Journal of Mechanical Engineering*, 61(6), 409-418.
- Yih-Fong, T., & Fu-Chen, C. (2005). Investigation into some surface characteristics of electrical discharge machined SKD-11 using powder-suspension dielectric oil. *Journal of Materials Processing Technology*, 170(1-2), 385-391.





Review of Channel Modelling for Optical Wireless Links

Miglani, R.^{1*} and Malhotra, J. S.²

¹*Department of Electronics and Communication systems, Lovely Professional University and Research Scholar, IKG P.T.U, Phagwara, Punjab 144111, India*

²*Department of Electronics and Communication Engineering, DAV Institute of Engineering and Technology, Jalandhar, Punjab 144008, India*

ABSTRACT

Atmospheric adversities impacts on the performance of free space optical (FSO) links, with turbulence-induced fading being the most prominent among them. Since FSO links involve transmission of optically modulated signal through atmosphere, it is crucial to have well defined mathematical model to understand and map association of atmospheric turbulence with channel link characteristics. To model a reliable optical wireless communication link, it is important to have an accurate probability density function (PDF) of received intensity, as it allows us to understand the atmospheric factors and magnitude of their impact that may lead to impairment of the link. It was observed that the variation in turbulence has a direct impact on channel behaviour and in turn affects the PDF of received intensity. This paper also analyses the performance of different channel models by contrasting their PDF for varying degrees of turbulence.

Keywords: Atmospheric turbulence, channel fading, channel modelling, Cumulative Distribution Function (CDF), Irradiance Probability Density Function (PDF), variance

INTRODUCTION

An exponential rise in demand for higher bandwidth has led to a scenario where we have to look for something beyond Radio Frequency (RF) links which have reached saturation levels in delivering higher data rates to serve the bandwidth-starved smart device era. The Free space optical (FSO) communication is technology which has been experimentally tested to provide data rates as high as 10 Gbps (Willebrand, Ghuman, 2001) which can serve as reliable solution. It transmits optically modulated data using visible or IR part of frequencies which is essentially non-licensed. The FSO transmission being line of sight offers unprecedented security and privacy. Being optically modulated using very narrow

Article history:

Received: 29 December 2016

Accepted: 21 April 2017

E-mail addresses:

rajan.16957@lpu.co.in (Miglani, R.),

jmalhotra292@gmail.com (Malhotra, J. S.)

*Corresponding Author

wavelengths, FSO links are not only immune to co-channel interference and but also immune to RF interferences (Leitgeb, Awan, Brandl, Plank, Capsoni, Nebuloni, Loschnigg; 2009; Hogan, 2013).

However, the link can be a major dampener, namely degrading the performance of free space optical communication links. This is because the atmospheric and metrological conditions such as wind, rain, fog, temperature variations may impair the link owing to scatter and absorption of light. In comparison to atmospheric conditions, the turbulence effect of atmosphere can cause serious damages to the link over time. The atmosphere is composed of absorption, turbulence induced fading and scattering (Kedar & Arnon, 2004). Due to absorption and scattering, light is unable to reach its destination with full intensity because it gets scattered by water molecules. As mentioned above, the most dominating effect which weakens the link is turbulence-induced fading (Andrews & Phillips, 2005) which occurs in clear atmosphere due to temperature variations whereby the air's refractive index changes. The turbulence effect causes fluctuations in modulated signal phase and amplitude which may make it either difficult or impossible for the receiver to extract information, and this effect is known as fading. The Kolmogorov theory explains the concept of turbulence-induced fading as discussed by Tatarskii, Zavorotnyi, (1985) using parameters which characterise the turbulence: the inner and outer scale turbulence l_0 and L_0 , respectively and index of refraction C^2_n . It is worth mentioning that for the given link atmospheric, turbulence is never constant i.e. its strength may vary from weak to strong, depending upon dynamic link and atmospheric conditions. To describe the extent of turbulence, the factor scintillation index (SI) is used as standard, which is defined in equation 1 and explained by Khalighi and Uysal (2014):

$$\sigma^2_I = E\{I^2\}/E\{I\}^2 - 1 \quad (1)$$

where I is intensity of optical wave and $E\{.\}$ defines the expected value of I . To define the quantum of loss of signal intensity due these channel fluctuations, various models have been proposed over the years. The main focus of this paper is to analyse effective channel modelling technique that allows transmission of optically modulated data through the turbulent conditions with minimum fading effects. In the recent past, channel modelling techniques such as Log Normal distribution, Rayleigh distribution, Rician distribution, Negative exponential distribution have been proposed but these models consider turbulence effects either as weak or strong general models which only define the turbulence effect either as weak or strong (Al-Habash, Andrews, Phillips, 2001). Additionally, other models such as Gamma-Gamma and Weibull are based on doubly stochastic theory discussed (Chatzidiamantis, Sandalidis, Karagiannidis, Kotsopoulos, Matthaiou, 2010; Kashani, Uysal and Kavehrad, 2013). These models are capable of describing fading effects of turbulence in all regimes ranging from weak to strong turbulences as cited by Navas, Balsells, Paris and Notario, (2011). The performance of these channel models has been studied and contrasted by determining the probability density function (PDF) of received irradiance in different turbulence regimes. As a rule of thumb, channel turbulence has a direct impact on PDF of received intensity. To model a reliable and interference free optical wireless communication it is very important to build an accurate PDF of received intensity using a channel model that ensures that minimum fading effects are

induced on channel. In this paper, the Cumulative Distribution Function of received intensity has also been taken into consideration when developing these channel models. *Section I* of this paper explains the introductory concepts related to free space optical links and channel modelling. Mathematical models to define these channels have been described in *Section II* while qualitative analysis, calculation and interpretation of effect of turbulence on channel fading is described in *Section III*. *Section IV* contains discussion and conclusive remarks.

A simplified schema of a free space optical communication link along with its basic subsystems is illustrated in Figure 1. The information source is suitably modulated onto optical modulator using laser diode. This signal, known as optically modulated signal, is then transmitted over atmospheric channel to remote destinations using line of sight communication.

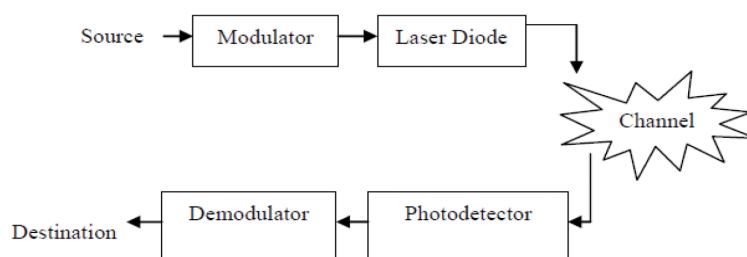


Figure 1. Basic block diagram of free space optical communication system

On the receiver side, the signal is optically collected using photo detectors which convert the optical signals back to electrical information. The free space optical communication provides large bandwidth to support more users than radio frequency (RF) communication.

METHODS

Lognormal Distribution

This model is used to define the fading effect in FSO channel and is best suited to simulate weak atmospheres turbulence (Zhu & Kahn, 2002; Ghassemlooy, Popoola, & Leitgeb, 2007). The turbulence is characterised using Rytov variance denoted by σ_I^2 and the turbulence is essentially considered having values of $\sigma_I^2 < 1.2$ (Popoola & Ghassemlooy, 2009) also the Rytov variance is defined as

$$\sigma_I^2 = 1.23 C_n^2 K^{7/6} L^{11/6}$$

where L is link distance, k is wave number and C_n^2 is refractive index parameter. The Probability density function (PDF) of Lognormal is given in equation. 2 cited from works of Ghassemlooy et al., (2007), Popoola, Ghassemlooy, Allen, Leitgeb, and Gao, (2008), and Yang and Cheng, (2016);

$$p(I) = \frac{1}{(\sqrt{2\pi\sigma_I^2})^I} \exp\left\{-\frac{(\ln(\frac{I}{I_0}) + \frac{\sigma_I^2}{2})^2}{2\sigma_I^2}\right\}, I > 0 \tag{2}$$

Where I is irradiance I_0 is irradiance without scintillation. The cumulative distribution function (CDF) of Lognormal is given in equation 3.

$$P(I) = (1/2)\operatorname{erfc}\left\{-\frac{\ln\left(\frac{I}{I_0}\right) + \sigma_I^2/2}{\sqrt{2}\sigma}\right\} \quad (3)$$

Rayleigh Distribution

The Rayleigh distribution can be effectively used to model fading effects of moderate to strong values of turbulence. As the value of variance fluctuates between high and low, link performance degrades as PDF of received intensity decreases. This distribution is used to express channel gain. For convenience, the scintillation index for this model was assumed as unity. The probability density function (PDF) for Rayleigh distribution is given in equation 4.

$$p(I) = \frac{I}{2\sigma^2} \exp\left\{-\frac{I}{2\sigma^2}\right\}, I > 0 \quad (4)$$

Where, I is the irradiance, σ^2 is the variance. The cumulative distribution function of Rayleigh is given in equation 5.

$$P(I) = 1 - \exp\left\{-\frac{I^2}{\sigma^2}\right\}, I > 0 \quad (5)$$

Negative Exponential Distribution

The negative exponential model, describes turbulence under strong regime of fading effects only; this is because negative exponential model gives optimum values at negative region only (Al-Habash et al., 2001). The probability density function (PDF) of negative exponential is given in equation 6 and is cited from Al-Habash et al. (2001) and Nistazakis, Stassinakis, Muhammad, Tombras, (2014).

$$p(I) = \frac{1}{I_0} \exp\left[\frac{-I}{I_0}\right], I > 0 \quad (6)$$

where I_0 is the average value of irradiance, $E[I] = I_0$. The cumulative distribution function of negative exponential distribution is given in equation 7.

$$P(I) = 1 - \exp\left[\frac{-I}{I_0}\right] \quad (7)$$

Rician Distribution

The Rician distribution is used to model the effects of strong turbulence. It is principally based on realization that along with direct path between sources to destination there exists multipath component as well. The probability density function (PDF) of Rician distribution as described by Papoulis (1991) is given in equation 8:

$$p(I) = \frac{1}{\sigma^2} \exp\left\{-\frac{I^2 + k_d^2}{2\sigma^2}\right\} I_0 \left(\frac{Ik_d}{\sigma^2}\right), I > 0 \quad (8)$$

where I is irradiance, $\sigma^2 = 1.23 C^2 n K^{7/6} L^{11/6}$ and Rician factor = K (dB) = $10 \log_{10}(k_d^2 / 2\sigma^2)$. The cumulative distribution function of Rician distribution is given in equation 9 where k_d is the strength of direct component

$$P(I) = 1 - Q\left(\frac{k_d}{\sigma}, \frac{I}{\sigma^2}\right) \tag{9}$$

where Q is Marcum function.

Gamma-Gamma Distribution

The Gamma-Gamma distribution models turbulent atmosphere, in which the light fluctuations consists of both small scale effects which are basically scattered and large effects of refraction. This distribution is based on doubly stochastic theory. The received irradiance I is the function of two random processes I_x and I_y . Where I_x and I_y irradiance arises from small and large turbulence eddies. The probability density function (PDF) of Gamma-Gamma distribution is given in equation 10 as explained recently by Anees and Bhatnagar, (2015), and Bhatnagar and Ghassemlooy (2015, 2016).

$$p(I) = \frac{2(\alpha\beta)^{\frac{(\alpha+\beta)}{2}}}{\Gamma(\alpha)\Gamma(\beta)} I^{((\alpha+\beta)/2)-1} K_{\alpha-\beta}(2\sqrt{\alpha\beta I}), I > 0 \tag{10}$$

$$\alpha = \frac{1}{\exp\left[\frac{0.49\sigma^2}{(1+1.11\sigma^{12/5})^{7/6}}\right]-1} \tag{11}$$

$$\beta = \frac{1}{\exp\left[\frac{0.51\sigma^2}{(1+0.69\sigma^{12/5})^{5/6}}\right]-1} \tag{12}$$

Where I is irradiance $\Gamma(.)$ is gamma function $K(\alpha, \beta)$ is Bessel function of second order.

RESULTS AND DISCUSSION

The probability density function and cumulative distribution function for various channel models have been studied for their variation in PDF and CDF. The scintillation index is considered as 1. The analytical results were obtained using MATLAB. The plot of PDF versus irradiance is shown in Figure 2 as analysed previously in equation 2 for log normal link model. It was shown that for various values of variance, the link delivers higher values of PDF for weak turbulence condition only. Figure 3 illustrates behaviour of channel modelled using Rayleigh link conditions. This link gives low irradiance PDF values at different values of variance, hence it can be concluded such links are heavily affected in strong turbulence conditions. The PDF for negative exponential distribution is shown Figure 4. The slope of this graph is negative which means that the negative exponential distribution has its optimum values in negative region and this model, like Rayleigh, performs miserably in conditions of strong turbulence.

The plot in Figure 5 shows PDF versus irradiance of Rician distribution based on equation. 8 and under strong turbulence regions low PDF values were obtained. Figure 5 illustrates variation in PDF with respect to irradiance for different values of Rician factor K_d .

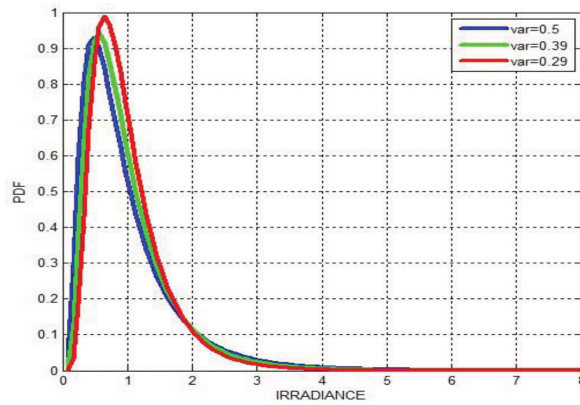


Figure 2. Probability Density Functions (PDF) vs. irradiance for lognormal model

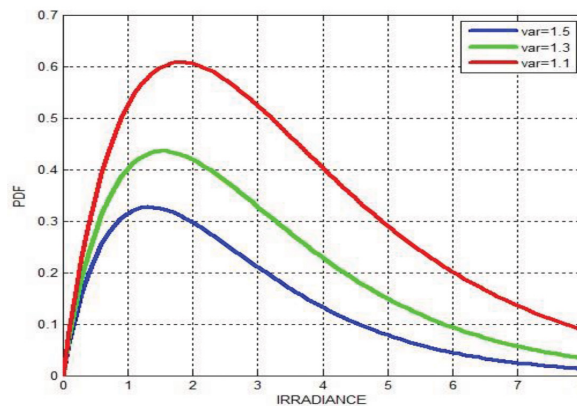


Figure 3. Probability Density Functions (PDF) vs. irradiance for Rayleigh model

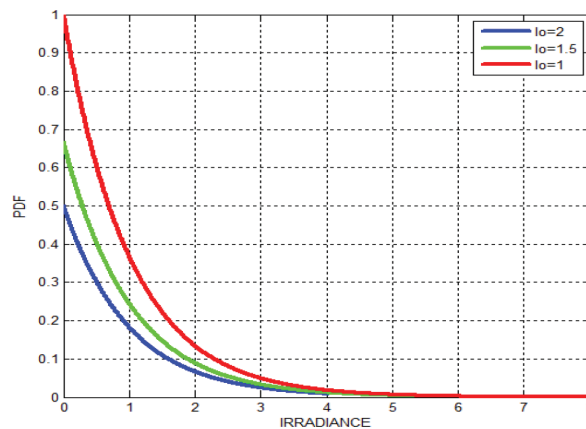


Figure 4. Probability Density Functions (PDF) vs. irradiance for Negative exponential model

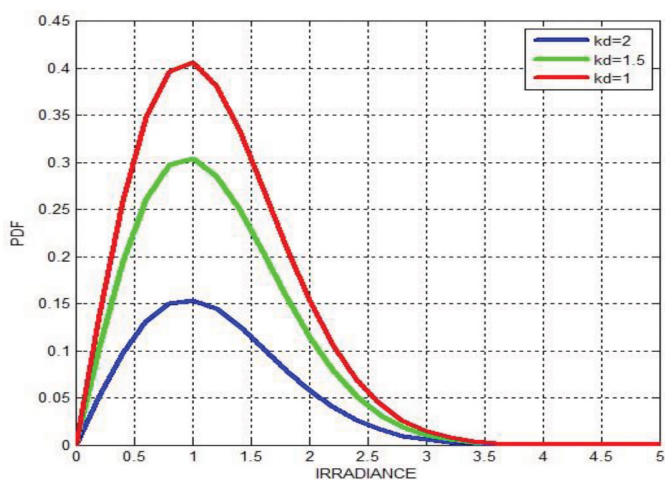


Figure 5. Probability Density Functions (PDF) vs. Irradiance for Rician model

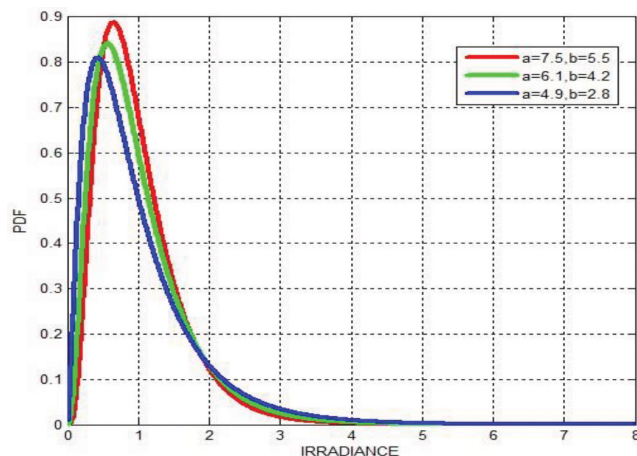


Figure 6. Probability Density Functions (PDF) vs. irradiance for Gamma-Gamma model

The plot in Figure 6 is based on equation 10 and illustrates the PDF variation for Gamma-Gamma link model. In this analysis, the effect of both small and large scale eddy are considered. It can be seen that appreciable PDF of irradiance can be obtained in weak-to-strong turbulence conditions. Figure 7 gives compares performance of different channels models under turbulent atmospheric conditions. It was an obvious observation that channel model is the most appropriate model for describe fading effects and determination of irradiance PDF, irrespective of turbulence regimes. Table 1 defines the PDF values of different channel models, assuming irradiance to be unity. As shown in Table 1, the negative exponential and Rician distribution have lower value (0.38) of PDF in strong turbulence conditions indicating such links would fail to perform in strong turbulence, whereas lognormal and Rayleigh can be used to define weak turbulence and strong turbulence. The Gamma-Gamma analysis gave best results at irradiance equal to unity. It delivered PDF of 0.99 which is higher compared with other channel models.

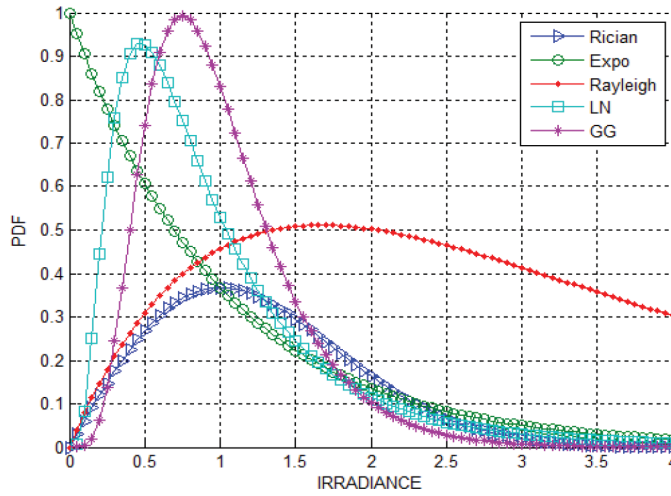


Figure 7. Probability Density Functions (PDF) vs. irradiance of different channel models

Table 1
PDF based comparison of different models

Channel model	Key factor	PDF(at intensity=1)
Lognormal	Variance(σ^2)	0.52
Rayleigh	Variance(σ^2) σ^2)	0.47
Negative exponential	Average irradiance(I_0)	0.38
Rician	k_d	0.38
Gamma-Gamma	Alpha (α or a), beta (β or b)	0.99

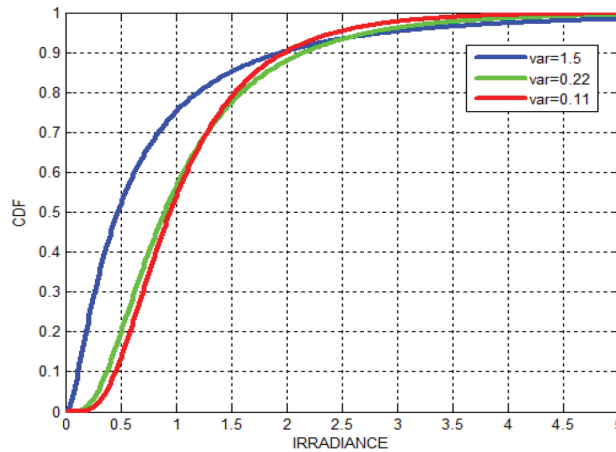


Figure 8. Cumulative Distribution Functions (CDF) vs. irradiance for Log normal model

The plot in Figure 8 is based on equation 3 and it gives CDF values at different variance. As variance decreases, the CDF increases. The CDF determination is also one of the tools to understand the fading effects in channel model for a range of turbulence. In Figure 8 and 9, CDF for Lognormal (LN) and Rayleigh channel model is determined for different values of variance. Clearly, increase in variance decreases the CDF associated with received irradiance.

The plot in Figure 10 is based on 7 and it provides CDF values at different values of I_0 . Figure 11 is CDF of Rician distribution and it is an analysis of equation 9. Figure 12 compares the performance of different channel models on the basis on CDF for received irradiance and it has been noted that Lognormal channel model has higher CDF value of 0.80 at intensity =1 indicating that these models explain only weak turbulence condition whereas Negative exponential and Rician have lower values of CDF corresponding to a strong turbulence regime. Table 2 shows the CDF values of different channel models at irradiance=1. The Table 2 represent comparative picture of analysed results.

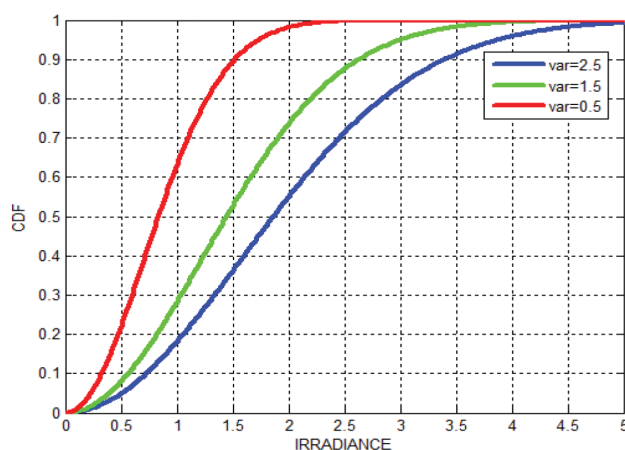


Figure 9. Cumulative Distribution Functions (CDF) vs. irradiance for Rayleigh model

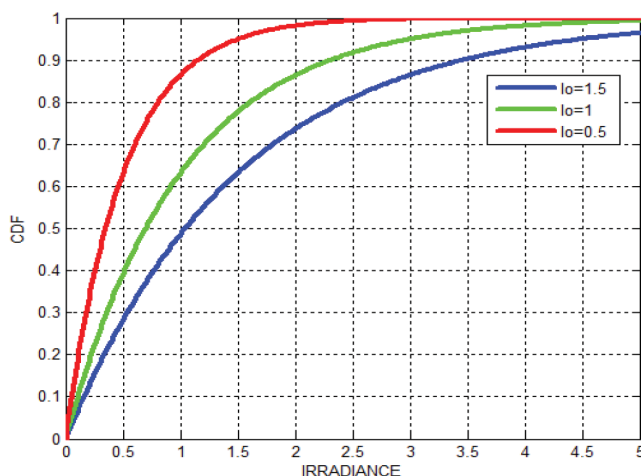


Figure 10. Cumulative Distribution Function (CDF) vs. irradiance for Negative-exponential model

The lognormal modelled channel experiences highest CDF of 0.80 at the receiver which essentially means it can be used to quantify weak turbulence conditions. Table 3 shows the turbulence condition for all channel models and the key factors on which the performance of channel models depends.

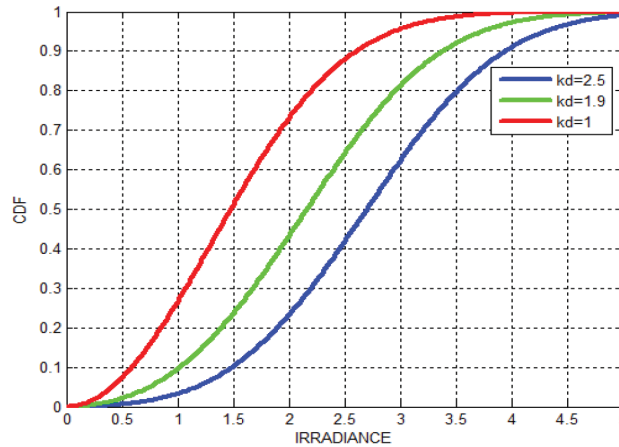


Figure 11. Cumulative Distribution Function (CDF) vs. irradiance for Rician model

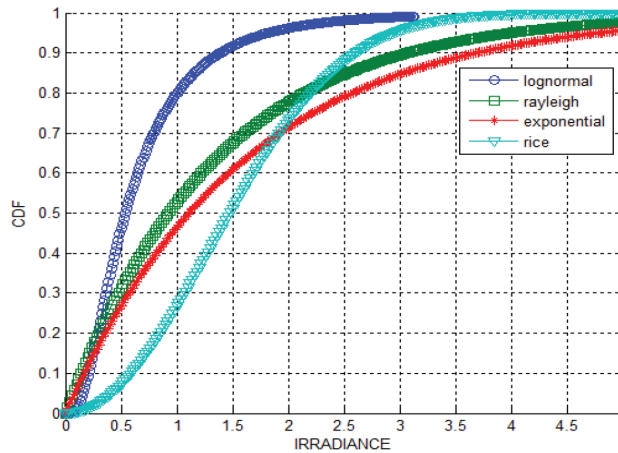


Figure 12. Plot of cumulative distribution functions vs. irradiance of different channel models

Table 2
CDF based comparison of different models

Channel model	Key factor	CDF (at intensity=1)
Lognormal	Variance (σ^2)	0.80
Rayleigh	Variance (σ^2)	0.53
Negative exponential	Average irradiance (I_0)	0.47
Rician	k_d	0.28

CONCLUSION

This paper analysed the performance of different channel models used in free space optical communication. The scintillation index was unity while PDF associated with irradiance and atmospheric turbulence was used as a benchmark to determine performance for various categories of link modelling. It can be concluded that Lognormal, Rayleigh and Rician channel models are suitable to model channel conditions for weak or strong turbulence conditions only.

Table 3

Turbulence condition of different channel models on basis of PDF and CDF

Channel model	Key factor	Turbulence condition
Lognormal	σ^2	Weak
Rayleigh	σ^2	Strong
Negative exponential	I_0	Very strong
Rician	k_d	Strong
Gamma-gamma	α, β	Weak to strong

However, the negative exponential and Gamma-Gamma model are valid for mapping weak to strong turbulence regime with optimum values for the former in the negative region. The paper thus concludes that the Gamma-Gamma model is an appropriate choice as it takes into account effect both large and small turbulence eddies. Effective link modelling allows reducing drastically, if not rule out, the effect of atmospheric turbulences on FSO links.

REFERENCES

- Al-Habash, M. A., Andrews, L. C., & Phillips, R. L. (2001). Mathematical model for the irradiance probability density function of a laser beam propagating through turbulent media. *Optical Engineering*, 40(8), 1554-1562.
- Andrews, L. C., & Phillips, R. L. (2005). *Laser beam propagation through random media* (Vol. 1). Bellingham, WA: SPIE press.
- Anees, S., & Bhatnagar, M. R. (2015). Performance evaluation of decode-and-forward dual-hop asymmetric radio frequency-free space optical communication system. *IET Optoelectronics*, 9(5), 232-240
- Bhatnagar, M. R., & Ghassemlooy, Z. (2015, June). Performance evaluation of FSO MIMO links in Gamma-Gamma fading with pointing errors. In *International Conference on Communications (ICC), 2015 IEEE* (pp. 5084-5090). IEEE.
- Bhatnagar, M. R., & Ghassemlooy, Z. (2016). Performance analysis of Gamma-Gamma fading FSO MIMO links with pointing errors. *Journal of Lightwave Technology*, 34(9), 2158-2169.

- Chatzidiamentis, N. D., Sandalidis, H. G., Karagiannidis, G. K., Kotsopoulos, S. A., & Matthaiou, M. (2010, April). New results on turbulence modeling for free-space optical systems. In *17th International Conference on Telecommunications (ICT), 2010 IEEE* (pp. 487-492). IEEE.
- Ghassemlooy, Z., Popoola, W. O., & Leitgeb, E. (2007, July). Free-space optical communication using subcarrier modulation in gamma-gamma atmospheric turbulence. In *9th International Conference on Transparent Optical Networks, ICTON'07, 2007* (Vol. 3, pp. 156-160). IEEE.
- Hogan, H. (2013). Data Demands: Drive Free-Space Optics. *Photonics Spectra*, 47(2), 38-41.
- Kashani, M., Uysal, M., & Kavehrad, M. (2013). A novel statistical model of turbulence-induced fading for free space optical systems. *15th International Conference on Transparent Optical Networks (ICTON)* (pp. 1-5). IEEE.
- Kedar, D., & Arnon, S. (2004). Urban optical wireless communication networks: the main challenges and possible solutions. *IEEE Communications Magazine*, 42(5), S2-S7.
- Khalighi, M. A., & Uysal, M. (2014). Survey on free space optical communication: A communication theory perspective. *IEEE Communications Surveys and Tutorials*, 16(4), 2231-2258.
- Leitgeb, E., Awan, M. S., Brandl, P., Plank, T., Capsoni, C., Nebuloni, R., ... & Loschnigg, M. (2009, June). Current optical technologies for wireless access. In *10th International Conference on Telecommunications, ConTEL 2009* (pp. 7-17). IEEE.
- Navas, A. J., Balsells, J. M. G., Paris, J. F., & Notario, A. P. (2011). A unifying statistical model for atmospheric optical scintillation. In J. Awrejcewicz (Ed.), *Numerical Simulations of Physical and Engineering Processes* (pp. 181-206). Rijeka, Croatia: InTech.
- Nistazakis, H. E., Stassinakis, A. N., Muhammad, S. S., & Tombras, G. S. (2014). BER estimation for multi-hop RoFSO QAM or PSK OFDM communication systems over gamma gamma or exponentially modeled turbulence channels. *Optics and Laser Technology*, 64, 106-112.
- Papoulis, A., & Pillai, S. U. (2002). *Probability, random variables, and stochastic processes*. United Kingdom, UK: McGraw-Hill Education.
- Popoola, W. O., & Ghassemlooy, Z. (2009). BPSK subcarrier intensity modulated free-space optical communications in atmospheric turbulence. *Journal of Lightwave Technology*, 27(8), 967 -973.
- Popoola, W. O., Ghassemlooy, Z., Allen, J. I. H., Leitgeb, E., & Gao, S. (2008). Free-space optical communication employing subcarrier modulation and spatial diversity in atmospheric turbulence channel. *IET optoelectronics*, 2(1), 16-23.
- Tatarskii, V. I., & Zavorotnyi, V. U. (1985). Wave propagation in random media with fluctuating turbulent parameters. *JOSA A*, 2(12), 2069-2076.
- Willebrand, H. A., & Ghuman, B. S. (2001). Fiber optics without fiber. *IEEE spectrum*, 38(8), 40-45.
- Yang, F., & Cheng, J. (2016, February). Recent results on correlated lognormal atmospheric turbulence channels. In *International Conference on Computing, Networking and Communications (ICNC), 2016* (pp. 1-6). IEEE.
- Zhu, X., & Kahn, J. M. (2002). Free-space optical communication through atmospheric turbulence channels. *IEEE Transactions on communications*, 50(8), 1293-1300.



Dealing with Interdependency among NFR using ISM

Kaur, H.* and Sharma, A.

*Institute of Engineering and Technology, Department of Computer Engineering & Applications,
GLA University, Mathura, Uttar Pradesh 281406, India*

ABSTRACT

Non-Functional Requirements (NFRs) determine the utility and effectiveness of a framework. Due to the subjective nature and complexity of NFRs, it is quite unrealistic to concentrate on each NFR. Consequently, agreement between groups of cross-utilitarian and cross functional decision makers are important. This paper models NFRs in the form of Soft Goal Interdependency Digraph (SID). The SID is based on Interpretive Structural Modelling (ISM) method which in turn utilises MICMAC (Matrices Impacts Croise's Multiplication Appliquée a UN Classement) and AHP (Analytic Hierarchy Process) approaches for identification of critical NFRs. These objectives allow the analysts and developers to accept the best possible trade off choices among NFRs. This is discussed using a general case of cafeteria ordering framework. The proposed model contrasts well with other positioning methodologies.

Keywords: Analytic Hierarchy Process, Interpretive Structural Modelling, Matrices Impacts Croise's Multiplication Appliquée a UN Classement, Non-Functional requirements, sensitivity analysis

INTRODUCTION

Non-functional requirements (NFRs) assume a pivotal role in determining the most critical requirements when presented with an array of choices. The expression "Non-functional requirements" are utilised to allude to the greater part of the data framework other than the sought and desired functional prerequisites. However, surprisingly, NFRs have are often incorporated very late into the process of framework design (Chung et al., 2009). To add to system woes, NFRs are hidden inside computer software program specifications as remarks. Over the years, numerous strategies and procedures have been proposed to enhance their elicitation, documentation, and approval. Yet, at the same time, it is impractical to allocate same amount time on each NFR during program development and improvement stages as they are complex. Thus, there is a need to settle for best possible choice among the NFRs.

Article history:

Received: 29 December 2016

Accepted: 21 April 2017

E-mail addresses:

harsimran.31@gmail.com (Kaur, H.),

ashish.sharma@gla.ac.in (Sharma, A.)

*Corresponding Author

The NFRs are unpredictable (Chung et al., 2009) and thus this paper considers the issues related to identifying critical NFRs and determining degree of mutual reliance between them to help software analysts in managing such NFRs for their programs.

This paper also examines the integration between ISM and AHP, in order to show interdependencies between NFRs. It does this by generating Softgoal Interdependency Digraph (SID) and MICMAC analysis to showcase critical NFRs.

The validity and favourable circumstances of the proposed methodology are discussed using model. In order to examine the credibility of this proposed model, it was initially analysed individually before it is compared with others built up and noticeable methodologies proposed in the past.

There are many definitions of NFR in the literature. Chung et al. (2009) questions that “in the presence of so many different definitions on NFR how should we proceed”. In their paper, they define it as: $f: I \rightarrow O$ (e.g., sum: $\text{int} \times \text{int} \rightarrow \text{int}$), just about anything that addresses characteristics of f , I , O or relationships between I and O will be considered NFRs. As per IEEE (2010) “non-functional requirement (NFR) – in software system engineering, a software requirement that describes not what the software will do, but how the software will do it, for example, software performance requirements, software external interface requirements, design constraints, and software quality attributes”.

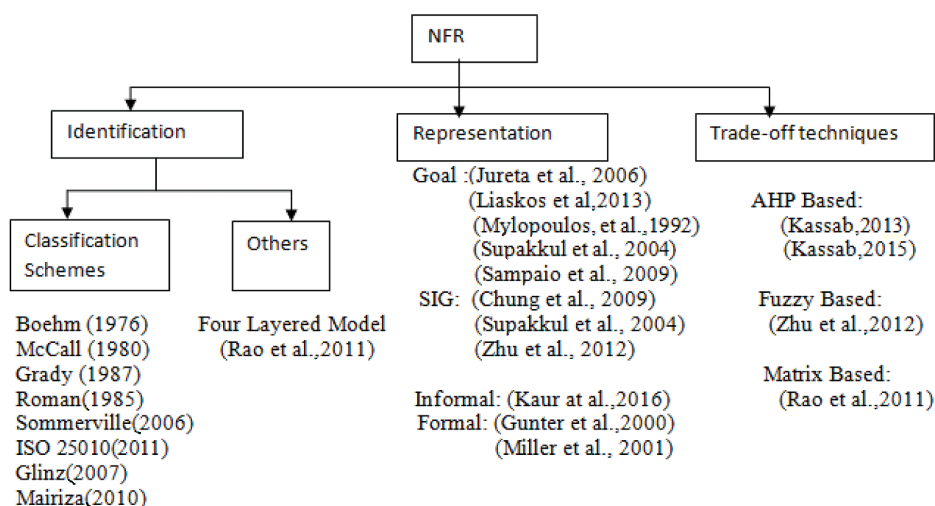


Figure 1. Different NFR schemes from literature

Boehm (1976), McCall (1980), Roman (1985), Grady (1987), Sommerville (2006), Glinz (2007), Mairiza (2010), Chung (2009) addressed ways to identify and classify NFRs. Boehm proposed both quality and quantitative approach to software quality while McCall attempted to bridge the gap between users and developers by focusing on a number of software quality factor that reflect both the users’ views and the developers’ priorities. Roman focused on consumer-oriented attributes such as performance, design and adaptation as well as on technically-oriented attributes such as functional scope Grady proposed FURPS which has

two categories of requirement: Functional (F) and Non-Functional (URPS). At present, the ISO 25010 (2011) model is considered as the standard model for identification of NFRs. Glinz proposed a rethink of the notion of NFRs as there is no fact which explains the meaning of NFR. Some prominent schemes for identification, representation and trade-off for NFR are shown in Figure 1. Not one of the models was able to solve unpredictability associated with managing assorted qualities in number of NFRs and their entomb reliance on each other that an analyst faces during initial phase of software development.

The NFR are represented separately from functional requirements, usually in the form of simple sentences. It is contained under section 3 of IEEE recommended practice for software requirement specifications. Many other initial approaches such as NFR Framework (Juteta et al., 2006) and UML which deals with NFRs informally have been discussed in literature. To address the changing needs of many different classes of users related to NFR a novel approach is discussed by Kaur et al. (2016). It is difficult to determine the degree of mutual reliance between them when there are large number of NFRs with the above representation techniques.

There have been only a few studies on NFR ranking in software systems to date but those are very specific to the particular software application. Some of the ranking techniques for NFR are discussed here. Karlsson, Wohlin, and Regnell (1998) concluded AHP technique to be the most promising method to prioritize requirements. Liaskos, Jalman, and Aranda (2013) used AHP in their model by mapping every OR-decomposition in the goal model into a separate decision problem. They treated all NFRs as mandatory which is not possible in praxis. Elahi and Yu (2011) describe the Requirements Hierarchy Approach (RHA), a quantifiable method to measure and manipulate the effects that NFRs have on a system without focusing on NFR interdependencies. Firesmith (2004) discussed various prioritisation techniques in his paper but did not prioritise it mathematically. Kassab (2013, 2015) provides a set of specialised guidelines to transform the hierarchy that visualise the NFR framework into an AHP decision hierarchy. It focused on pragmatic solution to rank the alternative operationalisations that satisfy NFRs while considering their interdependencies. But there is need to check for inconsistency of the priorities calculated by AHP. Zhu et al. (2012) proposes a fuzzy qualitative and quantitative soft goal interdependency graphs (FQQSIG) model for non-functional requirement correlations analysis in Trustworthy Software and presents a tool based on Matlab. It used the Relation Matrix algorithm that to cope with the negative impact along with the positive impact among NFRs. In this proposed model, ISM is integrated with AHP to generate soft goal digraph for identified NFR.

This paper proposes a model which generates soft goal interdependency digraph. The model integrates qualitative and quantitative methods to describe, analyse, calculate, and evaluate the critical NFRs for a particular system. Finally, it gives the choice result for decision-makers to select critical NFRs as discussed in next section.

METHODS

The proposed methodology is one that coordinates ISM (Digalwar, 2013) and AHP (Saaty, 2008) procedures to manage mutual correlation among critical NFR; it does this by producing Soft-Goal Inter-Dependency Digraph. The proposed model involves a five-stage method as shown in Figure 2.

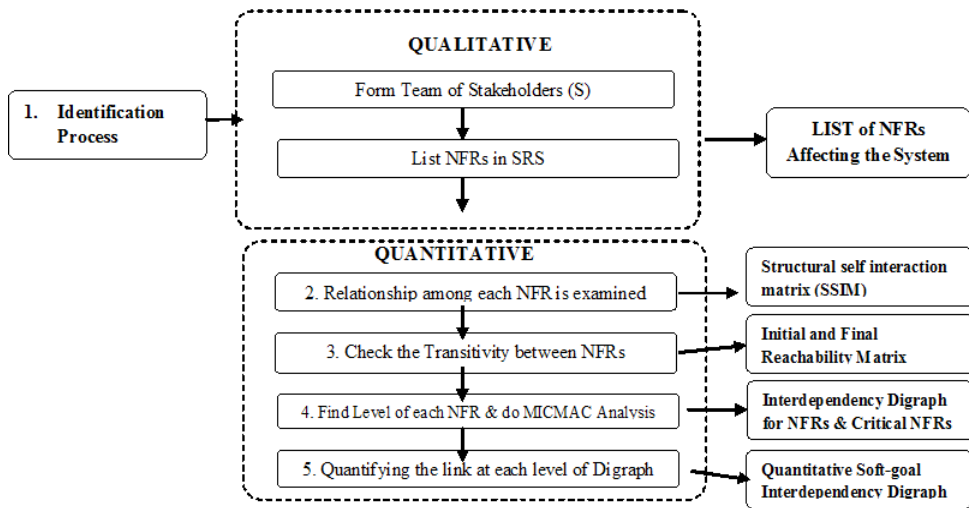


Figure 2. Model process (Five-Step Analysis)

Identification Process

It is important to discuss the NFR choice procedure. There is a group of cross-functional partners that assume diverse roles in programming advancement process for managing NFRs. In this paper, the partner (specialists) constitutes two academicians in the area of program building and program design respectively from a software company. Critical NFRs recognised using Software Requirement Specification (SRS) are then investigated by group of specialists to determine the relationship among NFRs.

Relationship among each NFR

For a strategic analysis of NFRs, it is important to identify and recognise the relationship between each NFR. This leads to accomplishment of Self-Connection Grid (SSIM). The specialists (as discussed in section 3.1) are then consulted to indicate the relevant correlations among the NFRs. Relationship between these N elements can be then represented in a matrix known as Structural Self-Interaction Matrix (SSIM), which is developed on the basis of pairwise comparison of variables which is in turn based on a set of rules specified below:

$$A = (a_{ij})_{N \times N} \cdot a_{ij} = 1$$

$$NFR = \{n_i | (i=1, 2, \dots, n)\}$$

V – NFR i will depend on NFR j .

A – NFR j depends on NFR i .

X – NFR i and j depend on each other.

O – NFR i and j are unrelated NFR's

(1)

Reachability matrix can be then framed from the SSIM and which is later analysed for transitivity.

Check Transitivity between NFRs

The fundamental assumption made in ISM is about transitivity of contextual relationships of NFRs and the transitivity closure of A is defined as

$$\hat{A} = A \oplus A^2 \oplus A^3 \oplus \dots \oplus A^P \tag{2}$$

while reachability matrix is defined as

$$R = \hat{A} \oplus I = (A + I)^P \tag{3}$$

To evaluate the transitivity between NFRs, SSIM was transformed into a binary matrix, also better known as Initial Reachability Matrix by simply replacing V, A, X and O by 1 and 0 as per the rules (Digalwar, 2013).

MICMAC ANALYSIS

Once the final Reachability Matrix has been designed, then segmentations are done keeping in mind the goal of discovering the chain of command for each of the NFR. The Reachability and predecessor set for each NFR was determined; it essentially incorporates NFR and other NFRs on which it might rely upon. The antecedent set comprises NFR itself and alternate NFRs which rely on it. At this point, the convergence of these sets is inferred for all NFRs. The NFR for which the reachability and intersection point sets are same, assume top-level NFR position in the ISM hierarchy. Once the top-level NFRs are recognised, they are then isolated from all other NFRs and, the same procedure is then repeated for the next level. With \hat{A} and R, Soft Goal Interdependency Diagram of components is plotted and MICMAC is inferred by summing up the samples of all possible conceivable outcomes of interactions in the row. The reliance of the NFR is determined by computing the sum of sections of potential outcomes of collaborations in the columns. The NFRs are arranged into four groups as shown in Table 1, also better known as Cross Impact Matrix Multiplication (MICMAC Analysis).

Table 1
Different classification of NFRs made during MICMAC Analysis [3]

Groups	Description
Autonomous NFR (Not Critical)	The NFRs are relatively disconnected from the system framework and thus, they can be ignored
Dependant NFRs (Critical NFR)	These NFRs are totally dependent on other NFRs
Linkage NFRs (Most Critical NFRs)	Any activity on these NFRs will affect alternate NFRs; furthermore, feedback may have an impact on them, which may intensify with any moves or measures
Independent NFRs (Less Critical)	These NFRs can also be put on hold in case of limited resources.

The driving force of the NFR can be inferred by summing the sections of potential outcomes of collaborations in rows, while the reliance power of the NFR is dictated by summing samples of conceivable outcomes of connections in the column of Reachability Matrix.

Quantifying the Link at each Level of Diagraph

AHPs are utilised to evaluate the priority of NFRs at every level using a digraph (Saaty, 2008). It is an effective tool for managing complex decision making, and may help the decision maker to set needs and settle for the best possible choice. Pair-wise correlation between NFRs is performed at every level chosen by ISM. A pair wise comparison matrix **A** is then created using AHP, where **A** represents a real matrix of dimension $m \times m$, where m represents total evaluation criterions weighed. Every element m_{jk} of matrix A , speaks about the significance of j th criterion in respect to k th one subjected to condition that if $a_{jk} < 1$, then the j th basis is less critical than the k th paradigm. On the off chance that two criteria have the same significance, then the passage a_{jk} is 1 i.e. $a_{jk}.a_{kj}=1$

$$A=[a_{jk}]_{n \times n} = \begin{bmatrix} 1 & a_{12} \dots & a_{1n} \\ \frac{1}{a_{12}} & 1 \dots & a_{2n} \\ \vdots & \vdots & \vdots \\ \frac{1}{a_{1n}} & \frac{1}{a_{2n}} \dots & 1 \end{bmatrix} \tag{4} [26]$$

Subject to $a_{kj}=1/a_{jk}$

$$\begin{bmatrix} \frac{w_1}{w_1} & \frac{w_1}{w_2} & \dots & \frac{w_1}{w_n} \\ \frac{w_2}{w_1} & \frac{w_2}{w_2} & \dots & \frac{w_2}{w_n} \\ \vdots & \vdots & \ddots & \vdots \\ \frac{w_n}{w_1} & \frac{w_n}{w_2} & \dots & \frac{w_n}{w_n} \end{bmatrix} * \begin{bmatrix} w_1 \\ \vdots \\ w_n \end{bmatrix} = n \begin{bmatrix} nw_1 \\ \vdots \\ nw_n \end{bmatrix} \tag{5}[26]$$

$$A \times W = n.W$$

Consistency ratio has not been calculated as the consistency and transitivity has already been sorted by ISM. The Complete approach is discussed in the later section using relevant examples.

RESULTS

Lucid variant of Cafeteria Ordering System (COS) (Weigers et al., 2013) that allows Process Impact workers to request supper from the company cafeteria which are ordered on-line and to

be delivered to specific requested destinations has been discussed in the earlier section. Here, NFRs have been taken (effectively recognised) from Software Requirement Specification (SRS), hence Identification Process of this Model was deliberately skipped. A rundown of NFRs distinguished in SRS for COS is seen in Table 2. The complete procedure for Cafeteria Ordering System is discussed below.

1. Two academicians were consulted simultaneously to draw a line of distinction between NFRs. In creating SSIM (Table 4), four symbols (V, A, X, 0) were used to represent the degree of coherence between two NFRs, *i* and *j*.

Table 2
NFRs in COS

NFR	NFR requirements	Referred As
Performance	PE-1: The system shall oblige 400 clients during the peak time usage window from 8 am to 10am, with normal average session span of 8 minutes.	N1
	PE-2: All Web pages created by the system framework should be completely downloadable in close to 10 seconds over a 40KBps modem association.	N2
	PE-3: Reactions to questions should not take more than 7 seconds to stack onto the screen after the client presents the inquiry	N3
	PE-4: The framework should show affirmation messages to clients 4 seconds after the latter submit an initial information to the framework	N4
Security	SE-1: network transactions which may be either financial of personal identifiable, must be encrypted per BR-33 standard.	N5
	SE-2: Clients will be required to sign in to the specially designed Cafeteria Ordering System for all operations except menu options.	N6
	SE-3: Benefactors should log in into the restricted computer system access policy as per the BR-35 standard.	N7
	SE-4: The system must privilege cafeteria staff individuals only who are listed approved Menu Managers to make or alter menus, per BR-24 standard.	N8
	SE-5: Only the users who have been authorised for home access to the corporate Intranet may utilise the COS from non-organisation areas.	N9
	SE-6: The system should allow Patrons to view only their placed orders while the order history of any other patron should be restricted from any unauthorised persons.	N10
Robustness	On the off chance that the association between the client and the system terminates before a request is being either confirmed or scratched off, the Cafeteria Ordering System must empower the user to recoup an incomplete request.	N11
Availability	The Cafeteria Ordering System should be accessible to clients on the corporate Intranet and to dial-in clients with an up-time of 99.9% for local time between 5 am and 12 am and with compromised time of about 95% for duration between 12 midnight and 5am.	N12

Table 3
Structural Self-Interaction Matrix (SSIM)

	N12	N11	N10	N9	N8	N7	N6	N5	N4	N3	N2	N1
N1	X	V	0	X	0	V	V	V	V	V	V	X
N2	V	V	0	X	0	V	V	V	V	V	X	
N3	V	X	0	V	0	V	V	V	0	X		
N4	V	X	0	V	0	V	V	V	X			
N5	V	X	0	0	0	X	0	X				
N6	V	0	0	A	0	X	X					
N7	V	A	X	X	X	X						
N8	0	0	0	0	X							
N9	V	A	A	X								
N10	V	0	X									
N11	V	X										
N12	X											

Table 4
Initial Reachability Matrix

	N1	N2	N3	N4	N5	N6	N7	N8	N9	N10	N11	N12
N1	1	1	1	1	1	1	1	0	1	0	1	1
N2	0	1	1	1	1	1	1	0	1	0	1	1
N3	0	0	1	1	1	1	1	0	1	0	1	1
N4	0	0	1	1	1	1	1	0	1	0	1	1
N5	0	0	0	0	1	0	0	0	0	0	1	1
N6	0	0	0	0	0	1	1	0	0	0	0	1
N7	0	0	0	0	0	0	1	1	0	0	0	0
N8	0	0	0	0	0	0	1	1	0	0	0	0
N9	1	1	0	0	0	1	1	0	1	0	0	1
N10	0	0	0	0	0	0	1	0	1	0	0	1
N11	0	0	1	1	1	0	1	0	1	0	1	1
N12	1	0	0	0	0	0	0	0	0	0	0	1

Table 5
Final Reachability Matrix

	N1	N2	N3	N4	N5	N6	N7	N8	N9	N10	N11	N12	Driver Power
N1	1	1	1	1	1	1	1	0	1	0	1	1	10
N2	0	1	1	1	1	1	1	0	1	0	1	1	9
N3	0	0	1	1	1	1	1	0	1	0	1	1	8
N4	0	0	1	1	1	1	1	0	1	0	1	1	8
N5	0	0	0	0	1	0	(1)	0	0	0	1	1	4
N6	0	0	0	0	0	1	1	0	(1)	0	0	1	4
N7	0	0	0	0	0	0	1	1	0	0	0	0	5
N8	0	0	0	0	0	0	1	1	0	0	0	0	2
N9	1	1	0	0	0	1	1	0	1	0	0	1	6
N10	0	0	0	0	0	0	1	0	1	0	0	1	5
N11	0	0	1	1	1	0	1	0	1	0	1	1	8
N12	1	0	0	0	0	0	0	0	0	0	0	1	2
Dependence Power	3	3	5	5	6	9	11	1	9	2	6	11	

1. The SSIM has been changed over into a binary grid, named Initial Reachability Matrix as shown in Table 4, by substituting V, A, X, O with either 1 or 0. By applying the tenets discussed in section 3, an underlying reachability framework for the NFRs to execute COS is acquired. The last reachability matrix is then acquired by including transitivity as discussed before (Table 5 shows the final outcomes of above mentioned operations).
2. The driving force and the reliance power of every hindrance have likewise been compiled in the Table 6 while Soft goal interdependency digraph generated on the basis of Table 7 is shown in Figure 5.

Table 6
Level of Objective Criteria

NFRs	Reachability set	Antecedent Set	Intersection Set	Level
N1	1,2,3,4,5,6,7,9,11,12	1,9,12	1,9,12	1
N2	2,3,4,5,6,7,9,11,12	1,2,9,12	2,9	2
N3	3,4,5,6,7,9,11,12	1,2,3,4,11	3,4,11	4
N4	3,4,5,6,7,9,11,12	1,2,3,4,11	3,4,11	4
N5	5,7,11,12	1,2,3,4,5,11	5,11	5
N6	6,7,9,12	1,2,3,4,6,7,9	6,7,9	5
N7	6,7,9,12	1,2,3,4,5,6,7,8,9,10,11	6,7,9	6
N8	7,8	8	8	1
N9	1,2,6,7,9,12	1,2,3,4,6,7,9,10	1,2,6,7,9	4
N10	7,9,10,12	7,10	7	3
N11	3,4,5,7,9,11,12	1,2,3,4,5,11	3,4,5,11	3
N12	1,12	1,2,3,4,5,6,7,9,10,11,12	1,12	7

The links between the NFRs are drawn as per the relationships shown in the reachability matrix. A simpler version of the initial digraph is obtained by eliminating the transitive relationships step-by-step by examining their interpretation from the knowledge base as shown in Figure 3.

Further NFRs are classified as autonomous, dependent, linkage and independent NFRs which are in turn based on estimations of dependence and driver power as shown in Figure 4. The present study showed robustness, Availability and Security were the critical NFRs which cannot be overlooked regardless of situation; they can easily compromise with Performance parameter which is a less critical NFR. The disentangled digraph after filtering out Autonomous NFRs is shown in Figure 5 while Figure 6 represents the remaining ones after removal of independent NFRs.

Dealing Interdependency among NFR using ISM

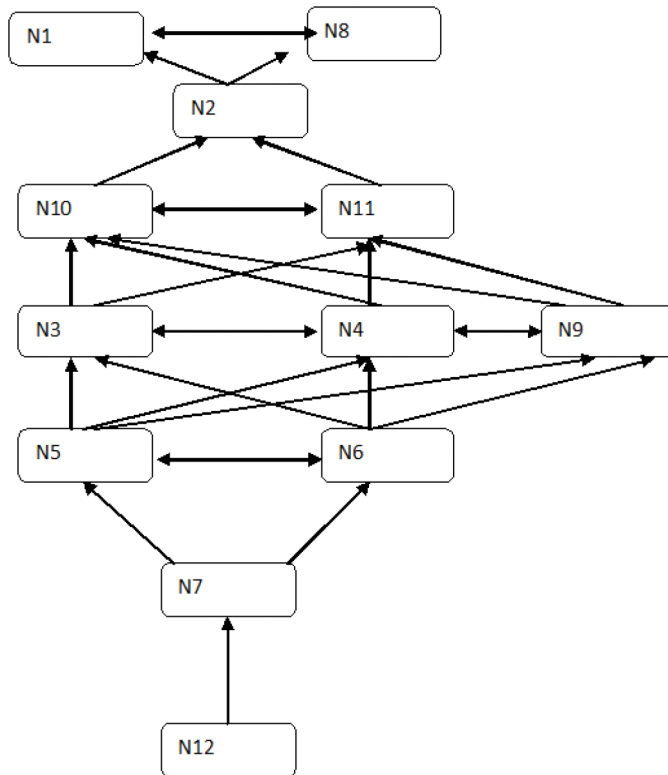


Figure 3. Softgoal interdependency digraph for NFRs

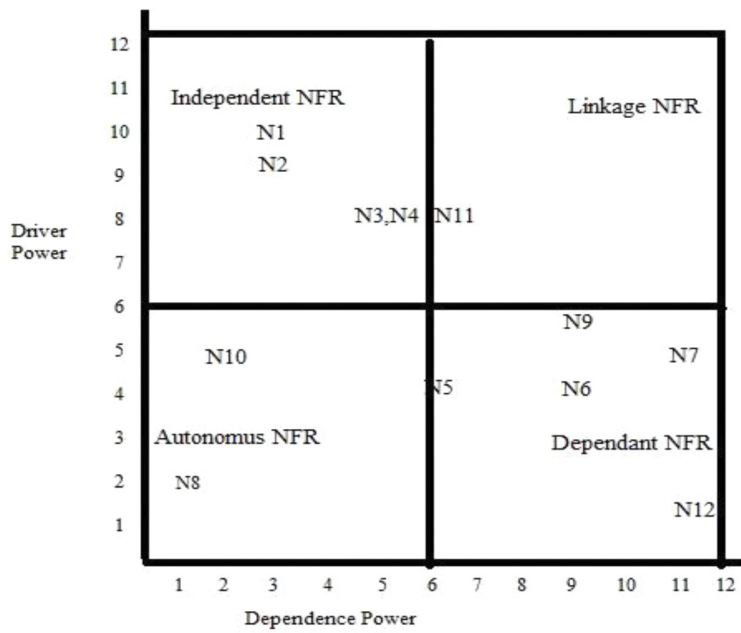


Figure 4. NFR classification

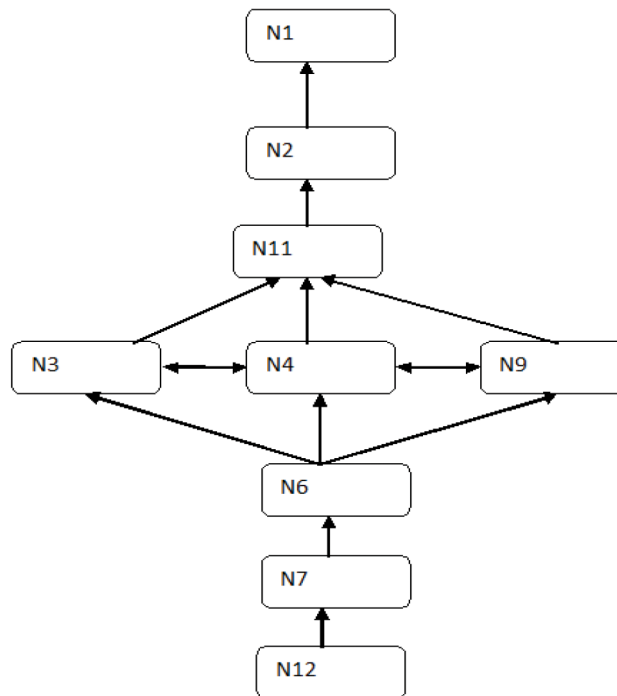


Figure 5. Simplified softgoal interdependency digraph on removing autonomous NFR

Final Simplified graph shows that there is only one NFR at each level as seen in Fig 8, but in cases where there are more than one NFR at each level then AHP may be applied to prioritise NFR at each level of hierarchy.

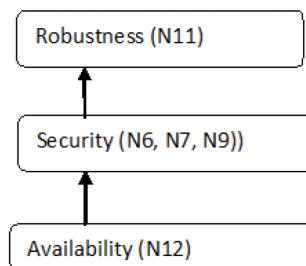


Figure 6. Normalized softgoal interdependency digraph on removing independent

Critical Findings of Application of Proposed Approach on COS

1. Approach helps the members in creating and elucidating the Non-Functional Requirements that are to be organized.
2. Ranks of the criteria, in view of their driving powers showcase that the strength and accessibility are the key functionalities of this model while security and performance are other complimentary criteria.

3. Autonomous NFRs: These NFRs are relatively disengaged from the system framework and can be overlooked. N5, N8 and N10 are self-sufficient NFRs in this illustration.
4. Dependent NFRs: These NFRs are having solid reliance and frail driver, thus they can't be overlooked. N6, N7, N9 and N12 were observed to be the Dependant NFR.
5. Linkage NFRs: These NFRs are having solid driving and reliance power, so they should be considered in every phase of programming development and improvement. In this example N11 characterizes as Linkage NFR.
6. Independent NFRs: These NFRs condition the various NFRs, while being unaffected by them consequently. These NFRs can likewise be put on hold in the event of constrained resources. N1, N2, N3, N4 were observed to be the autonomous NFRs for this particular case study.
7. Also from the map, it was observed that Robustness (N11) was in-fact the top-notch basis while Security traits can be considered as secondary level parameter followed by accessibility and then later with miscellaneous criterions occupying lowers levels on priority hierarchy.

DISCUSSION

In contrasting the present assessment model with the ones proposed by Karlsson, Wohlin, and Regnell (1998), this study found AHP system to be the most encouraging strategy to exchange off necessities. In the current study, NFRs alongside their interdependencies were handled by applying coordinated methodology of ISM and AHP. Liaskos (2013) connected AHP to the goal model by mapping each OR-decomposition in the objective model into a distinct decision making problem. They regard all non-useful necessities as obligatory which is not essentially conceivable; thus, the present study used MICMAC to discover basic NFRs so they are not disregarded even if there occurs a case of restricted assets. Zhu et al. (2012) proposes a fuzzy quantitative and quantitative soft goal interdependency charts (FQQSIG) model with an objective of determining NFRs' correlations using Trustworthy Software and present them using Matlab based tool. The Relation Matrix calculation has been extensively used to determine its negative and the positive effects on NFRs. This was further simplified by adopting MICMAC investigation and analysis methodology by highlighting the reliance and driving force between NFRs.

In this paper, PriEst (Siraj, 2013), was used as an intuitive choice bolster tool to estimate needs from pairwise correlation judgments to contrast with existing exchange off methodologies available in literature. This tool permits clients to choose distinctive prioritisation strategies to gauge inclinations from the same arrangement of judgments. Likewise, it also offers additional techniques to enhance the decision maker's understanding and permit strategy assessment simultaneously. Table 6 shows an analysis of positioning Techniques AHP, Fuzzy, Traceability Matrix(TM) and Proposed Approach based on six parameters.

In the first place the parameters are positioned with the assistance of PriEsT tool. The weights for parameters ascertained by utilising eigenvector technique (EV) and geometric mean (GM) are listed in Table 7. Managing Interdependencies (wp3) and Modelling Structure to manage interdependencies (wp6) were found to be the most essential measure for looking at four different alternative methods for Trade-off for NFR as shown in Figure 7.

Table 6
Analysis of various ranking methods for NFRs based on multiple parameters

	AHP	Fuzzy	Traceability Matrix	Proposed Approach
Concept	Expressive	Expressive, logic based, formal	Simple Goal and Rule Based	visible, well-defined models
Individual Concerns of Stakeholders	Negligible	Negligible	Less	Negligible
Subjectivity	Very high	Very high	Less	Moderate
Dealing Interdependencies	Yes	Limited	No	Yes
Find Criticality of NFRs	Negligible	Negligible	Find critical NFRs	Find further categorisation of critical NFRs
Quantitative	Yes	Yes	No	Yes
Modelling Structure to deal with Interdependencies	Hierarchical tree	Does not deal	Does not deal	Interdependency Diagraph

The proposed Technique is considered the most preferred on the basis of parameters (P1-P6) with weight of 46.7% followed by fuzzy with weight around 25.8% as shown in Table 8 and Table 9. It is represented graphically in Figure 8.

Table 7
Estimated values for the parameter weights

	Individual Concerns of Stakeholders w_{P1} (%)	Subjectivity Required w_{P2} (%)	Dealing Interdependencies w_{P3} (%)	Finding Criticality of NFRs w_{P4} (%)	Quantitative w_{P5} (%)	Modelling Structure to deal with Interdependencies w_{P6} (%)
EV	5.3	4.5	31.3	5.3	12.7	40.8
GM	5.3	4.5	31.3	5.3	12.7	40.8

Dealing Interdependency among NFR using ISM

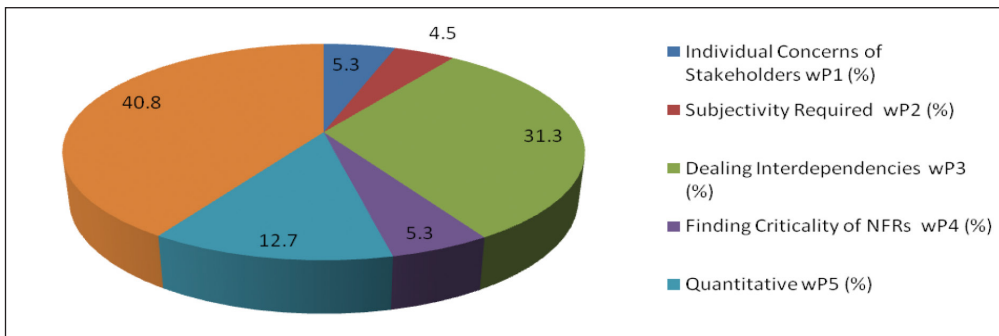


Figure 7. Chart on the basis of weights calculated for different parameters

Table 8

Estimated weights for the available ranking techniques for NFR

		AHP	Fuzzy	Traceability Matrix	Proposed Technique
P1	GM	0.25	0.25	0.25	0.25
	EV				
P2	GM	0.25	0.25	0.25	0.25
	EV				
P3	GM	.117	.223	.082	.578
	EV	.116	.223	.082	.578
P4	GM	.116	.122	.245	.517
	EV	.116	.122	.244	.518
P5	GM	.321	.321	.036	.321
	EV				
P6	GM	.17	.285	.073	.472
	EV	.17	.284	.073	.473
Overall		.177	.258	.098	.467

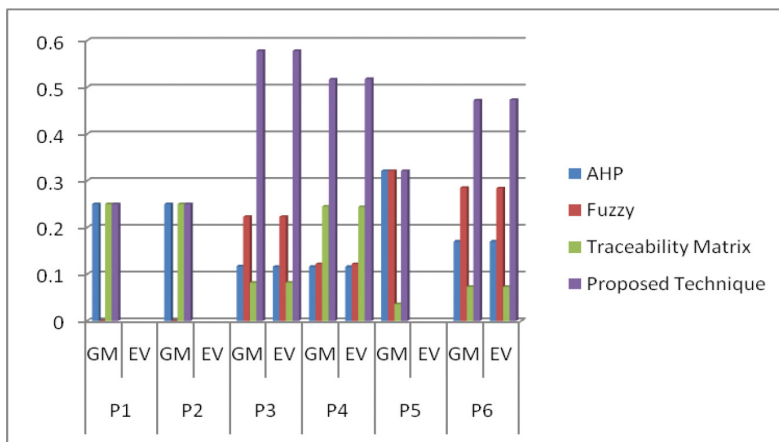


Figure 8. Comparison graph for different trade-off analysis technique

Table 9

Weights suggested by PriEsT for selecting best Trade-off technique

Ranking Techniques	AHP	Fuzzy	Traceability	Proposed
%	17.7%	25.8%	9.8%	46.7

The methodology for finding a suitable procedure is subjective as there can be irregularities in the analysis of the specialists. Such irregularities can be effectively tackled by applying multi-rule technique PrInt on PriEsT tool. Sensitivity investigation is accomplished by taking diverse arrangement of parameters at given time, as shown in Figure 9. The Uniform Distribution view in Figure 9(a) demonstrates Fuzzy and Proposed approach at the same level when viewed on the basis of parameters P1, P2, P3 and P4. Figure 9(b) indicates AHP and Proposed positioning equivalent if contrasted in terms of P3, P4, P5 and P6. Parameter P3 and P6 were weighted as vital parameters as seen in Table 9. At the same point when sensitivity investigation is done on the premise of these parameters, the proposed methodology is considered as the most favoured positioning strategy as shown in Figure 9(c). From the above, it can be concluded that proposed approach supersedes other approaches discussed in the literature on array of parameters and which can be utilised to discover critical NFRs and model their interdependency on each other.

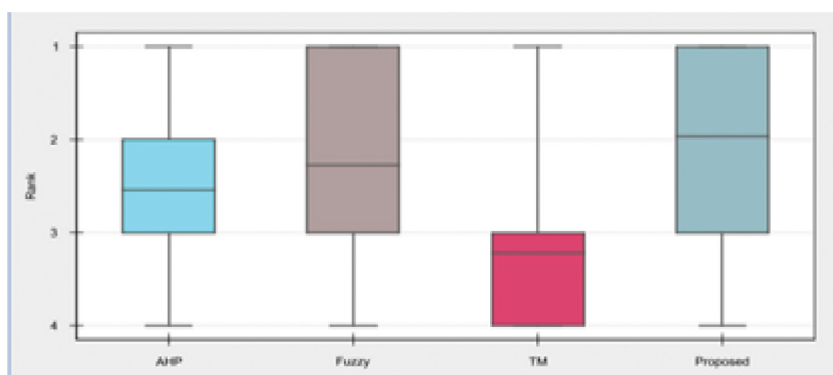


Figure 9(a). Comparison on the basis of parameters P1, P2, P3 and P4

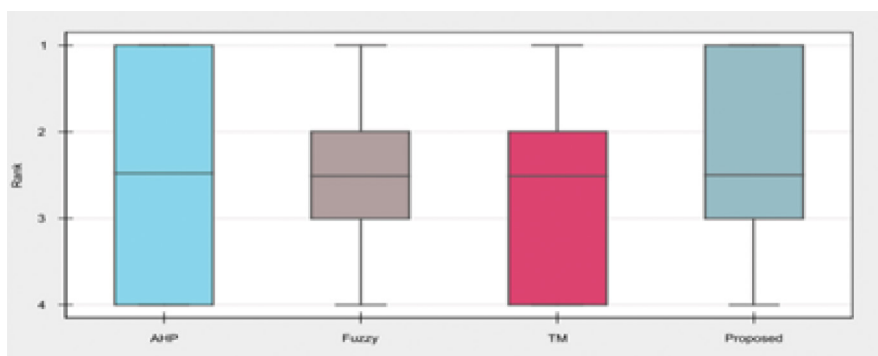


Figure 9(b). Comparison on the basis of parameters P3, P4, P5 and P6

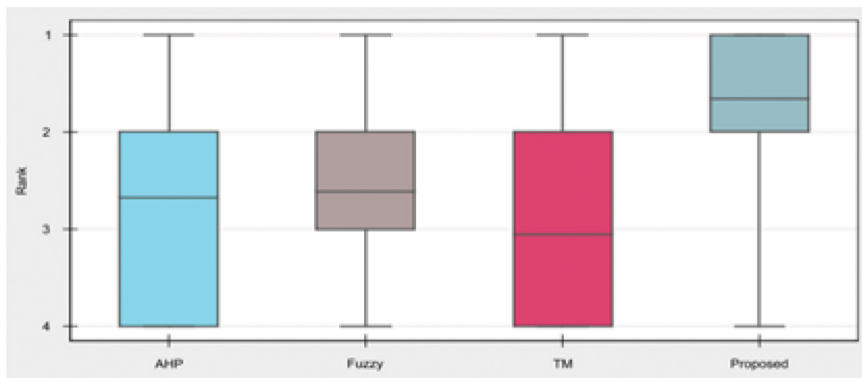


Figure 9(c). Comparison on the basis of P3 and P6

CONCLUSION

Non-Functional Requirements (NFRs) determine the success or failure of a software framework product. As NFR concerns are ordinarily managed at configuration and usage level this methodology often results in the disappointment in the frameworks. Hence, it is good to identify and model suitable NFRs, instead of incorporating them straightaway. A good way is to build up a model that distinguishes critical NFRs from the rest and then look out for potential clashes among them before the prerequisite investigation and analysis. Thus, the most critical non-functional requirements (NFRs) are addressed immediately. The paper proposed a five-step trade off analysis method by using ISM which identified the critical NFRs; dealt with their interdependency by SID; and NFRs classification. The findings of this paper will be greatly beneficial to software development organisations by improving associations involving desired Non-Functional Requirements that will add to programming quality in a financially savvy way.

REFERENCES

- Boehm, B. W., Brown, J. R., & Lipow, M. (October). Quantitative evaluation of software quality. In *Proceedings of the 2nd international conference on Software engineering* (pp. 592-605). IEEE Computer Society Press.
- Chung, L., & do Prado Leite, J. (2009). On non-functional requirements in software engineering. *Conceptual modeling: Foundations and applications*, 5600, 363-379.
- Chung, L., & Supakkul, S. (2004). Integrating FRs and NFRs: A Use Case and Goal Driven Approach. In *2nd International Conference on Software Engineering (SERA'04)* (pp. 30-37).
- Digalwar, A. K., & Giridhar, G. (2015). Interpretive structural modeling approach for development of electric vehicle market in India. *Procedia CIRP*, 26, 40-45.
- Elahi, G., & Eric, S. K. (2011). A semi-automated tool for requirements trade-off analysis. In *CAiSE Forum* (pp. 9-16).
- Fan, Z. P., & Liu, Y. (2010). A method for group decision-making based on multi-granularity uncertain linguistic information. *Expert systems with Applications*, 37(5), 4000-4008.

- Firesmith, D. (2004). Prioritizing Requirements. *Journal of Object Technology*, 3(8), 35-48.
- Glinz, M. (2007, October). On non-functional requirements. In *15th IEEE International Conference on Requirements Engineering, RE'07, 2007* (pp. 21-26). IEEE.
- Grady, R. B., & Caswell, D. L. (1987). *Software metrics: establishing a company-wide program*. Upper Saddle River, NJ: Prentice Hall.
- Gunter, C. A., Gunter, E. L., Jackson, M., & Zave, P. (2000). A reference model for requirements and specifications. *IEEE Software*, 17(3), 37-43.
- IEEE. (1993). *Recommended Practice for Software Requirements Specifications* (pp. 830-1993). IEEE Xplore Digital Library.
- ISO/IEC 25010:2011. (2011). *Software Engineering - Product Quality - Part 1: Quality Model*. International Organization for Standardization: Geneva, Switzerland.
- Jureta, I. J., Faulkner, S., & Schobbens, P. Y. (2006, November). A more expressive softgoal conceptualization for quality requirements analysis. In *International Conference on Conceptual Modeling* (pp. 281-295). Springer Berlin Heidelberg.
- Karlsson, J., Wohlin, C., & Regnell, B. (1998). An evaluation of methods for prioritizing software requirements. *Information and software technology*, 39(14-15), 939-947.
- Kassab, M. (2013). An integrated approach of AHP and NFRs framework. In *IEEE Seventh International Conference on Research Challenges in Information Science (RCIS), 2013* (pp. 1-8). IEEE.
- Kassab, M., & Kilicay-Ergin, N. (2015). Applying analytical hierarchy process to system quality requirements prioritization. *Innovations in Systems and Software Engineering*, 11(4), 303-312.
- Kaur, H., & Sharma, A. (2016, March). A measure for modelling non-functional requirements using extended use case. In *3rd International Conference on Computing for Sustainable Global Development (INDIACom), 2016* (pp. 1101-1105). IEEE.
- Liaskos, S., Jalman, R., & Aranda, J. (2012, September). On eliciting contribution measures in goal models. In *20th IEEE International Conference on Requirements Engineering (RE), 2012* (pp. 221-230). IEEE.
- Mairiza, D., Zowghi, D., & Nurmuliani, N. (2010, March). An investigation into the notion of non-functional requirements. In *Proceedings of the 2010 ACM Symposium on Applied Computing* (pp. 311-317). ACM.
- McCall, J. A., & Matsumoto, M. T. (1980). *Software Quality Measurement Manual, Vol. II. Rome Air Development Center*. RADC-TR-80-109-Vol-2.
- Miller, S. P., & Tribble, A. C. (2001, October). Extending the four-variable model to bridge the system-software gap. In *20th Conference Digital Avionics Systems, 2001, DASC*. (Vol. 1, pp. 4E5-1). IEEE.
- Moreira, A., Rashid, A., & Araujo, J. (2005, August). Multi-dimensional separation of concerns in requirements engineering. In *Proceedings of 13th IEEE International Conference on Requirements Engineering, 2005* (pp. 285-296). IEEE.
- Mylopoulos, J., Chung, L., & Nixon, B. (1992). Representing and using nonfunctional requirements: A process-oriented approach. *IEEE Transactions on software engineering*, 18(6), 483-497.
- Pressman, R. S. (2005). *Software engineering: a practitioner's approach*. New York, NY: Palgrave Macmillan.

- Rao, A. A., & Gopichand, M. (2011). Four layered approach to non-functional requirements analysis. *International Journal of Computer Science Issues*, 8(6), 371-379.
- Roman, G. C. (1985). A Taxonomy of Current Issues in Requirements Engineering. *IEEE computer*, 18(4), 14-23.
- Saaty, T. L. (2008). Relative measurement and its generalization in decision making why pairwise comparisons are central in mathematics for the measurement of intangible factors the analytic hierarchy/network process. *Revista de la Real Academia de Ciencias Exactas, Fisicas y Naturales. Serie A. Matematicas*, 102(2), 251-318.
- Siraj, S., Mikhailov, L., & Keane, J. A. (2015). PriEsT: an interactive decision support tool to estimate priorities from pairwise comparison judgments. *International Transactions in Operational Research*, 22(2), 217-235.
- Sommerville, I. (2006). *Software Engineering* (6th Ed.). Boston, MA: Addison-Wesley Longman Publishing Co., Inc.
- Wieggers, K., & Beatty, J. (2013). *Software requirements*. United States, USA: Pearson Education.
- Yen, J., & Tiao, W. A. (1997, January). A systematic tradeoff analysis for conflicting imprecise requirements. In *Proceedings of the Third IEEE International Symposium on Requirements Engineering, 1997* (pp. 87-96). IEEE.
- Zhu, M. X., Luo, X. X., Chen, X. H., & Wu, D. D. (2012). A non-functional requirements tradeoff model in trustworthy software. *Information Sciences*, 191, 61-75.





DNA and Bernoulli Random Number Generator Based Security Key Generation Algorithm

Sodhi, G. K. and Gaba, G. S.*

Discipline of Electronics and Communication Engineering, Lovely Professional University, Jalandhar 144411, India

ABSTRACT

Security is a major concern for the communication sector. The technique presented in this paper provides a novel security key generation mechanism. The proposed technique aims to generate a security key using the biological characteristics of the human body and the mathematically generated pseudo random sequences, thus producing different keys for different individuals. The final key is produced through the fusion of deoxyribonucleic acid (DNA) sequence of 1024 characters and Bernoulli Random Number Generator sequence of 256 bits. The performance of produced keys is evaluated using National Institute of Standards and Technology (NIST) tests and uniqueness is verified through avalanche test.

Keywords: Authentication, Bernoulli random number generator, biometrics, communication, confidentiality, DNA, integrity, security

INTRODUCTION

Security is critical in communication networks following the growth of the internet. Biometrics and integrity are two mechanisms which can improve security considerations. Biometrics ensures the identification and authentication of individuals by observing their personal unique features (Hao, Anderson, & Daugman, 2006). A practical system that integrates the iris biometrics into cryptographic applications can be found in Hao et al. 2006. A system that works using audio fingerprints has also been proposed by (Brown & Seberry, 2001; Chouakri, Bereksi, Ahmaidi, Fokapu, 2005; Covell & Baluja, 2007. Ktata, Ouni, Ellouze, 2009) studied the use of electrocardiogram (ECG) signals for enhanced security. Baluja, Covell, 2007 proposed to create personal signatures for authentication. Chen & Chandran, 2007) did a study on identification based on image processing is carried out by various researchers.

DNA has been used in many cryptographic algorithms to provide confidentiality (Chang, Kuo, Lo, & Wei, 2012). Bernoulli random

Article history:

Received: 29 December 2016

Accepted: 21 April 2017

E-mail addresses:

gurpreetsodhi123@gmail.com (Sodhi, G. K.),

er.gurjotgaba@gmail.com (Gaba, G. S.)

*Corresponding Author

number generator (BRNG) is used to make the technique more efficient and effective. The BRNG works on a secret seed value which ensures the generation of a different sequence for each seed value provided. The work reported in this paper is based on the idea of unique and random attributes of DNA and Bernoulli random number generator sequence.

The approach to generate a security key is implemented through numeric coding of the DNA sequence and the Bernoulli random sequence generated with the secret seed value. The output of key generating algorithm is tested using NIST tests of randomness as well as the strict avalanche criterion, the results of which are formulated in Table 4 and Table 5 respectively. Results point out the applicability of the proposed approach in areas where security is a concern.

The paper is organized as follows; characteristics of DNA and Bernoulli random number generator are described in Section 2. In Section 3, proposed algorithm for the 256-bit key generation is presented where the DNA data is taken from the MIT-BIH database, followed by result and analysis in Section 4. Finally, conclusions and future work are reported in Section 5.

Characteristics of DNA and BRNG

Progress in the field of biotechnology has made the DNA sequencing more effective. DNA sequencing for various organisms has been done with higher accuracy (Goldberger, Amaral, Glass, Hausdorff, Ivanov, Mark, Mietus, Moody, Peng & Stanley, 2000). Investigating the biological relationships of different species is known as analysing the DNA sequence.

The internet provides various databases of DNA sequences which can be easily accessed from the World Wide Web (Ensembl Genome Browser, NCBI databases). The DNA is composed of two polymeric strands made of monomers that include a nitrogenous base (A-adenine, C-cytosine, G-guanine, and T-thymine), deoxyribose sugar and a phosphate group. According to most of the techniques a DNA sequence is taken as symbolic data that is composed of four characters A, C, G and T corresponding to the four types of nucleic acids present. The DNA samples from a genome are sequenced using a Genome Sequencer, the signals created in the sequencing process are then analysed by the software to generate millions of sequenced bases.

The backbone of each strand located on the surface of the DNA is formed by the sugar and phosphate groups, while the inside of the structure is made of bases. There exists a weak hydrogen bond between the complementary bases of each strand (i.e. between A and T and between C and G) giving rise to pairing of bases, this pairing holds the two strands together. DNA sequences are unique for every individual, including the identical twins. The pattern formed by a DNA sequence specifically represents an individual and its characteristics. Hence, there is no possibility of duplicity in the DNA sequences.

To strengthen the bond of security, a random sequence is generated by Bernoulli random number generator. This sequence is generated with a seed value that is secretly given by the user. BRNG computes n^{th} Bernoulli number for a given integer n . Bernoulli numbers are a sequence B_n of rational numbers defined by the Taylor expansion.

Bernoulli numbers have a prominent place in mathematics, for instance they appear in Taylor expansion of tangent and in Euler-Maclaurin formula. Equation (1) represents the BRNG method for generation of random sequences.

$$\sum_{n=0}^{\infty} \frac{B_n}{n!} x^n = \frac{x}{e^x - 1} \quad (1)$$

The fusion of BRNG and DNA sequence forms a very strong 256-bit key which is less susceptible to attacks and thus provides higher level of security.

The Key Generation Mechanism

The proposed key is generated by combining DNA sequence of an individual and the random sequence obtained through BRNG using a secret seed value. The method of the generation of these keys is devised into three subsequent subsections and the hierarchical structure is portrayed in Figure 1.

DNA sequence formulation

- 1) Obtaining a DNA sequence of 1024 characters from the DNA database [9]:
The DNA sequence consists of 1024 characters forming base pairs 'agct'.
- 2) Obtaining the binary sequence from DNA characters:
Each character of the DNA sequence is represented by 8 bit ASCII code. Hence, resulting in a DNA sequence of length 8192 bits.
- 3) Framing a DNA sequence of 256 bits:
 - (i) The DNA sequence is then divided into equal halves.
 - (ii) Apply exclusive-or operation on the obtained sequences.
 - (iii) The result is further divided into two equal parts and exclusive-or operation is applied again.

The step (iii) is repeated till a sequence is obtained whose length is 256 bits. The whole procedure is summarized in the flow chart (Figure 1).

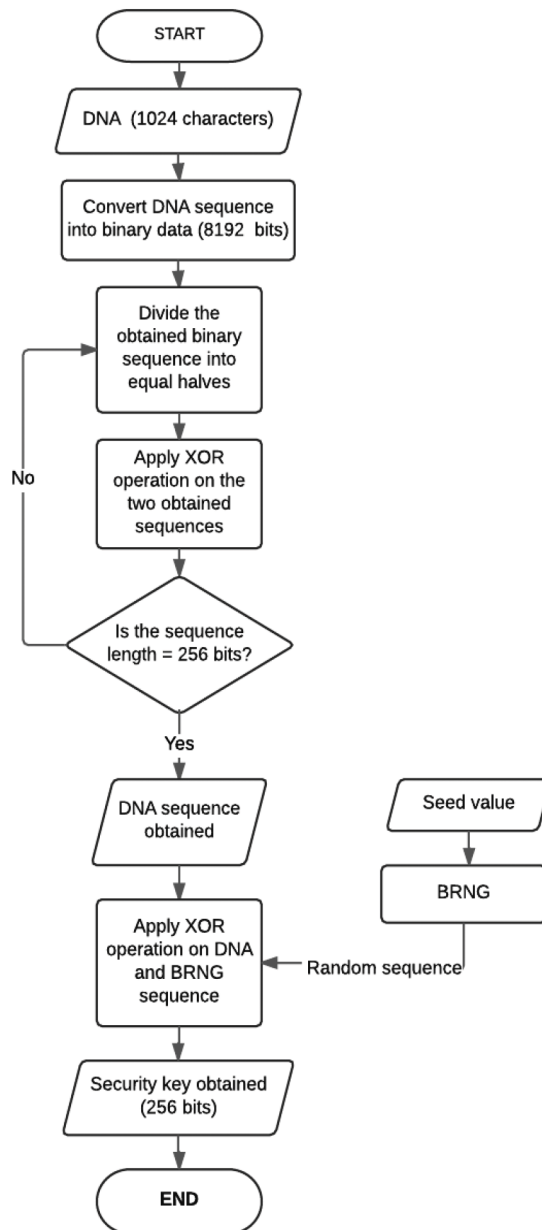


Figure 1. Key generation process

The conversion from ‘agct’ sequence of 1024 characters to 256-bit binary DNA sequence is given in Table 1.

Table 1
DNA sequence formulation

	DNA sequence (1024 characters)	DNA sequence (8192 bits)	DNA sequence (256 bits)
D ₁	gcacaatcagaagcaggcggaggagacggcg gccttcgaggaggtcatgaaggacctgacctg ac.....gcaca gaggcaaggcgtcagcagcatgccaccct gtctccgctgtcaccatcactcaggctgtagcc atg.	011001110110001101100001 011000110110000101100001 0111010001100011.....01 110100011000010110011101 100011011000110110000101 11010001100111	00000100000000000001010100 01011100000010000001100001 01010000010000000110000001 10000001100000011000010011 00000000000000000001001100 0000000000010000001100000 0000000011000000110000001 0000000011000000110000001 00000000100001001100000110 00000010000000000000010000 00000000100110000000
D ₂	ccacgcgtccggcgagaagatggcgacttcg aacaatccgcggaaatcagcagagaagatcgc gct.....ggcgtcagcc ccctgtccctgagcacagaggcaaggcgtcag caggcatcgcggccctgtcccgctgcacc at.	011000110110001101100001 011000110110011101100011 0110011101110100.....0 111010001100011011000010 110001011000110110001101 10000101110100	00000010000000100000001000 00001000000110000101110000 01 000001011100000100000000 0000000000000000000000110 00000010000001100001010100 01001100000010000000000000 0000000001000010011000001 100000000000000001000000110 00000110000000100000000000 0101110000010000000100
D ₃	agcccttaggggaagatcctgctgtgctgtg atgctccagctccagaaatccagctacctgcaac tg.....tctggagcagcagctg ccctacgcctctctcaccagggcggctcccagc agccaccgcccagcagcccccagccccgccc	011000010110011101100011 011000110110001101110100 0111010001100001.....1 000110110001101100011011 000110110011101100011011 0001101100111	00010101000000000000001000 01011100000100000101110000 00000000001000000100000001 10000000000000010000010101 00000010000001000000000000 00000000010101000000100000 00100000000000000100000000 00000101110000001000010011 00010011000001100000000000 0101110001001100010011

*D₁, D₂, D₃: DNA sequences, NCBI Database

Random sequence generation through BRNG. Three sequences are generated using three different seed values. A seed value is a secret input given by the user at the beginning of generator operation. The obtained random sequences along with the corresponding seed value are summarized as in Table 2.

Table 2
BRNG sequence

Seed value	Bernoulli random sequence (256 bits)
B ₁ 1231	101100110000001101011010011000010101001000010111011101110011101000 0000110000011010101101000101011011101010001101110101010101100000001 1001110110100000110110011001011110111001010001000101100100000000101 1100001111011010111011110000011011110000110010010010110
B ₂ 101355	0001011010010001010100011001011001110000001101011111001111010101110 0010010110010100001110110111001110000100110011001101101101001011100 1101110100011000001101111100111111100110100000111110011001001001100 010001000110011011100100100100101010110101101010001
B ₃ 2114	01110101000011010011000001010101000000010001000010101010101000001 10101111010101010011010011010010100000110001000101011100000001000111 0011100010000110010010111110001011100010100110101110111110101100011 00011000101110110010110100100100001111011110001101011

*B₁, B₂, B₃: Three BRNG sequences

Fusion of DNA sequence and BRNG sequence. To enhance the strength of security and randomness in the key, exclusive-or logic is applied between each DNA and BRNG sequence. The resultant key has length of 256 bits and is strong enough to survive critical attacks on networks. The process is repeated for two other DNA and BRNG sequences. Therefore, three 256 bit keys are obtained as shown in Table 3.

Table 3
Security keys

KEY ₁	0001001010010001010001001000000101110010001100111110110011101110110010001 0111110100010110110001001010110100110011001101101010010101110011011110001 11100011011111001001111111110100100111110111000000101100100001000010011011 100100000100101010111100001010001
------------------	---

KEY ₂	10110001000000010101100001100010101011110001110010111001110110011000010011 0000011010101101000101011010001010000101110011010000110001000000111001010 00001101100110010110101100001100011101011001000000011011101101111000010111 00111000001101010110011011001001111
------------------	--

KEY ₃	0110000000001101001100100100001000000101000001111010101010101010001100011 1101100101001101001111001000101011000000010111110000000100011100110010000 0111010010101110001011100000100110101110010001010111001110000000010001100 01110100100100100001010111101111000
------------------	--

The final key is a combination of true random source (DNA) and pseudo random source (BRNG). The keys obtained have unique and random characteristics and thus can be useful in maintaining security.

RESULTS AND DISCUSSION

A security key is said to be efficient if it is random and unique. The National Institute of Standards and Technology (NIST) tests discuss some aspects of selecting and testing random number generators. The outputs of these generators may be used in most of the security applications for the generation of security keys. The generators that are to be used for security applications should meet stronger requirements than those to be used for other applications. To be precise, their outputs need to be unpredictable for unknown inputs. These tests may be useful for determining if a generator is suitable for a particular security application. The randomness of a key is evaluated on the bases of its P-value, which must be greater than 0.01 for a random sequence.

NIST Tests

The keys obtained are evaluated on the basis of seven NIST randomness verification tests and the P-value is calculated for each test with respect to the security key. An overview of the NIST tests used for evaluating the sequences is given as:

Runs test. The purpose of applying this test is to calculate the number of runs in an entire sequence, where run specifies the number of uninterrupted sequence of identical bits (Rukhin et al., 2010). The results in Table 4 clearly depict that the proposed algorithm has higher rate of interruptions.

Frequency Test. Frequency test is used for determining the proportion of number of ones and zeros in an entire sequence. It is used to check the closeness between the number of ones and number of zeros. A sequence is said to be random if the proportion of zeros and ones are close to each other (Rukhin et al., 2010). The results in Table 4 clearly depict that the proposed algorithm produces better proximity between the count of ones and zeros as compared to the traditional techniques.

Approximate Entropy Test. This test deals with the frequency of all the overlapping bit patterns across the entire sequence. The aim of this test is to compare the frequency of overlapping blocks of two consecutive/adjacent lengths with the expected result for a random sequence.

Discrete Fourier Transform Test (DFT). The DFT test is used to find the peak heights in the Discrete Fourier Transform of a sequence. The aim of this test is to detect periodic features (i.e. repetitive patterns) in the tested sequence that indicates a deviation from the assumed randomness. The goal is to detect if the number of peaks exceeding the 95 % threshold are significantly different than 5%.

Binary Derivative Test. The test is performed using exclusive-or operation between successive bits until only one bit is left. Afterwards, the ratio of number of ones to the length of entire sequence in each case is calculated. Finally, the average of the ratio of all the sequences is observed, and where the value lies near to 0.5, then the sequence is considered as a random sequence (Rukhin et al., 2010). The results in Table 4 show that the output of proposed algorithm is random.

Maurer's "Universal Statistical" Test. The aim of this test is to detect if a sequence can be significantly compressed without any loss of information. The number of bits between matching patterns are calculated. A sequence that is significantly compressible is considered to be non-random. This test is also known as Universal test (Rukhin et al., 2010).

Random Excursion Variant Test. The test focuses on the total number of times a particular state occurs in a cumulative sum random walk. It detects the deviations from the expected number of visits. The P-value specifies if the sequence is random or not. This test considers successive sums of the binary bits as a one-dimensional random walk (Rukhin et al., 2010).

$$P_{value} = erfc \times \frac{(|\xi(x) - j|)}{\sqrt{(2 \times j \times ((4 \times |x|) - 2))}} \quad (1)$$

Where,

erfc: the error function

ξ : the total number of times the state x occurs

x : the state occurred

j : the total number of cycles

The P-value must be greater than 0.01 for a sequence to be random (Rukhin et al., 2010).

It is observed that the proposed technique produces better results in terms of randomness of the keys. The efficiency of the proposed technique is evaluated by comparing it with other traditional biometric techniques used for authentication and security key generation. The tests have been performed on KEY₁ and results are tabulated in Table 4.

Table 4
Comparison and analysis

S. No	Input Source of random number generator	Key Length (bits)	Runs Test		Frequency Test	Approximate Entropy Test	DFT Test	Binary Derivative Test	Maurer's Test	Random Excursion Variant Test
			P-value	P-value	P-value	P-value	P-value	P-value	P-value	
1.	ECG	128	0.1262	0.2487	0.5468	0.0294	0.5039	0.9428	Random	
2.	Image	256	0.0809	0.8026	0.9759	0.4220	0.4887	0.9780	Random	
3.	Iris sequence	128	0.1254	0.3768	0.9409	0.3304	0.5021	0.9062	Random	
4.	Finger print	128	0.3345	0.3041	0.3345	0.7597	-	0.2757	Random	
5.	DNA & BRNG	256	0.0438	0.9005	0.9340	0.8185	0.5090	0.9920	Random	

It can be observed that the P-value obtained for the keys generated for all the seven tests is significantly greater than 0.01. Thus, it can be concluded that the keys generated are random in nature and hence fulfil the basic criteria required for security keys.

Avalanche test has also been performed on the keys obtained. The purpose of this test is to check the avalanche effect, which is a desirable property of the security keys. Wherein if the input is changed slightly the output changes significantly. It gives the percentage of bits flipped with a change in the input. It is a desirable property of security keys.

The test is performed on three sets of DNA and BRNG sequences:

Case 1: In the initial set, two security keys are generated through two DNA sequences while keeping the same BRNG sequence.

Case 2: The second set involves generation of two security keys through the same DNA sequence and two BRNG sequences.

Case 3: In the third set, two security keys are generated through two DNA and BRNG sequences.

Further, the avalanche effect is calculated for each of the three sets and results are tabulated in Table 5, Table 6 and Table 7 respectively, this is done to know the amount of randomness the proposed technique produces on changing the input.

The avalanche effect can be calculated using the formula given in equation (3).

$$Avalanche\ effect = \frac{No.of\ bits\ flipped\ in\ the\ sequence}{Total\ no.of\ bits\ in\ the\ sequence} \times 100 \tag{3}$$

The result of avalanche effect on changing the inputs is summarized in tabular form, where D₁, D₂, D₃ represent the DNA sequences as taken from Table 1 and B₁, B₂, B₃ represent the BRNG sequences characterized by the seed values, as taken from Table 2.

Table 5
Avalanche test analysis: Case 1

DNA Sequences (D _n)	Seed Value	Bernoulli Random Sequence (B _n)	Key Generated K= D _n xor B _n	Avalanche Result of Key (K)	
				No. of bits flipped	Avalanche Effect
D ₁	1231	B ₁	1011011100000011010011110111011001	58	22.65 %
			010000000100010110111010011001000		
			001111000010101010000100011001100		
			1110010001101110101010111111000001		
			100111010010000101011001100101100		
			011100011000101010110011000010001		
			111001111101111011101111000011101		
			1110000111011110010110		
D ₂	1231	B ₁	101100010000000101011000011000110	58	22.65 %
			10101000000000001111111000101000		
			000101100000110101011010001010110		
			110110100010011101100101110010001		
			010101110100100000110110011001011		
			100111101100001011101100100000000		
			001110011111010110111010110000011		
			011011110110000010010010		

* Refer Table 1 for D₁, D₂, D₃ and Table 2 for B₁, B₂, B₃

** Different DNA sequences - Same BRNG sequence

Table 6
Avalanche test analysis: Case 2

DNA Sequence (D _n)	Seed Value	Bernoulli Random Sequence (B _n)	Key Generated K= D _n xor B _n	Avalanche Result of Key (K)	
				No. of bits flipped	Avalanche effect
D ₁	1231	B ₁	101101110000001101001111011101100 101000000010001011011101001100100 000111100001010101000010001100110 01110010001101110101010111110000 011001110100100001010110011001011 000111000110001010101100110000100 01111001111101110111011110000111 011110000111011110010110	124	48.43 %
	101355	B ₂	000100101001000101000100100000010 1110010001100111110110011101110111 0010001011111010001011011000100101 0110100110011001101101010010101110 0110111110001111000110111110010011 111111101001001111101110000001011 0010000100001001101110010000010010 1010111100001010001		

* Refer Table 1 for D₁, D₂, D₃ and Table 2 for B₁, B₂, B₃

** Same DNA sequences - Different BRNG sequences

Table 7
Avalanche test analysis: Case 3

DNA Sequence (D _n)	Seed Value	Bernoulli Random Sequence (B _n)	Key Generated K= D _n xor B _n	Avalanche Result of Key (K)	
				No. of bits flipped	Avalanche Effect
D ₁	1231	B ₁	10110111000000110100111101110110 01010000000100010110111010011001 00000111100001010101000010001100 11001110010001101110101010111111 00000110011101001000010101100110 01011000111000110001010101100110 00010001111001111101111011101111 000011101111000011101111001011011	58	22.65 %
	D ₂	101355	B ₂	00010100100100110101001110010100 01110110001000101111110111111011 110011001011001010000111011011100 111110010011101100101110101111010 01111110111100011000001101111100 1101111010101001101111100110010 00001100100001001010011010100100 100100000100110111101010101	

*Refer Table 1 for D₁, D₂, D₃ and Table 2 for B₁, B₂, B₃

**Different DNA sequences – Different BRNG sequences

The avalanche test results indicate that a slight change in the inputs leads to a significant change in the output. The higher the percentage value of avalanche effect, the more is the uniqueness of the key. As the seed value may vary according to the user's choice and the DNA being unique to an individual, it can be assumed that the security system built has higher efficiency and is less susceptible to attacks.

CONCLUSION

In this work, a novel algorithm is proposed to generate biometric security keys for authentication using an individual's DNA sequence and BRNG sequence. DNA being the most unique characteristic of an individual when collaborated with the Bernoulli seed is more efficient. The proposed key finds its application in various areas where maintaining the sender's confidentiality as well as retaining the original message are important. Most of the security system researches have been carried out on fingerprint, facial, iris and voice recognition; while those focused on the DNA are rare. A system that computes a 256-bit biometric security key through the fusion of DNA and BRNG is presented and analysed using NIST Tests. Results indicate this method is superior to more traditional techniques.

REFERENCES

- Baluja, S., & Covell, M. (2007, April). Audio fingerprinting: Combining computer vision & data stream processing. *IEEE International Conference on Acoustics, Speech and Signal Processing, 2007, ICASSP 2007* (Vol. 2, pp. II-213). IEEE.
- Brown, L., & Seberry, J. (1990). On the design of permutation P in DES type cryptosystems. In G. Brassard (Ed.), *Advances in Cryptology—EUROCRYPT'89* (pp. 696-705). Germany: Springer Berlin/Heidelberg.
- Chang, H. T., Kuo, C. J., Lo, N. W., & Lv, W. Z. (2012). DNA sequence representation and comparison based on quaternion number system. *DNA Sequence*, 3(11), 39-46.
- Chen, B., & Chandran, V. (2007, December). Biometric based cryptographic key generation from faces. In *9th Biennial Conference of the Australian Pattern Recognition Society on Digital Image Computing Techniques and Applications* (pp. 394-401). IEEE.
- Chouakri, S. A., Bereksi-Reguig, F., Ahmaldi, S., & Fokapu, O. (2005, September). Wavelet denoising of the electrocardiogram signal based on the corrupted noise estimation. *Computers in Cardiology, 2005* (pp. 1021-1024). IEEE.
- Covell, M., & Baluja, S. (2007, April). Known-audio detection using waveprint: spectrogram fingerprinting by wavelet hashing. *IEEE International Conference on Acoustics, Speech and Signal Processing, 2007, ICASSP 2007* (Vol. 1, pp. I-237). IEEE.
- Ensembl. (n.d.). *Ensembl Genome Browser*. Retrieved from <http://www.ensembl.org/index.html>
- Garcia-Baleon, H. A., Alarcon-Aquino, V., & Starostenko, O. (2009, August). A wavelet-based 128-bit key generator using electrocardiogram signals. *52nd IEEE International Midwest Symposium on Circuits and Systems, 2009, MWSCAS'09* (pp. 644-647). IEEE.

- Goldberger, A. L., Amaral, L. A., Glass, L., Hausdorff, J. M., Ivanov, P. C., Mark, R. G., ... & Stanley, H. E. (2000). Physio bank, physio toolkit, and physio net. *Circulation*, *101*(23), e215-e220.
- Hao, F., Anderson, R., & Daugman, J. (2006). Combining crypto with biometrics effectively. *IEEE transactions on computers*, *55*(9), 1081-1088.
- Hedayatpour, S., & Chuprat, S. (2011, September). Hash functions-based random number generator with image data source. *IEEE Conference on Open Systems (ICOS), 2011* (pp. 69-73). IEEE.
- Khokher, R., & Singh, R. C. (2015, May). Generation of security key using ECG signal. *International Conference on Computing, Communication and Automation (ICCCA), 2015* (pp. 895-900). IEEE.
- Ktata, S., Ouni, K., & Ellouze, N. (2009). A novel compression algorithm for electrocardiogram signals based on wavelet transform and SPIHT. *International Journal of Signal Processing*, *5*(4), 32-37.
- NCBI. (n.d.). *National Center for Biotechnology Information*. Retrieved from <http://www.ncbi.nlm.nih.gov/Entrez>
- NCBI. (n.d.). *National Center for Biotechnology Information*. Retrieved from <http://www.ncbi.nlm.nih.gov/nuccore/3327045?report=genbank>
- NCBI. (n.d.). *National Center for Biotechnology Information*. Retrieved From <http://www.ncbi.nlm.nih.gov/nuccore/20380066?report=genbank>
- NCBI. (n.d.). *National Center for Biotechnology Information*. Retrieved from <http://www.ncbi.nlm.nih.gov/nuccore/33874586?report=genbank>
- Rukhin, A., Soto, J., Nechvatal, J., Barker, E., Leigh, S., Levenson, M., ... & Smid, M. (2010). *Statistical test suite for random and pseudorandom number generators for cryptographic applications*. Gaithersburg: NIST Special Publication.
- Wei, W., & Jun, Z. (2013, November). Image encryption algorithm based on the key extracted from iris characteristics. In *IEEE 14th International Symposium on Computational Intelligence and Informatics (CINTI), 2013* (pp. 169-172). IEEE.
- Ying, L., Shu, W., Jing, Y., & Xiao, L. (2010, December). Design of a random number generator from fingerprint. In *International Conference on Computational and Information Sciences (ICCIS), 2010* (pp. 278-280). IEEE.



Analysis of MIMO FSO over different Modulation Techniques

Kaur, K.¹, Miglani, R.^{1*} and Malhotra, J. S.²

¹*School of electronics and electrical engineering, Lovely Professional University, Phagwara, Punjab 144411, India*

²*Department of Electronics and Communication Engineering, DAV Institute of Engineering and Technology, Jalandhar, Punjab 144008, India*

ABSTRACT

Atmospheric turbulence is the main impairment in free space optical communication links. To mitigate the effect of turbulence spatial diversity techniques are used. In this paper, we analyse the performance of Gamma-Gamma channel model with spatial diversity and compare it with K-distribution. The modulation techniques assumed here are on-off keying, binary PPM and binary phase shift keying and the bit error rate and Gain performance with single input single output (SISO), single input multiple output (SIMO), multiple input single output (MISO) and multiple input multiple output (MIMO) are presented.

Keywords: Binary Phase Shift Keying (BPSK), Bit Error Rate (BER), Gamma-Gamma channel model, K-distribution model, Multiple Input Multiple Output (MIMO), Multiple Input Single Output (MISO), Single Input Multiple Output (SIMO), spatial diversity

INTRODUCTION

Radio frequency links have reached a saturation level with the demand for higher data rates opens up the era Free space optical communication which experimentally claims to provide higher data rates up to 160Gbps provided by Willebrand and Ghuman (2001). The visible and infrared frequency ranges used in FSO does not require license from government agencies. In FSO transmission the data is optically modulated with narrow wavelengths to provide security and privacy as explained by Bhatnagar and Ghassemlooy (2016). The main impairment in FSO is associated with atmospheric conditions and turbulence induced fading. Turbulence

may be caused by variations in temperature or turbulence induced fading creates fluctuations in phase and amplitude of a transmitted signal. Tatarskii and Zavorotnyi (1985); Khalighi and Uysal (2014) has been explained turbulence theory using Kolomogorov model by relating it with parameters such as: the refractive

Article history:

Received: 29 December 2016

Accepted: 21 April 2017

E-mail addresses:

sidhhukulvir18@gmail.com (Kaur, K.),

rajan.16957@lpu.co.in (Miglani, R.),

jmalhotra292@gmail.com (Malhotra, J. S.)

*Corresponding Author

index σ_I , inner scale of turbulence l_0 and outer scale of turbulence L_0 . To describe the extent of turbulence, the scintillation index (SI) is used as standard which is defined in Eq. 1 as

$$\sigma_I^2 = E\{I^2\}/E\{I\}^2 - 1 \tag{1}$$

Where I is the irradiance and $E\{.\}$ is expectation of irradiance, I .

The impact of turbulence of FSO channel link can be modelled using: Lognormal model, K-distribution, and Gamma-Gamma and Rayleigh distribution. While Zhu and Kahn (2002), explained that lognormal model is valid only for low turbulence condition, the K-distribution model is applicable for strong turbulence. The Gamma-Gamma is valid for all levels of turbulence as pointed out by Chatzidiemantis, Sandalidis, Karagiannidis, Kotsopoulos and Matthaïou (2010). The Gamma-Gamma model is based on doubly stochastic theory that takes into account the effect of small and large turbulence eddies. In this paper the two basic models have been considered Gamma-Gamma and K-distribution model. In section I below FSO communication is discussed. In section II system models and their mathematical notations are presented.

System Model

FSO links are the line of sight (LOS) communication links in which optically modulated data is transmitted as physical media. The transmitters used for this purpose are lasers and light emitting diodes (LED) while to facilitate reception the data is demodulated using optical detectors. The free space optical communication provides more security than RF and it serves large users because of high bandwidth.

The received optical signal is given as equation 2:

$$y = \eta \times I + n \tag{2}$$

In equation 2 x represents information bits it can be either 0 or 1. Where n is additive white Gaussian noise with mean = 0 and variance = $N_0/2$. I is the normalised irradiance. The optical to electrical conversion is denoted by η .

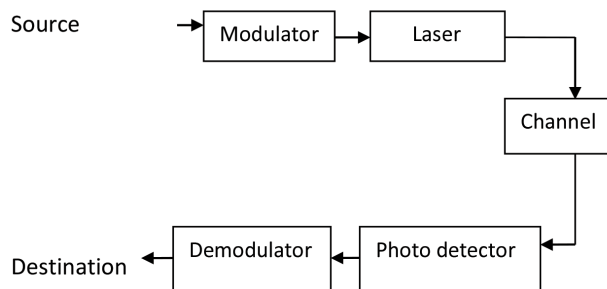


Figure 1. Basic block diagram of free space optical communication system

The losses occur in channel which are mainly misalignment losses which occurs due to building motion also known as building sway and beam wander, the reason for atmospheric losses are fog, rain etc. and atmospheric turbulence induced fading is the phenomenon which occurs due to fluctuations of signal because of variable temperature and amplitude, which degrades the performance of FSO links so it is necessary to design a channel with good performance to make the efficient communication. There are various channel models in FSO to define channel losses.

METHODS

Statistics of Channel Models

Gamma-Gamma channel model. The Gamma-Gamma channel model is widely accepted model as it is fit for all kinds of turbulence scenarios. The received irradiance (I) estimation for this model is based on product of two gamma random processes I_x and I_y which arises from small turbulence and large turbulent eddies. The probability density function (PDF) of irradiance (I) in Gamma-Gamma distribution is given by equation 3 given by Al-Habash, Andrews, and Phillips (2001); Yang, Gao, and Alouini (2014).

$$f(I) = \frac{2(\alpha\beta)^{\frac{(\alpha+\beta)}{2}}}{\Gamma(\alpha)\Gamma(\beta)} I^{(\alpha+\beta)/2-1} K_{\alpha-\beta}(2\sqrt{\alpha\beta I}), I > 0 \quad (3)$$

Where

I is irradiance

$\Gamma(\cdot)$ is gamma function

$K(\alpha, \beta)$ is Bessel function of second order.

The α and β are numbers of small and large turbulence cells and given by equation no. 4 and 5 respectively:

$$\alpha = \frac{1}{\exp\left[\frac{0.49\sigma^2}{(1+1.11\sigma^{12/5})^{7/6}}\right]-1} \quad (4)$$

$$\beta = \frac{1}{\exp\left[\frac{0.51\sigma^2}{(1+0.69\sigma^{12/5})^{5/6}}\right]-1} \quad (5)$$

Where σ^2 represents variance.

The scintillation index (SI) which can be applied to Gamma-Gamma channel describes the impact of turbulence is given as:

$$\sigma^2 = (1/\alpha) + (1/\beta) + (1/\alpha\beta). \quad (6)$$

By considering the Gamma-Gamma channel model some special cases are derived. The K-distribution is obtained by setting $\beta=1$ and another case in which β is set at infinity.

K- distribution channel model. The K-distribution model is valid for strong turbulence condition as explained by Tsiftsis, Sandalidis, Karagiannidis, and Uysal (2009); Kaur, Jain, and Kar (2016). The probability density function of K-distribution is obtained from equation 3 as a special case by setting $\beta=1$, the derived PDF is 7:

$$f(I) = \frac{2(\alpha)^{\frac{(\alpha+1)}{2}}}{\Gamma(\alpha)} I^{((\alpha-1)/2)} K_{\alpha-1}(2\sqrt{\alpha I}), I > 0 \tag{7}$$

Where I is irradiance, $\Gamma(\cdot)$ is gamma function and $K(\alpha, 1)$ is Bessel function of second order.

Performance Analysis of SISO Channels

BER Analysis. BER (bit error rate) is the parameter used in communication to analyse the performance of those systems which transmits digital data. It is defined as the ratio of bits in error to the total transmitted bits. In this section BER analysis of OOK, BPPM and BPSK is done. For binary modulation schemes the BER P_b is directly linked with PEP (posterior error probability) $P_e(d)$ which depends only on Euclidean distance. The Euclidean distance between the constellation points s and \hat{s} is denoted by d , the mathematical expression of $d = \|s - \hat{s}\|$ and the PEP $P_e(d, I) = Q(\sqrt{\gamma d^2 I^2 / (4\sigma^2)})$ which depends on SNR that is denoted by γ and irradiance I . From this formula, the PEP over a turbulent media has been derived, as given in equation 8.

The PEP over the turbulent channel is:

$$P_e(d) = Q\left(\sqrt{\frac{\gamma d^2}{4\sigma^2}} I\right) f(I) dI \tag{8}$$

Where γ is SNR and d represents the Euclidean distance for modulation techniques and $f(I)$ is the PDF for both the models. The performance is analysed for OOK (on-off keying) which is a basic form of ASK (amplitude shift keying) in which for binary 1 the carrier is present and for binary zero there is no carrier. The comparison of OOK is presented with BPPM which is binary pulse position modulation; for this technique, the two bits in a symbol are used to transmit the data and with BPSK (binary phase shift keying) in which two symbols are 0 and 1 at phase of 180 degree are considered.

Diversity and combining Gain. The diversity combining gains is a technique to extract the information from various transmitted signals over different paths. This method gives a single improved signal by combining the various signals. To characterize a turbulence fading channel the terms diversity gain G_d and combining gain G_c are used. The diversity and combining gain for SISO Gamma-Gamma turbulence channel is obtained in equation 9 and 10 given by Bayaki, Schober and Mallik (2009):

$$G_d = \min(\alpha/2, \beta/2) \tag{9}$$

$$G_c = \left(\frac{d}{2\sqrt{2}\alpha\beta\sigma}\right)^2 X \left(\frac{2\sqrt{\pi}(\max\{\alpha, \beta\})\Gamma(2G_d+1)}{\Gamma(|\alpha-\beta|)\Gamma(G_d+\frac{1}{2})}\right)^{1/G_d} \tag{10}$$

For k-distribution we consider the $\beta=1$ in diversity and combining gains and the final equations for gains are

$$G_d = \min(\alpha/2, 1/2) \tag{11}$$

$$G_c = \left(\frac{d}{2\sqrt{2}\alpha\sigma}\right)^2 X \left(\frac{2\sqrt{\pi}(\max\{\alpha,1\})\Gamma(2G_d+1)}{\Gamma(|\alpha-1|)\Gamma(G_d+\frac{1}{2})}\right)^{1/G_d} \tag{12}$$

In this section the mathematical analysis for MIMO FSO system is done. The MIMO system is known as multiple input and multiple output and used in wireless communication. The multiple antennas at both ends are used to reduce the errors and to increase the transmission speed.

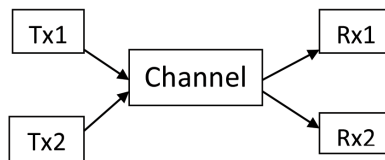


Figure 2. MIMO diversity (2x2)

Performance Analysis of MIMO FSO Channel

MIMO Gamma-Gamma channel. The probability density function (PDF) of irradiance (I) in Gamma-Gamma distribution in MIMO system is written as in equation 13 given by Luong and Pham (2014), where I is the function of M and N and denoted by $I(MN)$:

$$f(I(M, N)) = \frac{2(\alpha_1\beta_1/MN)^{\frac{(\alpha_1+\beta_1)}{2}} I^{(\alpha_1+\beta_1)/2-1} K_{\alpha_1-\beta_1}(2\sqrt{I\alpha_1\beta_1/MN})}{\Gamma(\alpha_1)\Gamma(\beta_1)}, I>0 \tag{13}$$

Where $\alpha_1=MN\alpha$ and $\beta_1=MN\beta$ are the new shaping parameters for MIMO Gamma-Gamma model. The numbers of transmitters are represented by M and where N is number of receive apertures. The case in which the M and N is 1, represents the SISO case as given in equation 3.

MIMO K- distribution channel. The probability density function of $I(MN)$ for K-distribution in MIMO system is given in equation 14.

$$f(I(MN)) = \frac{2(\alpha_1/MN)^{\frac{(\alpha_1+1)}{2}} I^{(\alpha_1-1)/2} K_{\alpha_1-1}(2\sqrt{I\alpha_1/MN})}{\Gamma(\alpha_1)}, I>0 \tag{14}$$

BER and Gain performance in MIMO

1) *BER Analysis:* For MIMO BER analysis the PDF $f(I(MN))$ from equation 13 and 14 is considered for the formula given in equation 8 for both Gamma-gamma and K-distribution. The final BER for MIMO system is given in equation 15:

$$P_e(d) = Q \left(\sqrt{\frac{\gamma d^2}{4\sigma^2}} I^2 \right) f(I(MN)) dI \tag{15}$$

2) *Diversity and Combining Gains:* The diversity gain and combining gain for MIMO Gamma-Gamma and K- channel is given in equation 16 as explained by Tsiftsis et al. (2009).

$$G(M, N) = \frac{G_C^{MRC}}{G_C^{EGC}} = N \left(\frac{2\Gamma(2MG_d)}{\Gamma(MG_d)} \right)^{1/MG_d} \times \left(\frac{\Gamma(MNG_d+1)}{\Gamma(2MNG_d+1)} \right)^{1/MNG_d} \tag{16}$$

RESULTS

In this section the analysis of BER and Gain of Gamma-Gamma and K-distribution channel is presented for SISO and MIMO systems.

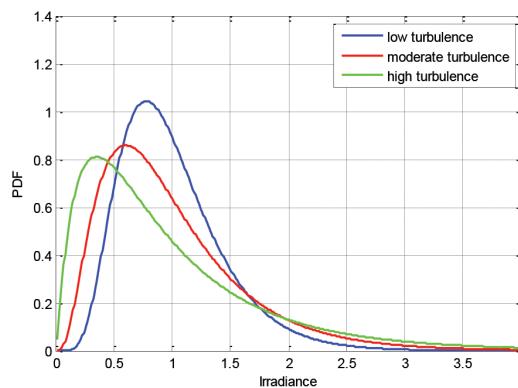


Figure 3. Probability density function vs. irradiance for Gamma-gamma model

Figure 3 represents the variation of probability density function with respect to irradiance for Gamma-Gamma turbulent channel under different turbulence regimes assuming the contribution of both large and small turbulence eddies and it has been shown that the PDF decreases with increase in turbulence. In Figure 4 the PDF vs. irradiance graph is presented for K-channel model for different turbulence scenarios. It has been shown that as the value of (alpha) which is no. of discrete scatters decreases the turbulence increases and the PDF decreases. The value for PDF only occurs at negative slope as in negative exponential distribution. This represents that K-distribution has very high turbulence condition.

MIMO FSO over different Modulation Techniques

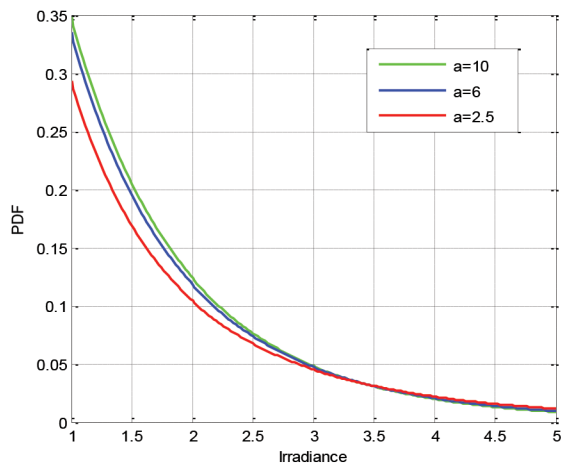


Figure 4. Probability density function vs. irradiance for K-distribution model

Table 1
Parameters and PDF for different turbulence regimes

Turbulence	α (G-G)	β (G-G)	α (k-dist.)	PDF (G-G)	PDF (k-dist.)
Weak	11	10	10	0.9	0.14
Moderate	7.1	4.5	6	0.65	0.12
Strong	4.4	4.2	2.5	0.45	0.1

In Table 1 the values for different parameters of both Gamma-Gamma and K-distribution are given and the PDF for Gamma-Gamma at irradiance =1 for all turbulence regimes is included in this table, where PDF at irradiance =2 is included for K-distribution model.

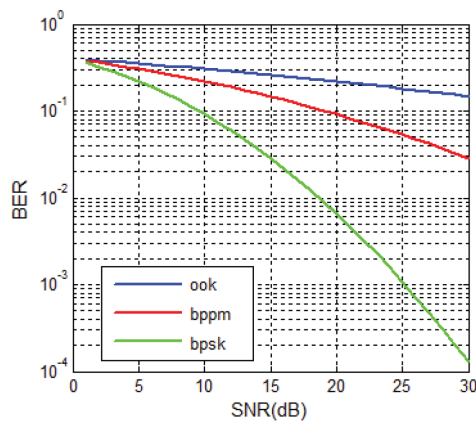


Figure 5. BER vs. SNR for SISO Gamma-gamma model under different modulation techniques

In Figure 5 the BER vs. SNR graph is presented for different modulation schemes and it can be concluded that the BPSK modulation gives appreciable results in comparison of other binary modulation techniques for SISO Gamma-Gamma model. As shown in graph in order to achieve the BER of order 10^{-1} the corresponding SNR for BPSK is 9.8dB and for BPPM the SNR is 19.7dB which shows that BPSK performs better.

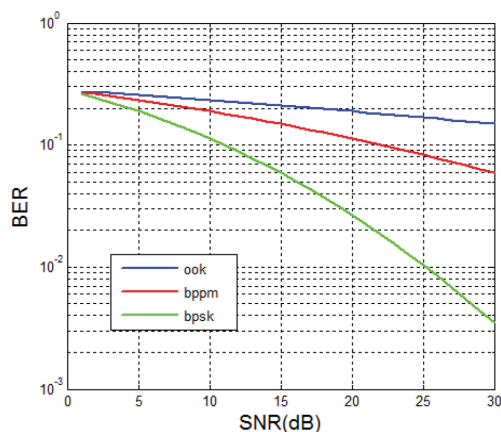


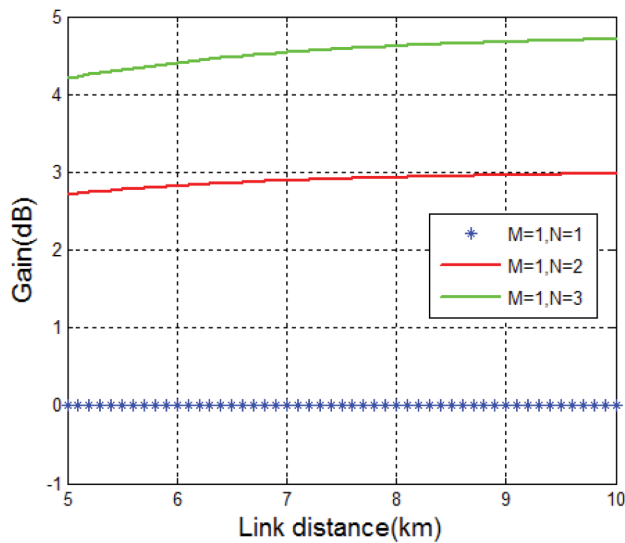
Figure 6. BER vs. SNR for SISO K-distribution model under different modulation techniques

The Figure 6 represents the performance of K-distribution with respect to BER vs. SNR for different modulation techniques. The performance of BPSK is better from other techniques. To achieve $BER = 10^{-1}$, the SNR required for BPPM is 21dB where for BPSK the SNR is 10.8dB. In comparison to Gamma-Gamma channel model for same modulation technique the K-distribution requires large SNR which concludes that Gamma-Gamma channel model is better and all the parameters are presented in table 2 below.

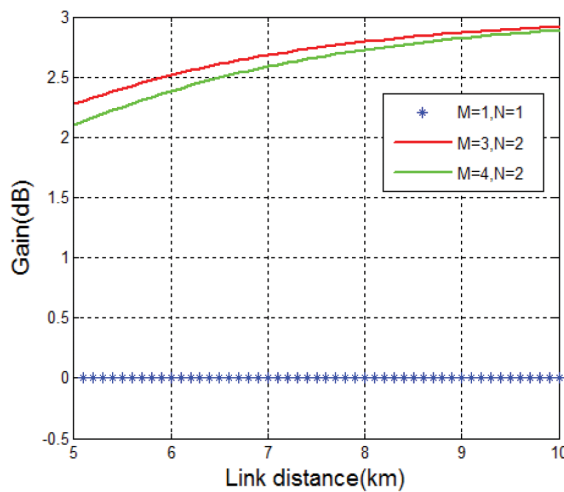
Table 2

Comparison of different modulation schemes for SISO Gamma-Gamma and K-distribution channel

Modulation	SNR for BER	SNR for BER
	10^{-1} (Gamma-Gamma)	10^{-1} (K-distribution)
BPSK	9.8dB	10.8dB
BPPM	19.7dB	21dB
OOK	More than 30dB	More than 30dB



(a)



(b)

Figure 7. Plot of Gain with Link distance for Gamma-gamma model (a) Receiver diversity (b) Transmit diversity

In Figure 7 the performance of diversity systems in terms of gain is analysed and the conclusion drawn indicates the gain of system increases as the number of receiver aperture (receiver diversity) increases. In Figure 7(a) the system which has $M=1, N=3$ diversity gives improved gain up to 4.2dB where low diversity order has Gain=2.8dB. In Figure 7(b) the transmitter diversity system is considered and concluded that by increasing the number of transmitters the performance of gain decreases, the exact results shown in Table 3.

Table 3
Performance comparison of Gain for different diversity systems in Gamma-Gamma channel model

Diversity	Gain at L=6km	Gain at L=9km
M=1,N=2	2.9dB	3db
M=1,N=3	4.4dB	4.8dB
M=3,N=2	2.5dB	2.9dB
M=4,N=2	2.35dB	2.89dB

The plot in Figure 8 is presenting the comparison analysis of gain vs. link distance for gamma-gamma channel model and K-distribution. The performance of gamma-gamma in SIMO (M=1, N=3) diversity has better result than SISO. Where the K-distribution with same SIMO diversity has less gain than Gamma-Gamma distribution as given in Table 4.

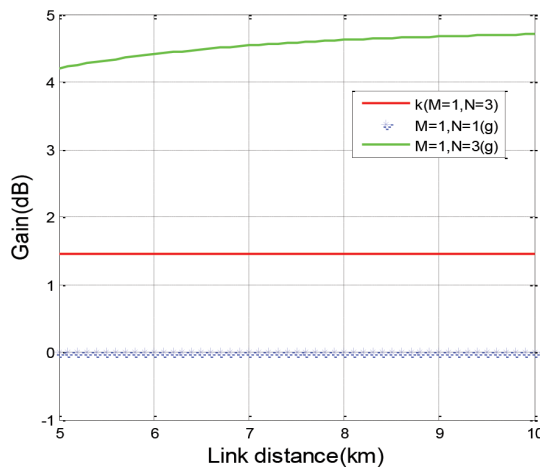


Figure 8. Comparison of Gain vs. Link distance for Gamma-gamma and K-distribution

Table 4
Gain comparison for Gamma-Gamma and K-distribution

Channel Model	Diversity	Gain(dB) at L=6km	Gain(dB) at L=9km
Gamma- Gamma	M=1,N=3	4.4	4.8
K- distribution	M=1,N=3	1.5	1.5

Table 5 is based on Figure 9 in which the MIMO Gamma-Gamma channel model with OOK and BPPM modulation is presented. The BER calculated for M=1 and N=3 diversity system. To achieve the BER = 10^{-3} the SNR for BPPM is required up to 37.5dB where for OOK it is more than 40dB.

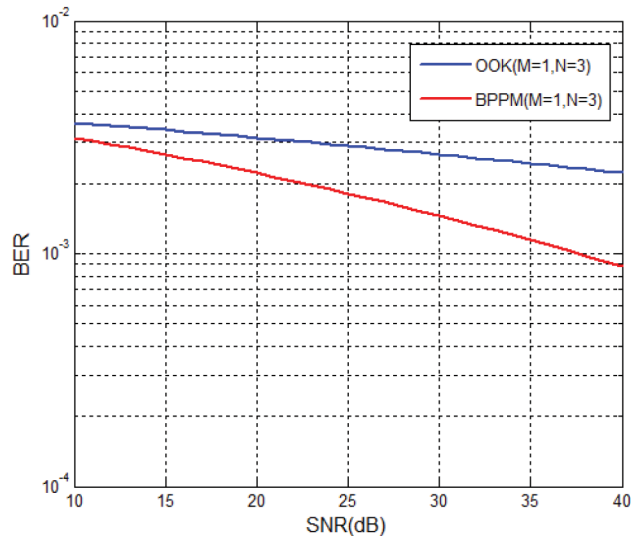


Figure 9. BER vs. SNR for MIMO Gamma-Gamma channel model with modulation

Table 5

Performance comparison for MIMO Gamma-Gamma model for OOK and BPPM

Channel Model	Diversity	Modulation	SNR at BER (10^{-3})
Gamma- Gamma	M=1,N=3	OOK	>40dB
	M=1, N=3	BPPM	37.5dB

In Figure 10 the comparison for BPPM and BPSK is carried out for M=2 and N=2 diversity order. It is analysed that to achieve BER= 10^{-5} the required SNR for BPSK is 25.1dB where for BPPM it is more than 40dB. Thus, it can be concluded that BPSK performs better than BPPM and BPPM performs better than OOK. Table 6 is based on Figure 10 allowing us to conclude that the BPSK is a better technique.

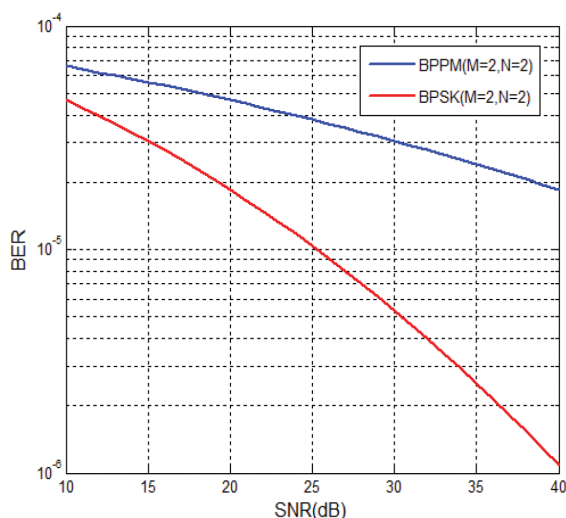


Figure 10. BER vs. SNR for MIMO Gamma-Gamma channel model with modulation

Table 6

Performance of MIMO Gamma-Gamma model for BPPM and BPSK

Channel Model	Diversity	Modulation	SNR at BER (10^{-5})
Gamma-	M=2, N=2	BPPM	>40dB
Gamma	M=2, N=2	BPSK	25.1dB

Figure 11 represents the performance of MIMO K-distribution channel with OOK and BPPM modulation techniques. The performance analyses presented for OOK and BPPM with M=1 and N=3 diversity order the SNR required to achieve BER = 10^{-2} is more than 40dB in case of OOK modulation where for BPPM SNR is 29.6dB.

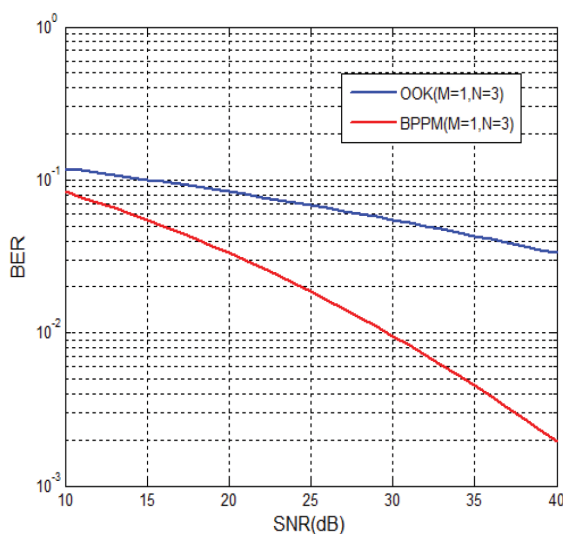


Figure 11. BER vs. SNR for MIMO K-distribution channel model with modulation

MIMO FSO over different Modulation Techniques

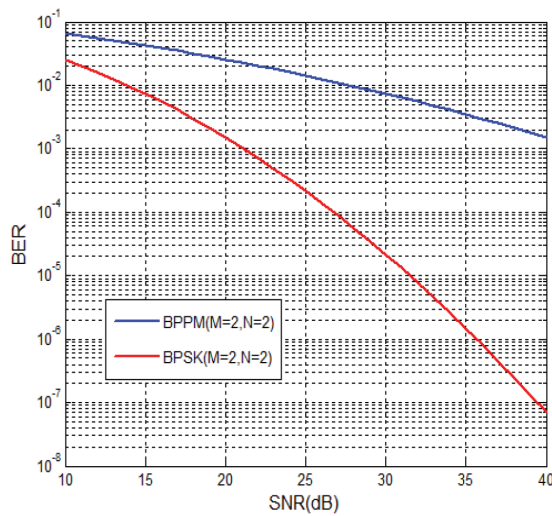


Figure 12. BER vs. SNR for MIMO K-distribution channel model with modulation

The Table 7 is based on Figure 11 in which the performance of K-distribution is analysed for MIMO system by considering OOK and BPPM diversity and concluded that BPPM performs better.

Table 7
Performance of MIMO K-distribution model for OOK and BPPM

Channel Model	Diversity	Modulation	SNR at BER (10^{-2})
K-distribution	M=1, N=3	OOK	>40dB
	M=1, N=3	BPPM	29.6dB

On basis of Figure 12 the Table 8 is presented in which two modulation techniques BPPM and BPSK are analysed over K-distribution channel model by considering M=2 and N=2 diversity order and it is analysed that to achieve BER = 10^{-3} the SNR required for BPPM modulation is >40dB and with BPSK 21dB.

Table 8
Performance of MIMO K-distribution model for BPPM and BPSK

Channel Model	Diversity	Modulation	SNR at BER (10^{-3})
K-distribution	M=2, N=2	BPPM	>40dB
	M=2, N=2	BPSK	21dB

DISSCUSION

In this paper, Gamma-Gamma and K-distribution channel models were analysed for SISO and MIMO FSO links with the objective of determining the impact of turbulence on optical wireless link. The analysis was done by determining the Gain and BER performance of Gamma-Gamma and K-distribution. The probability density function of irradiance is also plotted and it is concluded that as the turbulence increases the pdf decreases for both the channels as in Gamma-Gamma for large turbulence the PDF at intensity 1 is 0.45 and for small turbulence 0.9. Similarly, for K-distribution the PDF for large turbulence at intensity 2 is 0.1 and for small 0.14. It is concluded that the BER for MIMO system is less than other diversities in both channel models but Gama-Gamma model gives better results than K-model. Analysis of the gain with link distance for both the channel models showed that the gain for Gamma-Gamma channel is 4.4dB where for K- distribution model it is 1.5dB for same diversity order. By comparing the different diversity orders, it is shown that the Gamma-Gamma channel performs better than K-distribution in all types of turbulence scenarios.

CONCLUSION

There are some digital modulation techniques OOK, BPPM, BPSK are also compared in this paper and it is concluded that the BPSK performance better than others. The Gamma-Gamma channel model is declared as better model than K-model.

REFERENCES

- Al-Habash, M. A., Andrews, L. C., & Phillips, R. L. (2001). Mathematical model for the irradiance probability density function of a laser beam propagating through turbulent media. *Optical Engineering*, 40(8), 1554-1562.
- Bayaki, E., Schober, R., & Mallik, R. K. (2009). Performance analysis of MIMO free-space optical systems in gamma-gamma fading. *IEEE Transactions on Communications*, 57(11), 3415-3424.
- Bhatnagar, M. R., & Ghassemlooy, Z. (2016). Performance analysis of gamma-gamma fading FSO MIMO links with pointing errors. *Journal of Lightwave Technology*, 34(9), 2158-2169.
- Chatzidiamantis, N. D., Sandalidis, H. G., Karagiannidis, G. K., Kotsopoulos, S. A., & Matthaiou, M. (2010, April). New results on turbulence modelling for free-space optical systems. In *IEEE 17th International Conference on Telecommunications (ICT), 2010* (pp. 487-492). IEEE.
- Kaur, P., Jain, V. K., & Kar, S. (2016). Performance of free space optical links in presence of turbulence, pointing errors and adverse weather conditions. *Optical and Quantum Electronics*, 48(1), 65-77.
- Khalighi, M. A., & Uysal, M. (2014). Survey on free space optical communication: A communication theory perspective. *IEEE Communications Surveys and Tutorials*, 16(4), 2231-2258.
- Luong, D. A., & Pham, A. T. (2014, June). Average capacity of MIMO free-space optical gamma-gamma fading channel. In *IEEE International Conference on Communications (ICC), 2014* (pp. 3354-3358). IEEE.
- Tatarskii, V. I., & Zavorotnyi, V. U. (1985). Wave propagation in random media with fluctuating turbulent parameters. *JOSA A*, 2(12), 2069-2076.

- Tsiftsis, T. A., Sandalidis, H. G., Karagiannidis, G. K., & Uysal, M. (2009). Optical wireless links with spatial diversity over strong atmospheric turbulence channels. *IEEE Transactions on Wireless Communications*, 8(2), 951-957.
- Willebrand, H. A., & Ghuman, B. S. (2001). Fiber optics without fiber. *IEEE spectrum*, 38(8), 40-45.
- Yang, L., Gao, X., & Alouini, M. S. (2014). Performance analysis of free-space optical communication systems with multiuser diversity over atmospheric turbulence channels. *IEEE Photonics Journal*, 6(2), 1-17.
- Zhu, X., & Kahn, J. M. (2002). Free-space optical communication through atmospheric turbulence channels. *IEEE Transactions on communications*, 50(8), 1293-1300.





Performance Evaluation of Compressive Sensing based Channel Estimation Techniques in OFDM System for Different Channels

Jha, A., Kansal, L. and Gaba, G. S.*

School of Electronics and Electrical Engineering, Lovely Professional University, Phagwara, Punjab 144411, India

ABSTRACT

Data transfer in wireless communication systems requires higher data rate, transmission capability, high bandwidth and robustness. Orthogonal frequency division multiplexing (OFDM) is mainly used in regard with Multipath fading and delay. To increase the systems performance various pilot assisted method was discovered and studied. We have used compressed sensing to estimate the channel coefficients of the fading channel; then we have performed the compressive sensing (CS) recovery algorithm to estimate the channel and to nullify the fading effect, the thus much better result are obtained in the simulation which satisfies the better performance of the system as compared to the traditional method.

Keywords: Compressed sensing, channel estimation, LS, MMSE, OFDM

INTRODUCTION

The demand for flexible higher data rates has been increased due to rapid growth in technology. The frequency selective multipath fading that results in inter-symbol interference is affecting the performance of high data rates communication systems as suggested in Bajwa, Haupt, Sayeed, and Nowak (2010). In one development study (Donoho, 2006), presented an idea that OFDM is a multi-carrier modulation technique, which divides the present spectrum into some parallel subcarriers and where each subcarrier is modulated by a low rate data stream. The traditional OFDM system uses inverse fast Fourier transform (IFFT) and fast Fourier transform (FFT) for multiplexing the signals and hence removes the complexity both at transmitter and receiver. OFDM is used in areas

such as, Digital Audio and Video Broadcasting, wireless local area network (WLAN) and high performance local area network (HIPERLAN). In OFDM the original data signal will be split into multiple signals which are independent and each independent signal, is modulated at a different frequency as demonstrated by (Cheng et al., 2013).

Article history:

Received: 29 December 2016

Accepted: 21 April 2017

E-mail addresses:

jha.ashish256256@gmail.com (Jha, A.),

lavish.15911@lpu.co.in (Kansal, L.),

er.gurjotgaba@gmail.com (Gaba, G. S.)

*Corresponding Author

Channel estimation is broadly classified into two categories: blind and non-blind. The blind channel estimation requires statistical behavior of the received signals, whereas the non-blind channel estimation method requires portions of the transmitted signals as discussed by Xiong, Jiang, Gao, and You (2013). The advantage of blind channel techniques is presented by (Tropp & Gilbert, 2008) as the possible elimination of training sequences cutting the system bandwidth efficiency. In some applications training sequences need to be transmitted periodically thus causing further loss of the channel throughput. Due to these reasons blind channel estimations require a prominent concern as we have to remove the no of training sequences. On the other hand, non-blind channel estimation techniques can be implemented by giving pilot tones to all the subcarriers with a period of insertion or pilot tones into some of the carriers for each OFDM symbols. The first case is also known as block type estimation and required for slow fading channel which is further divided into LS estimation and MMSE estimation. LS estimation has less complex but its performance is not good in comparison with the MMSE estimator. From the entire estimator MMSE provides best mean-square-error (MSE) performance knowing full knowledge of channel statistics and operating signal to noise ratio (SNR) as presented by (Donoho, 2006). However if the channel statistics are not known MMSE estimator is more complex that is to be realized in the practical system. The discrete cosine transform (DCT) based channel estimation with hexagonal pilot pattern taking Doppler frequency and virtual subcarriers into considerations are shown by (Chen, Wen & Ting, 2013). The requirement of channel estimation in OFDM system to provide high data transmission and immunity to the multipath fading environment. Due to this reason, (Qi & Wu, 2011) proposed channel estimation method to provide an accurate and efficient channel to reduce the problem caused by discrete Fourier transform (DFT) transformation and to eliminate the computational complexity. An improved channel estimation method based on pilots and its performance has been checked for OFDM system. This method is very useful in mobile communication as described by (Tropp & Gilbert, 2008). The cascading approach which checked the performance of the system is presented by (Bajwa, Haupt, Raz, & Nowak, 2008). The implementation of the sparse time dispersive channel using atomic norm minimization is done having gain path and the grid of path and grid less estimation of arbitrary delay is done by (Hsieh & Wei, 2011). In the next section, we describe the various kinds of techniques in CS, channels estimation schemes, and comparison between LS, MMSE, and CS techniques as proposed by (Zhou, Tong & Zhang, 2017). The final section consists of an s of analysis of the results and the conclusion.

Model Description

We studied various estimation schemes to determine the channel coefficients and to nullify the fading components of the channel. Fourier Transform is one of the most popular transforms for obtaining frequency spectrum of signals. To find the Discrete Fourier Transform in a faster way and with reduced complexity we use Fast Fourier Transform. For the signals whose frequency does not change with time will mostly use this technique. The bit stream data that was generated will be modulated using m-ary phase shift keying (M-PSK) modulator to map input data into the symbols as described by Bajwa et al., (2010). Now, IFFT block will generate N - parallel stream using these symbols which will be transmitted over the sub carriers by OFDM as shown

in Figure 1. We can define the sequence of data as, $x(n), n = 0 \text{ to } N - 1$.

The output frequency domain $X[k]$ is defined as:

$$X[k] = \sum_{n=0}^{N-1} x[n] e^{-jk\left(\frac{2\pi}{N}\right)n} \quad k = 0 \text{ to } N - 1 \quad (1)$$

The output of passing the symbols over N- Parallel streams will be determined as

$$X_k(n) = \frac{1}{\sqrt{N}} \sum_{k=0}^{N-1} X[k] e^{jk\left(\frac{2\pi}{N}\right)n} \quad (2)$$

Conventionally $X[k]$ and $X_k(n)$ are referred to as ‘ Frequency domain data’ and ‘time domain data’ respectively. For simplicity, we define the FFT and IFFT when considering the various FFT algorithms as:

$$FFT_N(k, f) = \sum_{n=0}^{N-1} f(n) e^{-\frac{j2\pi kn}{N}} = \sqrt{N} F(k) \quad (3)$$

$$IFFT_N(n, F) = \sum_{k=0}^{N-1} F(k) e^{\frac{j2\pi kn}{N}} = \sqrt{N} F(k) \quad (4)$$

We consider OFDM with IFFT at transmission end and the FFT at receiver end of the system.

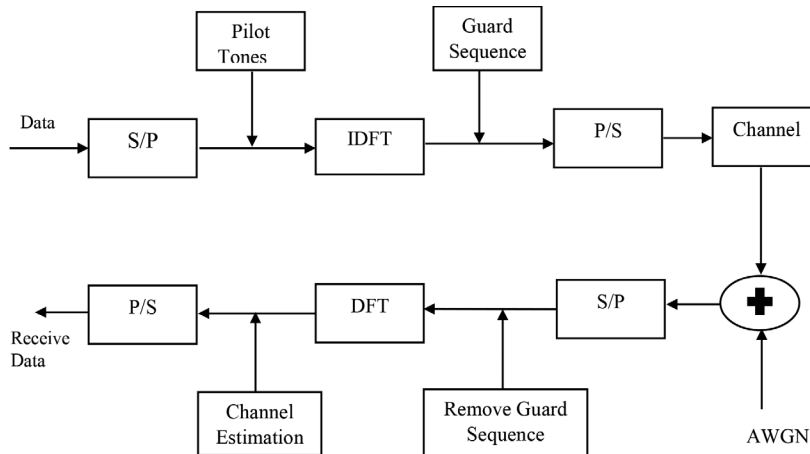


Figure 1. OFDM System model

Whereas:

R- Symbols / Sec

M – Number of data output lines in parallel

N – Samples of time domain

Lp – Prefix of length samples

Brief description is as follows:

Compress Sensing Approach. The compressed sensing is restricted to the theory that, through optimization the sparsity of a signal can be exploited using the small amount of samples required. The recovery operation is based on the two conditions. They are: sparsity in which the signal to be sparse must be in the same domain. The latter one is the incoherence that was applied through the property of isomerism must be sufficient to sparse signals. We used CS in DCT domain and to create the DCT matrix we applied the following equations:

DCT Matrix

$$y(k) = w(k) \sum_{n=1}^N x(n) \cos\left(\frac{\pi}{2N}(2n-1)(k-1)\right) \tag{5}$$

Where the values of k are from (1 to N) & for k=1, $w(k) = \frac{1}{\sqrt{N}}$, else $w(k) = \frac{\sqrt{2}}{\sqrt{N}}$

IDCT Matrix

$$y(M, l) = \sum_{k=1}^M w(k) u(k, l) \cos \pi(2M-1)(k-1) \tag{6}$$

Where for k=1, $w(k) = \frac{1}{\sqrt{M}}$, else $w(k) = \frac{2}{\sqrt{M}}$

The CS comprises of several methods that are used for the estimation. They are explained below:

Undetermined Linear Systems. These types of linear equation systems have more unknowns and have an infinite number of solutions. Therefore, there is a need of implying extra conditions or constrains on the system as presented by Cheng et al. (2013). Now, with under the determining system of linear equations we consider a sparse vector is $S_{n \times 1}$ observed in linear mixing system where $m < n$, cannot be uniquely recovered from the infinite number of solutions described by Bajwa et al. (2008).

Solution/ Reconstruction Method. The redundancy in the signals is taken as an advantage in compressed sensing as described by Hsieh and Wei (2011). In particular, many signals may have coefficients equal to zero, when represented in the same domain. By taking the weighted linear combination of samples, the compressed sensing technique will typically start as demonstrated by Xiong et al. (2013). The least-square solution to such a problem is the minimization of L^2 norm – which defines the minimum amount of energy in the system. When solving the undetermined system of linear equations, we have to minimize the number of non-zero components of the solution as presented by Tropp and Gilbert (2008). We define the function that counts the number of non-zero counts as L^0 norm. As L^0 is not computable, we will move to its closest convex L^1 as demonstrated by Chen et al., (2013). The L^1 solution is stable due to its convex nature. The basic equation can be formed as:

$$\min \|s\|_{L^1} \text{ s.t. } x = A.s \tag{7}$$

Smoothed L^0 Norm Method. As discussed earlier, we have formulated the minimization criterion for sparsity of L^0 norm as

$$\min \|s\|_{l_0} \text{ s.t. } x = A \cdot s \tag{8}$$

The L^0 form is having a disadvantage of combinatorial search and sensitivity to the noise. The basic idea of smoothed L^0 method is to the L^0 normal form with function

$$f_\sigma(s) \triangleq e^{-\frac{s^2}{2\sigma^2}} \tag{9}$$

Where, σ – Determines the quality of the approximation

Now we have,

$$\lim_{\sigma \rightarrow 0} f_\sigma(s) = \begin{cases} 1 & \text{if } s=0 \\ 0 & \text{if } s \neq 0 \end{cases} \tag{10}$$

For the vector s , we have

Where,

$$F_\sigma(s) = \sum_{i=1}^n f_\sigma(s_i) \tag{11}$$

As the values of f_σ is non – smooth for smaller values its maximization is not global over $A \cdot s = x$. Hence, we decrease the sequence of σ which gives the minimum L^0 norm solution.

Least Square estimation. OFDM channel estimation symbols will be transferred periodically in block-type pilot-based channel estimation. In this type based on the pilot signals and received signals estimating the channel conditions will be done. The receiver uses the estimated channel condition to decode the data inside the block. The least-square estimator minimizes the parameter:

$$(\bar{Y} - \underline{X}\bar{H})^H (\bar{Y} - \underline{X}\bar{H}) \tag{12}$$

Where,

$(.)^H$ – Conjugate transpose operation

\bar{Y} – received signals

\underline{X} Pilot signal specified by matrix

Then, the LS estimator of \bar{H} is given by

$$\hat{H}_{LS} = \underline{X}^{-1} \bar{Y} = [(X_k/Y_k)]^T \quad (k=0, \dots, N-1) \tag{13}$$

The LS estimator can calculate the channel conditions even without having any knowledge about the statistics of the channel with very low complexity for calculation. But these calculations are suffering from high mean square error.

MMSE Estimation. The MMSE method minimizes the mean square error by employing second – order statistics of the channel conditions as presented by Bajwa et al. (2008). Assuming that the channel vector \bar{g} and the noise \bar{N} are uncorrelated, it is derived that:

$$R_{HH} = E\{H^T H\} = F R_g g F H \tag{14}$$

$$R_{gY} = E\{\bar{g} \bar{Y}^T H\} = R_g g, F H X H \tag{15}$$

$$R_{YY} = E\{\bar{Y} \bar{Y}^T H\} \tag{16}$$

$$= X F R_g g F H X H + \sigma^2 N I N \tag{17}$$

R_{aa}, R_{HH}, R_{YY} – Represents auto-covariance matrix of $\bar{g}, \bar{H}, \bar{Y}$ respectively

R_{gY} – Represents the cross-covariance matrix between \bar{g} and \bar{Y}

σ_N^2 – Represents the noise variance

By assuming that the auto-covariance matrix and noise variance are known at the receiver in advance, and the MMSE estimator is of \bar{g} is given by \hat{g}_{MMSE} may not be a minimum mean square error. At last, it is calculated that:

$$\hat{g}_{mmse} = R_{gY}^{-1} Y^{HH} \tag{18}$$

$$\hat{H}_{mmse} = F \hat{g}_{mmse} \tag{19}$$

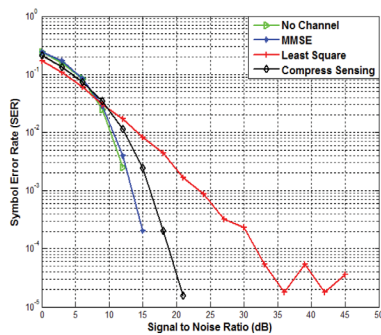
The MMSE estimator surely yields much better performance than the LS estimator, but the only major drawback is its high computational complexity.

RESULTS AND DISCUSSION

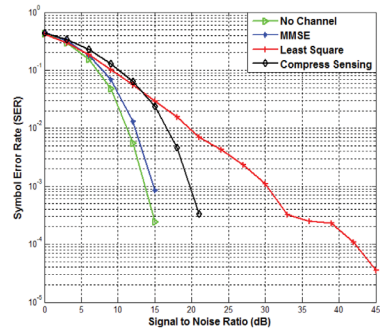
In this section, we have depicted the compressed sensing techniques using DCT transform and evaluated its performance in different channel models, comparing it with traditional techniques like LS, MMSE and with no channel. The comparison is shown in Table 1. We have given the simulation results to compare the performance of the proposed LS, CS and MMSE techniques both at Rayleigh and Rician channel for OFDM system. The data sequences are modulated by M-PSK modulation. The compressed sensing techniques use DCT transform for compressing the data thus, performance is evaluated at particular channel respectively. Here all these estimation schemes are done over Rayleigh channel thus for each modulation schemes graph has been shown below from Figure 2 (a-h). At higher modulation, it becomes difficult to recover the signal from sparse property thus the performance of the CS based estimator deteriorates this is shown in Figure 2(f-h). We observe that SNR required to achieve the symbol error rate (SER) up to 10^{-3} for different estimation schemes at Rayleigh channel are: For LS estimation, it takes about 23dB while for MMSE it takes only 14dB. CS require 16dB and for no channel condition, it takes only 13dB to achieve the same for binary phase shift keying (BPSK) modulation. Similarly, we observed for quadrature phase shift keying (QPSK) modulation that SNR required for LS estimation is 30dB, MMSE is 15dB while for no channel it is 14dB and CS required 20dB to achieve that SER. Similarly, this is also observed for higher order modulation to validate the estimators' performance.

Table 1
BER performance in Rayleigh & Rician Channel

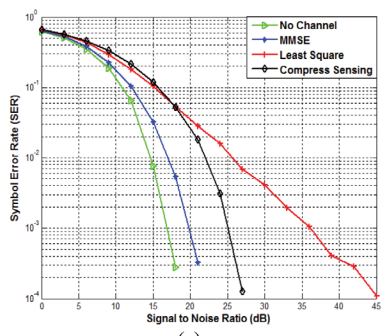
M-PSK	SNR VALUE TO ACHIEVE BER UPTO 10^{-3} (dB)							
	RAYLEIGH Channel				RICIAN Channel			
	NO Channel	LS	MMSE	CS	NO Channel	LS	MMSE	CS
2	13	23	14	16	13	25	35	16
4	14	30	15	20	14	32	18	20
8	17	35	20	25	18	37	27	25
16	22	40	27	32	22	42	32	33
32	26	45	32	42	27	46	28	42
64	32	>45	35	>45	32	48	41	>45
128	37	>45	>45	>45	37	>45	40	>45
256	42	>45	>45	>45	43	>45	45	>45



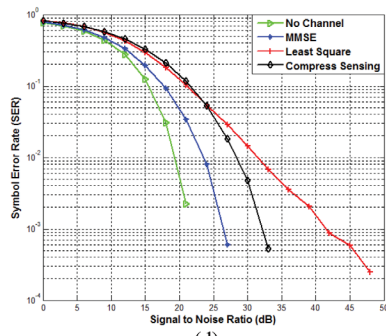
(a)



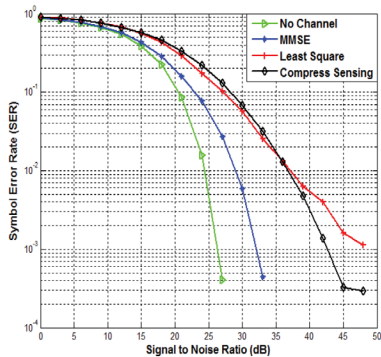
(b)



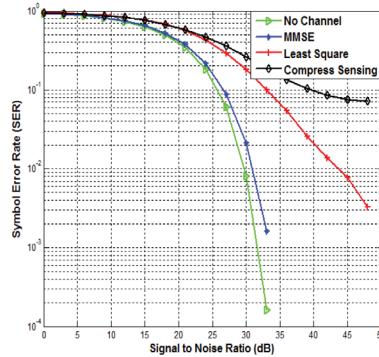
(c)



(d)



(e)



(f)

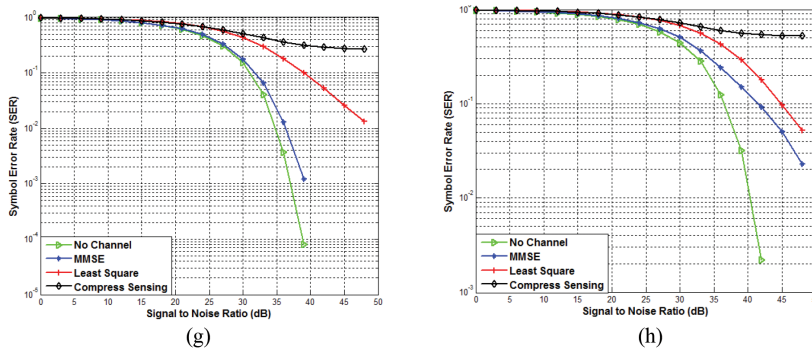
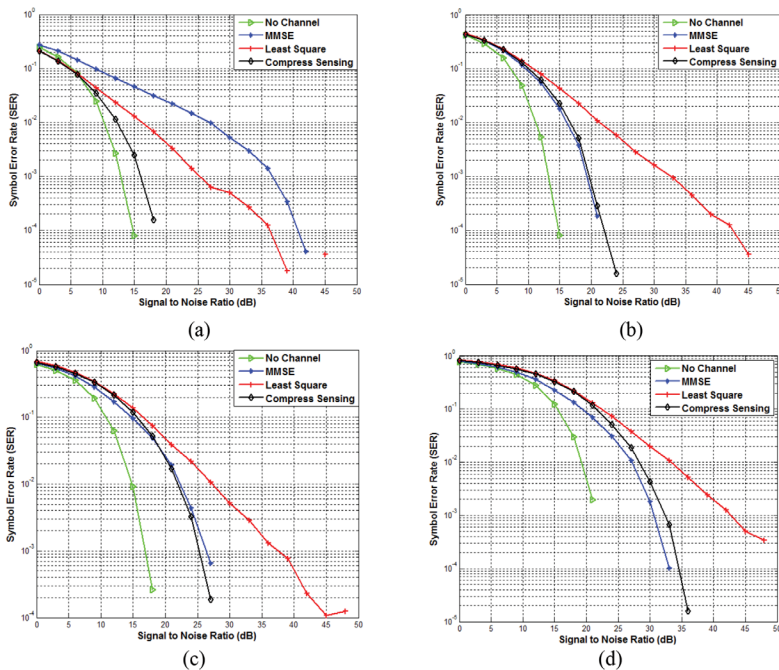


Figure 2 (a-h). SER & SNR comparison for LS, MMSE & CS-DCT estimating technique in Rayleigh Channel (a) BPSK (b) QPSK (c) 8-PSK (d) 16-PSK (e) 32-PSK (f) 64-PSK (g) 128-PSK (h) 256-PSK

Figure 3(a-h). shows the performance of the estimation schemes over Rician channel at which CS based estimation shows a better response at low SNR and at high SNR it matches to LS estimation and its performance deteriorates. In rician channel also, the performance of the LS estimation Scheme is worst. MMSE being the best and CS shows a better response at low SNR as SNR is increased cs performance matches to LS estimation. At higher modulation, it's become difficult to recover the signal from sparse property thus the performance of the CS based estimator deteriorates this is shown in Figure 3(f-h). We observe that SNR required to achieve the SER up to 10^{-3} for different estimation schemes at Rician channel are: For LS estimation, it takes about 25dB while for MMSE it takes only 35dB. CS require 16dB and for no channel condition, it takes only 13dB to achieve the same for BPSK modulation. Similarly, we observed for QPSK modulation that SNR required for LS estimation is 32dB, MMSE is 18dB while for no channel it is 14dB and CS required 20dB to achieve that SER. Similarly, this is also observed for higher order modulation to validate the estimators' performance.



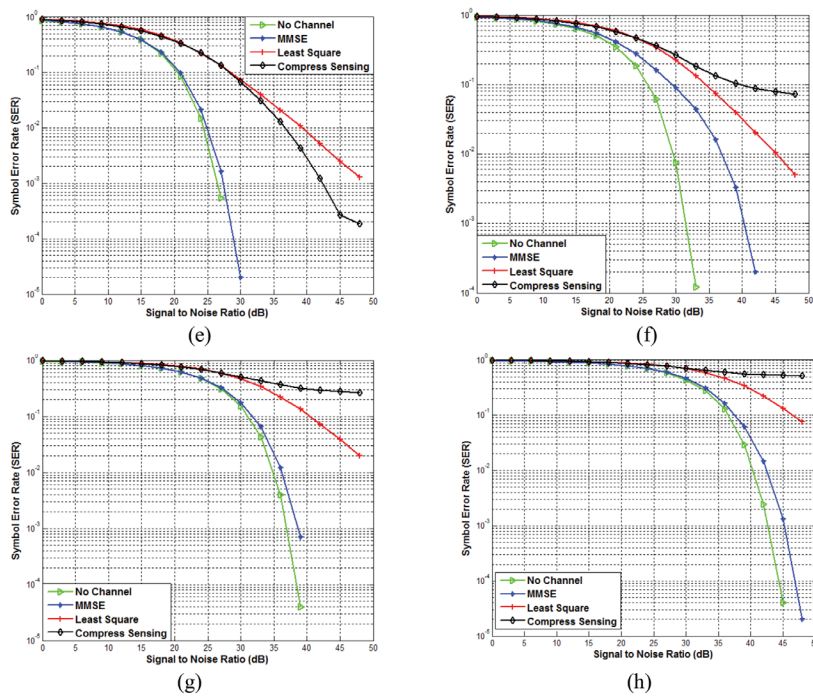


Figure 3 (a-h). SER & SNR comparison for LS, MMSE & CS-DCT estimating technique in Rician Channel (a) BPSK (b) QPSK (c) 8-PSK (d) 16-PSK (e) 32-PSK (f) 64-PSK (g) 128-PSK (h) 256-PSK

CONCLUSION

In this paper the channel estimation schemes based on compressed sensing theory was studied. We first showed the performance evaluation of LS, MMSE and CS method based on M-PSK modulation. Based on channel statistics we made a comparison of the listed schemes on different channel and plot has been made between SNR & SER to show the estimator performance. Through simulation, we concluded that LS estimation was the worst as it required much SNR to achieve the fixer error rate while MMSE was the best. But practically knowing channel state information is not possible so implemented a CS based approach which depicts that at the low value of SNR CS gives the best response but as SNR increases the performance of the CS based estimation deteriorates as proved in higher modulation types. The estimation schemes can be tested for other digital modulation schemes.

REFERENCES

Bajwa, W. U., Haupt, J., Raz, G., & Nowak, R. (2008, March). Compressed channel sensing. In *42nd Annual Conference on Information Sciences and Systems, 2008, CISS 2008* (pp. 5-10). IEEE.

Bajwa, W. U., Haupt, J., Sayeed, A. M., & Nowak, R. (2010). Compressed channel sensing: A new approach to estimating sparse multipath channels. *Proceedings of the IEEE*, 98(6), 1058-1076.

- Chen, J. C., Wen, C. K., & Ting, P. (2013). An efficient pilot design scheme for sparse channel estimation in OFDM systems. *IEEE Communications Letters*, 17(7), 1352-1355.
- Cheng, P., Chen, Z., Rui, Y., Guo, Y. J., Gui, L., Tao, M., & Zhang, Q. T. (2013). Channel estimation for OFDM systems over doubly selective channels: A distributed compressive sensing based approach. *IEEE Transactions on Communications*, 61(10), 4173-4185.
- Donoho, D. L. (2006). Compressed sensing. *IEEE Transactions on information theory*, 52(4), 1289-1306.
- Hsieh, M. H., & Wei, C. H. (1998). Channel estimation for OFDM systems based on comb-type pilot arrangement in frequency selective fading channels. *IEEE Transactions on Consumer Electronics*, 44(1), 217-225.
- Qi, C., & Wu, L. (2011). Optimized pilot placement for sparse channel estimation in OFDM systems. *IEEE Signal Processing Letters*, 18(12), 749-752.
- Tropp, J. A., & Gilbert, A. C. (2007). Signal recovery from random measurements via orthogonal matching pursuit. *IEEE Transactions on information theory*, 53(12), 4655-4666.
- Xiong, X., Jiang, B., Gao, X., & You, X. (2013). DFT-based channel estimator for OFDM systems with leakage estimation. *IEEE Communications Letters*, 17(8), 1592-1595.
- Zhou, Y. H., Tong, F., & Zhang, G. Q. (2017). Distributed compressed sensing estimation of underwater acoustic OFDM channel. *Applied Acoustics*, 117, 160-166.



Cost Estimation Model for Web Applications using Agile Software Development Methodology

Soni, D.* and Kohli, P. J.

Department of Computer Science and Engineering, Jaypee Institute of Information Technology, Noida, Uttar Pradesh 201301, India

ABSTRACT

There are many sophisticated models available for estimating the effort of the software project. However, estimation using existing model developed with agile software is questionable, making it necessary to develop a distinct model for web applications. This paper proposes a model that will evaluate cost of web applications developed through agile methodology and discusses the difference between the conventional software development and web application development.

Keywords: Agile software, cost estimation, function point, Kalman Filter, web objects

INTRODUCTION

Conventional software projects are developed through traditional software development life cycle models as given by Lazić and Mastorakis (2010). However, traditional models are not suitable for projects with changing requirements and rapid changes in application methods. For the development of web applications, different development methodology need to be used. Web applications can adopt agile methodology, which also supports rapid application development. In agile web development, professionals join for building blocks and reusable components using rapid application development process and continuous prototyping (Ziauddin & Zia, 2012). As the methodology opted for development is different for web applications estimation models are needed as suggested by Ochoa (Bastarrica & Parra, 2003).

For the successful completion of a web- based project it is essential to have a good predictor of time and cost in agile environment with limited resources.

In this paper, we introduced a Cost Estimation Model of Web Applications using Agile Software Development Methodology. The model is based on “Model-based Dynamic Cost Estimation and Tracking Method for Agile Software Development”. Section 2 of

Article history:

Received: 29 December 2016

Accepted: 21 April 2017

E-mail addresses:

devpriya.soni@jiit.ac.in (Soni, D.),

kohli@jiit.ac.in (Kohli, P. J.)

*Corresponding Author

the paper, compares the Agile methodology with traditional, RAD and DevOps. In the Section 3 we have presented traditional cost estimation model and agile cost estimation models along with the Characteristic of Agile Based Web Development Projects. The section 4 has the result content which emphasizes on the issues related to web cost estimation and problems associated with the existing models, thereafter, describes the proposed cost estimation model for web applications using agile development methodology.

Comparison of Agile with Traditional Methodology, Rapid Application Development (RAD) and DevOps

Traditional software development is based on factors such as requirement, analysis, design, implementation, testing, deployment and testing whereas agile is based on iterations which operate on confirmed requirements, develop, test system then release and start working on next project. RAD is based on prototype designing and then improving on the code. If there are new requirements traditional development does not have ways to handle it while agile process can keep the system running. Agile divide the solution into features. Devops is a new methodology compared with agile but it is complementary to agile as it is more about deployment and management rather than development. Agile development methodology differs with other methodologies in several ways therefore the estimation model incorporated for traditional methods should also be different for agile method.

METHODS

Traditional Cost Estimation Model

The primary focus of software developers and stakeholders is the time and cost estimation of the software at the time of project commencement. . Cost estimation models can be categorized in two types: 1. algorithmic, 2. non-algorithmic (Kumari & Pushkar, 2013a).

Algorithmic estimation method. Empirical formula are used to estimate the cost of algorithmic models (Kumari & Pushkar, 2013b). Most popular algorithmic software cost estimation models include Source line of codes (SLOC), Object points, Function Point(FP)(Albrecht & Gaffney, 1983), Constructive Cost Model-I (COCOMO-I)(Boehm,1981) and Constructive Cost Model-II (COCOMO-II) (Boehm, Madachy, & Steece, 2000).

Non-Algorithmic estimation methods. Many of the non-algorithmic cost estimation techniques rely on analytical comparison of similar projects done earlier and expert experience (Khatibi & Jawawi, 2011). Most are expert judgment, Analogy, Delphi technique, top-down, thumb rule, bottom-up, price-to-win and Wideband Delphi, Parkinson's Law.

Agile Cost Estimation Models. With the invention of agile methodology new opportunities have emerged. This methodology gained popularity because it emphasized collaboration with customers, communication among developers, fast delivery of product and on demand change

of requirements (Cao, 2008; Schmietendorf, Kunz & Dumke, 2008). Extreme programming, scrum, crystal, feature driven development and learn development are some of the commonly used agile development techniques.

Agile methodology emphasizes team work rather than the individual which contribute to collective effort and work is quantified in terms of effort not in terms of time and changing requirements depending on demand. Various researchers have come up with cost estimation models which are suitable for agile method. Most common is planning poker (Cohn, 2005). Planning poker is simple to implement and it is non-algorithmic model. Other estimation models introduced by researchers are constructive agile estimation algorithm (Bhalerao & Ingle, 2009; Litoriya & Kothari, 2013), although these models have not been evaluated empirically yet (Munialo & Muketha, 2016).

Characteristic of Agile based web development projects. Developers are using various development technologies such as HTML, Java script and java applets, PHP for the development of web based projects. With the Agile process model, various web projects were evolved and became functional in a few months. This rapid development raised several issues. Web based projects were estimated for schedule and cost as the agile method came into existence.

“Agile software development paradigm with component-based software development, visual technologies, and systematic reuse, Reifer (2000)” is illustrated in Table 1. The priority of the companies is to get their software to the market first hence the desire for rapid development. Waterfall model software based on the requirement whereas, agile based Web development is based on iterative and incremental development, rapid application development and continuous prototyping which provided working software with building blocks and reusable components. Web development cost can be determined through Functional Metrics, (David Consulting Group) in Agile Estimation. Estimation of Agile Web developments are also difficult to estimate.

Table 1
Characteristics of conventional versus agile web development projects, Reifer (2000)

	Conventional Approach	Agile Web-based challenges
Estimating process	Use analogy supplemented by lessons gathered from past experience	Job costing done ad hoc based on inputs from the developers.
Size estimation	SLOC or function points are used. Separate models are used for COTS and reused software.	Applications are built using templates and a variety of web-based objects (html, applets, components, building blocks).
Effort estimation	Effort is estimated via regression formulas customized by cost drivers.	Effort is estimated by breaking the job down into tasks and identifying what is needed to do the work.
Schedule estimation	Schedule is estimated using a cube root relationship with effort.	Schedule is estimated based upon analogy. Models typically estimate schedules high because cube root relationship doesn't hold.
Model calibration	Measurements from past projects are used to calibrate models.	Measurements from past projects are used to identify myths.

Note. Table is an adaptation from Estimating Web Development Costs: There Are Differences by Reifer (2000)

RESULTS

Issues Related to Web Cost Estimation

Conventional software development is different than web project development. Agile methodology makes the web development more diverse. Table 2 compares conventional estimation approach and agile web cost estimation challenges (Reifer, 2000).

Estimation of size and duration are the key issues. There is a need to evolve a new metrics for size so that Web objects, building blocks and reusable components can be taken into account. With these many challenges, cube root laws don't seem fit for web applications. Therefore, we need to produce a new model.

Problems associated with the existing models. Characteristics of web based project are discussed with the agile method in Table 1. We cannot apply the prevailing estimation models to web based project developed by agile methodology because of the divers issues related to these models.

1) Model which are taking agile methodology into consideration are not treating web based project separately. Like "Model-Based dynamic cost estimation and tracking method for agile software development" proposed by Kang, Choi and Baik (2010) is the model which has resolved issues related to agile method but characteristics of web based project are not discussed.

Table 2
Challenges of agile web development Reifer (2000)

Characteristics	Conventional Development	Agile Web Development
Key objective	Build quality software products at minimum cost	Bring worth products to market as rapidly as possible under varying requirements of clients
Project size	Medium to large (hundreds of team members)	Small (5 - 7 team members)
Costing	In millions	In thousands
Development approach employed	Classical, requirements-based, water fall or incremental delivery, uses cases, documentation-driven	Rapid application development, gluing building blocks less paper work, XP
Major engineering technologies used	Object oriented methods, generators, modern programming languages (C++), CASE tools, and so forth	Web object based methods, fourth- and fifth-generation technologies like JAVA. Net framework PHP etc.
Processes employed	Capability maturity model-based	Ad hoc

Note: Table is an adaptation from Estimating Web Development Costs: There Are Differences by Reifer (2000)

- 2) Story points are used by many estimation models which are unable to determine the time duration required, Logue, McDaid and Greer (2007).
- 3) A story point is not quantitative measure it is a relative measure, its value changes depending upon the baseline story. Therefore, we require a cost metric whose value does not changes with time, Kang et al. (2010). Model proposed by Kang et al. (2010) have determined function point instead of story point but they have not evaluated the cost involved in web objects.
- 4) Kang et al. (2010) proposed “a function point based daily estimation as cost metric and model based cost estimation and tracking of agile project”. Similar tracking for web component is also required.

Various models have not considered web objects during estimation, which is an important component in estimating the web based project with agile characteristics. Therefore, we proposed a model where web characteristics and agile characteristics are taken into account.

Proposed Model for Web Applications based on Agile Software Methodology

This paper presents a model for estimation of cost of a Web Application using agile software methodology that utilizes function points and web object as the base of measurement. All the function points and web objects are decided at the initial phase of the project. Further, this aggregated value is used as an input to the model proposed by, Kang et al. (2010). Model is used to evaluate the cost of time required by the project through the estimation of the size. Plan of the project can be determined through calculating the function point and web objects then estimation model is generated for rest of the function points and web objects then plan for the project is decided based on duration of the project. Thereafter, velocity is measured on daily basis and growth is traced. The model uses Kalman filter for day-to-day tracking.

Working of model. From estimation model depicted in Figure 1 the function points and value of web objects for the required features were calculated and the model function points obtained. Value of the web objects can be calculated as suggested by Reifer (2000) through Number of XML, HTML, query language links, multimedia Files, scripts, and Web building blocks. The project team decides the duration from release, iteration and day. The duration of release lasts a few months, iteration a few weeks and day to a day. After the velocity is measured for, every day and progress is tracked. The Kalman filter is incorporated for tracking the project. Cost estimation of the software is determined by evaluating the effort involved in developing the software. Function point and web object corresponds to the effort required to develop the software. Therefore, Function point and web object as sizing factors can be used to evaluate the cost of the software. None of the existing estimation model had considered web objects with the function point as a method to provide better estimates for web applications.

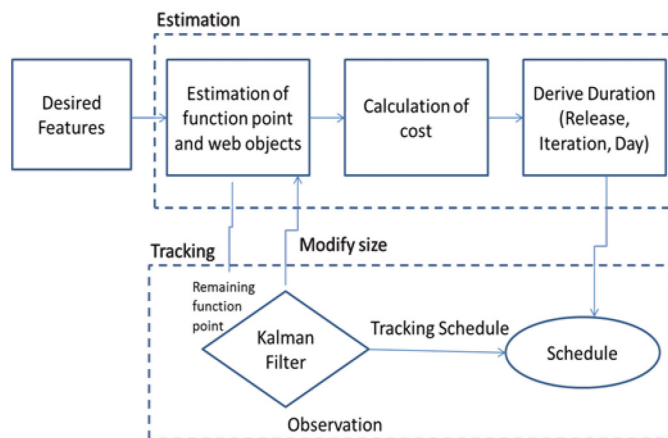


Figure 1. Model for cost estimation of web application using agile development methodology

Day-to-day Tracking. Kalman filtering is an estimating and tracking algorithm used in computer graphics (Welch & Bishop, 2001). Kang et al. (2010) have proposed “a state space model for historical data which estimate the future value of data using Kalman filter algorithm”. If there is a change in the requirement by customer, then the scope changes accordingly and new function point and web objects would be added to the existing ones. This new value is given as input to the Kalman filter and which calculate the cost for new requirements.

Following formula is used to evaluate the estimation of the “state space model” at time t+1.

$$F_t = A_t F_t + W_t \tag{1}$$

Cost estimation can be done through the “state space model”. The above formula can be used to evaluate the cost in terms of persons/month or LOC (lines of code). Equation for the same is given as follows:

$$X_t = H_t F_t + V_t \tag{2}$$

CONCLUSION

Agile methodology emphasizes rapid application development. Web based project developed through agile method are short-term projects. Developing a web based project using agile method allows the incorporation of existing estimation models. In this paper, we have discussed various open issues associated with web development particularly while opting for agile software development. We proposed a model for the estimation of cost for Web Applications developed using agile development methodology. The model used function points and web objects as base of measurement, which can be quantitatively measured rather than a relative measure like story point so it will produce accurate estimation. Empirical validation of the model remains to be done.

REFERENCES

- Albrecht, A. J., & Gaffney, J. E. (1983). Software function, source lines of code, and development effort prediction: A software science validation. *IEEE transactions on software engineering*, 9(6), 639-648.
- Bhalerao, S., & Ingle, M. (2009). Incorporating vital factors in Agile estimation through Algorithmic Method. *International Journal of Computer Science and Applications*, 6(1), 85-97.
- Boehm, B. W. (1981). *Software engineering economics* (Vol. 197). Englewood Cliffs (NJ): Prentice-hall.
- Boehm, B. W., Madachy, R., & Steece, B. (2000). *Software cost estimation with Cocomo II with Cdrom*. Upper Saddle River, NJ: Prentice Hall PTR.
- Cao, L. (2008). Estimating agile software project effort: An empirical study. In *Proceedings of the Fourteenth Americas Conference on Information Systems, Toronto, ON, Canada* (pp. 1-10). AMCIS.
- Cohn, M. (2005). *Agile estimating and planning*. United States of America, USA: Pearson Education.
- Kang, S., Choi, O., & Baik, J. (2010, August). Model-based dynamic cost estimation and tracking method for agile software development. In *IEEE/ACIS 9th International Conference on Computer and Information Science (ICIS), 2010* (pp. 743-748). IEEE.
- Khatibi, V., & Jawawi, D. N. (2011). Software cost estimation methods: A review 1. *Journal of Emerging Trends in Computing and Information Sciences*, 2(1), 21-29.
- Kumari, S., & Pushkar, S. (2013a). Performance analysis of the software cost estimation methods: A review. *International Journal of Advanced Research in Computer Science and Software Engineering*, 3(7), 229-238.
- Kumari, S., & Pushkar, S. (2013b). Comparison and analysis of different software cost estimation methods. *International Journal of Advanced Computer Science and application*, 4(1), 153-157.
- Lazić, L., & Mastorakis, N. E. (2010). Two novel effort estimation models based on quality metrics in web projects. *WSEAS Transactions on Information Science and Applications*, 7(7), 923-934.
- Litoriya, R., & Kothari, A. (2013). An efficient approach for agile web based project estimation: AgileMOW. *Journal of software engineering and Applications*, 6(06), 297-303.
- Logue, K., McDaid, K., & Greer, D. (2007, May). Allowing for task uncertainties and dependencies in agile release planning. In *4th Proceedings of the Software Measurement European Forum* (pp. 275-284).
- Munialo, S. W., & Muketha, G. M. (2016). A review of Agile software effort estimation methods. *International Journal of Computer Applications Technology and Research*, 5(9), 612-618.
- OchoaOchoa, S. F., Bastarrica, M. C., & Parra, G. (2003, November). Estimating the development effort of Web projects in Chile. In *Proceedings of First Latin American Web Congress, 2003* (pp. 114-122). IEEE.
- Reifer, D. J. (2000). Web development: Estimating quick-to-market software. *IEEE Software*, 17(6), 57-64.
- Schmietendorf, A., Kunz, M., & Dumke, R. (2008, May). Effort estimation for agile software development projects. In *5th Software Measurement European Forum* (pp. 113-123). Milan.
- Welch, G., & Bishop, G. (1995). *An introduction to the Kalman filter*: (Technical Report). University of North Carolina, Chapel Hill, NC, USA

Soni, D. and Kohli, P. J.

Ziauddin, S. K. T., & Zia, S. (2012). An effort estimation model for agile software development. *Advances in Computer Science and Its Applications (ACSA)* 314, 2(1), 314-324.

Understanding Consumer Preferences using IoT SmartMirrors

Gaur, L.¹, Singh, G.¹ and Ramakrishnan, R.^{2*}

¹*Amity International Business School, Amity University, Noida, Uttar Pradesh 226010, India*

²*Uflex Limited, Noida, 201301 Uttar Pradesh, India*

ABSTRACT

Internet of things (IoT) has so far been considered to be a complex network of objects speaking to each other across a digital network transmitting information and broadcasts about themselves and their surroundings through an assembly of sensors, actuators and motors. In this paper we present a use case for IoT to understand and record consumer behavior. In essence the paper attempts to classify how humans and IoT devices can learn from each other. In this paper retail smart devices can help salespersons understand more accurately a consumer or shoppers preferences and suggest more suitable options.

Keywords: Human – IoT bridge, Indian enterprises, Intelligent gesture recognition, Internet of Things, Knowledge recording, SmartMirrors

INTRODUCTION

Internet of Things (IoT) refers to the growing cyber physical development of augmenting physical devices with computing and communication capabilities to collectively gather information on real time basis (Guo, Zhang, Wang, Yu, & Zhou, 2013).

With Internet of Things as a global network allowing communication between objects-objects and objects-humans a unique identity for each and every object (Aggarwal & Das, 2012) new technology horizons have opened up.

Ferguson, T. (2002) has emphasized the importance of objects having the ability to communicate can speed up processes, reduce error, prevent theft, and incorporate complex and flexible organizational systems through IoT.

Numerous research papers illustrate comprehensively that customers' requirements play a key role in product performance in conceptual design (Häubl & Murray, 2001). The textile sector in India is one of the oldest industries in the economy contributing

Article history:

Received: 29 December 2016

Accepted: 21 April 2017

E-mail addresses:

gsingh@amity.edu (Gaur, L.),

lgaur@amity.edu (Singh, G.),

ravi.ramakrishnan@gmail.com (Ramakrishnan, R.)

*Corresponding Author

11 per cent of total exports (USD41.4 billion in 2014-15) and employing a huge population (Ministry of Textiles, Tech Sci-Research Note).

India has a sizeable chunk of millennial and is one of the biggest fashion markets and shopping trends have changed from open markets to mom and-pop stores to multi-storied shopping malls. SmartMirrors are highly functional advanced mirrors manufactured by integrating embedded electronics such as displays, cameras, and sensors. SmartMirrors offer an array of features such as Internet connectivity and some products offer touch screen option. Globally, the SmartMirror market is witnessing significant growth due to increasing demand for the SmartMirror in major shopping outlets & malls. By connecting IoT to SmartMirror, it is possible to implement a variety of application services. SmartMirror that has been linked with IoT platform is friendly and variety provides information to user (Moon, et al., 2015). The global SmartMirror market has been estimated to be valued at USD386.8 million in 2015, and is expected to witness a healthy compound annual growth rate (CAGR) from 2016 to 2022 (Persistence Market Research, 2017). The IoT powered SmartMirrors offers retailers opportunities in three areas: improving customer experience, measuring product or apparel acceptability / trials / converts, and new channels and revenue streams.

This article provides an exploratory research on the use of SmartMirrors in the retail garments shopping to determine their efficacy in influencing customer shopping and also increasing shop seller's productivity by reducing number of actual trials and identifying potential sales and non-materialized sales.

Literature Review

Bellman, Lohse, and Johnson (1999) described some factors that predict customer buying behavior. Laudon and Traver (2001) list some aspects of consumer profile to explain customer online behavior. In the context of online shopping to attract more customers' purchasing, Haubl and Murray (2001) believe that a selective recommendation agent can play a prominent role to persuade consumers' purchase decision. Their findings suggest, "An electronic agent have the potential, whether intentionally or unintentionally, to persuade users that certain alternatives are preferable to others."

Solima, Della Peruta and Maggioni (2015) has presented a strong case backed by exploratory research on using IoT devices as a visual aid for museum visitors. It has been shown that implementing IoT solution introduces a plethora of new products, services and business models for guides and cultural events.

Ceipidor et al. (2011) has explained a ShopLovers solution as tool to use interconnected objects powered by Radio-frequency identification (RFID) to enhance social connect of customers and brands which runs on mobile devices and transforms the shopping experience using Near Field Communication (NFC) and other technologies. This solution helps customers coordinate actions in a retain environment such as checking out products and making payments or referring choices to friends and ask their advice.

Ching, Yue and Lee (2016) has explained technical feasibility of developing a tele-presence robot which can adopt social expressions with facial contours and gestures. These can be used for ad-hoc conversations in offices or as a guided tour for retail shoppers.

Randelli, Bonanni, Iocchi and Nardi (2012) has explained the aspect of knowledge acquisition through interaction between humans and robots. It is argued that a robot due to their limited understanding of their surroundings restricts their capabilities and utility in real world situations. However, using speech technologies and vision based systems and established AI algorithms human skills can be learnt by robots leading to accomplishment of more tasks.

Guo et al. (2013) has demonstrated the concept of opportunistic IoT (which is a decentralized ad-hoc human centric networks e.g. customers connecting Bluetooth over a coffee shop) which is the observed close relation between human and smart objects enabling information forwarding. Information so captured by this interaction can be carried forward to other opportunistic IoT communities. Weiser (1991) prophesized that pervasive computing can learn and adapt to human needs.

IoT consists of three capabilities user awareness (personal contexts and behaviors), ambient awareness (space status) and social awareness (group level detection of patterns) (Guo et al., 2013).

METHODS

Technical Layout - SmartMirror

The proposed solution suggests the following applications of a Smart Meter in engaging customers and ensuring a higher trial to sales ratio in the case of readymade apparels (Figure 1).

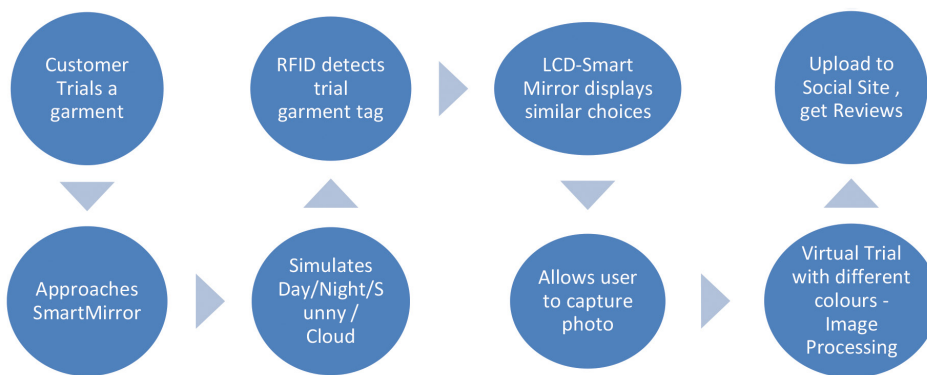


Figure 1. Process flow SmartMirror

- A SmartMirror made of acrylic or glass with adjustable lighting (two-way mirror). These mirrors allow a Liquid Crystal Display (LCD) to be fitted behind while retaining the properties of a Mirror to be used in retail trial external rooms. The mirrors have a Light Emitting Diode (LED) background lighting which can be dimmed to simulate day light, night light or cloudy or sunny environment.
- Raspberry PI device for computing power with WI-FI access and RFID tag reader. The raspberry Pi allows limited processing power; powered by a Linux OS it allows Data retrievals, image processing and content display.

- Kinect Camera for 3d Sensing and tracking user gesture, this can be for an advanced model to detect a customer's touch preferences on the mirror and accordingly simulate actions such as dimming lights for a specific selection using finger movements, simulating a like or dislike again using gestures.
- LCD display behind the Mirror for content and image display. The LCD will display matching images of similar costumes while also allowing consumers to take photographs and upload the content to their social networking sites to get reviews.
- Software for coordination and orchestration and connecting to back end inventory system. The software performs a myriad of activities including reading the RFID tag of the clothes being tried and then getting data from the back-end systems matching the tag category as suggestions. The software keeps track of user preferences and final selection to constantly give better choices and thereby increase sale converts from trials.
- RFID tags attached to the garments for identification uniquely, this allows grouping of similar tags apparels.
- Integration between social networking sites, content (Application Programming Interface, API).

The process consists of all garments being tagged with a RFID tag, the SmartMirror being enclosed in an open Kiosk, and each consumer being given a RFID card (to be used dually as a brand loyalty card). The consumer tries a ready-made garment, approaches the SmartMirror which detects the garment using the tag and the consumer identity using the card. The SmartMirror collects data of past purchases to give many upsell and cross sell ideas to the consumer through a complex algorithm consisting of his past purchase trends and the other consumer trends on same age group or profile and also the other similar options available in the store. The consumer also has an option to click a photo and upload to connected social network sites and with friends to get their opinion resulting in a higher acceptance and sale. Finally, the SmartMirror also has options to adjust lighting to give different appearance of a sunny bright day, night or evening, cloudy or winter to help users understand the clothes appearance in diverse weather conditions.

The SmartMirror gets insights with the number of customer usage and it provides a ready to use data mine for number of trials, most accepted or tried garment set and the garments which face rejection due to size or color limitations to the merchant. Thereby allowing the seller to understand the reasons for non-converted sales and work towards having a fast selling stock reducing capital lock in in no moving items.

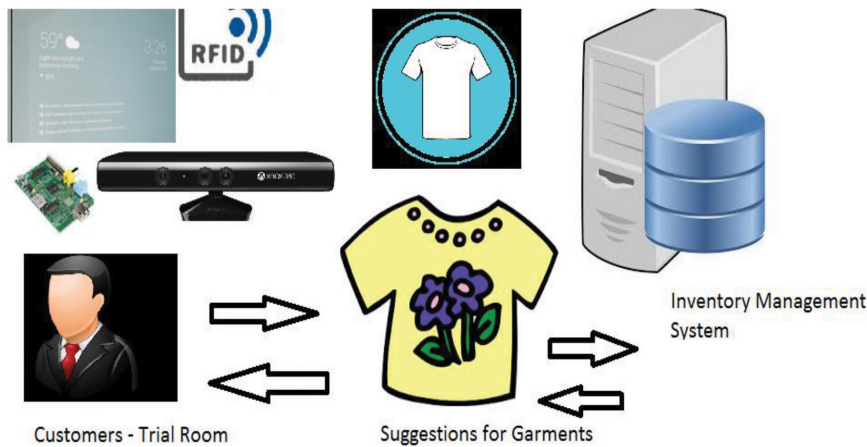


Figure 2. SmartMirror suggesting a customer

The SmartMirror can further use AI to superimpose different costumes on the person's mirror reflection there by reducing time for trials, effort in cleaning up tried garments and also pilferage or damage to clothes.

The above process helps a consumer simulate virtually based on suggestions given by the SmartMirror backed by analytics, this is a combination of machine intelligence (adaptive intelligence) and user preferences. The following analytics are of significance from customer and retailer point of view.

Consumer gets insights based on his current selection, what other consumers have purchased or liked there by providing real time insights.

Retailer gets insights on customer's preferences for each garment including his level of likes and dislikes thereby stocking more preferred items and also having a higher trial to convert ratio.

The system can be enhanced by identifying using facial recognition or a IoT wearable the exact customer approaching the Smart Meter thereby giving him a personalized offering and also keep his history of transactions and preferences in the past thereby getting valuable insights into changing trends at an individual customer level (Figure 2).

RESULTS AND DISCUSSIONS

To motivate our research, we did a secondary data analysis using literature review of existing implementation cases.

First, a high-street shop Neiman Marcus, San Francisco which has installed a Memory Mirror the major benefit to customers being a reduction in the long process of trying and re-trying on clothes. The Memory Mirror shows you a 360-degree view of customers with the outfit on and allows comparing outfits side-by-side. It also snaps photos of customer with the outfit to share with friends on Facebook to ask for their opinion before making a purchase.

Second, Ralph Lauren, New York, with a SmartMirror inside the changing room, mirror is programmed to transform the lighting and also change the outfit colors and size and try out virtually using interactive touch. It also allows integration with smartphone of the helpers who

can bring the desired color and size. The mirror also recommends other items which can go with the original choice. Following this a trial was conducted for limited set of respondents on whether they found the study satisfactory or value adding. Based on both of this the paper arrives at a logical conclusion.

Michelleti (2003) asserts women drive consumer activism than men primarily because they do daily shopping, they are more concerned about the impact on family and finally because they have had to work more due to historical exclusion from decision making.

To understand the premise for such as SmartMirror need, the researchers used the Observation method in a leading retail garment shop to identify on random days the pattern of buying. As part of this daily two families or individual was observed ever since they entered the shop till the time they exited and on subsequent days to eliminate bias. Observation sheets were structured and standardized It was observed after consolidating observation sheets of 25 families that:

- Clothes purchased were similar in design/ fabric to what the customer was currently wearing in other words current clothing pattern could predict buying pattern.
- Across age group clothing trends were similar or could be related logically.
- Color choices were very distinct either dark or light and it also had a bearing on one of the clothes of the purchaser or the family member.
- Lastly purchases spend over 80% of the time locating clothes of right sizing, similar design but different colors and around 20% of the time in trials
- Trials rooms on an average took almost 8-10 minutes per buyer for trying out and usually 3 sets of clothes were tried out at the same time.
- The attendants spend roughly 5 minutes repacking, restoring to original place the tried-out clothes.

The above observations could be addressed in a scientific manner using the SmartMirrors as per the researchers.

- The SmartMirror using Cognitive algorithms could predict the buyers age, current clothing sense and colors to predict matching designs and patterns
- SmartMirror algorithms could be used for virtual trails reducing the need for packing and replacing and also blocking the trial rooms for a longer period.
- Lastly SmartMirrors could serve as virtual shopping assistant thereby suggesting stocks in place in the store rather than for endless searching and not finding a matching garment.

Table 1
Descriptive statistics on sample

		Age Group			
		<i>Frequency</i>	<i>Percent</i>	<i>Valid Percent</i>	<i>Cumulative Percent</i>
Valid	<30	32	58.2	58.2	58.2
	>30	23	41.8	41.8	100.0
Total		55	100.0	100.0	

The researchers tied up with a SmartMirror manufacturer and the system put on trial in a controlled environment with around 55 women participants. Each participant was briefed on the technology and their responses recorded to create a clothes inventory with RFID tags. Actual evaluation was conducted and based on 6 close ended questions were presented to help review perception of the systems usability. A 5 point Likert scale was used to develop an ordinal ranking of preferences concerning the perceived utility of the SmartMirror and its contribution in and motivation in using this technology. The survey was administered in person over one week day and one week end. Descriptive statistics were calculated and there after the data was analyzed and using factor analysis it was seen if we can reduce them to one variable “buyer and seller utility”. The following graphs show the descriptive statistics of this survey sample.

The descriptive statistics shows that the sample has comparable sizes on population from both age group segments below 30 and above 30.

Table 2
Measures of central tendency

		Statistics				
		<i>Age Group</i>	<i>Faster Selection</i>	<i>Faster Trial</i>	<i>Better Feedback</i>	<i>More Informed on Stock Status</i>
N	Valid	55	55	55	55	55
	Missing	0	0	0	0	0
	Mean	1.4182	3.4182	3.4909	3.9273	4.2182
	Median	1.0000	3.0000	3.0000	4.0000	4.0000
	Mode	1.00	2.00	3.00	4.00	4.00

We do a test for the normality of data across the two groups. Since the sig value is less than .05 hence normality of data cannot be concluded.

Table 3
Tests of Normality

		<i>Kolmogorov-Smirnov^b</i>			<i>Shapiro-Wilk</i>		
		<i>Statistic</i>	<i>df</i>	<i>Sig.</i>	<i>Statistic</i>	<i>Df</i>	<i>Sig.</i>
<i>Age</i>	Neutral	.417	12	.000	.608	12	.000
<i>Group</i>	Agree	.485	15	.000	.499	15	.000

a. *Age Group is constant when Faster Selection = Disagree. It has been omitted.*

b. *Lilliefors Significance Correction*

c. *Age Group is constant when Faster Selection = Strongly Agree. It has been omitted.*

The analysis of survey results shows that the SmartMirror has definitely resulted in a better feedback mechanism for the sellers on customer preferences and made the buyers more aware of stock after making the initial selection of different colors and designs. The results on faster trials or faster cloth selection are not very clear though it holds potential for future. Further it was shown that SmartMirrors using advanced cognitive image processing algorithms could reasonably well detect the buyers profile, current clothing and color preference, age and gender and together with a robust integration could reduce time to buy significantly, convert more trials to sales and finally reduced the maintenance for replacing tried out garments. The biggest benefit came from the less time spent in the shop thereby reducing crowd and keeping space for potential customers.

There are number of challenges in the proposed solution. Technically security can be a major challenge as more and more objects start intruding privacy and identity in a cyber-physical space. Additionally, whether the virtual simulation though gives a lot of comfort will be it fulfilling in terms of garments trials. However, this point can be mitigated as we see increasing volumes of ecommerce garment purchase just by viewing the pictures of the garment online. Ensuring number of such mirrors will also be a challenge however it is evident that the number of trial rooms though limited is able to satisfy the demand even with increasing footfalls. It needs to be seen whether the mirrors can perform myriad other revenue generating functions like advertisements or display boards when they are not in use using their wireless content broadcast and accepting architecture.

From the research aspect the small sample size may not meet population mean expectations and the questions may be too general in nature. Factors such as longitudinal effects, cultural effects, gender effects and segments such as high end designer clothes have not been taken into account and could affect research results. The earlier observation is very limited in scope and may vary for stores with attendants and with higher technology advancements. The research also suffers from limited field survey and convenience sample.

CONCLUSION AND FUTURE SCOPE

Cyber physical machines have huge potential in health care, retail, manufacturing, energy to name a few. IoT objects such as SmartMirrors have the potential to bridge the current knowledge divide between sellers and consumers especially in the case of readymade garments and track

the trial of clothes and the ratio between trials and converted sales. While trials of garments give an indication of customer's purchase interest most instances trials do not convert to sales due to color issues, design issues, lack of correct sizing and fitting and thereby influencing choice decision. This paper shows how SmartMirrors can capture data on trials and reduce time spent searching for alternatives by giving suggestions intelligently or alerting support staff. Technologically IoT devices embedded in utility appliances like mirrors can help decision making and with the integration of data. In future SmartMirrors may have capabilities to recognize a prospective buyer. Integration with other social channels like social media can further add value by real time sharing of information. The trend is visible across age groups as seen from the survey results which confirms quantitatively the use of SmartMirrors and hence can be adopted to successfully replace traditional mirrors. Worldwide there are many cases of SmartMirrors implementation but there are more informative than transactional. A blended solution with instructiveness and intuitive solutions like facial recognition, speech recognition, and emotion recognition and finally preference recording and suggestions will lead to faster adoption and better customer benefits.

REFERENCES

- Aggarwal, R., & Das, M. L. (2012, August). RFID security in the context of internet of things. In *Proceedings of the First International Conference on Security of Internet of Things* (pp. 51-56). ACM. New York, NY, USA.
- Bellman, S., Lohse, G. L., & Johnson, E. J. (1999). Predictors of online buying behavior. *Communications of the ACM*, 42(12), 32-38.
- Ceipidor, U. B., Medaglia, C. M., Volpi, V., Moroni, A., Sposato, S., & Tamburrano, M. (2011, September). Design and development of a social shopping experience in the IoT domain: The Shop Lovers solution. In *19th International Conference on Software, Telecommunications and Computer Networks (Soft COM), 2011* (pp. 1-5). IEEE, Split, Croatia.
- Ching, P. W., Yue, W. C., & Lee, G. S. G. (2016, April). Design and development of edgar-a telepresence humanoid for robot-mediated communication and social applications. *IEEE International Conference on Control and Robotics Engineering (ICCRE), 2016* (pp. 1-4). IEEE, Singapore.
- Ferguson, G. T. (2002, June). Have your objects call my object. *Harvard Business Review*. Retrieved from <https://hbr.org/2002/06/have-your-objects-call-my-objects>
- Guo, B., Zhang, D., Wang, Z., Yu, Z., & Zhou, X. (2013). Opportunistic IoT: Exploring the harmonious interaction between human and the internet of things. *Journal of Network and Computer Applications*, 36(6), 1531-1539.
- Haubl, G., & Murray, K. B. (2001, October). Recommending or persuading? The impact of a shopping agent's algorithm on user behavior. In *Proceedings of the 3rd ACM conference on Electronic Commerce* (pp. 163-170). ACM. Florida, FL, USA.
- Laudon, K., & Traver, C. (2001). *Business. Technology. Society*. Boston, New York, NY: Addison-Wesley Longman Publishing Co., Inc.
- Michelletti, M. (2003). *Individuals, consumerism and collective actions*. New York, NY: Palgrave Macmillan.

- Moon, Y. B., Oh, S. W., Kang, H. J., Lee, H. S., Kim, S. J., & Bang, H. C. (2013, September) Smart Mirror Health Management Services based on IoT Platform. In *Proceedings of the 14th International Conference on Applications of Computer Engineering*, (pp. 87-89). Seoul, South Korea.
- Randelli, G., Bonanni, T. M., Iocchi, L., & Nardi, D. (2013). Knowledge acquisition through human-robot multimodal interaction. *Intelligent Service Robotics*, 6(1), 19-31.
- Solima, L., Della Peruta, M. R., & Maggioni, V. (2016). Managing adaptive orientation systems for museum visitors from an IoT perspective. *Business Process Management Journal*, 22(2), 285-304.

Investigation on Tapping of Al6061-SiC Metal Matrix Composite with HSS Taps

Melvin Paious¹, Raviraja Adhikari² and Nagaraja^{2*}

¹*Department of Mechanical Engineering, Saint Thomas College of Engineering and Technology, Kannur, Kerala State 700027, India*

²*Department of Mechanical and Manufacturing Engineering, Manipal Institute of Technology, Manipal University, Karnataka State, 576104 India*

ABSTRACT

The present study deals with tapping of Al6061/SiC metal matrix composite. Stir casting technique was used for the fabrication of composite. Castings were produced by varying weight percentage of SiC (5, 7.5 and 10 wt. %) of 23 μm size in Al6061. The fabricated specimens were characterized for their hardness and tensile strength. It was found that hardness increases by the addition of SiC. Images from Scanning Electron Microscope (SEM) and metallurgical microscope showed the fair distribution of reinforcement. Due to the presence of SiC reinforcement that is highly abrasive in nature makes machining difficult and produces high rate of tool wear. After drilling, tapping experiments were conducted for the machinability study of Al6061/SiC metal matrix composite by using M8 HSS machine tap. Tapping operation was performed under dry condition with different cutting speed (12, 14 and 16 m/min) and constant feed rate equal to the pitch of thread. Torque required for tapping was measured using strain gauge based two-component cutting tool dynamometer. Microstructure and surface morphology of thread surfaces was analyzed using Metallurgical Microscope and Scanning Electron Microscope (SEM) respectively. Estimation of progressive flank wear of machine taps was undertaken using profile projector. The performance of HSS machine taps was evaluated in terms of tapping torque, tool flank wear and surface characteristics of thread surfaces.

Keywords: Al6061, flank wear, machine tap, metal matrix composite, stir casting, tapping

Article history:

Received: 11 January 2017

Accepted: 21 April 2017

E-mail addresses:

melvinpaious@gmail.com (Melvin Paious),
ravi.adhikari@manipal.edu (Raviraja Adhikari),
nag_mech@manipal.edu (Nagaraja)

*Corresponding Author

INTRODUCTION

Aluminium based composites are increasingly being used in the transport, aerospace, marine, automobile industries, owing to their improved strength, stiffness and wear resistance properties. The widely used reinforcing materials for these composites

are silicon carbide, aluminium oxide and graphite in the form of particles or whiskers (Kumar, Rao, Selvaraj & Bhagyashekar, 2010). Stir casting is the most economical, flexible and easy method to prepare aluminium silicon carbide metal matrix composite. It involves melting of the matrix material, followed by introducing reinforcement material into the melt, obtaining a suitable dispersion through stirring (Soltani et al., 2015).

Metal matrix composite materials are one of the most difficult to machine due to their inherent inhomogeneity, abrasive nature of reinforcements and anisotropic nature resulting in high tool wear and subsurface damage. The extensive tool wear is caused by the very hard and abrasive reinforcements (Wilson & Harvey, 1959). The main reason for wear is the direct contact between the reinforcing particles and the cutting edge which causes both a mechanical and a thermal load on the cutting edge (Kilickap, Cakir, Aksoy & Inan, 2005). The dominant wear mechanism is abrasion generated by impacts at the cutting edge and by the sliding motion of the particles relative to the rake and clearance face. Additionally, thermal load stresses the cutting edge. This thermal load results from hot spots which are generated by micro contacts between the cutting edge and the reinforcement.

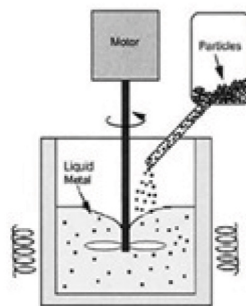


Figure 1. Schematic diagram of stir casting setup (Chawla & Chawla, 2006)

From previous studies it can be discerned that the reinforcement material, type of reinforcement, weight percentage of the reinforcement and matrix properties as well as the distribution of these particles in the matrix are the factors that affect the overall machinability of these composites (Hung, Boey, Khor, Phua & Lee, 1996). Cutting speed, feed and depth of cut have a similar effect on tool life and surface finish in machining of metal matrix composites (Sahoo, Pradhan & Rout, 2013).

The reinforced particles tend to dislodge themselves from the matrix and roll in front of the cutting edge, to plough through the machined surface and generating grooves on it (Sekhar & Singh, 2015) The tool life decreases while the surface finish improves only slightly with an increase in cutting speed, since the tool temperature increases with cutting speed, thereby softening the tool material.

A tap is simply a hardened steel screw with lengthwise grooves, called flutes, milled or ground across the threads. In a machine tap, flutes form a series of teeth and provide chip room along the entire length of the threaded portion of the tap.

When a tap is turned into a hole of proper diameter, the teeth cut into the wall of the hole and remove material to form threads of the same pitch as the threads found in the tap. The majority of tapping process is done by the teeth on the chamfer portion and the first full following thread (Drozda & Wick, 1983).

The common failures of tapping are tap breakage and poor thread quality. From the metallurgical point of view, the shape of a tap causes very high surface stress concentrations as it is subjected to both torsional and bending loads (Sha & Wu, 1990). Generally, tap breakage may be caused by overload, material fatigue, inadequate heat treatment etc. The quality of the thread is decided by the size and surface finish. The threaded hole may be undersized or oversized. In a threading operation, surface finish is usually not crucial, if the thread is to be used for a fastener. But, the burr on the entry or exit of the hole can cause a significant problem. The major causes of the above symptoms are tap wear, error in size of hole, misalignment, and poor lubrication. Information available on the tapping of metal matrix composite is very rare and incomplete.

Extensive research work has been done on turning and drilling of Al6061/SiC metal matrix composite. However, there has been little attempt on studies involving tapping of Al6061/SiC metal matrix composite. Therefore, it is essential to create more knowledge about tapping on Al6061/SiC metal matrix composite. The aim of the present study is to bring out the influence of varying percentage of presence of SiC in the matrix, cutting speed on tool wear and surface roughness of the threaded hole.

METHOD

Fabrication of Specimens

The matrix material selected for the present studies was Al6061 alloy and was procured from HINDALCO Industries Limited, India. The chemical composition of Al6061 alloy, as provided by the supplier is given in Table 1.

Silicon carbide particles of size 23 microns was used as reinforcement material having properties such as high hardness and strength, chemical and thermal stability, high melting point, oxidation resistance and high erosion resistance.

The schematic diagram of the setup used for fabrication of metal matrix composite is shown in Figure 1. Al6061 rods were melted at a temperature of 800°C using an electric furnace. Preheating of silicon carbide particles was done at 600°C for an hour to remove the moisture and gases from the surface of the particulates. The aluminium melt is degassed at a temperature of 750°C using nitrogen gas. Degassing eliminates a variety of impurities which could pose serious problems in the production of quality castings. At the forefront of these impurities is hydrogen. The solubility of hydrogen in molten aluminium increases with temperature. Solidifying metal must reject the hydrogen. Otherwise resultant castings will suffer from porosity. To increase the wettability of the silicon carbide particles in the matrix material, 2 wt. % magnesium ribbons was added to the molten metal. Stirring of molten metal with SiC particles added slowly was done for 10 minutes.

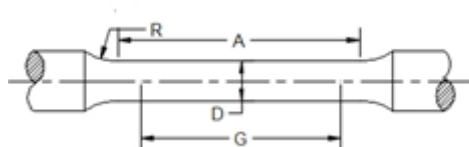
Table 1
Chemical composition of Al6061

Contents	Weight Percentage
Al	97.547
Si	0.773
Fe	0.22
Mn	0.068
Mg	0.922
Cu	0.276
Ti	0.22
Cr	0.072

CHARACTERISATION OF SPECIMENS

Vickers Hardness and Tensile Test

Specimens for Vicker's hardness test were prepared from round castings by turning and polishing with different grades of abrasive paper. Hardness test was carried out using Micro Vicker's Hardness Tester (Matsuzawa make). Five sample points were taken for averaging the hardness test value. The tensile test specimens were prepared according to ASTM E8/E8M-11 standard, as shown in the Figure 2. The tensile test was performed on an electronic tensometer.



$$A = 36 \text{ mm}, D = 6 \text{ mm}, G = 30 \text{ mm}, R = 6 \text{ mm}$$

Figure 2. Tensile test specimen

Micro Structure and Surface Morphology

The microstructure plays an important role in the overall performance of a composite and the physical properties depend on the microstructure, reinforcement particle size, shape and distribution in the alloy. Microstructure study of the composites was done using Trinocular Inverted Metallurgical Microscope. The surface morphology of the work materials was captured by using EVO MA18 Scanning Electron Microscope (SEM).

EXPERIMENTATION

Setup

The tapping experiments were conducted on Computer Numerical control (CNC) vertical machining centre (M/s Ace Manufacturing Systems, Bangalore, India) at constant feed rate of 1.25 mm/rev (pitch of thread) with speeds 12, 14 and 16 m/min. The material behavior of Al6061/SiC composite was expected to be in between aluminium alloy and cast iron. The cutting speed for the tapping operation was selected between the tapping speed for cast iron (9-12m/min) and aluminium (19-22 m/min) (C. M. T. I., 1987). High Speed Steel (HSS) machine taps M8X1.25 with three flutes was used for tapping operation. Before tapping, the specimens were pre-drilled with 6.8 mm diameter drill bit. Figure 3 shows the arrangement used for conducting tapping experiments on composites.



Figure 3. Arrangement used for conducting tapping experiments on composites

A strain gauge based Drill tool dynamometer (IEICOS, Bangalore, India) was used for measuring thrust force and torque produced on the work piece during the tapping operation. IEICOS digital multi component force indicator which comprises digital displays calibrated for force and torque measurement with two component drill tool dynamometer was used for measuring the values.

Measurement of Flank Wear

The wear pattern of the machine tap was obtained using a Profile Projector (METZER, India) with a magnification of 20X. The profile of the tap before and after tapping was compared for variations in the profile. The reduction in the height of cutting tooth (h) in the chamfer section is used as a measure of flank wear, as shown in Figure 4.

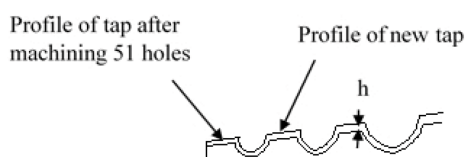


Figure 4. Profile of the chamfer portion of tap

Measurement of Surface Roughness

Surface roughness of the thread surface of tapped hole (hole no: 1,13,26,38 and 51) for all composites (5 wt. %,7.5 wt. % and 10 wt. % of SiC) was measured using Surtronic 3+ surface roughness measuring instrument. For surface roughness test, sampling length of 0.25 mm and average of 3 readings was taken.

Surface Morphology and Microstructure Analysis of Machine Tap and Tapped Hoe Surface

Microstructures of thread surface were taken from the Trinocular Inverted Metallurgical Microscope. The surface morphology of the thread surface was captured by using EVO MA18 (Zeiss) Scanning Electron Microscope (SEM). Thread surface analysis will reveal information such as, effect of tool wear and flow of work piece material during tapping on the thread surface.

RESULTS AND DISCUSSIONS

Hardness Test

Table 2 shows the hardness values of metal matrix composites having different percentage of SiC. The hardness value increased with increase in weight percentage of SiC reinforcement. The increase in hardness was expected, since SiC particles being very hard contribute positively to the hardness of the composite (Su et al., 2010) Nearly one third increase in the hardness value was recorded for the 10% SiC reinforced composite in contrast with those of 5% SiC. This increased hardness could be attributed to the hard SiC particle acting as barriers to the movement of dislocations within the Al6061 matrix (Kannan & Kishawy, 2008).

Table 2
Vickers micro hardness test results

Material wt. %	Vicker's Hardness Number (VHN)
Al+ 5SiC	68.08
Al+7.5SiC	80.53
Al+ 10%SiC	99.7

Tensile Test

From Table 3, it was observed that the ultimate tensile strength (UTS) measured using a tensometer (Khudal Instruments, Pune, India) increased with the addition of SiC. This increase in UTS may be due to the increased presence of SiC particle that acting as barriers to dislocation in microstructure (Kannan & Kishawy, 2008).

Table 3

Tensile test results

Material Wt. %	Avg. Ultimate Tensile Strength(MPa) (Standard:ASTME08)
Al+ 5SiC	113.25
Al+7.5SiC	135.6
Al+ 10SiC	151.32

Surface Morphology and Microstructure Analysis of Composite

The surface morphology and microstructure of the composite are shown in Figure 5 and 6. The microstructure of the composites at 100X magnification shows satisfactory dispersion of SiC particles in the matrix. The uniform distribution of particles is positively reflected in tensile and hardness test values. The dark spots are the discrete SiC particles embedded in Al6061 matrix. There is no agglomeration of reinforcements in the matrix. The microstructure does not reveal the existence of blowholes. The achievement of uniform dispersion of SiC particles in the microstructure of Al based matrix composites has been used as a strong measure of the quality of composites (Teti, 2002).

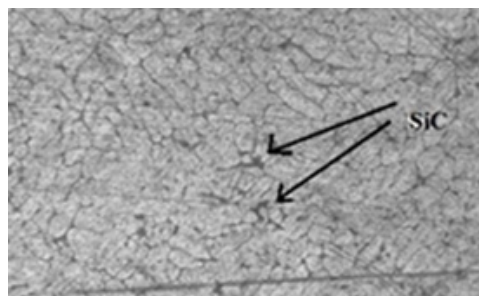
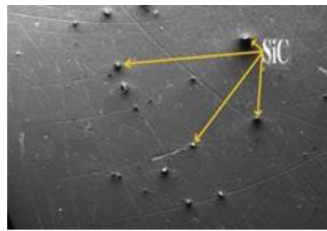
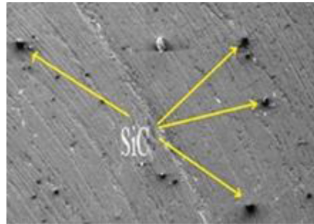


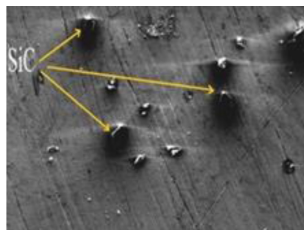
Figure 5. Images from metallurgical microscope showing SiC reinforcement (100X)



(a)



(b)



(c)

Figure 6. SEM image of Al6061-SiC metal matrix composite with (a) 5%SiC (b) 7.5%SiC (c) 10% SiC (400X)

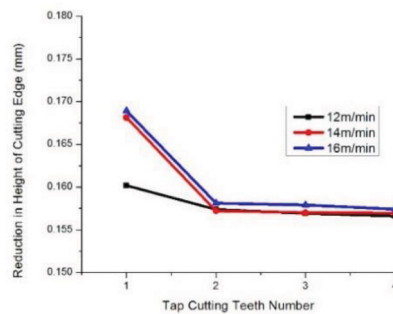
Flank Wear

From Figure 7, it was observed that increase in weight percentage of SiC in Al/SiC composite increased the tool wear. Increase in percentage of SiC increased the hardness of the composite and hence tool's wear. For a particular percentage of SiC particles it was observed that increases in speed increased the flank wear. Since abrasion is expected to be the major form of tool wear when cutting hard particle reinforced aluminium matrix composites, the important factors affecting tool life are the hardness, weight percentage of reinforcement particles in the composites and the speed of machining.

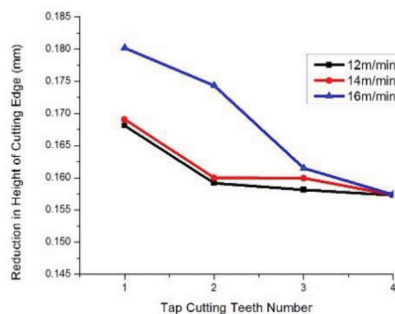
It was also observed that the flank wear increased with increase in the number of holes tapped. As tapping of holes progressed, tapping tool lost its sharpness of cutting edge and became dull. To perform tapping of holes further using the same tool needs higher magnitude of energy. This would induce cascading effect on the rate of tool wear. Therefore, there would be a significant progressive wear of tool with the increase in number of holes.

Flank wear results in reduction of relief angle on the clearance face of the tool. This gives rise to increased frictional resistance. It produces wear land on the side and end flanks of the tool, on account of the rubbing action of the machined surface. In the beginning, the tool is

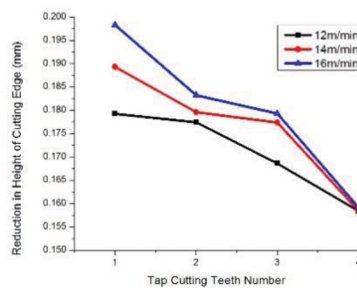
sharp and the wear land on the flank has zero width. However very soon the wear land develops and grows in size on account of abrasion, adhesion, shear, etc. (Teti, 2002). The maximum value of flank wear (0.1983 mm) was found on tapping tool for 10% SiC at the speed of 16 m/min after tapping 51st hole. It was evident that the rate of flank wear was higher for tapping speed of 16 m/min for all weight percentage of SiC, when compared with the same for speed of 12 m/min and 14 m/min. Hence, it may be inferred that the cutting speed in the range of 12 to 14 m/min is more satisfactory with 5% to 10% SiC aluminium composite.



(a)



(b)



(c)

Figure 7. Reduction in height of the cutting edge of the tap after tapping 51 holes on Al/SiC specimen with (a) 5 wt. % (b) 7.5 wt. % (c) 10 wt. % SiC

From the microscopic image (Figure 8), the area on the flank that has undergone wear can be seen. The increased torque at higher tapping speed and higher weight percentage of SiC indicated the higher energy used during the tapping operation. This also indicated the increases in flank wear at higher tapping speed and weight percentage of SiC.

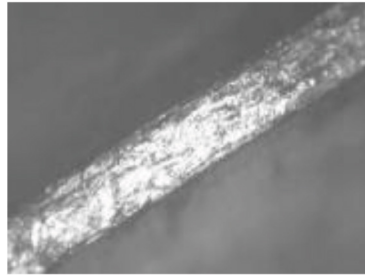


Figure 8. Image of (100X) tool flank after machining 51 holes on 10% SiC MMC at speed of 16 m/min

Figure 9 shows the sticking of aluminium between the cutting edges of the teeth and flute of the tap. The material stuck on the flute surface of the tool would obstruct the smooth passage of chips, leading to clogging of flute and cutting edges of tap. This would create artificial cutting edges inferior to actual cutting edges, producing poor quality of threads (Steininger, Siller, & Bleicher, 2015)



Figure 9. Aluminium stuck between the cutting edges of the tap

Torque

It was observed that increase in weight percentage of SiC particles increased the torque during machining. There was a significant increase in hardness and strength of the composite while increasing weight percentage of SiC. This could be attributed as one of the main reasons for the increase in torque. It was observed that, at tapping on a specimen with 5 wt. % SiC at 16 m/min, the torque was 15 Nm while it was the same with 10 wt. %SiC was 27.4 Nm.

It was also observed that for a particular percentage of SiC in composite, higher the speed, higher is the torque required. Increase in speed produces more flank wear on cutting edges

which could cause consumption of more energy during the tapping process resulting in higher magnitude of torque. It was observed that at tapping on a specimen with 10 wt. % SiC at 12 m/min, the torque was 4 Nm while the same with 14m/min was 19 Nm.

It was found the torque required increased with increase in the number of holes tapped as the tool loses its sharpness and becomes dull from progressive wear. A few deviations from this trend was observed when reinforcing particles in the composite were not uniform, resulting from lack of or absence of particles in the region of tapping of specified holes.

Surface Roughness Measurement

From the results, it was evident that for a particular weight percentage of SiC, the surface roughness value of the machined thread surface increases as speed increases. At 5 wt. % SiC, and speed of 12 m/min, the surface roughness value of the threaded surface of the hole was $6.68 \mu\text{m}$ while the same for 16 m/min was $6.8 \mu\text{m}$. It was also observed that increase in speed increases the flank wear on the tool. Flank wear affects the geometry and cutting action of the tool. This would lead to the poor surface finish of the tapped hole. It was also noticed that the surface roughness of the thread surface increased with increase in weight percentage of SiC in metal matrix composite. At 5 wt. % SiC, and speed of 16 m/min, the surface roughness value of the threaded surface of the hole was $6.8 \mu\text{m}$ while the same for 10 wt. % SiC was $8.8 \mu\text{m}$. Hard reinforcing particles in the matrix of composites would not get sheared off when they come across the cutting edge of the tool. They would either remain embedded to the surface or get dislodged from the surface creating dents on the threaded surface. In either of these cases, the quality of thread surface is affected due to the increase in surface roughness.

It was observed that the surface roughness of the tapped hole increased progressively with the increase in number of holes at all speeds and weight percentages of SiC particles. The magnitude and rate of flank wear of the tapping tool increased with increase in speed and weight percentage of SiC. The progressively damaged portions of the cutting edges of machine tap which interact with surface of the hole affect the surface finish of machined threads.

From SEM image (Figure 10 and 11) and cut section view of the threaded hole (Figure 12 (a) and (b)) it is evident that for higher percentage of SiC and higher speed the threaded surface gets damaged and surface roughness also increases.

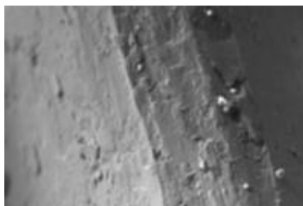


Figure 10. SEM image (300X) of tapped surface at 5 wt. % SiC and 12 m/min speed

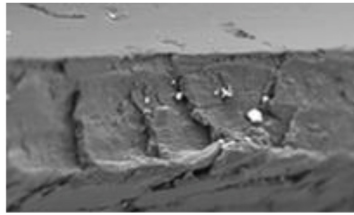


Figure 11. SEM image (300X) of tapped surface at 10 wt. % SiC and 16 m/min speed



(a)



(b)

Figure 12. (a) Cut section view of the tapped hole at 5% SiC and 12 m/min speed, Ra value 6.8 μm
(b) at 10% SiC and 16 m/min speed, Ra value 8.8 μm

CONCLUSIONS

The following conclusions are drawn based on an analysis of experimental investigations.

1. Increase in the weight percentage of SiC particles result in an increase of hardness and tensile strength of composite.
2. Increase in weight percentage of SiC particles and tapping speed would increase the torque required for tapping, rate of flank wear of tool and surface roughness of the threaded holes.
3. Clogging of aluminium material in the space between the cutting edges and sticking of aluminium on the flute surface could be the main reason for poor surface finish of thread surface and increased torque while tapping with higher speed and percentage of SiC.

REFERENCES

- Chawla, N., & Chawla, K. K. (2006). *Metal matrix composites*. United States of America, USA: Springer US.
- CMTI. (1987). *machine tool design handbook*. Central Machine Tool Institute. New Delhi: Tata McGraw-Hill.
- Drozda, E. J., & Wick, C. (1983). *Tool and manufacturing engineers handbook, Vol. I – Machining* (4th Ed.). New York, NY: Society of Manufacturing Engineers.

- Hung, N. P., Boey, F. Y. C., Khor, K. A., Phua, Y. S., & Lee, H. F. (1996). Machinability of aluminum alloys reinforced with silicon carbide particulates. *Journal of Materials Processing Technology*, 56(1-4), 966-977.
- Kannan, S., & Kishawy, H. A. (2008). Tribological aspects of machining aluminium metal matrix composites. *Journal of Materials Processing Technology*, 198(1), 399-406.
- Kilickap, E., Cakır, O., Aksoy, M., & Inan, A. (2005). Study of tool wear and surface roughness in machining of homogenised SiC-p reinforced aluminium metal matrix composite. *Journal of Materials Processing Technology*, 164, 862-867.
- Kumar, G. V., Rao, C. S. P., Selvaraj, N., & Bhagyashekar, M. S. (2010). Studies on Al6061-SiC and Al7075-Al₂O₃ metal matrix composites. *Journal of Minerals and Materials Characterization and Engineering*, 9(01), 43-55.
- Sahoo, A. K., Pradhan, S., & Rout, A. K. (2013). Development and machinability assessment in turning Al/SiCp-metal matrix composite with multilayer coated carbide insert using Taguchi and statistical techniques. *Archives of Civil and Mechanical Engineering*, 13(1), 27-35.
- Sekhar, R., & Singh, T. P. (2015). Mechanisms in turning of metal matrix composites: a review. *Journal of Materials Research and Technology*, 4(2), 197-207.
- Sha, J. L., & Wu, S. M. (1990). Diagnosis of the tapping process by information measure and probability voting approach. *Journal of Engineering for Industry*, 112(4), 319-325.
- Soltani, S., Khosroshahi, R. A., Mousavian, R. T., Jiang, Z. Y., Boostani, A. F., & Brabazon, D. (2015). Stir casting process for manufacture of Al-SiC composites. *Rare Metals*, 0(0), 1-10.
- Steininger, A., Siller, A., & Bleicher, F. (2015). Investigations regarding process stability aspects in thread tapping Al-Si alloys. *Procedia Engineering*, 100, 1124-1132.
- Su, H., Gao, W., Zhang, H., Liu, H., Lu, J., & Lu, Z. (2010). Optimization of stirring parameters through numerical simulation for the preparation of aluminum matrix composite by stir casting process. *Journal of Manufacturing Science and Engineering*, 132(6), 061007.
- Teti, R. (2002). Machining of composite materials. *CIRP Annals-Manufacturing Technology*, 51(2), 611-634.
- Wilson, F. W., & Harvey, P. D. (1959). *Tool engineers handbook*. American Society of Tool Engineers: McGraw Hill Book Company, Inc.





Dynamic Performance Characteristics of Finite Journal Bearings Operating on TiO₂ based Nanolubricants

Binu, K. G.¹, Yathish, K.^{1*}, Shenoy, B. S.², Rao, D. S.³ and Pai, R.³

¹Department of Mechanical Engineering, St Joseph Engineering College, Vamanjoor, Mangaluru, Karnataka, 575028, India

²Department of Aeronautical, Manipal Institute of Technology, Manipal, 576104, Karnataka, India

³Department of Mechanical Engineering, Manipal Institute of Technology, Manipal, 576104, Karnataka, India

ABSTRACT

Dynamic stiffness and damping coefficients of a finite journal bearing operating on TiO₂ based nanolubricant are obtained using the linear perturbation approach. Time dependent version of governing Reynolds equation is modified to consider the couple stress effect of TiO₂ nanoparticle lubricant additives. The viscosity variation of lubricant with varying concentrations of nanoparticle additives is simulated using a modified Krieger-Dougherty model. The modified Reynolds equation is solved using linear perturbation approach to obtain the dynamic pressures and dynamic coefficients. Threshold stability maps are plotted depicting stable operating regions of journal bearing operating on TiO₂ nanolubricants. Results reveal an increase in stiffness and damping coefficients, and a corresponding improvement in whirl instability characteristics of journal bearings, with increase in TiO₂ nanoparticle concentration.

Keywords: Couple Stress Fluids, Dynamic Characteristics, Journal bearings, Nanofluids, TiO₂ nanoparticle additives, Viscosity model

INTRODUCTION

The severity of operating conditions on modern day support elements, such as, journal bearings, have promoted renewed interest in tribological research aimed at increasing the bearing's load carrying capacity. The inherent issue of whirl instability in fluid film bearings has also received great attention. Solution models generated over the years to address these issues could be generally categorized

Article history:

Received: 11 January 2017

Accepted: 21 April 2017

E-mail addresses:

binu.tribology@gmail.com (Binu, K. G.),

yathsa2k@gmail.com (Yathish, K.),

satishshenoyb@yahoo.com (Shenoy, B. S.),

ds.rao@manipal.edu (Rao, D. S.),

rbpai@yahoo.com (Pai, R.)

*Corresponding Author

into two. Firstly, modifying the geometry of bearings and secondly, the use of lubricant additives to enhance the tribological properties of operating lubricants. The first approach has resulted in journal bearings with modified geometry, such as, externally adjustable pad bearings (Shenoy & Pai, 2009, 2010, 2011). The second approach has led to development of lubricants with chemical additives, which are activated at higher temperatures to generate sacrificial tribo-films to reduce friction and wear. However, stringent environment norms and the desire to develop additives, which are chemically stable and environment friendly, has led to researchers focusing on alternative additive technologies, such as, nanoparticles.

Chemically stable ceramic and metallic nanoparticles have found to function effectively as lubricant additives with significant increase in journal bearing load capacity (Li, Wang, Liu & Xue, 2006; Li, Zheng, Cao & Ma, 2011; Battez et al., 2007; Joly-Pottuz et al., 2008; Rico, Minondo & Cuervo, 2007; Peng et al., 2007; Peng, Kang, Hwang, Shyr & Chang, 2009; Mosleh, Atnafu, Belk & Nobles, 2009). Few theoretical studies have also shown an improvement in stability of journal bearings running on such nano-oils (Babu, Nair & Krishnan, 2012; Nair, Ahmed & Al-qahtani, 2009). However, a generalized theory to simulate the performance characteristics of journal bearings operating on nanoparticle additives is yet to be developed. Binu, Shenoy, Rao and Pai (2011) has presented an analytical model, which does consider additive concentrations, in modelling the static characteristics of journal bearings operating on engine oil dispersed with TiO_2 nanoparticles. This analytical model considers the couple stress effect of nanoparticle additives by using the nanoparticle size as the control parameter. The influence of nanoparticle additive concentration on viscosity of base fluid was integrated into the governing Reynolds equation using a modified Krieger-Dougherty viscosity model to simulate the viscosity variation.

Stability characteristics in journal bearings is important because the journal centre motion governs the oil film thickness and decides the operability of journal bearings for specific applications. Previous studies have reported improvement in journal bearing stability due to the presence of long chain polymer additives. These lubricants were characterized as couple stress fluids with the polymer molecule length of the additives being considered as couple stress factor. Binu et al. (2011) has reported an increase in the stability of journal bearings by conducting a non-linear transient analysis on journal bearings operating on couple stress fluids (Binu et al., 2011).

In this study, the analytical model developed by Binu et al. (2011) is used in studying the influence of TiO_2 nanoparticle additives on the dynamic characteristics of journal bearings. The governing Reynolds equation is modified to consider the variation in viscosities of nanolubricant samples due to varying nanoparticle concentration. The linear perturbation method is used to obtain the dynamic stiffness and damping characteristics. The influence of nanoparticle concentration on critical speeds and mass parameter of journal bearings are studied.

METHODS

Numerical Formulation

General governing equation. The governing equation for the analysis is the time-dependent form of Reynolds equation in two-dimensions for a couple stress fluid. The equation is expressed as shown below (Binu et al., 2011; Guha, 2004).

$$\frac{\partial}{\partial x} \left(f(h, d) \frac{\partial p}{\partial x} \right) + \frac{\partial}{\partial z} \left(f(h, d) \frac{\partial p}{\partial z} \right) = 6\mu U \frac{\partial h}{\partial x} + 12\mu \frac{\partial h}{\partial t} \tag{1}$$

Where, $f(h, d) = h^3 - 12hd^2 + 24d^3 \tanh\left(\frac{h}{2d}\right)$

The couple stress effect of nanoparticle additives on lubricant film thickness *h* is studied using standard couple stress parameter $d = \sqrt{\frac{\eta}{\mu_{bf}}}$. In the above equation, the size of nanoparticle additive is taken as the couple stress parameter with $[\eta]$ being the material property responsible for couple stresses and μ_{bf} being the viscosity of base lubricant.

The governing equation is obtained in dimensionless form using the following standard non-dimensional parameters (Binu et al., 2011; Guha, 2004).

$$\theta = \frac{x}{R}; \quad \bar{z} = \frac{z}{L}; \quad \bar{h} = \frac{h}{C}; \quad \bar{d} = \frac{d}{C};$$

$$\bar{t} = \omega t; \quad \bar{p} = \frac{pC^2}{\mu\omega R^2}; \quad \bar{\mu} = \frac{\mu_{nf}}{\mu_{bf}}; \quad \lambda = \frac{L}{D}$$

The dimensionless form of equation-1 is written as:

$$\frac{\partial}{\partial \theta} \left(\bar{f}(\bar{h}, \bar{d}) \frac{\partial \bar{p}}{\partial \theta} \right) + \frac{1}{4\lambda^2} \frac{\partial}{\partial \bar{z}} \left(\bar{f}(\bar{h}, \bar{d}) \frac{\partial \bar{p}}{\partial \bar{z}} \right) = \dots$$

$$\dots 6\bar{\mu} \frac{\partial \bar{h}}{\partial \theta} + 12\bar{\mu} \frac{\partial \bar{h}}{\partial \bar{t}} \tag{2}$$

Where, $\bar{f}(\bar{h}, \bar{d}) = \bar{h}^3 - 12\bar{d}^2\bar{h} + 24\bar{d}^3 \tanh\left(\frac{\bar{h}}{2\bar{d}}\right)$

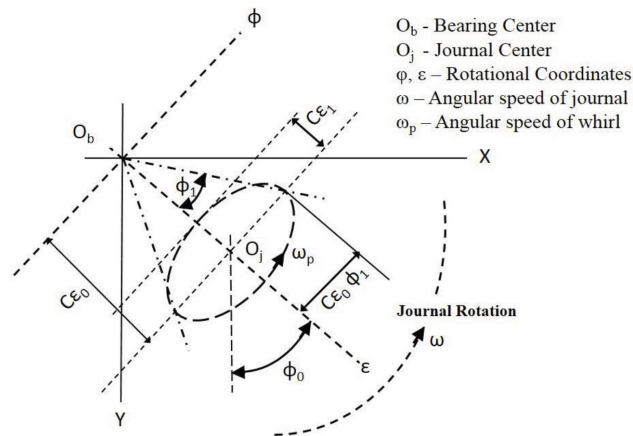


Figure 1. Rotational coordinate system

The rotational coordinate system for the journal centre is shown in Figure 1. Introducing the rotational coordinate system to equation (2), the governing non-dimensional form of Reynolds equation for dynamic analysis is presented below (Binu et al., 2011; Guha, 2004).

$$\frac{\partial}{\partial \theta} \left(\bar{f}(\bar{h}, \bar{d}) \frac{\partial \bar{p}}{\partial \theta} \right) + \frac{1}{4\lambda^2} \frac{\partial}{\partial z} \left(\bar{f}(\bar{h}, \bar{d}) \frac{\partial \bar{p}}{\partial z} \right) = \dots$$

$$\dots 6\bar{\mu}(1 - 2\dot{\phi}) \frac{\partial \bar{h}}{\partial \theta} + 12\bar{\mu} \frac{\partial \bar{h}}{\partial t}$$
(3)

Where, $\bar{f}(\bar{h}, \bar{d}) = \bar{h}^3 - 12\bar{d}^2 \bar{h} + 24\bar{d}^3 \tanh\left(\frac{\bar{h}}{2\bar{d}}\right)$

Dynamic journal Bearing Characteristics. By considering small harmonic whirling of the journal centre within the bearing with whirl frequency ω_p , the instantaneous location of the journal centre is expressed using the equations provided below.

$$\epsilon = \epsilon_0 + \epsilon_1 e^{i\Omega t}$$

$$\phi = \phi_0 + \phi_1 e^{i\Omega t}$$
(4)

For the first order perturbation, the corresponding film pressure and film thickness can be expressed in non-dimensional form as:

$$\bar{p} = \bar{p}_0 + (\epsilon_1 \bar{p}_\epsilon + \epsilon_0 \phi_1 \bar{p}_\phi) e^{i\Omega t}$$

$$\bar{h} = \bar{h}_0 + (\epsilon_1 \cos \theta + \epsilon_0 \phi_1 \sin \theta) e^{i\Omega t}$$
(5)

In the above equation (4), \bar{p}_0 is the steady state pressure; \bar{p}_ε and \bar{p}_ϕ are the perturbed pressures and $\Omega = \frac{\omega_p}{\omega}$ is the whirl frequency ratio.

Performing an order analysis as explained in Guha, (2004), Majumdar, Pai and Hargreaves (2004) and Lahmar (2005), the non-dimensional stiffness and damping coefficients are computed as shown below.

$$\begin{bmatrix} Z_{\varepsilon\varepsilon} & Z_{\varepsilon\phi} \\ Z_{\phi\varepsilon} & Z_{\phi\phi} \end{bmatrix}^T = - \int_0^1 \int_0^{2\pi} \begin{Bmatrix} \bar{p}_\varepsilon \\ \bar{p}_\phi \end{Bmatrix} \times (\cos \theta : \sin \theta) d\bar{z} d\theta \quad (6)$$

Where, $Z_{i,j} = A_{i,j} + i\Omega B_{i,j}$ and $(i,j) = (\varepsilon, \phi)$.

The non-dimensional stiffness and damping coefficients are presented below (Lahmar, 2005).

$$\begin{aligned} \bar{K}_{\varepsilon\varepsilon} &= \text{Real}(Z_{\varepsilon\varepsilon}) = -\text{Re} \int_0^1 \int_0^{2\pi} \bar{p}_\varepsilon \cos \theta d\bar{z} d\theta; \\ \bar{K}_{\phi\varepsilon} &= \text{Real}(Z_{\phi\varepsilon}) = -\text{Re} \int_0^1 \int_0^{2\pi} \bar{p}_\varepsilon \sin \theta d\bar{z} d\theta; \\ \bar{K}_{\varepsilon\phi} &= \text{Real}(Z_{\varepsilon\phi}) = -\text{Re} \int_0^1 \int_0^{2\pi} \bar{p}_\phi \cos \theta d\bar{z} d\theta; \\ \bar{K}_{\phi\phi} &= \text{Real}(Z_{\phi\phi}) = -\text{Re} \int_0^1 \int_0^{2\pi} \bar{p}_\phi \sin \theta d\bar{z} d\theta; \end{aligned} \quad (7)$$

$$\begin{aligned} \bar{D}_{\varepsilon\varepsilon} &= \text{imag}(Z_{\varepsilon\varepsilon}) = -\text{Im} \int_0^1 \int_0^{2\pi} \bar{p}_\varepsilon \cos \theta d\bar{z} d\theta; \\ \bar{D}_{\phi\varepsilon} &= \text{imag}(Z_{\phi\varepsilon}) = -\text{Im} \int_0^1 \int_0^{2\pi} \bar{p}_\varepsilon \sin \theta d\bar{z} d\theta; \\ \bar{D}_{\varepsilon\phi} &= \text{imag}(Z_{\varepsilon\phi}) = -\text{Im} \int_0^1 \int_0^{2\pi} \bar{p}_\phi \cos \theta d\bar{z} d\theta; \\ \bar{D}_{\phi\phi} &= \text{imag}(Z_{\phi\phi}) = -\text{Im} \int_0^1 \int_0^{2\pi} \bar{p}_\phi \sin \theta d\bar{z} d\theta; \end{aligned} \quad (8)$$

Stability parameters. The stability of journal bearings is then analysed using the stiffness and damping coefficients obtained in section B (Majumdar et al., 2004; Lahmar, 2005).

At the threshold of stability, the critical mass \bar{M}_c and whirl ratio Ω_{cr} are expressed as (Lahmar, 2005):

$$\begin{aligned} \bar{M}_c &= \frac{M_c \omega^2 C}{W_0} = \frac{A_{eq}}{\Omega_{cr}^2} \\ \Omega_{cr}^2 &= \left(\frac{\omega_p}{\omega} \right)^2 = \frac{(\bar{K}_{XX} - A_{eq})(\bar{K}_{YY} - A_{eq}) - \bar{K}_{XY} \bar{K}_{YX}}{D_{XX} D_{YY} - D_{XY} D_{YX}} \end{aligned} \quad (9)$$

Where, $A_{eq} = \frac{\bar{K}_{XX} \bar{D}_{YY} + \bar{K}_{YY} \bar{D}_{XX} - \bar{K}_{XY} \bar{D}_{YX} - \bar{K}_{YX} \bar{D}_{XY}}{\bar{D}_{XX} + \bar{D}_{YY}}$

The non-dimensional threshold speed of the rotor is then expressed as (Lahmar, 2005):

$$\bar{\omega}_{cr} = \omega_c \sqrt{\frac{M_c C}{W_0}} = \sqrt{\bar{M}_c} \quad (10)$$

Therefore, a journal bearing system is asymptotically stable when the journal mass c is less than \bar{M}_c . Likewise, a system is asymptotically stable when the operating speed of the rotor is less than $\bar{\omega}_{cr}$. A negative value of \bar{M}_c means that the journal will always be stable for all values of journal mass \bar{M}_c . Similarly, a negative value of Ω_c^2 implies the absence of whirl (Lahmar, 2005).

Viscosity Model

Adding TiO₂ nanoparticles to engine oil is found to increase the viscosity of lubricant samples. The authors of this current paper have reported in a previously published study (Binu, Shenoy, Rao & Pai, 2014), the suitability of a modified Krieger-Dougherty viscosity model in simulating the dynamic viscosities of engine oil samples dispersed with TiO₂ nanoparticles. The study reports good agreement of experimental viscosities obtained using a rheometer with theoretical viscosities simulated using modified Krieger-Dougherty viscosity model. The modified Krieger-Dougherty viscosity model also considers the nanoparticle packing fraction, which is the ratio of aggregate particle size to the primary particle size. TiO₂ nanoparticle dispersions in engine oil showed an aggregate particle size distribution of 777 nm in the DLS particle size analysis that was performed and reported in the publication by Binu et al. (2014). The TiO₂ nanoparticles used in the study were of 100 nm primary particle size.

Therefore, the relative viscosities $\bar{\mu}$ of TiO₂ dispersions in engine oil simulated using modified Krieger-Dougherty equation is expressed as (Binu et al., 2014):

$$\bar{\mu} = \frac{\mu_{nf}}{\mu_{bf}} = \left(1 - \frac{\phi_a}{\phi_m} \right)^{-2.5\phi_m} \quad (11)$$

In which, the packing fraction is obtained as:

$$\phi_a = \phi \left(\frac{a_a}{a} \right)^{3-D} \quad (12)$$

a_a and a are the aggregate and primary particle size respectively. D is the fractal index having a typical value of 1.8 for nanofluids (Binu et al., 2014).

RESULTS AND DISCUSSIONS

The modified Reynolds equation (2), presented in section II of this paper, incorporates parameters which enable us to study the influence of TiO₂ nanoparticle concentration on dynamic bearing characteristics. The relative viscosity term $\bar{\mu}$, computed using the modified Krieger-Dougherty equation (11), integrates the effects of TiO₂ nanoparticle additive concentration on the dynamic characteristics of journal bearings.

The computational code developed for the analysis is validated by comparing the values of stiffness and damping coefficients with previously published results by Guha (2004). For Newtonian fluids ($\bar{d} = 0$), the stiffness and damping coefficients obtained for increasing eccentricity ratio using the developed code is shown in Figure 2 and Figure 3. The dynamic coefficients are found to be in good agreement with the values presented in Guha (2004).

Upon validating the computational code, dynamic coefficients are computed for different values of nanoparticle concentrations. Table-1 provides the values of various operating parameters used in the analysis.

Table 1
Operating parameters

Bearing Details
L/D Ratio: 1.0
Bearing Angle: $\theta = 360^\circ$ Full Bearing
Bearing Type: Plain Compliant Bearing
Bearing Clearance: 25 microns
Lubricant Details
Type: Couple stress fluid
Additives: TiO ₂ nanoparticles
Couple stress parameter: $\bar{d} = \frac{d}{C} = 0.03108$ corresponding to aggregate nanoparticle size of 777 nm and bearing clearance of 25 microns.
TiO ₂ nanoparticle concentrations: $\phi = 0.001, 0.005, 0.01, 0.02$

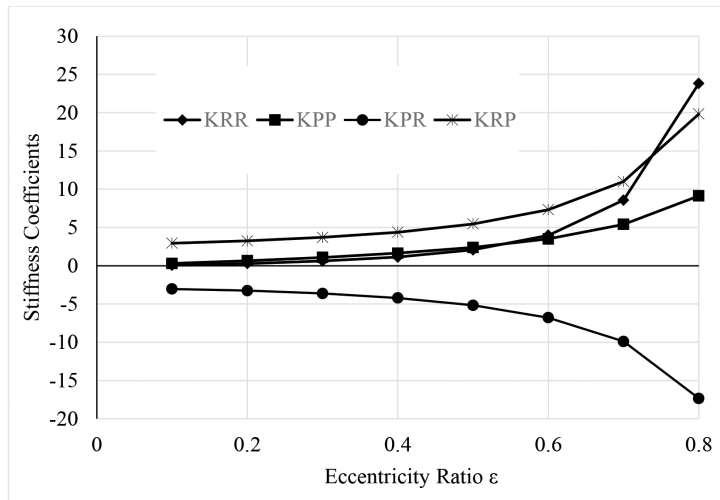


Figure 2. Stiffness Coefficients for Newtonian Lubricant $\bar{d} = 0$

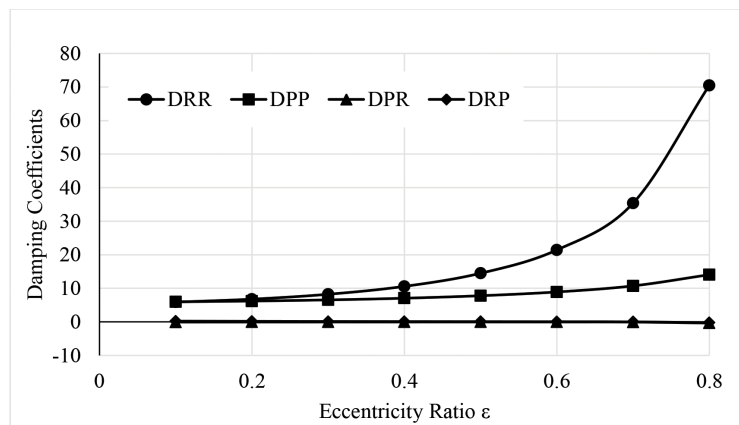


Figure 3. Damping Coefficients for Newtonian Lubricant $\bar{d} = 0$

The validated computational code was then used to obtain the dynamic characteristics of journal bearings operating on TiO₂ nanolubricants at different TiO₂ nanoparticle concentrations. Figure 4 and Figure 5 provides the variation in dynamic coefficients of TiO₂ nanoparticle dispersions of aggregate particle size 777 nm, which results in a couple stress parameter of 0.03108, with TiO₂ additive concentrations varying from 0.001 to 0.02. Results reveal an increase in dynamic coefficients with increasing nanoparticle additive concentrations.

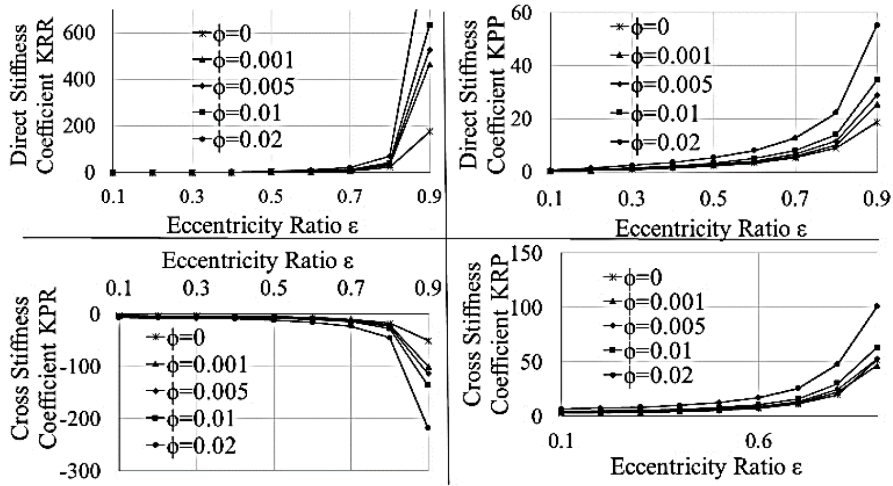


Figure 4. Stiffness coefficients at couple stress parameter $\bar{d} = 0.03108$ (aggregate TiO₂ particle size of 777 nm) for varying TiO₂ volume fractions

The increment in stiffness and damping coefficients with TiO₂ nanoparticle concentration is discussed below.

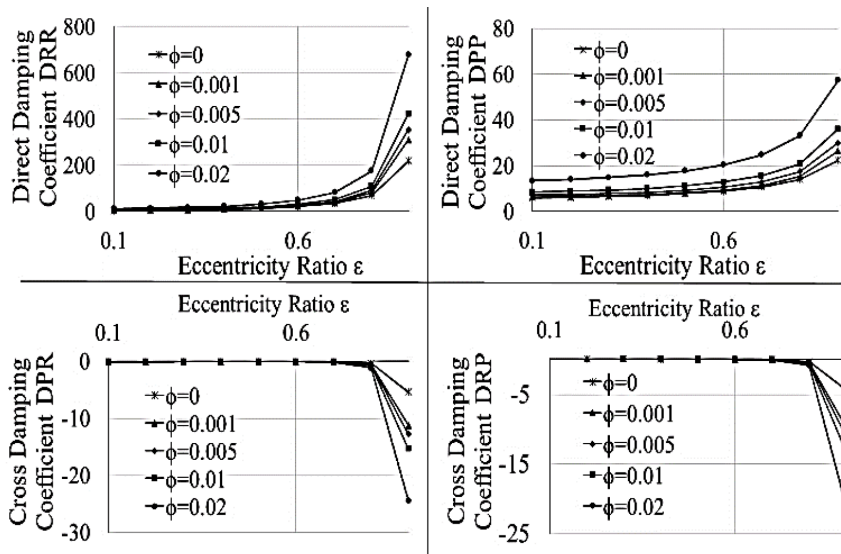


Figure 5. Damping coefficients at couple stress parameter $\bar{d} = 0.03108$ (aggregate TiO₂ particle size of 777 nm) for varying TiO₂ volume fractions

As observed in Figure 4 and Figure 5, the stiffness coefficients are considerably higher for nano lubricants in comparison to plain oil. This increase in stiffness coefficients being more prominent at higher eccentricities. A similar observation was also obtained for damping

coefficients. When the TiO₂ nanoparticle size is kept constant at 777 nm and is added at a volume fraction of 0.001, the cross stiffness KRP is found to increase by 10% in comparison to plain oil.

The results also help us to understand the influence of volume fraction on the dynamic coefficients. Considering the cross-stiffness coefficient KRP at an eccentricity ratio of 0.8, it is observed that adding TiO₂ nanoparticle additives of aggregate size 777 nm (corresponding to $\bar{d} = 0.03108$), at a volume fraction $\phi=0.01$, will increase the cross stiffness by 51% in comparison to plain oil. This increase in cross stiffness is more pronounced when TiO₂ nanoparticles are added at higher volume fractions.

Addition of 0.01 and 0.02 volume fractions increases the cross-stiffness parameter KRP by 51% and 140% respectively. However, it has to be mentioned that higher particle sizes and volume fractions will change the flow behavior and physical interactions of the particles leading to quicker sedimentation. Optimum values of TiO₂ nanoparticle sizes and volume fractions for acceptable dispersion stability has to be determined. Experimentation to determine optimum values are necessary. It also needs to be mentioned that, considering the changes in viscosity due to temperature variation will also provide a more accurate picture. The viscosity variations dealt with in this study does not account for the temperature variation prevalent in bearing area for high load and high speed applications. Hence a thermo hydrodynamic analysis of dynamic characteristics will offer more insights.

Influence of TiO₂ nanoparticle concentration on whirl instability of journal bearings is studied and presented below. The stability parameters comprising critical mass parameter, critical threshold speed (angular), and whirl ratio are computed and their variation with concentration of TiO₂ nanoparticle additives are studied.

Influence of TiO₂ nanoparticle concentration of a constant particle size of 777 nm on critical mass parameter \bar{M}_{cr} is studied and the results are shown in Figure 6. As seen in Figure 6, stability of journal bearing systems is found to improve with addition of TiO₂ nanoparticles at increasing concentrations. The increase in stability is more prominent at eccentricity ratio more than 0.5.

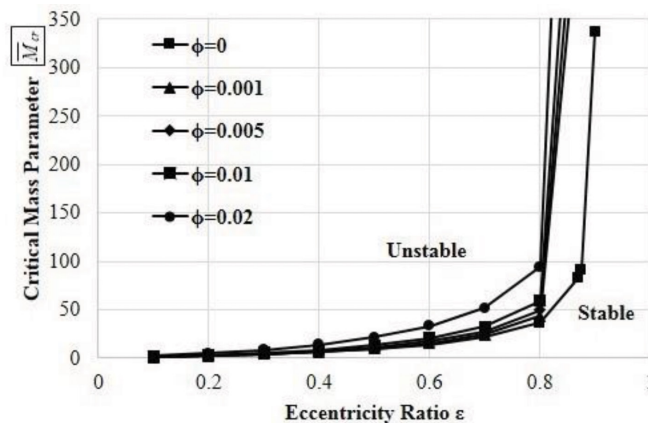


Figure 6. Variation in Critical Mass Parameter with nanoparticle volume fraction ϕ at constant couple stress parameter $\bar{d} = 0.03108$

Improvement in stability of journal bearing system as seen in Figure 6 is further analysed by plotting the threshold stability maps for varying nanoparticle concentrations.

The threshold stability map for varying TiO₂ nanoparticle concentrations at a constant particle size of 777 nm is shown in Figure 7.

The improvement in stability of journal bearing system due to the addition of TiO₂ nanoparticles at higher eccentricities is evident in threshold stability map Figure 7. This fact can also be seen in Figure 8, which shows the variation of critical whirl ratio for various TiO₂ nanoparticle concentrations.

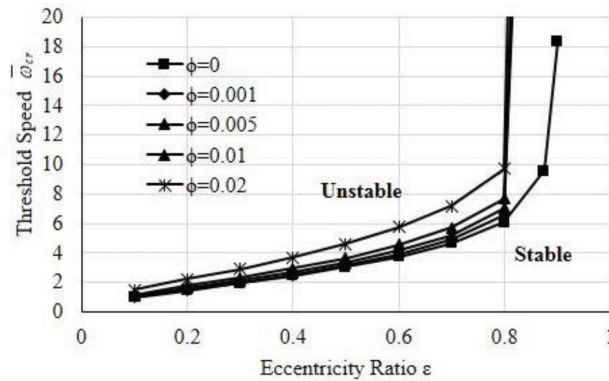


Figure 7. Threshold stability map for varying TiO₂ volume fractions at $\bar{d} = 0.03108$

Reason for pronounced influence of TiO₂ nanoparticle additives on stability characteristics of journal bearings at higher eccentricities can be attributed to comparable nanoparticle size and film thickness at higher eccentricities. Reduced film thickness associated with higher eccentricities could permit increased physical interactions between particles and between particles and surfaces, resulting in pronounced damping coefficients. However, its true influence will also be greatly influenced by dispersion stability and temperature reduction of oil film viscosity.

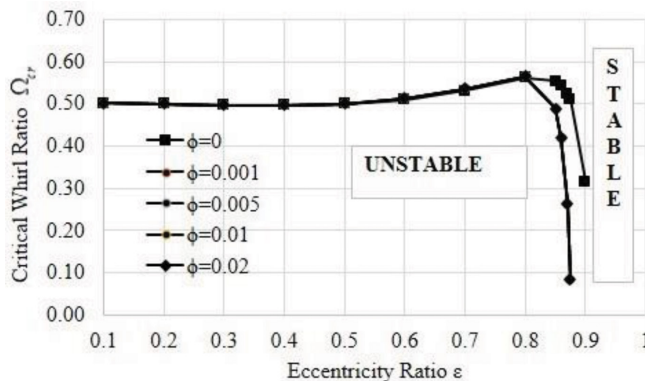


Figure 8. Critical whirl ratio for varying TiO₂ volume fractions at $\bar{d} = 0.03108$

As observed in Figure 8, there is negligible change in critical whirl ratio with increasing nanoparticle concentrations. However, Figure 7 shows that the threshold speed of journal bearing system is increasing with TiO₂ volume fractions. Therefore, even though the whirl ratio does not reveal significant variation with volume fraction, there is a significant reduction in unstable operating region at higher eccentricities due to the addition of nanoparticle additives.

Threshold stability maps and whirl ratio variation shown in Figure 7 and Figure 8 reveals that, the presence of TiO₂ nanoparticle additives clearly demonstrates an increase in stable operating region of journal bearing systems.

CONCLUSIONS

In this study, dynamic characteristics of journal bearing systems operating on TiO₂ nanoparticle dispersions in engine oil was obtained using linear perturbation approach. A modified Reynolds equation was developed integrating the influence of TiO₂ nanoparticle additive concentration on the dynamic characteristics of journal bearing systems. The results reveal a significant increase in stiffness and damping coefficients of journal bearing system due to the addition of nanoparticle additives. The threshold stability maps reveal an increase in stable operating region due to the volume fraction influence of TiO₂ nanoparticle additives. Results also reveal the influence of nanoparticle additives in stability is more relevant at higher eccentricities experienced during heavy-load and high-speed operations.

Further experimental studies focused on nanoparticle interaction within the oil film and the temperature influence on viscosity will generate more insights into the functioning of nanoparticle additives.

ACKNOWLEDGEMENTS

The First Author of this paper would like to acknowledge The Management of St Joseph Engineering College – Vamanjoor, Mangaluru for sponsoring his Research and for their continued support. The Authors would also like to thank the Applications Lab of AIMIL India Pvt. Ltd, for their support in the Rheological studies.

REFERENCES

- Babu, K. S., Nair, K. P., & Krishnan, P. R. (2012). Analysis of static and dynamic performance characteristics of THD journal bearing operating under lubricants containing nanoparticles. *International Journal of Precision Engineering and Manufacturing*, 13(10), 1869-1876.
- Battez, A. H., Gonzalez, R., Felgueroso, D., Fernandez, J. E., Fernandez, M. R., Garcia, M. A., & Penuelas, I. (2007). Wear prevention behaviour of nanoparticle suspension under extreme pressure conditions. *Wear*, 263(7), 1568-74.
- Binu, K. G., Shenoy, B. S., Rao, D. S., & Pai, R. (2011). Stability characteristics of journal bearing systems lubricated with couple stress fluids using the nonlinear transient approach. *Journal of Tribology and Surface Engineering*, 3(1-2), 51-66.

- Binu, K. G., Shenoy, B. S., Rao, D. S., & Pai, R. (2014). Static characteristics of a fluid film bearing with TiO₂ based nanolubricant using the modified Krieger–Dougherty viscosity model and couple stress model. *Tribology International*, 75, 69-79.
- Guha, S. K. (2004). A theoretical analysis of dynamic characteristics of finite hydrodynamic journal bearings lubricated with coupled stress fluids. *Proceedings of the Institution of Mechanical Engineers, Part J: Journal of Engineering Tribology*, 218(2), 125-33.
- Joly-Pottuz, L., Vacher, B., Mogne, T. L., Martin, J. M., Mieno, T., & He, C. N. (2008). The role of Nickel in Ni-containing nanotubes and onions as lubricant additives. *Tribology Letters*, 29(3), 213-219.
- Lahmar, M. (2005). Elastohydrodynamic analysis of double-layered journal bearings lubricated with couple-stress fluids. *Proceedings of the Institution of Mechanical Engineers, Part J: Journal of Engineering Tribology*, 219(2), 145-171.
- Li, B., Wang, X., Liu, W., & Xue, Q. (2006). Tribochemistry and antiwear mechanism of organic-inorganic nanoparticles as lubricant additives. *Tribology Letters*, 22(1), 79-84.
- Li, W., Zheng, S., Cao, B., & Ma, S. (2011). Friction and wear properties of ZrO₂/SiO₂ composite nanoparticles. *Journal of Nanoparticle Research*, 13(5), 2129-37.
- Majumdar, B. C., Pai, R., & Hargreaves, D. J. (2004). Analysis of water-lubricated journal bearings with multiple axial grooves. *Proceedings of the Institution of Mechanical Engineers, Part J: Journal of Engineering Tribology*, 218(2), 135-146.
- Mosleh, M., Atnafu, N. D., Belk, J. H., & Nobles, O. M. (2009). Modification of sheet metal forming fluids with dispersed nanoparticles for improved lubrication. *Wear*, 267(5), 1220-1225.
- Nair, K. P., Ahmed, M. S., & Al-qahtani, S. T. (2009). Static and dynamic analysis of hydrodynamic journal bearing operating under nano lubricants. *International Journal of Nanoparticles*, 2(1-6), 251-262.
- Peng, D. X., Kang, Y., Hwang, R. M., Shyr, S. S., & Chang, Y. P. (2009). Tribological properties of diamond and SiO₂ nanoparticles added in paraffin. *Tribology International*, 42(6), 911-17.
- Peng, Y., Hu, Y., & Wang, H. (2007). Tribological behaviours of surfactant-functionalized carbon nanotubes as lubricant additive in water. *Tribology Letters*, 25(3), 247-253.
- Rico, E. F., Minondo, I., & Cuervo, D. G. (2007). The effectiveness of PTFE nanoparticle powder as an EP additive to mineral base oils. *Wear*, 262(11), 1399-1406.
- Shenoy, B. S., & Pai, R. (2009). Theoretical investigations on the performance of an externally adjustable fluid-film bearing including misalignment and turbulence effects. *Tribology International*, 42(7), 1088-1100.
- Shenoy, B. S., & Pai, R. (2010). Stability characteristics of an externally adjustable fluid film bearing in the laminar and turbulent regimes. *Tribology International*, 43(9), 1751-1759.
- Shenoy, B. S., & Pai, R. (2011). Effect of turbulence on the static performance of a misaligned externally adjustable fluid film bearing lubricated with couple stress fluids. *Tribology International*, 44(12), 1774-1781.

NOMENCLATURE

a	Radii of primary TiO ₂ nanoparticles (nm)
a_a	Radii of aggregate TiO ₂ nanoparticles (nm)
C	Bearing clearance (mm)
D	Fractal Index
D_{xx}	Damping coefficients
d	Couple stress parameter
\bar{d}	Non-dimensional couple stress parameter
e	Eccentricity (m)
h	Film thickness (m)
\bar{h}	Non-dimensional film thickness
K_{xx}	Stiffness coefficients
L	Bearing length (m)
M	Mass parameter
M_c	Critical mass parameter
p	Hydrodynamic film pressure (N/m ²)
\bar{p}	Non-dimensional Hydrodynamic film pressure
t	Time (s)
\bar{t}	Non-dimensional time
U	Tangential velocity of journal (m/s)
W_0	Static load capacity
x	Circumferential bearing coordinates
z	Axial bearing coordinates
μ_{bf}	Viscosity of base fluid
μ_{nf}	Viscosity of nanofluids
$\bar{\mu}$	Relative viscosity
ϕ	Nanoparticle volume fraction
ϕ_a	Effective volume fraction
ϕ_m	Maximum particle packing fraction
ε	Eccentricity ratio
θ	Angular coordinates (rad)
ω	Angular velocity (rad/s)
ω_{cr}	Critical threshold speed
ω_p	Journal whirl speed
$[\eta]$	Intrinsic velocity
η	Material constant (couple stress)
Ω	Whirl ratio
Ω_{cr}	Critical Whirl ratio

Modal Behaviour of Vertical Axis Wind Turbine Comprising Prestressed Rotor Blades: A Finite Element Analysis

Torabi Asr, M.^{1*}, Masoumi, M. M.² and Mustapha, F.³

¹ Department of Mechanical Engineering, Faculty of Engineering, Universiti Putra Malaysia, 43400 UPM, Serdang, Selangor, Malaysia

² Department of Civil Engineering, Islamic Azad University, Science and Research Branch, Fars, 1477893855, Iran

³ Department of Aerospace Engineering, Faculty of Engineering, Universiti Putra Malaysia, 43400 UPM, Serdang, Selangor, Malaysia

ABSTRACT

Pre-stressing is a concept used in many engineering structures. In this study prestressing in the form of axial compression stress is proposed in the blade structure of H-Darrieus wind turbine. The study draws a structural comparison between reference and prestressed configurations of turbine rotor with respect to their dynamic vibrational response. Rotordynamics calculations provided by ANSYS Mechanical is used to investigate the effects of turbine rotation on the dynamic response of the system. Rotation speed ranging between 0 to 150 rad/s was examined to cover the whole operating range of commercial instances. The modal analysis ends up with first six mode shapes of both rotor configurations. As a result, the displacement of the proposed configurations reduced effectively. Apparent variations in Campbell diagrams of both cases indicate that prestressed configuration has its resonant frequencies far away from turbine operation speeds and thus remarkably higher safety factor against whirling and probable following failures.

Keywords: Finite element analysis, H-Darrieus blade, prestressed blade, modal analysis, rotor dynamics, vertical axis wind turbine

Article history:

Received: 11 January 2017

Accepted: 21 April 2017

E-mail addresses:

mahditorabiasr@gmail.com (Torabi Asr, M.),

mehdiscientist@gmail.com (Masoumi, M. M.),

faizalms@upm.edu.my (Mustapha, F.)

*Corresponding Author

INTRODUCTION

The increasing demand for renewable energy, particularly wind energy, has seen the development of different types of wind turbines (Torabi Asr, 2016; Torabi Asr, Zal, Mustapha, & Wiriadidjaja, 2016). One of two ordinary types of wind turbines is the vertical axis wind turbine, shortly VAWT.

Darrieus turbines in their various forms, namely troposkien shape and H-shape, are the most conventional types of VAWTs (Paraschivoiu, 2002; Sutherland, Berg & Ashwill, 2012; Brusca, Lanzafame & Messina, 2014). VAWTs and specifically H-Darrieus-type rotors are easy to fabricate, easy to maintain and produce less noise than other conventional propeller-type turbines (Pathade, Pandhare, Saskar, Chaudhari, & Bairagi, 2016). More importantly, they can function independently of wind direction and thus do not require complicated yawing systems (Torabi, Osloob, & Mustapha, 2016; Al-Maaitah, 1993). Besides the advantages these class of wind turbines offer, their structure is exposed to large variation in torque with each revolution (Roy & Mohiuddin, 2015).

This study provides a pioneering approach in the load-bearing optimization of the turbine rotor by introducing prestress on the rotor blades. It suggests prestressed structure improves the integrity, stability and structure behavior. The aim of this paper is to draw a comparison of the dynamic behavior between the turbine rotors with prestress-reinforced blades and the original design.

METHODS

Finite Element Analysis

A conventional type H-Darrieus turbine rotor was modelled employing commercial finite element software ANSYS for conducting a modal analysis. As shown in Figure 1 the rotor comprising of three blades and a radial arm connecting the blades to the central column which is mounted on a supporting rigid part which acts as the bearing. Blades were of the so-called NACA 0018 airfoil in length. More detailed description of turbine rotor can be found in Table 1.

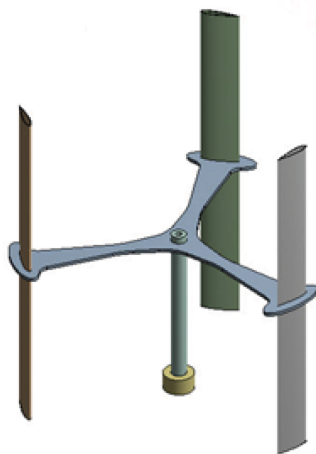


Figure 1. Test bed turbine model

Table 1
Test Bed Turbine Specifications

Quantity	Magnitude
Blade chord length	100 mm
Blade profile thickness	2.5 mm
Blade length	1000 mm
Rotor radius	400 mm
Radial arm thickness	10 mm
Blade mass	0.3 kg
Total rotor mass	3.2 kg

Aluminium alloy material which properties are shown in Table 2 was assigned to all parts excluding the supporting part which selected as a rigid body.

For the simulations conducted in this work, Hex Dominant method was used for the purpose of grid generation. A final mesh with approximately 34,000 elements was verified after conducting a grid study. Mesh cells start at 3 mm on blade edges and the maximum length of mesh cells did not to exceed 10 mm.

Table 2
Material properties (aluminium alloy)

Quantity	Magnitude
Young's modulus	71 GPa
Tensile yield strength	460 MPa
Shear modulus	26.7
Poisson's ratio	0.33

Simulations performed in this work can be categorized into two groups, namely reference and prestressed configurations. The latter group proposed a design in which turbine blades are initially reinforced by axial compression prestress of 10 MPa along their length. The choice of 10 MPa was selected after a preliminary study of several values ranging 5-15 MPa to provide an illustrative comparison between reference and prestressed configurations.

In order to juxtapose the structural dynamic behavior of these two configurations modal analysis, structure vibration responses, natural frequencies, and corresponding mode shapes were calculated. Of particular importance, due to the rotary operation of turbines, these structures are highly suspected to face resonance effect which can lead to whirling in some specific operational speeds and likely hazardous failures. Rotordynamics calculations provided by ANSYS Mechanical was used, and 25 rad/s-interval of rotation speed ranging between 0 to 150 rad/s were examined.

RESULTS AND DISCUSSIONS

Modal analysis has been performed on the turbine structure both for the reference configuration and the proposed prestressed. Figure 2 demonstrates the mode shapes for the reference configuration in the parked condition. As expected the rotor experienced considerable deformation, with a maximum displacement value of about 48 mm in the fourth mode shape.

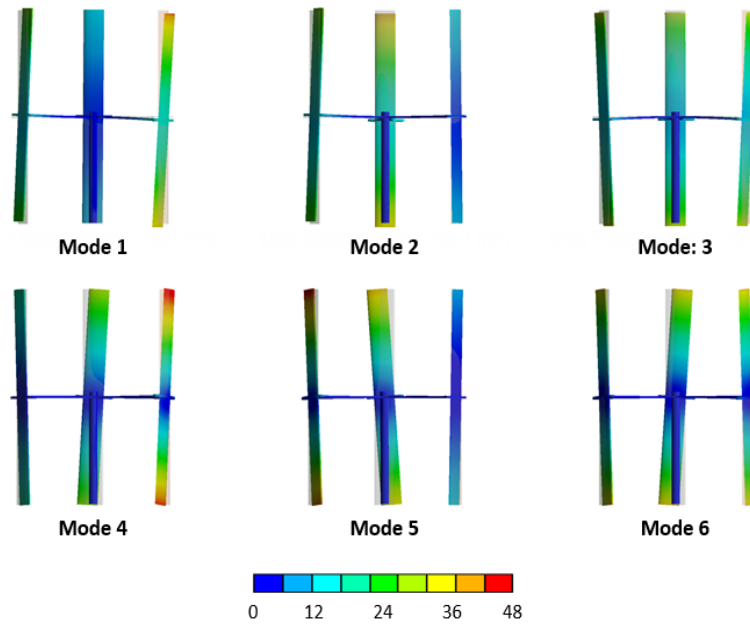


Figure 2. First six mode shapes for reference configuration coloured by total displacement [mm] representing variation from initial

More detailed information on the vibrational behavior of these two configurations is shown in Figure 3. It indicates employing the prestressed blades can offer an overall decrease in deformation amplitude at nearly all rotation speeds. In this respect, an average reduction factor of 20% was calculated for the maximum displacement.

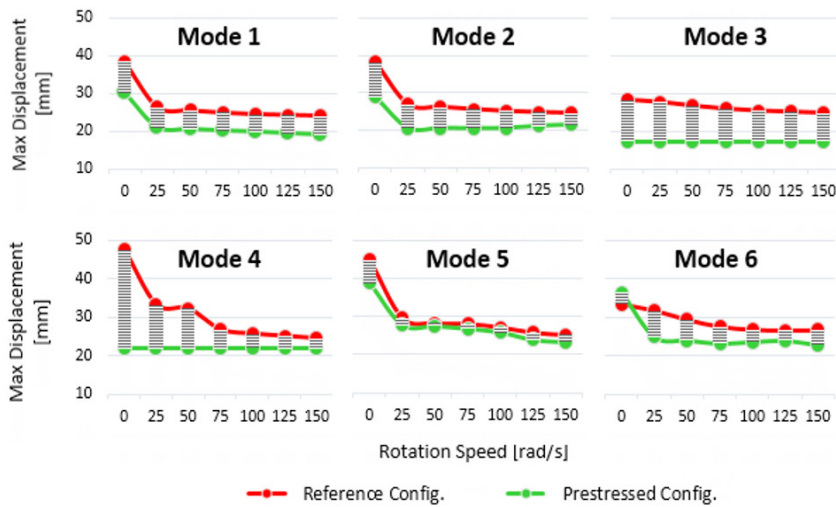


Figure 3. Maximum displacement occurred on turbine rotor over different rotation speeds at first six mode shapes

Based on the simulation results, increased rotation speed in turn, results in relatively less deformation once natural frequencies are expected to occur; however, the risk of resonance phenomenon can still be a concern. Regarding this issue, Campbell diagrams were plotted for both cases showing how the frequency of the different modes varies with the turbine rotation speed (see Figure 4). Intersection points where the Ratio=1 line crosses the curves considered as critical speed, in which rotor operational frequency comes in context with natural frequencies of turbine structure, the resonance phenomenon occurs and the response of the rotor shows a peak. In rotor dynamics, this is called as whirling and more specifically synchronous whirl, where the frequency of whirling is the same as the rotation speed.

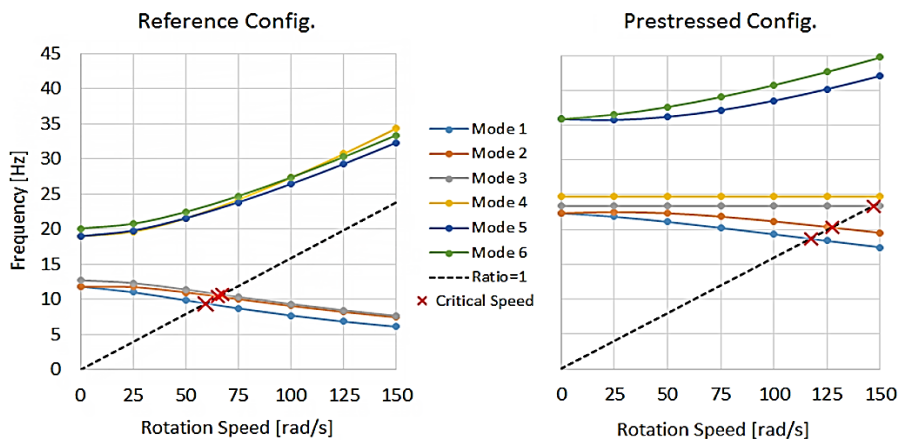


Figure 4. Campbell diagram for reference and prestressed configurations

Comparing these two Campbell diagrams, a considerable rise in natural frequencies or resonant frequencies can be seen for all speeds in prestressed blades. Moreover, the critical speeds from the original configuration ranging between 60 and 67 rad/s, corresponding to the first three mode shapes, shifted up significantly in the proposed design. A two-fold variation of lowest critical speed about 117 rad/s was observed which is fairly away from the normal operating condition of the commercial H-Darrieus turbines. The improved design contributes to greater protection from whirling and probable following failures. This is, in fact, in line with apparent growth in resonant frequencies of the structure due to the application of prestress-reinforced blades.

CONCLUSIONS

Results from the modal analysis show that applying a certain amount of axial pre-stress on turbine blades can significantly affect the dynamic response of the turbine structure. A one-fifth less average of maximum deformation which rotor structure is prone to while facing its resonant frequencies, as well as a wider whirling-free operational zone for the turbine with respect to its rotation speed (approximately up to 120 rad/s) are the advantages of employing prestress-reinforced blades. Prestressing can also be applied to all sizes and categories of Darrieus turbines.

ACKNOWLEDGEMENTS

The authors gratefully acknowledge the Ministry of Education, Malaysia, for sponsoring this research project through Universiti Putra Malaysia (Grant no. ERGS-5524501).

REFERENCES

- Al-Hassan, A. Y., & Hill, D. R. (1987) *Islamic technology: an illustrated history*. Cambridge: Cambridge University Press.
- Al-Maaitah, A. (1993). The design of the Banki wind turbine and its testing in real wind conditions. *Renewable Energy*, 3(6-7), 781-786.
- Brusca, S., Lanzafame, R. & Messina, M. (2014). Design of a vertical-axis wind turbine: how the aspect ratio affects the turbine's performance. *International Journal of Energy and Environmental Engineering*, 4(5), 333-340. doi:10.1007/s40095-014-0129-x.
- Jha, A. R. (2010). *Wind turbine technology*. Boca Raton, FL: CRC Press.
- Nawy, E. G. (2005). *Prestressed concrete: a fundamental approach* (5th Ed.). Upper Saddle River, NJ: Prentice Hall.
- Nilson, A. H. (1987). *Design of prestressed concrete*. New York, NY: John Wiley & Sons.
- Paraschivoiu, I. (2002). *Wind turbine design* (1st Ed.). Montréal: Polytechnic International Press.
- Pathade, H., Pandhare, P., Saskar, R., Chaudhari, R., & Bairagi, P. (2016). Design and fabrication of vertical axis wind turbine (VAWT). *International Journal of Advanced Engineering Research and Technology*, 4(5), 168-170.
- Price, T. (2005) James Blyth - Britain's first modern wind power engineer. *Wind Engineering*, 29(3), 191-200. doi:10.1260/030952405774354921.
- Roy, A. N., & Mohiuddin, S. (2015). Design and fabrication of vertical axis economical wind mill. *International Journal on Recent and Innovation Trends in Computing and Communication*, 2(3), 133-139.
- Sutherland, H. J., Berg, D. E., & Ashwill, T. D. (2012). *A retrospective of VAWT technology*. United States of America, USA: Sandia National Laboratories.
- Torabi Asr, M. (2016). *Improved performance of H-Darrieus vertical axis wind turbine with emphasis on start-up behaviour*. (Unpublished Master's Thesis). Universiti Putra Malaysia, Malaysia. doi:10.13140/RG.2.2.33999.48803
- Torabi Asr, M., Zal N. E., Mustapha, F., & Wiriadidjaja, S. (2016). Study on start-up characteristics of H-Darrieus vertical axis wind turbines comprising NACA 4-digit series blade airfoils. *Energy*, 112, 528-537. doi:10.1016/j.energy.2016.06.059
- Torabi Asr, M., Osloob, R., & Mustapha, F. (2016). Double-stage H-Darrieus wind turbine—rotor aerodynamics. *Applied Mechanics and Materials*, 829, 21-26. doi:10.4028/www.scientific.net/AMM.829.21
- Wittry, J. (2006). *NASA's Glenn Research Center*. Wind Energy Research Reaps Rewards. Retrieved from http://www.nasa.gov/vision/earth/technologies/wind_turbines.html

A Review Study on Diesel and Natural Gas and Its Impact on CI Engine Emissions

Hayder A. Alrazen^{1,2*} and K. A. Ahmad³

¹Department of Mechanical Engineering, Faculty of Engineering, Universiti Putra Malaysia, 43400 UPM, Serdang, Selangor, Malaysia

²Technical Institute/Qurna, Southern Technical University, Qurna, Basra, Iraq

³Department of Aerospace Engineering, Faculty of Engineering, Universiti Putra Malaysia, 43400 UPM, Serdang, Selangor, Malaysia

ABSTRACT

Diesel engines produce high emissions of nitrogen oxide, smoke and particulate matter. The challenge is to reduce exhaust emissions but without making changing their mechanical configuration. This paper is an overview of the effect of natural gas on the diesel engine emissions. Literature review suggests that engine load, air-fuel ratio, and engine speed play a key role in reducing the pollutants in the diesel engine emissions with natural gas enrichment. It is found that increasing the percentage of natural gas (CNG) will affect emissions. Nitrogen oxide (NO_x) is decreased and increased at part loads and high loads respectively when adding CNG. The reduction in carbon dioxide (CO₂), particulate matter (PM) and smoke are observed when adding CNG. However, carbon monoxide (CO) and unburned hydrocarbon (HC) are increased when CNG is added.

Keywords: CO, CO₂, Diesel, Engine, Emissions, HC, Natural gas (CNG), NO_x

INTRODUCTION

One of the problems associated with petrol engine is its high emissions such as carbon dioxide, carbon monoxide, hydrocarbons, particulate matter and nitric oxides (Adnan, Masjuki & Mahlia, 2009; Alrazen, Talib, & Ahmad, 2016a; Sahoo, Sahoo, & Saha, 2009), which can contaminate the environment. In order to reduce emissions, Diesel Particulate Filter (DPF) and Selective Catalytic Reduction (SCR) have been used to reduce PM and NO_x emissions respectively. These As expensive

Article history:

Received: 11 January 2017

Accepted: 21 April 2017

E-mail addresses:

hayderalrazen@yahoo.com (Hayder A. Alrazen),

aekamarul@upm.edu.my (K. A. Ahmad)

*Corresponding Author

metals are used as catalysts and to retrofit the engines alternative fuels are being developed and promoted to achieve the goals of reducing air pollution emissions (Alrazen, Talib, Adnan, & Ahmad, 2016b; Ibrahim & Bari, 2008; Karavalakis et al., 2013; Korakianitis, Namasivayam, & Crookes, 2011b).

The cleanest alternative fuel is the natural gas. Natural gas (NG) is an excellent fuel for heating and , power, due to its less harmful environmental side effects compared with conventional fuels. It is also an abundant source of clean energy.(Namasivayam, Korakianitis, Crookes, Bob-Manuel, & Olsen, 2010). Natural gas produces lower levels of emissions, such as CO_2 and NO_x , compared with traditional fuels like oil and coal (Alrazen et al., 2016a). Additionally, no particulate matter or sulphur dioxide are produced by NG and it is extensively used in the automobile and consumer goods sector, as a chemical feedstock in the manufacture of plastics and other commercially important organic chemicals (Papagiannakis & Hountalas, 2004; Ramamurthy, 2006).

The NG which contains between 85% and 95% methane is gas extracted from the earth. It is a naturally occurring hydrocarbon gas mixture and includes varying amounts of other higher alkanes. It is formed when layers of decomposing plant and animal matter are exposed to intense heat and pressure under the surface of the Earth over millions of years. The energy that the plants originally obtained from the sun is stored in the form of chemical bonds in the gas.

It is usually found trapped among the rock in the earth's crust and located in close proximity with liquid petroleum. The NG has a broad flammability range between 5% and 15% allowing for lean burn. Additionally, it has high octane rating (>120) with increased compression ratio (Korakianitis, Namasivayam, & Crookes, 2011a; Williams, 2004). The aim of this review paper is to investigate the impact of natural gas in diesel fuel engines.

EFFECTS OF CNG ON NO_x EMISSION

Nitrogen oxides (NO_x), released during coal burning, consists of nitric oxide (NO) and nitrogen dioxide (NO_2), known as NO_x ; the latter is released through ignition and includes NO (90%-95%) and NO_2 (5%-10%) (Alrazen et al., 2016b).

Abhishek Paul et al. (2013) reported a reduction of NO_x emission with CNG-diesel combination. Figure 1 shows at 80% load condition, the emission of NO_x diminishes with increased CNG for all load conditions. When the CNG injection durations increase from 4000 sac to 7500 sac, 12,000 μSec , 15,000 μSec and 18,000 μSec , it results in a maximum reduction in NO_x emission by 33%, 47.43%, 61.3%, 68.57% and 66.49% respectively (Paul et al., 2013). This is primarily because of cool gas entering the cylinder, so that it reduces ignition temperature (Kalam et al., 2009). Further, nonappearance of overabundant oxygen because of CNG supplanting admission air produces lower NO_x emission.

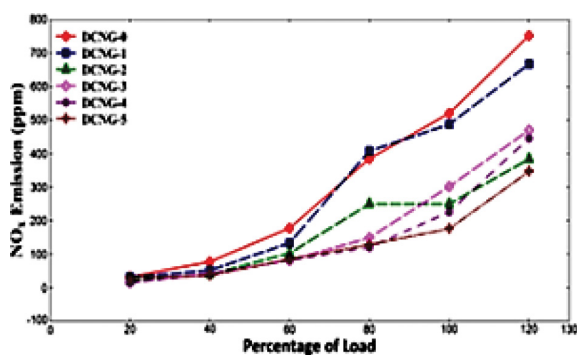


Figure 1. Variation of NO_x emission with load for D-CNG combination (Paul et al., 2013)

Lounici et al. (2014) found (see Figure 2) at low and medium loads, NO_x emission in dual mode is lower compared with traditional fuels. The development of thermal NO_x is for the most part supported by two parameters: high oxygen fraction and high charge temperature (Wang, Deng, He & Zhou, 2007). For these loads, the g temperatures for both modes are almost the same (see Figure 3(a)). Higher oxygen concentrations (see Figure 3(b)) results in higher level of NO_x emissions (Lounici et al., 2014). At high loads, the authors reported that the NO_x emission in dual fuel mode is higher than using diesel fuel alone. (Figure 3a). The higher temperature is due to release of heat in the premixed burning stage, which is the consequence of the fuel ignition at those loads (Lounici et al., 2014).

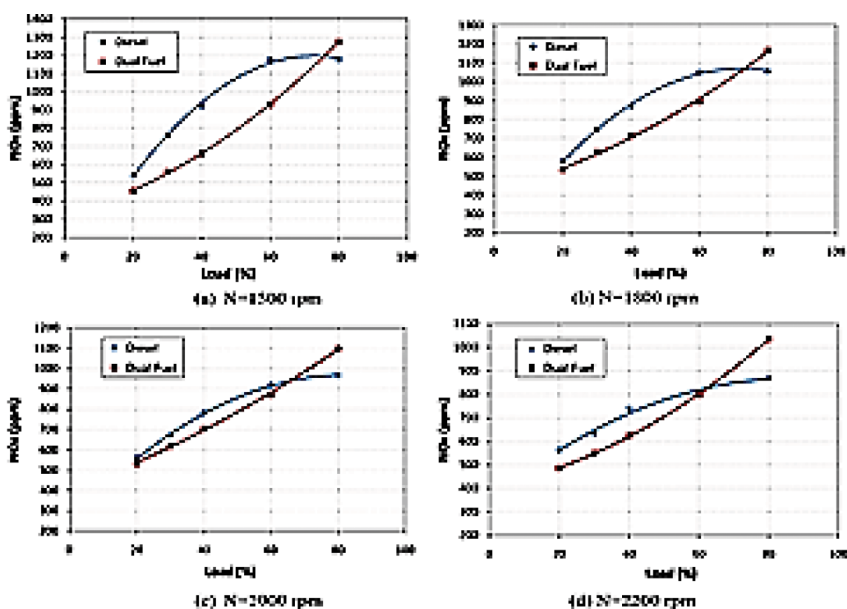


Figure 2. Variation of NO_x emission according to load at different engine speeds (Lounici et al., 2014)

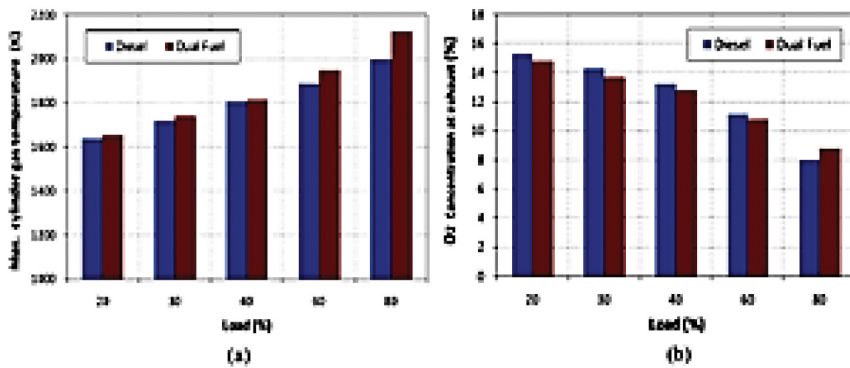


Figure 3. Maximum cylinder gas temperature (a) and oxygen concentration (b) at various loads (N = 2000 rpm) (Lounici et al., 2014)

EFFECTS OF CNG ON PARTICULATE MATTER (PM) & SMOKE

Particulate matter and smoke are an outcome of poor ignition (Saravanan & Nagarajan, 2008; Zhou, Cheung, & Leung, 2014). Exhaust smoke is considered as the contrast in the middle of development and oxidation of soot (Khan, Greeves, & Wang, 1973). Soot is formed amid ignition at high temperature. Fuel pyrolysis is portrayed as chain fracture of hydrocarbon when there is no oxygen. Such fractures along these lines transform into nucleation destinations which result in hydrocarbons and sulphates residue particles. In like manner, soot oxidation happens during high temperatures (Masood, Ishrat, & Reddy, 2007). Paul et al. (2013) noted different exhaust smoke related to distinctive fuel blends at diverse load conditions (see Figure 4). Figure 4 shows that use of CNG reduces emissions at all load conditions. At 40% load condition, CNG (15,000 μ Sec injection duration) demonstrates smoke haziness of 13%, which is half that of diesel. At full load condition, CNG (4,000 μ Sec injection duration) indicated smoke darkness of 17.4%, lower than that that of diesel (Paul et al., 2013).

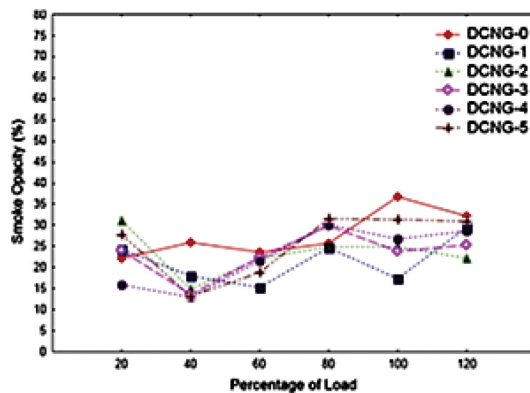


Figure 4. Variation of smoke opacity with load for D-CNG combination (Paul et al., 2013)

Lounici et al. (2014) measured soot emission for 1500, 1800, 2000 and 2200 rpm for the two engine modes. Figure 5 presents results for two engine speeds (1500 and 2000 rpm). It is clear that dual fuel mode is an effective strategy to lessen soot emission particularly at high loads. Soot emission in dual fuel mode is much lower compared with normal diesel especially for high loads. Use of Natural gas results in reduced soot emission as the former contains high methane levels which are responsible in producing small amounts of soot (Ibrahim & Bari, 2008; Lounici et al., 2014; Zhou et al., 2014).

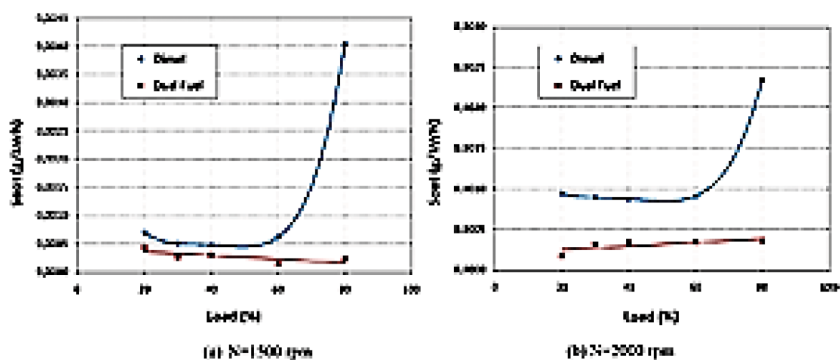


Figure 5. Soot emissions at various loads for both dual fuel and conventional diesel modes at different engine speeds (Lounici et al., 2014)

EFFECTS OF CNG ON UNBURNED HYDROCARBON

Unburnt hydrocarbon emissions are the consequences of inadequate burnings (Alla, Soliman, Badr, & Rabbo, 2002). Numerous studies have shown that dual fuel mode emits higher HC in contrast to using traditional diesel mode, especially at part load conditions (Abdelaal & Hegab, 2012; Zhou et al., 2014). This is a direct result of the blend of gaseous fuel and air at such conditions and poor fuel efficiency since much of the natural gas escapes from the ignition procedure increasing the HC emissions. At high loads, the blend and the change in the fuel use reduces HC, but it is higher than using traditional diesel mode (Abdelaal & Hegab, 2012). Paul et al. (2013) reported that (Figure 6), the unburned hydrocarbon was increased along with adding natural gas into diesel. They discovered the most noteworthy unburned hydrocarbon outflow of 352 ppm was seen with most astounding CNG infusion at 20% load, which is 311 ppm (just about 8.5 times) higher than that of diesel at the same load condition. This could be because methane is slower to respond than hydrocarbon and the burning velocity may be too moderate for burning at extremely lean blend. With expanding load, the mean viable weight rises, bringing about a higher exhaust temperature, which results in decrease of unburnt hydrocarbons (Bedoya, Arrieta, & Cadavid, 2009).

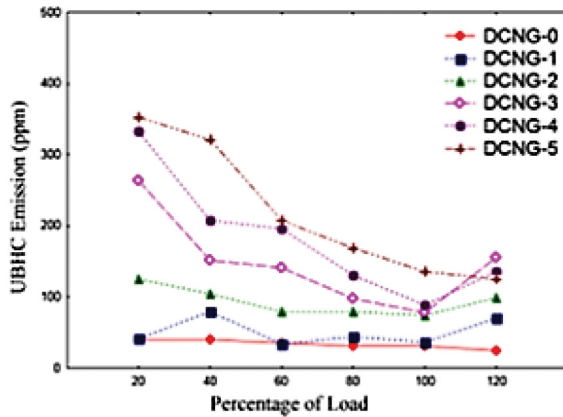


Figure 6. Variation of UBHC emission with load for D-CNG combination (Paul et al., 2013)

Lounici et al. (Lounici et al., 2014) analysed unburned hydrocarbon emissions, as a component of engine load, for the two modes at 1500, 1800, 2000 and 2200 rpm engine speeds (Figure 8). They found that the pattern of aggregate hydrocarbon (THC) outflow is comparable. At any engine load, THC emissions for dual mode are significantly higher compared with using diesel. At low load, the low temperature and the high air-fuel proportion of gaseous fuel blend result in weak ignition. Thus, the level of methane does not influence ignition. On the other hand, at lower loads, regardless of the fact that the ignition conditions are not positive, (see Figure 7), the THC outflows are lower. At the point when the load increases, the emissions increases as ignition quality is not adequate to bring down the THC outflows. For high loads, higher charge temperature and increased gaseous fuel result in a further change in the ignition process, and a reduction in the unburned hydrocarbon outflows (Alla et al., 2002).

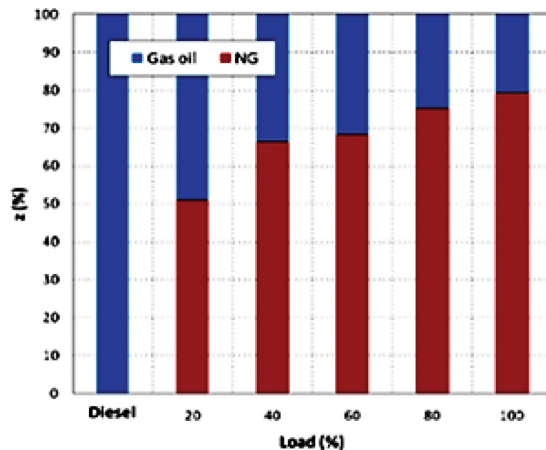


Figure 7. Variation of the participation rate (Z) as a function of load, N = 1500 rpm (Lounici et al., 2014)

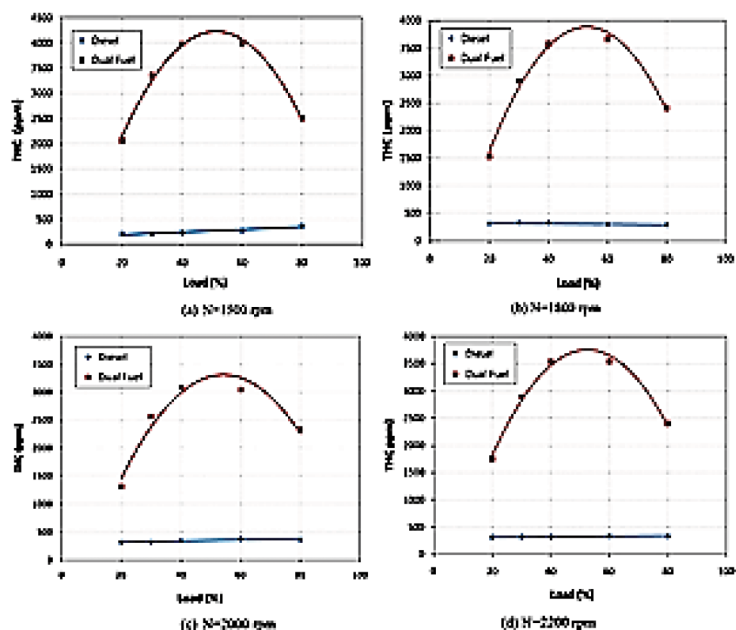


Figure 8. Unburned hydrocarbon emissions at various loads for both dual fuel and conventional diesel modes for different engine speeds (Lounici et al., 2014)

EFFECTS OF CNG ON CARBON MONOXIDE

Carbon monoxide (CO) is a component of the unburned gaseous fuel and blend temperature, both of which control the rate of fuel disintegration and oxidation (Heywood, 1988; Turns, 1996). CO is released through the ignition process with rich fuel-air blends and when there is lack of oxygen to completely burn all the carbon in the fuel to CO₂ (Alrazen et al., 2016a). Paul et al. (2013) studied different load conditions for all fuel combinations to see their effect on the CO emission (Figure 9). It is clear at 40% load, CO emissions is increased by 41.37%, 70% at 80% load, and 94.21% at 120% load (Paul et al., 2013). This increase in CO emissions when CNG is increased is a sign of deficient oxygen inside the cylinder through combustion. Kalam et al. (2009) had similar findings.

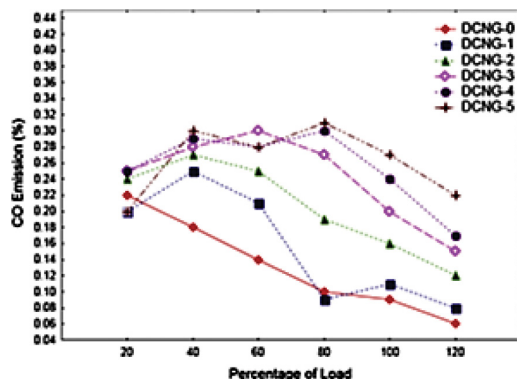


Figure 9. Variation of CO emission with load for D-CNG combination (Paul et al., 2013)

Lounici et al. (Lounici et al., 2014) reported the variation of carbon monoxide emissions under diesel mode and CNG-diesel dual mode and 1500 and 2000 rpm, as a function of engine load. As illustrated in Figure 10, CO outflows are higher for dual fuel mode at low and medium loads. On the other hand, CO for dual mode diminishes when engine load is increased as a consequence of gaseous fuel use. Then again, for high loads, in light of extremely rich blends in traditional diesel, which bring about bad burning, the CO outflows are fundamentally higher (Lounici et al., 2014). In brief, it can be seen that CO emissions with dual mode is consistently higher. This is due to the fact dual fuel mode experiences a poor fuel usage that prompts deficient ignition and high HC emission. That is, fuel disintegration and oxidation is not upgraded, and hence, CO emissions are increased. I Increasing the load diminishes CO emissions; as more fuel results in a complete ignition.

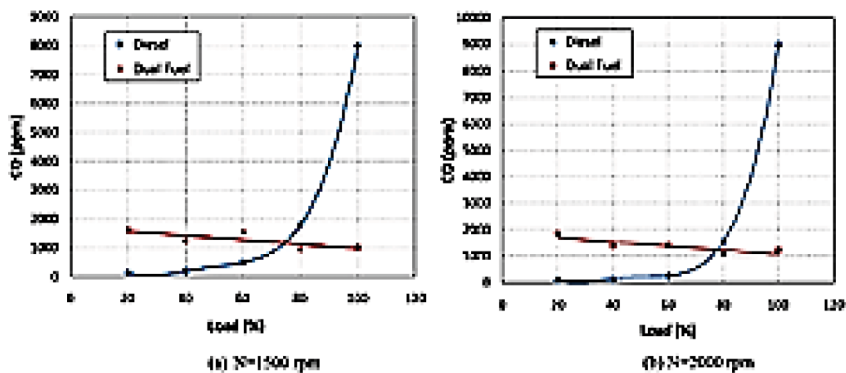


Figure 10. Variation of the CO emissions according to load, for various engine speeds (Lounici et al., 2014)

EFFECTS OF CNG ON CARBON DIOXIDE

Carbon dioxide (CO₂) is the most noticeable human made Greenhouse gas emission. (Alrazen et al., 2016a). Natural gas has one of the least carbon substance among hydrocarbons, bringing about a capability of lower CO₂ emission than that of clean diesel (Caillol, Berardi, Brecq, Ramspacher, & Meunier, 2004). Most studies affirmed that the utilisation of natural gas in a dual fuel engine at high loads as a good strategy to reduce climate change (Lounici et al., 2014). Lounici et al. (2014) compared conventional diesel mode and CNG-diesel dual mode under two engine speeds as shown in Figure 11. They showed that the CO₂ emission for diesel mode was higher compared with CNG-diesel mode. At low loads, the contrast between CO₂ emissions for traditional diesel and dual fuel mode is not significant. As for higher loads, because of the increase of engine load under dual fuel mode which is accomplished by expanding the measure of natural gas, the distinction is clearer. In this situation, the important role of natural gas to reduce the CO₂ emissions is clear (Martínez, Mahkamov, Andrade, & Lora, 2012; Lounici et al., 2014).

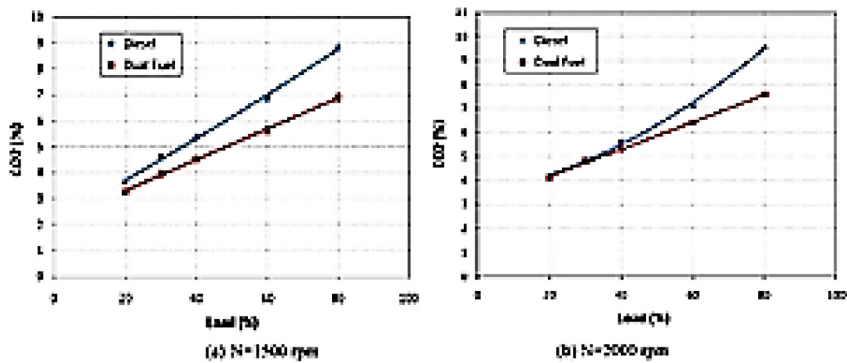


Figure 11. Variation of the CO₂ emissions according to load, for various engine speeds (Lounici et al., 2014)

Thus, it can be seen that dual fuel mode emits lower CO₂ in contrast with diesel mode. This is due to the perfect way of burning of the natural gas, lower carbon-to-hydrogen proportion (C/H); for one reason. The other reason may be the high HC outflow of dual fuel mode and the abnormal burning, as uncovered by the high CO emit; especially at part load (Alrazen et al., 2016a). At high load, on the other hand, the change in the burning procedure causes CO₂ emissions to increment, however its worth stays substandard compared to that of diesel ignition (Abdelaal & Hegab, 2012).

CONCLUSIONS

There are five significant findings in this review paper:

- moderate and low loads, NO_x emissions of CNG-diesel dual fuel mode are lower compared with using diesel fuel alone. At high loads, however, the emissions of NO_x of CNG-diesel dual fuel mode is higher compared with that of diesel one. This is due to heat released in the early premixed burning stage, which is the consequence of the fuel ignition change at those loads.
- The utilisation of natural gas results in dramatically reduced soot emission. This reduction is due to methane which is the main component of natural gas.
- Dual fuel mode leads to greater HC emissions compared with traditional diesel mode, especially at part load conditions. This is a direct result of the blend of gaseous fuel and air at such conditions as well as poor fuel efficiency; much of the natural gas escapes from the ignition procedure leading to greater HC emissions.
- Majority of studies have reported that CO emission with dual mode is always higher than conventional diesel mode. The reason for this is due poor fuel utilisation leading to abnormal combustion and high level of CO emission.
- Dual fuel mode produces significantly reduced CO₂ emissions in contrast with using diesel mode alone. This is due to perfect burning of the natural gas and the lower carbon-to-hydrogen proportion (C/H). Additionally, dual fuel mode and the abnormal burning produces high levels CO emit, especially at part load. At high load, on the other hand, the change in the burning procedure leads to higher CO₂ emissions; however, it is lower compared with that of diesel ignition.

Further experiments are need to study the actual emission styles for example, the NO_x-HC trade-off, engine parameter choices, different engine configurations, and combustion regimes.

REFERENCES

- Abdelaal, M., & Hegab, A. (2012). Combustion and emission characteristics of a natural gas-fueled diesel engine with EGR. *Energy Conversion and Management*, *64*, 301-312.
- Adnan, R., Masjuki, H., & Mahlia, T. (2009). An experimental investigation of unmodified DI diesel engine with hydrogen addition. In *3rd International Conference on Energy and Environment, 2009, ICEE 2009* (pp. 45-49). UPM, Malaysia.
- Alla, G. A., Soliman, H., Badr, O., & Rabbo, M. A. (2002). Effect of injection timing on the performance of a dual fuel engine. *Energy Conversion and Management*, *43*(2), 269-277.
- Alrazen H. A., Talib, A. A., & Ahmad, K. A. (2016a). A two-component CFD studies of the effects of H₂, CNG, and diesel blend on combustion characteristics and emissions of a diesel engine. *International Journal of Hydrogen Energy*, *41*(24), 10483-10495.
- Alrazen, H. A., Talib, A. A., Adnan, R., & Ahmad, K. (2016b). A review of the effect of hydrogen addition on the performance and emissions of the compression-Ignition engine. *Renewable and Sustainable Energy Reviews*, *54*, 785-796.
- Bedoya, I. D., Arrieta, A. A., & Cadavid, F. J. (2009). Effects of mixing system and pilot fuel quality on diesel-biogas dual fuel engine performance. *Bioresource Technology*, *100*(24), 6624-6629.
- Caillol, C., Berardi, G., Brecq, G., Ramspacher, M., & Meunier, P. (2004). A simulation tool for evaluating gas composition effects on engine performance. *International Gas Research Conference*, (pp. 1-19).
- Heywood, J. B. (1988). *Internal combustion engine fundamentals*. New York, NY: Mcgraw-hill.
- Ibrahim, A., & Bari, S. (2008). Optimization of a natural gas SI engine employing EGR strategy using a two-zone combustion model. *Fuel*, *87*(10), 1824-1834.
- Kalam, M., Masjuki, H., Mahlia, T., Fuad, M., Halim, K., Ishak, A., ... & Shahrir, A. (2009). Experimental test of a new compressed natural gas engine with direct injection. In *SAE 2009 International Powertrains, Fuels and Lubricants Meeting, 2009* (pp. 1-7). Florence, Italy. doi:10.4271/2009-01-1967
- Karavalakis, G., Hajbabaie, M., Durbin, T. D., Johnson, K. C., Zheng, Z., & Miller, W. J. (2013). The effect of natural gas composition on the regulated emissions, gaseous toxic pollutants, and ultrafine particle number emissions from a refuse hauler vehicle. *Energy*, *50*, 280-291.
- Khan, I. M., Greeves, G., & Wang, C. H. T. (1973). *Factors affecting smoke and gaseous emissions from direct injection engines and a method of calculation* (No. 730169). SAE Technical Paper.
- Korakianitis, T., Namasivayam, A., & Crookes, R. (2011a). Diesel and rapeseed methyl ester (RME) pilot fuels for hydrogen and natural gas dual-fuel combustion in compression-ignition engines. *Fuel*, *90*(7), 2384-2395.
- Korakianitis, T., Namasivayam, A., & Crookes, R. (2011b). Natural-gas fueled spark-ignition (SI) and compression-ignition (CI) engine performance and emissions. *Progress in Energy and Combustion Science*, *37*(1), 89-112.

- Lounici, M. S., Loubar, K., Tarabet, L., Balistrrou, M., Niculescu, D., & Tazerout, M. (2014). Towards improvement of natural gas-diesel dual fuel mode: An experimental investigation on performance and exhaust emissions. *Energy*, *64*, 200-211.
- Martínez, J. D., Mahkamov, K., Andrade, R. V., & Lora, E. E. S. (2012). Syngas production in downdraft biomass gasifiers and its application using internal combustion engines. *Renewable Energy*, *38*(1), 1-9.
- Masood, M., Ishrat, M., & Reddy, A. (2007). Computational combustion and emission analysis of hydrogen–diesel blends with experimental verification. *International Journal of Hydrogen Energy*, *32*(13), 2539-2547.
- Namasivayam, A., Korakianitis, T., Crookes, R., Bob-Manuel, K., & Olsen, J. (2010). Biodiesel, emulsified biodiesel and dimethyl ether as pilot fuels for natural gas fuelled engines. *Applied Energy*, *87*(3), 769-778.
- Papagiannakis, R., & Hountalas, D. (2004). Combustion and exhaust emission characteristics of a dual fuel compression ignition engine operated with pilot diesel fuel and natural gas. *Energy Conversion and Management*, *45*(18), 2971-2987.
- Paul, A., Bose, P. K., Panua, R. S., & Banerjee, R. (2013). An experimental investigation of performance-emission trade off of a CI engine fueled by diesel–compressed natural gas (CNG) combination and diesel–ethanol blends with CNG enrichment. *Energy*, *55*, 787-802.
- Ramamurthy, B. (2006). *Design of a catalyst system with periodic flow reversal for lean burn natural gas engines*. (Master's thesis). University of Tennessee, Knoxville.
- Sahoo, B., Sahoo, N., & Saha, U. (2009). Effect of engine parameters and type of gaseous fuel on the performance of dual-fuel gas diesel engines—A critical review. *Renewable and Sustainable Energy Reviews*, *13*(6), 1151-1184.
- Saravanan, N., & Nagarajan, G. (2008). An experimental investigation of hydrogen-enriched air induction in a diesel engine system. *International Journal of Hydrogen Energy*, *33*(6), 1769-1775.
- Turns, S. R. (1996). *An introduction to combustion* (3rd Ed.). New York, NY: McGraw Hill.
- Wang, X., Deng, K., He, F., & Zhou, Z. (2007). A thermodynamics model for the compression and expansion process during the engine's motoring and a new method for the determination of TDC with simulation technique. *Applied Thermal Engineering*, *27*(11), 2003-2010.
- Williams, A. M. (2004). *Lean NOx trap catalysis for lean burn natural gas engines*. (Master's Thesis). University of Tennessee, USA. Retrieved from http://trace.tennessee.edu/utk_gradthes/2224
- Zhou, J., Cheung, C., & Leung, C. (2014). Combustion, performance and emissions of a diesel engine with H₂, CH₄ and H₂–CH₄ addition. *International Journal of Hydrogen Energy*, *39*(9), 4611-4621.



Stability of water lubricated bearing using linear perturbation method under turbulent conditions

R. Mallya^{1*}, B. S. Shenoy², R. S. Pai² and R. Pai³

¹*Department of Mechanical Engineering, Canara Engineering College, Benjanapadavu, Karnataka 574219, India*

²*Department of Aeronautical and Automobile Engineering, Manipal Institute of Technology, Manipal University, Karnataka 576104, India*

³*Department of Mechanical and Manufacturing Engineering, Manipal Institute of Technology, Manipal University, Karnataka 576104, India*

ABSTRACT

The stability of a bearing is influenced by the turbulent conditions encountered during its operation. In this paper, a linearised perturbation method is used to theoretically investigate the stability of a three-axial groove water lubricated bearing. The stiffness and the damping coefficients are plotted for different eccentricity ratios of the bearing, for groove angles of 36° and 18°. The mass parameter and the whirl ratio, which are a measure of stability, are also plotted against the bearing number for different values of Reynolds number. The bearing shows very good stability at higher eccentricity ratios. The stiffness and damping coefficients as well as the mass parameter increase as the Reynolds number increases. The whirl ratios are unaffected by the change in Reynolds number.

Keywords: Axial groove, hydrodynamic pressure, journal bearing, stability, turbulent regime, water lubrication

INTRODUCTION

Fluid film bearings are susceptible to instability to certain extent. Litwin (2009) states that strict environmental laws, the growing awareness of environmental conservation, penalties

for discharging toxic substances to the ocean, and economical estimates have resulted in enhancing the use of water-lubricated bearings. These bearings consist of a flat region called staves or lands which support the load. The flat regions are separated by axial grooves called flutes. The instability of a fluid film bearing is influenced by many

Article history:

Received: 11 January 2017

Accepted: 21 April 2017

E-mail addresses:

ravindramallya@gmail.com (R. Mallya),

satishshenoyb@yahoo.com (B. S. Shenoy),

ramamohan.pai@manipal.edu (R. S. Pai),

rbpai@yahoo.com (R. Pai)

*Corresponding Author

parameters. To prevent instability in plain cylindrical bearings, and enhance the stable speed range of the equipment designers have considered different geometries like multi-lobe, tilting pad, pressure dam, wave bearing design etc (Kakoty & Majumdar 1999). The mass of fluid is generally ignored in the study of bearing instability because of the negligible inertia effect in the calculation of the fluid film forces. The use of low viscosity fluids like water and the high-speed conditions of present day machinery make it necessary to consider the effects of fluid film inertia. The effects of turbulence and inertia of the lubricant film on bearing behavior increase as the Reynolds number increases.

The dynamic stability of a rotor supported by fluid film bearings can be studied by two different approaches, linear perturbation analysis and non-linear transient analysis. A small perturbation is assumed to be imposed on the journal centre around its equilibrium position in the linear perturbation theory. This method calculates the stiffness and damping coefficients that characterizes the equilibrium position at the shaft centre. The calculated coefficients are subsequently used to compute the critical mass and the whirl frequency. The set of stiffness and damping coefficients established, evaluates the vibration characteristics of the hydrodynamic film. The coefficients are computed from the solutions of the Reynolds equation as stated by Stachowiak and Batchelor (2013). Majumdar, Pai and Hargreaves (2004) in their analysis of water lubricated journal bearing with three axial grooves have concluded that smaller groove angle increase both load capacity and stability.

Kakoty and Majumdar (2000) in their linear perturbation analysis concluded that fluid inertia was independent of the steady state characteristics. Shenoy and Pai (2010) incorporated laminar and turbulence effects in externally adjustable fluid film bearing and observed that both in laminar as well as in turbulent flow the load capacity increases as the film thickness reduces. For a particular eccentricity value and misalignment, the shaft attitude angle and the friction value increased. Capone, Russo and Russo (1991) have theoretically analysed the influence of inertia and turbulence on the dynamic characteristics of bearings for various values of Reynolds number. From the different plots, it was observed that the direct stiffness coefficients changed their trend as the Reynolds number was varied. It was also observed that, the cross-coupled stiffness coefficients were affected by turbulence and fluid inertia. Pai, Rao, Shenoy and Pai (2012) in their study on tri taper journal bearing found the critical mass parameter increased with the increase in the ramp size to contribute to an improvement in the stability of the bearing. The variation in film thickness of the lubricant also affected the performance characteristics of the bearing. Rao and Sawicki (2002) have theoretically analyzed the effect of cavitation on fluid film bearing using linear stability analysis. Their theoretical results were in close agreement with the experimental published work. The study validated the significance of incorporating cavitation flow modelling in linear stability analysis of journal bearing. Hashimoto and Wada (1982a) in their analysis on dynamic characteristics of turbulent journal bearings observed that the whirl frequencies decreased with turbulence for all slenderness ratios, but the inertial effects were different for each slenderness ratio. The frequencies of infinitely short bearings became higher with the inertia forces at high eccentricities and decreased with changes in the slenderness ratio. Kumar and Mishra (1996) used Constantinescu's turbulent lubrication theory to investigate the stability of hydrodynamic worn journal bearings in turbulent conditions. It was observed that stability decreases initially with the wear depth parameter and then improves

when the wear depth parameter is increased. With an increase in L/D ratio, the stability of the worn bearings deteriorates when operating in turbulent lubrication regime. Worn bearings with lower L/D ratios were relatively more stable. The dynamic characteristics in journal bearing incorporating turbulence and inertia effects were studied by Hashimoto and Wada (1982b). It was found that the Sommerfeld number decreased by turbulence effects and the attitude angles increased by inertia effects. Lahmar (2005) has theoretically investigated the double-layered journal bearings lubricated with couple-stress fluids and discussed the combined effects of flow and fluid–solid interaction on the stability of double-layered journal bearings. It was observed that the peak pressure, the load capacity, stability region of the bearing increased with the couple stress parameter. In the present study, the dynamic coefficients for 3 axial water lubricated bearing in the turbulent regime are computed using the linearized bearing reaction method for groove angles 18° and 36° . The whirl ratio and mass parameter are also plotted for different values of bearing number for different eccentricity ratios.

METHODS

Procedure

Dynamic characteristics. The Reynolds equation governs the pressure distribution in the clearance space between journal and bearing. To study the turbulent flow in a fluid film, the Reynolds equation is modified by introducing ‘turbulence coefficients’. The equation [1] shows the modified Reynolds equation.

$$\frac{\partial}{\partial x} \left[\frac{1}{k_\theta} h^3 \frac{\partial p^*}{\partial x} \right] + \frac{\partial}{\partial z} \left[\frac{1}{k_z} h^3 \frac{\partial p^*}{\partial \theta} \right] = \frac{1}{2} U \eta \frac{\partial h}{\partial x} + \eta \frac{\partial h}{\partial t} \quad [1]$$

The governing equation [1] in non-dimensional form, reduces to

$$\frac{1}{k_\theta} \left[\frac{\partial}{\partial \theta} \left((\bar{h}^3) \frac{\partial \bar{p}}{\partial \theta} \right) \right] + \frac{1}{k_z} \left(\frac{R^2}{L^2} \right) \left[\frac{\partial}{\partial \bar{z}} \left((\bar{h}^3) \frac{\partial \bar{p}}{\partial \bar{z}} \right) \right] = \frac{1}{2} \frac{\partial \bar{h}}{\partial \theta} \quad [2]$$

The turbulence model used is Ng – Pan where the coefficients k_θ and k_z are calculated as

$$k_\theta = 12 + k_x (Re_L)^{n_x} \quad [3]$$

$$k_z = 12 + k_{zz} (Re_L)^{n_z} \quad [4]$$

The values for k_x, n_x, k_{zz} and n_z are listed in the table 1 as suggested by Taylor & Dowson (1974).

Table 1
Turbulence parameters from Taylor and Dowson (1974)

	k_x	n_x	k_{zz}	n_z
$Re_L \geq 50,000$	0.0388	0.80	0.0213	0.80
$10,000 \leq Re_L < 50,000$	0.0250	0.84	0.0136	0.84
$5,000 \leq Re_L < 10,000$	0.0250	0.84	0.0088	0.88
$Re_L < 5,000$	0.0039	1.06	0.0021	1.06

The boundary conditions used are the Reynolds boundary conditions, i.e. $\bar{p} = 0$, when $\frac{\partial \bar{p}}{\partial \theta} = 0$. It is assumed that journal moves in a periodic movement with small amplitude of $\Re(\mathcal{C}\varepsilon_1 e^{i\tau})$ along the line of centres and $\Re(\mathcal{C}\varepsilon_0 \phi_1 e^{i\tau})$ perpendicular to the line of centres. The journal moves around its steady state position of ε_o and ϕ_o . When the instability of the journal begins, the initial position of the journal centre can be termed as a steady state value (ε_o, ϕ_o) together with a harmonic vibration of frequency ω_p thus

$$\varepsilon = \varepsilon_o + \varepsilon_1 e^{i\tau}, \phi = \phi_o + \phi_1 e^{i\tau}$$

Where, $|\varepsilon_1| \ll \varepsilon_o, |\phi_1| \ll \phi_o$.

When the journal is functioning under very small amplitude of vibration, first order perturbation method will be applicable. The pressure and film thickness equations are written as

$$\bar{p} = \bar{p}_o + \varepsilon_1 e^{i\tau} \bar{p}_1 + \varepsilon_o \phi_1 e^{i\tau} \bar{p}_2 \tag{5}$$

$$\bar{h} = \bar{h}_o + \varepsilon_1 e^{i\tau} \cos \theta + \varepsilon_o \phi_1 e^{i\tau} \sin \theta \tag{6}$$

Substitution of equation [5] and [6] in equation [2] and holding on to first linear terms will result in the equations [7], [8] and [9].

$$\varepsilon_o \left[\frac{12}{k_\theta} \left[\bar{h}_o^3 \frac{\partial^2 \bar{p}_o}{\partial \theta^2} + 3\bar{h}_o^2 \frac{\partial \bar{h}_o}{\partial \theta} \frac{\partial \bar{p}_o}{\partial \theta} \right] + \frac{12}{k_z} \left(\frac{R}{L} \right)^2 \bar{h}_o^3 \frac{\partial^2 \bar{p}_o}{\partial z^2} - \Lambda \frac{\partial \bar{h}_o}{\partial \theta} - 2\lambda \Lambda \frac{\partial \bar{h}_o}{\partial \tau} \right] = 0 \tag{7}$$

$$\varepsilon_1 e^{i\tau} \left[\frac{12}{k_\theta} \left[\bar{h}_o^3 \frac{\partial^2 \bar{p}_1}{\partial \theta^2} + 3\bar{h}_o^2 \cos \theta \frac{\partial \bar{h}_o}{\partial \theta} \frac{\partial^2 \bar{p}_o}{\partial \theta^2} - 3\bar{h}_o^2 \sin \theta \frac{\partial \bar{p}_o}{\partial \theta} + \frac{6\bar{h}_o}{\partial \theta} \frac{\partial \bar{h}_o}{\partial \theta} \frac{\partial \bar{p}_o}{\partial \theta} \cos \theta + 3\bar{h}_o^2 \frac{\partial \bar{h}_o}{\partial \theta} \frac{\partial \bar{p}_1}{\partial \theta} \right] + \frac{12}{k_z} \left(\frac{R}{L} \right)^2 \left[\bar{h}_o^3 \frac{\partial^2 \bar{p}_1}{\partial z^2} + 3\bar{h}_o^2 \cos \theta \frac{\partial^2 \bar{p}_o}{\partial z^2} \right] \right] \tag{8}$$

$$+ \Lambda \sin \theta - 2i\lambda \Lambda \cos \theta = 0$$

$$\varepsilon_o \phi_1^{i\tau} \left[\frac{12}{k_\theta} \left[\bar{h}_o^3 \frac{\partial^2 \bar{p}_2}{\partial \theta^2} + 3\bar{h}_o^2 \sin \theta \frac{\partial^2 \bar{p}_o}{\partial \theta^2} + 3\bar{h}_o^2 \cos \theta \frac{\partial \bar{p}_o}{\partial \theta} + 6\bar{h}_o \frac{\partial \bar{h}_o}{\partial \theta} \frac{\partial \bar{p}_o}{\partial \theta} \sin \theta + 3\bar{h}_o^2 \frac{\partial \bar{h}_o}{\partial \theta} \frac{\partial \bar{p}_2}{\partial \theta} \right] + \frac{12}{k_z} \left(\frac{R}{L} \right)^2 \left[\bar{h}_o^3 \frac{\partial^2 \bar{p}_2}{\partial z^2} + 3\bar{h}_o^2 \sin \theta \frac{\partial^2 \bar{p}_o}{\partial z^2} \right] \right] + \Lambda \cos \theta - 2i\Lambda \lambda \sin \theta = 0 \tag{9}$$

The dynamic movement of the centre of the journal, $Re(C\varepsilon_1 e^{i\tau})$ being in the parallel and $Re(C\varepsilon_o \phi_1 e^{i\tau})$ in the perpendicular direction of the line of centres will be used to compute the dynamic pressures \bar{p}_1 and \bar{p}_2 . The load components of the dynamic pressures along and at right angles to the line of centres are mentioned in equations [10] and [11].

$$(W_1)_r = \int_0^L \int_0^{2\pi} p_1 R \cos \theta d\theta dz \tag{10}$$

$$(W_1)_\phi = \int_0^L \int_0^{2\pi} p_1 R \sin \theta d\theta dz \tag{11}$$

The equations [12] to [15] are used to compute the stiffness and the damping values of the journal bearing

$$\bar{K}_{rr} = -Re \left(\int_0^1 \int_0^{2\pi} \bar{p}_1 \cos \theta d\theta d\bar{z} \right) \tag{12}$$

$$\bar{K}_{\phi r} = -Re \left(\int_0^1 \int_0^{2\pi} \bar{p}_1 \sin \theta d\theta d\bar{z} \right) \tag{13}$$

$$\bar{D}_{rr} = -Im \left(\frac{\int_0^1 \int_0^{2\pi} \bar{p}_1 \cos \theta d\theta d\bar{z}}{\lambda} \right) \tag{14}$$

$$\bar{D}_{\phi r} = -Im \left(\frac{\int_0^1 \int_0^{2\pi} \bar{p}_1 \sin \theta d\theta d\bar{z}}{\lambda} \right) \tag{15}$$

Where $\bar{K}_{ij} = \frac{K_{ij}C}{LDp_s}$ and $\bar{D}_{ij} = \frac{D_{ij}C\omega}{LDp_s}$

Similarly, equations [16] to [19] give the stiffness and damping values considering the dynamic movement of the centre of the shaft along the ϕ direction,

$$\bar{K}_{\phi\phi} = -Re \left(\int_0^1 \int_0^{2\pi} \bar{p}_2 \sin \theta d\theta d\bar{z} \right) \tag{16}$$

$$\bar{K}_{r\phi} = -Re \left(\int_0^1 \int_0^{2\pi} \bar{p}_2 \cos \theta d\theta d\bar{z} \right) \tag{17}$$

$$\bar{D}_{\phi\phi} = -Im \left(\frac{\int_0^1 \int_0^{2\pi} \bar{p}_2 \sin \theta d\theta d\bar{z}}{\lambda} \right) \tag{18}$$

$$\bar{D}_{r\phi} = -Im \left(\frac{\int_0^1 \int_0^{2\pi} \bar{p}_2 \cos \theta d\theta d\bar{z}}{\lambda} \right) \tag{19}$$

Stability criteria. The rotor is assumed to be stiff or inelastic and considered to have mass M . The stability of the rotating journal is evaluated by computing the film forces F_r and F_ϕ , which is obtained by combining the equations of motion [20] and [21].

$$F_r + W \cos \phi - MC \left[\frac{d^2 \varepsilon}{dt^2} - \varepsilon \left(\frac{d\phi}{dt} \right)^2 \right] = 0 \tag{20}$$

$$F_\phi - W \sin \phi - MC \left[\varepsilon \frac{d^2 \phi}{dt^2} + 2 \frac{d\varepsilon}{dt} \frac{d\phi}{dt} \right] = 0 \tag{21}$$

After substituting ε, ϕ and non-dimensionalising and simplifying,

$$\bar{M} = \frac{1}{\lambda^2 (\bar{D}_{\phi\phi} + \bar{D}_{rr})} \left[\frac{(\bar{D}_{rr} \bar{K}_{\phi\phi} + \bar{K}_{rr} \bar{D}_{\phi\phi}) - (\bar{K}_{\phi r} \bar{D}_{r\phi} + \bar{D}_{\phi r} \bar{K}_{r\phi})}{\varepsilon_o} + \bar{W} (\bar{D}_{rr} \cos \phi_o - \bar{D}_{\phi r} \sin \phi_o) \right] \tag{22}$$

$$\begin{aligned} \bar{M}^2 \lambda^4 - \lambda^2 \left[\bar{M} \left(\frac{\bar{W} \cos \phi_o}{\varepsilon_o} + \bar{K}_{\phi\phi} + \bar{K}_{rr} \right) + (\bar{D}_{rr} \bar{D}_{\phi\phi} - \bar{D}_{\phi r} \bar{D}_{r\phi}) \right] \\ + (\bar{K}_{rr} \bar{K}_{\phi\phi} - \bar{K}_{\phi r} \bar{K}_{r\phi}) + \frac{\bar{W}}{\varepsilon_o} (\bar{K}_{rr} \cos \phi_o - \bar{K}_{\phi r} \sin \phi_o) = 0 \end{aligned} \quad [23]$$

Equations [22] and [23] use the computed stiffness and damping coefficients to evaluate the stability of a rigid journal held by the bearing. \bar{M} and λ are the solutions calculated from equations [22] and [23] which are linear algebraic equations. The threshold speed of journal is calculated from this value of \bar{M} . The bearing system will be unstable if the speed of the system goes beyond the limiting speed. The rotating speed of the shaft centre can be found from the whirl ratio. The rotation of the shaft and the rotation of its centre are in the same direction.

Solution Procedure

The solution method used here is similar to that of Majumdar et al. (2004). A second-order finite difference method was used for solving the governing Reynolds equation incorporated with the turbulent coefficients. A programmable code in MATLAB R2012b was written to calculate the non-dimensional dynamic pressure. The circumferential coordinate θ for an axial groove bearing is considered from the region of maximum film thickness. Initially, an arbitrary value of attitude angle is considered, the solution converges when the arbitrary value and the calculated value of attitude angle for a given accuracy is achieved. The calculated attitude angle is considered by the program to compute the dynamic non-dimensional pressure. The aspect ratio of the grid was kept equal; increment in θ direction $\delta\theta$, and increment in the z direction δz , both were kept equal to 0.0524. The iterative procedure of calculation with an accuracy value of 0.0001 at the nodes was used for the convergence of the pressure. A relaxation factor of 1.3 was implemented to accelerate the convergence of dynamic pressure. The dynamic loads are calculated using the equations [10] and [11]. The program computes both the stiffness and damping coefficients, given in the equations [12] to [19]. The stability criterion of the bearing is analysed using equations [22] and [23] where the mass parameter and the whirl ratio are calculated. The L/D value is taken as 1 for both the groove angles.

Validation

Figure 1 and 2 show the validation of the codes used. The results of the codes are validated with the published data from Majumdar et al. (2004). The plots from the present analysis in the Figure 1 are of critical mass parameter and whirl ratio considering the flow of the lubricant in the laminar regime. The nature of the plots in Figure 1 and Figure 2 are in good agreement, with little variation in the values.

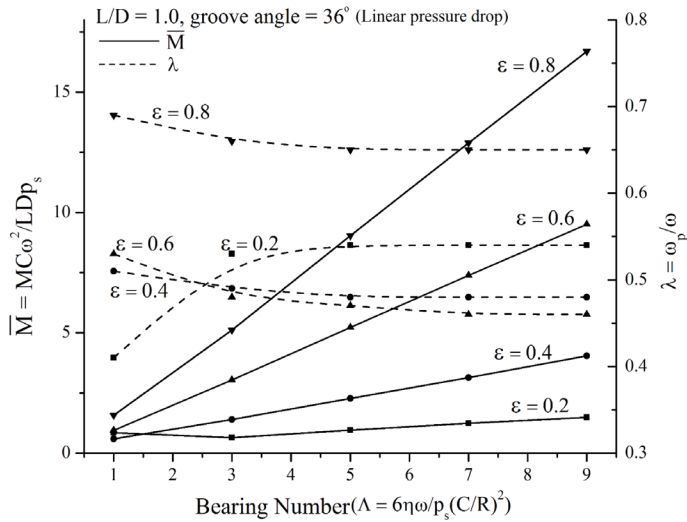


Figure 1. Effect of Critical Mass variable (\bar{M}) and whirl ratio (λ) with bearing no. for different eccentricity ratios (Present analysis)

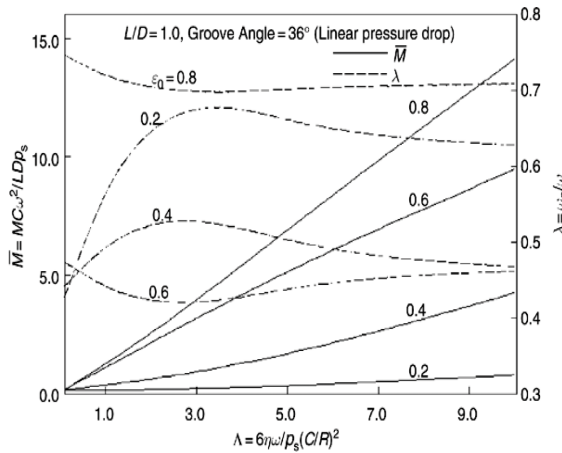


Figure 2. Effect of Mass variable (\bar{M}) & whirl ratio (λ) with various bearing no. for different eccentricity ratios, from Majumdar et al. (2004)

RESULTS AND DISCUSSIONS

Figure 3, 4 and 5 are the graphs for mass parameter versus bearing number for different values of eccentricity ratios. The whirl ratio versus bearing number is also plotted in the same graph. The groove angle considered is 18° with values of Re varying from 4000 to 55,000. Figure 6, 7 and 8 are the similar plots for groove angle 36° . The major factors responsible for whirl instability are the two coefficients calculated from the codes, stiffness coefficients \bar{K}_{ij} and damping coefficients \bar{D}_{ij} . The individual coefficients of either stiffness or damping do not indicate stability characteristics. The computed coefficient values are substituted in the equations of motion to obtain threshold or limiting speed of the bearing. The threshold speed

is the limiting speed within which the bearing has to operate. The bearing becomes unstable if the speed of the bearing goes beyond the threshold speed. The value of mass parameter, \bar{M} gives the threshold speed. The whirl speed is established from the whirl ratio λ for a given journal speed. \bar{M} and λ , are the factors used to quantify the stability of the bearing. The upper region of the curve in all the figures 3 to 8 of \bar{M} versus bearing number are unstable. The journal bearing system should function within the stable region. The stable region of the bearing increases as the eccentricity ratio is increased. The axial groove journal bearings, irrespective of the turbulent conditions and groove angles, show higher values of \bar{M} , thereby revealing that; theoretically, the bearings become stable when they are operating in high eccentricities. It can also be observed that for the same value of Reynolds number, the \bar{M} value for the bearing with the 18° groove angle is more than that for 36° groove angle. This indicates that a bearing having smaller groove angle is more stable than that with a higher groove angle. The stability of the bearing improved with the increase in the Reynolds number and increase in eccentricity ratio as seen from all the plots. The values of the whirl ratios reduce when the bearing is operating in the higher eccentricity as seen from all the graphs. The value of λ decreases for both the groove angles for $\epsilon = 0.8$ and $\epsilon = 0.6$. Theoretically, the influence of turbulent flow affects the stability of the bearing as seen from all the plots.

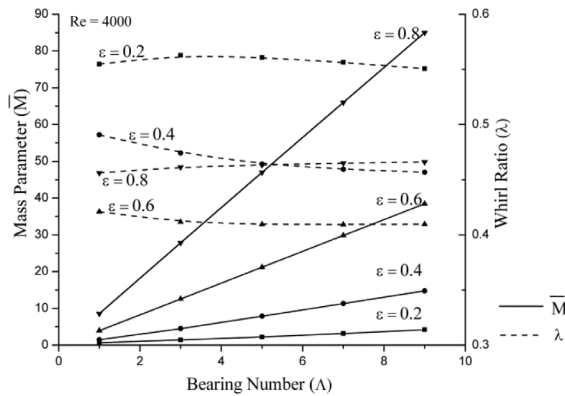


Figure 3. Effect of Reynolds Number ($Re = 4000$) on Mass variable, whirl ratio with various bearing no. for various ϵ for groove angle 18°

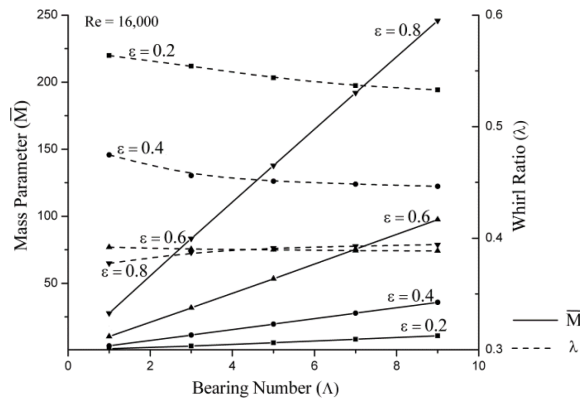


Figure 4. Effect of Reynolds Number ($Re = 16,000$) on Mass variable, whirl ratio with various bearing no. for various ϵ for groove angle 18°

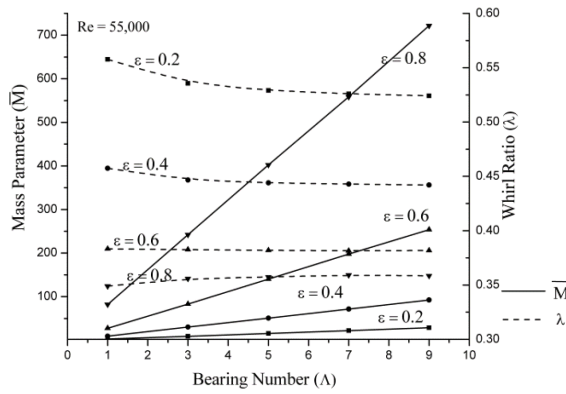


Figure 5. Effect of Reynolds Number ($Re = 55,000$) on Mass variable, whirl ratio with various bearing no. for various ϵ for groove angle 18°

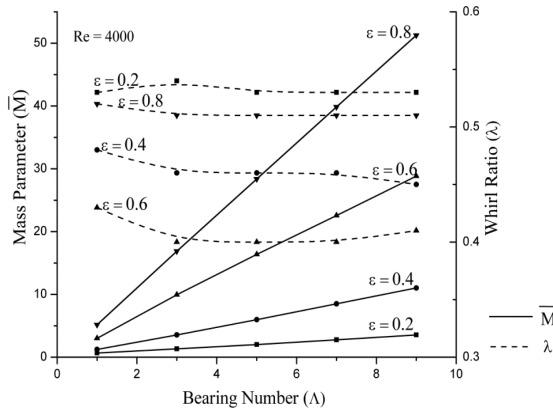


Figure 6. Effect of Reynolds Number ($Re = 4000$) on Mass variable, whirl ratio with various bearing no. for various ϵ for groove angle 36°

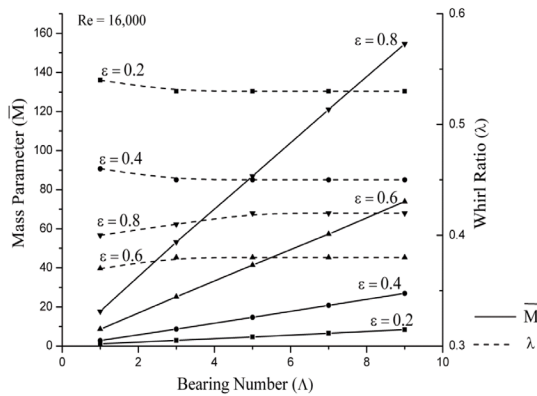


Figure 7. Effect of Reynolds Number ($Re = 16,000$) on Mass variable, whirl ratio with various bearing no. for various ϵ for groove angle 36°

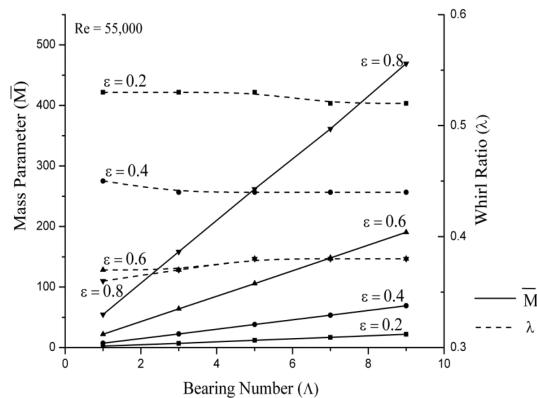


Figure 8. Effect of Reynolds Number ($Re = 55,000$) on Mass variable, whirl ratio with various bearing no. for various ϵ for groove angle 36°

CONCLUSIONS

It can be concluded that turbulence can affect the stability of the bearing. As the Reynolds number increases, it is seen that the stability region for the bearing improves. Irrespective of the groove angle and the Reynolds number at which the bearing is operating there is no significant changes in the whirl ratio for the range of eccentricity ratios considered. The groove angles considered do not result in a large variation of the calculated Mass parameter for the various Reynolds numbers at which the analysis has been performed.

REFERENCES

- Cabrera, D. L., Woolley, N. H., Allanson, D. R., & Tridimas, Y. D. (2005). Film pressure distribution in water-lubricated rubber journal bearings. *Proceedings of the Institution of Mechanical Engineers, Part J: Journal of Engineering Tribology*, 219(2), 125-132. doi: 10.1243/135065005X9754
- Capone, G., Russo, M., & Russo, R. (1991). Inertia and turbulence effects on dynamic characteristics and stability of rotor-bearings systems. *Journal of Tribology*, 113(1), 58-64. doi:10.1115/1.2920604
- Hashimoto, H., & Wada, S. (1982a). An analysis of dynamic characteristics of turbulent journal bearings considering inertia forces. *Bulletin of JSME*, 25(208), 208-15. Retrieved from <http://doi.org/10.1299/jsme1958.25.1601>
- Hashimoto, H., & Wada, S. (1982b). An influence of inertia forces on the stability of turbulent journal bearings. *Bulletin of JSME*, 25(202), 202-223. doi:10.1299/jsme1958.25.653
- Kakoty, S. K., & Majumdar, B. C. (1999). Effect of fluid inertia on stability of flexibly supported oil journal bearings: linear perturbation analysis. *Tribology International*, 32(4), 217-228. doi:10.1016/S0301-679X(99)00036-5
- Kakoty, S. K., & Majumdar, B. C. (2000). Effect of fluid inertia on the dynamic coefficients and stability of journal bearings. *Proceedings of the Institution of Mechanical Engineers, Part J: Journal of Engineering Tribology*, 214(3), 229-240. doi:10.1243/1350650001543133

- Kumar, A., & Mishra, S. S. (1996). Stability of a rigid rotor in turbulent hydrodynamic worn journal bearings. *Wear*, 193(1), 25-30. doi:10.1016/0043-1648(95)06654-3
- Lahmar, M. (2005). Elastohydrodynamic analysis of double-layered journal bearings lubricated with couple-stress fluids. *Proceedings of the Institution of Mechanical Engineers, Part J: Journal of Engineering Tribology*, 219(2), 145-165. doi:10.1243/135065005X9835
- Litwin, W. (2009). Water lubricated bearings of ship propeller shafts– problems, experimental tests and theoretical investigations. *Polish Maritime Research*, 16(4), 42-50. doi: 10.2478/v10012-008-0055-z
- Majumdar, B. C., Pai, R., & Hargreaves, D. J. (2004). Analysis of water-lubricated journal bearings with multiple axial grooves. *Proceedings of the Institution of Mechanical Engineers, Part J: Journal of Engineering Tribology*, 218(2), 135-146. doi: 10.1177/135065010421800208
- Pai, R., Rao, D. S., Shenoy, B. S., & Pai, R. S. (2012). Stability characteristics of a tri-taper journal bearing: A linearized perturbation approach. *Journal of Materials Research and Technology*, 1(2), 84-90. doi: 10.1016/S2238-7854(12)70016-9
- Rao, T. V. V. L. N., & Sawicki, J. T. (2002). Linear stability analysis for a hydrodynamic journal bearing considering cavitation effects. *Tribology Transactions*, 45(4), 450-456. doi:10.1115/1.1828451
- Shenoy, B. S., & Pai, R. (2010). Stability characteristics of an externally adjustable fluid film bearing in the laminar and turbulent regimes. *Tribology International*, 43(9), 1751-1759. doi:10.1016/j.triboint.2010.04.015
- Stachowiak, G., & Batchelor, A. W. (2013). *Engineering Tribology*. United States of America, USA: Butterworth-Heinemann
- Taylor, C. M., & Dowson, D. (1974). Turbulent lubrication theory – application to design. *Journal of Lubrication Technology*, 96(1), 36-47. doi:10.1115/1.3451905

NOMENCLATURE

C	Clearance between shaft and bearing (m)
D	Bearing Diameter (m)
$D_{rr}, D_{\phi\phi}, D_{\phi r}, D_{r\phi}$	Damping coefficient (Ns/m)
$\bar{D}_{rr}, \bar{D}_{\phi\phi}, \bar{D}_{\phi r}, \bar{D}_{r\phi}$	Non dimensional damping coefficient, $\bar{D}_{i,j} = D_{i,j} C \omega / LDp_s$
F_r	Dynamic force of lubricant film along the radial direction (N)
F_ϕ	Dynamic force of lubricant film along ϕ the direction (N)
h, \bar{h}	film thickness (m), $\bar{h} = h / C$
$K_{rr}, K_{\phi\phi}, K_{\phi r}, K_{r\phi}$	Stiffness coefficient (N/m)
$\bar{K}_{rr}, \bar{K}_{\phi\phi}, \bar{K}_{\phi r}, \bar{K}_{r\phi}$	Non dimensional stiffness coefficient $\bar{K}_{i,j} = K_{i,j} C / LDp_s$
M, \bar{M}	Mass of the Rotor (kg), mass variable $\bar{M} = \frac{MC\omega^2}{LDP_s}$
p, \bar{p}	Lubricant film pressure (Pa), $\bar{p} = pC^2 / \eta UR$, $\bar{p} = p / p_s$
p_s	Lubricant supply pressure (Pa)
\bar{p}_1, \bar{p}_2	Perturbed pressure
R	Journal radius (m)
Re	Global Reynolds Number
x	Coordinates in circumferential direction
U	Journal velocity = ωR (m/s)
W	Load during steady state (N)
W_r, W_t	Load components along and perpendicular to the line joining the centres respectively (N)
z	Axial direction coordinate axis (m)
ε	Eccentricity Ratio = e/C

ε_1, ϕ_1	Perturbation parameters
η	Absolute viscosity coefficient (Pa-s)
θ, \bar{z}	Non dimensional coordinates measured from the line joining the centers, $\theta = x / R, \bar{z} = z / L$
θ^*	Circumferential coordinate measured from the centre of the groove
λ	Whirl ratio = ω / ω_p
Λ	Bearing number = $6\eta\omega / [p_s(C/R)^2]$
τ	Non-dimensional time, $\omega_p t$
ϕ	Attitude angle (rad)
ω	Rotation speed of journal (rad/s)
ω_p	Journal vibration frequency (rad/s)
$()_o$	Steady state value



Estimation and Validation of Nearshore Current at the Coast of Carey Island, Malaysia

Fitri, A.^{1,2*}, Hashim, R.² and Motamedi, S.³

¹Department of Civil Engineering, Faculty of Civil Engineering and Planning, Universitas Internasional Batam (UIB), Batam, Kepulauan Riau, 29442, Indonesia

²Department of Civil Engineering, Faculty of Engineering, University of Malaya, 50603, Kuala Lumpur, Malaysia

³Faculty of Engineering, Environment and Computing, School of Energy, Construction and Environment, Coventry University, Coventry, CV1 5FB, United Kingdom

ABSTRACT

This study simulates the nearshore current characteristics at Carey Island by using *MIKE 21 Hydrodynamic FM*. The model simulations are calibrated and validated against measured conditions by adjusting the values of bed resistant over the stipulated computation domain. To evaluate the accuracy of the simulation results, three statistical parameters, namely RMSE, R Squared, and Thiel's inequality coefficients are calculated to compare the observed and simulated results. The results indicate that the current speeds during the spring tide are approximately between 0 m/s and 0.64 m/s which come from Northwest to southeast direction. A good agreement between observed and simulated values of current speeds, current direction and water level with R squared of approximately 0.92 to 0.95 are obtained. Results suggest that the bed resistant is an important parameter in the hydrodynamic simulation using *MIKE 21 Hydrodynamic FM*.

Keywords: Bed resistant, current characteristics, estimation, validation, MIKE 21 Hydrodynamic FM

INTRODUCTION

Coastal hydrodynamics is important in the calculation of sediment transport and morphological evolution (Fairley, Davidson, & Kingston, 2009; Fitri, Hashim, Song, & Motamedi, 2016; Hashim, Fitri, Motamedi, & Hashim, 2013; Nam, Larson, & Hanso, 2011; Ranasinghe, Symonds, Black, & Holman, 2004; Roberts, Hir, & Whitehouse, 2000). This information is vital for many coastal engineering design and applications for new retrofitting measures of coastal defence structures. Initially,

Article history:

Received: 11 January 2017

Accepted: 21 April 2017

E-mail addresses:

arniza@uib.ac.id (Fitri, A.),

roslan@um.edu.my (Hashim, R.),

ac5172@conventry.ac.uk (Motamedi, S.)

*Corresponding Author

characteristic of the coastal hydrodynamics is studied through physical models. However, these models have certain limitations such as selecting the appropriate scale, high cost, randomness of natural phenomena, and non-availability of complete understanding of coastal hydrodynamic behaviour. Therefore, estimations of coastal hydrodynamics rely largely on numerical models supported by physical experiments (Kim & Wang, 1996; Nicholson et al., 1997; Shamji, 2011; Zanuttigh, 2007).

Hydrodynamic numerical models are used to examine the complex systems of the multiple processes in the coastal areas that may occur simultaneously (Toorman, 2001). These models are important for the study of hydraulics (Bolaños, Sørensen, Benetazzo, Carniel, & Sclavo, 2014). Due to the nonlinearity of these systems and irregular domains in the coastal water bodies, a number of numerical models have been developed based on flexible mesh approach which can handle such irregular domains (DHI, 2013; Jones, Petersen, & Kofoed-Hansen, 2007; Wu, Sánchez, & Zhang, 2011).

The main objective of this study was to simulate the current speeds and current directions at the Coast of Carey Island; this information would be useful in designing proper coastal structures around the coastline of Carey Island. The simulations of current characteristics have been carried out using the software package - *MIKE 21 Hydrodynamic FM* (DHI, 2013). In order to provide the best performances of the simulation results, the model was initially calibrated and validated against the measured conditions by adjusting the manning number in the computational domain.

METHODS

Model Input

Data required for the modelling of *MIKE 21 Hydrodynamic FM* consists of bathymetry data from computational domain, wind speeds and wind directions, significant wave heights, mean wave directions and bed resistant. Wind speeds, wind directions, significant wave heights and mean wave directions at the range of latitude 2° to 3°30' N and longitude 100° to 102° were obtained from Meteorology Department of Malaysia.

Bathymetry

Bathymetry survey with fine resolution was conducted along Langat river and around the coast of Carey Island covering an area of approximately 17.5 km x 7 km. The survey activities were carried out during the spring tide from 8th until 12th December 2014. In addition, bathymetry data of the ocean region was generated using C-MAP 2014.

Boundary Condition

Tidal levels at Lumut station (obtained from Department of Survey and Mapping, Malaysia) and Belawan station (obtained from Dinas Hidro-Oceanography, Indonesia) were spatially interpolated to obtain the values of water levels at the north boundary condition, while

tidal levels at Tanjung Keling station (obtained from Department of Survey and Mapping, Malaysia) and Dumai station (obtained from Dinas Hidro-Oceanography, Indonesia) were spatially interpolated to find the values of water levels at the south boundary condition (Figure 1).

Model Calibration and Validation

Two units of Acoustic Wave and Current Profiler (AWAC) with 600 KHz frequency were installed at two locations at Carey Island coast between 23th December 2014 and 7th January 2015 (covering spring tide and neap tide). The device was utilised to measure the current characteristics (current speeds and current directions) and water level at 10-minute intervals. Table 1 shows the location of the AWAC.

The current characteristics and water levels recorded at latitude 02° 48' 40.02" N and longitude 101° 20' 11.18" E (AWAC 1) were used for model calibration purposes. Current characteristics and water levels at latitude 02° 49' 26" N and longitude 101° 18' 58.14" E (AWAC 2) were used for validating the calibrated model. Figure 1 shows the flexible mesh in computation domain, boundary condition, locations of the AWAC and locations of the tide stations.

Table 1
Co-ordinate locations of AWAC 1 and AWAC 2

Station	Longitude	Latitude	Depth (m)
AWAC 1	101° 20' 11.18"E	02° 48' 40.02" N	10.324
AWAC 2	101° 18' 58.14" E	02° 49' 26" N	12.557

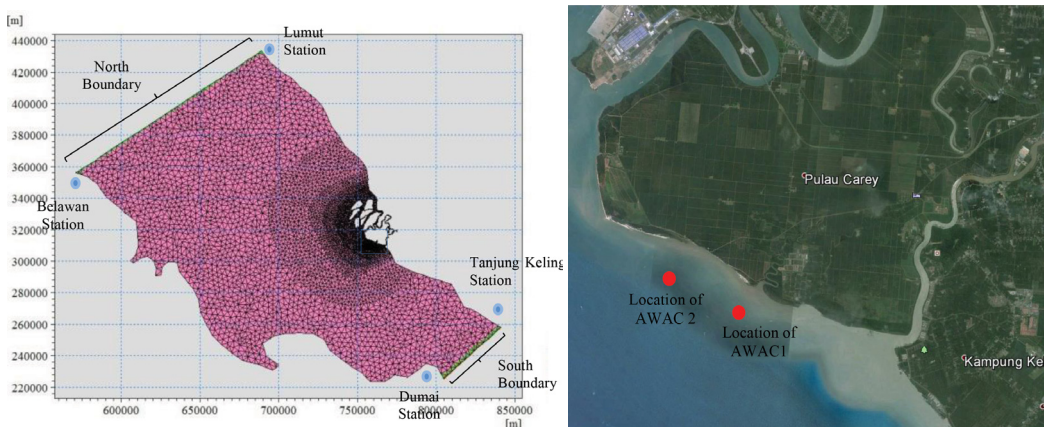


Figure 1. Computational domain used for hydrodynamic simulation and locations of the AWAC and tidal stations

Numerical Model

MIKE 21 Hydrodynamic FM is the basic model of the MIKE 21 software package for free surface flows based on flexible mesh approach. It simulates unsteady two-dimensional (2D) water level variations and flows in the coastal area (DHI, 2013). The flows are calculated in x and y direction based on the solution of depth integrated equations of conservations of volume and momentum. The following equations are the conservation of volume and momentum which describe the flow and water level variations in x and y direction:

X direction of momentum:

$$\frac{\partial p}{\partial t} + \frac{\partial}{\partial x} \left(\frac{p^2}{h} \right) + \frac{\partial}{\partial y} \left(\frac{pq}{h} \right) + gh \frac{\partial \zeta}{\partial x} + \frac{gp\sqrt{p^2 + q^2}}{C^2 h^2} - \frac{1}{\rho_w} \left[\frac{\partial}{\partial x} (h\tau_{xx}) + \frac{\partial}{\partial y} (h\tau_{xy}) \right]$$

$$-\Omega q - fVV_x + \frac{h}{\rho_w} \frac{\partial}{\partial x} (Pa) = 0 \quad [1]$$

Y direction of momentum:

$$\frac{\partial p}{\partial t} + \frac{\partial}{\partial y} \left(\frac{q^2}{h} \right) + \frac{\partial}{\partial x} \left(\frac{pq}{h} \right) + gh \frac{\partial \zeta}{\partial y} + \frac{gq\sqrt{p^2 + q^2}}{C^2 h^2} - \frac{1}{\rho_w} \left[\frac{\partial}{\partial y} (h\tau_{yy}) + \frac{\partial}{\partial x} (h\tau_{xy}) \right]$$

$$-\Omega q - fVV_y + \frac{h}{\rho_w} \frac{\partial}{\partial y} (Pa) = 0 \quad [2]$$

$$C = Mh^{1/6} \quad [3]$$

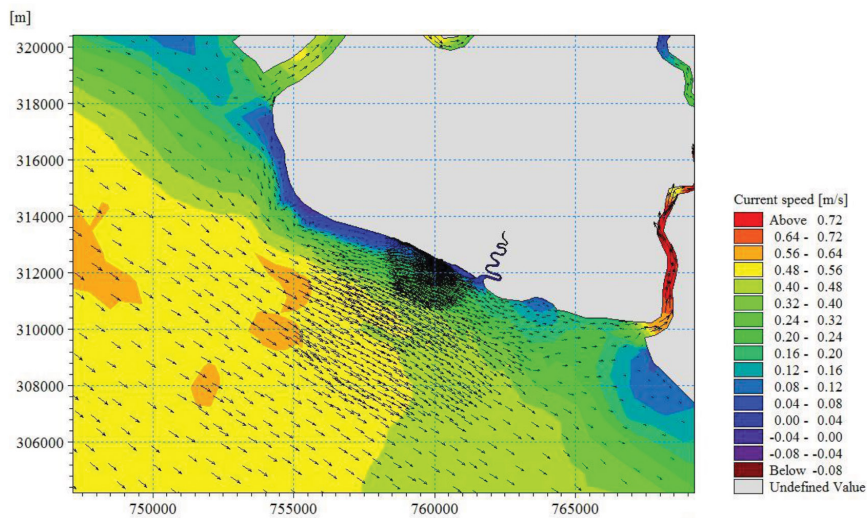
The equation of continuity:

$$\frac{\partial \zeta}{\partial t} + \frac{\partial p}{\partial x} + \frac{\partial q}{\partial y} = \frac{\partial d}{\partial t} \quad [4]$$

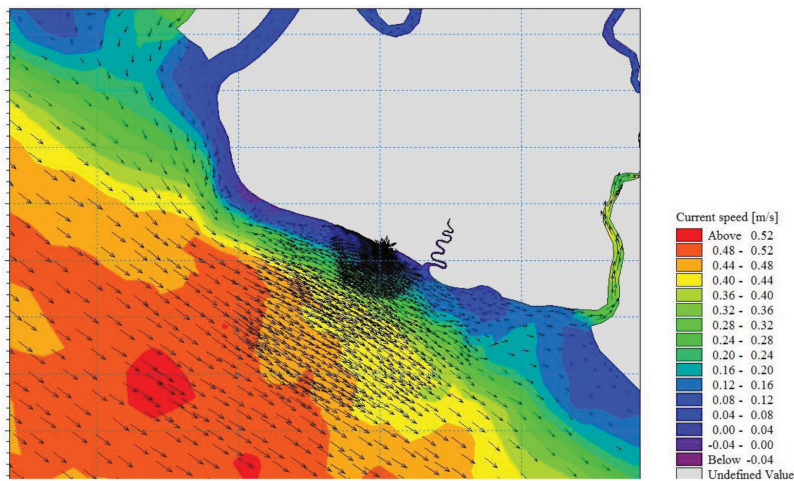
Where, x, y is space coordinate or direction components, ζ is surface elevation (m), h is water depth (m), d is time varying water depth (m), C is chezy resistance ($m^{1/2}/s$), while M is manning number or bed roughness ($m^{1/3}/s$)., f(V) is wind friction factor while V is wind speed (m/s), g is acceleration due to gravity (m/s^2), Pa is atmospheric pressure (kg/m^2), ρ_w is density of water (kg/m^3) and τ is shear stress.

RESULTS AND DISCUSSIONS

Figure 2 shows the current characteristics at the coast of Carey Island during spring tide and neap tide between 23rd December 2014 and 7th January 2015. Figure 3 summarises the comparison of predicted and measured current speeds, current directions and water levels at latitude 02° 48' 40.02" N and longitude 101° 20' 11.18" E. In addition, Figure 4 presents the comparison of predicted and measured current speeds, current directions and water levels at latitude 02° 49' 26" N and longitude 101° 18' 58.14" E. In order to produce the best performance of the simulation results in hydrodynamic model of *MIKE 21 Hydrodynamic FM* model, the values of bed roughness (Table 2) were used in the computation domain.

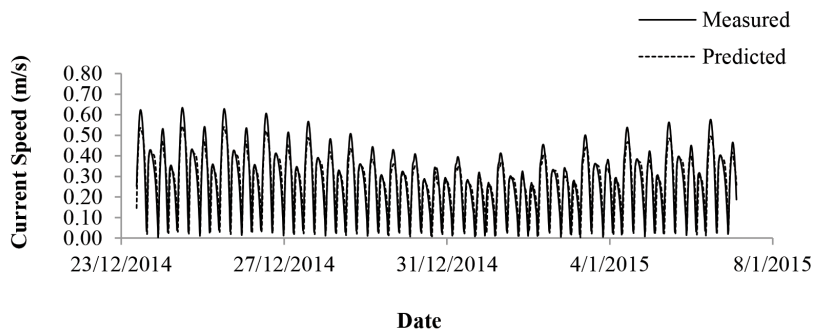


(a)

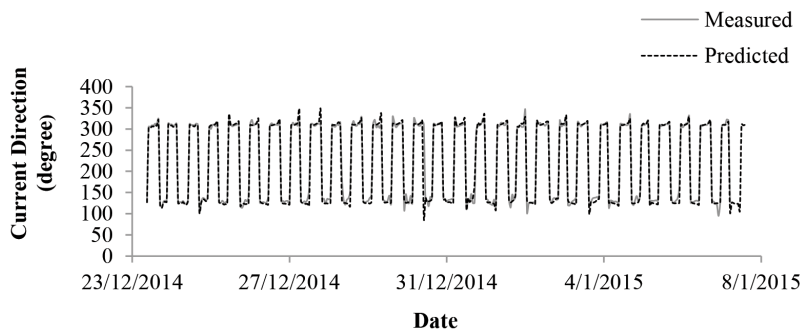


(b)

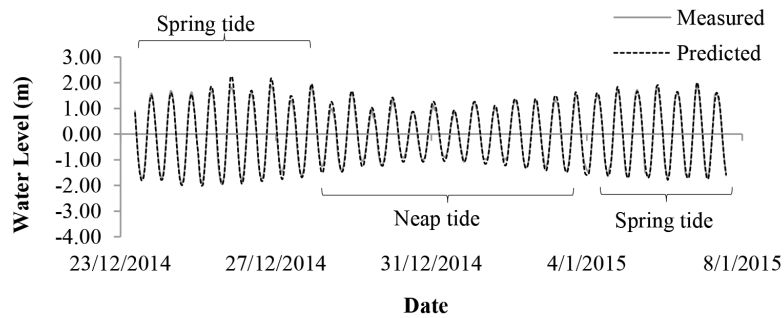
Figure 2. Current characteristics at the coast of Carey Island, (a) during spring tide, (b) during neap tide



(a)



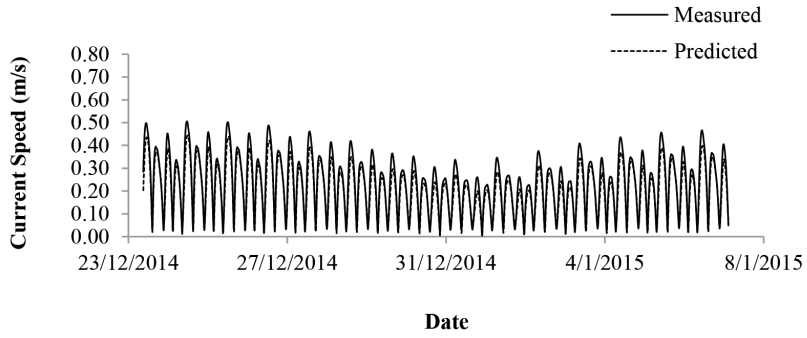
(b)



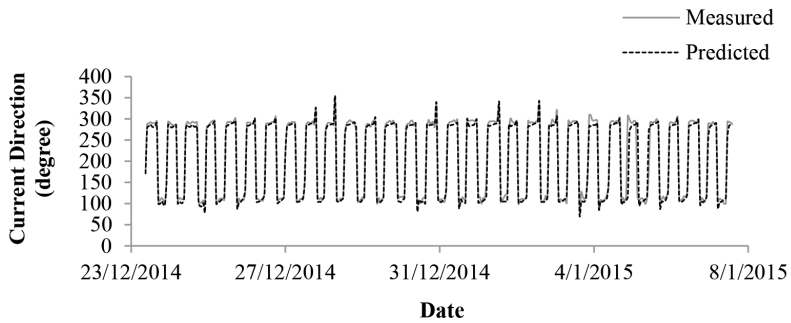
(c)

Figure 3. Comparison between measured and predicted of (a) current speeds, (b) current directions and (c) water levels on 23th December 2014 to 7th January 2015 at latitude 02° 48' 40.02" N and longitude 101° 20' 11.18" E

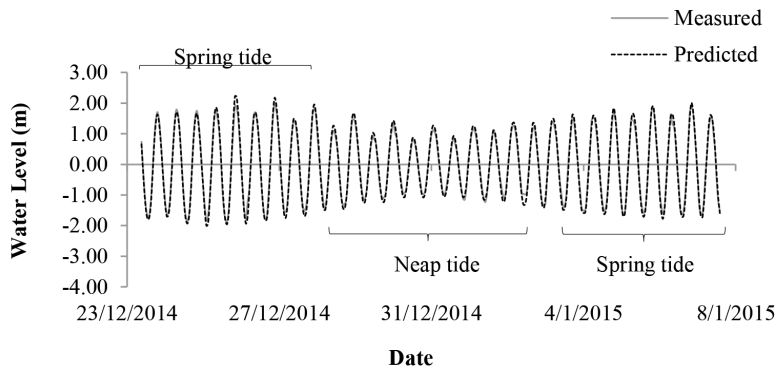
Coastal Hydrodynamic Characteristics



(a)



(b)



(c)

Figure 4. Comparison between measured and predicted of (a) current speeds, (b) current directions and (c) water levels on 23th December 2014 to 7th January at latitude 02° 49' 26" N and longitude 101° 18' 58.14" E

Table 2
Bed Roughness used in the computational domain

No	Depth (m)	Manning Number ($m^{1/3}/s$)
1	Less than 15	45
2	15 to 50	40
3	Greater than 50	35

Based on Figure 2, it is evident that the current speeds at the coast of Carey Island during spring tide and neap tide conditions were approximately 0 to 0.64 m/s and 0 to 0.52 m/s, respectively which come from the northwest to southeast direction (125°). According to Figure 3 and Figure 4, the current speeds, current directions and water levels obtained from hydrodynamic simulations have a good agreement with the field measurement.

Table 3 summarises the minimum values of *RMSE*, R Squared, and Theil's inequality coefficients in model calibration and validation process. The minimum values of *Root Mean Squared Error (RMSE)* for calibration and validation of current speeds and current direction are 0.07 m/s & 15° and 0.08 m/s & 17° respectively. Based on standard error allowed for hydraulic study by DID (2013), the *RMSE*, R Squared and Theil's inequality coefficients values prove that the model is well calibrated and validated.

Table 3
Statistical Metrics for hydrodynamic model performance

No	Type of Statistical Metrics	Calibration Process			Validation Process		
		Current Speed (m/s)	Current Direction (degree)	Water Level (m)	Current Speed (m/s)	Current Direction (degree)	Water Level (m)
1	RMSE Values	0.07	15°	0.11	0.08	17°	0.10
2	R Squared	0.92	0.91	0.94	0.91	0.92	0.95
3	Theil's inequality Coefficient	0.08	0.09	0.06	0.08	0.09	0.05

CONCLUSIONS

In this study, we found that the Manning values around the coast of Carey Island are between 35 and $45 m^{1/3}/s$ according to water depths between 0 and 60 m. Based on the simulation results, it can be seen that the current speeds at the coast of Carey Island between 23th December 2014 and 7th January 2015 are less than 0.64.

ACKNOWLEDGEMENT

This study is supported by University of Malaya, HIR-MOHE under Grant no. UM.C/HIR/MOHE/ENG/34.

REFERENCES

- Bolaños, R., Sørensen, J. V. T., Benetazzo, A., Carniel, S., & Sclavo, M. (2014). Modelling ocean currents in the northern Adriatic Sea. *Continental Shelf Research*, 87(1), 54-72.
- DHI. (2013). *MIKE 21 Hydrodynamic FM module*. Danish Hydraulic Institute. User Guide and Reference Manual (ed. 2013). Denmark.
- DID. (2013). *Guidelines for preparation of coastal engineering hydraulic study and impact evaluation*. Department of Irrigation and Drainage Guidelines 1/97, Malaysia.
- Fairley, I., Davidson, M., & Kingston, K. (2009). The morphodynamics of a beach protected by detached breakwaters in a high energy tidal environment. *Journal of Coastal Research*, 56(4), 598 - 607.
- Fitri, A., Hashim, R., Song, K. I., & Motamedi, S. (2016). Evaluation of morphodynamic changes in the vicinity of low-crested breakwater on cohesive shore of Carey Island, Malaysia. *Coastal Engineering Journal*, 57(4), 1-27.
- Hashim, R., Fitri, A., Motamedi, S., & Hashim, A. M. (2013). Modeling of coastal hydrodynamic associated with coastal structures: A review. *Malaysian Journal of Science*, 32(4), 149-154.
- Jones, O. P., Petersen, O. S., & Kofoed-Hansen, H. (2007). Modelling of complex coastal environments: some considerations for best practice. *Coastal Engineering*, 54(10), 717-733.
- Kim, T., & Wang, H. (1996). Numerical modeling of nearshore morphological changes under a current-wave field. In *Coastal Engineering 1996* (pp. 3830-3845). ASCE American Society of Civil Engineers.
- Nam, P. T., Larson, M., & Hanson, H. (2011). A numerical model of beach morphological evolution due to waves and currents in the vicinity of coastal structures. *Coastal Engineering*, 58(9), 863-876.
- Nicholson, J., Broker, I., Roelvink, J. A., Price, D., Tanguy, J. M., & Moreno, L. (1997). Intercomparison of coastal area morphodynamic models. *Coastal Engineering*, 31(1), 97-123.
- Ranasinghe, R., Symonds, G., Black, K., & Holman, R. (2004). Morphodynamics of intermediate beaches: a video imaging and numerical modelling study. *Coastal Engineering*, 51(7), 629-655.
- Roberts, W., Hir, P. L., & Whitehouse, R. J. S. (2000). Investigation using simple mathematical models of the effect of tidal currents and waves on the profile shape of intertidal mudflats. *Continental Shelf Research*, 20(10), 1079-1097.
- Shamji, V. R. (2011). *Studies on beach morphological changes using numerical models*. (Doctoral dissertation). Cochin University of Science and Technology, Thiruvananthapuram.
- Toorman, E. A. (2001). Cohesive sediment transport modeling: European perspective. In W. H. McAnally, & A. J. Mehta (Eds.), *Coastal and Estuarine Fine Sediment Processes* (pp. 1-18). The Netherlands: Gulf Professional Publishing.
- Wu, W., Sánchez, A., & Zhang, M. (2011). An implicit 2-D shallow water flow model on unstructured quadtree rectangular mesh. *Journal of Coastal Research*, 8(2), 15-26.
- Zanuttigh, B. (2007). Numerical modelling of the morphological response induced by low-crested structures in Lido di Dante, Italy. *Coastal Engineering*, 54(1), 31-47.





A Computational Fluid Dynamics Study of Combustion and Emission Performance in an Annular Combustor of a Jet Engine

M. Zuber^{1*}, M. S. B. Hisham², N. A. M. Nasir², A. A. Basri² and S. M. A. Khader³

¹Department of Aeronautical and Automobile Engineering, Manipal Institute of Technology, Manipal University, Manipal 576104, India

²Department of Aerospace Engineering, Faculty of Engineering, Universiti Putra Malaysia, 43400 UPM, Serdang, Selangor, Malaysia

³Department of Biochemistry, School of Biomedical Sciences, The University of Hong Kong, Pokfulam, Hong Kong

ABSTRACT

This paper is a Computational Fluid Dynamics (CFD) study of the performance of a jet engine annular combustor that was subjected to various loading conditions. The aim is to comprehend the effect of various genuine working conditions on ignition and emission performance. The numerical models utilized for fuel ignition is the feasible $k-\omega$ model for turbulent stream, species transport (aviation fuel and air) with eddy-dissipation reaction modelling and pollution model for nitrogen oxides (NO_x) emission. The results obtained confirm the findings described in the literature.

Keywords: Annular combustor, CFD, combustor loading, jet engine, gas emission

INTRODUCTION

Gas turbines operating at simple cycle have low efficiencies due to the loss of energy to the atmosphere (Alves & Nebra, 2003). The combustor is the hottest part of the gas turbine thus frequent use affects its lifespan (Li, Peng, & Liu, 2006). Many studies have been carried out to improve the performance of a gas turbine (Alves & Nebra, 2003; Carapellucci & Milazzo,

2005; Luo, Zhang, Lior, & Lin, 2011; Han, Jin, Zhang, & Zhang, 2007). Li et al., 2006 utilized the CFD model to analyse the ignition and cooling in an air motor combustor. Wang, Luo, Lu and Fan (2011) considered the structure of a hydrogen/air premixed fire in a small-scale combustor using the direct numerical simulation method. Gobbato, Masi, Toffolo and Lazzaretto (2011) performed a

Article history:

Received: 11 January 2017

Accepted: 21 April 2017

E-mail addresses:

mdzubairmanipal@gmail.com, mohammad.zuber@manipal.edu

(M. Zuber),

syafiqbad94@gmail.com (M. S. B. Hisham),

athrhnsr@gmail.com (N. A. M. Nasir),

adi.azriff@gmail.com (A. A. Basri),

smak.quadri@gmail.com (S. M. A. Khader)

*Corresponding Author

CFD reproduction on a hydrogen fuelled single can gas turbine combustor. Ghenai (2010) completed a numerical examination on the combustion of syngas fuel blend in gas turbine can combustor. The impact of syngas fuel composition and lower heating value on the fire shape, gas temperature, and nitrogen oxides per unit of energy generation were also studied. Zhang, Fu, Lin and Li (2012) examined the NO_x emanation in a model commercial aircraft motor combustor using CFD. The present study investigates the can annular combustor in order to understand its working at various loading conditions and examine the NO_x and CO₂ emissions during operation.

METHOD

Governing Equations

The mathematical equations to show combustion depend on the equations of conservation of mass, momentum, and energy together with other supplementary equations for the turbulence and combustion. The SST k- ω turbulence model is utilized as a part of this study. The equations for the turbulent kinetic energy k and the specific dissipation rate of the turbulent kinetic energy ω are solved. The reaction model is activated with species transport. The radiation effects are ignored. The equations are as follows (Mujeebu, Abdullah, & Zubair, 2013; Ismail et al., 2013).

Mass Conservation Equation:

$$\frac{\partial \rho}{\partial t} + \nabla \cdot (\rho \vec{V}) = S_m \quad (1)$$

Where the S_m is the mass added to the continuous phase from the dispersed second phase.

Continuity Equation:

$$\frac{\partial \rho}{\partial t} + \frac{\partial}{\partial x}(\rho v_x) + \frac{\partial}{\partial r}(\rho v_r) + \frac{\rho v_r}{r} = S_m \quad (2)$$

Where x is the axial coordinate, r is the radial coordinate, v_x is the axial velocity, and v_r is the radial velocity.

Momentum Conservation Equations:

$$\frac{\partial}{\partial t}(\rho \vec{v}) + \nabla \cdot (\rho \vec{v} \vec{v}) = -\nabla \rho + \nabla \cdot (\vec{\tau}) + \rho \vec{g} + \vec{F} \quad (3)$$

Where $\vec{\tau}$ is the stress tensor, $\rho \vec{g}$ and \vec{F} are the gravitational body force and external body forces, respectively.

Species Transport Model:

$$\frac{\partial}{\partial t}(\rho Y_i) + \nabla \cdot (\rho \vec{v} \bar{Y}_i) = -\nabla \cdot \bar{J}_i + R_i + S_i \quad (4)$$

Where R_i the net is rate of production by chemical reaction and S_i is the rate of creation by addition from the dispersed phase plus any user defined sources.

Transport Equations for the SST k- ω model:

$$\frac{\partial}{\partial t}(\rho k) + \frac{\partial}{\partial x_i}(\rho k u_i) = \frac{\partial}{\partial x_j} \left(\Gamma_k \frac{\partial k}{\partial x_j} \right) + G_k - Y_k + S_k \quad (5)$$

$$\frac{\partial}{\partial t}(\rho \omega) + \frac{\partial}{\partial x_j}(\rho \omega u_j) = \frac{\partial}{\partial x_j} \left(\Gamma_\omega \frac{\partial \omega}{\partial x_j} \right) + G_\omega - Y_\omega + D_\omega + S_\omega \quad (6)$$

Where the term G_k represents the production of turbulence kinetic energy, and is defined in the same manner as in the standard k- ω model. G_ω represents the generation of ω . Γ_k and Γ_ω represent the effective diffusivity of k and ω , respectively. Y_k and Y_ω represent the dissipation of k and ω due to turbulence. D_ω represents the cross-diffusion term. S_k and S_ω are user-defined source terms.

$$\sigma_{k1} = 0.85, \sigma_{k2} = 1, \sigma_{\omega1} = 0.5, \sigma_{\omega2} = 0.856$$

Geometry, Boundary Conditions, Mesh and Numerical Method

The basic geometry of the gas turbine annular combustor is shown in the Figure 1(a). The size of the combustor is 0.341 m in the Y direction and 0.65 m in the X direction. The dimensions of the combustor were obtained from the works of (Chaudhari, Kulshreshtha, & Channiwala, 2012). A quality mesh was generated for the annular combustor and the mesh dependency study resulted in the mesh count of 41605 elements.

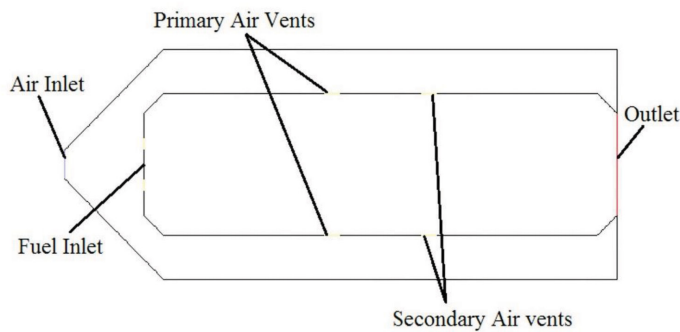


Figure 1. 2D model of the gas turbine annular combustor

The finite volume method and the second order upwind method were used to solve the governing equations. The convergence criteria were set to 10^{-4} for the mass, momentum, turbulent kinetic energy, dissipation rate of turbulent kinetic energy and the mixture fraction.

For the energy and the pollution equations, the convergence criteria were set to 10^{-6} . The boundary conditions of the air and fuel are similar to the one presented by Gang and Hongtao (2013) and are shown in Table 1.

Table 1
Combustor conditions

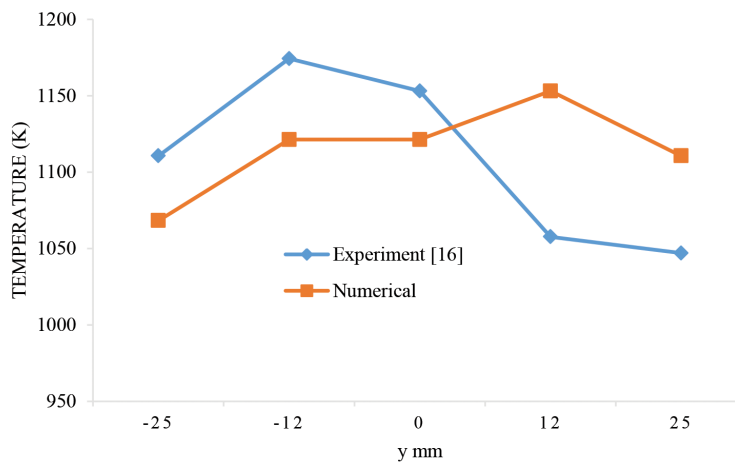
Condition	Mass flow rate of air (kg/s)	Temperature of air (K)	Mass flow rate of fuel (kg/s)	Temperature of fuel (K)	Combustor load %
1	2.7568	645.4	0.04184	305	30
2	3.3458	693.2	0.05939	305	50
3	3.8096	726.8	0.07552	305	70
4	4.016	742	0.08382	305	80
5	4.3865	769.9	0.09987	305	100

The experiment data of Dang (2009), was utilized to validate the numerical findings. In the experimental and numerical cases, the fuel of aviation kerosene was considered. The boundary condition of the experimental and numerical cases are follows: the temperature is 500K, mass flow rate of air 0.24 kg/s,, mass flow rate of fuel 0.0624 kg/s, and the fuel temperature 305K.

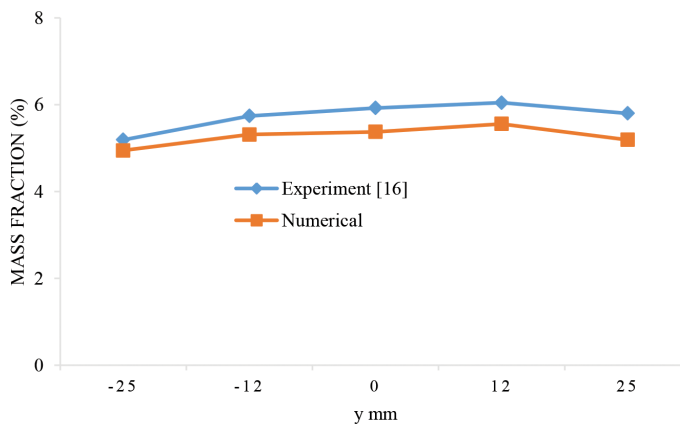
RESULTS AND DISCUSSIONS

Validation with Literature

The CO₂ mass fraction and the temperature radial profiles at the combustor outlet was compared with the results of Dang (2009), in Figure 2, respectively. The value of CO₂ mass fraction and temperature in the present results and the experimental results of Dang (2009), were similar.



(a) Temperature



(b) CO₂ mass fraction

Figure 2. CO₂ mass fraction radial profile and temperature at combustor outlet

Flow field

The velocity field in the combustor under condition 5 is shown in Figure 3. The streamlines indicate the path followed by the air and fuel under conditions 1 to 5 are identical with only a marginal difference. In this study, only the streamlines for condition 5 are depicted. Air flow from the inlet to the combustor outlet can be divided into two zones, namely primary zone, and secondary zone.

In the primary zone, the air leaves the inlet to the combustor liner at high velocity. The air mixes with fuel injected from the nozzle, flows forward and entraps the air in the centre of the combustor liner while the downstream air refills the region. As a result, a central recirculation zone with a counter rotating vortex pair forms in the head of the combustor liner, and ensures the burning and stable combustion in the combustor liner. Due to symmetry of the shell, the air flow rates into the combustor liner from the upper and lower surfaces are also symmetric.

In the downstream area of the primary zone, strong fresh air is injected into the combustor liner from the primary holes; as a result, the primary zone is cut off by the fresh air. Although a small amount of gas is inhaled into the primary zone, most of it flows downstream to mix with the cold air from the secondary zone. This results in more uniform flow in the combustor.

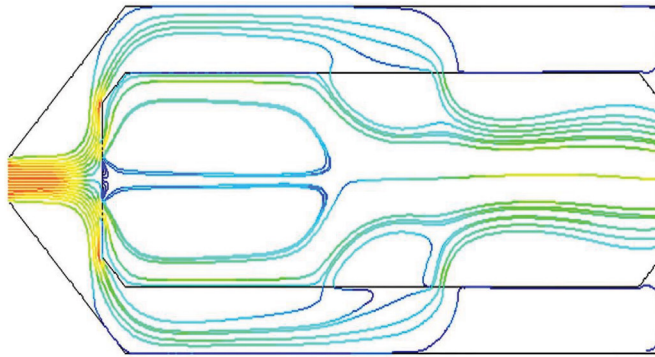


Figure 3. Streamline velocity of condition 5

The air flow distribution is a fundamental issue in combustor configuration and advancement. It influences the combustor ignition, combustion productivity, fire stability, absolute pressure loss, wall cooling, as well as the outlet temperature distribution. Figure 4 demonstrates the extent of primary zone air conveyance. It can be seen from the figure, the proportion of air circulation under various conditions are similar: air inlet=15%, primary air = 29.5%. It can be presumed that the air circulation is for the most part dictated by the combustor structure, not the working conditions.

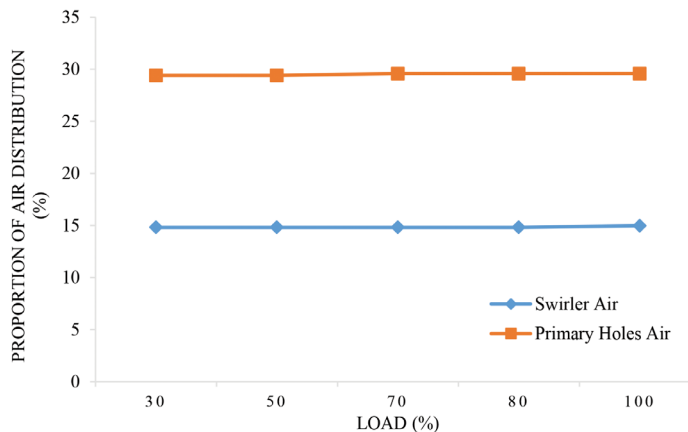


Figure 4. Flow distribution of air in different conditions

Temperature Field

The contours of the anticipated gas temperature for the combustion of fuel aviation kerosene in combustor are explained in Figure 5. The highest gas temperature is mostly concentrated at the tail end of the exit of the combustor. The temperature at the primary combustion zone is in the range of 1900 to 2100K for all the loading conditions. At higher loads, the combustor temperature is quite less and the maximum temperature region is pushed towards the exit tail. It is on the grounds that more fuel is burned in the combustor under the high load. The temperature of the gas close to the lower surface of the combustor liner is lower than that close to the upper surface in the centre zone and mixing zone

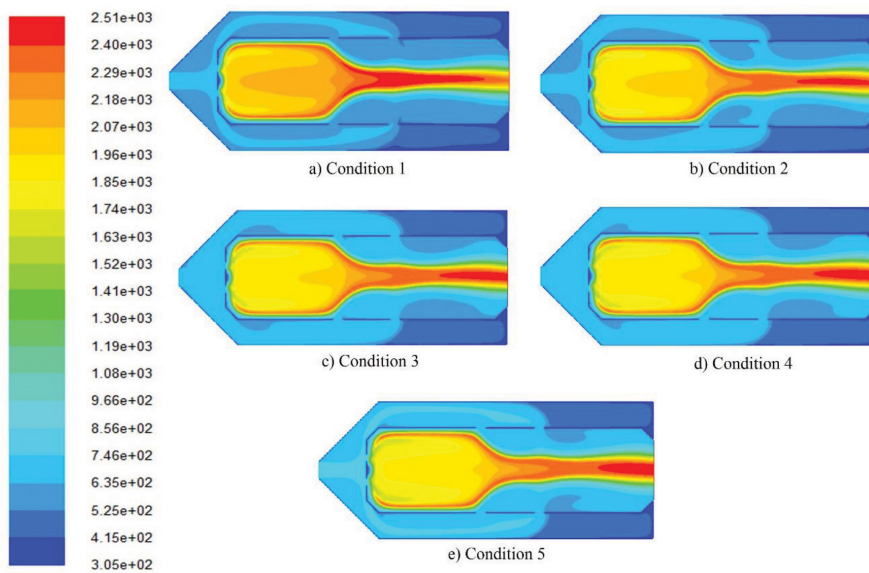


Figure 5. Contour of Temperature

As seen from Figure 5, there are two high temperature zones in the combustor. One is at the centre and where the temperature increases with the load along the central axis of combustor liner. The other located behind the primary zones, which only exists when the air-fuel mixture is above 30% load, and gets higher as the load increases. No significant change in the temperature along the central axis of the combustor as observed as per Figure 6. This shows that, higher loads have less effect on the performance of the combustor. However, there is a significant increase downstream suggesting higher load increases the exit temperature of the combustor gases.

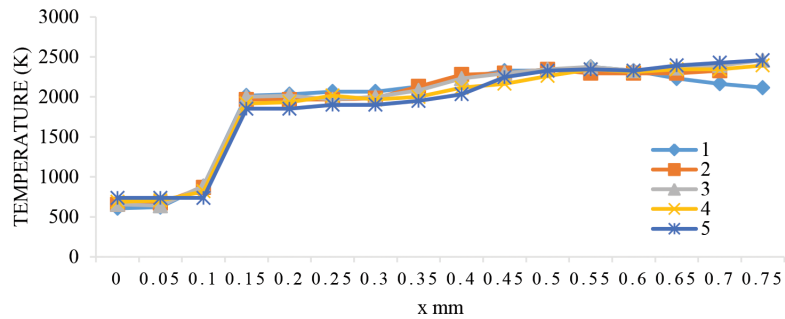


Figure 6. Central axis of temperature distribution

Emission

NO_x Emission. Figure 7 shows the production of NO_x discharge at combustor outlet for different operating conditions indicated in Table 1. The least NO_x outflow is 444.44 ppm at condition 1 and the most elevated is 623.98 ppm at condition 5. The higher temperature in the primary zone can increase the production of NO_x and is evident with increased temperature associated with condition 5, more NO_x was produced.

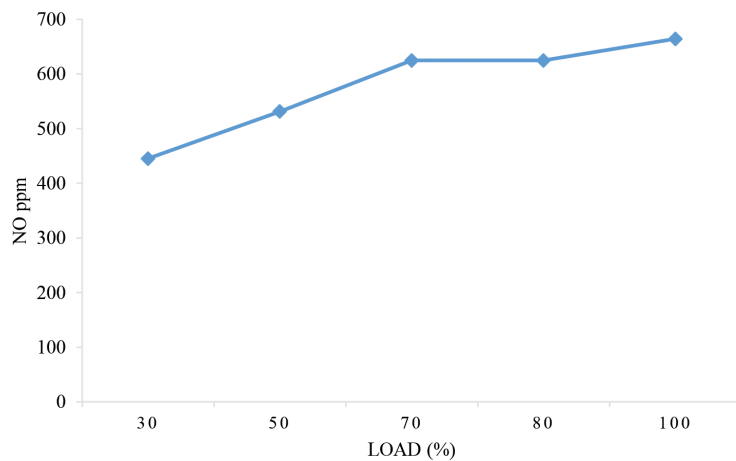


Figure 7. Emission of NO_x at outlet in different condition

CO₂ Emission. Figure 8 shows the mass fraction of CO₂ in the core of combustor in 100% load (Condition 5). It can be inferred that CO₂ distribution follows the similar pattern as that of temperature and maximum CO₂ can be observed at the downstream region. The increase in load also increases the CO₂ production as observed from the Figure 9. The mass fraction of CO₂ having maximum of 0.0746 kg was obtained at condition 5 and lowest of 0.0537 kg at condition 1.

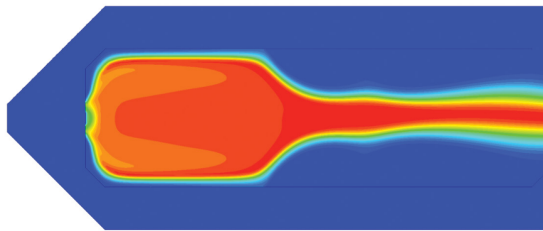


Figure 8. Contour of mass fraction CO₂ (Condition 5)

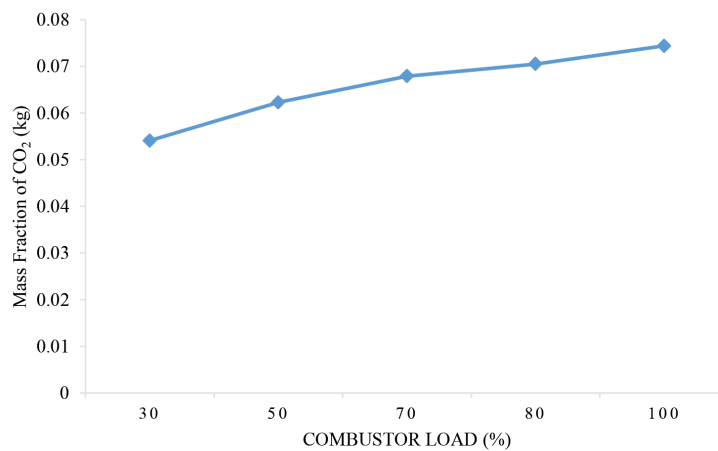


Figure 9. Mass fraction of CO₂ at the outlet in various condition

CONCLUSIONS

The two-dimensional CFD study of combustion in jet engine annular combustor performed in this study are as follows:

- 1) The combustor burns fuel viably under various conditions. A core of combustor chamber with different angle of primary and secondary inlet could improve the flame stability under different conditions.
- 2) Because of the symmetrical flow field, the temperature conveyance in combustor is symmetrical too. The gas temperatures close to the upper and lower surfaces of combustor liner are identical, and the greatest temperature contrast is around 100K in the centre zone for each condition, which is helpful to secure the liner. Hence, a symmetrical stream field in the combustor may expand the life of the combustor liner.
- 3) The estimations of the NO_x outflow are 623.98 ppm and 444.4 ppm under 100% load and 30% load respectively. It is also observed that there is an increase in CO₂ emission with increase in the load.

ACKNOWLEDGEMENTS

The authors would like to thank Universiti Putra Malaysia (UPM) for providing funds through the UPM GP –IPM/2014/9444000 grant.

REFERENCES

- Alves, L. G., & Nebra, S. A. (2003). Thermoeconomic evaluation of a basic optimized chemically recuperated gas turbine cycle. *International Journal of Thermo-dynamics*, 6(1), 13–22.
- Carapellucci, R., & Milazzo, A. (2005). Thermodynamic optimization of a reheat chemically recuperated gas turbine. *Energy Conversion and Management*, 46(18-19), 2936–2953.
- Chaudhari, K. V., Kulshreshtha, D. B., & Channiwala, S. A. (2012). Design and CFD simulation of annular combustion chamber with kerosene as fuel for 20 kW gas turbine engine. *International Journal of Engineering Research and Applications (IJERA)*, 2(6), 1641-1645.
- Chen, J. C., & Chen, W. (2012). How flow becomes turbulent. *IAENG International Journal of Applied Mathematics*, 42(2), 99–110.
- Danao, L. A., Edwards, J., Eboibi, O., & Howell, R. (2013). A numerical investigation into the effects of fluctuating wind on the performance of a small scale vertical axis wind turbine. *Engineering Letters*, 21(3), 149–157.
- Dang, X. X. (2009). *Experimental investigation and numerical simulation of a gas turbine annular combustor with dual-stage swirler*. (Doctoral thesis). Nanjing University of Aeronautics and Astronautics.
- Gang, P., & Hongtao, Z. (2013). Combustion and emission performance in a can annular combustor. *Engineering Letters*, 22(1), EL_22_1_03.
- Ghenai, C. (2010). Combustion of syngas fuel in gas turbine can combustor. *Advances in Mechanical Engineering*, 2010, 1–13.
- Gobbato, P., Masi, M., Toffolo, A., & Lazzaretto, A. (2011). Numerical simulation of a hydrogen fuelled gas turbine combustor. *International Journal of Hydrogen Energy*, 36(13), 7993–8002.
- Han, W., Jin, H., Zhang, N., & Zhang, X. (2007). Cascade utilization of chemical energy of natural gas in an improved CRGT cycle. *Energy*, 32(4), 306–313.
- Ismail, A. K., Abdullah, M. Z., Zubair, M., Ahmad, Z. A., Jamaludin, A. R., Mustafa, K. F., & Nazir, A. M. (2013). Application of porous medium burner with micro cogeneration system. *Energy*, 50, 131-142.
- Li, L., Peng, X. F., & Liu, T. (2006). Combustion and cooling performance in an aero-engine annular combustor. *Applied Thermal Engineering*, 26(16), 1771–1779.
- Luo, C., Zhang, N., Lior, N., & Lin, H. (2011). Proposal and analysis of a dual-purpose system integrating a chemically recuperated gas turbine cycle with thermal seawater desalination. *Energy*, 36(6), 3791–3803.
- Mujeebu, M. A., Abdullah, M. Z., & Zubair, M. (2013). Experiment and CFD simulation to develop clean porous medium surface combustor using LPG. *Journal of Thermal Science and Technology, Isi Bilimi ve Teknigi Dergisi/Journal of Thermal Science & Technology*, 33(1), 55-61.
- Wang, H., Luo, K., Lu, S., & Fan, J. (2011). Direct numerical simulation and analysis of a hydrogen/air swirling premixed flame in a micro combustor. *International Journal of Hydrogen Energy*, 36(21), 13838–13849.
- Zhang, M., Fu, Z., Lin, Y., & Li, J. (2012). CFD Study of NOX emissions in a model commercial aircraft engine combustor. *Chinese Journal of Aeronautics*, 25(6), 854–863.

Effect of Silica Nanoparticles in Kenaf Reinforced Epoxy: Flexural and Compressive Properties

F. Bajuri¹, N. Mazlan^{1,2*} and M. R. Ishak¹

¹ Department of Aerospace Engineering, Faculty of Engineering, Universiti Putra Malaysia, 43400 UPM, Serdang, Selangor, Malaysia

² Institute of Tropical Forestry and Forest Products (INTROP), Universiti Putra Malaysia, 43400 UPM, Serdang, Selangor, Malaysia

ABSTRACT

Kenaf natural fibre is used as a sustainable form of material to reinforce polymeric composite. However, natural fibres usually do not perform as well as synthetic fibres. Silica nanoparticle is a material with high surface area and its high interfacial interaction with the matrix results in its improvement. In this research, silica nanoparticles were introduced into epoxy resin as a filler material to improve the mechanical properties of the kenaf-reinforced epoxy. They were dispersed into the epoxy using a homogeniser at 3000 rpm for 10 minutes. The composites were fabricated by spreading the silica filled epoxy evenly onto the kenaf mat before hot pressing the resin wet kenaf mat. The results show for flexural properties, composites with higher fibre and silica volume content generally had better properties with specimen 601 (60 vol% kenaf and 1 vol% silica) having the highest strength at 68.9 MPa. Compressive properties were erratic with specimen 201 (20 vol% kenaf and 1 vol% silica) having the highest strength at 53.6 MPa.

Keywords: Compressive, flexural, kenaf, nanoparticles, nanosilica

INTRODUCTION

Natural plant fibres such as kenaf have been extensively studied as an environmentally sustainable replacement to synthetic fibres such as glass and carbon fibres (Ochi, 2008; Xue et al., 2009). This is due to the natural fibre's biodegradability, resistance, reduced dermal and

respiratory irritation, low cost, renewability, low density which contributes to its high specific strength and non-abrasive nature making the natural fibre easy to be processed and filled (Akil et al., 2011; Lee et al., 2009; Marques et al., 2015). Natural fibres have also garnered attention in the automotive world

Article history:

Received: 11 January 2017

Accepted: 21 April 2017

E-mail addresses:

farid.bajuri@yahoo.com (F. Bajuri),

norkhairunnisa@upm.edu.my (N. Mazlan),

mohdridzwan@upm.edu.my (M. R. Ishak)

*Corresponding Author

(Asumani et al., 2012; Xue et al., 2009). Compared with other natural fibres, kenaf (*Hibiscus cannabinus* L.) has a significantly high ability to fixate CO₂ and is able to absorb CO₂ 1.4 times its weight (Serizawa et al., 2006). It can be easily grown and adapts to different climate. Kenaf has a high growth rate, reaching up to three metres in height within three months and is considered mature between five and six months of age (Nishino et al., 2003; Sallih et al., 2014; Summerscales et al., 2013).

Using natural fibre as a reinforcing material has challenges, namely the incompatibility between hydrophilic natural fibre and hydrophobic matrix which reduces the interfacial adhesion. This causes stress transfer between the materials ultimately reducing their mechanical properties of the composites (Lee et al., 2009). Thus, in order to improve surface compatibility between fibres and matrices, surface treatment such as alkalisation (Meon et al., 2012), silane coupling agent treatment (Herrera-Franco & Valadez-Gonzalez, 2005) and silance treatment with pre-impregnation process of the HDPE/xylene solution. The presence of Si-O-cellulose and Si-O-Si bonds on the lignocellulosic surface confirmed that the silane coupling agent was efficiently held on the fibres surface through both condensation with cellulose hydroxyl groups and self-condensation between silanol groups. The fiber-matrix interface shear strength were examined (Asumani et al., 2012). Alkali treatment increases the surface roughness of the fibre to improve mechanical bonding while silane treatment improves the degree of cross-linking in the interface area and increases the fibre surface area (Asumani et al., 2012). While improving the properties of the composite, the total cost of the composite production may increase. Addition of silica nanoparticle as filler which is derived from cheap source of rice husk ash is an alternative material to improve composite properties. It is highly porous and due to the small porous structure, it has high surface area of about 1500 m²/g, which have active function and high interfacial interaction with resin (Bajuri et al., 2016; Basri et al., 2015). With such properties, it has ability to enhance a composite's mechanical, physical and optical properties while being able to protect against environmental stress such as cracking and aging (Zayed et al., 2014). Moreover, inclusion of nanoparticles may improve the toughness and other mechanical properties of a composite by enhancing the energy crack propagation, the increment of hard-particle interactions or by changing the properties of the polymer nearby the particle surface (Chen et al., 2008). Due to their large surface area to volume ratio, the area of contact between the nanoparticles and matrix will increase and in turn, the stress concentration around the filler will be reduced (Gendre et al., 2015). This study has achieved its objective to show the importance of silica nanoparticles as filler materials. to improve the flexural and compressive properties of kenaf-reinforced epoxy.

METHODOLOGY

Materials

The resin used for fabrication was Epoxamite 100 with 103 SLOW Hardener, manufactured by Smooth-On. The resin-to-hardener ratio was 100:28.4 by weight as suggested by the manufacturer. Pot life and curing time of the epoxy were 55 minutes and 20~24 hours respectively. The kenaf mat used provided by Zkk Sdn Bhd. The fibre's orientation was

random with the fibres compressed into mat form. Hydrophilic silica nanoparticles, derived from rice husk ash, were used as filler and provided by Maerotech Sdn. Bhd., Malaysia. The average diameter of the silica nanoparticle was 324 nm as determined by particle size analyser.

Material Preparations

Specimens with loading of 20 to 60 vol % of kenaf were prepared. 1 and 5 vol % of silica were also prepared to be added into the epoxy/kenaf. Table 1 lists all the composition of kenaf, epoxy and silica nanoparticle in making composite. For the specimen name, the first two numbers indicate kenaf's loading and the last number indicates silica nanoparticles' loading. As an example, specimen 405 is the specimen with 40% vol kenaf, 60% vol epoxy and an extra 5% vol silica nanoparticles from kenaf and epoxy's total volume percentages. The mat-like fibres were cut into 150 mm × 150 mm. They were used by combining the mats until the desired amount is reached.

Table 1
List of specimens fabricated

Specimen Name	Kenaf's Loading [vol%]	Epoxy's Loading [vol%]	Silica Nanoparticles' Loading [vol%]
200	20	80	0
300	30	70	0
400	40	60	0
500	50	50	0
600	60	40	0
201	20	80	1
301	30	70	1
401	40	60	1
501	50	50	1
601	60	40	1
205	20	80	5
305	30	70	5
405	40	60	5
505	50	50	5
605	60	40	5

Specimen Fabrication

Silica nanoparticles were dispersed into epoxy using a homogeniser at 3000 rpm for 10 minutes. The hardener was then added into the mixture before it is applied evenly onto kenaf layers using a paint brush. The resin wet kenaf layers were then placed inside a 150 mm × 150 mm × 3 mm mould and hot pressed for 20 minutes at 80°C under 40 tonne pressure. Further cold press for five minutes under 40 tonne pressure was applied onto the specimens. The specimens were left for 24 hours to be cured before being post-cured at 80°C for two hours. Finally, the specimens were conditioned into respective dimensions needed for each test using a composite cutter.

Flexural Test

A 3-point-bending test was conducted using 5 kN INSTRON Universal Testing Machine according to ASTM D790-03. The samples were conditioned into 125 mm × 12.7 in length and width. As the composites fabricated used mat type fibres, even after being compressed, the thickness of specimens with different loading varied. The thickness variation of samples with the same loading rate was miniscule. A total of 10 samples per loading were tested. The loading rate (R) in mm/min used is written in [1] where Z is the straining rate, L is the support span and d is the depth of the specimen.

$$R = ZL^2/6d \quad [1]$$

Here, a straining rate of 0.01 mm/mm/min and a support span-to-depth ratio of 16:1 were used. Flexural strength is the maximum stress obtained from the stress strain curve while flexural modulus is the slope of the linear section of the same curve.

Compressive Test

The compressive tests were done according to ASTM D695-02a using 5 kN INSTRON Universal Testing Machine. The samples' length and width were 1.275 mm × 1.275 mm. A total of 5 samples per loading were tested. The loading rate used was 2 mm/min. The specimen was placed on top of the compressive jig with the thickness sections of the specimen lightly touching the jig before pressure is applied. The compressive strength and compressive modulus will be discussed in the report.

RESULTS AND DISCUSSIONS

Flexural Properties

Figure 1 shows the mean flexural strength while Figure 2 shows the mean flexural modulus of kenaf reinforced epoxy (KRE) and silica nanoparticles infused kenaf reinforced epoxy (SIKRE). It can be seen that by increasing the fibre volume fraction, the flexural strength of the KREs increased too. For each kenaf's loading the flexural strength increased too with the

inclusion of silica nanoparticles, except for specimen 201 as its strength is lower than specimen 200. Furthermore, other than specimens with 60% vol kenaf, generally, the inclusion of 5% vol silica nanoparticles had specimens with better strength. Specimen 601 had the highest flexural strength at 68.9 MPa, 1~33% stronger than other specimens. From Figure 2 similar trend can be seen for flexural modulus of every loading. However, it is interesting to note that although specimen 601 had the highest strength when compared with other specimens with the same fibre content, its flexural modulus is not the highest. This indicates that although specimen 601 was strongest in term of strength it is not the stiffest specimen and can withstand less deformation than some other specimens such as specimen 405, 501, 505, 600, and 605 before breaking. Specimen 605 had the highest modulus at 4.35 GPa, 4~49% higher than other specimens. Overall, generally it can be seen that the inclusion of silica nanoparticles improved the flexural properties of the KREs. Inclusion of silica nanoparticles caused some volume of matrix surrounding the nanoparticles to become immobilised due to the binding of the matrix with the particles' surface which caused the matrix to be stiffer (Zhang et al., 2003). Hence, improving the elastic property of the KREs.

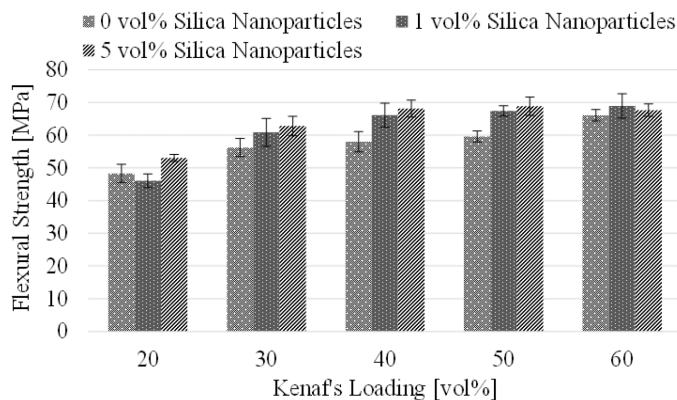


Figure 1. Flexural strength of SIKRE

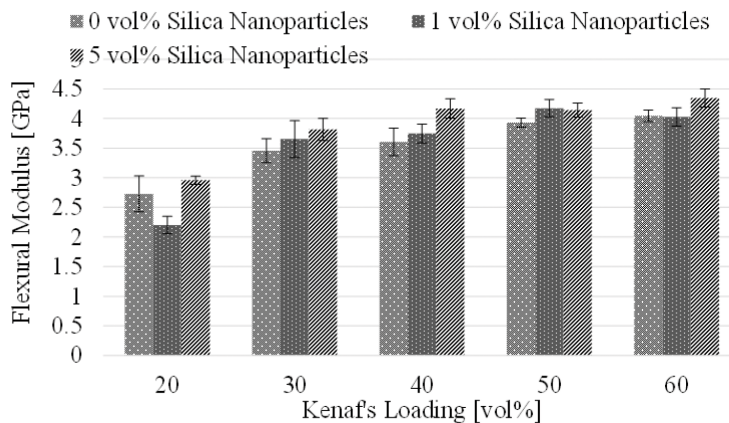


Figure 2. Flexural modulus of SIKRE

Compressive Properties

For compressive strength, contrary to flexural strength, specimens with 20% vol kenaf had the highest strengths with specimen 201 being the best (Figure 3). Specimen 201's compressive strength was 53.6 MPa, 5~34% stronger than other specimens. However, from the same figure it can be seen that if we ignore specimens 200, 201 and 205, the results are similar to those of flexural strength results as discussed in the previous section. Fibres are strong in the direction they are pulled but they do not provide much support in the opposite direction, like the case in compressive test. This may be the reason why specimens with 20% vol kenaf were stronger than other specimens. The fibre's volume content was low enough that instead of relying on kenaf, the specimens rely mostly on the epoxy matrix instead for support. From 30% vol onward, the fibre content was high enough to affect the overall compressive strength. The increment of fibre content also means that the fibres will be more compressed inside the composite. The compressed kenaf in turn will provide support to the whole composite increasing its strength as kenaf's load is increased. The inclusion of silica nanoparticles did not seem to have a significant effect, with some specimen's strength increased and some lowered when compared with specimens without silica nanoparticles. For compressive modulus, based on Figure 4, other than specimens with 20% and 30% vol kenaf, the results are quite erratic. However, specimen 201 has the highest modulus. It is interesting to note, the results showed low standard deviation; however, the results for compressive modulus had high deviations. The behaviour of the compressive modulus indicates that different sections of the same plate that was fabricated possess different level of stiffness. This may be due to the usage of randomly orientated kenaf mat. Due to the random nature of the fibre, there is a possibility that the parts used for the test may be of different length and orientation which has an effect on how the specimen behaves. It has to be noted that the specimen size for the compressive tests were small. The fibre might be aligned to an orientation which provides better properties at some parts of the plate.

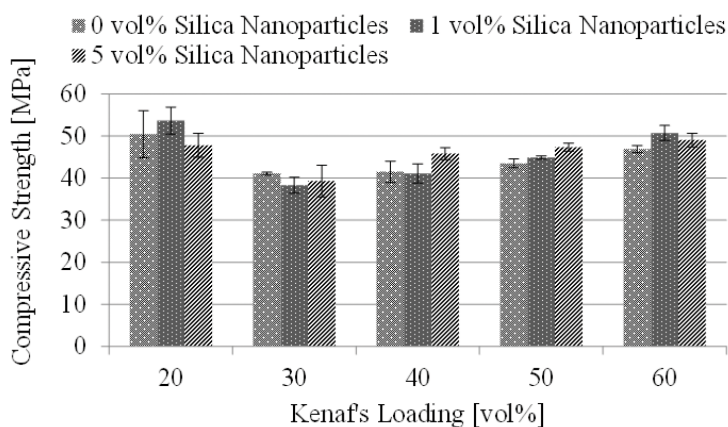


Figure 3. Compressive strength of SIKRE

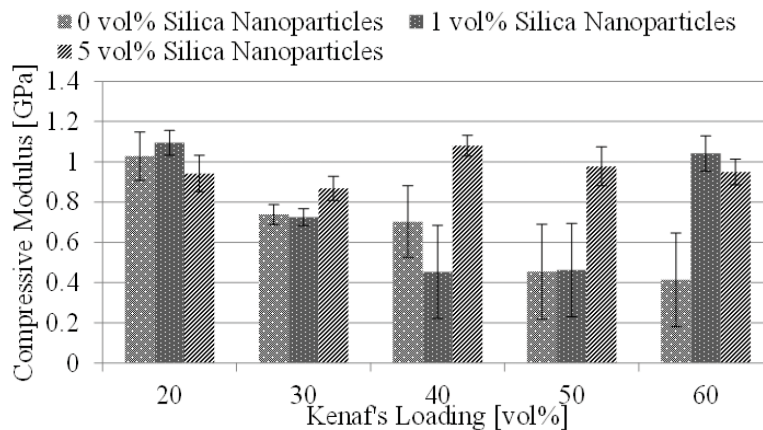


Figure 4. Compressive modulus of SIKRE

CONCLUSIONS

The findings of this study indicate that for flexural properties, increase in kenaf fibre volume content increased the specimen strength and modulus while increase in silica nanoparticles also generally improved the properties, except for specimen 201 and 605. For compressive strength, other than specimens with 20% vol (having the highest strength) kenaf, increase in fibre volume content had a positive impact. Inclusion of silica nanoparticles did not produce much difference compared with KREs without the nanoparticles. For compressive modulus, the results were erratic. As a whole, the inclusion of silica nanoparticles had a positive impact in terms of improving the mechanical properties of KREs.

ACKNOWLEDGEMENT

The authors would like to thank Universiti Putra Malaysia (UPM) for its grant (9463900) that enabled research and publication of this work.

REFERENCES

- Akil, H. M., Omar, M. F., Mazuki, A. A. M., Safiee, S., Ishak, Z. A. M., & Abu, B. A. (2011). Kenaf fiber reinforced composites: A review. *Materials and Design*, 32(8–9), 4107–4121. Retrieved from <https://doi.org/10.1016/j.matdes.2011.04.008>
- Asumani, O. M. L., Reid, R. G., & Paskaramoorthy, R. (2012). The effects of alkali-silane treatment on the tensile and flexural properties of short fibre non-woven kenaf reinforced polypropylene composites. *Composites Part A: Applied Science and Manufacturing*, 43(9), 1431–1440. Retrieved from <https://doi.org/10.1016/j.compositesa.2012.04.007>
- Bajuri, F., Mazlan, N., & Ridzwan, M. (2016). Flexural and compressive properties of hybrid kenaf / silica nanoparticles in epoxy composite. *Procedia Chemistry*, 19, 955–960. Retrieved from <https://doi.org/10.1016/j.proche.2016.03.141>

- Basri, M. S. M., Mazlan, N., & Mustapha, F. (2015). Effects of stirring speed and time on water absorption performance of silica aerogel / epoxy nanocomposite. *Asian Research Publishing Network*, 10(21), 9982–9991.
- Chen, C., Justice, R. S., Schaefer, D. W., & Baur, J. W. (2008). Highly dispersed nanosilica-epoxy resins with enhanced mechanical properties. *Polymer*, 49(17), 3805–3815. Retrieved from <https://doi.org/10.1016/j.polymer.2008.06.023>
- Gendre, L., Njuguna, J., Abhyankar, H., & Ermini, V. (2015). Mechanical and impact performance of three-phase polyamide 6 nanocomposites. *Materials and Design*, 66(PB), 486–491. Retrieved from <https://doi.org/10.1016/j.matdes.2014.08.005>
- Herrera-Franco, P. J., & Valadez-Gonzalez, A. (2005). A study of the mechanical properties of short natural-fiber reinforced composites. *Composites Part B: Engineering*, 36(8), 597–608. Retrieved from <https://doi.org/10.1016/j.compositesb.2005.04.001>
- Lee, B. H., Kim, H. S., Lee, S., Kim, H. J., & Dorgan, J. R. (2009). Bio-composites of kenaf fibers in polylactide: Role of improved interfacial adhesion in the carding process. *Composites Science and Technology*, 69(15–16), 2573–2579. Retrieved from <https://doi.org/10.1016/j.compscitech.2009.07.015>
- Marques, M. D. F. V., Melo, R. P., Araujo, R. D. S., Lunz, J. D. N., & Aguiar, V. D. O. (2015). Improvement of mechanical properties of natural fiber-polypropylene composites using successive alkaline treatments. *Journal of Applied Polymer Science*, 132(12), 1–12. Retrieved from <https://doi.org/10.1002/app.41710>
- Meon, M. S., Othman, M. F., Husain, H., Remeli, M. F., & Syawal, M. S. M. (2012). Improving tensile properties of kenaf fibers treated with sodium hydroxide. *Procedia Engineering*, 41(Iris), 1587–1592. Retrieved from <https://doi.org/10.1016/j.proeng.2012.07.354>
- Nishino, T., Hirao, K., Kotera, M., Nakamae, K., & Inagaki, H. (2003). Kenaf reinforced biodegradable composite. *Composites Science and Technology*, 63(9), 1281–1286. Retrieved from [https://doi.org/10.1016/S0266-3538\(03\)00099-X](https://doi.org/10.1016/S0266-3538(03)00099-X)
- Ochi, S. (2008). Mechanical properties of kenaf fibers and kenaf/PLA composites. *Mechanics of Materials*, 40(4–5), 446–452. Retrieved from <https://doi.org/10.1016/j.mechmat.2007.10.006>
- Sallih, N., Lescher, P., & Bhattacharyya, D. (2014). Factorial study of material and process parameters on the mechanical properties of extruded kenaf fibre/polypropylene composite sheets. *Composites Part A: Applied Science and Manufacturing*, 61, 91–107. Retrieved from <https://doi.org/10.1016/j.compositesa.2014.02.014>
- Serizawa, S., Inoue, K., & Iji, M. (2006). Kenaf-fiber-reinforced poly(lactic acid) used for electronic products. *Journal of Applied Polymer Science*, 100(1), 618–624. Retrieved from <https://doi.org/10.1002/app.23377>
- Summerscales, J., Virk, A., & Hall, W. (2013). A review of bast fibres and their composites: Part 3 - Modelling. *Composites Part A: Applied Science and Manufacturing*, 44(1), 132–139. Retrieved from <https://doi.org/10.1016/j.compositesa.2012.08.018>
- Xue, Y., Du, Y., Elder, S., Wang, K., & Zhang, J. (2009). Temperature and loading rate effects on tensile properties of kenaf bast fiber bundles and composites. *Composites Part B: Engineering*, 40(3), 189–196. Retrieved from <https://doi.org/10.1016/j.compositesb.2008.11.009>

- Zayed, S. M., Alshimy, A. M., & Fahmy, A. E. (2014). Effect of surface treated silicon dioxide nanoparticles on some mechanical properties of maxillofacial silicone elastomer. *International journal of biomaterials*, 2014(2014), 1-7.
- Zhang, M. Q. I. U., Rong, M. I. N. Z. H. I., Zhang, H. A. I. B. O., & Rich, K. F. (2003). Mechanical properties of low nano-silica. *Polymer Engineering and Sciences*, 43(2), 490-500. Retrieved from <https://doi.org/10.02/pen.10040>



REFEREES FOR THE PERTANIKA JOURNAL OF SCIENCE AND TECHNOLOGY

VOL. 25 (3) JUL. 2017

The Editorial Board of the Journal of Science and Technology wishes to thank the following for acting as referees for manuscripts published in this issue of JST.

Abdullah Sani Mohamed <i>(UKM, Malaysia)</i>	Low Heng Chin <i>(USM, Malaysia)</i>	Seripah Awang Kechil <i>(UiTM, Malaysia)</i>
Adi Irfan Che Ani <i>(UKM, Malaysia)</i>	Michael Khoo Boon Chong <i>(USM, Malaysia)</i>	Shailesh Tiwari <i>(ABESEC, India)</i>
Ahmad Hamdan Bin Ariffin <i>(UPM, Malaysia)</i>	Mohamed Thariq Bin Hameed Sultan <i>(UPM, Malaysia)</i>	Sherif Mohamed <i>(Griffith University, Australia)</i>
Ahmad Kamal Ismail <i>(UnikL, Malaysia)</i>	Mohan Reddy Moola <i>(Curtin University, Malaysia)</i>	Siti Rahmah Awang <i>(UTM, Malaysia)</i>
Ali Dehghanbanadaki <i>(IAU, Iran)</i>	Nagaraj S Nayak <i>(CCE, Oman)</i>	Song Ki Il <i>(Inha University, Korea)</i>
Amit Wason <i>(Ambala College, India)</i>	Nipun Sharma <i>(Quest Group of Institutions, India)</i>	Srinivasa Pai P <i>(NMAMIT, India)</i>
Baharudin Abdullah <i>(USM, Malaysia)</i>	Nor Aishah Ahad <i>(UUM, Malaysia)</i>	Surender Singh Saini <i>(CSIO, India)</i>
Chandrakant Kini <i>(MIT, India)</i>	Norazan Mohamed Ramli <i>(UiTM, Malaysia)</i>	Sushil Kumar <i>(MAU, India)</i>
Chia Chay Tay <i>(UiTM, Malaysia)</i>	Normala Halimoon <i>(UPM, Malaysia)</i>	Suzina Sheikh Ab Hamid <i>(USM, Malaysia)</i>
Devpriya Soni <i>(JIIT, India)</i>	Norshahida Shaadan <i>(UiTM, Malaysia)</i>	Syazwani Idrus <i>(UPM, Malaysia)</i>
Dinesh Arora <i>(CEC, India)</i>	Pooja Sahni <i>(CEC, India)</i>	Tee Boon Tuan <i>(UTeM, Malaysia)</i>
Fatimah Othman <i>(MOH, Malaysia)</i>	Pramod Kumar <i>(Tula's Institute, India)</i>	Vijay GS <i>(MIT, India)</i>
Fernando JR. O. Paras <i>(UPLB, Philippines)</i>	Ravi Prakash <i>(Amity University, India)</i>	Yap Tze Chuen <i>(Herriot-Watt University, Malaysia)</i>
Geeta Appannah <i>(UPM, Malaysia)</i>	Ravikrian Kadoli <i>(NIT, India)</i>	Yong Zulina Zubairi <i>(UM, Malaysia)</i>
Hazizi Abu Saad <i>(UPM, Malaysia)</i>	Rizal Zahar <i>(UPM, Malaysia)</i>	Yumn Suhaylah Yusoff <i>(USIM, Malaysia)</i>
Jagannath Rao <i>(MIT, India)</i>	Sandeep Jindal <i>(CEC, India)</i>	Zalilah Mohd Shariff <i>(UPM, Malaysia)</i>
Loveleen Gaur <i>(Amity University, India)</i>		

ABESEC	ABES Engineering College	MIT	Madras Institute of Technology	UPLB	University of the Philippines Los Baños
Ambala College	Ambala College of Engineering and Applied Research	MOH	Ministry of Health	UPM	Universiti Putra Malaysia
CCE	Caledonian College Of Engineering	NIT	National Institute Of Technology	USIM	Universiti Sains Islam Malaysia
CEC	Chandigarh Engineering College	NMAMIT	NMAM Institute of Technology	USM	Universiti Sains Malaysia
CSIO	Central Scientific Instruments Organization	UiTM	Universiti Teknologi MARA	UTeM	Universiti Teknikal Malaysia Melaka
IAU	Islamic Azbad University	UKM	Universiti Kebangsaan Malaysia	UTM	Universiti Teknologi Malaysia
JIIT	Jaypee Institute of Information Technology	UM	Universiti Malaya		
MAU	Maharaja Agrasen University	UnikL	Universiti Kuala Lumpur		

While every effort has been made to include a complete list of referees for the period stated above, however if any name(s) have been omitted unintentionally or spelt incorrectly, please notify the Chief Executive Editor, *Pertanika* Journals at nayan@upm.my.

Any inclusion or exclusion of name(s) on this page does not commit the *Pertanika* Editorial Office, nor the UPM Press or the University to provide any liability for whatsoever reason.



Pertanika Journals

Our goal is to bring high quality research to the widest possible audience

INSTRUCTIONS TO AUTHORS (Manuscript Preparation & Submission Guide)

Revised: June 2016

Please read the Pertanika guidelines and follow these instructions carefully. Manuscripts not adhering to the instructions will be returned for revision without review. The Chief Executive Editor reserves the right to return manuscripts that are not prepared in accordance with these guidelines.

MANUSCRIPT PREPARATION

Manuscript Types

Pertanika accepts submission of mainly **four** types of manuscripts for peer-review.

1. REGULAR ARTICLE

Regular articles are full-length original empirical investigations, consisting of introduction, materials and methods, results and discussion, conclusions. Original work must provide references and an explanation on research findings that contain new and significant findings.

Size: Generally, these are expected to be between 6 and 12 journal pages (excluding the abstract, references, tables and/or figures), a maximum of 80 references, and an abstract of 100–200 words.

2. REVIEW ARTICLE

These report critical evaluation of materials about current research that has already been published by organizing, integrating, and evaluating previously published materials. It summarizes the status of knowledge and outline future directions of research within the journal scope. Review articles should aim to provide systemic overviews, evaluations and interpretations of research in a given field. Re-analyses as meta-analysis and systemic reviews are encouraged. The manuscript title must start with "Review Article:".

Size: These articles do not have an expected page limit or maximum number of references, should include appropriate figures and/or tables, and an abstract of 100–200 words. Ideally, a review article should be of 7 to 8 printed pages.

3. SHORT COMMUNICATIONS

They are timely, peer-reviewed and brief. These are suitable for the publication of significant technical advances and may be used to:

- (a) report new developments, significant advances and novel aspects of experimental and theoretical methods and techniques which are relevant for scientific investigations within the journal scope;
- (b) report/discuss on significant matters of policy and perspective related to the science of the journal, including 'personal' commentary;
- (c) disseminate information and data on topical events of significant scientific and/or social interest within the scope of the journal.

The manuscript title must start with "*Brief Communication:*".

Size: These are usually between 2 and 4 journal pages and have a maximum of three figures and/or tables, from 8 to 20 references, and an abstract length not exceeding 100 words. Information must be in short but complete form and it is not intended to publish preliminary results or to be a reduced version of Regular or Rapid Papers.

4. OTHERS

Brief reports, case studies, comments, concept papers, Letters to the Editor, and replies on previously published articles may be considered.

PLEASE NOTE: NO EXCEPTIONS WILL BE MADE FOR PAGE LENGTH.

Language Accuracy

Pertanika **emphasizes** on the linguistic accuracy of every manuscript published. Articles must be in **English** and they must be competently written and argued in clear and concise grammatical English. Contributors are strongly advised to have the manuscript checked by a colleague with ample experience in writing English manuscripts or a competent English language editor.

Author(s) **must provide a certificate** confirming that their manuscripts have been adequately edited. A proof from a recognised editing service should be submitted together with the cover letter at the time of submitting a manuscript to Pertanika. **All editing costs must be borne by the author(s)**. This step, taken by authors before submission, will greatly facilitate reviewing, and thus publication if the content is acceptable.

Linguistically hopeless manuscripts will be rejected straightaway (e.g., when the language is so poor that one cannot be sure of what the authors really mean). This process, taken by authors before submission, will greatly facilitate reviewing, and thus publication if the content is acceptable.

MANUSCRIPT FORMAT

The paper should be submitted in one column format with at least 4cm margins and 1.5 line spacing throughout. Authors are advised to use Times New Roman 12-point font and *MS Word* format.

1. Manuscript Structure

Manuscripts in general should be organised in the following order:

Page 1: Running title

This page should **only** contain the running title of your paper. The running title is an abbreviated title used as the running head on every page of the manuscript. The running title should not exceed 60 characters, counting letters and spaces.

Page 2: Author(s) and Corresponding author information.

This page should contain the **full title** of your paper not exceeding 25 words, with name(s) of all the authors, institutions and corresponding author's name, institution and full address (Street address, telephone number (including extension), hand phone number, and e-mail address) for editorial correspondence. First and corresponding authors must be clearly indicated.

The names of the authors may be abbreviated following the international naming convention. e.g. Salleh, A.B.¹, Tan, S.G^{2*}., and Sapuan, S.M³.

Authors' addresses. Multiple authors with different addresses must indicate their respective addresses separately by superscript numbers:

George Swan¹ and Nayan Kanwal²

¹Department of Biology, Faculty of Science, Duke University, Durham, North Carolina, USA.,

²Office of the Deputy Vice Chancellor (R&I), Universiti Putra Malaysia, Serdang, Malaysia.

A **list** of number of **black and white / colour figures and tables** should also be indicated on this page. Figures submitted in color will be printed in colour. See "5. Figures & Photographs" for details.

Page 3: Abstract

This page should **repeat** the **full title** of your paper with only the **Abstract** (the abstract should be less than 250 words for a Regular Paper and up to 100 words for a Short Communication), and **Keywords**.

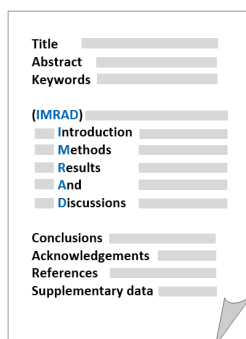
Keywords: Not more than eight keywords in alphabetical order must be provided to describe the contents of the manuscript.

Page 4: Introduction

This page should begin with the **Introduction** of your article and followed by the rest of your paper.

2. Text

Regular Papers should be prepared with the headings *Introduction, Materials and Methods, Results and Discussion, Conclusions, Acknowledgements, References, and Supplementary data* (if available) in this order.



Title _____
 Abstract _____
 Keywords _____
 (IMRAD)
 Introduction _____
 Methods _____
 Results _____
 And _____
 Discussions _____
 Conclusions _____
 Acknowledgements _____
 References _____
 Supplementary data _____

MAKE YOUR ARTICLES AS CONCISE AS POSSIBLE

Most scientific papers are prepared according to a format called IMRAD. The term represents the first letters of the words Introduction, Materials and Methods, Results, And, Discussion. It indicates a pattern or format rather than a complete list of headings or components of research papers; the missing parts of a paper are: Title, Authors, Keywords, Abstract, Conclusions, and References. Additionally, some papers include Acknowledgments and Appendices.

The Introduction explains the scope and objective of the study in the light of current knowledge on the subject; the Materials and Methods describes how the study was conducted; the Results section reports what was found in the study; and the Discussion section explains meaning and significance of the results and provides suggestions for future directions of research. The manuscript must be prepared according to the Journal's instructions to authors.

3. Equations and Formulae

These must be set up clearly and should be typed double spaced. Numbers identifying equations should be in square brackets and placed on the right margin of the text.

4. Tables

All tables should be prepared in a form consistent with recent issues of Pertanika and should be numbered consecutively with Roman numerals. Explanatory material should be given in the table legends and footnotes. Each table should be prepared on a new page, embedded in the manuscript.

When a manuscript is submitted for publication, tables must also be submitted separately as data - .doc, .rtf, Excel or PowerPoint files- because tables submitted as image data cannot be edited for publication and are usually in low-resolution.

5. Figures & Photographs

Submit an **original** figure or photograph. Line drawings must be clear, with high black and white contrast. Each figure or photograph should be prepared on a new page, embedded in the manuscript for reviewing to keep the file of the manuscript under 5 MB. These should be numbered consecutively with Roman numerals.

Figures or photographs must also be submitted separately as TIFF, JPEG, or Excel files- because figures or photographs submitted in low-resolution embedded in the manuscript cannot be accepted for publication. For electronic figures, create your figures using applications that are capable of preparing high resolution TIFF files. In general, we require **300 dpi** or higher resolution for **coloured and half-tone artwork**, and **1200 dpi or higher** for **line drawings** are required.

Failure to comply with these specifications will require new figures and delay in publication.

NOTE: Illustrations may be produced in colour at no extra cost at the discretion of the Publisher; the author could be charged Malaysian Ringgit 50 for each colour page.

6. References

References begin on their own page and are listed in alphabetical order by the first author's last name. Only references cited within the text should be included. All references should be in 12-point font and double-spaced.

NOTE: When formatting your references, please follow the **APA reference style** (6th Edition). Ensure that the references are strictly in the journal's prescribed style, failing which your article will **not be accepted for peer-review**. You may refer to the *Publication Manual of the American Psychological Association* for further details (<http://www.apastyle.org/>).

7. General Guidelines

Abbreviations: Define alphabetically, other than abbreviations that can be used without definition. Words or phrases that are abbreviated in the introduction and following text should be written out in full the first time that they appear in the text, with each abbreviated form in parenthesis. Include the common name or scientific name, or both, of animal and plant materials.

Acknowledgements: Individuals and entities that have provided essential support such as research grants and fellowships and other sources of funding should be acknowledged. Contributions that do not involve researching (clerical assistance or personal acknowledgements) should **not** appear in acknowledgements.

Authors' Affiliation: The primary affiliation for each author should be the institution where the majority of their work was done. If an author has subsequently moved to another institution, the current address may also be stated in the footer.

Co-Authors: The commonly accepted guideline for authorship is that one must have substantially contributed to the development of the paper and share accountability for the results. Researchers should decide who will be an author and what order they will be listed depending upon their order of importance to the study. Other contributions should be cited in the manuscript's Acknowledgements.

Copyright Permissions: Authors should seek necessary permissions for quotations, artwork, boxes or tables taken from other publications or from other freely available sources on the Internet before submission to Pertanika. Acknowledgement must be given to the original source in the illustration legend, in a table footnote, or at the end of the quotation.

Footnotes: Current addresses of authors if different from heading may be inserted here.

Page Numbering: Every page of the manuscript, including the title page, references, tables, etc. should be numbered.

Spelling: The journal uses American or British spelling and authors may follow the latest edition of the Oxford Advanced Learner's Dictionary for British spellings.

SUBMISSION OF MANUSCRIPTS

Owing to the volume of manuscripts we receive, we must insist that all submissions be made electronically using the **online submission system ScholarOne™**, a web-based portal by Thomson Reuters. For more information, go to our web page and [click "Online Submission"](#).

Submission Checklist

1. **MANUSCRIPT:** Ensure your MS has followed the Pertanika style particularly the first four pages as explained earlier. The article should be written in a good academic style and provide an accurate and succinct description of the contents ensuring that grammar and spelling errors have been corrected before submission. It should also not exceed the suggested length.

COVER LETTER: All submissions must be accompanied by a cover letter detailing what you are submitting. Papers are accepted for publication in the journal on the understanding that the article is **original** and the content has **not been published** either **in English** or **any other language(s)** or **submitted for publication elsewhere**. The letter should also briefly describe the research you are reporting, why it is important, and why you think the readers of the journal would be interested in it. The cover letter must also contain an acknowledgement that all authors have contributed significantly, and that all authors have approved the paper for release and are in agreement with its content.

The cover letter of the paper should contain (i) the title; (ii) the full names of the authors; (iii) the addresses of the institutions at which the work was carried out together with (iv) the full postal and email address, plus telephone numbers and emails of all the authors. The current address of any author, if different from that where the work was carried out, should be supplied in a footnote.

The above must be stated in the cover letter. Submission of your manuscript will not be accepted until a cover letter has been received

2. **COPYRIGHT:** Authors publishing the Journal will be asked to sign a copyright form. In signing the form, it is assumed that authors have obtained permission to use any copyrighted or previously published material. All authors must read and agree to the conditions outlined in the form, and must sign the form or agree that the corresponding author can sign on their behalf. Articles cannot be published until a signed form (*original pen-to-paper signature*) has been received.

Please do **not** submit manuscripts to the editor-in-chief or to any other office directly. Any queries must be directed to the **Chief Executive Editor's** office via email to nayan@upm.my.

Visit our Journal's website for more details at <http://www.pertanika.upm.edu.my/home.php>.

HARDCOPIES OF THE JOURNALS AND OFF PRINTS

Under the Journal's open access initiative, authors can choose to download free material (via PDF link) from any of the journal issues from Pertanika's website. Under "**Browse Journals**" you will see a link, "*Current Issues*" or "*Archives*". Here you will get access to all current and back-issues from 1978 onwards.

The **corresponding author** for all articles will receive one complimentary hardcopy of the journal in which his/her articles is published. In addition, 20 off prints of the full text of their article will also be provided. Additional copies of the journals may be purchased by writing to the Chief Executive Editor.



Why should you publish in

Pertanika?

BENEFITS TO AUTHORS

PROFILE: Our journals are circulated in large numbers all over Malaysia, and beyond in Southeast Asia. Our circulation covers other overseas countries as well. We ensure that your work reaches the widest possible audience in print and online, through our wide publicity campaigns held frequently, and through our constantly developing electronic initiatives such as Web of Science Author Connect backed by Thomson Reuters.

QUALITY: Our journals' reputation for quality is unsurpassed ensuring that the originality, authority and accuracy of your work are fully recognised. Each manuscript submitted to Pertanika undergoes a rigid originality check. Our double-blind peer refereeing procedures are fair and open, and we aim to help authors develop and improve their scientific work. Pertanika is now over 38 years old; this accumulated knowledge has resulted in our journals being indexed in SCOPUS (Elsevier), Thomson (ISI) Web of Science™ Core Collection, Emerging Sources Citation Index (ESCI), Web of Knowledge [BIOSIS & CAB Abstracts], EBSCO, DOAJ, ERA, AGRICOLA, Google Scholar, ISC, TIB, Journal Guide, Citefactor, Cabell's Directories and MyCite.

AUTHOR SERVICES: We provide a rapid response service to all our authors, with dedicated support staff for each journal, and a point of contact throughout the refereeing and production processes. Our aim is to ensure that the production process is as smooth as possible, is borne out by the high number of authors who prefer to publish with us.

CODE OF ETHICS: Our Journal has adopted a Code of Ethics to ensure that its commitment to integrity is recognized and adhered to by contributors, editors and reviewers. It warns against plagiarism and self-plagiarism, and provides guidelines on authorship, copyright and submission, among others.

PRESS RELEASES: Landmark academic papers that are published in Pertanika journals are converted into press-releases as a unique strategy for increasing visibility of the journal as well as to make major findings accessible to non-specialist readers. These press releases are then featured in the university's UK and Australian based research portal, ResearchSEA, for the perusal of journalists all over the world.

LAG TIME: The elapsed time from submission to publication for the articles averages 3 to 4 months. A decision on acceptance of a manuscript is reached in 3 to 4 months (average 14 weeks).



Address your submissions to:
The Chief Executive Editor
Tel: +603 8947 1622
nayan@upm.my

Journal's Profile: www.pertanika.upm.edu.my/

Call for Papers 2017-18

now accepting submissions...

Pertanika invites you to explore frontiers from all key areas of agriculture, science and technology to social sciences and humanities.

Original research and review articles are invited from scholars, scientists, professors, post-docs, and university students who are seeking publishing opportunities for their research papers through the Journal's three titles; JTAS, JST & JSSH. Preference is given to the work on leading and innovative research approaches.

Pertanika is a fast track peer-reviewed and open-access academic journal published by Universiti Putra Malaysia. To date, Pertanika Journals have been indexed by many important databases. Authors may contribute their scientific work by publishing in UPM's hallmark SCOPUS & ISI indexed journals.

Our journals are open access - international journals. Researchers worldwide will have full access to all the articles published online and be able to download them with zero subscription fee.

Pertanika uses online article submission, review and tracking system for quality and quick review processing backed by Thomson Reuter's ScholarOne™. Journals provide rapid publication of research articles through this system.

For details on the Guide to Online Submissions, please visit http://www.pertanika.upm.edu.my/guide_online_submission.php

About the Journal

Pertanika is an international multidisciplinary peer-reviewed leading journal in Malaysia which began publication in 1978. The journal publishes in three different areas — Journal of Tropical Agricultural Science (JTAS); Journal of Science and Technology (JST); and Journal of Social Sciences and Humanities (JSSH). All journals are published in English.

JTAS is devoted to the publication of original papers that serves as a forum for practical approaches to improving quality in issues pertaining to tropical agricultural research- or related fields of study. It is published four times a year in *February, May, August* and *November*.

JST caters for science and engineering research- or related fields of study. It is published twice a year in *January* and *July*.

JSSH deals in research or theories in social sciences and humanities research. It aims to develop as a flagship journal with a focus on emerging issues pertaining to the social and behavioural sciences as well as the humanities, particularly in the Asia Pacific region. It is published four times a year in *March, June, September* and *December*.



An Award-winning
International-Malaysian Journal
— CREAM AWARD, MoHE
—Sept 2015





Performance Evaluation of Compressive Sensing based Channel Estimation Techniques in OFDM System for Different Channels <i>Jha, A., Kansal, L. and Gaba, G. S.</i>	921
Cost Estimation Model for Web Applications using Agile Software Development Methodology <i>Soni, D. and Kohli, P. J.</i>	931
Understanding Consumer Preferences using IoT SmartMirrors <i>Gaur, L., Singh, G. and Ramakrishnan, R.</i>	939
Selected Papers from the International Conference On Computational Methods In Engineering and Health Sciences (ICCMEH 2015)	
Guest Editor: Kamarul Ariffin Ahmad, Mohammad Zuber, Mohamad Ridzwan Ishak & Norkhairunnisa Mazlan	
Guest Editorial Board: Azmin Shakrine Mohd Rafie, Mohamed Thariq Hameed Sultan, Raghuvir Pai, Masaaki Tamagawa, Satish Shenoy, S. M. Abdul Khader & Satoshi Iikubo	
Investigation on Tapping of Al6061-SiC Metal Matrix Composite with HSS Taps <i>Melvin Paious, Raviraja Adhikari and Nagaraja</i>	949
Dynamic Performance Characteristics of Finite Journal Bearings Operating on TiO ₂ based Nanolubricants <i>Binu, K. G., Yathish, K., Shenoy, B. S., Rao, D. S. and Pai, R.</i>	963
Modal Behaviour of Vertical Axis Wind Turbine Comprising Prestressed Rotor Blades: A Finite Element Analysis <i>Torabi Asr, M., Masoumi, M. M. and Mustapha, F.</i>	977
A review study on diesel and natural gas and its impact on CI engine emissions <i>Hayder A. Alrazen and K. A. Ahmad</i>	983
Stability of water lubricated bearing using linear perturbation method under turbulent conditions <i>R. Mallya, B. S. Shenoy, R. S. Pai and R. Pai</i>	995
Estimation and Validation of Nearshore Current at the Coast of Carey Island, Malaysia <i>Fitri, A., Hashim, R. and Motamedi, S.</i>	1009
A Computational Fluid Dynamics Study of Combustion and Emission Performance in an Annular Combustor of a Jet Engine <i>M. Zuber, M. S. B. Hisham, N. A. M. Nasir, A. A. Basri and S. M. A. Khader</i>	1019
Effect of Silica Nanoparticles in Kenaf Reinforced Epoxy: Flexural and Compressive Properties <i>F. Bajuri, N. Mazlan and M. R. Ishak</i>	1029

Relative Risk Estimation for Dengue Disease Mapping in Malaysia based on Besag, York and Mollié Model <i>Samat, N. A. and Pei Zhen, W.</i>	759
Effects of Baseline Correction Algorithms on Forensic Classification of Paper Based on ATR-FTIR Spectrum and Principal Component Analysis (PCA) <i>Lee, L. C., Liong, C-Y., Khairul, O. and Jemain, A. A.</i>	767
Deriving Partial Differential Equation for the Value of Salam Contract with Credit Risk <i>Hisham, A. F. B., Jaffar, M. M. and Othman, J.</i>	775
Combination of Forecasts with an Application to Unemployment Rate <i>Muniroh, M. F., Ismail, N. and Lazim, M. A.</i>	787
Complexity Index for Decision Making Method <i>Hanif, H. M., Mohamad, D. and Dom, R. M.</i>	797
Evaluation of Risk Factors for Prolonged Invasive Mechanical Ventilation in Paediatric Intensive Care Unit (PICU) <i>Ismail, I., Yap, B. W. and Abidin, A. S. Z.</i>	811
The Control Chart Technique for the Detection of the Problem of Bad Data in State Estimation Power System <i>Zahid Khan, Radzuan B. Razali, Hanita Daud, Nursyarizal Mohd Nor and Mahmud Fotuhi-Firuzabad</i>	825
Selected Papers from the International Conference on Science, Engineering, Law and Management (ICSELM 2017)	
Guest Editor: Hardeep Singh & Acmad Choerudin	
Guest Editorial Board: Pooja Sahni, Amit Wason, Surender Singh Saini, Elsanosy M. Elamin & Tolga Ensari	
Internet of Things – Technology Adoption Model in India <i>Singh, G., Gaur, L. and Ramakrishnan, R.</i>	835
Effect of Maghemite (γ -Fe ₂ O ₃) Nano-Powder Mixed Dielectric Medium on Tool Wear Rate (TWR) During Micro-EDM of Co- Cr-Mo <i>Elsiti, N. M., Noordin, M. Y. and Idris, A.</i>	847
Review of Channel Modelling for Optical Wireless Links <i>Miglani, R. and Malhotra, J. S.</i>	859
Dealing with Interdependency among NFR using ISM <i>Kaur, H. and Sharma, A.</i>	871
DNA and Bernoulli Random Number Generator Based Security Key Generation Algorithm <i>Sodhi, G. K. and Gaba, G. S.</i>	891
Analysis of MIMO FSO over different Modulation Techniques <i>Kaur, K., Miglani, R. and Malhotra, J. S.</i>	905

Contents

Foreword	i
<i>Nayan Deep S. Kanwal</i>	
Review Article	
Implementation of Building Information Modelling (BIM) in Malaysia: A Review	661
<i>Nuzul Azam Haron, Raja Putri Zarifah Ana Raja Soh and Aizul Nahar Harun</i>	
Regular Articles	
Reliability, Technical Error of Measurement and Validity of Height Measurement Using Portable Stadiometer	675
<i>Azli Baharudin, Mohamad Hasnan Ahmad, Balkish Mahadir Naidu, Nurul Rufaidah Hamzah, Nor Azian Mohd Zaki, Ahmad Ali Zainuddin and Noor Safiza Mohd Nor</i>	
The value of ¹⁸ F-fluorodeoxyglucose –positron emission tomography/computed tomography (¹⁸ F- FDG PET/CT) in the staging and impact on the management of patients with nasopharyngeal carcinoma	687
<i>Sethu Thakachy Subha, Fathinul Fikri Ahmad Saad, Abdul Jalil Nordin and Saraiza Abu Bakar</i>	
Design of a Movable Swine Roasting Machine	697
<i>Bunkrachang, N. and Kitthawee, U.</i>	
Effect of inoculums content and screening of significant variables for simultaneous COD removal and H ₂ production from tapioca wastewater using Plackett-Burman Design	707
<i>Thanwised, P.</i>	
Comparison of Scoring Functions on Greedy Search Bayesian Network Learning Algorithms	719
<i>ChongYong, Chua and HongChoon, Ong</i>	
Selected Papers from the 2nd International Conference on Statistics in Science, Business and Engineering (ICSSBE 2015)	
Guest Editors: Yap Bee Wah & Sayang Mohd Deni	
Analysis of Malaysia's Single Stock Futures and Its Spot Price	735
<i>Marzuki, R. M., Mohd, M. A., Nawawi, A. H. M. and Redzwan, N. M.</i>	
Projecting Input-Output Table for Malaysia: A Comparison of RAS and EURO Method	745
<i>Shuja', N., Lazim, M. A. and Yap, B. W.</i>	



Pertanika Editorial Office, Journal Division
Office of the Deputy Vice Chancellor (R&I),
1st Floor, IDEA Tower II,
UPM-MTDC Technology Centre
Universiti Putra Malaysia
43400 UPM Serdang
Selangor Darul Ehsan
Malaysia

<http://www.pertanika.upm.edu.my/>
E-mail: executive_editor.pertanika@upm.my
Tel: +603 8947 1622/1620

PENERBIT
UPM
UNIVERSITI PUTRA MALAYSIA
PRESS

<http://penerbit.upm.edu.my>
E-mail : penerbit@putra.upm.edu.my
Tel : +603 8946 8855/8854
Fax : +603 8941 6172

